IAEA-TECDOC-1178

Handbook on photonuclear data for applications
Cross-sections and spectra

Final report of a co-ordinated research project
1996–1999

INTERNATIONAL ATOMIC ENERGY AGENCY

31 / 47

October 2000

L

HANDBOOK ON PHOTONUCLEAR DATA FOR APPLICATIONS:
CROSS-SECTIONS AND SPECTRA
IAEA, VIENNA, 2000
IAEA-TECDOC-1178
ISSN 1011–4289

Please be aware that all of the Missing Pages in this document were originally blank pages

FOREWORD

Nuclear data for applications constitute an integral part of the IAEA's programme of activities. In recent years, the traditional emphasis on energy applications, in terms of nuclear power reactors and related neutron reaction data, has been gradually shifting towards non-energy applications. This shift could be viewed as a response to increasing user demands for data describing nuclear interactions with charged particles and photons.

Photons are commonly produced as bremsstrahlung radiation by electron accelerators. These are relatively simple machines present in many hospitals, industries and laboratories. Photonuclear data, describing interactions of photons with atomic nuclei, are of importance for a variety of applications. These applications span from radiation shielding and radiotherapy to inspection technologies and possibly nuclear waste transmutation.

In response to growing needs for photonuclear data, in the 1990s, a number of laboratories worldwide became engaged in the development of their own or national photonuclear data libraries. There was no international co-ordination of this effort, and consequently no effort to create an internationally recognized photonuclear data library.

In this situation the IAEA initiated a Co-ordinated Research Project (CRP) on Compilation and Evaluation of Photonuclear Data for Applications. The project, coordinated by the IAEA between 1996 and 1999, produced three major results: the IAEA Photonuclear Data Library; the present Handbook on Photonuclear Data for Applications; and additions of compiled experimental photonuclear cross-sections in the EXFOR database.

The IAEA wishes to thank all the participants of the CRP and other scientists for their work that led to the creation of the Photonuclear Data Library and for their contributions to the present TECDOC. The assistance of M.B. Chadwick (chair), A.I. Blokhin, T. Fukahori, Y.-O. Lee, M.N. Martins, V.V. Varlamov, B. Yu, as well as Y. Han, S.F. Mughabghab, and J. Zhang in the preparation of this publication is gratefully acknowledged. The responsible IAEA staff member for this report was P. Obložinský, Division of Physical and Chemical Sciences.

CONTENTS

Chapter 1

Introduction

Photons are commonly produced as bremsstrahlung radiation by electron accelerators. These are relatively simple machines (generally small linear accelerators, sometimes microtrons) present in many laboratories, industries and hospitals. For example, electron accelerators with energies up to 25 MeV are used to produce bremsstrahlung beams in many radiation oncology facilities worldwide.

Photo-induced reaction cross-section data are of importance for a variety of current or emerging applications. Among them are:

- Radiation shielding design and radiation transport analyses (of particular concern are photoneutrons produced by photons with energies above the neutron separation energy – typically above about 8 MeV),

- Calculations of absorbed dose in the human body during radiotherapy,

- Physics and technology of fission reactors (influence of photoreactions on neutron balance) and fusion reactors (plasma diagnostics and shielding),

- Activation analyses, safeguards and inspection technologies (identification of materials through radiation induced by photonuclear reactions using portable bremsstrahlung devices),

- Nuclear waste transmutation, and

- Astrophysical nucleosynthesis.

Other areas where accurate photonuclear data are needed are reactor in–core dosimetry (to take into account contributions from photofission events in monitor foils), radiation damage estimates in reactor structural materials (both for displacement and transmutation calculations), safeguards (for taking into account photon induced neutron production on light nuclei) and fast reactor calculations (impact on uranium–thorium cycle).

In the past, several activities were carried out which aimed to provide reliable photonuclear data for these applications. One of the most important was the project by the Photonuclear Data Center of the US National Bureau of Standards during the period 1955-1982. This project culminated in the voluminous 15 issues by E.G. Fuller and H. Gerstenberg "Photonuclear Data - Abstract Sheets 1955-1982", published between 1983 and 1986 [1]. Given the technologies available at the time, these data were collected and published as hardcopies from the original literature in the form of abstracts, tables and graphs. Another pioneering work was undertaken by B.L. Berman in his 1975 "Atlas of Photoneutron Cross-Sections Obtained by Monoenergetic Photons" [2], followed by the update coauthored with S.S. Dietrich in 1988 [3].

Despite these efforts, there has been a lack of evaluated photonuclear data. Users often rely on raw photonuclear data, primarily reaction cross-sections from different (and often discrepant) measurements. However, many applications need evaluated cross-sections and emission spectra for transport calculations. Generally, data for structural, shielding, and bremsstrahlung conversion target materials are most important, followed by biologically-important materials. In terms of incident energies, the giant dipole resonance region is most important. i.e. photon energies below about 25-30 MeV.

The evaluation of nuclear reaction data consists of several systematic steps. These include a bibliographic compilation. a compilation of experimental data. followed by a critical analysis of the measurement techniques used, together with evaluations based on theoretical nuclear reaction modeling. The present status of photonuclear data compilations and evaluations is described below.

Bibliography compilations can be considered as satisfactory. In the past, several laboratories, mainly LLNL Livermore (USA). CEN Saclay (France) and MSU Moscow (Russia). have reported a large body of experimental data. These data were partly compiled into the internationally available computerized library EXFOR. This major task is not yet complete (only about 20% of the published data were compiled as of the end of 1996).

The need for evaluation methods for photonuclear data arises because it is difficult to develop a complete photonuclear data file on the basis of measured cross-sections alone. These data were often obtained from different kinds of photon sources, causing significant systematic discrepancies. and there is a lack of data in a number of important cases. Nevertheless, recent developments both in methods to resolve experimental discrepancies and in nuclear reaction theory are promising for use in the generation of evaluated photonuclear data.

During the 1990s, several laboratories began to be engaged in large-scale evaluations of photonuclear data. For example, in Japan, JAERI (Tokai) was developing a Photonuclear Data File up to 140 MeV. In Russia, a series of evaluations were performed at the Centre for Photonuclear Experiments Data, MSU Moscow, and IPPE Obninsk was working on the photonuclear BOFOD library up to 20 MeV. In China, the Chinese Nuclear Data Center (Beijing) was developing methods to calculate photonuclear reactions. In the USA, LANL (Los Alamos) was working on theoretical models for emission spectra and angular distributions from photonuclear reactions. and on databases for simulations of (nucleon-induced) accelerator-driven technologies.

Considering the above research activities, the pressing needs for evaluated data, and the promising recent developments in evaluation methods (both experimental and theoretical in origin), it was felt to be timely and useful to initiate a co-ordinated effort to develop an internationally agreed-upon file of evaluated photonuclear data. Such a Co-ordinated Research Project (CRP), endorsed by the International Nuclear Data Committee at its 1993 and 1995 Meetings in Vienna, was approved and initiated by the IAEA in 1996 under the title *"Compilation and Evaluation of Photonuclear Data for Applications"*. The ultimate goal of the CRP was to develop an internationally recognized data file of evaluated photonuclear reaction cross-sections for use in transport simulation codes (such as MCNP [4], used for example in recent calculations of absorbed dose in photon therapy [5]).

The most important incident-energy range is up to 25 MeV, the upper energy of most electron/photon accelerators, which also corresponds to the energy range of photoab-

sorption primarily via the giant dipole resonance. Photonuclear data up to energies of approximately 50 MeV are useful for some new medical accelerator technologies under development that utilize higher energy photons. Additionally, it is also desirable to have evaluated photonuclear data up to an incident energy of approximately 150 MeV due to their use in emerging accelerator-driven transmutation technologies. to complement the neutron and proton high-energy libraries that are being implemented in fully-coupled neutron-photon-charged-particle radiation transport simulations [6].

The list of the most important materials (43 elements) for which photonuclear data are needed is summarized below. The list starts with structural, shielding and bremmsstrahlung target materials. followed by biological, and fissionable materials. It should be noted that the CRP focused on the major 40 isotopes of the first three groups comprising 29 elements. Thanks to the impressive efforts of the Nuclear Data Laboratory, KAERI. S. Korea, this project also generated evaluated data for an additional 124 isotopes, comprising largely the elements shown in the fourth category below.

1. Structural. shielding, and bremsstrahlung target materials
   Be, Al. Si, Ti, V, Cr, Fe, Co. Ni, Cu, Zn, Zr, Mo, Sn, Ta. W. Pb
   Note: Beryllium bremsstrahlung targets are used in special
      clinical accelerators to produce narrow photon beams.
2. Biological materials
   C, N, O, Na, S, P, Cl, Ca
3. Fissionable materials
   Th. U, Np, Pu
4. Other materials
   H, K, Ge, Sr, Nb, Pd, Ag, Cd, Sb, Te, I, Cs, Sm, Tb.

The present TECDOC is primarily designed for users of photonuclear data, aimed to fill-in a substantial gap in the scientific and technical literature on photonuclear reactions. In addition to production cross-sections, energy and angular distributions of the emitted particles are provided (these are needed for transport calculations). The TECDOC provides users with an up-to-date overview of photonuclear reaction data. The material is presented in a systematical way, covering experimental data and their compilation; an introduction to relevant parts of nuclear reaction theory; an exposition of evaluation methodology used to generate evaluations; an intercomparison of different evaluations; and finally a description of the IAEA Photonuclear Data Library.

The TECDOC is organized as follows. For the reader's convenience we first summarize definitions and notations in Chapter 2. Then, we proceed with a description of available experimental data in Chapter 3. Chapter 4 is devoted to a description of nuclear reaction models that constitute the basic tool for an evaluation of photonuclear reaction data. Then, Chapter 5 is devoted to a summary and description of the evaluations, including one of the key novel aspects of the present project – emission spectra. This is followed by the ultimate highlight of the whole project: a description of the IAEA Photonuclear Data Library in Chapter 6. The concluding Chapter 7 summarizes recommendations for users as well as possible directions for future research work. Finally, Appendix A reproduces a tabular part of the Atlas of Giant Dipole Resonances [7], and Appendix B shows graphical presentation of the IAEA Photonuclear Data Library.

Chapter 2

Definitions and Notation

2.1 General

There are two basic methods for the experimental study of photonuclear reactions: the measurement of the residual activity of the final nucleus, if radioactive; and the direct detection of outgoing particle(s).

In certain cases the first method allows the details of all reaction products (light particles and heavy residual nuclei) to be determined unambiguously, and therefore the exclusive reaction cross-section (see below) can be determined. An example is the measurement of the activity of ^{62}Cu ($T_{1/2}$ = 9.74 min) for studying the reaction ^{63}Cu$(\gamma, n)^{62}$Cu. At higher energies, when multiparticle emission processes become energetically possible, in some cases this method cannot be used since more than one combination of light-particle ejectiles may lead to the same radioactive product nuclide. As, for example, in the case of ^{63}Cu$(\gamma, 2n)$ and $(\gamma, 2p)$ reactions, which produce ^{61}Cu and ^{61}Co, respectively, both decaying to the same final nucleus ^{61}Ni.

The second method, in its basic form, measures inclusive reaction cross-sections (see below) since in general a number of exclusive reaction channels may contribute to the production of the outgoing particle of interest. For instance, the exclusive reactions (γ, n), (γ, np), $(\gamma, 2n)$, etc. may all be open and therefore contribute to the measured inclusive neutron production. So, in general, the exact reaction studied depends upon the experimental methods employed. This may lead to uncertainties in the interpretation of experimental results when the authors do not specify exactly what was measured. For example, in certain papers, authors indicate that they measure the (γ, n) reaction, while actually measuring the $[(\gamma, n) + (\gamma, np)]$ reaction, which can be significantly different especially for light target nuclei where charged-particle emission channels are not small.

The term *exclusive cross-section* is used to indicate an individual nuclear reaction of a specific, unique type. For example, $(\gamma, 2n)$, (γ, α), and (γ, np) each indicate particular exclusive reactions, where all the secondary particles (ejectiles, including the residual nucleus) are known. Analogously, the term *inclusive cross-section* is used to designate a process that includes all nuclear reactions leading to production of a particular emission product. Such emission products might be, for example, neutrons, protons, gamma-rays, or a particular residual nucleus formed in several different exclusive reactions. For instance, the inclusive photoneutron yield cross-section (written as (γ, xn), where x indicates any combination of emitted particles) might involve the sum of exclusive reactions such as (γ, n), (γ, np), $(\gamma, n\alpha)$, $2(\gamma, 2n)$, etc., that lead to emission of a neutron.

The term *evaluated* is used in this text to describe cross-sections or other data that have been determined by: (1) assessing the most probable value from a collection of ex-

perimental data; (2) performing theoretical calculations with models and parameters that have been optimized to experimental data; or, (3) using a combination of experimental data and theoretical calculations to ascertain best or recommended values. Similarly, the term *evaluation* is used here to describe a computer file of evaluated nuclear data (cross-sections, angular distributions, energy distributions, *etc.*) that provides complete coverage over a specific energy range of all quantities needed in a typical nuclear analysis calculation (for example, calculations of particle transport, radiation damage, energy deposition, *etc.*)

If neutrons are detected in an inclusive emission measurement, then the cross-section measured is the inclusive photoneutron yield cross-section, and includes the multiplicity of neutrons emitted in each reaction event:

$$
\begin{aligned}
\sigma(\gamma, xn) \quad = \quad & \sigma(\gamma, n) + \sigma(\gamma, np) + \sigma(\gamma, n2p) + \\
+ \quad & 2\sigma(\gamma, 2n) + 2\sigma(\gamma, 2np) + 3\sigma(\gamma, 3n) + \cdots + \\
+ \quad & \bar{\nu}(\gamma, F),
\end{aligned}
\tag{2.1}
$$

where $\bar{\nu}$ is the average multiplicity of photofission neutrons.

In several cases, authors use special methods to infer the photoneutron multiplicity (so called "ring-ratio" methods, statistical methods, theory calculations, *etc.*), and give data for the total photoneutron cross-section:

$$
\begin{aligned}
\sigma(\gamma, sn) \quad = \quad & \sigma(\gamma, n) + \sigma(\gamma, np) + \sigma(\gamma, 2n) + \\
+ \quad & \sigma(\gamma, 2np) + \sigma(\gamma, n2p) + \sigma(\gamma, 3n) + \cdots + \\
+ \quad & \sigma(\gamma, F).
\end{aligned}
\tag{2.2}
$$

The sum of this reaction with the photo-charged-particle reaction cross-section will give the total photoabsorption reaction cross-section:

$$
\begin{aligned}
\sigma(\gamma, abs) \quad = \quad & \sigma(\gamma, sn) + \sigma(\gamma, p) + \sigma(\gamma, 2p) + \cdots + \\
+ \quad & \sigma(\gamma, d) + \sigma(\gamma, dp) + \cdots + \sigma(\gamma, \alpha) + \cdots
\end{aligned}
\tag{2.3}
$$

It should be noted that for heavy nuclei photoabsorption cross-section can be approximated by the first term of the above equation

$$
\sigma(\gamma, abs) \cong \sigma(\gamma, sn).
\tag{2.4}
$$

2.2 Symbols

For the reader's convenience, the most important symbols used throughout the present document are summarized below.

$\sigma(\gamma, abs)$	Photoabsorption cross-section
$\sigma(\gamma, 1n)$	Single photoneutron cross-section
$\sigma(\gamma, 1nx)$	Sum of cross-sections that have a single neutron in the final state $(1n + 1np + 1n\alpha + 1n \cdots)$
$\sigma(\gamma, 2n)$	Double photoneutron cross-section
$\sigma(\gamma, 2nx)$	Sum of cross-sections that have two neutrons in the final state $(2n + 2np + 2n\alpha + 2n \cdots)$
$\sigma(\gamma, sn)$	Total photoneutron cross-section, also known as $\sigma(\gamma, tot\ n)$
$\sigma(\gamma, xn)$	Photoneutron yield or production cross-section
$\sigma(\gamma, f)$	First-chance photofission cross-section
$\sigma(\gamma, nf)$	Second-chance photofission cross-section
$\sigma(\gamma, F)$	Total photofission cross-section
E_γ	Photon energy, given in the laboratory reference frame and expressed in MeV
E_o	Electron or positron kinetic energy, given in the laboratory reference frame and expressed in MeV
$m_o c^2$	Electron or positron rest energy
Γ	Width of the giant dipole resonance
K	Bremsstrahlung spectrum

2.3 Abbreviations

BOFOD	Biblioteka Fotoyadernykh Dannykh(Library of Photonuclear Data, in Russian)
CDFE	Centr Dannykh Fotoyadernykh Eksperimentov (Center for Photonuclear Experiments Data, in Russian)
CNDC	China Nuclear Data Center, Beijing, China
ENDF-6	Format for storing evaluated nuclear cross-section data
EPNDL	Evaluated Photonuclear Data File developed by CDFE
EXFOR	Library of experimental nuclear cross-section data in the EXchange FORmat
FWHM	Full width at half maximum
GDR	Giant dipole resonance
IFUSP	Institute of Physics, University of São Paulo, Brazil
IPPE	Institute of Physics and Power Engineering, Obninsk, Russia
JAERI	Japan Atomic Energy Research Institute, Tokai, Japan
JENDL	Japan Evaluated Nuclear Data Library
KAERI	Korea Atomic Energy Research Institute, Taejon, Rebublic of Korea
LANL	Los Alamos National Laboratory, Los Alamos, USA
MF	File type under ENDF-6
MSU	Moscow State University, Moscow, Russia
MT	Reaction type under ENDF-6
QD	Quasi-deuteron

Chapter 3

Available Experimental Data

The experimental data on photonuclear reactions available today were obtained from several types of measurements, spanning a wide range of probes and detected particles. The largest bulk of data is, nonetheless, of photoneutron cross-sections, obtained by counting the emitted neutrons. The next section presents a brief description of the most frequently used experimental procedures.

3.1 Experiments

In a determination of the cross-section for any nuclear process, it is necessary to make absolute measurements both of the number of reaction products and of the flux of incident particles. In some cases, for instance those involving continuum bremsstrahlung spectra, the cross-section is not determined directly, and so a third necessity is added: an analysis of the yield curve to give the cross-section.

In the case of (γ, x) reactions, the number of reactions can be determined in one of two ways: either by direct detection of the emitted particle, x, or by counting the activity of the residual nucleus, in the cases where this nucleus is not stable. The determination of the incident photon flux can be done with an ionization chamber (usually the case in measurements where a bremsstrahlung beam is used) or by scintillators or solid state detectors (usually in the case of monochromatic, quasi-monochromatic or tagged photons).

3.1.1 Bremsstrahlung

The first measurements of photonuclear cross-sections were done using, as the source of radiation, the continuous bremsstrahlung spectrum produced by striking a radiator target with an electron beam from an accelerator (initially betatrons and synchrotrons, and later, linacs).

The use of a continuous spectrum of photon energies means that the measured quantity is a yield, a convolution of the photonuclear cross-section with the bremsstrahlung spectrum over the photon energies:

$$Y(E_0) = N_R \int\limits_{Threshold}^{E_0} \sigma(E_\gamma) K(E_0, E_\gamma) \frac{dE_\gamma}{E_\gamma}, \tag{3.1}$$

where E_0 is the energy of the electron beam, E_γ is the photon energy, σ is the photonuclear cross-section, and $K(E_0, E_\gamma)$ is the bremsstrahlung absolute intensity spectrum.

Stepping the electron beam energy in small increments allows the experimenter to obtain a yield curve, which, submitted to an "unfolding" procedure (see below), produces the photonuclear cross-section.

There are two main problems associated with this technique. The first one is related to a sufficiently accurate knowledge of the bremsstrahlung spectrum for all electron energies. The second problem is intrinsic to the experimental method. Accurately measuring a yield curve in small energy steps requires great stability in the accelerator parameters, and large counting statistics. The process of differentiation of the yield curve introduces correlations between the experimental points and the deconvoluted cross-section may exhibit fluctuations that have no physical meaning. This kind of problem is aggravated when energies above the peak of the giant dipole resonance are reached, because the yields increase much more slowly and the results are obtained from small differences between two large numbers.

Several laboratories around the world (mostly in Russia, Canada and Australia) used this technique to obtain a large set of data. Discrepancies between results from different laboratories are probably due to the use of different bremsstrahlung spectrum and/or to differences in the deconvolution methods. Some of the most important and widely used deconvolution methods are briefly described below.

The Photon Difference Method [8] uses the fact that the difference of two bremsstrahlung spectra having slightly different end-point energies can be interpreted as a spectrum close to monoenergetic. Some improvements to this method were developed, such as the linear combination of three points [9].

In the Penfold-Leiss method [10] the integral expression (3.1) is substituted by a set of linear equations for a given bin of analysis. A modification of the Penfold-Leiss method [11] uses the bin of analysis as a parameter depending on the accuracy of the yield.

Several kinds of regularization methods are widely used. In these methods the mean square difference between the cross-section and its estimator is minimized under the assumption of the cross-section smoothness. The choice of the regularizator produces the differences among the regularization methods available. Some of them are: Tikhonov's Method [12], Cook's Least Structure Method [13], the Second Difference Method, [14] and the Statistical Regularization Method [15].

All methods above try to extract the smoothest possible cross-section. The advantage of using bremsstrahlung is the large intensity of the beam. This results in reasonable statistics even for relatively small cross-sections.

3.1.2   Positron Annihilation in Flight

This is the method that, during the sixties and seventies, mostly in Saclay (France) and Livermore (United States), was used to produce quasi-monochromatic photon beams with variable energy. The method consists [16] in producing a beam of fast positrons, with definite energy E_0, transporting it to the experimental area and making it impinge upon a thin, low-Z target, thus producing a bremsstrahlung spectrum plus a peak of annihilation photons. Positrons are created by pair production from the bremsstrahlung generated
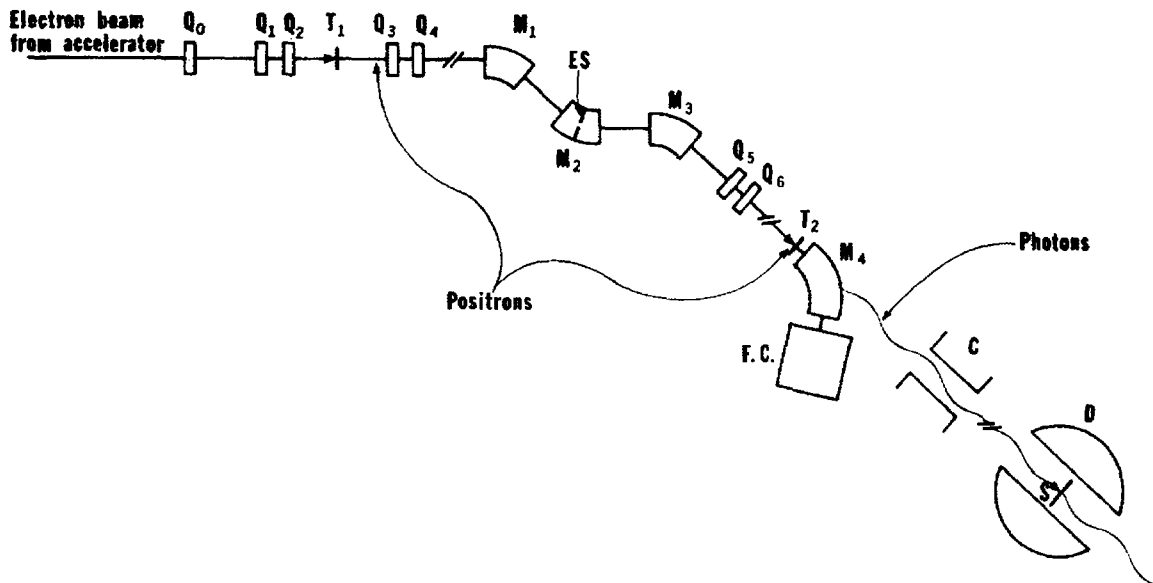
8

Figure 3.1: *Schematic diagram of the annihilation photon beam facility at Saclay. M_i - bending magnets; Q_i - quadrupole magnets; ES - energy analyzing slit; T_1 - positron converter target; T_2 - annihilation target; FC - Faraday cup; C - collimator; S - nuclear sample; D - neutron detector. Taken from Ref. [17].*

when the intense beam of high energy electrons from the accelerator hits a thick, high-Z converter.

Positrons have been produced either along the accelerator (Livermore case) or at the end of the accelerator (Saclay case). Figure 3.1 shows a schematic view of the Saclay facility. In this case the positrons of the desired energy are filtered by magnetic fields and defining slits. The energy of the positron beam can be adjusted by a change in the magnetic fields.

In the Livermore system, the converter target is placed between two sections of the linac. Positrons emerging from the target are focused into the next accelerator section, which is operated with the microwave frequency nearly 180° out phase with that normally used for electrons. The energy of the positrons can be selected by adjusting the power in the linac section. After acceleration, the beam is energy analyzed (magnetic fields and defining slits) and transported to the experimental area and the annihilation target.

The annihilation target is usually made of a low-Z material in order to maximize the relation between the annihilation peak and the bremsstrahlung tail. To subtract the bremsstrahlung contribution, the experimental measurements are repeated with incident electrons instead of positrons. To the first Born approximation, the same number of electrons with the same kinetic energy crossing the annihilation target will produce the same bremsstrahlung spectrum without the annihilation peak. Figure 3.2 shows photon spectra produced by beams of 16.5 MeV positrons and electrons striking a 0.13 mm thick Be target. The annihilation photon peak is broadened by the resolution of the 20 x 20 cm^2 NaI(Tℓ) spectrometer used in the measurement.
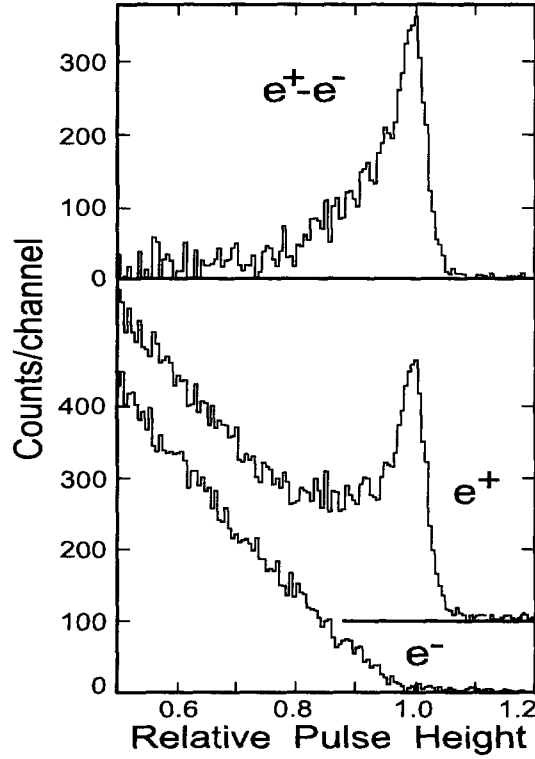
Figure 3.2: *Bottom: photon spectra produced by beams of 16.5 MeV electrons (e^- data) and positrons (e^+ data) striking a 0.13 mm thick Be target. Notice that the e^+ spectrum was shifted upwards by 100 counts/channel for visualization. Top: annihilation photon peak obtained from the difference between e^+ and e^- spectra. The annihilation photon peak is broadened by the NaI(Tℓ) spectrometer resolution. Taken from Ref. [17].*

The photonuclear measurement is a two-step process: first one determines the number of counts, $N^+(E_0)$, obtained with the γ-spectrum produced by the positron beam of energy E_0; the second step is the measurement of the number of counts, $N^-(E_0)$, produced by the γ-spectrum from the electron beam of the same energy E_0. The photonuclear cross-section is then proportional to the difference $N^+(E_0) - N^-(E_0)$, divided by the number of "quasi-monochromatic" photons that irradiated the target, $N_\gamma(E_0)$, without any deconvolution procedure. The effective photon spectrum lineshape is still different from the ideal delta-function. It may be asymmetric and present a tail extending to the low energy side. The disadvantage of this method (as compared to bremsstrahlung) is associated with the low intensity of the photon beam, since the positron production and conversion processes both present small cross-sections.

3.1.3 Bremsstrahlung Tagging

Following the development of high duty-cycle electron accelerators, perhaps the most successful method of producing monochromatic photons has become the tagging of bremsstrahlung photons [18]. The bremsstrahlung tagging technique is conceptually simple, as illustrated in Figure 3.3. A monochromatic electron beam of energy E_0 incident on a thin radiator produces a continuum bremsstrahlung photon spectrum in the forward direction. Since the radiator is very thin (about 0.1% of a radiation length) the primary beam passes through the radiator practically undisturbed and is deflected by the magnetic
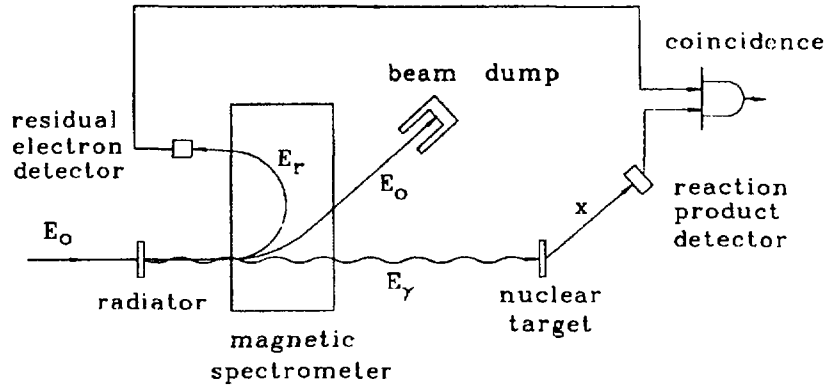
Figure 3.3: *Schematic representation of the bremsstrahlung tagging technique.*

spectrometer to the beam dump. A small fraction of the beam is scattered in the radiator, losing a significant part of its energy. The electrons that have final momenta within the acceptance range of the spectrometer are deflected to an array of detectors placed in the focal plane of the spectrometer. The signal produced by one of those detectors, from an electron with energy $E_{residual}$, announces the presence of a photon with energy

$$E_\gamma = E_0 - E_{residual}.$$ (3.2)

A time coincidence between this signal and a signal from the nuclear reaction product detector indicates that the reaction was produced by a photon of energy E_γ.

With this method part of the continuous bremsstrahlung spectrum is selected (the energy bin corresponding to the momentum acceptance of the spectrometer) and divided into smaller parts, depending on the number of detectors in the focal plane. So the energy resolution of the tagger depends on the optics of the magnetic spectrometer and on the spatial distribution of the detectors on the focal plane. This method presents a draw-back, which is the low intensity of the photon beam (typically 10^6 - 10^7 s^{-1} in order to keep the accidentals rate acceptable), associated with difficulties that are intrinsic to coincidence measurements. The typical apparatus function (effective photon spectrum) for a photon tagger is close to a Gaussian line.

3.1.4 Electron-induced Reactions

An electrodisintegration experiment, or (e, x), is one in which an outgoing nuclear fragment or radioactivity is detected. It is the experiment complementary to electron scattering, (e, e'), where the scattered electron is detected. In the (e, x) case, the scattered electron is not observed, so the experiment integrates over all its final states, see section 4.4.

Electrodisintegration experiments are usually analyzed using the virtual photon technique. The basic premise of this technique is that we can express the electrodisintegration cross-section, $\sigma_{e,x}(E_0)$, in terms of the photonuclear cross-sections, $\sigma_{\gamma,x}^{\lambda L}(E_\gamma)$, associated
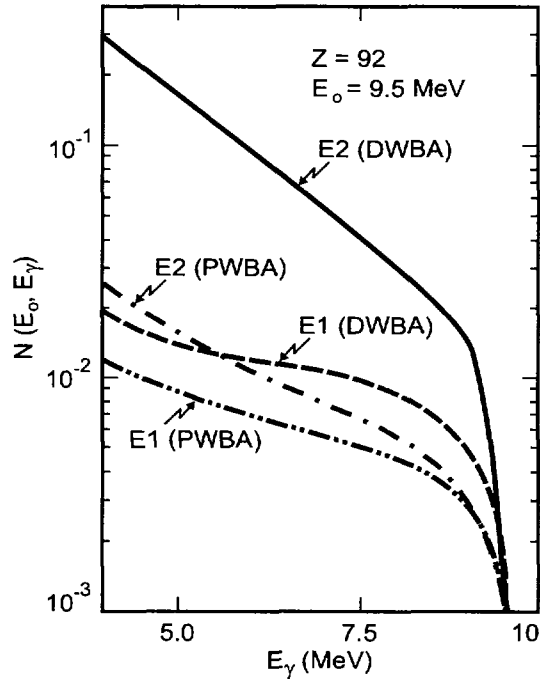
Figure 3.4: *E1 and E2 PWBA and DWBA virtual photon spectra for 9.5 MeV electrons scattered by a uranium nucleus. Taken from Ref. [19].*

with the absorption of real photons of multipolarity λL, through an integral over the corresponding virtual photon spectra, $N^{\lambda L}(E_0, E_\gamma, Z)$:

$$\sigma_{e,x}(E_0) = \int\limits_{Threshold}^{E_0} \sum_{\lambda L} \sigma_{\gamma,x}^{\lambda L}(E_\gamma) N^{\lambda L}(E_0, E_\gamma, Z)\frac{dE_\gamma}{E_\gamma}. \tag{3.3}$$

In this expression E_0 stands for the total electron energy, E_γ for the virtual photon energy, and Z for the atomic number of the target nucleus. The validity of this expression stems from the cancellation of the reduced matrix elements for photo and electrodisintegration, which is exact in the limit of low momentum transfers. This method will surely fail for large momentum transfers, where the long wavelength approximation breaks down (see section 4.4).

Several groups (mainly in Brazil, Germany, Scotland and the United States) used this method in order to separate the multipole components of the photonuclear cross-section, using the substantial difference between the virtual photon spectra of different multipolarities. Figure 3.4 shows E1 and E2 plane wave Born approximation and distorted wave Born approximation virtual photon spectra for 9.5 MeV electrons scattered by a Z=92 nucleus. The E2 virtual photon spectrum, already enhanced with respect to the E1 in the plane wave solution, is further increased when Coulomb distortion is taken into account. Combining the measurement of electrodisintegration cross-sections and electro plus photodisintegration yields, experimenters could change the multipole composition of the photons seen by the target.

This kind of measurement suffers from the same problems as those using bremsstrahlung, *i.e.*, the photonuclear cross-sections are obtained from the solution of integral equations and so are subject to strong uncertainties in the shape. Nevertheless the integrated

cross-section is obtained with high accuracy. Figures 3.5 and 3.6 show typical results obtained with this method.
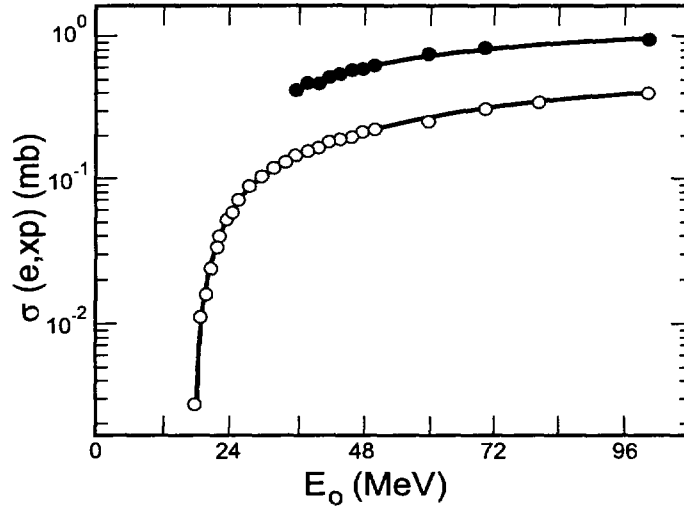
Figure 3.5: *Electrodisintegration cross-section for proton production, $\sigma_{e,xp}(E_0)$, for ^{56}Fe (light circles) and electro plus photodisintegration yield, $Y_{e,xp}(E_0)$, (full circles). The smooth curves are the best simultaneous fit to the data and were obtained by combining the E1 and E2 photonuclear proton production cross-sections, shown in Fig. 3.6. Taken from Ref. [20].*

3.2   Compiled Data

3.2.1   Bibliographic Data

There are several well known photonuclear reaction bibliographies dealing with the results obtained from the interaction of electromagnetic radiation with atomic nuclei. As a rule they cover the most important aspects of the studies on photonuclear reactions and
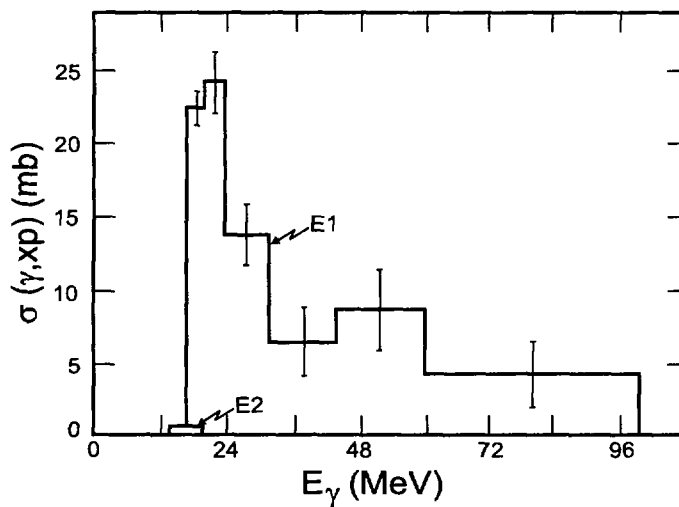
Figure 3.6: *E1 and E2 photonuclear proton production cross-sections, (γ, xp), represented by histograms. Obtained from the simultaneous analysis of the electrodisintegration cross-section and electro plus photodisintegration yield shown in Fig. 3.5. Taken from Ref. [20].*

their inverse processes: photon induced disintegration and fission, photon absorption and scattering, electro-disintegration, electron scattering, and the radiative capture of various particles. The most widely used of these bibliographies are briefly reviewed below.

The 10-th edition of the IAEA Bibliographical Series [21] includes references for both theoretical and experimental works taken from the literature in the period 1948-1963. The references are classified into 15 categories: photodisintegration, photofission, electrodisintegration, absorption, scattering, etc. In the main categories the material is distributed according to the type of reaction. Generally the references are supplied with abstracts. For ease of reference an Author Index and a Subject Index are included.

Two comprehensive bibliographies, Photonuclear Data Index 1955-1972 and Photonuclear Data Index 1973-1982 were prepared E.G. Fuller and others at the Photonuclear Data Center of the National Bureau of Standards (current National Institute for Standards and Technology, Washington DC, USA), confer Ref. [1]. In both books the experimental data are presented in tabular form for all nuclei that have been measured. Organized by element and isotope, each entry in the Index deals with a specific reaction reported in a given reference. Information is given on the type of measurement, excitation energies studied, source type and energies, detector type and angular range covered. Annotated data indices and bibliographies are also given.

Using the above bibliograhies, 15 volumes of the Photonuclear Data - Abstract Sheets 1955-1982 were published during the period of 1983-1986 by the National Bureau of Standards [1]. These volumes cover most classes of experimental photonuclear data. The sheets are ordered by target element, isotope, and by an assigned bibliographic reference code. Information is given on the type of measurement, excitation energies studied, source type and energies, detector type, and angular range covered. For a given reference, the relevant figures and tables are mounted on a separate sheet for each nuclide studied.

An Index [22] prepared at the Centre for Photonuclear Experiments Data (CDFE) of the Institute of Nuclear Physics of the Moscow State University, includes a table of experimental photonuclear data, in which the results of research published in the period 1976-1995 are systematized. For the period previous to 1982 the data of [1] were also used. The data are ordered by isotope and reaction studied, and by a bibliographic reference code. Information is given on the source type, excitation energies and angles studied. Detailed descriptions of the physical results obtained in the paper are given, using special codes to present the general quantities measured, deduced, or reviewed. A reference list of the papers, an author index, and a table of abundances of isotopes and particle separation energies are presented. The Index also includes a table with the main parameters of the giant dipole resonance, in which the energy positions, absolute values, widths, integrated cross-sections, and integrated cross-section first moments for the resonances observed in the reactions are listed together with the relevant references. The Index is presented both in book and ASCII file forms.

The Bibliographic Index [23] to Photonuclear Reaction Data (1955-1992), prepared by the Japan Atomic Energy Research Institute (JAERI) also exists in book and ASCII file forms. The Index was prepared using JAERI compilations together with the compilations of [1] and [7], covering the period 1955-1992. The Index contains information on target nucleus, incident beam, type of reaction and quantity, energy range of the incident beam, laboratory, type of work, reference citations, first author's name, and a short comment.

14

A combined photonuclear data bibliographic file was produced by the CDFE Moscow using indexes [22] and [23]. These 2 sources were merged and duplications excluded. The resulting file is available at the Web, in the site: http://depni.npi.msu.su/cdfe.

3.2.2 EXFOR Library

EXFOR [25] is the computerized library of experimental nuclear reaction data maintained by the worldwide Network of Nuclear Reaction Data Centers [26]. Its origin is the EXchange FORmat designed to allow a large variety of numerical nuclear reaction data tables with explanatory and bibliographic information to be transmitted in a general computer-readable format among the members of the Network, and from the Nuclear Reaction Data Centers to the users. EXFOR library stores data for reactions induced by neutrons, charged particles and photons. In addition to numerical experimental data and bibliographic information, EXFOR stores information on uncertainties, status, and history of the data, including updates which have been made, and correlations to other data sets.

Only two groups are currently actively compiling photonuclear data into the EXFOR format: CDFE (Centre Dannykh Fotoyadernykh Eksperimentov - Centre for Photonuclear Experiments Data). Moscow, Russia, and the Photonuclear Data Group, University of Sao Paulo, Brazil.

An EXFOR entry, based on one paper and its updates, is uniquely characterized by a 5-digit accession number. The entry may be subdivided into several subentries that deal with specific reactions, each subentry being characterized by an additional 3-digit number.

A total of 669 entries, representing 4 197 subentries, presently exist in the photonuclear part of the EXFOR library. These are mostly from works published after 1976. For this period, approximately 25 % of the works are available in EXFOR, for works published before 1976 the situation is poorer. During 1996-1999, the present project contributed to the above statistics by 115 entries, representing 634 subentries. To summarize, there are 4 series of entries:

The L series with 58 entries (L0001-L0035 and L0037-L0059) was compiled by B.L. Berman and coworkers from the Lawrence Livermore National Laboratory (LLNL, Livermore, USA) and revised by V.V. Varlamov from the CDFE. The M series with 595 entries (M0001-M0595) was compiled by V.V. Varlamov and coworkers from the CDFE Moscow. The G0 series with 12 entries (G0001-G0008, G0010-G0013) was compiled by the Nuclear Data Section, IAEA Vienna. Finally, the G3 series with 4 entries (G3001-G3004) was compiled by M.N. Martins at the University of Sao Paulo.

3.2.3 Atlases of Cross-Sections and GDR Parameters

There are several publications presenting complete overviews of photonuclear reaction data. The most relevant ones will be briefly described below.

One should have in mind that the most probable result from the photoabsorption process in a heavy nucleus in the GDR energy region (E_γ about 8-30 MeV) is the emission of one or more neutrons. However, other processes such as the emission of charged particles might be important in medium and especially in light nuclei, where photoproton cross-sections can even be larger than photoneutron cross-sections.

Photoneutron cross-section data (and some photofission and photoproton data as well), measured with quasimonoenergetic photons, have been presented in graphic form in the Atlases authored by Dietrich, Berman, and Fultz, Refs. [17], [27], [3]. These publications also present tables, containing the GDR integrated cross-sections and their moments, and the parameters of Lorentz curves fitted to the data.

There is not such a publication for data obtained with bremsstrahlung photons. Nevertheless, several reaction cross-sections and also such quantities as photonuclear reaction products, angular distributions, energy spectra and other, obtained using both bremsstrahlung and quasimonoenergetic photons have been presented in [28]. The data are shown in the form of tables and graphs, taken from the original papers (quasimonoenergetic photon data [17], [27] have also been used).

Graphs of experimental and evaluated photoneutron reaction data for selected nuclides have been published [29] using the international nuclear data library EXFOR.

The most recent publication is presented as tabulated data in Varlamov's Atlas [7], see the Annex of this document. This table includes parameters of the GDR observed in photonuclear reactions measured by bremsstrahlung, quasimonoenergetic and tagged photons (selected evaluated cross-sections are also presented). Cross-section data for the whole GDR region are presented. Data relevant to specific parts of the resonance, for example for a photofission cross-section near the threshold, are omitted. Table entries are organized by element, isotope and reaction (ordered by product from neutron to alpha). Relevant parameters deduced from the cross-sections, such as total photoabsorption, neutron yield, single, double, triple, and total neutron production, charged particle emission and fission are included. The table contains information on the GDR parameters derived from the data for 82 elements (220 isotopes and natural compositions) with atomic numbers between 1 and 95. The entries for almost all 600 photoneutron cross-sections obtained with quasimonoenergetic photons [3] are also included. There are altogether 1317 entries.

3.2.4   Additional Data in Other Formats

In addition to the EXFOR photonuclear library, there is a compilation prepared before 1987 by the photonuclear data group of E.G. Fuller at the US National Bureau of Standards (current NIST). This compilation includes about 1500 data sets for several photonuclear reaction cross-sections for nuclei from ^{2}H to ^{237}Np, published in [1]. Parts of this compilation have already been included in the EXFOR L- or M-series by the CDFE Moscow group.

3.3   Access to Data

Access to the EXFOR library is possible using the Web services provided cost-free by the Nuclear Data Section. IAEA. Vienna at

http://www-nds.iaea.or.at/.

A CD-ROM version of the complete EXFOR library is also available. It can be obtained, cost-free, from the IAEA Nuclear Data Section using the address given at the cover page of the present TecDoc. Also, it can be requested via e-mail sent to

services@iaeand.iaea.or.at.

Retrievals from the Atlas of giant dipole resonance parameters and graphs of photonuclear reaction cross-sections can be obtained from the Web site operated by the CDFE Moscow

http://depni.npi.msu.su/cdfe.

Chapter 4

Nuclear Models

This chapter provides an overview of the nuclear reaction mechanisms that occur in photonuclear reactions below the pion threshold. The emphasis is on nuclear theories and models that are implemented in the nuclear modeling codes used by the participants in the present project.

4.1 Photoabsorption Model

A model of photonuclear reactions must account for the different nuclear reaction mechanisms involved in the initial photonuclear excitation process, and the subsequent decay of the excited nucleus by particle and gamma-ray emission. At low energies, below about 30 MeV, the Giant Dipole Resonance (GDR) is the dominant excitation mechanism, where a collective bulk oscillation of the neutrons against the protons occurs. At higher energies up to approximately 150 MeV, where the wavelength of the photon decreases, the phenomenological model of photoabsorption on a neutron-proton (quasi-deuteron, QD), which has a large dipole moment, becomes important. An illustration of the different photoabsorption mechanisms is shown in Fig 4.1 below.
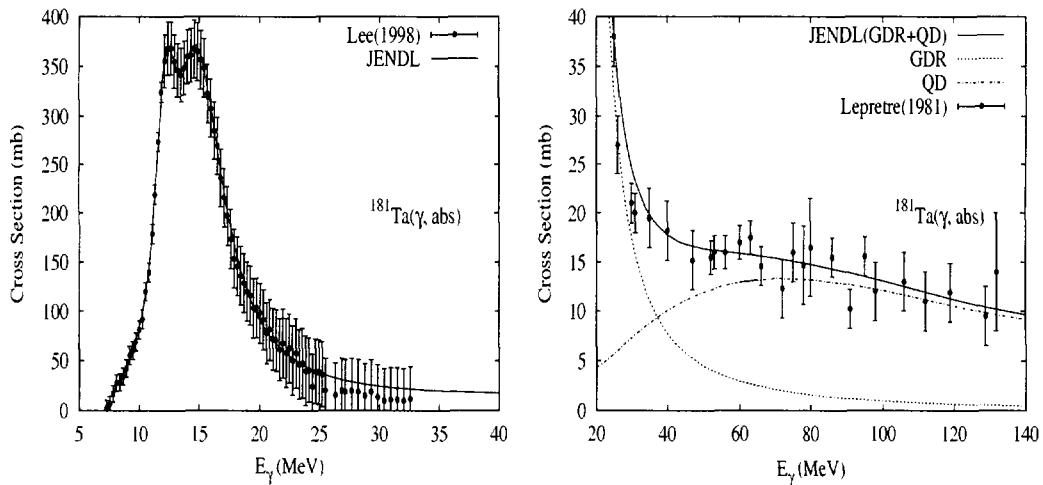
Figure 4.1: *Illustrative example of the nuclear photoabsorption cross-section. Shown to the left is the GDR component. Shown to the right is the quasideuteron component along with the GDR tail and their sum. Taken from [35, 31].*

Models of photonuclear reactions typically begin with a determination of the photoabsorption cross-section, and this can be done in one of two ways: (1) An evaluation based on experimental data, if data exist; and (2) A model calculation of photoabsorption. These methods are discussed in more detail below.

18

If experimental data exist for the total photoabsorption cross-section, they can be used as input into most codes which model the subsequent particle emission reactions. The most useful type of experimental data here are from photon absorption experiments which measure the total photoabsorption cross-section. For heavy nuclei, compilations of photoneutron total cross-section such as that of Dietrich and Berman [3] can be used to approximate the photoabsorption cross-sections, since contributions from photoproton reactions (and other reactions producing complex charged particles) are suppressed by the Coulomb barrier. However, in light nuclei this approach cannot be used since the photoproton cross-section is no longer small, and in some cases exceeds the photoneutron cross-section. In such cases one should rely only on absorption-type data. The evaluation of measured total photoabsorption data is discussed in Chapter 5.1.

An alternative way to obtain the photoabsorption cross-section is to calculate it theoretically as a sum of two components [31]

$$\sigma_{abs}(E_\gamma) = \sigma_{GDR}(E_\gamma) + \sigma_{QD}(E_\gamma). \tag{4.1}$$

The GDR component, $\sigma_{GDR}(E_\gamma)$, is given by a Lorentzian shape, with parameters describing the total absorption of the giant dipole resonance. A relation to be used reads

$$\sigma_{GDR}(E_\gamma) = \sum_i \sigma_i \; \frac{(E_\gamma \Gamma_i)^2}{(E_\gamma^2 - E_i^2)^2 + (E_\gamma \Gamma_i)^2}, \tag{4.2}$$

where σ_i, E_i and Γ_i are the GDR peak cross-section, energy and width, respectively. The summation is limited to $i = 1$ for spherical nuclei, while for deformed nuclei the resonance is split and one uses $i = 1, 2$. As a rule, the parameters are derived from fits to experimental data or from systematics (see Kishida [32]).

The QD component, $\sigma_{QD}(E_\gamma)$, is taken from the model of Chadwick et al. [31], which uses a Levinger-type theory. It relates the nuclear photoabsorption cross-section to the experimental deuteron photodisintegration cross-section $\sigma_d(E_\gamma)$,

$$\sigma_{QD}(E_\gamma) = L \; \frac{NZ}{A} \; \sigma_d(E_\gamma) \; f(E_\gamma). \tag{4.3}$$

Here, the Levinger parameter was derived to be $L = 6.5$ [31], and $f(E_\gamma)$ is the Pauli-blocking function, which reduces the free deuteron cross-section $\sigma_d(E_\gamma)$ to account for Pauli-blocking of the excited neutron and proton by the nuclear medium. The experimental deuteron photodisintegration cross-section was parameterized as

$$\sigma_d(E_\gamma) = 61.2 \; \frac{(E_\gamma - 2.224)^{3/2}}{E_\gamma^3}, \tag{4.4}$$

with E_γ in MeV and σ_d in units of mb. The Pauli-blocking was derived by Chadwick et al. to be a multidimensional integral whose solution could be well approximated in the energy range $20 - 140$ MeV by the polynomial expression

$$f(E_\gamma) = 8.3714 \times 10^{-2} - 9.8343 \times 10^{-3} E_\gamma + 4.1222 \times 10^{-4} E_\gamma^2$$

$$- 3.4762 \times 10^{-6} E_\gamma^3 + 9.3537 \times 10^{-9} E_\gamma^4, \tag{4.5}$$

with E_γ in MeV. In Ref. [31] the Pauli-blocking function was not parameterized below 20 MeV, where it tends to zero, or above 140 MeV, where it tends to unity. Still, as the contribution needs to be defined at all energies considered, we use an exponential shape $f(E_\gamma) = \exp(-D/E_\gamma)$ for energies below 20 MeV, and above 140 MeV, with $D = -73.3$ for $E_\gamma < 20$ MeV and $D = 24.2$ for $E_\gamma > 140$ MeV. This form has the correct behavior in that it tends to zero at $E_\gamma = 0$, and unity for large E_γ and is continuous with Eq. (4.5) at 20 and 140 MeV.

Photoabsorption calculations using the above model are common [33, 32, 34, 35]. In some cases, authors have treated the Levinger parameter as an adjustable parameter to obtain best agreement with measurements in the 50 - 150 MeV photon energy region.

Finally, we note a method sometimes used by evaluators to infer the total absorption cross-sections when no measured data exist, and when the absorption cross-section cannot be equated to measured photoneutron cross-sections. This situation sometimes arises for light nuclei. This method involves using a nuclear model calculation to estimate the ratio of (γ, xn) to (γ, abs) cross-sections; and inferring the total absorption cross-section (γ, abs) such that the calculated (γ, xn) agrees with measurements. This procedure has been described in model detail in Refs. [32, 36].

4.2 Reaction Models

In this subsection, nuclear models for describing particle emission following photonuclear absorption are discussed. Nuclear theories and models that are implemented within the computer codes described in Chapter 4.3 are emphasized.

4.2.1 Preequilibrium Emission

Preequilibrium reaction mechanisms become important for incident photon energies above 10-15 MeV. In the photoabsorption mechanisms described in the previous section, the initial nuclear excitation can be understood in terms of particle-hole excitations ($1p1h$ for the GDR; $2p2h$ or $2p1h$, as discussed later, for QD processes) and thus it is natural to use a preequilibrium theory of particle-hole excitations to describe the processes of preequilibrium emission, and damping to equilibrium, during the evolution of the reaction. Such models can be used to calculate photonuclear reactions for incident photons with energies up to about 140 MeV, which is the threshold for pion production.

Semiclassical preequilibrium models, such as the exciton and hybrid models, have proved to be powerful tools for predicting particle emission spectra with a high degree of reliability, and in a computationally-fast manner [37, 38, 33, 35]. Semiclassical models make use of detailed balance, and phase space considerations, to calculate emission rate probabilities from particle-hole states. By working in terms of emission rates, and not quantum mechanical transition amplitudes, some information is lost, particularly concerning observables sensitive to interference effects such as angular distributions and an-

alyzing powers. Additionally, such models typically do not account for correlations in the particle-hole excitations. However, these deficiencies are to some extent compensated by the ease of implementation and high predictive power of the semiclassical theories. Semiclassical intranuclear cascade photonuclear models have also been developed [39, 36, 40]. These models have much in common with preequilibrium models. They differ, though, by following the trajectories of the excited nucleons in coordinate and momentum space (semiclassical preequilibrium models usually just follow the excitations in energy space), and by assuming that free nucleon-nucleon scattering cross-sections can be used for in-medium nucleon scatterings. In practice, it is only the semiclassical preequilibrium models that have been implemented for photonuclear reactions, and the quantum multistep preequilibrium models [41] have not yet been extended for calculating these processes.

Two works in particular have demonstrated the usefulness of semiclassical preequilibrium models in describing photonuclear reactions: Wu and Chang's paper [37] on an exciton model; and Blann et al.'s studies [38] using the hybrid model; both of which utilize a Weisskopf-Ewing evaporation theory to describe the subsequent equilibrium decay. A more recent work [33], which describes new capabilities recently built into the GNASH modeling code [42], makes use of many of the ideas from these papers, but with the following new features:

- Full angular momentum and parity conservation is included in a Hauser-Feshbach treatment of equilibrium emission, accounting for the fact that an E1-photon brings in one unit of angular momentum;

- Multiple-preequilibrium emission processes, where more than one fast preequilibrium ejectile is emitted in the reaction, are included using the theory of Ref. [43].

In semiclassical preequilibrium models, particle and hole excitations are produced in the nucleus following photoabsorption. Particle emission can occur from such a state yielding the typically high-energy preequilibrium emission; or alternatively, a nucleon-nucleon interaction may occur producing more particle-hole excitations. The composite nuclear system passes through such stages of increasing complexity towards equilibrium, and the total preequilibrium emission is the sum of contributions from all the preequilibrium stages.

Wu and Chang [37] and Blann et al [38] have successfully applied preequilibrium physics modeling to describe the emission of high-energy nucleons following photoabsorption. Wu and Chang used an initial $2p2h$ state in the preequilibrium cascade, while Blann argued that the two holes are correlated through the quasi-deuteron mechanism, and therefore can be approximately treated as one degree of freedom, i.e. a $2p1h$ initial state. Also, calculations by Ryckbosch et al. [44] indicated a preference for an initial $2p1h$ state when analyzing emission spectrum data at 60 MeV. Therefore the calculations of Chadwick et al. [33] using GNASH, like those of Kishida et al. [32] based on ALICE, also follow Blann's prescription. In the case of the GNASH calculations, the Kalbach exciton model in GNASH [42] is used to calculate the preequilibrium emission of fast nucleons. Once the incident photon energy exceeds about 50 MeV, multiple preequilibrium emission becomes important, where more than one fast particle is emitted. For this the generalized multiple preequilibrium emission model of Ref. [43] is used. For both primary and multiple preequilibrium emission, the neutron-proton distinguishability factors were modified

to reflect the initial particle-hole type appropriate for the quasi-deuteron mechanism (i.e. of the two particles, one is a neutron and the other a proton).

4.2.2 Compound Nucleus Equilibrium Emission

Following the possible emission of preequilibrium particles, the remaining nuclear system reaches equilibrium, after which it decays by sequential particle or gamma-ray emission (or possibly fission) until the residual nucleus ground state is reached.

Generally, the calculation of these equilibrium decay processes do not present any particular theoretical difficulties (with the exception of fission, which is described in more detail below). The Hauser-Feshbach theory, which includes angular momentum and parity conservation, or the more simple Weisskopf-Ewing theory, may be applied. In the case of the former theory, the angular momentum of the photon projectile should be specifically accounted for. The principal uncertainty entering these calculations is in the input information needed to compute equilibrium decay rates: nuclear level densities, optical model transmission coefficients and inverse reaction cross-sections, and gamma-ray strength functions. The IAEA Reference Input Parameter Library (RIPL) [45] provides extensive guidance on the choice of these quantities.

It should be noted that isospin conservation can play a role in photonuclear reactions on lighter nuclei. For instance, for a $T = 1$ photon projectile and a $T = 0$ targets, one would expect the emission of alpha particles, which are also $T = 0$, to be supressed in certain reactions near threshold (cases where the low-lying residual nuclei are also $T = 0$). Since the nuclear reaction codes we use do not include isospin conservation, our evaluations have addressed this issue in a somewhat ad-hoc manner by suppressing the alpha channel when measurements indicate the presence of isospin conservation effects. One expects that a formally correct treatment with isospin conservation would lead to equivalent final results by applying appropriate isospin mixing coefficients.

4.2.3 Illustrative Comparisons with Experiment

A difficulty in testing photonuclear reaction theories that model nucleon emission spectra is the lack of experimental data to compare the model predictions against. While photoneutron and photoproton emission spectra from bremsstrahlung photon sources are not uncommon, such measured spectra from monoenergetic ("monochromatic") photon incident beams are sparse. A few monoenergetic photon-induced experiments do exist though [46, 44], and in addition, quasi-monoenergetic photon-induced spectra have been inferred using the difference-technique, where two bremsstrahlung-induced emission spectra, with different end-points, are subtracted to approximate the spectrum due to a monoenergetic source.

One way to circumvent problems in validating emission spectra calculations given the lack of differential monoenergetic photon-induced measurements, is to test the theoretical predictions of partial exclusive reaction channels (e.g. $(\gamma, 1n), (\gamma, 2n)$, etc), along with neutron emission multiplicities, against experimental measurement. These measurements indirectly test the calculated emission spectra. This is because the shape of the calculated
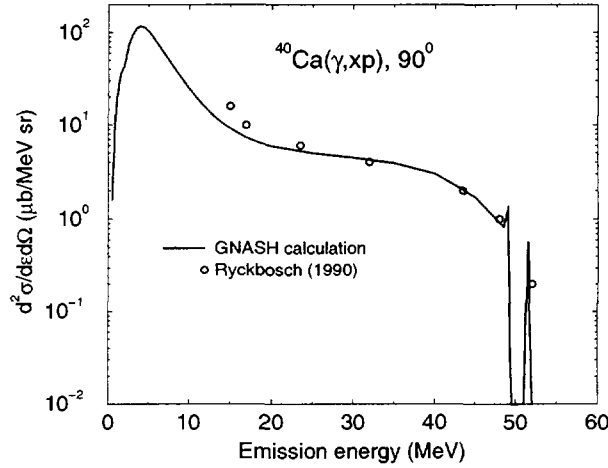
Figure 4.2: *Emission spectrum of protons at 90-degrees in the 60 MeV $^{40}Ca(\gamma, xp)$ reaction. Taken from Ref. [47].*
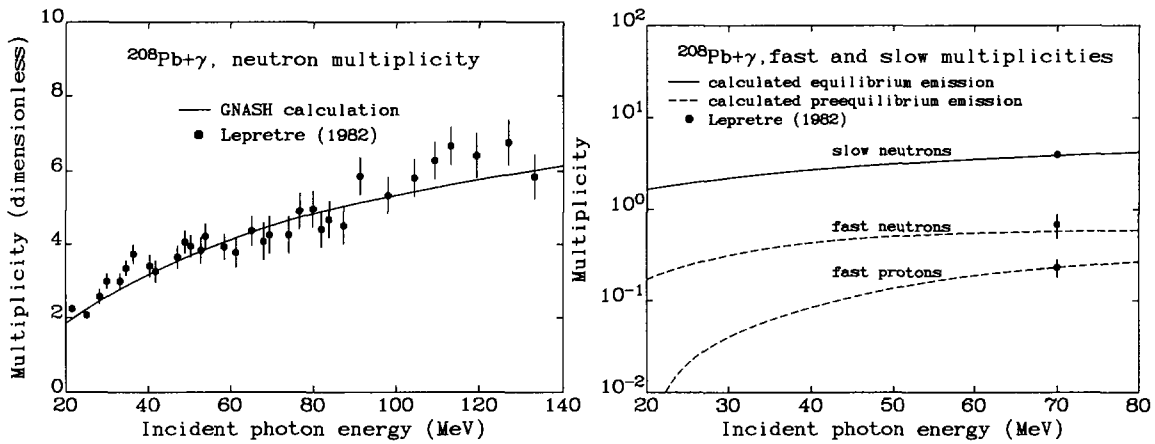

Figure 4.3: *Average multiplicity of emitted particles in photonuclear reactions on lead, compared with model calculations. Shown to the left is total neutron multiplicity; shown to the right are fast (preequilibrium) and slow (equilibrium) multiplicities. Taken from Ref. [33].*

photon emission spectra strongly influences the exclusive reaction channels populated, by energy balance. Likewise, multiplicities of particles emitted are influenced by the kinetic energies carried away by the light-particle ejectiles in the reactions. We provide some illustrative examples of calculations of emission spectra and multiplicities along with comparisons with experimental data.

Figure 4.2 shows an example of calculated 60 MeV proton emission spectra at 90-degrees compared with data [44], for the $^{40}Ca(\gamma, xp)$ reaction at 60 MeV. The angular variation was obtained using the Chadwick-Oblozinsky theory, described in Refs. [33, 48] and Sec. 4.2.4 below. The calculated photoproton emission spectrum describes the measurements well. This is important because there are very few sets of measured emission spectra data for monoenergetic incident photons to test the theory. Other tests of the calculated emission spectra were presented in Ref. [48], using the carbon experimental data of McGeorge *et al.* [46].

As an illustrative example of the use of neutron emission multiplicities to test the model calculations, Fig. 4.3 shows calculated multiplicities for particle emission compared with the measurements of Lepretre *et al.* [49]. The left-hand figure shows the average neutron multiplicity, which is well described by the calculations. The right-hand figure shows the measured fast and slow multiplicities at an incident photon energy of 70 MeV, compared with calculations. The fast multiplicity refers to the preequilibrium particles, while the slow multiplicity refers to the compound nucleus particles, and the calculations are seen to describe the correct partitioning of ejectiles among preequilibrium and equilibrium emission, and between neutrons and protons. These measurements are invaluable for testing the preequilibrium modeling in the calculation, since direct measurements of the nucleon emission spectra from monoenergetic photons do not exist for lead. The large Coulomb barrier in lead is responsible for the excess of fast preequilibrium neutrons compared to protons; at the highest energies the differences are reduced. In general the slow neutron multiplicity is much larger than the fast multiplicities, since preequilibrium decay accounts for at most the first two emissions, with the subsequent sequential particle decays coming from compound-nucleus emission. There is a nice discussion in Lepretre's paper [49] commenting on the slope of the average neutron multiplicity curve, which is worth repeating: If preequilibrium emission did not occur, each emitted neutron would require approximately 10 MeV (separation energy plus evaporation kinetic energy), and so the multiplicity curve would increase at a slope of 1 unit for every 10 MeV incident energy. The data in Fig. 4.3 show such a steep slope at the lowest incident energies, but for higher energies a much smaller slope occurs due to the higher kinetic energy carried by preequilibrium ejectiles.

The ALICE code photonuclear reaction calculations have been extensively benchmarked against measured data by Blann [38], and more recently by Kishida [32].

4.2.4   Angular Distributions

A knowledge of the angular distribution of the ejectiles in photonuclear reactions is essential for radiation transport studies, but most nuclear modeling codes (certainly those described in this report), in their basic form yield only angle-integrated results. In nucleon-induced reactions, the Kalbach systematics [50] have been widely used for obtaining double-differential emission spectra. They are particularly attractive for use in evaluation work since for each emission energy one need only specify the preequilibrium fraction (f_{MSD}) for the angular distribution to be defined, allowing a compact representation of angle-energy correlated cross-sections. However, as originally formulated they cannot be applied in photonuclear reactions. Ideally, for applications it would be useful to parameterize measured angular distributions in monochromatic photon-induced reactions in QD and GDR regimes, but an extensive experimental data set does not yet exist (larger amounts of experimental information exist for incident photons with a bremsstrahlung spectrum, but these data are not directly usable).

Below we describe an applications-oriented method [48] for determining continuum photonuclear angular distributions for emission of light particles (n, p, d, t, ^{3}He, and α) for energies up to 150 MeV. Based on theoretical considerations by Chadwick and Oblozinsky [43] for the angular forward-peaking in preequilibrium reactions, Kalbach's 1988 angular distribution systematics [50] for a neutron projectile are modified for use in photon-induced reactions. This results in photonuclear angular distributions which

are less forward-peaked than their nucleon-induced counterparts in the quasideuteron regime, due to the small momentum carried by a photon. In the GDR regime, a simple approximation of isotropy is assumed.

Giant-Dipole Resonance Region

At present, no general prescription is available for nuclear data evaluators for describing the angular distribution of secondary particles emitted in photonuclear reactions in the GDR regime. Experimental angular distributions for emitted nucleons from such collective excitations often show a dipole shape (peaking at 90-degrees), but nuclear structure effects are important in determining the detailed angular distribution and it is not clear that accurate systematics can be developed to describe them.

One of the main problems is that most measurements are for an incident bremsstrahlung spectrum, and not for monoenergetic photons. This is a problem because angular distributions are incident-energy dependent, and are also angle-energy correlated (i.e., the angular distribution varies for different secondary emission energies). Given this situation, two options appear available for evaluators:

- Include angular distribution information based on available measured data

- Assume isotropy in the GDR regime, for simplicity

The evaluations described in this report follow the latter approach except for certain light nuclei where angular distributions were represented with Legendre polynomials. It is hoped that for most applications, this is a reasonable starting point, and hopefully future work will result in a more accurate angular distribution representation within ENDF files.

Quasideuteron Region

Chadwick et al. [48] presented an approach for calculating the angular distribution of secondary ejectiles emitted in photonuclear reactions in the quasideuteron regime. The approach made use of the theoretical basis for the forward-peaking parameter a in the Kalbach systematics (originally developed for nucleons) [33, 51], which was found to be dependent upon the momentum of the projectile. The low momentum of photons, compared to nucleons of the same energy, results in angular distributions which are much less forward-peaked than their nucleon counterparts.

This approach, which is presented below, allows evaluators to make use of the Kalbach systematics developed for nucleon projectiles, with a straightforward modification to the a-parameter.

Recommended Systematics for Use in Evaluations

We recommend the applications-oriented method (Ref. [48]) to calculate continuum angular distributions of light particles $(n, p, d, t, {}^3\text{He}, \text{ and } \alpha)$ produced in photonuclear reactions based on Kalbach's 1988 systematics and the theoretical considerations given in Ref. [51]. The procedure for obtaining photonuclear angular distributions for a photon of

energy $\leq$ 150 MeV in (γ, y) reactions, where y may represent all light ejectiles with mass ≤ 4, consists of the following 3 steps:

- Determine the a^{ν} parameter for (n, y) reactions, for an incident neutron with energy E_{inc} from Kalbach's 1988 systematics.

- Obtain the photon-projectile a using:

$$a = a^{\nu}[\sqrt{E_{inc}/2m}]\ [min(4, max(1, 9.3/\sqrt{E_{em}}))], \tag{4.6}$$

where m is the neutron mass in MeV and the a^{ν} parameter is taken from Kalbach's 1988 paper [50] for an incident neutron of the same energy as the photon projectile. The first modification factor to a^{ν} accounts for the lower photon momentum compared to a neutron, while the second factor approximately accounts for differences in refraction effects, and an upper limit of 4 for this correction to prevent it becoming unphysically large at low emission energies [48].

- Apply this a value in the following formulae:

$$\frac{d^2\sigma}{d\epsilon d\Omega} = \frac{d\sigma}{d\epsilon}\left[(1 - f_{MSD}(\epsilon))\frac{1}{4\pi} + f_{MSD}(\epsilon)g(\theta)\right], \tag{4.7}$$

where $d\sigma/d\epsilon$ is the angle–integrated spectrum and $f_{MSD}(\epsilon)$ is the fraction of the emission spectrum at emission energy ϵ coming from preequilibrium processes. An isotropic distribution for the non-precompound contribution is assumed. The quasideuteron angular distribution shape is given by:

$$g(\theta) = \frac{1}{4\pi}\frac{2a}{e^a - e^{-a}}\exp(a\ \cos\theta). \tag{4.8}$$

4.2.5 Photofission

Introduction to Fission

Nuclear fission is a complex phenomenon which, although discovered as early as 1939, is far from being completely understood. The importance of this process for fundamental physics and for the production of nuclear energy has stimulated many experimental and theoretical studies. The large amount of experimental data that has been accumulated on fission has been useful for the phenomenological description of many aspects of this reaction and has been realized in the production of nuclear energy. Nevertheless, in all of this time, there has not emerged a fully-satisfactory unified understanding of the fission process on the basis of fundamental theoretical models.

The original concept introduced by A. Bohr [52] – that nuclear fission takes place through definite transition states, with well-defined quantum numbers on the top of a one-hump barrier – has undergone rapid development. The properties of these intermediate states allowed the determination of several features of the fission process. But they could not describe the intermediate structure of the fission cross-sections in the sub-barrier energy range. The concept of the double-hump barrier, introduced by Strutinsky [53] in

26

the late 1960s, was a major breakthrough in the field of fission and provided an explanation for many fission results which could not be otherwise understood. The double-humped barrier arises from a combination of "macroscopic" liquid-drop effects, and "microscopic" shell effects, on the variation of the potential energy with deformation, and is particularly important in the actinide region.

Such a barrier shape is now currently used in fission cross-section calculations but still cannot be obtained to the required accuracy from theory alone – the most sophisticated theories can only predict barrier heights with an uncertainty of 0.5 MeV, or more, which is generally insufficiently accurate for fission cross-section calculations. Fits to the experimental fission cross-section data are needed in order to obtain the fission barrier parameters. The combination of the Bohr theory of fission exit channels and the phenomenological Strutinsky prescription of the parameters of the double-hump barrier play a major role both for the understanding of the fission process and for the calculation of fission cross-sections.

The different stages of the fission process are as follows. In the initial stage a nucleus undergoes a series of large vibrations until it becomes so strongly deformed that it breaks into (usually) two primary fragments (this break is called scission). Although the initial nucleus is highly excited with closely spaced levels, the resulting transition state nucleus is relatively "cold" since most of the initial excitation energy is expended as deformation energy. This effect is well supported by fission fragment angular distributions, and the result is that only a few channels determine the statistical properties of fission widths. The spectrum of the excited states in the transition nucleus is expected to be analogous to the low-energy spectrum of a deformed heavy nucleus. These levels are well understood in terms of the collective model where each level is characterized by the quantum numbers, I, π, and K (projection of I on the nuclear symmetry axis). After scission, the fragments repel each other due to the long-range Coulomb force. During their mutual repulsion, these fragments de-excite by prompt-neutron and prompt-γ-ray emissions. These de-excitation processes are called "prompt", and the residual fragments are called the fission products. The fission products are generally far from the line of β-stability and they decay to stable nuclei by β-radioactivity followed by γ and even particle (neutron) emission. These processes are usually described as the "delayed" processes. The total energy released in the fission process is about 200 MeV.

Photofission Cross-Sections

Our concern here is the photofission process, which can occur in heavy target elements. The excitation curves found for the photofission of uranium and transuranic elements such as americium, neptunium and plutonium exhibit a sharp and important peak at giant resonance energies between 10 and 20 MeV for the incident photons. At higher photon energies the photofission cross-section decreases by two orders of magnitude up to 100 MeV. Above 100 MeV it increases again sharply due to a new mechanism of fission. This mechanism can be ascribed either to the neutron field in the quasi-deuteron disintegration mechanism, or to the incipient production of photopions in the nucleus, or to both.

Modern theories of the photofission process at γ-ray energies which are not too high are based on the hypothesis of the compound nucleus introduced by N. Bohr in 1936. The photofission process at low energies is assumed to be a two-step process. The nucleus absorbs a photon and the compound nucleus thus created decays by fission, by neutron

emission, or by γ-deexcitation. The model is developed on the assumption that the fission process is governed only by barrier transmission. The two-step fission cross-section formula is given by

$$\sigma_f(E_\gamma) = \sum_{I,\pi,K} \sigma_{\gamma,abs}^{I,\pi}(E_\gamma) P_f(I,\pi,K,E_\gamma). \tag{4.9}$$

where I and π are the spin and the parity of transition states, K is the spin projection on the symmetry axis, P_f is the fission probability that contains information derived from the fission barriers. and $\sigma_{\gamma,abs}^{I,\pi}$ is the photoabsorption cross-section.

Whereas photoabsorption cross-section is well understood over a wide energy range (up to 1 GeV), the dependence of the fissility on the excitation energy has only been studied in the giant resonance region (below 20 MeV). In our further description, we restrict ourselves to γ-ray energies up to 30 MeV where one can neglect proton emission. In the frame of the statistical model the fissility, for first-chance, second chance, etc. fission, can be written as

$$P_f(I,\pi,K,E_\gamma) = \frac{\Gamma_f^{I,\pi,K}}{\Gamma_f^{I,\pi,K} + \Gamma_\gamma^{I,\pi} + \Gamma_n^{I,\pi}} \quad +$$

$$\frac{\Gamma_n^{I,\pi,K}}{\Gamma_f^{I,\pi,K} + \Gamma_\gamma^{I,\pi} + \Gamma_n^{I,\pi}} \times \frac{(\Gamma_f^{I,\pi,K})'}{(\Gamma_f^{I,\pi,K})' + (\Gamma_\gamma^{I,\pi})' + (\Gamma_n^{I,\pi})'} + \ldots \tag{4.10}$$

where the symbols $\Gamma_f^{I,\pi,K}$, $\Gamma_\gamma^{I,\pi}$ and $\Gamma_n^{I,\pi}$ denote, respectively, the widths for fission, γ-deexcitation and neutron emission. The primed quantities describe the decay widths for the nucleus produced after one neutron is emitted from the initial compound nucleus. For γ-ray energies below the fission barrier the neutron emission width $\Gamma_n^{I,\pi}$ is generally taken to be equal to zero. The widths $\Gamma_f^{I,\pi,K}$, $\Gamma_\gamma^{I,\pi}$ and $\Gamma_n^{I,\pi}$ are related to the corresponding transmission coefficients T as

$$\Gamma_i^{I,\pi,K} = \frac{D_{I,\pi}}{2\pi} \times T_i^{I,\pi,K}, \tag{4.11}$$

where $D_{I,\pi}$ is the average spacing of excited states with spin and parity I,π.

The neutron transmission coefficients T_n can be calculated within statistical models, using for example the Weisskopf model [54] in which parameters are those of the level density formulas.

The electric dipole radiation of γ-rays gives the main part in the total radiation width. Usually in practical calculations, magnetic dipole and quadrupole electric transitions also are taken into account. The γ-ray transmission coefficients for electric dipole radiation can be estimated in the frame of the Brink-Axel giant resonance model [55]. For further details see, for example, Chapter 4 in Ref. [56].

28

For the one-dimensional model of fission the fission transmission coefficients T_f can be determined from numerical solution of the Schrodinger equation. The calculations of the fission transmission coefficients within the framework of the double-humped fission barrier are described in detail in Ref. [57].

The ratio Γ_n/Γ_f is an important parameter in a calculation of photofission cross-sections. From analyses of experimental data obtained for example in [58, 59], it was determined that the ratio is approximately constant for excitation energies up to 30 MeV. At the same time the fissionability increases with excitation energy and increases by a step when a new next chance-fission channel opens. In Ref. [59] the Γ_n/Γ_f values were measured and analyzed as a function of the nuclear fissionability Z^2/A together with previously obtained experimental data. It was shown that the values for Γ_n/Γ_f decrease approximately exponentially with the nuclear fissionability. These data can be approximated by the equation

$$log_{10} \frac{\Gamma_n}{\Gamma_f} = 36.82 - 1.02 \frac{Z^2}{A}.$$

(4.12)

This result can be used to guide the choice of fission-channel and neutron-channel level density parameters. This is particularly important for multi–chance fission where there may be little experimental information on the fissionability.

Average Number of Prompt Neutrons

The prompt neutron emission multiplicity in photofission process is an important quantity that influences the importance of the photoneutron source in applications. The average number of prompt neutrons $\bar{\nu}_p$, as a function of the incident photon energy, was measured for photofission on ^{233,234}U, ^{237}Np, and ^{239}Pu in Ref. [59], and ^{235,236,238}U and ^{232}Th in Ref. [60]. As for neutron-induced fission, $\bar{\nu}_p$ increases with increasing incident energy. The increase is approximately linear up to 20 MeV, with the exception of ^{232}Th which exhibited a more complex relationship.

The spectrum of prompt fission neutrons has been difficult to determine from a theoretical point of view, though certain advances have been made [61]. In practice, the experimentally-measured spectra of prompt fission neutrons have a rather simple form which can be fitted by theoretical shapes derived from crude phenomenological models. Usually two shapes are considered for presentation of the prompt fission spectrum: (i) the Maxwell spectrum, which can be derived simply by assuming that all neutrons are emitted by a single nucleus at rest and excited at a temperature T. This spectrum contains only one adjustable parameter, the temperature T, which has no real physical significance; (ii) the Watt spectrum, which can be derived assuming that all the neutrons are emitted by the moving fragments at the same nuclear temperature T, and all fragments have the same kinetic energy per nucleon. This two-parameter Watt spectrum of prompt fission neutrons gives provides a slightly better approximation to the experimental data than the Maxwell form, perhaps because the physical hypotheses are more realistic, but also for the reason that the Watt spectrum contains two adjustable parameters instead of only one for the Maxwell spectrum.

Photofission Product Yield

The distribution of the fission products from the photofission process has been studied also as a function of the incident photon energy. Whereas the cross-section studies provide information on the "static" properties of the fissioning nuclei, the study of fragment characteristics (mass, charge, and energy distributions) instruct us also about the "dynamic" properties on the path from the saddle to the scission point. Most of the first results on fragment characteristics obtained in photofission have been summarized in Refs. [62, 63]. Recent measurements on fragment characteristics for the photofission of ^{235,238}U, ^{240,242,244}Pu, with 12-, 15-, 20-, 30-, and 70-MeV bremsstrahlung the have been performed in Ref. [64]. In these works a systematic study of mass, charge, and kinetic energy distributions has been investigated as a function of initial photon energy. It was shown that for all photon energies between 10 and 100 MeV, the fission product distribution is seen to have two well-marked humps, in contrast with the chain yield distributions found for fission with high energy neutrons, protons and complex nuclei where the two-hump distribution gradually transitions to a one-hump distribution with increasing excitation energy of the fissile system. For the photofission process the two-humped structure appears to remain regardless of the excitation energy.

4.3 Nuclear Modeling Codes

In this section, brief overviews are given of the nuclear reaction modeling codes that have been used in this Coordinated research Program to predict cross-section data for evaluated photonuclear data libraries.

4.3.1 GNASH (Los Alamos)

The Los Alamos GNASH code [65] treats a nuclear reaction as proceeding through an initial preequilibrium phase (calculated from the exciton model with a $2p1h$ initial configuration), from which high-energy ejectiles can be emitted, followed by a process of sequential particle emission from decaying compound nuclei, until the final residual nucleus attains its ground state via particle or gamma-ray emission. The Hauser-Feshbach theory is used to calculate emission from the compound nucleus, with a full conservation of spin and parity. Production cross-sections and emission spectra of secondary light particles, γ-rays, and recoil nuclides are obtained from the calculations.

The photoabsorption model described in Sec. 4.1 is implemented, as are the photonuclear emission models described in Sec. 4.2. Full details can be found in Ref. [33], and in the GNASH code manual [65].

4.3.2 ALICE-F and MCPHOTO (Tokai)

The ALICE-F code [66] is a version of Blann's ALICE code that has been developed by Fukahori of JAERI. A number of extensions have been made to the original code, including a capability to model reactions at energies up to many hundreds of MeV.

This code applies the hybrid and geometry-dependent-hybrid preequilibrium models [67], with equilibrium decay calculated from the Weisskopf-Ewing evaporation model. Initial exciton configurations of $2p1h$ or $2p2h$ can be used in the quasideuteron regime, and $1p1h$ in the GDR region. The photoabsorption and emission models follows the descriptions above in Secs. 4.1, 4.2. The ALICE-F code's role in photonuclear data evaluation is described by Kishida in Ref. [32], and its use in a recent evaluation for tantalum has been described by Lee, Fukahori, and Chang [35].

The MCPHOTO code is a version of the MCEXCITON [68] code that has been developed by Kishida *et al.* to calculate photo-induced reaction data. This code applies the Random Walk Exciton Model [69] with equilibrium decay calculated following the treatment of Ref. [69] using the Monte-Carlo method. This code has been used to calculation of particle decay process after photon absorbed by certain nuclei, at the JAERI laboratory.

4.3.3 GUNF and GLUNF (Beijing)

The GUNF code, developed by Zhang *et al.* at the Chinese Nuclear Data Center, applies the exciton model for preequilibrium emission processes, and the Hauser-Feshbach theory for compound nucleus decay. Recoil effects in multi-stage emission processes are included. The preequilibrium exciton model is implemented using the master-equation approach. This model was generalized to include angular momentum and parity conservation, which allows a unified treatment of preequilibrium and equilibrium emission. Preequilibrium cluster emission processes are also included. Again, the photoabsorption and emission processes are computed using the approaches outlined in Secs. 4.1, 4.2. Full details can be found in the GUNF code manual [70].

A specific version of the above code was developed to calculate photonuclear reactions on light nuclei. In particular, GLUNF (GL stands for "Gamma Light") calculates reactions $\gamma + {}^9Be$ up to 30 MeV. At low energies, the giant dipole resonance is the dominant reaction mechanism and isotropy is used for the angular distributions of outgoing particles. Because of relatively strong recoil effects in light nucleus reactions, the energy balance is strictly taken into account in expressions for spectra of the outgoing particles. Based on the unified Hauser–Feshbach and exciton models, emission ratios for each specific excited level can be calculated. The expressions for double differential cross-sections are explicitly provided for discrete levels in sequential two–body reactions, three–body breakup process and two–body cluster separation. The GLUNF code calculates the following quantities:

- Photoabsorption cross-sections

- Cross-sections for all reactions

- Energy spectra of outgoing particles for each reaction channel

- Total neutron spectrum.

The code converts the calculated quantities into the ENDF-6 format. The relevant expressions can be found in Ref. [71].

4.3.4 XGFISS (Obninsk)

The XGFISS code [72] has been developed by A. Blokhin of IPPE for calculations of photofission and photoneutron cross-sections in the frame of the statistical model, using neutron emission decay from the Weisskopf evaporation model [54], and the fission probabilities from the penetrability of double(triple)-humped fission barriers, see Sec. 4.2.5. The photoabsorption cross-sections are calculated using the approaches described in Secs. 4.1. The input consists of the following quantities:

- Parameters of two (one) Lorenz curves or tables of photoabsorption cross-section. Default: the photoabsorption cross-section is calculated using the systematics of Lorenz parameters adopted within the code,

- Level density parameters or their systematics.

- Neutron binding energies,

- Parameters for double(triple)-humped fission barrier, and

- Nucleus-target, spin, parity and deformation of the ground state, γ-ray energy range and energy step.

Output is arranged into tables with $(\gamma, abs), (\gamma, xn), (\gamma, 1n), (\gamma, 2n), (\gamma, F), (\gamma, f), (\gamma, nf)$ and $(\gamma, 2nf)$ cross–sections for the γ–ray energy range up to 20 MeV. The results of calculations are presented in the ENDF-6 format. Theoretical models used in the code are described in Ref. [72].

4.4 Relation Between Electron and Photon Induced Reactions

Consider scattering with an electron with initial energy E_0 and momentum P_0, final energy E_f and momentum P_f, with transferred energy $E = E_0 - E_f$ and transferred momentum $\vec{q} = \vec{P_0} - \vec{P_f}$. In inelastic electron scattering experiments the scattered electron is detected at some angle θ with respect to the incident beam, having transferred momentum q and energy E, to the nucleus. As a result of the nuclear excitation, other kinds of nuclear debris may be emitted, but the experiment integrates over all the final states of these outgoing particles, since only the electron is detected. The photonuclear cross-section is the low-q limit, $q \to E$, of the electron scattering cross-section. When real photons are absorbed, only the very first few multipoles are involved; whereas the absorption of virtual photons, i.e., electron scattering, can involve higher multipoles, the complexity of the electron scattering spectrum growing with q.

On the other hand, an electrodisintegration experiment is one in which an outgoing nuclear fragment or a radioactivity is detected. Since the outgoing electron is not observed, the experiment integrates over all of its final states. The electrodisintegration cross-section includes all the multipoles excited in electron scattering, but it emphasizes the transverse

parts of the interaction, because it is dominated by the very forward angles (that are never sampled in electron scattering experiments).

The cross-section [73], [74], [75] in Born approximation for the inelastic scattering of an electron of initial energy E_0 and final energy E_f into a solid angle $d\Omega$ and providing an excitation of energy E, and multipole order λL, is given by:

$$\frac{d\sigma}{d\Omega} = 8\pi\alpha^2 \ (\frac{P_f}{P_0}) \ \frac{1}{\eta q_\mu^4} \ \left[V_C(\theta) \sum_{L=0}^\infty \left[F_C^L(q) \right]^2 + V_T(\theta) \sum_{L=1}^\infty \left[F_T^L(q) \right]^2 \right], \tag{4.13}$$

where $q_\mu^2 = q^2 - E^2$. V_C and V_T are coefficients depending only on kinematical variables, and $F_C(q)$ and $F_T(q)$ are related to the reduced matrix elements of the Coulomb and transverse operators, connecting the nuclear ground state, I_0, with some excited state, I_k.

$$\left[F_C^L(q) \right]^2 = \frac{1}{2I_0 + 1} \ | < I_k||M_L(q)||I_0 > |^2 \tag{4.14}$$

and

$$\left[F_T^L(q) \right]^2 = \frac{1}{2I_0 + 1} \ \left[| < I_k||T_L^{el}(q)||I_0 > |^2 + | < I_k||T_L^{mag}(q)||I_0 > |^2. \right] \tag{4.15}$$

The electron scattering cross-section is dominated by small-angle, low-q, transverse photon-like transitions owing to the $(q^2 - E^2)^2$ factor in the denominator of eq.(4.13).

The virtual photon spectra, required for the analysis of electrodisintegration experiments, are obtained by comparing the electron scattering cross-section of eq.(4.13) with the photonuclear cross-section, integrated over the level:

$$\int \sigma_\gamma(E_\gamma) \, dE_\gamma =$$

$$= (\frac{\alpha}{E_\gamma}) \ \frac{(2\pi)^3}{2I_0 + 1} \ \sum_L \left[| < I_k||T_L^{el}(E_\gamma)||I_0 > |^2 + | < I_k||T_L^{mag}(E_\gamma)||I_0 > |^2 \right] =$$

$$= (\frac{\alpha}{E_\gamma}) \ (2\pi)^3 \ \sum_L \left[F_T^L(E_\gamma) \right]^2,$$

which is proportional to the electron scattering cross-section as $q \to E_\gamma$. So that one can define:

$$\frac{dN^{\lambda L}}{d\Omega} = \frac{E_\gamma}{\int \sigma_\gamma(E_\gamma) dE_\gamma} \frac{d\sigma}{d\Omega}. \tag{4.16}$$

Then

$$\frac{dN^{EL}}{d\Omega} = \frac{\alpha}{\pi^2} \frac{E_\gamma^2}{q_\mu^4} \frac{P_f}{P_0} \left[\frac{F_T^{EL}(q)}{F_T^{EL}(E_\gamma)} \right]^2 V_T(\theta),$$

$$\frac{dN^{ML}}{d\Omega} = \frac{\alpha}{\pi^2} \frac{E_\gamma^2}{q_\mu^4} \frac{P_f}{P_0} \left[\frac{F_T^{ML}(q)}{F_T^{ML}(E_\gamma)} \right]^2 V_T(\theta).$$

Even though the Coulomb operator cannot be responsible for excitations by real photons, a similar expression can be written for these excitations through the use of Siegert's theorem, which connects $F_T^{EL}(q)$ and $F_C^L(q)$, as $q \to E_\gamma$:

$$F_T^{EL}(q) \overset{q \to E_\gamma}{=} -\frac{E_\gamma}{q} \left[\frac{L+1}{L} \right]^{1/2} F_C^L(q). \tag{4.17}$$

In the long wavelength limit, $qr \ll 1$, where r is the nuclear radius, the transition probabilities can be cancelled and the electric and magnetic virtual photon spectra can be calculated. The basic premise of the virtual photon technique is that we can express the electrodisintegration cross-section for the emission of a particle x, $\sigma_{e,x}(E_0)$, in terms of the corresponding photonuclear cross-section, $\sigma_{\gamma,x}^{\lambda L}(E_\gamma)$, associated with the absorption of real photons of multipolarity λL, through the virtual photon spectrum, $N^{\lambda L}(E_0, E_\gamma, Z)$, by:

$$\sigma_{e,x}(E_0) = \int_{Threshold}^{E_0} \sum_{\lambda L} \sigma_{\gamma,x}^{\lambda L}(E_\gamma) N^{\lambda L}(E_0, E_\gamma, Z) \frac{dE_\gamma}{E_\gamma}. \tag{4.18}$$

The validity of this expression stems from the cancellation of the reduced matrix elements for photo and electrodisintegration, which is exact in the limit $q \to E_\gamma$.

Chapter 5

Evaluations

This Chapter describes evaluations of photonuclear reactions. We start with evaluations based on experimental data, proceed with evaluations based on model calculations, and end up with methods used for producing evaluated photonuclear libraries.

5.1 Evaluations Based on Experimental Data

An absence of sufficiently intense beams of monoenergetic photons is one of the main problems in experimental studies of photonuclear reactions. There are several methods aiming at circumventing this problem. In particular, one can use

- Data obtained using continuous bremsstrahlung beams. The corresponding photonuclear cross-section is derived by unfolding the observed data, and

- Quasi-monoenergetic beams produced most often by annihilation of relativistic positrons or tagged photons.

The resulting differences in actual spectral distributions of photons as well as their substantial deviations from a delta function cause serious challenges for the comparison of different experiments and for the evaluation of data: systematic disagreements have been observed between data obtained by bremsstrahlung and quasi-monoenergetic beams [76]. In addition, significant discrepancies in absolute values of cross-sections, as well as in the positions of the resonance peaks, have been observed [77], [78]. This was supported by a systematic study of more than 500 experimental total photoneutron reaction cross-sections [79], where discrepancies in shape, absolute values and average energies were found and analyzed.

These discrepancies were attributed to three aspects of experimental procedure: actual difference in photon spectra; absolute normalization of cross-sections; and calibration of photon energies. An evaluator is challenged to resolve these discrepancies, or disregard parts of the data. To this end, an evaluation procedure to handle experimental photonuclear data has been developed by the CDFE Moscow group.

The first step of the CDFE procedure is to transform experimental data obtained by different methods (different photon spectra) so that they can be treated as reasonable approximations of data measured by monoenergetic beams, allowing them to be directly compared. To achieve this, data are reduced to the same quasi-monoenergetic photon spectrum, employing a so-called "method of reduction" of experimental data. The second step consists of removing systematical discrepancies caused by normalization (absolute
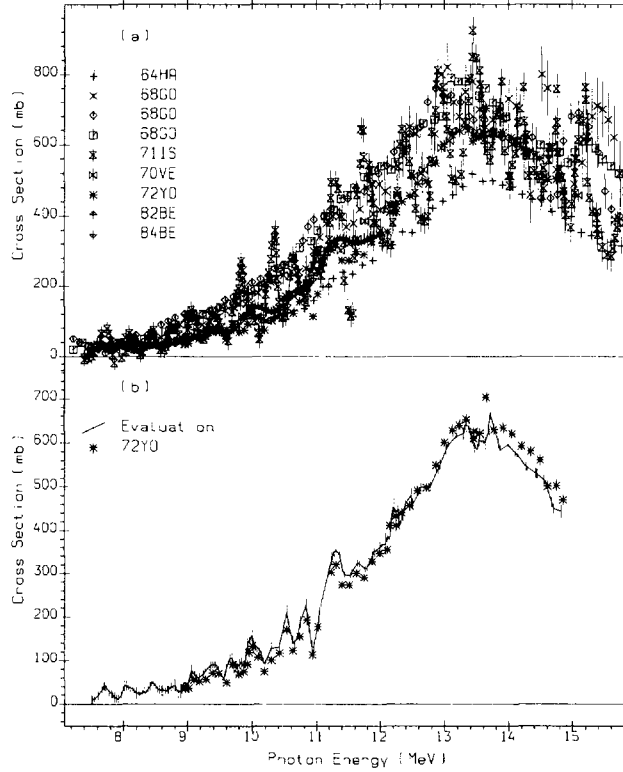
Figure 5.1: *Experimental and evaluated cross-sections for the $^{208}Pb(\gamma, xn)$ reaction. (a) Experimental data compiled from 9 papers published in the period 1964-1984. (b) Evaluated data obtained by the method of reduction with the 120 keV resolution (line with error bars) compared with the fine resolution experiment using tagged photons (stars) [80].*

values of cross-section) and by energy shifts due to energy calibration. These two steps are briefly explained below.

The observed cross-section, $\sigma^{observed}(E'_\gamma)$, at the photon energy E'_γ, is related to the true cross-section, $\sigma^{true}(E_\gamma)$, at the energy E_γ as

$$\sigma^{observed}(E'_\gamma) = \int W(E'_\gamma, E_\gamma)\sigma^{true}(E_\gamma)dE_\gamma + \mu(E'_\gamma), \tag{5.1}$$

where $W(E'_\gamma, E_\gamma)$ is the spectrum of photons (apparatus function), and μ is the error (additive noise). This equation can be schematically written in operator form

$$\sigma^{observed} = W\sigma^{true} + \mu. \tag{5.2}$$

The method of reduction represents a technique of statistical mathematics [81, 82] to transform $\sigma^{observed}$ into a quantity relevant to a quasi-monoenergetic photon spectrum U. This is achieved by applying an appropriate operator R to the above equation. Defining $\sigma^{reduced} = R\sigma^{observed}$, $U = RW$ and $\tilde{\mu} = R\mu$ one gets

$$\sigma^{reduced} = U\sigma^{true} + \tilde{\mu}. \tag{5.3}$$

36

The first step of the procedure consists in finding a realistic quasi-monoenergetic photon spectrum U, usually a Gaussian with a sufficiently narrow width, and deducing the operator R (see Ref. [78] for more details). In this way, a set of different measurements can be reduced to the same photon spectrum that satisfies the requirement of being quasi-monoenergetic. The unfolding of Eq.(5.1) is thus avoided, which represents an advantage. A disadvantage is that $\sigma^{reduced}$ rather than σ^{true} is obtained.

The second step of the evaluation procedure consists of removing discrepancies between data sets assumed to be caused by absolute normalization of cross-sections and by calibration of photon energies. Adopting a simple linear renormalization and a simple additive recalibration (photon energy shift), this second step is achieved by applying a transformation of the type

$$\sigma^{evaluated}(E_\gamma) = a + (1 + b)\sigma^{reduced}(E_\gamma + c). \qquad (5.4)$$

Actual values of the renormalization parameters a, b and the photon energy shift c are found by a least squares fitting over all experimental points to minimize discrepancies between data sets (for more details see Ref. [78], with refinements explained in Ref. [83]).

As an illustrative example, $^{208}Pb(\gamma, xn)$ cross-sections are shown on Figure 5.1. Part (a) (upper figure) shows initial experimental data, and part (b) (lower figure) compares evaluated cross-sections with the fine resolution results obtained using tagged photons [80].

The described procedure was applied by the CDFE Moscow group to evaluate 26 materials constituting the Evaluated Photonuclear Data Library, EPNDL:

- Materials: ^{2}H, ^{6,7}Li, ^{9}Be, ^{nat}C, ^{nat,16}O, ^{20,22}Ne, ^{nat}Al, ^{28}Si, ^{nat}Ca, ^{52}Cr, ^{54,56}Fe, ^{nat,58,60}Ni, ^{63,65}Cu, ^{nat}Zr, ^{141}Pr, ^{nat}Pb, ^{nat,235,236}U

- Energy: giant dipole resonance range, up to 20-30 MeV

- Data types: mostly (γ,abs), partly $(\gamma, 1n), (\gamma, 1p), (\gamma, 2n)$ and (γ, np).

5.2 Evaluations Based on Model Calculations

Theory plays a key role in essentially all evaluations that can be utilized by radiation transport codes, since a nuclear model code is capable of providing the comprehensive cross-section information that is needed, $i.e.$ emission spectra, angular distributions, $etc.$, in addition to cross-sections. Furthermore, a nuclear model code provides all this information in a way that automatically satisfies the conservation laws of energy, momentum, unitarity, and so on.

However, it is important to stress that model-based evaluations also crucially rely on experimental data in a number of ways. Experimental information usually guides the evaluated absorption cross-section. Likewise, researchers place a great importance on accurately modeling measured $(\gamma, 1n)$, $(\gamma, 2n)$, $etc.$ excitation functions. Having modeled

these processes accurately, one may then rely with more confidence on the emission spectra of secondary ejectiles predicted by theory.

Details of the nuclear theory and models used in photonuclear evaluations were provided in Chapter 4. In this subsection, general procedures that are used in model-based evaluations are summarized. The information provided below is, by necessity, rather general in nature, since specific details vary from laboratory to laboratory. Further details can be obtained from publications by individual evaluators, and by studying the documentation included within an ENDF file.

The major steps in an evaluation consist of:

1. Develop theoretical and computational tools to calculate photonuclear reaction cross-sections. See, for instance, the physical models described in Chapter 4, along with the computer codes that have been developed.

2. Collect together all available experimental data that has been measured for photonuclear reactions on the target material of interest. Compilations of information on experiments, such as the work of Varlamov [22] (see the Annex of this TEC-DOC), and Dietrich and Berman [3], are particularly useful. See Chapter 3.2 for detailed discussions of all the experimental information that is available.

3. Based on the above experimental information, evaluate the photoabsorption cross-section, which is usually taken as an input to the subsequent nuclear reaction calculation. This evaluation may be based upon available total photonuclear absorption experimental data; on the experiment-based evaluations of the Moscow EPNDL library; or on model calculations using giant-resonance and quasideuteron mechanisms, as described in Chapter 4.1

4. Calculate the $(\gamma, 1n)$, $(\gamma, 2n)$, $(\gamma, 1p)$ etc. excitation functions, and compare against available experimental data. If different experiments are discrepant with one another, establish methods to assess which experiment is most likely to be accurate. (In some cases, experimentalists have already addressed these discrepancies).

5. If the calculated excitation functions, described above, disagree with the measured values, consider studying the sensitivity of the model calculations to some of the input parameters used. For instance, the calculated excitation functions can depend sensitively on the level densities, and optical potentials, that are used. Adjust these input parameters within their ranges of known validity to optimize agreement between calculation and experiment.

6. If photofission can occur, model calculations are most reliable when photofission cross-section measurements are available. This allows the fission barrier heights and widths to be inferred from the data, for first-chance, second-chance, ... fission. Calculated fission cross-sections depend sensitively on these parameters, as well as on the level densities used to describe the transition states.

7. When an acceptable representation of available measured data is obtained, use the model calculations to predict cross-sections, and emission spectra, for a fine incident and emission energy grid.

8. Convert the calculated results into the ENDF-6 format, and document the methods used to arrive at the evaluated results

5.2.1 Emission Spectra

An important aspect to the present project has been the generation of photonuclear data describing the emission spectra of the secondary ejectiles. This information was obtained from the preequilibrium and equilibrium decay models described in chapter 4. The inclusion of emission spectra data allows the evaluated ENDF files to be used in radiation transport computer simululations, which need such information for describing and tracking the secondary ejectiles as they undergo further interactions with matter.

As discussed in Chapter 4.2.3. very few measurements exist for the spectra of secondary particles from monoenergetic source photons. An example was provided in Figure 4.2 for photons incident on calcium. Nevertheless, one may have confidence in the accuracy of the evaluated spectra in cases where the agreement between the calculated and measured channel cross-sections (γ, 1n), (γ, 2n), etc., is good. This is because the energy dependence of the emission spectrum stronly influences the relative population of various product nuclides when multiparticle emission is possible.
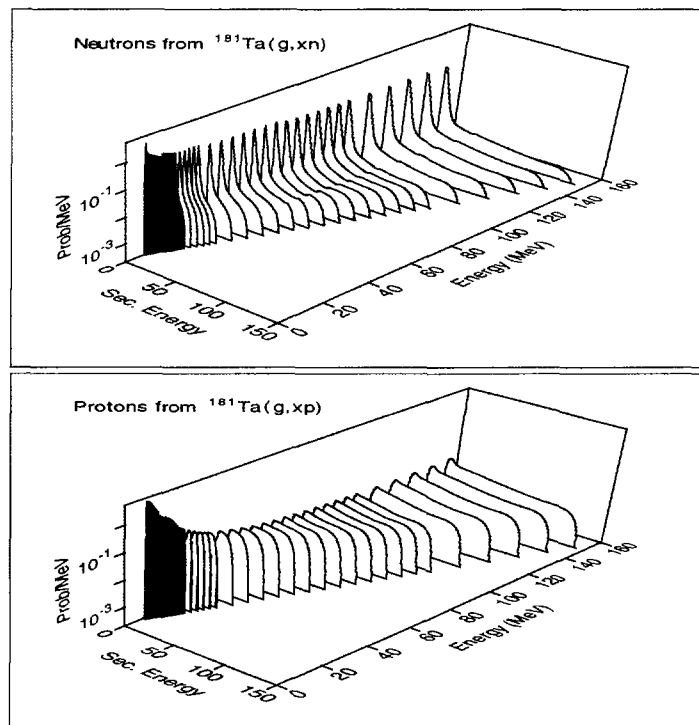

Figure 5.2: *The probability distributions for neutron (upper graph) and proton (lower graph) emission spectra, for photons incident on* ^{181}*Ta. These 3D perspective graphs show the probability distributions as a function of both secondary particle energy and incident photon energy.*

All the ENDF evaluations generated by this project include emission spectrum data. An example is given above in Figure 5.2 for the angle-integrated spectra of neutrons (upper figure) and protons (lower figure), from photons incident on ^{181}Ta. The 3D perspective plots show the spectra as a function of the secondary particle emission energy, for various incident energies up to 150 MeV. The spectra are given as probability distributions normalized to unit area. The increasing role of high-energy preequilibrium ejectiles with increasing incident energy is clearly seen. Also, for neutrons one sees a large probability for the emission of low-energy evaporation neutrons, whereas for protons the coulomb barrier suppresses low-energy emission.

5.3 Methods Used for Producing Evaluated Libraries

This section provides summaries of the approaches used to produce evaluated photonuclear data libraries that have been adopted by various laboratories in the present project. The libraries are arranged alphabetically according to their acronyms: BOFOD, CNDC, EPNDL, JENDL, KAERI and LANL.

5.3.1 Obninsk Library (BOFOD)

The BOFOD photonuclear data library is a special purpose file of the Russian general purpose data file BROND. The initial contents of the BOFOD library included photonuclear data up to 20 MeV as described in Ref. [84]. In 1994-1999, new evaluated photonuclear data were prepared and included into the updated BOFOD library (also called BOFOD-99). This updated library is aimed at applications in radiation transport and radioisotope production.

The library consists of the following 70 materials:

1. 39 materials (36 isotopes and 3 natural compositions), with data for transport calculations, up to γ energy 20 MeV:
   ^{23}Na, ^{50,52,53,54}Cr, ^{55}Mn, ^{54,56,57,58}Fe, ^{nat}Ni, ^{58,60,62,64}Ni, ^{88}Sr, ^{nat}Zr, ^{90,91,92,94,96}Zr, ^{nat}Pb, ^{209}Bi, ^{232}Th, ^{233,234,235,236,238}U, ^{237}Np, ^{238,239,241}Pu, ^{241,243}Am and ^{243,244,245}Cm.

2. 2 materials, up to γ energy 70 MeV, with evaluated data for neutron production (cross-sections and energy distributions):
   ^{9}Be and ^{181}Ta.

3. 19 materials, up to γ energy 20 MeV, with photoabsorption cross-sections:
   ^{92,94,96,98,100}Mo, ^{114,116,118,120,122,124}Sn, ^{120,122,124,126,130}Te and ^{182,184,186}W.

4. 10 materials with specific production cross-sections for positron emitters, for positron-electron tomography (PET). The data are up to γ energy 70 MeV, produced by combining fitted experimental data and model calculations. The list includes:
   ^{12}C(γ, n), ^{14}N(γ, n), ^{16}O(γ, n), ^{19}F(γ, n), ^{nat}Ne$(\gamma, 2n + p)$, ^{32}S(γ, np), ^{63}Cu(γ, n), ^{65}Cu(γ, n), ^{nat}Ga(γ, n) and ^{141}Pa(γ, n).

The BOFOD-99 library is in the ENDF-6 format and it can be identified by NLIB=42. The following MT numbers were used for representing the photonuclear reactions:

MT	Quantity
3	Photoabsorption cross-section
4	Single neutron emission cross-section $(\gamma, 1n)$
5	(γ, sn)
16	Double neutron emission cross-section $(\gamma, 2n + 2np)$
18	Photofission cross-sections (γ, f)
28	(γ, np)

5.3.2 Beijing Library (CNDC)

The Beijing Photonuclear Library, also called the China Evaluated Photonuclear Data File, is being developed by the China Nuclear Data Center (CNDC). The library includes data up to γ-ray energy of 30 MeV, namely (γ, γ), $(\gamma, 1n)$, $(\gamma, 1p)$, $(\gamma, 1\alpha)$, $(\gamma, 1\,^3He)$, $(\gamma, 1t)$, $(\gamma, 2n)$, (γ, np), $(\gamma, n\alpha)$ and $(\gamma, 3n)$, both spectra and angular distributions of outgoing particles.

The CNDC Beijing evaluated photonuclear data for the following 24 nuclides: ^{9}Be, ^{27}Al, ^{51}V, ^{50,52,53,54}Cr, ^{54,56,57,58}Fe, ^{63,65}Cu, ^{90,91,92,94,96}Zr, ^{180,182,183,184,186}W, and ^{209}Bi.

Evaluation Methods

The evaluation methodology is based upon a critical analysis of experimental data combined with theoretical calculations. The experimental photonuclear database was obtained from the EXFOR master file of the IAEA Nuclear Data Section. Experimental data for materials under evaluation were retrieved, collected and analyzed. In general, these experimental data cover the photon energy range from threshold up to 30 MeV.

In order to calculate photonuclear data, the best neutron optical potential parameters were searched automatically using the code AUTOOPT. Based on the fitting of the experimental data including total cross-sections, nonelastic scattering, elastic scattering, and their angular distributions, a set of optimum neutron parameters was obtained. The optical model parameters for charged particles $(p, \alpha, d, \,^3He$ and $t)$ were taken from the relevant references.

Using the code DREAM, a set of discrete levels, pairing corrections, level density parameters and giant dipole resonance parameters as well as relevant ground state masses and J^π values was taken from the Chinese Evaluated Nuclear Parameter Library CENPL. Afterwards, photonuclear reactions were calculated using the reaction codes GUNF and GLUNF.

The total photoneutron cross-section $(\gamma, 1n)$ was obtained by summing of photoneutron excitations to the ground state, higher excited states and continuum. GDR parameters were adjusted automatically with the code GUNF or GLUNF by fitting the experimental cross-sections for $(\gamma, 1n)$, $(\gamma, 1nx)$, $(\gamma, 2n)$, (γ, abs) and other reaction channels. Calculated cross-sections for many channels were in good agreement with existed experimental data, giving some confidence to cross-sections where experimental data are not available.

Format

The checking and testing of evaluated data in the ENDF-6 format was carried out using computer codes of the CNDC and the US National Nuclear Data Center. This included format, consistency between the total and the sum of partial cross-sections, physics parameters and energy balance between incident γ and emitted particles.

The resulting data were arranged into computer files using the ENDF-6 format with the following specifications:

MF	MT	Quantity
1	451	Description and Dictionary
3	3	Photoabsorption cross-section
3	4	Cross-section for $(\gamma, 1n)$
3	16	Cross-section for $(\gamma, 2n)$
3	17	Cross-section for $(\gamma, 3n)$
3	50,51.....66.....91	Cross-sections for partial excited states, from ground state to the highest state and continuum
3	102.....107,111	Cross-sections for (γ, γ), $(\gamma, 1p)$, $(\gamma, 1d)$, $(\gamma, 1t)$, $(\gamma, 1\,^3He)$, $(\gamma, 1\alpha)$ and $(\gamma, 2p)$
6	16,17,22,28,91	Double differential cross-sections for $(\gamma, 2n)$, $(\gamma, 3n)$, $(\gamma, n\alpha)$, (γ, np) and $(\gamma, n$ continuum$)$

5.3.3 Moscow Library (EPNDL)

The evaluation methods used here were described in some detail in Section 5.1, and so we do not repeat them here. Note that this method focuses on reconciling discrepant experimental data, to arrive at an evaluated result based on measurements alone. The method does not address secondary emission spectrum data.

5.3.4 JENDL Library (JENDL)

The JENDL Photonuclear Library, also called JENDL Photonuclear Data File, contains γ-ray induced reaction data up to 140 MeV (pion threshold). The library is provided for applications such as neutron shielding, radiation therapy and estimation of radioactive isotopes produced in electron accelerators. The photon absorption cross-section is evaluated with the giant dipole resonance model and quasi-deuteron model, and the decaying processes are estimated with the statistical model with pre-equilibrium correction by using MCPHOTO [85] and ALICE-F [66] codes.

Nuclei included in the JENDL Photonuclear Data File (30 elements, 51 isotopes): ^{2}H, ^{9}Be, ^{12}C, ^{14}N, ^{16}O, ^{23}Na, ^{24,25,26}Mg, ^{27}Al, ^{28,29,30}Si, ^{40,48}Ca, ^{46,48}Ti, ^{51}V, ^{52}Cr, ^{55}Mn, ^{54,56}Fe, ^{59}Co, ^{58,60,61,62,64}Ni, ^{63,65}Cu, ^{64}Zn, ^{90}Zr, ^{93}Nb, ^{92,94,96,98,100}Mo, ^{133}Cs, ^{160}Gd, ^{181}Ta, ^{182,184,186}W, ^{197}Au, ^{206,207,208}Pb, ^{209}Bi, ^{235,238}U.

Evaluation Methods

Evaluation of the JENDL Photonuclear Data File was performed by making use of combination of experimental data and model calculation, because of a lack of experimental data for all quantities of interest. Some of the experimental data for photonuclear reactions are available in the Atlases of photonuclear cross-sections and in the EXFOR library. JNDC has also compiled a Photonuclear Reaction Data Index [23]. Data obtained by a least squares fitting procedure and model calculations are combined to evaluate photoabsorption and photoneutron cross-section. The fitting function for the photoabsorption cross-section is based on a sum of GDR and quasi-deuteron components. In the GDR region, multiple Lorentz resonance curves are used, whereas for the quasi-deuteron regime the formalism by Chadwick et al. [31] was adopted, see Sec. 4.1.

If experimental data for the photoabsorption cross-section are not available but data for the photoneutron cross-sections exist, then theoretical predictions for the ratio of the photoneutron absorption cross-section to the total absorption cross-section are used. This allows the total absorption cross-section to be inferred from the available photoneutron data. In cases where no experimental data are available, systematics and parameter compilations for the GDR were used. For energy spectra, angular distributions and double differential cross-sections for emitted light particles and isotope production cross-sections, the codes MCPHOTO and ALICE-F were used with GDR and quasi-deuteron models. Angular distributions of emitted particles were obtained with the formalism described in Sec. 4.2.4.

Format

Major applications at intermediate energies require a knowledge of isotope production cross-sections and double differential light particle spectra. For most applications it is sufficient to represent the particles emitted as inclusive emission spectra, $i.e.$ production cross-sections and spectra. In the ENDF-6 format, physical quantities of importance can be classified into two files, namely, MF=3 for cross-sections and MF=6 for double differential particle emission spectra. As concerns cross-sections, total absorption, photoneutron, and isotope and particle production cross-sections should be included. In addition, MF=1 contains evaluation information and comments, and MF=33 contains covariances. The structure of the file is summarized below.

MF	MT	Quantity
1	451	Description and dictionary
3	3	Total photoabsorption cross-section
3	5	Total isotope production cross-section
3	18	Fission cross-section
3	201	Neutron production cross-section
3	203	Proton production cross-section
3	204	Deuteron production cross-section
3	205	Triton production cross-section
3	206	^3He production cross-section
3	207	alpha production cross-section
6	5	Branching ratios (yields) for isotope production cross-section
6	201, 203-207	Normalized double-differential cross-section for light particles
33	3	Covariance of total photoabsorption cross-section

5.3.5 KAERI Library (KAERI)

KAERI is building a photonuclear data library [35, 86, 87, 86], which currently includes 143 isotopes of 38 elements for incident photon energies below 140 MeV. The list is as follows:

- Structural, Shielding and Bremsstrahlung Target Materials:
  $^{24,25,26}Mg$, ^{27}Al, $^{50,52,53,54}Cr$, ^{55}Mn, $^{54,56,57,58}Fe$, ^{59}Co, $^{58,60,61,62,64}Ni$, $^{63,65}Cu$, $^{64,66,67,68,70}Zn$, $^{90,91,92,94,96}Zr$, $^{92,94,95,96,97,98,100}Mo$,

$^{112,114,115,116,117,118,119,120,122,124}Sn$, $^{120,122,123,124,125,126,128,130}Te$, ^{141}Pr, ^{165}Ho, ^{197}Au, ^{209}Bi.

- Biological Materials:
  $^{12,13}C$, $^{14,15}N$, $^{16,17,18}O$, ^{23}Na, $^{32,33,34,36}S$, $^{35,37}Cl$, $^{40,42,43,44,46,48}Ca$.

- Nuclear Waste Transmutation:
  $^{84,86,87,88,90}Sr$, ^{93}Zr, $^{93,94}Nb$, $^{102,104,105,106,107,108}Pd$, $^{107,108,109}Ag$, $^{127,129}I$, $^{133,135,137}Cs$, $^{144,147,148,149,150,151,152,154}Sm$, $^{158,159}Tb$.

- Activation Analysis:
  $^{27,28,29,30}Si$, $^{36,38,40}Ar$, $^{39,40,41}K$, $^{46,47,48,49,50}Ti$, $^{70,72,73,74,76}Ge$, ^{110}Pd, $^{106,108,110,111,112,113,114,116}Cd$, $^{121,123}Sb$.

Evaluation Methods

Available experimental data were collected and their discrepancies were analyzed to select or reconstruct the representative data set. Then, the photoabsorption cross-sections were evaluated by applying the Giant Dipole Resonance (GDR) model for energies below about 30 MeV, and the quasi-deuteron model for higher energies, up to 140 MeV. The GDR parameters were adjusted automatically with the GUNF code [70] by fitting the experimental data of photoabsorption cross-sections or photoneutron cross-sections, as described in Sec. 4.1. In the discrete resonance regions in some light nuclei where the GDR model can not be applied, experimental data were fitted with the least squares procedure.

The resulting representative photoabsorption data were given as input for theoretical calculations for the emission process of neutron, proton, deuteron, triton, ^3He, α particles and γ rays using GNASH code [33, 65] (see Secs. 4.2 and 4.3).

Format

The KAERI library utilizes MF3-MT5 and MF6-MT5 combinations of the ENDF-6 format to provide a complete representation of the photonuclear reaction data. Photoabsorption cross-section, which is equal to total nonelastic cross-section, is tabulated in MF3-MT5. Exclusive reaction cross-sections, e.g. $(\gamma,1n)$, $(\gamma, 2n)$, ... are not explicitely tabulated in MT3 but can be inferred from the cross-sections of heavy recoil products tabulated in MT5. The inclusive production cross-sections and emission spectra for neutron, proton, deuteron, triton, alpha particles, and all residual nuclides are tabulated by use of MT=5 in the file MF=6. The description of the ENDF-6 format for the photonuclear data is summarized in Sec. 6.4.

5.3.6   Los Alamos Library (LANL)

The 12 isotopes included in the Los Alamos Photonuclear Library (LANL, sometimes also known as LA150.G) are documented in detail in Ref. [47]. Evaluations have been performed for isotopes of the following elements:

44

- Structural, shielding and bremsstrahlung target materials: Al, Si, Ca, Fe, Cu, Ta, W, Pb

- Biological materials: C, O

The nuclear models used in the GNASH code [65], and the evaluation techniques employed, largely follow the descriptions given in Secs. 4.2, 4.3, and 5.2. Below are given a few general details regarding these evaluations that are not described elsewhere in this TECDOC.

Evaluation Methods

The reader is pointed to the MF=1 documentation given at the beginning of each ENDF evaluation for full details of the evaluation methods used, together with experimental data that guided the evaluation. An accurate modeling of photoneutron emission was given a high priority in the LANL evaluations, due to the practical importance of neutron-production in many applications, though there was an attempt to model charged-particle production accurately too, particularly for light target nuclei where these channels are important. Where emission spectra measurements were available in addition to the usual excitation function data, they were used to validate the preequilibrium and equilibrium emission models.

One feature of the Los Alamos photonuclear evaluations is that they extend up to 150 MeV. The reason for this is that there has been an interest at Los Alamos in preequilibrium reaction physics, and these processes become important in the 15-150 MeV region. Additionally, certain applications need data up to 150 MeV. Specifically, there has been a recent interest at Los Alamos in developing neutron- and proton-induced (LA150 library) ENDF evaluations up to 150 MeV for accelerator-driven technologies (for waste transmutation, energy-production, tritium production etc.) [6]. For the MCNP and MCNPX codes to perform radiation transport simulations of these technologies in a fully coupled manner, photonuclear libraries are also needed up to 150 MeV.

For the light biologically-important target materials included in the LA150.G library (C, O), certain experiment-based evaluation methods were applied, that are worth highlighting here. In particular, unlike photonuclear reactions on medium and heavy nuclei, direct reactions, where a neutron or proton is emitted leaving the residual nucleus in its ground or low-lying discrete state, become important and account for a large fraction of the reaction processes, particularly in the giant dipole region. Theories describing these direct reactions have traditionally poorly accounted for the measured cross-sections. Therefore, the LA150.G evaluations involved a determination of these direct reactions to the ground-state (n_0 and p_0 emission) from experiment; the remaining photonuclear absorption flux was then made available for preequilibrium and compound nucleus decay in the usual manner. This procedure is described in detail in Refs. [33, 47], and allows a more accurate modeling of the neutron and proton emission processes.

Another feature unique to the LANL and also to the KAERI GNASH-based evaluations is the inclusion of emission spectra as well as the production cross-sections of the heavy recoil nuclear fragments, in addition to the light ejectiles. This recoil information is not very important for most applications, but the information was straightforward to include due to the physics models and computational tools already developed for nucleon

reactions [6] (where the recoil information is very important for quantifying radiation heating and damage). The recoil velocities are calculated in a coupled manner as the sequential particle and gamma-ray decay processes occur, following the kinematics of the emission processes. The recoil spectra information is useful for analyzing processes where a high-concentration of energy deposition by nuclear fragments in a small volume is important – e.g. radiation damage, including single-event upsets in microelectronics, and the relative biological effectiveness of radiotherapy beams.

Format

The LANL evaluations use a very simple ENDF format representation, making use exclusively of MT=5, together with file-3 and file-6 (MF=3 and MF=6). The photoabsorption cross-section, which equals the total nonelastic cross-section, is tabulated in file-3 MT=5, whereas emission multiplicities (yields) and spectra of all light charged particles, gamma-rays, and heavy nuclear products, are tabulated in file-6 MT=5.

What this means in practice, for readers who are not ENDF-format *aficionados*, is that the evaluations made use of inclusive production cross-sections, e.g. (γ, xn), rather than separately tabulating each exclusive reaction, e.g. $(\gamma, 1n)$, $(\gamma, 2n)$, ... The use of this representation at higher energies is driven by practical considerations, since the number of exclusive reactions possible at higher energies increases combinatorially. Furthermore, there are few applications where the exclusive reaction information is really needed, and the inclusive production cross-section information tabulated in LA150.G is quite adequate for almost all applications.

Whilst, for instance, $(\gamma, 1n)$ and $(\gamma, 2n)$ cross-sections are not specifically tabulated in the LA150.G files as MT=4 and MT=16, this same information is, in fact, available in the file by looking at the production cross-section tabulated in MT=5 for the corresponding heavy recoil product. This situation, though, is not true for cases where the light ejectiles cannot be uniquely identified by knowing the heavy reaction product – for instance, the (γ, np) and $(\gamma, 1d)$ reactions both produce the same heavy product.

46

Chapter 6

IAEA Photonuclear Data Library

The IAEA Photonuclear Data Library represents a computerized data file containing evaluations of photonuclear cross-section data. The library bears the name "IAEA", indicating that it aims to be an internationally recognized data file. The library was selected by participants of the present project from amongst all the sources of evaluated photonuclear data available. However, only data that can be used in radiation transport codes were considered, that is, data that are complete and include information on the spectra of emitted particles.

Below we describe the procedures adopted to select the evaluations. This is followed by a summary of the contents of the library; some comparisons of evaluations with measurements to illustrate the selection methods; a discussion of the format in which the cross-sections are stored; and information regarding access to the library.

A graphical presentation of the library, where comparisons are made between evaluation and experiment for all materials that are included in the library, can be found in Appendix B.

6.1 Selection Procedure

The selection procedure consisted of three major steps: collection of evaluations from various laboratories after their due completion; intercomparison of evaluations for each material; and selection of the best evaluations.

Step 1: Collection. The following 6 photonuclear data libraries were collected, intercompared and subjected to consideration for selection:

- BOFOD library, by IPPE Obninsk, Russia [88]

- CNDC library, by CNDC Beijing, China [89]

- EPNDL library, by CDFE Moscow, Russia [90]. *These are purely experimental cross-sections obtained by the method of reduction, without emission spectra, and are therefore not the subject of selection.*

- JENDL library, by JAERI Tokai, Japan [91]

- KAERI library, by KAERI Taejon, Rep. of Korea [92]

- LANL library, by LANL Los Alamos, USA [47]

The names of these libraries represent abbreviations that are either related to the name of the laboratory of its origin or to the specific name of the library or file. Thus, BOFOD is derived from the Russian 'Bibliotheka Fotoyadernykh Dannykh' meaning Library of Photonuclear Data. CNDC stands for the China Nuclear Data Center. EPNDL means Evaluated Photonuclear Data File. JENDL stands for the Japan Evaluated Nuclear Data File, including the Photonuclear Data File that we actually have in mind in the present project. KAERI means Korean Atomic Energy Research Institute. Finally, LANL refers to the Los Alamos National Laboratory evaluations that extend up to 150 MeV.

Step 2: Intercomparison. Intercomparison was applied individually to each material (target isotope and/or element). It consisted of the following steps:

- Available evaluated data were compared against each other and also against the measured data taken from the experimental cross-section library EXFOR [93] (the US alias name for this library is CSISRS). To this end, plots were produced for (γ, abs), (γ,xn) and (γ, F) cross-sections as needed.

- Results of this intercomparison were discussed by the CRP participants at two meetings (Los Alamos 1998, and Tokai 1999).

- Problems were identified and resolved by additional technical activity as needed.

Step 3: Selection. The following criteria were applied to determine which evaluation should be recommended in cases where more than one evaluation exists.

The two most important criteria were:

- Quality of evaluation. In particular, the extent to which the evaluation agrees with measured data was considered. For this purpose, comparison was also made with cross-sections incorporated in the Moscow library EPNDL.

- Completeness of evaluation. The evaluations were primarily intended for use in radiation transport codes, and therefore it is important that they include descriptions of, for instance, the energy spectra of photoneutrons.

Additional criteria that were considered:

- Energy range. The upper energy limit should be as high as possible. Thus, for instance, a 140-150 MeV maximum energy was considered preferable to 20-30 MeV, all other things being equal.

- Processing. The evaluations should be processable by the well-established and internationally recognized processing code NJOY [94], for use by a transport code such as MCNPX/MCNP [95, 4].

48

For final selection the following criterion was applied:

- Consensus. Selection of the data judged to be the best was reached by consensus of all CRP participants.

The above procedure was applied to each of the 164 isotopes included into the IAEA Photonuclear Data Library. In practice, competing evaluations were available mostly for 40 isotopes considered as priority materials (see Chapter 1), while for most of the remaining isotopes only a single evaluation was available.

To illustrate various aspects of our selection procedure employed, we show four specific examples for the nuclei ^{181}Ta, ^{12}C, ^{51}V and ^{235}U.
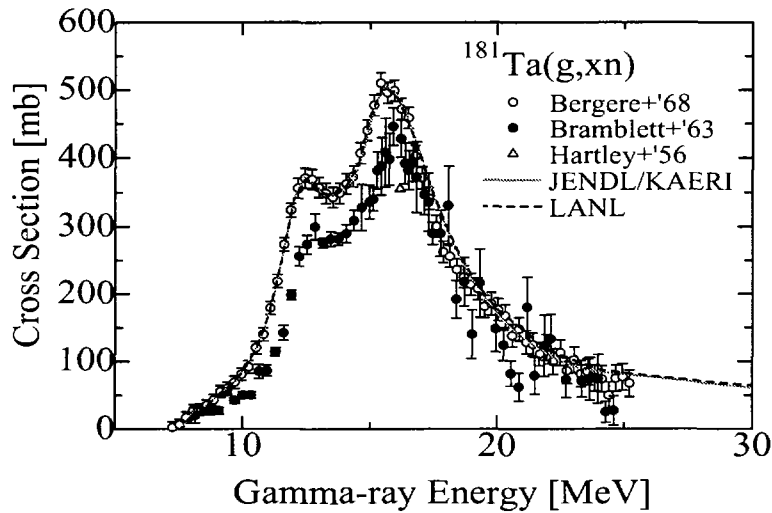
Figure 6.1: *Evaluated cross-sections for* ^{181} *Ta(γ, xn) compared with measurements*

Figure 6.1 shows ^{181}Ta (γ, xn), which is a dominant reaction for such a heavy nucleus. Experimental data are compared with evaluations from LANL and JENDL/KAERI. In this case the evaluated results are in very close agreement, even though they were obtained with different modeling codes (GNASH and ALICE-F repsectively). Notice that both evaluations agree with the higher data from Saclay, rather than the lower Livermore values. Since the calculated ^{181}Ta results, together with reasons for adopting the Saclay (γ, xn) data, were first published by Lee et al. [35] in a journal publication, we selected the JENDL/KAERI evaluation here.
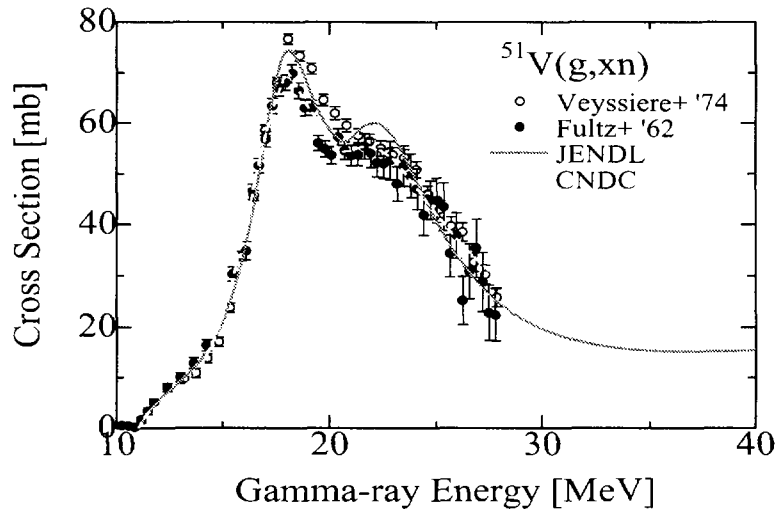
Figure 6.2: *Evaluated cross-sections for* $^{51}V(\gamma, xn)$ *compared with measurements*

Figure 6.2 shows ^{51}V (γ, xn), which is an important reaction for this medium-mass nucleus. Experimental data are compared with evaluations from CNDC and JENDL. Both evaluations provide a good representation of the experimental data, which are somewhat discrepant amongst one another. The Chinese CNDC evaluation was selected here.
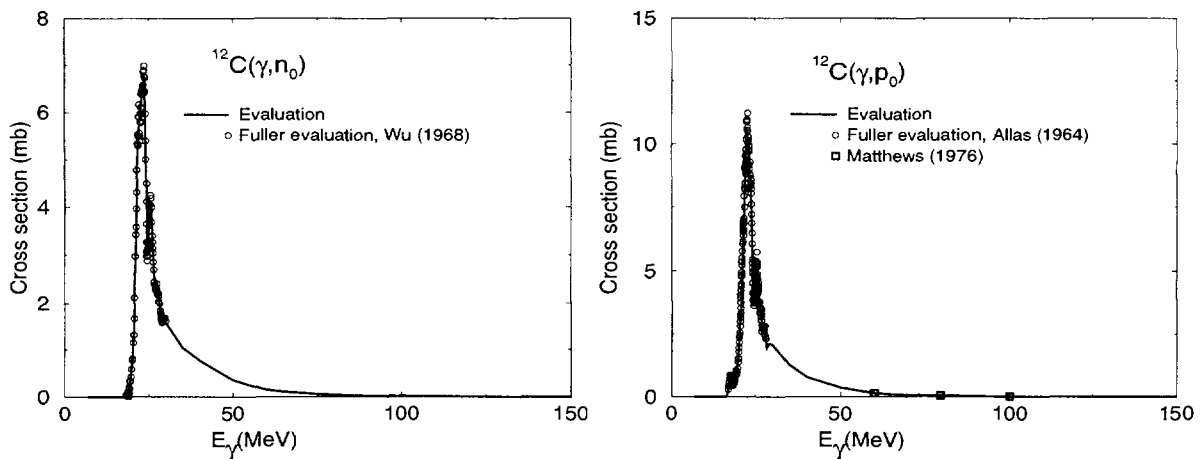
Figure 6.3: *Evaluated cross-sections for* ^{12}C (γ, n_0) *and* ^{12}C (γ, p_0) *compared with measurements.*

Figure 6.3 shows ^{12}C (γ, n_0) and (γ, p_0) reactions, where the residual nuclei are left in their ground states. These are specific reaction channels of importance in light nuclei, and the evaluations are based on the measured data shown in the figures. Only the LANL evaluation includes this detail in its light-nucleus evaluations, and also includes legendre-coefficients for the angular distributions of the emitted particles. Therefore the LANL evaluation was selected. (A more detailed figure showing these data is given in Appendix B).
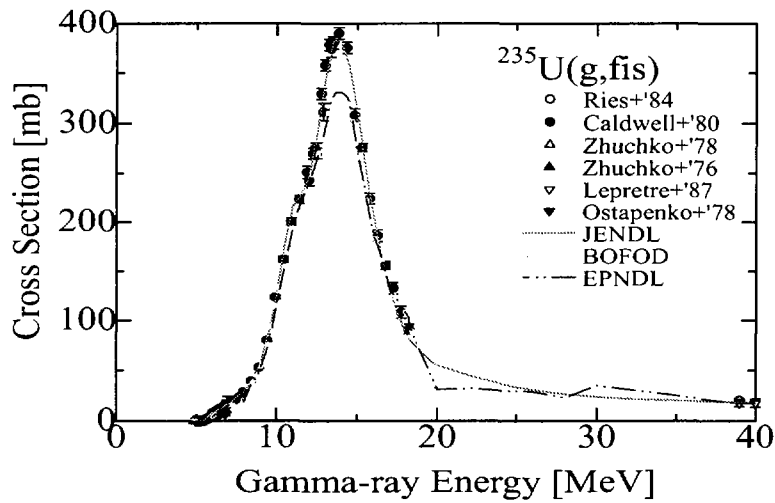
Figure 6.4: *Evaluated cross-sections for* $^{235}U(\gamma, F)$ *compared with measurements*

Figure 6.4 shows ^{235}U (γ, F) total fission, which is an important reaction channel for actinide nuclei. Experimental data are compared with evaluations from BOFOD, EPNDL and JENDL. The BOFOD evaluation was selected since it is the most complete evaluation and includes information on the fission neutron average multiplicity and spectra, which are important for transport calculations.

A summary of photonuclear evaluations used for intercomparisons and selection is given in Table 6.1. The table lists 164 nuclei, showing MT numbers of the ENDF-6 format for evaluations in 5 national libraries. The name of the library which supplied recommended evaluation is given in the last column. Comparison with experimental data can be found in Appendix B.

Table 6.1:   SUMMARY OF PHOTONUCLEAR EVALUATIONS

Listed are evaluations from 5 national libraries used in intercomparison and selection. Columns 2-6 show MT numbers of these evaluations, column 7 identifies selected evaluation.

Nucleus	BOFOD ≤ 20MeV	CNDC ≤ 30MeV	JENDL ≤ 140MeV	LANL ≤ 150MeV	KAERI ≤ 140MeV	Selected Evaluation
H-2			3,4,50			JENDL
Be-9	4,201	3,16,28,29,102-106	3,5,201,203-207			CNDC
C-12	4		3,5,201,203-207	5,50,600	5	LANL
C-13					5	KAERI
N-14	4		3,5,201,203-207		5	JENDL
N-15					5	KAERI
O-16	4		3,28,201,203-207	5	5	LANL
O-17					5	KAERI
O-18					5	KAERI
Na-23	4		Planned		5	KAERI
Mg-24			Planned		5	KAERI
Mg-25			Planned		5	KAERI
Mg-26			3,5,201,203-207		5	KAERI
Al-27		3,4,16,22,28,50-79,91,102-107,111	3,5,201,203-207	5	5	LANL
Si-27					5	KAERI
Si-28			3,5,201,203-207	5	5	KAERI
Si-29			3,5,201,203-207		5	KAERI
Si-30			3,5,201,203-207		5	KAERI
S-32	28				5	KAERI
S-33					5	KAERI
S-34					5	KAERI
S-36					5	KAERI
Cl-35					5	KAERI
Cl-37					5	KAERI
Ar-36					5	KAERI
Ar-38					5	KAERI
Ar-40					5	KAERI
K-39					5	KAERI
K-40					5	KAERI
K-41					5	KAERI
Ca-40			3,5,201,203-207	5	5	LANL
Ca-42					5	KAERI
Ca-43					5	KAERI
Ca-44					5	KAERI
Ca-46					5	KAERI
Ca-48			Planned		5	KAERI
Ti-46			Planned		5	KAERI
Ti-47					5	KAERI
Ti-48			Planned		5	KAERI
Ti-49					5	KAERI
Ti-50					5	KAERI
V-51		3,4,16,22,28,103-107,111	3,5,201,203-207			CNDC
Cr-50	3	3,4,16,22,28,50-56,91,102-107,111			5	CNDC
Cr-52	3,4	3,4,16,22,28,50-68,91,102-107,111	Planned		5	CNDC
Cr-53		3,4,16,22,28,50-71,91,102-107,111			5	CNDC
Cr-54	3	3,4,16,22,28,50-68,91,102-107,111			5	CNDC
Mn-55	4		Planned		5	KAERI
Fe-54	3,28	3,4,16,22,28,50-55,91,102-107,111	3,5,201,203-207		5	JENDL
Fe-56	3	3,4,16,22,28,50-59,91,102-107,111	3,5,201,203-207	5	5	JENDL
Fe-57		3,4,16,22,28,50-61,91,102-107,111			5	KAERI
Fe-58	3	3,4,16,22,28,50-55,91,102-107,111			5	KAERI
Co-59			Planned		5	KAERI
Ni-58	3		3,5,201,203-207		5	JENDL
Ni-60	3		3,5,201,203-207		5	KAERI
Ni-61			3,5,201,203-207		5	KAERI
Ni-62	3		3,5,201,203-207		5	KAERI
Ni-64	3		3,5,201,203-207		5	KAERI
Cu-63	4	3,4,16,22,28,50-65,91,102-107,111	3,5,201,203-207	5	5	LANL
Cu-65	4	3,4,16,17,22,28,50-63,91,102-107,111	3,5,201,203-207		5	JENDL
Zn-64			3,5,201,203-207		5	JENDL
Zn-66					5	KAERI
Zn-67					5	KAERI
Zn-68					5	KAERI
Zn-70					5	KAERI
Ge-70					5	KAERI
Ge-72					5	KAERI
Ge-73					5	KAERI
Ge-74					5	KAERI
Ge-76					5	KAERI
Sr-84					5	KAERI
Sr-86					5	KAERI
Sr-87					5	KAERI
Sr-88	3				5	KAERI
Sr-90					5	KAERI
Zr-90	3	3,4,16,22,28,103-107,111	3,5,201,203-207		5	KAERI
Zr-91	3	3,4,16,22,28,103-107,111			5	CNDC
Zr-92	3	3,4,16,22,28,103-107,111			5	CNDC
Zr-93					5	KAERI

Nucleus	BOFOD ≤ 20MeV	CNDC ≤ 30MeV	JENDL ≤ 140MeV	LANL ≤ 150MeV	KAERI ≤ 140MeV	Selected Evaluation
Zr-94	3	3,4,16,17,22,28,103-107,111			5	KAERI
Zr-96	3	3,4,16,17,22,28,103-107			5	CNDC
Nb-93			3,5,201,203-207		5	KAERI
Nb-94					5	KAERI
Mo-92	3,4		Planned		5	KAERI
Mo-94	3,4,16		3,5,201,203-207		5	KAERI
Mo-95					5	KAERI
Mo-96	3,4,16		3,5,201,203-207		5	KAERI
Mo-97					5	KAERI
Mo-98	3,4,16		3,5,201,203-207		5	KAERI
Mo-100	3,4,16		Planned		5	KAERI
Pd-102					5	KAERI
Pd-104					5	KAERI
Pd-105					5	KAERI
Pd-106					5	KAERI
Pd-107					5	KAERI
Pd-108					5	KAERI
Pd-110					5	KAERI
Ag-107					5	KAERI
Ag-108					5	KAERI
Ag-109					5	KAERI
Cd-106					5	KAERI
Cd-108					5	KAERI
Cd-110					5	KAERI
Cd-111					5	KAERI
Cd-112					5	KAERI
Cd-113					5	KAERI
Cd-114					5	KAERI
Cd-116					5	KAERI
Sn-112					5	KAERI
Sn-114	3				5	KAERI
Sn-115					5	KAERI
Sn-116	3				5	KAERI
Sn-117	3				5	KAERI
Sn-118	3				5	KAERI
Sn-119	3				5	KAERI
Sn-120	3				5	KAERI
Sn-122	3				5	KAERI
Sn-124	3				5	KAERI
Sb-121					5	KAERI
Sb-123					5	KAERI
Te-120	3				5	KAERI
Te-122	3				5	KAERI
Te-123					5	KAERI
Te-124	3				5	KAERI
Te-125					5	KAERI
Te-126	3				5	KAERI
Te-128	3				5	KAERI
Te-130	3				5	KAERI
I-127					5	KAERI
I-129					5	KAERI
Cs-133			3,5,201,203-207		5	KAERI
Cs-135					5	KAERI
Cs-137					5	KAERI
Pr-141	4				5	KAERI
Sm-144					5	KAERI
Sm-147					5	KAERI
Sm-148					5	KAERI
Sm-149					5	KAERI
Sm-150					5	KAERI
Sm-151					5	KAERI
Sm-152					5	KAERI
Sm-154					5	KAERI
Tb-158					5	KAERI
Tb-159					5	KAERI
Ho-165					5	KAERI
Ta-181	201		3,5,201,203-207	5		JENDL
W-180		3,4,16,17,22,28,103-107,111				CNDC
W-182	4	3,4,16,17,22,28,103-107	3,5,201,203-207			JENDL
W-183		3,4,16,17,22,28,103-107				CNDC
W-184	4	3,4,16,17,22,28,103-107	3,5,201,203-207	5		LANL
W-186	4,16	3,4,16,17,22,28,103-107	3,5,201,203-207			JENDL
Au-197			Planned		5	KAERI
Pb-206			3,5,201,203-207	5		LANL
Pb-207			3,5,201,203-207	5		LANL
Pb-208			3,5,201,203-207	5		LANL
Bi-209	4,10,16	3,4,16,17,22,28,50-64,	3,5,201,203-207		5	CNDC
Th-232	3,4,16,18					BOFOD
U-233	3,4,16,18					BOFOD
U-234	3,4,10,18					BOFOD
U-235	3,4,16,18		3,5,18,201,203-207			BOFOD
U-236	3,4,16,18					BOFOD
U-238	3,4,16,18		3,5,18,201,203-207			BOFOD
Pu-238	3,4,16,18					BOFOD
Pu-239	3,4,16,18					BOFOD
Pu-241	3,4,16,18					BOFOD
Selected	9	12	10	9	124	164

6.2 Contents of the Library

The library contains evaluated photonuclear data arranged in two categories. Under **recommended**, a user will find selected evaluations, judged to be the best available. Under **other_files**, one finds data files of all evaluations submitted to the IAEA by laboratories participating in the present project.

Recommended. Recommended evaluations are provided for a total of 164 isotopes. This reflects a complete wish list defined at the beginning of the project and discussed in Chapter 1.

Other_files. Included are photonuclear data libraries submitted to the IAEA by 6 laboratories participating in the present project. These libraries are BOFOD (part of files submitted), CNDC (all files submitted), EPNDL (all files submitted), JENDL (part of files submitted), KAERI (all files submitted) and LANL (all files submitted). The libraries differ substantially in terms of materials (isotopes and/or elements), data types (reaction channels), energy range of incident photons, and partly also evaluation methodology. Although each of these libraries provides data in the ENDF-6 format, there are differences in the structure and organization of files.

An actual overview can be obtained from README files in the FTP photonuclear site of the IAEA Nuclear Data Section. Table 6.2 shows the contents of the relevant directory, UD4:[PHOTONUCLEAR], of the DEC Alpha computer where the library is actually stored. This is followed by some more details on each of 6 libraries involved.

Table 6.2:   CONTENTS OF THE DIRECTORY UD4:[PHOTONUCLEAR]

Subdirectory	Contents
RECOMMENDED	IAEA library, 164 materials selected
	from libraries listed in OTHER_FILES
OTHER_FILES	Libraries submitted by 6 laboratories
OTHER_FILES.BOFOD	27+36+9 materials, including 9 selected
OTHER_FILES.CNDC	24 materials, including 12 selected
OTHER_FILES.EPNDL	26 materials
OTHER_FILES.JENDL	18 materials, including 10 selected
OTHER_FILES.KAERI	143 materials, including 124 selected
OTHER_FILES.LANL	12 materials, including 9 selected

1. BOFOD, Obninsk

- Number of materials: 27+36+9
    - 27 materials: ^{9}Be, ^{23}Na, ^{52}Cr, ^{55}Mn, ^{nat}Ni, ^{nat}Zr, ^{92,94,96,98,100}Mo, ^{182,184,186}W, ^{nat}Pb, ^{209}Bi, ^{232}Th, ^{233,234,235,236,238}U, ^{237}Np, ^{239,241}Pu, ^{241,243}Am
    - 36 materials: ^{50,52,54}Cr, ^{54,56,58}Fe, ^{56,58,60,62,64}Ni, ^{88}Sr, ^{90,91,92,94,96}Zr, ^{92,94,96,98,100}Mo, ^{114,116,117,118,119,120,122,124}Sn, ^{120,122,124,126,128,130}Te

54

- 9 materials: ^{232}Th, ^{233,234,235,236,238}U, ^{238,239,241}Pu

- Energy: Up to 20 MeV

- Data types: (γ, n) and partly (γ, f) for 27 materials; (γ, abs) for 36 materials; all for 9 materials

- Methodology: Model calculations and experimental data

- Available from IAEA: Part of files (Compare with a more recent list given in Sec. 5.3.1)

2. CNDC, Beijing

- Number of materials: 24
  ^{9}Be, ^{27}Al, ^{50,52,53,54}Cr, ^{63,65}Cu, ^{54,56,57,58}Fe, ^{51}V, ^{90,91,92,94,96}Zr, ^{180,182,183,184,186}W, ^{209}Bi

- Energy: Up to 30 MeV

- Data types: All

- Methodology: Model calculations adn experimental data

- Available from IAEA: All files

3. EPNDL, Moscow

- Number of materials: 26
  ^{2}H, ^{6,7}Li, ^{9}Be, ^{nat}C, ^{nat,16}O, ^{20,22}Ne, ^{nat}Al, ^{28}Si, ^{nat}Ca, ^{52}Cr, ^{54,56}Fe, ^{nat,58,60}Ni, ^{63,65}Cu, ^{nat}Zr, ^{141}Pr, ^{nat}Pb, ^{nat,235,236}U

- Energy: Giant dipole resonance range, up to 20-30 MeV

- Data types: Mostly (γ, abs), partly (γ, n), (γ, p), $(\gamma, 2n)$ and (γ, np)

- Methodology: Method of reduction of experimental data

- Available from IAEA: All files

4. JENDL, Tokai

- Number of materials: 50
  ^{2}H, ^{12}C, ^{14}N, ^{16}O, ^{23}Na, ^{24,25,26}Mg, ^{nat}Al, ^{28,29,30}Si, ^{40,48}Ca, ^{46,48}Ti, ^{51}V, ^{52}Cr, ^{55}Mn, ^{54,56}Fe, ^{59}Co, ^{58,60,61,62,64}Ni, ^{63,65}Cu, ^{64}Zn, ^{90}Zr, ^{93}Nb, ^{92,94,96,98,100}Mo, ^{137}Cs, ^{160}Gd, ^{181}Ta, ^{182,184,186}W, ^{197}Au, ^{206,207,208}Pb, ^{209}Bi, ^{235,238}U

- Energy: Up to 140 MeV

- Data types: All

- Methodology: Model calculations and experimental data

- Available from IAEA: Part of files

5. KAERI, Taejon

- Number of materials: 143
  For the list see Sec. 5.3.5.

- Energy: Up to 140 MeV

- Data types: All

- Methodology: Model calculations and experimental data

- Available from IAEA: All files

6. LANL, Los Alamos

- Number of materials: 12
  ^{12}C, ^{16}O, ^{27}Al, ^{28}Si, ^{40}Ca, ^{56}Fe, ^{63}Cu, ^{181}Ta, ^{206,207,208}Pb, ^{184}W

- Energy: Up to 150 MeV

- Data types: All

- Methodology: Model calculations and experimental data

- Available from IAEA: All files

6.3 ENDF-6 Format

The ENDF-6 format [96] developed by the US Cross-Section Evaluation Working Group (CSEWG), is the internationally recognized standard format to store evaluated nuclear reaction data for applications. The format itself is complicated and allows various solutions as to how to store specific data. Therefore, the adopted solution for photonuclear data, as described below, was accepted after a thorough discussion involving experts on nuclear data processing codes.

The ENDF-6 format uses a hierarchical organization of information. The most important terms and notations are explained in Table 6.3, in particular the material MAT, the file MF and section MT.

The format adopted to represent the photonuclear data is summarized in Table 6.4. It should be noted that majority of evaluations selected for the IAEA Photonuclear Data Library actually makes use of MT=5, where one puts all data of interest for transport (energy-angle distributions of emitted particles), as well as production cross-sections of radioactive nuclei, into inclusive reaction channels.

56

Table 6.3: BASIC TERMS AND NOTATIONS OF THE ENDF-6 FORMAT

Term	Notation	Explanation
Material	MAT	Reaction target, each material (isotope or composition of isotopes) is designed unique identification number
File	MF	Subdivision of material (MAT). Each file contains data for certain classes of information:

<div style="margin-left:2em">

MF = 1	General information
MF = 3	Reaction cross-sections
MF = 4	Angular distributions for emitted particles
MF = 5	Energy distributions for emitted particles
MF = 6	Energy-angle distributions for emitted particles
...	

</div>

Term	Notation	Explanation
Section	MT	Subdivision of file (MF). Each section describes particular reaction type:

<div style="margin-left:2em">

MT = 3	Total absorption or total reaction cross-section
MT = 4	Production of one neutron
MT = 5	Sum of all reactions not given explicitly in another MT number, excluding photofission(MT3=MT5+MT18). MT5 can be used to represent inclusive emission spectra, e.g. (n,xn), using MF3 (file3) for reaction cross-section and MF6 (file6) for yields and energy-angle distributions
MT = 16	Production of two neutrons
MT = 18	Fission
MF = 50	Production of neutron leaving residual nucleus in its ground state
MT = 51	Production of neutron leaving residual nucleus in the 1-st excited state
MT =103	Production of a proton
MT =104	Production of a deuteron
MT =105	Production of a triton
MT =106	Production of a 3-He
MT =107	Production of an alpha particle
MT =600	Production of proton leaving residual nucleus in its ground state
MT =601	Production of proton leaving residual nucleus in the 1-st excited state
MT =650	Production of deuteron leaving residual nucleus in the ground state
MT =700	Production of triton leaving residual nucleus in the ground state
...	

</div>

Table 6.4:   ADOPTED ENDF-6 FORMAT FOR PHOTONUCLEAR DATA

MF	MT	Explanation
1	451	Descriptive information and dictionary
1	452	Total number of neutrons per photofission
1	455	Number of delayed neutrons per photofission
1	456	Number of prompt neutrons per photofission
1	458	Energy released per photofission
3	1	Total photoabsorption cross-section
3	4	Total (g.1n) cross-section
3	5	Photoabsorption cross-section from which production c.s. for particles and isotopes are determined using yields in MF6-MT5
3	16	Total $(\gamma, 2n)$ cross-section
3	18	Total (γ, f) cross-section
3	103	Total (γ, p) cross-section
	...	
3	107	Total (γ, α) cross-section
4	18	Photofission
5	18	Prompt photoneutrons
5	455	Delayed photoneutrons
6	5	Yields (also known as branching ratios or multiplicities) and possibly also double-differential cross-sections for light particles $(n, p, d, ..., \gamma)$ and residual isotopes
6	16	DDX for $(\gamma, 2n)$
6	18	DDX for (γ, f)
6	103	Discrete and continuum levels
	...	
6	107	Discrete and continuum levels
6	600	Discrete and continuum levels
	...	
6	850	Discrete and continuum levels

6.4   Access to the Library

All nuclear data libraries stored at the IAEA Nuclear Data Section, including the IAEA Photonuclear Data Library, are available cost-free to users from all Member States of the International Atomic Energy Agency.

The IAEA Photonuclear Data Library, physically located at the DEC Alpha server operated by the IAEA Nuclear Data Section, can be conveniently accessed using the Web interface or by FTP. The address of the Web site reads

http://www-nds.iaea.or.at/photonuclear/

While for FTP (read-only) one should use

```
ftp iaeand.iaea.or.at
username: photonuclear                         59
```

with no password required. The Library, along with the present Handbook, is also available on a CD-ROM, cost-free upon request by e-mail to

```
services@iaeand.iaea.or.at.
```

The Handbook is furthermore available as a hardcopy, cost-free, upon request from the IAEA Nuclear Data Section (see address on the back of the cover page of the present document).

Chapter 7

Recommendations to Users and Evaluators

The participants of the present project have the following recommendations to users of the IAEA Photonuclear Data Library and to evaluators of photonuclear data:

1. The IAEA Photonuclear Data Library is recommended for use in applications involving simulations of neutron production, and other photon-induced nuclear reactions. In cases where more than one evaluation exists for a given material, we recommend that users also study the sensitivity of their results to the use of other evaluations, contained in the individual laboratory photonuclear libraries.

2. The IAEA Photonuclear Data Library described in this TECDOC allows researchers to assess the importance of photonuclear reactions in a variety of applications, including medical accelerators, shielding needs, accelerator-driven systems, safeguards inspection technologies, etc.

3. The evaluated photonuclear libraries described in this TECDOC have been produced through extensive recent research activities. While they have been generally tested against available cross-section data, additional validation work is desirable. In particular, we recommend that users perform radiation transport benchmark simulations of integral experiments, including neutron production around medical linacs, to further validate the evaluations. Any discrepancies that are found, when related to the evaluators, may lead to future improvements in the evaluations.

4. The 1984 Report of the U.S. National Council on Radiation Protection and Measurements, NCRP No. 79, "Neutron Contamination from Medical Electron Accelerators", has been the primary source of information used to characterize dose to operating personnel and patients, and shielding needs, at medical therapy linacs. The photonuclear data described here, together with radiation transport codes that use these data, provide some of the tools needed for an update of the NCRP report.

5. For many materials, a variety of laboratories have performed photonuclear evaluations, and these were intercompared against one another before a selection was made for the IAEA Photonuclear Data Library. We recommend that laboratories undertake new evaluations for cases where only one choice was available. For instance, there is a need for additional evaluations of actinide nuclides.

6. Additional experiments are needed to better understand photonuclear reaction physics. In particular, there still exist only a few measurements of the emission spectra of secondary particles from monochromatic photon-induced reactions. Furthermore, there remains a surprising lack of measurements of photonuclear reactions on iron, a key material in many applications.

References

[1] E. G. Fuller and H. Gerstenberg, "Photonuclear data - abstract sheets 1955-1982," Report of the US National Bureau of Standards, NBSIR 83-2742, vol. I-XV (1983-1986), National Institute for Standards and Technology, Gaithersburg, MD.

[2] B. L. Berman, "Atlas of photoneutron cross-sections obtained with monoenergetic photons," Atomic Data and Nucl. Data Tables **15**, 319 (1975).

[3] S. S. Dietrich and B. L. Berman, "Atlas of photoneutron cross-sections obtained with monoenergetic photons," Atomic Data and Nuclear Data Tables **38**, 199 (1988).

[4] J. F. Briesmeister, "MCNP–a general Monte Carlo n-particle transport code. version 4 B," Technical Report No. LA-12625-M (1997), Los Alamos National Laboratory, Los Alamos, NM.

[5] I. Gudowska, A. Brahme, P. Andreo, W. Gudowski, and J. Kierkegaard, "Calculation of absorbed dose and biological effectiveness from photonuclear reactions in a bremsstrahlung beam of end point 50 MeV," Phys. Med. Biol. **44**, 2099 (1999).

[6] M. B. Chadwick, P. G. Young, S. Chiba, S. Frankle, G. M. Hale, H. G. Hughes, A. J. Koning, R. C. Little, R. E. MacFarlane, R. E. Prael, and L. S. Waters, "Cross-section evaluations to 150 MeV for accelerator-driven systems and implementation in MCNPX," Nucl. Sci. Eng. **131**, 293 (1999).

[7] A. V. Varlamov, V. V. Varlamov, D. S. Rudenko, and M. E. Stepanov, "Atlas of giant dipole resonance paramaters and graphs of photonuclear reaction cross-sections, " Technical Report No. INDC (NDS)-394 (1999), International Atomic Energy Agency, Vienna.

[8] O. V. Bogdankevich and F. A. Nikolaev, *Methods in Bremsstrahlung Research* (Academic Press, New York, USA, 1966).

[9] E. Van Camp, R. Van der Vyver, E. Kerhove, J. Ryckbosch, H. Ferdinande, P. Van Otten, and P. Berkvens, "Experimental determination of the proton escape width in the giant-dipole resonance of ^{89}Y," Phys. Rev. C **24**, 2499 (1981).

[10] A. S. Penfold and J. Leiss, "Analysis of photonuclear cross-sections," Phys. Rev. **144**, 1332 (1959).

[11] E. Bramanis, T. K. Deaque, R. S. Hicks, R. J. Hunger, E. G. Muirhead, R. H. Sambell, and R. J. J. Stewart, "The analysis of photonuclear yield curves," Nucl. Instr. and Methods **100**, 59 (1972).

[12] A. N. Tikhonov, V. G. Shevchenko, V. Galkin, B. I. Goryachev, P. N. Zaikin, B. S. Ishkhanov, and I. M. Kapitonov, "About the determination of photonuclear reaction cross-sections," Vestnik Moskovskogo Universiteta. Fizika. and Astronomia **2**, 208 (1970).

[13] B. C. Cook, "Least structure solution of photonuclear yield functions," Nucl. Instrum. and Methods **24**, 256 (1963).

[14] K. N. Geller and E. G. Muirhead, Phys. Rev. Lett. **11**, 371 (1963).

[15] I. F. Turchin, V. P. Kozlov, and M. S. Malkevich, "The method of mathematical statistics using for the uncorrect ill-posed task solving," Uspekhi Fizicheskikh Nauk **102**, 345 (1970).

[16] C. Tzara, Compt. Rend. Acad. Sci. (Paris) **56**, 245 (1957).

[17] B. L. Berman and S. C. Fultz, Rev. Mod. Phys. **47**, 713 (1975).

[18] L. S. Cardman, "Photon tagging: present practice and future prospects," Technical Report No. P/83/12/168 (1983), University of Illinois, Urbana-Champaign, Illinois, USA.

[19] I. C. Nascimento, E. Wolynec, and D. S. Onley, Nucl. Phys. A **246**, 210 (1975).

[20] W. R. Dodge, R. G. Leicht, E. Hayward, and E. Wolynec, "Electrodisintegration of ^{56}Fe, ^{59}Co, and ^{64}Zn," Phys. Rev. C **24**, 1952 (1981).

[21] V. I. Antonescu, "IAEA bibliographical series, photonuclear reactions," Technical Report No. 10 (1964), International Atomic Energy Agency, Vienna.

[22] V. V. Varlamov and V. V. Sapunenko, "Photonuclear data index 1976 - 1995," Technical Report No. Izdatel'stvo Moskovskogo Universiteta (1996), Moscow State University, Moscow, Russia.

[23] T. Asami and T. Nakagawa, "Bibliographic index to photonuclear reaction data (1955 - 1992)," Technical Report No. JAERI-M-93-195, INDC(JPN)- 167L (1993), Japan Atomic Energy Research Institute, Ibaraki-ken, Japan.

[24] V. V. Varlamov et al., "Photonuclear data index 1976 - 1980," Technical Report No. Izdatel'stvo Moskovskogo Universiteta (1982), Moscow State University, Moscow, Russia.

[25] V. McLane, "Exfor systems manual, nuclear reaction data exchange format," Technical Report No. BNL-NCS-63330 (1996), Brookhaven National Laboratory, National Nuclear Data Center, Upton, NY.

[26] H. D. Lemmel, "The Nuclear Data Centres Network, IAEA Nuclear Data Section," Technical Report No. INDC(NDS)-359 (1997), International Atomic Energy Agency, Vienna.

[27] B. L. Berman, "Atlas of photoneutron cross-sections obtained with monoenergetic photons," Technical Report No. UCRL-78482 (1976), Lawrence Livermore National Laboratory, Livermore, CA.

[28] B. Forkman and R. Petersson, "Photonuclear reaction cross-sections. Handbook on nuclear activation data," Technical Report Series No. 273 (1987), International Atomic Energy Agency, Vienna.

[29] A. I. Blokhin and S. M. Nasyrova, "Plots of the experimental and evaluated photoneutron cross-sections," Technical Report No. INDC(CCP)-337 (1991), International Atomic Energy Agency, Vienna.

[30] A. Lepretre, H. Beil, R. Bergere, P. Carlos, J. Fagot, A. De Miniac, and A. Veyssiere, "Measurements of the total photonuclear cross-section from 30 mev to 140 MeV for Sn, Ce, Ta, Pb, and U nuclei," Nucl. Phys. A **367**, 237 (1981).

[31] M. B. Chadwick, P. Oblozinsky, P. E. Hodgson, and G. Reffo. "Pauli blocking in the quasideuteron model of photoabsorption," Phys. Rev. C **44**, 814 (1991).

[32] N. Kishida, "Methods used in photonuclear data evaluation at JNDC," in *Proc. of the Symposium on Nuclear Data Evaluation Methodology*. Brookhaven National Laboratory, Upton, NY, 12-16 Oct. 1992, edited by C. Dunford (World Scientific, Singapore, 1993), p. 598.

[33] M. B. Chadwick and P. G. Young, "Preequilibrium model for photonuclear reactions up to the pion threshold," Acta Physica Slovaca **45**, 633 (1995).

[34] A. Fasso, A. Ferrari, and P. R. Sala, "Designing electron accelerator shielding with FLUKA," in *Proc. of 8th. International Conference on Radiation Shielding*, Arlington, Texas, April 24-28, 1994 (American Nuclear Society, La Grange Park, IL, 1994), pp. 643-649.

[35] Y.-O. Lee, T. Fukahori, and J. Chang, "Evaluation of photonuclear reaction data on tantalum-181 up to 140 MeV," Journal of Nuclear Science and Technology **35**, 685 (1998).

[36] A. Fasso, A. Ferrari, and P. R. Sala, "Total giant resonance photonuclear cross-sections for light-nuclei: A database for the FLUKA monte carlo transport code," in *Proc. of Third Specialists Meeting on Shielding Aspects of Accelerators, Targets, and Irradiation Facilities (SATIF-3)*, Tohoku University, Sendai, Japan, 12-13 May 1997 (Organization for Economic Cooperation and Development (OECD) Nuclear Energy Agency, Paris, France, 1998), pp. 61-74.

[37] J. R. Wu and C. C. Chang, "Pre-equilibrium particle decay in photonuclear reactions," Phys. Rev. C **16**, 1812 (1977).

[38] M. Blann, B. L. Berman, and T. T. Komoto, "Precompound-model analysis of photonuclear reaction," Phys. Rev. C **28**, 2286 (1983).

[39] T. A. Gabriel, "Intermediate-energy (40 MeV $\leq E_\gamma \leq$ 400 MeV) photonuclear interactions," Phys. Rev. C **13**, 240 (1976).

[40] N. V. Mokhov, S. I. Striganov, A. Van Ginneken, S. G. Mashnik, A. J. Sierk, and J. Ranft, "MARS code developments," in *Proc. of Fourth Specialists Meeting on Shielding Aspects of Accelerators, Targets, and Irradiation Facilities (SATIF-4) (LANL report LA-UR-5716 (1998))*, Knoxville, Tennessee, September 14-16 1998 (Organization for Economic Cooperation and Development (OECD) Nuclear Energy Agency, Paris, France, 1998).

[41] H. Feshbach, A. Kerman, and S. Koonin, "The statistical theory of multi-step compound and direct reactions," Ann. Phys. (N.Y.) **125**, 429 (1980).

[42] P. G. Young, E. D. Arthur, and M. B. Chadwick, "Comprehensive nuclear model calculations: Introduction to the theory and use of the GNASH code," Technical Report No. LA-12343-MS (1992), Los Alamos National Laboratory, Los Alamos, NM.

[43] M. B. Chadwick, P. G. Young, D. C. George, and Y. Watanabe, "Multiple pree-quilibrium emission in Feshbach-Kerman-Koonin analyses," Phys. Rev. C **50**, 996 (1994).

[44] D. Ryckbosch, L. Vanhoorebeke, R. Vandevyver, F. Desmet, J. O. Adler, D. Nilsson, B. Schroder, and R. Zorro, "Determination of the absorption mechanism in photon-induced preequilibrium reactions," Phys. Rev. C **42**, 444 (1990).

[45] International Atomic Energy Agency, *Handbook for Calculations of Nuclear Reaction Data: Reference Input Parameter Library*, IAEA-TECDOC-1034, Vienna, (1998).

[46] J. C. McGeorge *et al.*, "The $^{12}C(\gamma,p)$ reaction at E_γ=60 and E_γ=80 MeV," Phys. Lett. B **179**, 212 (1986).

[47] M. B. Chadwick, P. G. Young, R. E. MacFarlane, M. C. White, and R. C. Little, "Photonuclear physics in radiation transport: I. Cross-sections and spectra photonuclear cross-section evaluations to 150 MeV," Nucl. Sci. Eng. (2000, submitted).

[48] M. B. Chadwick, P. G. Young, and S. Chiba, "Photonuclear angular distribution systematics in the quasideuteron regime," Journal of Nuclear Science and Technology **32**, 1154 (1995).

[49] A. Lepretre, H. Beil, R. Bergere, P. Carlos, J. Fagot, A. Veyssiere, and I. Halpern, "Analysis of neutron multiplicities in photo-nuclear reactions from 30 to 140 MeV in heavy-elements," Nucl. Phys. A **390**, 221 (1982).

[50] C. Kalbach, "Systematics of continuum angular distributions: Extensions to higher energies," Phys. Rev. C **37**, 2350 (1988).

[51] M. B. Chadwick and P. Oblozinsky, "Continuum angular distributions in preequilibrium nuclear reactions: Physical basis for Kalbach systematics," Phys. Rev. C **50**, 2490 (1994).

[52] A. Bohr, "On the theory of nuclear fission," in *Proc. 1st UN Int. Conf. Peaceful Uses of Atomic Energy*, Geneva, 1955 (United Nations, New York. 1956), Vol. I, p. 151.

[53] V. M. Strutinsky, "Shell effects in nuclear masses and deformation energies," Nuclear Physics **A95**, 420 (1967).

[54] V. Weisskopf, Physical Review **52**, 295 (1937).

[55] P. Axel, "Electric dipole ground state transition width strength function and 7 MeV photon interaction," Physical Review **126**, 671 (1962).

[56] *The Nuclear Fission Process*, edited by C. Wagemans (CRC Press, 1991).

[57] A. Storozhenko, A. Blokhin, A. Ignatyuk, and A. Soldatov, "Theoretical investigation of subbarrier photofission of ^{232}Th," in *Proc. 5th Int. Seminar on Neutron-Nucleus Interactions (ISINN-5). Neutron Spectroscopy, Nuclear Structure and Related Topics*, Dubna, 1996 (JINR, Dubna, 1997), p. 337.

[58] A. Veyssiere, H. Bell, R. Bergere, P. Carlos, A. Leprete, and K. Kernbath, "A study of photofission and photoneutron processes in the giant dipole resonance of Th-232, U-238 and Np-237," Nuclear Physics **A199**, 45 (1973).

[59] B. L. Berman, J. T. Caldwell, E. J. Dowdy, S. S. Dietrich, P. Meyer, and R. A. Alvarez, "Photofission and photoneutron cross-sections and photofission neutron multiplicities for U-233, U-234, Np-237 and Pu-249," Physical Review **34(6)**, 2201 (1986).

[60] J. Caldwell, E. Dowdy, R. Alvarez, B. Berman, and P. Meyer, "Experimental determination of photofission neutron multiplicities for U-235, U-236, U-238 and Th-232 using monoenergetic photons," Nuclear Science and Engineering **73**, 153 (1980).

[61] D. G. Madland and J. R. Nix, "New calculation of prompt fission neutron-spectra and average prompt neutron multiplicities," Nucl. Sci. and Eng. **81**, 213 (1982).

[62] E. K. Hyde, "The nuclear properties of the heavy elements. vol. III," *The nuclear properties of the heavy elements. Vol. III* (Prentice-Hall, Englewood Cliffs, NJ, 1964).

[63] M. Y. Kondratenko and J. Petrzhak, Atomnaya Energiya **23(6)**, 559 (1967).

[64] E. Jacobs, A. De Clercq, and H. Thierens, "Fragment mass and kinetic energy distributions for the photofission of U-238 with 12-,15-,20-,30-, and 70-Mev bremsstrahlung," Phys. Rev. C **20**, 2249 (1979).

[65] P. G. Young, E. D. Arthur, and M. B. Chadwick, "Comprehensive nuclear model calculations: Theory and use of the GNASH code," in *Proc. of the IAEA Workshop on Nuclear Reaction Data and Nuclear Reactors - Physics, Design, and Safety*, Trieste, Italy, April 15 - May 17, 1996, edited by A. Gandini and G. Reffo (World Scientific Publishing, Ltd., Singapore, 1998), pp. 227–404.

[66] T. Fukahori, "ALICE-F calculation of nuclear data up to 1 GeV," in *Proc. of the Specialists' Meeting on High Energy Nuclear Data*, 3-4 October 1991, JAERI, Tokai, Japan (JAERI, Tokai, Ibaraki-ken, Japan, 1992), No. JAERI-M 92-039, p. 114.

[67] M. Blann, "A priori pre-equilibrium decay models," Nucl. Phys. A **213**, 570 (1973).

[68] N. Kishida and H. Kadotani, "On the validity of the intranuclear-cascade and evaporation model for high energy proton induced reactions," in *Proc. of the International Conference on Nuclear Data for Science and Technology*, Mito, Japan, May 30 - June 3, 1988, edited by S. Igarasi (Saikon Publishing Co. Ltd, Tokyo, 1988), p. 1209.

[69] K. K. Gudima, G. A. Osokov, and V. D. Toneev, "Model for pre-equilibrium decay of excited nuclei," Sov. J. Nucl. Phys. **21**, 138 (1975).

[70] J. Zhang, "Illustration on photonuclear data calculation with GUNF code," Communication of Nuclear Data Progress **19**, 33 (1998).

[71] J. Zhang, Y. Han, and L. Cao, "Summary of monoenergetic neutron beam sources for energies >14 MeV," Nucl. Sci. Eng. **133**, 1 (1999).

[72] A. Blokhin, "The XGFISS code for analysis of photonuclear cross-sections for actinide nuclei," Yadernye Konstanty **2**, in press (1999).

[73] H. Uberall, *Electron Scattering from Complex Nuclei, Part B* (Academic Press, New York, USA, 1971).

[74] J. M. Eisenberg and W. Greiner, *Excitation Mechanisms of the Nucleus* (North-Holland Publ. Co., Amsterdam, Netherlands, 1970).

[75] W. C. Barber, Ann. Rev. Nucl. Sci. **12**, 1 (1962).

[76] V. V. Varlamov, N. G. Efimkin, N. A. Lenskaja, and A. P. Chernjaev, "Investigation of the reasons for discrepancies in results of photonuclear experiments at the beams of bremsstrahlung and quasimonoenergetic gamma-quanta, the problem of interpretation," Technical Report No. MSU INP Preprint-89-66/14 (1989), Moscow State University, Moscow, Russia .

[77] E. G. Fuller, "Photonuclear reaction cross-sections for C-12, N-14 and O-16," Physics Reports **127**, 187 (1985).

[78] N. G. Efimkin and V. V. Varlamov, "The method of reduction as photonuclear data evaluation tool," in *Proc. of the Symposium on Nuclear Data Evaluation Methodology*, Brookhaven National Laboratory, Upton, NY, 12-16 Oct. 1992, edited by C. Dunford (World Scientific, Singapore, 1993), p. 585.

[79] V. V. Varlamov, N. G. Efimkin, B. S. Ishkhanov, and V. V. Sapunenko, Voprosy Atomnoi Nauki i Tekhniki. Seriya: Yadernye Konstanty **1**, 52 (1993).

[80] L. M. Young, PhD. thesis, University of Illinois, 1972.

[81] Y. P. Pyt'ev, Matematichesky Sbornik **118**, 19 (1982).

[82] Y. P. Pyt'ev, Vestnik Moskovskogo Universiteta. Fizika, and Astronomia **25**, 53 (1984).

[83] V. V. Varlamov, N. G. Efimkin, and B. S. Ishkhanov, "Simultaneous analysis of discrepant photonuclear data," in *Proc. of the International Conference on Nuclear Data for Science and Technology*, Gatlinburg, TN, 1994, edited by J. Dickens (American Nuclear Society, La Grange Park, IL, 1994), p. 662.

[84] A. Blokhin, N. Buleeva, S. Nasyrova, O. Pakhomova, S. Zabrodskaya, and A. Tsibulya, "Formation and application of evaluated photoneutron data libray BOFOD," Yadernye Konstanty **3**, 3 (1992).

[85] N. Kishida, Private Communication to T. Fukahori, 1988.

[86] Y. Lee, Y. Han, and J. Chang, "Evaluation of photonuclear data of Mo, Zn, S and Cl for medical and accelerator applications," in *Proc. of 9th International Conference on Radiation Shielding*, Tsukuba, Japan, Oct. 17-22, 1999.

[87] Y. Lee, Y. Han, J. Lee, and J. Chang, "Evaluated photonuclear data library in kaeri," in *Proc. of the Korean Nuclear Society Autumn Meeting*, Seoul, Korea, Oct. 29-30, 1999.

[88] A. Blokhin, Photonuclear Data Library BOFOD, private communication, October 1999.

[89] B. Yu, J. Zhang, and Y. Han, "Chinese evaluated photonuclear data file," Communication of Nuclear Data Progress **22**, 114 (1999).

[90] V. V. Varlamov, Photonuclear Data Library EPNDL, private communication, October 1999.

[91] Y.-O. Lee, Photonuclear Data File (PDF) of the JENDL Library, private communication, October 1999.

[92] Y.-O. Lee, Photonuclear Data Library KAERI, private communication, October 1999.

[93] V. McLane, CSISRS experimental nuclear data file, National Nuclear Data Center (NNDC), 1997, Brookhaven National Laboratory: WWW address: http://www.nndc.bnl.gov/.

[94] R. E. MacFarlane and D. W. Muir, "The NJOY nuclear data processing system, version 91," Technical Report No. LA-12740-M (1994), Los Alamos National Laboratory, Los Alamos, NM.

[95] H. G. Hughes, K. J. Adams, M. B. Chadwick, J. C. Comly, H. W. Egdorf, S. C. Frankle, J. S. Hendricks, R. C. Little, R. E. MacFarlane, S. G. Mashnki, R. E. Prael, A. J. Sierk, L. S. Waters, M. C. White, P. G. Young, F. X. Gallmeier, and E. C. Snow, "MCNPX for neutron-proton transport," in *Proc. of the Mathematics and Computation, Reactor Physics and Environmental Analysis in Nuclear Applications*, Madrid, Spain, September 27-30, 1999, edited by J. M. Aragones (Senda Editorial, S. A., Madrid, Spain, 1999), p. 939.

[96] V. McLane, "ENDF-102 data formats and procedures for the evaluated nuclear data file ENDF-6," Technical Report No. BNL-NCS-44945, Rev. 2/97, Brookhaven National Laboratory, National Nuclear Data Center, Upton, NY.

Appendix A

Atlas of Giant Dipole Resonances

Parameters of Photonuclear Reaction Cross Sections

As a part of the present project, an Atlas of Giant Dipole Resonances was produced by the Moscow group [A.1]. The Atlas consists of two parts:

- **Table** of parameters of giant dipole resonances observed in photonuclear reaction cross sections, and

- **Graphs** of photonuclear reaction cross sections from the international nuclear data library EXFOR.

For the user convenience, the Table is reproduced in the present Appendix. A reader interested in the Graphs is referred to the Web site of the CDFE, Moscow State University, $http : //depni.npi.msu.su/cdfe/$.

The Table is an updated (corrected and extended) version of the table *Parameters of the Giant Dipole Resonance* published in [A.2]. It includes parameters of the GDR observed in photonuclear reactions measured by bremsstrahlung, quasimonoenergetic, and tagged photons. These parameters were obtained directly, without any specific fitting procedure, from the cross sections for various photonuclear reactions, such as photoabsorption, neutron yield, total neutron production, single, double and triple neutron production, charged particle emission (proton, deuteron, triton, ^{3}He, alpha), and fission.

Table entries are organized by element, isotope, and reaction ordered by product from neutron to alpha. The Table contains information on the GDR parameters derived from the data for 82 elements (220 isotopes and natural compositions) with atomic numbers from 1 to 95. The entries for almost all the 600 photoneutron cross sections obtained with quasimonoenergetic photons [A.3] are also included. There are altogether 1317 entries.

Numerical data presented for the reaction cross section (peak energy and peak cross section, see notation table below) were obtained either directly from the relevant subentry (data set) of the EXFOR library, or estimated (together with the data for the peak width) using the graphs presented in the original papers (see reference and first author given in the table), or in the Photonuclear Data Abstract Sheets [A.4].

Numerical data for the integrated cross section and its first moment were obtained either by reading from the original papers (when available), or by deducing from the

max

max
(2nd line)

$\dfrac{\text{max}}{2}$

FWHM

E$_{max}$ E$_{max}$ E
(2nd line)
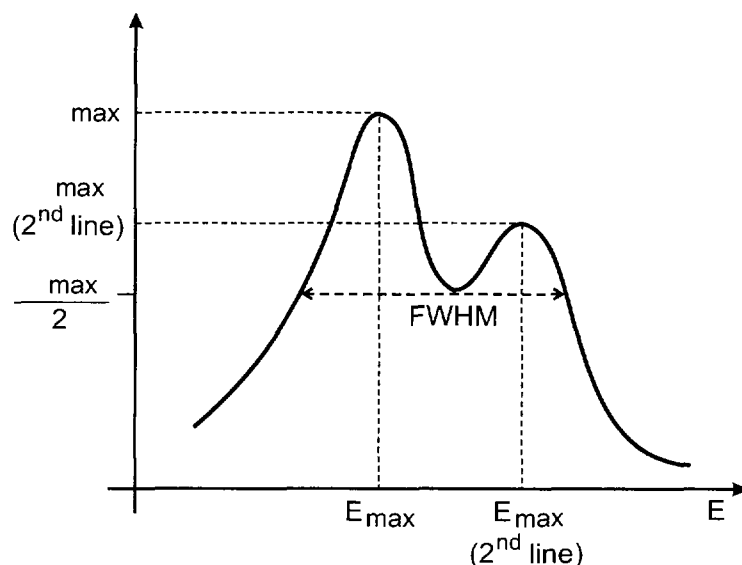
Figure Appendix A.1: *Schematical explanation of GDR parameters, describing experimental photonuclear reaction cross sections. Parameters were obtained directly from experimental curves, no fitting to Lorentzian shape was performed. Shown is the case with 2 peaks (peak energy and peak cross section of the second peak will appear at the 2nd line of an entry in the table). This case also illustrates that the FWHM may be larger than the width of any of two Lorentzians that would describe the curve. In cases where the experimental curve refers to a reaction channel with high threshold or where the curve is truncated by lack of high energy data, the FWHM may be smaller than the width of the Lorentzian curve.*

EXFOR data sets, or by reading from the appropriate Table in Ref. [A.2]. Data sources were the international nuclear data library EXFOR containing experimental cross sections described in Sec. 3.2.2. and the photonuclear data collections 1976-1995 [A.2] and 1955-1982 [A.4].

Besides the usual notation for reactions and reaction products described in Chapter 2, the following notation is used in the Table (see explanatory figure).

EXFOR	EXFOR 8-digit entry&subentry number
Nucl	Target nucleus (symbol)
A	Target nucleus (mass number)
Reac	Reaction
E$_{max}$	Energy at cross section maximum (peak energy) in MeV
σ_{max}	Peak cross section in mb
FWHM	Full width at half maximum in MeV
E$_{int}$	Upper limit of integration in MeV
σ_{int}	Integrated cross section in MeV * mb
σ_{int}^1	First moment of the integrated cross section in mb
Reference	Original paper
Author	Name of the first author

If the cross section presents more than one peak, then the E$_{max}$ column will have more than one line for the same entry.

70

EXFOR	Nucl	A	Reac	E_{max} MeV	σ_{max} mb	FWHM MeV	E_{int} MeV	σ_{int} MeV * mb	σ_{int}^{l} mb	Reference	Author
	1-H	2	γ,abs	4.48	2.5	18.1	30.00	29.	3.6	Ann.Phys.27.79(1964)	E.G.FULLER
							140.00	40.	3.7		
L0052004	1-H	3	γ,xn	17.211	2.66	>15.	23.40	32.3		Phys.Rev.C24,849(1981)	D.D.FAUL
	1-H	3	γ,sn	17.21	1.7		23.40	22.	1.48	Phys.Rev.C24,849(1981)	D.D.FAUL
L0052002	1-H	3	γ,n	12.555	.96	>15.	23.40	11.7		Phys.Rev.C24,849(1981)	D.D.FAUL
L0052002				17.211	.9						
L0052002				21.373	.89						
L0052003	1-H	3	$\gamma,2n$	16.43	.95	17.	23.40	10.2		Phys.Rev.C24,849(1981)	D.D.FAUL
L0052003				21.934	.8						
M0472002	1-H	3	γ,d	15.5	.78	13.	36.00	9.5	.4	Phys.Rev.C24,1791(1981)	D.M.SKOPIK
	1-H	3	γ,d	12.	.72	12.	33.00	12.	.78	Z.Physik,208,129(1968)	R.PFEIFER
L0052005	2-He	3	γ,xn	18.182	1.12	14.	25.80	14.1		Phys.Rev.C24,849(1981)	D.D.FAUL
	2-He	3	γ,xn	14.09	.97	14.	30.20	13.		Phys.Rev.C10,2221(1974)	B.L.BERMAN
L0052005	2-He	3	γ,sn	18.182	1.12	14.	25.80	14.1	.83	Phys.Rev.C24,849(1981)	D.D.FAUL
	2-He	3	γ,sn	14.09	.97	14.	30.20	13.	.77	Phys.Rev.C10,2221(1974)	B.L.BERMAN
L0052005	2-He	3	γ,n	18.182	1.12	14.	23.40	12.3		Phys.Rev.C24,849(1981)	D.D.FAUL
	2-He	3	γ,n	14.09	.97	14.	30.20	13.		Phys.Rev.C10,2221(1974)	B.L.BERMAN
L0018002	2-He	3	γ,n	14.092	.966	13.	30.00	13.	.77	Phys.Rev.L.24,1494(1970)	B.L.BERMAN
	2-He	3	γ,n	16.5	.96	15.	28.00	12.1	.68	Phys.Rev.144,B834(1966)	H.M.GERSTENBERG
M0479005	2-He	3	γ,np	17.	1.2	17.	120.00	43.6	1.42	Phys.Lett.11.137(1964)	A.N.GORBUNOV
	2-He	3	$\gamma,n2p$	19.5	.85	13.	30.00	13.4	.7	Nuov.Cim.A103,721(1990)	P.BELLI
							60.00	20.4	.9		
							100.00	23.8	1.		
							140.00	25.4	1.		
							170.00	26.1	1.		
M0479002	2-He	3	γ,p	11.	1.07	15.	117.00	26.1	1.3	Phys.Lett.11,137(1964)	A.N.GORBUNOV
	2-He	3	γ,d	12.	1.05	19.				Phys.Lett.46B,369(1973)	G.TICCIONI
	2-He	3	γ,d	12.5	1.06	18.	40.00	16.5	1.07	Phys.Rev.138,B372(1965)	J.R.STEWART
	2-He	3	γ,d	12.0	1.0	19.	170.00	26.5		ZHETF,47.30(1964)	A.T.VARFOLOMEEV
	2-He	3	γ,pd	10.5	.8	15.	30.00	12.4	.9	Nuov.Cim.A103,721(1990)	P.BELLI
							60.00	16.7			
							100.00	18.8			
							140.00	19.9			
							170.00	20.5			
M0040002	2-He	4	γ,abs	22.7	3.42	>20.	143.00	102.	2.9	Yad.Fiz.31.1400(1980)	YU.M.ARKATOV
M0019002	2-He	4	γ,abs	26.2	3.45	>20.	143.00	100.	2.5	Yad.Konst.4,55(1979)	YU.M.ARKATOV
	2-He	4	γ,xn	33.31	1.2	20.	47.30	23.5		Phys.Rev.C22,2273(1980)	B.L.BERMAN
L0023002	2-He	4	γ,xn	24.553	1.034	8.	31.40	7.9		Phys.Rev.C4,723(1971)	B.L.BERMAN
L0023002				27.443	1.021						
	2-He	4	γ,sn	33.31	1.2	20.	47.30	23.5	.73	Phys.Rev.C22,2273(1980)	B.L.BERMAN
L0023002	2-He	4	γ,sn	24.553	1.034	8.	31.40	7.9	.3	Phys.Rev.C4,723(1971)	B.L.BERMAN
L0023002				27.443	1.021						
L0051002	2-He	4	γ,n	33.311	1.2	20.	47.30	23.1		Phys.Rev.C22,2273(1980)	B.L.BERMAN
L0051002				24.302	1.09						
	2-He	4	γ,n	28.	1.45	16.				Nuov.Cim.38A,145(1977)	F.BALESTRA
L0023002	2-He	4	γ,n	24.553	1.034	8.	31.40	7.9		Phys.Rev.C4,723(1971)	B.L.BERMAN
L0023002				27.443	1.09						
M0489002	2-He	4	γ,n	24.5	1.96	14.	170.00	42.	1.1	Phys.Lett.27B.436(1968)	A.N.GORBUNOV
	2-He	4	γ,p	25.	1.7	15.				Nuov.Cim.38A,145(1977)	F.BALESTRA
M0489003	2-He	4	γ,p	26.5	1.86	14.	170.00	40.	1.1	Phys.Lett.27B.436(1968)	A.N.GORBUNOV
M0012002	2-He	4	γ,p	26.5	1.66	>15.	115.00	41.	1.2	Ukr.Fiz.Zh.23.1818(1978)	YU.M.ARKATOV
M0011002	2-He	4	γ,d	32.	.00511	>10.	65.00	.07	.002	Ukr.Fiz.Zh.23.919(1978)	YU.M.ARKATOV
M0034005	2-He	4	γ,d	32.2	.0052	>10.	65.00	.07	.002	Yad.Fiz.31.297(1980)	YU.M.ARKATOV
M0140016	3-Li	6	γ,abs	23.5	4.58	11.5	50.00	68.	3.4	CDFE/Li2.86	V.V.VARLAMOV
M0140016				1.5	1.71						
M0140016				41.	1.11						
L0008002	3-Li	6	γ,xn	11.63	1.681	13.	32.00	28.2		Phys.Rev.L.15,727(1965)	B.L.BERMAN
L0008002				30.21	1.043						
M0107002	3-Li	6	γ,xn	13.5	1.79	23.	60.00	53.	2.7	Nucl.Phys.68.191(1965)	E.B.BAZHANOV
M0107002				29.8	1.6						
M0107002				38.6	1.2						
M0235002	3-Li	6	γ,xn	16.27	1.79	>13.	20.00	17.7	1.5	Nucl.Phys.A430.214(1984)	N.DYTLEWSKI
M0235002				11.81	1.72						
M0251002	3-Li	6	γ,xn	16.26	2.3	>15.	29.00	36.1	2.4	Nucl.Phys.69.241(1969)	E.HAYWARD
M0251002				13.52	2.17						
M0251002				26.53	4.1						
	3-Li	6	γ,sn	14.	2.6		96.00	130.	3.8	Nuov.Cim.42B,382(1966)	S.COSTA
				11.	2.25						
M0140002	3-Li	6	γ,xn	11.5	1.71	37.	50.00	5.3	2.7	CDFE/Li2.86	V.V.VARLAMOV
M0140002				15.5	1.71						
M0140002				27.5	1.55						
M0140002				39.	1.12						
L0008005	3-Li	6	γ,sn	11.63	1.681	11.	32.00	27.8	1.91	Phys.Rev.L.15,727(1965)	B.L.BERMAN
L0008005				16.21	1.48						
L0008005				30.21	.98						
L0008003	3-Li	6	γ,n	11.63	1.681	11.	32.00	27.4		Phys.Rev.L.15,727(1965)	B.L.BERMAN
L0008003				16.21	1.48						
L0008003				30.22	.917						
	3-Li	6	γ,n	12.	.6	10.	20.00	3.2		Nucl.Phys.68.191(1965)	E.B.BAZHANOV
M0252002	3-Li	6	γ,n	14.	2.55		96.00	130.	3.8	Nuov.Cim.B42,382(1966)	S.COSTA
M0140008	3-Li	6	γ,np	8.	.4	12.	35.00	4.3	.4	CDFE/Li2.86	V.V.VARLAMOV
M0140008				17.5	.26						
M0104003	3-Li	6	γ,p	6.73	33.14	2.	11.00	32.2	4.6	Izv.AN SSSR,28,60(1964)	A.KH.SHARDANOV
M0140009	3-Li	6	γ,pd	23.5	2.57	1.5	50.00	9.6	.3	CDFE/Li2.86	V.V.VARLAMOV
L0008004	3-Li	6	$\gamma,2n$	31.12	.136	>4.	32.00	.4		Phys.Rev.L.15,727(1965)	B.L.BERMAN
L0008004				27.43	.087						
L0008004				29.72	.093						
M0107008	3-Li	6	γ,t	19.9	7.8	4.	24.00	28.3	1.3	Nucl.Phys.68.191(1965)	E.B.BAZHANOV
M0107008				21.9	7.7						
M0140013	3-Li	6	γ,t	20.	1.21	7.5	50.00	11.6	.5	CDFE/Li2.86	V.V.VARLAMOV
M0230002	3-Li	7	γ,abs	22.	3.1	>25.	217.00	187.5	4.4	Phys.Lett.B52,43(1974)	J.AHRENS
M0372002	3-Li	7	γ,abs	18.8	4.	25.	100.00	143.	4.64	Nucl.Phys.A251,479(1975)	J.AHRENS
M0372002							140.00	161.	4.79		
M0372002							210.00	206.	5.03		
M0214002	3-Li	7	γ,xn	19.5	3.21	>20.	56.00	101.	3.9	Phys.Rev.118,535(1960)	R.W.FAST
M0214002				47.5	2.13						
M0211003	3-Li	7	γ,xn	16.8	2.3	9.3	23.60	18.	1.3	Phys.Rev.110,1123(1958)	T.W.RYBKA
M0276002	3-Li	7	γ,xn	16.9	2.64	>10.	19.50	16.	1.	Nucl.Phys.A458.387(1986)	S.A.SIDDIQUI

EXFOR	Nucl	A	Reac	E_{max} MeV	σ_{max} mb	FWHM MeV	E_{int} MeV	σ_{int} MeV * mb	σ^1_{int} mb	Reference	Author
L0030002	3-Li	7	γ,xn	18.42	2.338	10.	30.50	30.2		Phys.Rev.129,2723(1963)	R.L.BRAMBLETT
M0251004	3-Li	7	γ,xn	22.75	4.06	13.	30.00	50.	2.6	Nucl.Phys.69,241(1965)	E.HAYWARD
M0251004				17.5	3.72						
M0109002	3-Li	7	γ,xn	35.	4.87	35.	50.00	85.	3.4	Dokl.AN.SSSR,171,549(1966)	E.B.BAZHANOV
M0109002				22.	3.39						
M0109002				24.	4.42						
M0109002				41.	2.79						
M0140017	3-Li	7	γ,xn	17.	3.29	25	50.00	87.8	3.7	CDFE/Li2,86	V.V.VARLAMOV
M0140017				22.5	2.81						
M0140017				30.5	2.55						
M0140017				35.	2.48						
L0030005	3-Li	7	γ,sn	14.75	1.565	13.	30.50	20.1	1.15	73PACIFI,1,175,73,P.175	R.L.BRAMBLETT
L0030003	3-Li	7	γ,sn	14.75	.932	8.	30.50	10.		73PACIFI,1,175,73	R.L.BRAMBLETT
L0030004	3-Li	7	$\gamma,2n$	19.06	.88	12.	30.50	10.1		73PACIFI,1,175,73	R.L.BRAMBLETT
M0247003	3-Li	7	γ,p	18.	1.35	20.	30.50	14.6	.8	Nucl.Phys.32,543(1962)	A.G.GREGORY
M0247003				27.	1.11						
M0102003	3-Li	7	γ,p	18.2	1.51	20.	30.00	13.9	.8	Izv.AN SSSR,27,1412(1963)	KUL'CHITSKIY
M0102003				14.1	1.27						
M0102003				16.2	1.51						
M0102003				21.7	1.52						
M0102003				25.2	.71						
M0113002	3-Li	7	γ,pt	24.5	.47	6.	27.00	1.	.03	Yad.Fiz.18,245(1973)	E.A.KOTIKOV
M0101007	3-Li	7	γ,t	19.4	.681	20.	25.80	7.5	.4	ZHETF,44,1153(1963)	KUL'CHITSKIY
M0102004	3-Li	7	γ,t	22.3	.771	20.	26.50	8.2	.4	Izv.AN SSSR,27,1412(1963)	KUL'CHITSKIY
M0102004				19.6	.718						
	3-Li	7	γ,t	17.	.2	20.	35.00	4.9		Nucl.Phys.69,241(1965)	E.HAYWARD
M0372003	4-Be	9	γ,abs	24.5	5.43	30.	100.00	173.	5.19	Nucl.Phys.A251,479(1975)	J.AHRENS
M0372003							140.00	189.	5.33		
M0372003							210.00	236.	5.58		
M0230003	4-Be	9	γ,abs	27.	5.19	30.	217.00	261.1	5.9	Phys.Lett.B52,43(1974)	J.AHRENS
M0451002	4-Be	9	γ,abs	20.5	9.	>20.	26.50	54.3	2.5	Nucl.Phys.31,570(1962)	U.MIKLAVZIC
M0451002				21.7	8.						
M0451002				25.5	8.5						
L0040004	4-Be	9	γ,xn	28.241	5.44	>20.	37.00	83.7		Nucl.Phys.A247,91(1975)	U.KNEISSL
	4-Be	9	γ,xn	26.	4.7	26.	70.00	220.	7.8	Nuov.Cim.42B,306,(1966)	S.COSTA
	4-Be	9	γ,sn	28.24	3.67	>15.	37.00	58.1	2.52	Nucl.Phys.A247,91(1975)	U.KNEISSL
L0040002	4-Be	9	γ,n	21.207	2.96	8.	37.00	32.5		Nucl.Phys.A247,91(1975)	U.KNEISSL
L0040003	4-Be	9	$\gamma,2n$	36.495	2.38	>12.	37.00	25.6		Nucl.Phys.A247,91(1975)	U.KNEISSL
L0040003				27.503	2.26						
M0440002	4-Be	9	γ,p	21.	1.79	8.	31.00	15.6	.67	Nucl.Phys.65,662(1964)	A.P.KOMAR
L0044004	5-B	10	γ,xn	22.001	5.73	19.	35.00	83.1		Nucl.Phys.A264.30(1976)	U.KNEISSL
M0498002	5-B	10	γ,xn	22.9	6.75	10.	27.10	51.5	2.7	Nucl.Phys.A215,147(1973)	R.J.HUGHES
M0498002				20.2	5.6						
	5-B	10	γ,xn	24.	6.5	10.5	29.00	67.		Nucl.Phys.69,241(1965)	E.HAYWARD
L0010002	6-C	12	γ,sn	22.179	6.8	6.	37.40	46.8	1.83	Phys.Rev.143.790(1966)	S.C.FULTZ
L0010002				25.353	4.2						
L0041002	6-C	12	γ,n	23.367	8.73	6.	32.10	51.6	2.08	Nucl.Instr.Meth.127,1(1975)	U.KNEISSL
L0041002				25.472	5.48						
L0041002				30.069	3.56						
L0038002	6-C	12	γ,n	22.24	8.14	6.	27.00	36.	1.47	Phys.Rev.141,1002(1966)	W.A.LOCHSTET
L0038002				23.07	8.04						
L0038002				25.6	5.9						
L0010002	6-C	12	γ,n	22.179	6.8	6.	37.40	46.8	1.83	Phys.Rev.143.790(1966)	S.C.FULTZ
L0010002				25.353	4.2						
M0319002	6-C	12	γ,n	23.5	11.5	>4.	26.30	28.7	1.2	Nucl.Instr.A127.1(1975)	U.KNEISSL
M0319002				21.	3.3						
M0319002				22.	8.1						
M0319002				25.	8.7						
M0273002	6-C	12	γ,n	23.	13.1	4.	27.00	43.6	1.9	Can.J.Phys.29.518(1951)	L.KATZ
M0241002	6-C	12	$\gamma,1n$	22.19	8.1	>5.	27.00	36.	1.5	Phys.Rev.141,1002(1966)	W.A.LOCHSTET
M0241002				23.13	8.						
M0241002				25.6	5.8						
M0033006	6-C	12	γ,np	41.	.65	20.	143.00	25.8	.4	Yad.Fiz.32,881(1980)	KHODYACHIKH
M0071003	6-C	12	γ,na	38.8	.446	10.	110.00	6.8	.2	Yad.Fiz.29.572(1979)	V.V.KIRICHENKO
M0013002	6-C	12	γ,p	22.75	13.85	5.	120.00	189	6.5	Yad.Fiz.27.588(1978)	V.V.KIRICHENKO
	6-C	12	γ,p	22.4	13.5	3.5				Phys.Rev.C14,456(1976)	R.CARCHON
	6-C	12	γ,pt	37.5	.25	22.	150.00	8.1		Yad.Fiz.49,790(1989)	V.I.VOLOSHCHUK
				55.	.22						
M0071002	6-C	12	γ,pa	29.8	.657	10.	110.00	9.7	.3	Yad.Fiz.29.572(1979)	V.V.KIRICHENKO
M0065002	6-C	12	γ,npa	54.	.245	35.	140.00	11.8	.1	Ukr.Fiz.Zh.10,1465(1989)	I.V.DOGYUST
	6-C	12	$\gamma,3a$	19.	.23	3.5				Nucl.Phys.50,561(1964)	M.E.TOMS
M0207002	5-B	10	γ,sn	23.81	5.93	>7.	25.30	44.6	2.4	Nucl.Phys.A469,381(1987)	M.H.AHSAN
M0207002				21.21	5.015						
	5-B	10	γ,sn	22.	5.73	17.	35.00	80.8	3.7	Nucl.Phys.A264.30(1976)	U.KNEISSL
L0044002	5-B	10	γ,n	22.001	5.55	17.	35.00	80.4		Nucl.Phys.A264.30(1976)	U.KNEISSL
L0044003	5-B	10	$\gamma,2n$	28.057	68	>20.	35.00	1.9		Nucl.Phys.A264.30(1976)	U.KNEISSL
L0044007	5-B	11	γ,xn	26.081	6.88	15.	35.10	84.1		Nucl.Phys.A264.30(1976)	U.KNEISSL
L0044007				19.749	4.06						
M0498003	5-B	11	γ,xn	25.5	8.95	>10.	27.50	58.8	2.8	Nucl.Phys.A215,147(1973)	R.J.HUGHES
	5-B	11	γ,xn	26.	7.5	11.	29.00	69.		Nucl.Phys.69,241(1965)	E.HAYWARD
	5-B	11	γ,sn	26.08	5.28	15.	35.10	69.2	2.93	Nucl.Phys.A264.30(1976)	U.KNEISSL
				19.75	3.95						
L0044005	5-B	11	γ,n	19.491	3.99	15.	35.10	54.3		Nucl.Phys.A264.30(1976)	U.KNEISSL
L0044005				21.503	3.66						
L0044005				26.58	3.79						
L0044006	5-B	11	$\gamma,2n$	26.081	1.92	11.	35.10	14.9		Nucl.Phys.A264.30(1976)	U.KNEISSL
	5-B	11	γ,p	25.	15.	10.	31.00	98.		Yad.Fiz.9.254(1969)	YU.I.SOROKIN
M0372004	6-C	12	γ,abs	22.7	21.36	6.	100.00	291.	8.81	Nucl.Phys.A251,479(1975)	J.AHRENS
M0372004							140.00	334.	9.18		
M0160002	6-C	12	γ,abs	22.57	17.8	3.2	28.00	84.	3.8	ZHETF,45,1694(1963)	N.A.BURGOV
M0160002				17.61	8.7						
M0160002				18.87	7.3						
M0160002				25.61	9.2						
L0041002	6-C	12	γ,xn	23.367	8.73	6.	32.10	51.6	2.08	Nucl.Instr.Meth.127,1(1975)	U.KNEISSL
L0041002				25.472	5.48						
L0041002				30.069	3.56						
	6-C	12	γ,xn	23.1	8.	>5.	27.00	36.	1.47	Phys.Rev.141,1002(1966)	W.A.LOCHSTET
	6-C	12	γ,xn	23.3	7.2	>4	25.50	29.4		J.Phisique.27.8(1966)	J.MILLER

EXFOR	Nucl	A	Reac	E_{max} MeV	σ_{max} mb	FWHM MeV	E_{int} MeV	σ_{int} MeV * mb	σ^1_{int} mb	Reference	Author
L0010002	6-C	12	γ, xn	22.798	7.22	6.	37.40	46.8	1.83	Phys.Rev.143,790(1966)	S.C.FULTZ
L0010002				25.353	4.2						
M0238002	6-C	12	γ, xn	22.972	12.12	>4.	24.20	24.8	1.1	Yad.Fiz.14,253(1971)	B.S.ISHKHANOV
M0238002				21.925	8.91						
M0238002				22.542	10.14						
M0238002				23.401	10.03						
M0238002				23.757	9.56						
L0041002	6-C	12	γ, sn	23.367	8.73	6.	32.10	51.6	2.08	Nucl.Instr.Meth.127,1(1975)	U.KNEISSL
L0041002				25.472	5.48						
L0041002				30.069	3.56						
L0038002	6-C	12	γ, sn	22.24	8.14	6.	27.00	36.	1.47	Phys.Rev.141,1002(1966)	W.A.LOCHSTET
L0038002				23.07	8.04						
L0038002				25.6	5.9						
	6-C	12	γ, sn	23.	7.	4.8	30.00	36.		Phys.Rev.143,790(1966)	S.C.FULTZ
L0048004	6-C	13	γ, xn	24.431	9.73		41.80	126.1	5.72	Phys.Rev.C19,1684(1979)	J.W.JURY
L0048004				13.817	3.94						
L0048004				20.976	6.6						
L0048004	6-C	13	γ, sn	24.431	9.73		41.80	126.1	5.72	Phys.Rev.C19,1684(1979)	J.W.JURY
L0048004				13.817	3.94						
L0048004				20.976	6.6						
L0048002	6-C	13	γ, n	24.431	9.71		41.80	121.3		Phys.Rev.C19,1684(1979)	J.W.JURY
L0048002				13.817	3.94						
L0048002				20.976	6.6						
M0363002	6-C	13	γ, n	23.77	8.11	>25.	25.00	41.	2.2	Nucl.Phys.A272,296(1976)	R.KOCH
M0363002				15.07	1.93						
M0363002				20.58	4.25						
L0048003	6-C	13	$\gamma, 2n$	35.065	.56	12.	41.80	4.7		Phys.Rev.C19,1684(1979)	J.W.JURY
	6-C	13	γ, p	19.75	3.4	7.	28.00	36.		Phys.Rev.C27,1957(1983)	D.ZUBANOV
L0056004	6-C	14	γ, xn	26.078	13.568		36.20	163.		Phys.Rev.C32,384(1985)	R.E.PYWELL
L0056004				15.417	9.531						
	6-C	14	γ, sn	15.42	9.53		36.20	126.	6.09	Phys.Rev.C32,384(1985)	R.E.PYWELL
				26.08	7.57						
L0056002	6-C	14	γ, n	15.417	8.956	10.	36.20	89.7		Phys.Rev.C32,384(1985)	R.E.PYWELL
L0056002				22.493	5.267						
L0056002				28.892	3.779						
L0056003	6-C	14	$\gamma, 2n$	26.078	5.737	5.	36.20	36.6		Phys.Rev.C32,384(1985)	R.E.PYWELL
	6-C	14	γ, p	5.6	2.5	1.	29.10	17.9		Phys.Rev.C44,1137(1991)	D.J.MCLEAN
				22.5	1.6						
	7-N	14	γ, abs	22.5	27.	7.	30.00	195.	8.4	Nucl.Phys.A128,426(1969)	N.BEZIC
M0214003	7-N	14	γ, xn	22.5	13.45	3.8	50.00	113.5	4.3	Phys.Rev.118,535(1960)	R.W.FAST
L0019002	7-N	14	γ, xn	23.343	14.65	7.	29.50	98.	4.36	Phys.Rev.C2,2318(1970)	B.L.BERMAN
L0019002	7-N	14	γ, sn	23.343	14.65	7.	29.50	98.	4.36	Phys.Rev.C2,2318(1970)	B.L.BERMAN
L0019002	7-N	14	γ, n	23.343	14.65	7.	29.50	98.	4.36	Phys.Rev.C2,2318(1970)	B.L.BERMAN
	7-N	14	γ, np	41.	.83	7.	45.00	54.2		Ukr.Fiz.Zh.34,511(1989)	V.I.VOLOSHCHUK
M0264003	7-N	15	γ, abs	25.43	22.49	7.2	27.00	129.7	6.2	Phys.Rev.C40,506(1989)	A.D.BATES
M0264003				19.85	11.76						
M0264003				21.75	12.52						
M0264002	7-N	15	γ, xn	25.89	14.86	3.9	26.50	78.9	2.8	Phys.Rev.C40,506(1989)	A.D.BATES
L0053004	7-N	15	γ, xn	22.964	11.78	7.	38.00	114.	4.65	Phys.Rev.C26,777(1982)	J.W.JURY
L0053004				25.106	10.58						
	7-N	15	γ, sn	22.96	11.78	7.	38.00	105.9	4.7	Phys.Rev.C26,777(1982)	J.W.JURY
M0264002	7-N	15	γ, sn	25.89	14.86	3.9	26.50	78.9	2.8	Phys.Rev.C40,506(1989)	A.D.BATES
L0053002	7-N	15	γ, n	22.964	11.68	7.	38.00	98.8		Phys.Rev.C26,777(1982)	J.W.JURY
L0053003	7-N	15	$\gamma, 2n$	30.818	1.01	7.	38.00	7.6		Phys.Rev.C26,777(1982)	J.W.JURY
L0053003				27.724	.94						
M0480002	7-N	15	$\gamma, 2n$	26.1	1.7	1.8	27.00	3.6	.1	Phys.Rev.C37,1403(1988)	K.G.MCNEILL
M0480002				22.9	.33						
M0372005	8-O	16	γ, abs	22.35	30.91	6.	100.00	432.	14.5	Nucl.Phys.A251,479(1975)	J.AHRENS
M0372005							140.00	508.	15.1		
M0345002	8-O	16	γ, xn	22.2	10.81	6.5	28.00	46.8	2.	Yad.Konst.1,52(1993)	V.V.VARLAMOV
M0345002				17.22	2.925						
M0345002				19.44	2.078						
M0345002				24.12	9.658						
L0054002	8-O	16	γ, xn	22.107	10.514	7.5	33.10	61.5	2.51	Phys.Rev.C27,1(1983)	B.L.BERMAN
L0054002				24.202	8.916						
L0041003	8-O	16	γ, xn	22.204	8.73	6.	37.00	62.9	2.4	Nucl.Instr.Meth.127,1(1975)	U.KNEISSL
L0041003				24.05	8.1						
L0039005	8-O	16	γ, xn	22.15	10.3	5.	37.10	80.1		Nucl.Phys.A227,513(1974)	A.VEYSSIERE
L0039005				24.05	9.7						
M0396002	8-O	16	γ, xn	22.46	14.79	>4.	25.00	32.12	1.6	Yad.Fiz.12,892(1970)	B.S.ISHKHANOV
M0396002				17.28	4.298						
M0396002				18.93	3.075						
M0396002				21.26	4.21						
M0396002				24.19	12.94						
	8-O	16	γ, xn	22.	10.5		26.50	41.5		J.Phisique.27,8(1966)	J.MILLER
				24.2	9.						
L0036002	8-O	16	γ, xn	22.372	8.91		28.00	41.5	1.76	Phys.Rev.L.15,976(1965)	J.T.CALDWELL
L0036002				24.223	8.11						
	8-O	16	γ, xn	22.2	42.	4.5	26.60	150.		ZHETF,43,70(1962)	N.A.BURGOV
L0051004	8-O	16	γ, xn	22.3	8.3	6.	33.10	61.5		Phys.Rev.C22,2273(1980)	B.L.BERMAN
L0051004				24.1	8.						
L0054002	8-O	16	γ, sn	22.107	10.514	7.5	33.10	61.5	2.51	Phys.Rev.C27,1(1983)	B.L.BERMAN
L0054002				24.202	8.916						
L0040005	8-O	16	γ, sn	22.2	8.73	6.	37.00	62.	2.4	Nucl.Phys.A247,91(1975)	U.KNEISSL
L0040005				24.05	8.1						
L0041003	8-O	16	γ, sn	22.204	8.73	6.	37.00	62.9	2.4	Nucl.Instr.Meth.127,1(1975)	U.KNEISSL
L0041003				24.05	8.1						
	8-O	16	γ, sn	22.15	10.3	5.	37.10	79.6	3.04	Nucl.Phys.A227,513(1974)	A.VEYSSIERE
				24.1	9.7						
	8-O	16	γ, sn	22.37	8.91		28.00	41.5	1.8	Phys.Rev.L.15,976(1965)	J.T.CALDWELL
				24.22	8.11						
L0036002	8-O	16	γ, sn	22.372	8.91		28.00	41.5	1.76	Phys.Rev.L.15,976(1965)	J.T.CALDWELL
L0036002				24.223	8.11						
L0051004	8-O	16	γ, sn	22.3	8.3	6.	30.00	53.8	2.51	Phys.Rev.C22,2273(1980)	B.L.BERMAN
L0051004				24.1	8.						
L0005002	8-O	16	γ, n	17.301	1.85	2.7				Phys.Rev.B133,869(1964)	R.L.BRAMBLETT
L0005002				19.646	1.6						
L0054002	8-O	16	γ, n	22.107	10.514	7.5	33.10	61.5		Phys.Rev.C27,1(1983)	B.L.BERMAN

EXFOR	Nucl	A	Reac	E_{max} MeV	σ_{max} mb	FWHM MeV	E_{int} MeV	σ_{int} MeV * mb	σ_{int}^1 mb	Reference	Author
L0054002				24.202	8.916						
L0041003	8-O	16	γ, n	22.204	8.73	6.	37.00	62.9	2.4	Nucl.Instr.Meth.127.1(1975)	U.KNEISSL
L0041003				24.05	8.1						
L0036002	8-O	16	γ, n	22.372	8.91		28.00	41.5	1.76	Phys.Rev.L.15.976(1965)	J.T.CALDWELL
L0036002				24.223	8.11						
L0039002	8-O	16	γ, n	22.15	10.3	5	37.10	78.9		Nucl.Phys.A227.513(1974)	A.VEYSSIERE
L0039002				24.05	9.7						
	8-O	16	γ, n	22.37	8.91		28.00	41.5		Phys.Rev.L.15.976(1965)	J.T.CALDWELL
				24.22	8.11						
L0051004	8-O	16	γ, n	22.3	8.3	6.	33.10	61.5		Phys.Rev.C22.2273(1980)	B.L.BERMAN
L0051004				24.1	8.						
L0039004	8-O	16	γ, np	30.82	1.7	8.5	37.10	11.		Nucl.Phys.A227.513(1974)	A.VEYSSIERE
L0039003	8-O	16	$\gamma, 2n$	32.72	.23		37.10	.6		Nucl.Phys.A227.513(1974)	A.VEYSSIERE
M0039002	8-O	16	γ, p	21.	7.28	10.	120.00	139.	5.6	Ukr.Fiz.Zh.25,229(1980)	KHODYACHIKH
	8-O	16	γ, α	13.	.02					Nucl.Phys.54,625(1964)	M.E.TOMS
				16.8	.013						
	8-O	16	$\gamma, 4\alpha$	20.5	.08	2.	21.50	.124		Nucl.Phys.54.625(1964)	M.E.TOMS
	8-O	17	γ, xn	23.19	13.28	6.	39.70	128.		Phys.Rev.C21.503(1980)	J.W.JURY
L0049002	8-O	17	γ, sn	23.19	13.28	6.	40.00	120.	5.22	Phys.Rev.C21.503(1980)	J.W.JURY
L0049003	8-O	17	γ, n	22.822	12.46	6.	39.70	111.		Phys.Rev.C21.503(1980)	J.W.JURY
L0049004	8-O	17	$\gamma, 2n$	34.915	1.03	16.	39.70	9.3		Phys.Rev.C21.503(1980)	J.W.JURY
L0049004				24.549	.74						
L0049004				31.213	.82						
L0047004	8-O	18	γ, xn	23.673	17.74	17.	41.80	275.		Phys.Rev.C19.1667(1979)	WOODWORTH
L0047004				11.453	9.01						
L0047004				14.813	13.13						
L0045004	8-O	18	γ, xn	23.33	16.83	18.	33.00	191.		Nucl.Phys.A272.125(1976)	U.KNEISSL
L0045004				11.315	6.25						
L0045004				14.507	10.84						
	8-O	18	γ, sn	23.43	12.54	18.	41.80	198.3	9.08	Phys.Rev.C19.1667(1979)	WOODWORTH
				11.45	9.						
				14.81	11.53						
	8-O	18	γ, sn	23.33	10.57	>18.	35.00	142.	6.9	Nucl.Phys.A272.125(1976)	U.KNEISSL
				14 51	9.						
L0047002	8-O	18	γ, n	11.453	9.	23.	41.80	121.5		Phys.Rev.C19.1667(1979)	WOODWORTH
L0047002				14.813	8.65						
L0047002				23.673	6.87						
L0047002				26.987	6.93						
L0045002	8-O	18	γ, n	30.752	8.07	>23.	35.00	93.		Nucl.Phys.A272.125(1976)	U.KNEISSL
L0045002				11.315	6.25						
L0045002				14.507	8.02						
L0045002				23.33	6.39						
	8-O	18	γ, np	27.5	1.2	8.	30.00	5.6	.21	Phys.Rev.C43.489(1991)	K.G.MCNEIL
							43.00	11.8	.39		
L0047003	8-O	18	$\gamma, 2n$	23.426	5.59	15.	41.80	76.7		Phys.Rev.C19.1667(1979)	WOODWORTH
L0047003				15.796	4.01						
L0045003	8-O	18	$\gamma, 2n$	23.164	5.35	11.	35.00	49.		Nucl.Phys.A272.125(1976)	U.KNEISSL
M0242002	8-O	18	γ, p	22.57	5.055	6.5	32.00	33.6	1.5	Nucl.Phys.A376.15(1982)	K.BANGERT
M0242002				23.57	4.994						
L0047005	8-O	18	γ, p	23.673	6.14	7.	41.80	44.		Phys.Rev.C19.1667(1979)	WOODWORTH
L0047005				17.517	1.22						
L0047005				19.938	1.81						
L0047005				26.754	3.39						
	8-O	18	γ, p	23.1	5.5	8.	30.60	29.8		Phys.Rev.L.36.1441(1976)	B.L.BERMAN
				25.2	3.3						
	9-F	19	γ, abs	24.	18.	14.	30.00	271.		Nucl.Phys.A128.426(1969)	N.BEZIC
L0039008	9-F	19	γ, xn	25.13	12.1	>10.	27.80	109.		Nucl.Phys.A227.513(1974)	A.VEYSSIERE
L0039008				12.26	3.7						
	9-F	19	γ, sn	24.86	11.1	>10.	27.80	104.	4.95	Nucl.Phys.A227.513(1974)	A.VEYSSIERE
L0039006	9-F	19	γ, n	23.77	10.4	>10.	27.80	99.		Nucl.Phys.A227.513(1974)	A.VEYSSIERE
L0039006				12.26	3.7						
	9-F	19	$\gamma, 2n$	24.7	.48	>40.	60.00	9.1		Nucl.Phys.A262.91(1976)	D.W.ANDERSON
				40.5	.25						
				56.6	.26						
L0039007	9-F	19	$\gamma, 2n$	27.03	1.7	>7.	27.80	5.2		Nucl.Phys.A227.513(1974)	A.VEYSSIERE
L0039007				25.13	1.2						
L0039011	10-Ne		γ, xn	20.52	8.3	8.	25.90	46.		Nucl.Phys.A227.513(1974)	A.VEYSSIERE
L0039011				17.81	3.6						
L0039011				25.13	5.9						
	10-Ne		γ, sn	19.17	6.6	8.	25.90	43.	1.98	Nucl.Phys.A227.513(1974)	A.VEYSSIERE
L0039009	10-Ne		γ, n	19.17	6.6	8.	25.90	40.		Nucl.Phys.A227.513(1974)	A.VEYSSIERE
L0039009				17.81	3.6						
L0039009				20.25	6.6						
L0039009				22.15	5.2						
L0039009				25.4	5.8						
L0039010	10-Ne		$\gamma, 2n$	20.52	1.1	3.	25.90	3.1		Nucl.Phys.A227.513(1974)	A.VEYSSIERE
M0369002	10-Ne	20	γ, n	19.	12.14	5.	28.40	58.2	2.6	Nucl.Phys.A357.171(1981)	P.D.ALLEN
M0369002				17.7	5.14						
M0369002				19.9	10.71						
	10-Ne	22	$\gamma, 2n$	20.7	13.	3.				Nucl.Phys.A227.513(1974)	A.VEYSSIERE
	11-Na	23	γ, abs	21.1	21.1	>13.	29.50	330.		Yad.Fiz.33.581(1981)	B.S.ISHKHANOV
				28.6	19.						
L0039014	11-Na	23	γ, abs	23.	15.	16.	30.00	200.	11.	Phys.Rev.137.B576(1965)	J.M.WYCKOF
L0022002	11-Na	23	γ, xn	26.62	12.1	14.	30.10	139.		Nucl.Phys.A227.513(1974)	A.VEYSSIERE
	11-Na	23	γ, xn	26.143	14.38	>15.	27.10	120.		Phys.Rev.C4.1673(1971)	R.A.ALVAREZ
L0022008	11-Na	23	γ, sn	26.76	12.5	14.	30.10	136.	6.18	Nucl.Phys.A227.513(1974)	A.VEYSSIERE
L0039012	11-Na	23	γ, sn	26.143	13.91	>15.	27.10	119.	5.74	Phys.Rev.C4.1673(1971)	R.A.ALVAREZ
L0022003	11-Na	23	γ, n	24.18	12.5	14.	30.10	133.		Nucl.Phys.A227.513(1974)	A.VEYSSIERE
L0039013	11-Na	23	γ, n	26.143	13.25	>15.	27.10	118.		Phys.Rev.C4.1673(1971)	R.A.ALVAREZ
L0022004	11-Na	23	$\gamma, 2n$	29.19	1.6	>5.	30.10	2.7		Nucl.Phys.A227.513(1974)	A.VEYSSIERE
	11-Na	23	$\gamma, 2n$	26.561	.56	>3.	27.10	.6		Phys.Rev.C4.1673(1971)	R.A.ALVAREZ
	11-Na	23	γ, p	20.6	30.1	>13.				Yad.Fiz.33.581(1981)	B.S.ISHKHANOV
				27.6	22.8						
	12-Mg		γ, abs	19.	24.	13.	30.00	225.	12.	Phys.Rev.137.B576(1965)	J.M.WYCKOFF
	12-Mg		γ, p	22.5	18.	11.	32.00	180.		Phys.Lett.9.162(1964)	B.S.ISHKHANOV
	12-Mg		γ, p	20.	13.5	6.	23.00	70.		J.Phys.Soc.Jap.17.735(1962)	K.SHODA
L0026002	12-Mg	24	γ, xn	19.16	9.9	8.	28.30	51.9	2.37	Phys.Rev.C4.149(1971)	S.C.FULTZ
L0026002				20.011	9.03						

EXFOR	Nucl	A	Reac	E_{max} MeV	σ_{max} mb	FWHM MeV	E_{int} MeV	σ_{int} MeV * mb	σ^1_{int} mb	Reference	Author
L0026002	12-Mg	24	γ,sn	19.16	9.9		28.30	51.9	2.37	Phys.Rev.C4,149(1971)	S.C.FULTZ
L0026002				20.011	9.03						
	12-Mg	24	γ,n	20.	12.					Nucl.Phys.A186,438(1972)	B.S.ISHKHANOV
				19.3	11.						
				24.6	8.						
L0026002	12-Mg	24	γ,n	19.16	9.9	8.	28.30	51.9	2.37	Phys.Rev.C4,149(1971)	S.C.FULTZ
L0026002				20.011	9.03						
M0001027	12-Mg	24	γ,p	19.3	25.29	7.	29.50	183.	8.4	Yad.Fiz.30,1185(1979)	V.V.VARLAMOV
M0001027				24.9	20.6						
L0022005	12-Mg	25	γ,xn	23.185	27.7	>11.	28.90	248.	12.	Phys.Rev.C4,1673(1971)	R.A.ALVAREZ
L0022009	12-Mg	25	γ,sn	23.185	27.7	9.	28.90	247.	11.5	Phys.Rev.C4,1673(1971)	R.A.ALVAREZ
L0022006	12-Mg	25	γ,n	23.185	27.7	9.	28.90	245.	11.	Phys.Rev.C4,1673(1971)	R.A.ALVAREZ
L0022007	12-Mg	25	$\gamma,2n$	28.099	0.8	>5.	28.90	1.5		Phys.Rev.C4,1673(1971)	R.A.ALVAREZ
	12-Mg	26	γ,xn	22.25	12.					Nucl.Phys.A186,438(1972)	B.S.ISHKHANOV
				17.5	17.						
				24.5	15.5						
L0026003	12-Mg	26	γ,xn	22.14	35.87	>10.	28.60	308.		Phys.Rev.C4,149(1971)	S.C.FULTZ
L0026003				17.646	22.84						
L0026006	12-Mg	26	γ,sn	22.14	25.12	>10.	28.60	236.	11.5	Phys.Rev.C4,149(1971)	S.C.FULTZ
L0026006				17.646	22.84						
L0026004	12-Mg	26	γ,n	17.646	22.84	>10.	28.60	164.		Phys.Rev.C4,149(1971)	S.C.FULTZ
L0026005	12-Mg	26	$\gamma,2n$	21.931	13.89	>8.	28.60	72.		Phys.Rev.C4,149(1971)	S.C.FULTZ
L0026005				24.858	12.23						
M0002013	12-Mg	26	γ,p	24.1	19.68	10.	27.00	101.3	4.6	Nucl.Phys.A313,317(1979)	B.S.ISHKHANOV
M0002013				17.8	5.07						
M0002013				20.7	10.05						
M0002013				21.8	15.1						
M0002013				23.4	18.97						
	12-Mg	26	γ,p	23.	20.	10.	29.00	140.		Nucl.Phys.A222,548(1974)	V.V.VARLAMOV
							20.10	10.5			
							26.00	18.			
M0372006	13-Al	27	γ,abs	20.8	41.6	9.	100.00	739.	25.7	Nucl.Phys.A251,479(1975)	J.AHRENS
M0372006							140.00	807.	26.3		
L0039017	13-Al	27	γ,xn	21.2	15.8	13.	30.30	152.	6.77	Nucl.Phys.A227,513(1974)	A.VEYSSIERE
	13-Al	27	γ,xn	22.	14.51	6.				Izv.AN SSSR,33,1742(1969)	B.S.ISHKHANOV
				19.	6.7						
				24.	5.83						
	13-Al	27	γ,xn	21.4	19.1	10.				Lett.Nuov.Cim.2,318(1969)	S.COSTA
L0010004	13-Al	27	γ,xn	21.25	14.54	14.	36.70	175.		Phys.Rev.143,790(1966)	S.C.FULTZ
	13-Al	27	γ,xn	22.	14.51	6.				Izv.AN SSSR,31,336(1967)	G.P.ANTROPOV
				19.	6.7						
				20.5	9.1						
				22.5	10.08						
L0039017	13-Al	27	γ,sn	21.2	15.8	13.	30.30	152.	6.77	Nucl.Phys.A227,513(1974)	A.VEYSSIERE
L0010007	13-Al	27	γ,sn	21.404	14.89	14.	36.70	167.	7.17	Phys.Rev.143,790(1966)	S.C.FULTZ
L0039015	13-Al	27	γ,n	21.2	15.8	13.	30.30	150.		Nucl.Phys.A227,513(1974)	A.VEYSSIERE
L0039015				19.84	14.3						
L0010005	13-Al	27	γ,n	21.404	14.89	11.	36.70	159.		Phys.Rev.143,790(1966)	S.C.FULTZ
M0267002	13-Al	27	$\gamma,1n$	20.62	5.52	6.5	24.60	31.5	1.6	Phys.Rev.141,1002(1966)	W.A.LOCHSTET
M0267002				18.54	4.97						
M0267002				19.62	5.31						
M0267002				21.38	5.46						
	13-Al	27	γ,p	19.9	17.5	>8.	23.00	110.		J.Phys.Soc.Jap.17,735(1962)	K.SHODA
L0039016	13-Al	27	$\gamma,2n$	29.74	.6		30.30	.6		Nucl.Phys.A227,513(1974)	A.VEYSSIERE
L0010006	13-Al	27	$\gamma,2n$	34.567	1.43	>8.	36.70	7.6		Phys.Rev.143,790(1966)	S.C.FULTZ
	13-Al	27	$\gamma,2p$	30.5	.29	10.	63.00	28.		Phys.Rev.110,1113(1958)	L.B.AULL
M0372007	14-Si		γ,abs	20.24	58.73	5.	29.80	392.8	18.7	Nucl.Phys.A251,479(1975)	J.AHRENS
M0372007				18.28	43.47						
M0372007				19.	48.31						
M0372007				21.42	58.09						
L0039018	14-Si		γ,xn	19.84	16.	4.	30.00	95.	4.25	Nucl.Phys.A227,513(1974)	A.VEYSSIERE
L0039018				18.9	11.2						
L0039018				20.79	15.8						
	14-Si		γ,xn	21.3	16.	5.				Lett.Nuov.Cim.2,318(1969)	S.COSTA
	14-Si		γ,xn	20.8	18.	4.				Yad.Fiz.7,1168(1968)	B.I.GORYACHEV
L0039018	14-Si		γ,sn	19.84	16.	4.	30.00	95.	4.25	Nucl.Phys.A227,513(1974)	A.VEYSSIERE
L0039018				18.9	11.2						
L0039018				20.79	15.8						
L0039018	14-Si		γ,n	19.84	16.	4.	30.00	95.	4.25	Nucl.Phys.A227,513(1974)	A.VEYSSIERE
L0039018				18.9	11.2						
L0039018				20.79	15.8						
L0055002	14-Si	28	γ,xn	20.774	14.487	4.	33.10	105.	4.46	Phys.Rev.C27,960(1983)	R.E.PYWELL
L0055002				18.87	11.269						
L0055002				19.822	13.212						
	14-Si	28	γ,sn	21.	15.	5.	31.00	93.		Nucl.Phys.A171,324(1971)	D.V.WEBB
L0055002	14-Si	28	γ,sn	20.774	14.487	4.	33.10	105.	4.46	Phys.Rev.C27,960(1983)	R.E.PYWELL
L0055002				18.87	11.269						
L0055002				19.822	13.212						
L0055002	14-Si	28	γ,n	20.774	14.487	4.	33.10	105.	4.46	Phys.Rev.C27,960(1983)	R.E.PYWELL
L0055002				18.87	11.269						
L0055002				19.822	13.212						
L0004002	14-Si	28	γ,n	19.86	11.05	4.5	33.00	68.	3.	Phys.Lett.6,213(1963)	J.T.CALDWELL
L0004002				20.77	10.64					Phys.Lett.6,213(1963)	J.T.CALDWELL
M0397002	14-Si	28	γ,n	20.78	18.95	4.5	29.50	102.9	4.6	Yad.Fiz.2,1168(1968)	B.I.GORYACHEV
M0397002				18.74	13.03						
M0397002				19.75	17.66						
M0397002				27.26	17.73						
M0345003	14-Si	28	γ,n	19.78	16.49	4.5	30.00	94.6	4.3	Yad.Konst.1,52(1993)	V.V.VARLAMOV
M0345003				18.18	7.468						
M0345003				18.74	11.5						
M0345003				20.78	15.73						
	14-Si	28	γ,p	21.	40.	5.	22.50	128.		Phys.Rev.C27,470(1983)	R.L.GULBRANSON
				19.	42.						
M0003025	14-Si	28	γ,p	20.1	45.75	4.5	28.00	265.7	12.4	Izv.AN SSSR,43,186(1979)	V.V.VARLAMOV
	14-Si	28	γ,p	18.7	31.4	4.	23.00	140.		J.Phys.Soc.Jap.17,735(1962)	K.SHODA
L0055003	14-Si	29	γ,xn	21.346	18.87	4.	33.10	194.5	8.65	Phys.Rev.C27,960(1983)	R.E.PYWELL
L0055003	14-Si	29	γ,sn	21.346	18.87	4.	33.10	194.5	8.65	Phys.Rev.C27,960(1983)	R.E.PYWELL
	14-Si	29	γ,sn	21.2	18.5	10.				Nucl.Phys.A369,141(1981)	R.E.PYWELL

EXFOR	Nucl	A	Reac	E_{max} MeV	σ_{max} mb	FWHM MeV	E_{int} MeV	σ_{int} MeV * mb	σ_{int}^1 mb	Reference	Author
				26.	13.5						
L0055003	14-Si	29	γ,n	21.346	18.87	4.	33.10	194.5	8.65	Phys.Rev.C27,960(1983)	R.E.PYWELL
	14-Si	30	γ,xn	20.2	23.65	13.	33.10	316.		Phys.Rev.C27,960(1983)	R.E.PYWELL
	14-Si	30	γ,xn	22.5	30	11.	28.00	264.		Nucl.Phys.A388,445(1982)	G.ODGERS
L0055006	14-Si	30	γ,xn	21.917	23.752	4.	33.10	316.		Phys.Rev.C27.960(1983)	R.E.PYWELL
L0055006	14-Si	30	γ,xn	15.634	13.866	4.	33.10	316.		Phys.Rev.C27.960(1983)	R.E.PYWELL
L0055006	14-Si	30	γ,xn	18.68	22.936	4.	33.10	316.		Phys.Rev.C27.960(1983)	R.E.PYWELL
L0055006	14-Si	30	γ,xn	20.203	23.648	4.	33.10	316.		Phys.Rev.C27.960(1983)	R.E.PYWELL
L0055006	14-Si	30	γ,xn	26.058	21.273	4.	33.10	316.		Phys.Rev C27.960(1983)	R.E.PYWELL
	14-Si	30	γ,sn	20.2	23.65	12.	33.10	249.	12.1	Phys.Rev.C27,960(1983)	R.E.PYWELL
L0055004	14-Si	30	γ,n	18.68	22.806	8.	33.10	181.		Phys.Rev.C27,960(1983)	R.E PYWELL
L0055004				30.818	8.78						
L0055005	14-Si	30	$\gamma,2n$	23.059	10.146	7.	33.10	67.5		Phys.Rev.C27,960(1983)	R.E.PYWELL
	15-P	31	γ,xn	23.6	22.53	9.	30.00	211.		Izv.AN SSSR,33.1742(1969)	B.S.ISHKHANOV
				19.4	18.66						
				21.3	21.12						
	15-P	31	γ,xn	22.	13.	11.5	28.00	127.		Phys.Rev.132,2251(1963)	L.N.BOLE
L0039022	15-P	31	γ,xn	21.2	19.8	12.	28.60	179.	8.34	Nucl.Phys.A227,513(1974)	A.VEYSSIERE
L0039019	15-P	31	γ,n	21.2	19.8	12.	28.60	178.	8.34	Nucl.Phys.A227,513(1974)	A.VEYSSIERE
M0273003	15-P	31	γ,n	19.	16.6	7.	25.00	115.3	6.	Can.J.Phys.29,518(1951)	L.KATZ
	15-P	31	$\gamma,1n$	19.5	19.	7.5				Can.J.Phys.41,180(1963)	W.J.MCDONALD
L0039020	15-P	31	γ,np	25.13	7.8	>10.	28.60	44.		Nucl.Phys.A227,513(1974)	A.VEYSSIERE
L0039021	15-P	31	$\gamma,2n$	28.11	.7	1.	28.60	1.1		Nucl.Phys.A227,513(1974)	A.VEYSSIERE
	15-P	31	γ,p	21.	43.	10.	32.00	350.		Phys.Lett.9.162(1964)	B.S.ISHKHANOV
	15-P	31	$\gamma,2p$	32.	.28	15.				Nucl.Phys.A150.625(1970)	D.W.ANDERSON
	15-P	31	$\gamma,2pN$	49.	.36	>15.				Nucl.Phys.A150.625(1970)	D.W.ANDERSON
	16-S		γ,abs	20.	50.	7.	30.00	400.	22.	Phys.Rev.137,B576(1965)	J.M.WYCKOFF
	16-S		γ,xn	21.5	15.3		30.00	749.		Yad.Fiz.7,1168(1968)	B.I.GORYACHEV
				19.	14.4						
	16-S		γ,xn	21.	15.19	5.				Izv.AN SSSR,31.336(1967)	G.P.ANTROPOV
				19.	8.36						
				22.5	12.15						
				24.5	6.49						
	16-S		γ,p	21.	50.	9.	32.00	370.		Phys.Lett.9,162(1964)	B.S.ISHKHANOV
	16-S	32	γ,xn	21.	16.	11.	32.00	137.		Nucl.Phys.A156,74(1970)	D.W.ANDERSON
L0039026	16-S	32	γ,xn	19.71	10.5	13.	32.20	98.	4.24	Nucl.Phys.A227,513(1974)	A.VEYSSIERE
L0039026				25.4	6.6						
L0039023	16-S	32	γ,n	19.71	10.5	13.	32.20	98.	4.24	Nucl.Phys.A227,513(1974)	A.VEYSSIERE
L0039023				25.4	6.6						
L0039025	16-S	32	γ,np	28.92	2.7	>10.	30.00	14.		Nucl.Phys.A227,513(1974)	A.VEYSSIERE
L0039024	16-S	32	$\gamma,2n$	30.	.1		29.47	.1		Nucl.Phys.A227,513(1974)	A.VEYSSIERE
M0510006	16-S	34	γ,abs	22.	66.34	7.5	26.00	446.5	22.8	Nucl.Phys.A460,455(1986)	Y.I.ASSAFIRI
M0510006				17.	39.51						
M0506002	16-S	34	γ,sn	17.6	36.88	8.	27.00	247.	13.1	Nucl.Phys.A413,416(1984)	Y.I.ASSAFIRI
M0506002				12.8	11.03						
M0506002				21.	31.16						
M0510003	16-S	34	γ,np	25.46	10.73	>5.	26.00	28.	1.	Nucl.Phys.A460,455(1986)	Y.I.ASSAFIRI
M0506003	16-S	34	$\gamma,2n$	25.8	11.36	6.	27.00	35.	1.5	Nucl.Phys.A413,416(1984)	Y.I.ASSAFIRI
M0506003				22.	7.83						
M0510002	16-S	34	γ,p	23.06	36.24	6.	26.00	213.	10.4	Nucl.Phys.A460,455(1986)	Y.I.ASSAFIRI
M0510002				16.91	13.76						
L0039029	17-Cl		γ,xn	22.96	30.3	12.	27.60	292.		Nucl.Phys.A227,513(1974)	A.VEYSSIERE
	17-Cl		γ,sn	22.96	26.3	12.	27.60	273.	13.3	Nucl.Phys.A227,513(1974)	A.VEYSSIERE
L0039027	17-Cl		γ,n	20.79	25.5	12.	27.60	254.		Nucl.Phys.A227,513(1974)	A.VEYSSIERE
L0039028	17-Cl		$\gamma,2n$	23.23	4.	4.	27.60	19.		Nucl.Phys.A227,513(1974)	A.VEYSSIERE
	17-Cl	35	γ,n	20.	14.	6.5	27.00	93.		J.Phys.Soc.Jap.17,1681(1962)	K.KURIYAMA
	17-Cl	37	$\gamma,2n$	23.	14.	>5.				Nucl.Phys.A227,513(1974)	A.VEYSSIERE
M0214004	18-Ar		γ,xn	21.5	41.51	10.	25.00	392.		Phys.Rev.118,535(1960)	R.W.FAST
M0214004							50.00	598.	25.		
	18-Ar	40	γ,abs	20.9	50.	10.	26.00	434.		Nucl.Phys.A398,415(1983)	R.A.SUTTON
				16.	42.						
	18-Ar	40	γ,abs	19.	42.	10.	32.00	450.		Z.Physik.187,210(1965)	D.EHHALT
L0039032	18-Ar	40	γ,xn	21.88	52.	10	26.80	538.		Nucl.Phys.A227,513(1974)	A.VEYSSIERE
L0039032				18.63	47.1						
M0346010	18-Ar	40	γ,xn	18.97	33.14	>10.	21.00	178.8	10.3	Can.J.Phys.51,1176(1973)	J.W.JURY
	18-Ar	40	γ,sn	17.4	40.	11.	27.00	382.		Nucl.Phys.A398,415(1983)	R.A.SUTTON
				20.9	40.						
	18-Ar	40	γ,sn	16.73	39.6	10.	26.80	390.	21.	Nucl.Phys.A227,513(1974)	A.VEYSSIERE
	18-Ar	40	γ,n	16.	38.	5.	27.00	232.		Nucl.Phys.A398,415(1983)	R.A.SUTTON
				20.9	15.						
L0039030	18-Ar	40	γ,n	16.73	33.7	6.	26.80	242.		Nucl.Phys.A227,513(1974)	A.VEYSSIERE
	18-Ar	40	γ,n	19.	37.	5.	32.00	200.		Z.Physik.187,210(1965)	D.EHHALT
	18-Ar	40	$\gamma,2n$	20.9	25.	7.	27.00	148.		Nucl.Phys.A398,415(1983)	R.A.SUTTON
L0039031	18-Ar	40	$\gamma,2n$	21.34	21.9	8.	26.80	148.		Nucl.Phys.A227,513(1974)	A.VEYSSIERE
	18-Ar	40	γ,p	23.4	21.4	3.	26.00	61.		Nucl.Phys.A398,415(1983)	R.A.SUTTON
				21.04	10.9						
L0039036	19-K		γ,xn	20.93	24.4	8.	31.60	218.	9.7	Nucl.Phys.A227,513(1974)	A.VEYSSIERE
L0039036	19-K		γ,sn	20.93	24.4	8.	31.60	217.	9.7	Nucl.Phys.A227,513(1974)	A.VEYSSIERE
L0039033	19-K		γ,n	20.93	24.4	8.	31.60	216.		Nucl.Phys.A227,513(1974)	A.VEYSSIERE
L0039035	19-K		γ,np	25.4	7.	4.	27.80	39.		Nucl.Phys.A227,513(1974)	A.VEYSSIERE
L0039035				21.34	6.7						
L0039034	19-K		$\gamma,2n$	31.09	.5	1.	31.60	1.1		Nucl.Phys.A227,513(1974)	A.VEYSSIERE
	19-K	39	γ,n	20.	16.	7.	30.00	102		Nucl.Phys.A171,324(1971)	D.V.WEBB
M0372008	20-Ca		γ,abs	19.77	97.06	5.	100.00	1120	45.5	Nucl.Phys.A251,479(1975)	J.AHRENS
M0372008							140.00	1290.	46.8		
	20-Ca	40	γ,abs	20.2	110.		28.50	920.	49.6	Phys.Lett.17,49(1965)	B.S.DOLBILKIN
	20-Ca	40	γ,abs	20.	105.	4.5				Phys.Rev.137,B576(1965)	J.M.WYCKOFF
L0039037	20-Ca	40	γ,xn	19.98	16.8	4.5	29.50	100.	4.55	Nucl.Phys.A227,513(1974)	A.VEYSSIERE
	20-Ca	40	γ,xn	20.2	16.5	5.5				Yad.Fiz.5,1138(1967)	B.I.GORYACHEV
	20-Ca	40	γ,xn	20.	14.9	3.5	26.00	73.		J.Phisique.27,8(1966)	J.MILLER
L0039037	20-Ca	40	γ,sn	19.98	16.8	4.5	29.50	100.	4.55	Nucl.Phys.A227,513(1974)	A.VEYSSIERE
L0039037	20-Ca	40	γ,n	19.98	16.8	4.5	29.50	100.	4.55	Nucl.Phys.A227,513(1974)	A.VEYSSIERE
M0397004	20-Ca	40	γ,n	20.26	20.41	5.	29.10	86.3	4.1	Yad.Fiz.2,1168(1968)	B.I.GORYACHEV
M0397004				19.24	14.86						
M0397004				21.25	13.97						
M0397004				23.34	12.34						
	20-Ca	40	γ,p	20.2	85.	4.	30.00	510.		Pisma ZHETF,5,225(1967)	B.I.GORYACHEV
				18.6	80.5						
	20-Ca	42	γ,p	19.7	50.5	7.5	27.00	256.		Nucl.Phys.A357,429(1981)	Y.I.ASSAFIRI

EXFOR	Nucl	A	Reac	E_{max} MeV	σ_{max} mb	FWHM MeV	E_{int} MeV	σ_{int} MeV * mb	σ^1_{int} mb	Reference	Author
				20.2	40.5						
	20-Ca	44	γ, sn	17.2	46.8	10.5				Austr.J.Phys.34.505(1981)	P.D.HARTY
	20-Ca	44	γ, p	22.	14.	>12.				Nucl.Phys.A277.301(1977)	S.OIKAWA
	20-Ca	48	γ, n	18.8	114.5	7.				Nucl.Phys.A469.239(1987)	G.J.O'KEEFE
	20-Ca	48	$\gamma, 2n$	22.6	50.	2.				Nucl.Phys.A469.239(1987)	G.J.O'KEEFE
	20-Ca	48	γ, p	24.9	19.5					Nucl.Phys.A469.239(1987)	G.J.O'KEEFE
				19.2	9.5						
				24.9	19.5						
L0039040	21-Sc	45	γ, xn	19.44	39.4	8.	28.10	399.		Nucl.Phys.A227.513(1974)	A.VEYSSIERE
	21-Sc	45	γ, xn	19.5	21.5	7.5	25.00	158.	8.4	Nucl.Phys.A205.139(1973)	R.H.SAMBELL
	21-Sc	45	γ, sn	19.44	39.4	8.	28.10	382.	19.6	Nucl.Phys.A227.513(1974)	A.VEYSSIERE
L0039038	21-Sc	45	γ, n	19.44	39.4	8.	28.10	365.		Nucl.Phys.A227.513(1974)	A.VEYSSIERE
L0039039	21-Sc	45	$\gamma, 2n$	25.4	3.9	>8.	28.10	17.		Nucl.Phys.A227.513(1974)	A.VEYSSIERE
	21-Sc	45	γ, p	2.2	47.	>12.				Nucl.Phys.A277.301(1977)	S.OIKAWA
	22-Ti		γ, xn	17.	60.	7.				Nuov.Cim.48B.461(1967)	S.COSTA
	22-Ti	46	γ, sn	20.5	31.	8.5	31.00	269.		Nucl.Phys.29.292(1962)	T.R.SHERWOOD
M0370002	22-Ti	46	$\gamma, 1n$	15.8	24.13	8.5	25.00	194.	9.9	Nucl.Phys.A318.461(1979)	R.E.PYWELL
M0370002				18.	23.87						
	22-Ti	46	γ, p	2.2	37.	9.				Nucl.Phys.A277.301(1977)	S.OIKAWA
M0532002	22-Ti	48	γ, sn	16.1	48.55	7.5	27.00	398.	20.8	Nucl.Phys.A339.125(1980)	R.SUTTON
M0532002				17.5	46.36						
M0532002				19.5	43.64						
	22-Ti	50	γ, xn	18.1	81.	8.5				Nucl.Phys.A318.461(1979)	R.E.PYWELL
				21.5	60.						
	22-Ti	50	γ, sn	18.1	81.	5.2				Nucl.Phys.A318.461(1979)	R.E.PYWELL
M0326002	22-Ti	50	γ, sn	18.27	82.	5.5	26.30	472.6	26.	Nucl.Phys.A325.116(1979)	R.E.PYWELL
M0326002				21.56	41.8						
L0039043	23-V	51	γ, xn	18.08	76.7	11.	27.80	689.		Nucl.Phys.A227.513(1974)	A.VEYSSIERE
	23-V	51	γ, xn	20.2	78.	8.	30.00	820.		Izv.AN SSSR.33.1736(1969)	B.I.GORYACHEV
	23-V	51	γ, xn	18.25	69.85	7.5	27.80	654.		Phys.Rev.128.2345(1962)	S.C.FULTZ
	23-V	51	γ, sn	18.08	76.7	10.	27.80	610.	31.2	Nucl.Phys.A227.513(1974)	A.VEYSSIERE
	23-V	51	γ, sn	20.2	78.	6.	30.00	600.		Izv.AN SSSR.33.1736(1969)	B.I.GORYACHEV
L0001002	23-V	51	γ, sn	18.251	69.85	6.5	27.80	552.	28.9	Phys.Rev.128.2345(1962)	S.C.FULTZ
L0039041	23-V	51	γ, n	18.08	76.7	10.	27.80	531.		Nucl.Phys.A227.513(1974)	A.VEYSSIERE
L0001003	23-V	51	γ, n	18.251	69.85	6.5	27.80	450.		Phys.Rev.128.2345(1962)	S.C.FULTZ
L0039042	23-V	51	$\gamma, 2n$	24.59	15.9	4.	27.80	79.		Nucl.Phys.A227.513(1974)	A.VEYSSIERE
L0001004	23-V	51	$\gamma, 2n$	25.319	22.16	5.	27.80	102.		Phys.Rev.128.2345(1962)	S.C.FULTZ
	23-V	51	γ, p	21.5	23.	>12.	29.00	205.		Nucl.Phys.A303.333(1978)	H.TSUBOTA
	24-Cr		γ, xn	17.8	88.	6.5				Austr.J.Phys.30.401(1977)	J.WEISE
M0093003	24-Cr	52	γ, xn	18.25	113.	6.5	31.80	734.6	36.6	Izv.AN SSSR.33.1736(1969)	B.I.GORYACHEV
M0093003				16.75	82.						
M0093003				19.25	104.						
M0067002	24-Cr	52	γ, p	20.2	32.8	4.	28.00	217.5	10.	Yad.Phys.11.485(1970)	B.S.ISHKHANOV
M0067002				15.9	8.2						
M0067002				18.7	14.3						
M0067002				26.2	22.4						
	25-Mn	55	γ, abs	17.5	100.	7.5	29.00	816.		Pisma ZHETF.10.365(1969)	B.S.DOLBILKIN
L0028002	25-Mn	55	γ, xn	20.64	71.87	12.5	36.50	902.		Phys.Rev.C20.128(1979)	R.A.ALVAREZ
L0028002				17.379	70.24						
	25-Mn	55	γ, xn	16.4	71.	11.	29.50	780.		Izv.AN SSSR.34.2228(1970)	B.S.ISHKHANOV
	25-Mn	55	γ, xn	16.8	90.	7.5	25.00	627.		Phys.Rev.120.1424(1960)	P.A.FLOURNOY
				19.75	77.						
L0028011	25-Mn	55	γ, sn	19.192	69.37	8.	36.50	733.	36.4	Phys.Rev.C20.128(1979)	R.A.ALVAREZ
L0028011				17.377	67.54						
L0028011				24.155	54.78						
	25-Mn	55	γ, sn	16.4	71.	11.	29.50	620.		Izv.AN SSSR.34.2228(1970)	B.S.ISHKHANOV
L0028003	25-Mn	55	γ, n	17.379	70.24	8.	36.50	567.		Phys.Rev.C20.128(1979)	R.A.ALVAREZ
L0028003				19.193	69.39						
L0028004	25-Mn	55	$\gamma, 2n$	22.699	22.81	7.	36.50	163.		Phys.Rev.C20.128(1979)	R.A.ALVAREZ
L0028005	25-Mn	55	$\gamma, 3n$	34.322	3.26		36.50	3.		Phys.Rev.C20.128(1979)	R.A.ALVAREZ
	25-Mn	55	γ, p	20.2	31.	7.				J.Phys.Soc.Jap.25.664(1968)	K.SHODA
	26-Fe		γ, abs	18.5	87.02	9.	26.50	735.		Yad.Fiz.9.675(1969)	B.S.DOLBILKIN
				12.2	79.						
	26-Fe		γ, xn	17.2	63.	7.				Nuov.Cim.51B.199(1967)	S.COSTA
M0507004	26-Fe	54	γ, abs	19.5	147.69	5.5	23.00	787.3	41.3	Austr.J.Phys.31.471(1978)	J.W.NORBURY
	26-Fe	54	γ, n	19.2	38.	6.9	31.00	290.		Austr.J.Phys.10.312(1957)	J.H.CARVER
M0273004	26-Fe	54	$\gamma, 1n$	19.	67.	7.	24.00	401.3	20.9	Can.J.Phys.29.518(1951)	L.KATZ
M0024002	26-Fe	54	γ, n	19.25	31.9	7.	26.50	215.8	10.6	Nucl.Phys.A285.71(1977)	B.S.RATNER
M0507002	26-Fe	54	$\gamma, 1n$	17.85	67.03	5.5	23.00	301.1	16.3	Austr.J.Phys.31.471(1978)	J.W.NORBURY
M0507002				19.64	55.17						
M0507003	26-Fe	54	γ, p	19.5	95.34	6.	23.00	487.3	25.2	Austr.J.Phys.31.471(1978)	J.W.NORBURY
	26-Fe	56	γ, p	20.	45.	5.				J.Phys.Soc.Jap.25.664(1968)	K.SHODA
	27-Co	59	γ, abs	18.6	92.	9.3	35.00	1030.	50.	Phys.Rev.137.B576(1965)	J.M.WYCKOFF
L0028006	27-Co	59	γ, xn	16.52	75.67	14.	36.50	965.		Phys.Rev.C20.128(1979)	R.A.ALVAREZ
L0028006				18.825	73.						
	27-Co	59	γ, xn	16.5	86.	7.5	30.00	1030.		Izv.AN SSSR.33.1736(1969)	B.I.GORYACHEV
				18.5	81.						
				20.5	76.						
	27-Co	59	γ, xn	17.5	69.	11.				Phys.Rev.128.2345(1962)	S.C.FULTZ
	27-Co	59	γ, xn	16.75	109.	6.	25.00	709.		Phys.Rev.120.1424(1960)	P.A.FLOURNOY
				18.75	92.						
M0541009	27-Co	59	γ, xn	16.5	72.	6.	28.00	657.		Nucl.Phys.67.178(1965)	G.BACIU
				19.	74.						
L0028008	27-Co	59	γ, n	16.52	75.67	7.	36.50	653.		Phys.Rev.C20.128(1979)	R.A.ALVAREZ
L0028008				18.825	73.04						
L0001006	27-Co	59	γ, n	17.64	68.5	6.	28.00	447.		Phys.Rev.128.2345(1962)	S.C.FULTZ
L0028009	27-Co	59	$\gamma, 2n$	22.209	19.16	7.	36.50	150.		Phys.Rev.C20.128(1979)	R.A.ALVAREZ
L0028009				26.574	13.31						
L0001007	27-Co	59	$\gamma, 2n$	25.93	24.2	7.	28.00	139.		Phys.Rev.128.2345(1962)	S.C.FULTZ
L0001007				22.86	22.						
	27-Co	59	$\gamma, 2n$	20.5	19.5.	7.5				Nucl.Phys.67.178(1965)	G.BACIU
				25.5	19.						
L0028010	27-Co	59	$\gamma, 3n$	36.136	4.52	>2.	36.50	4.		Phys.Rev.C20.128(1979)	R.A.ALVAREZ
	27-Co	59	γ, p	20.5	26.	>12.	29.00	353.		Nucl.Phys.A303.333(1978)	H.TSUBOTA
	28-Ni		γ, abs	18.7	89.	7.5	35.00	920.	44.	Phys.Rev.137.B576(1965)	J.M.WYCKOFF
	28-Ni		γ, xn	16.8	42.5	6.5	24.00	283.		Phys.Rev.L.21.1200(1968)	K.MIN
	28-Ni		γ, xn	17.8	43.	6.5				Nuov.Cim.54B.344(1968)	S.COSTA
	28-Ni		γ, xn	16.5	46.	5.	24.00	276.		Nucl.Phys.67.178(1965)	G.BACIU
							28.00	313.			
	27-Co	59	γ, sn	16.52	75.67	7.	36.50	807.	40.1	Phys.Rev.C20.128(1979)	R.A.ALVAREZ

EXFOR	Nucl	A	Reac	E_{max} MeV	σ_{max} mb	FWHM MeV	E_{int} MeV	σ_{int} MeV * mb	σ^1_{int} mb	Reference	Author
	27-Co	59	γ, sn	16.5	86.	7.5	30.00	740.		Izv.AN SSSR,33,1736(1969)	B.I.GORYACHEV
				18.5	81.						
				20.5	55.						
	27-Co	59	γ, sn	17.6	69.	7.5	28.00	586.		Phys.Rev 128,2345(1962)	S.C.FULTZ
	28-Ni		$\gamma, 2n$	23.	5.6	5.				Nucl.Phys.67,178(1965)	G.BACIU
	28-Ni	58	γ, xn	17.3	26.7	8.	33.50	294.		Phys.Rev.C10,608(1974)	S.C.FULTZ
	28-Ni	58	γ, xn	20.3	31.	7.	30.00	310.		Yad.Fiz.10,252(1969)	B.S.ISHKHANOV
				17.8	23.5						
	28-Ni	58	γ, xn	16.7	26.	6.	24.00	185.		Phys.Rev.L.21,1200(1968)	K.MIN
L0034002	28-Ni	58	γ, sn	17.298	26.7	8.	33.50	286.	13.8	Phys.Rev.C10,608(1974)	S.C.FULTZ
L0034002				22.623	23.16						
L0034003	28-Ni	58	γ, n	17.29	26.7	8.	33.50	278.		Phys.Rev.C10,608(1974)	S.C.FULTZ
L0034003				22.623	23.3						
M0273005	28-Ni	58	γ, n	19.	54.	6	22.00	316.	18.	Can.J.Phys.29,518(1951)	L.KATZ
	28-Ni	58	γ, np	19.5	125.	4.8	32.00	840.		Proc.Phys.Soc.73,585(1959)	J.H.CARVER
L0034004	28-Ni	58	$\gamma, 2n$	24.56	1.9	8.	33.50	7.7		Phys.Rev.C10,608(1974)	S.C.FULTZ
L0034004				29.522	1.51						
	28-Ni	58	γ, p	18.5	60.	9.5	30.00	570.		Yad.Fiz.11,485(1970)	B.S.ISHKHANOV
				16.6	48.5						
				23.3	46.5						
L0034005	28-Ni	60	γ, xn	16.33	74.94	11.	33.20	772.		Phys.Rev C10,608(1974)	S.C.FULTZ
	28-Ni	60	γ, xn	19.1	91.	6.5	30.00	620.		Yad.Fiz.10,252(1969)	B.S.ISHKHANOV
				16.3	73.5						
				17.5	80.5						
				20.6	63.5						
	28-Ni	60	γ, xn	16.8	82.	5.5	24.00	482.		Phys.Rev.L.21,1200(1968)	K.MIN
L0034008	28-Ni	60	γ, sn	16.33	74.95	7.	33.20	700.	35.4	Phys.Rev.C10,608(1974)	S.C.FULTZ
L0034006	28-Ni	60	γ, n	16.33	74.95	7.	33.20	628.		Phys.Rev.C10,608(1974)	S.C.FULTZ
	28-Ni	60	γ, np	19.	90.	5.5	30.00	940.		Yad.Fiz.11,485(1970)	B.S.ISHKHANOV
L0034007	28-Ni	60	$\gamma, 2n$	24.318	10.88	7.	33.20	72.		Phys.Rev C10,608(1974)	S.C.FULTZ
L0034007				28.312	8.71						
L0034007				31.338	5.49						
	28-Ni	60	γ, p	18.4	34.	8.5	30.00	320.		Yad.Fiz.11,485(1970)	B.S.ISHKHANOV
				16.4	26.						
				20.3	31.5						
				23.3	30.						
	29-Cu		γ, abs	17.5	94.	11.5	35.00	1036.	51.	Phys.Rev.137,B576(1965)	J.M.WYCKOFF
	29-Cu		γ, xn	17.8	116.79	13.5	30.00	1200.		Vestn.Mosk.Uni.6,606(1970)	B.S.ISHKHANOV
				16.1	114.72						
				21.4	109.51						
				23.8	105.07						
				25.2	102.15						
				27.4	78.14						
	29-Cu		γ, xn	17.7	86.	7.5	20.00	451.		Nucl.Phys.67,178(1965)	G.BACIU
							28.00	733			
	29-Cu		γ, xn	17.2	78.	8.	24.00	587.		J.Phys.Soc.Jap.25,655(1968)	T.TOMIMASU
L0006002	29-Cu		γ, xn	17.022	71.4	11.	27.80	710.		Phys.Rev.B133,1149(1964)	S.C.FULTZ
	29-Cu		γ, xn	16.1	90.3	>7.	19.60	450.		Nucl.Phys.32,236(1962)	J.MILLER
L0006011	29-Cu		γ, sn	17.022	71.4	8.	27.80	604.	33.8	Phys.Rev.B133,1149(1964)	S.C.FULTZ
	29-Cu		γ, sn	17.8	116.79	8.5				Vestn.Mosk.Uni.6,606(1970)	B.S.ISHKHANOV
				16.1	114.72						
				18.8	105.39						
				24.	53.49						
L0006003	29-Cu		γ, n	17.022	71.4	7.	27.80	498.		Phys.Rev.B133,1149(1964)	S.C.FULTZ
	29-Cu		γ, n	16.1	114.72	6.5	30.00	624.		Vestn.Mosk.Uni.6,606(1970)	B.S.ISHKHANOV
				21.	59						
				23.5	12						
	29-Cu		$\gamma, 2n$	25.5	44.57	8.5	30.00	288.		Vestn.Mosk.Uni.6,606(1970)	B.S.ISHKHANOV
	29-Cu		$\gamma, 2n$	23.	15.5	7.5				Nucl.Phys.67,178(1965)	G.BACIU
L0006004	29-Cu		$\gamma, 2n$	23.168	16.6	8.	27.80	106.		Phys.Rev.B133,1149(1964)	S.C.FULTZ
	29-Cu		γ, p	18.2	23.	>9.				Phys.Rev.119,748(1960)	R.E CHRIEN
L0006005	29-Cu	63	γ, xn	16.407	69.6	10.5	27.80	680.		Phys.Rev.B133,1149(1964)	S.C.FULTZ
L0006005				22.86	54.3						
	29-Cu	63	γ, sn	16.6	78.6					Yad.Fiz.58,387(1995)	V.V.VARLAMOV
				23.3	34.						
	29-Cu	63	γ, sn	16.5	63.	5.	28.00	764.	38.	Phys.Rev.B133,1149(1964)	S.C.FULTZ
L0006012	29-Cu	63	γ, sn	16.407	69.6	10.	27.80	604.	33.4	Phys.Rev.B133,1149(1964)	S.C.FULTZ
L0006012				22.86	41.5						
M0385002	29-Cu	63	γ, n	16.6	78.6	6.	25.00	510.3	30.	Yad.Fiz.58,387(1995)	V.V.VARLAMOV
L0006006	29-Cu	63	γ, n	16.407	68.5	8.	27.80	528.		Phys.Rev.B133,1149(1964)	S.C.FULTZ
L0006006				22.246	30.4						
L0006006				26.241	14.6						
M0273006	29-Cu	63	γ, n	18.	104.	6.	21.00	618.5	36.7	Can.J.Phys.29,518(1951)	L.KATZ
M0239004	29-Cu	63	γ, n	17.8	70.3	5.5	24.20	482.4	27.8	Yad.Phys.30,294(1979)	L.Z.DZHILAVYAN
M0385003	29-Cu	63	γ, np	23.5	17.5	5.	25.00	75.9	3.5	Yad.Fiz.58,387(1995)	V.V.VARLAMOV
M0026002	29-Cu	63	$\gamma, 1n$	17.77	69.15	6.5	24.30	484.5	27.9	Yad.Fiz.30,294(1979)	L.Z.DZHILAVYAN
	29-Cu	63	$\gamma, 1n$	16.7	92.	6.5				Nucl.Phys.A181,477(1972)	F.DREYER
L0013002	29-Cu	63	$\gamma, 1n$	16.79	78.	6.5	25.10	498.		Phys.Rev.176,1366(1968)	R.E.SUND
L0006007	29-Cu	63	$\gamma, 2n$	25.011	13.6	6.5	27.80	76.		Phys.Rev.B133,1149(1964)	S.C.FULTZ
L0013003	29-Cu	63	$\gamma, 2n$	23.7	10.	6.5	25.10	43.		Phys.Rev.176,1366(1968)	R.E.SUND
M0385004	29-Cu	63	γ, p	20.	34.2	6.	25.00	224.2	12.1	Yad.Fiz.58,387(1995)	V.V.VARLAMOV
L0006008	29-Cu	65	γ, xn	16.714	77.4	10.	27.80	817.		Phys.Rev.B133,1149(1964)	S.C.FULTZ
L0006008				19.787	76.3						
	29-Cu	65	γ, sn	16.8	88.	5.	28.00	766.	53.	Phys.Rev.B133,1149(1964)	S.C.FULTZ
L0006013	29-Cu	65	γ, sn	16.714	77.4	8.	27.80	619.	36.	Phys.Rev.B133,1149(1964)	S.C.FULTZ
L0006009	29-Cu	65	γ, n	16.714	77.5	5.	27.80	421.		Phys.Rev.B133,1149(1964)	S.C.FULTZ
M0273007	29-Cu	65	γ, n	18.	150.	6.5	22.00	1045.	61.9	Can.J.Phys.29,518(1951)	L.KATZ
M0450002	29-Cu	65	γ, n	17.	96.	5.	30.00	530.	30.	Phys.Rev.96,83(1954)	A.I.BERMAN
M0374006	29-Cu	65	γ, np	21.2	10.6	3.	24.40	26.5	1.3	Izv.RAN,54,222(1995)	V.V.VARLAMOV
L0006010	29-Cu	65	$\gamma, 2n$	22.246	30.4	7.	27.80	198.		Phys.Rev.B133,1149(1964)	S.C.FULTZ
L0006010				20.095	29.1						
M0450003	29-Cu	65	$\gamma, 2n$	25.	12.2	4.5	35.00	81.	3.1	Phys.Rev.96,83(1954)	A.I.BERMAN
M0374008	29-Cu	65	γ, p	25.	16.4	7.	28.00	126.6	5.8	Izv.RAN,54,222(1995)	V.V.VARLAMOV
M0374008				20.	11.4						
M0374008				22.2	12.3						
M0037408				27.6	10.8						
	29-Cu	65	γ, p	19.8	30.5	7.				ZHETF,38,780(1960)	N.V.LIN'KOVA
	30-Zn		γ, sn	16.7	91.	4.6	80.00	1607.	66.	Nuov.Cim.48B,461(1967)	S.COSTA
L0043004	30-Zn	64	γ, xn	16.73	71.8	14.	29.50	791.		Nucl.Phys.A258,365(1976)	P.CARLOS

78

EXFOR	Nucl	A	Reac	E_{max} MeV	σ_{max} mb	FWHM MeV	E_{int} MeV	σ_{int} MeV * mb	σ_{int}^{1} mb	Reference	Author
L0043004				18.9	71.3						
	30-Zn	64	γ, xn	16.2	52.	9.5				Izv.AN SSSR,39,134(1975)	A.M.GORYACHEV
				19.	49.						
	30-Zn	64	γ, xn	15.9	90.5	8.5.	27.00	800.		Yad.Fiz.20,433(1974)	B.S.ISHKHANOV
				18.	90.						
				20.2	76.						
	30-Zn	64	γ, sn	16.73	71.8	13.	29.50	750.	38.1	Nucl.Phys.A258,365(1976)	P.CARLOS
L0043002	30-Zn	64	γ, n	16.73	71.8	13.	29.50	703.		Nucl.Phys.A258,365(1976)	P.CARLOS
L0043002				18.9	70.7						
	30-Zn	64	γ, n	17.2	48.	7.	23.00	330.		Can.J.Phys.38,320(1960)	J.P.ROALSVIG
M0273008	30-Zn	64	γ, n	18.	123.	8.	23.00	93.	53.9	Can.J.Phys.29,518(1951)	L.KATZ
M0070002	30-Zn	64	γ, n	16.42	49.5	8.5	24.20	381.2	21.4	Vop.Teor.Y.Fiz.8,121(1982)	A.M.GORYACHEV
M0070002				19.02	44.2						
M0070002				22.42	33.1						
L0043003	30-Zn	64	$\gamma, 2n$	24.86	7.2	10.	29.50	44.		Nucl.Phys.A258,365(1976)	P.CARLOS
L0043003				22.96	6.5						
L0043003				28.11	6.4						
	30-Zn	66	γ, xn	16.2	80.	9.5				Izv.AN SSSR,39,134(1975)	A.M.GORYACHEV
				18.	61.						
M0070003	30-Zn	66	γ, n	16.42	76.6	7.	24.20	573.3	33.	Vop.Teor.Y.Fiz.8,121(1982)	A.M.GORYACHEV
M0042002	30-Zn	67	γ, n	16.62	93.9	7.	24.20	755.8	44.1	Izv.KAZSSR,6,16(1980)	A.M.GORYACHEV
M0070004	30-Zn	67	γ, n	17.02	93.7	6.5	24.40	755.8	44.1	Vop.Teor.Y.Fiz.8,121(1982)	A.M.GORYACHEV
	30-Zn	67	γ, p	22.	18.	8.	28.00	118.		Pisma ZHETF,11,452(1966)	V.G.IVANCHENKO
	30-Zn	68	γ, xn	16.2	92.	9.5				Izv.AN SSSR,39,134(1975)	A.M.GORYACHEV
	30-Zn	68	γ, xn	16.	150.	9.	27.00	1630.		Yad.Fiz.20,433(1974)	B.S.ISHKHANOV
				18.	117.						
				20.2	107.						
M0070005	30-Zn	68	γ, n	17.22	91.2	7.5	24.20	732.	42.6	Vop.Teor.Y.Fiz.8,121(1982)	A.M.GORYACHEV
M0042003	30-Zn	70	γ, n	17.25	97.7	7.	24.40	828.5	48.6	Izv.KAZSSR,6,16(1980)	A.M.GORYACHEV
M0070006	30-Zn	70	γ, n	17.25	97.7	7.	24.40	828.5	48.6	Vop.Teor.Y.Fiz.8,121(1982)	A.M.GORYACHEV
L0043007	31-Ga		γ, xn	16.97	113.4	11.	26.50	1108.		Nucl.Phys.A258,365(1976)	P.CARLOS
	31-Ga		γ, xn	16.5	115.	8.	28.00	947.		Nucl.Phys.67,178(1965)	G.BACIU
	31-Ga		γ, sn	16.97	115.4	8.	26.50	910.	52.	Nucl.Phys.A258,365(1976)	P.CARLOS
L0043005	31-Ga		γ, n	16.97	115.1	5.5	26.50	716.		Nucl.Phys.A258,365(1976)	P.CARLOS
L0043006	31-Ga		$\gamma, 2n$	20.49	33.1	7.5	26.50	196.		Nucl.Phys.A258,365(1976)	P.CARLOS
	32-Ge		γ, xn	17.5	158.		80.00	2495.	102.	Phys.Lett.10,324(1964)	S.COSTA
L0043010	32-Ge	70	γ, xn	15.89	91.6	10.	26.50	856.		Nucl.Phys.A258,365(1976)	P.CARLOS
	32-Ge	70	γ, xn	16.	92.	9.5				Izv.AN SSSR,39,134(1975)	A.M.GORYACHEV
	32-Ge	70	γ, sn	15.89	91.6	8.	26.50	780.	43.2	Nucl.Phys.A258,365(1976)	P.CARLOS
L0043008	32-Ge	70	γ, n	15.89	91.6	7.5	26.50	687.		Nucl.Phys.A258,365(1976)	P.CARLOS
	32-Ge	70	γ, n	17.5	158.	8.6				Nucl.Phys.15,436(1960)	F.FERRERO
M0070007	32-Ge	70	γ, n	15.82	90.1	7.5	24.20	717.8	41.4	Vop.Teor.Y.Fiz.8,121(1982)	A.M.GORYACHEV
M0070007				20.02	72.						
M0497003	32-Ge	70	γ, np	29.	7.	6.	42.00	46.9	1.6	Nucl.Phys.A213,371(1973)	J.J.MCCARTHY
M0497002	32-Ge	70	γ, p	24.	8.3	6.	40.00	92.	3.9	Nucl.Phys.A213,371(1973)	J.J.MCCARTHY
L0043009	32-Ge	70	$\gamma, 2n$	22.66	21.3	6.5	26.50	84.		Nucl.Phys.A258,365(1976)	P.CARLOS
L0043009				24.02	18.8						
L0043009				25.64	15.4						
L0043013	32-Ge	72	γ, xn	16.16	111.3	13.	26.50	1133.		Nucl.Phys.A258,365(1976)	P.CARLOS
L0043013				19.41	97.7						
L0043013				21.58	97.6						
	32-Ge	72	γ, xn	16.6	90.	9.5				Izv.AN SSSR,39,134(1975)	A.M.GORYACHEV
	32-Ge	72	γ, sn	16.16	111.3	10.	26.50	940.	53.5	Nucl.Phys.A258,365(1976)	P.CARLOS
L0043011	32-Ge	72	γ, n	16.16	111.3	7.5	26.50	737.		Nucl.Phys.A258,365(1976)	P.CARLOS
L0043011				21.85	32.4						
M0070008	32-Ge	72	γ, n	16.2	89.8	8.	24.20	732.5	43.9	Vop.Teor.Y.Fiz.8,121(1982)	A.M.GORYACHEV
M0070008				22.22	58.						
M0497004	32-Ge	72	γ, np	22.	5.6	5.5	40.00	38.9	1.6	Nucl.Phys.A213,371(1973)	J.J.MCCARTHY
L0043012	32-Ge	72	$\gamma, 2n$	21.04	36.7	7.	26.50	198.		Nucl.Phys.A258,365(1976)	P.CARLOS
M0042004	32-Ge	73	γ, n	17.02	92.3	8.	24.40	785.9	46.3	Izv.KAZSSR,6,16(1980)	A.M.GORYACHEV
M0070009	32-Ge	73	γ, n	17.02	92.3	8.	24.40	785.9	46.3	Vop.Teor.Y.Fiz.8,121(1982)	A.M.GORYACHEV
L0043016	32-Ge	74	γ, xn	19.41	128.1	13.	26.50	1322.		Nucl.Phys.A258,365(1976)	P.CARLOS
	32-Ge	74	γ, xn	16.2	115.	9.5				Izv.AN SSSR,39,134(1975)	A.M.GORYACHEV
	32-Ge	74	γ, sn	16.7	109.8	8.5	26.50	1020.	58.8	Nucl.Phys.A258,365(1976)	P.CARLOS
L0043014	32-Ge	74	γ, n	16.7	109.8	6.	26.50	704.		Nucl.Phys.A258,365(1976)	P.CARLOS
M0070010	32-Ge	74	γ, n	16.02	101.4	9.	24.20	899.8	53.	Vop.Teor.Y.Fiz.8,121(1982)	A.M.GORYACHEV
M0070010				22.62	72.3						
L0043015	32-Ge	74	$\gamma, 2n$	20.49	49.	7.5	26.50	309.		Nucl.Phys.A258,365(1976)	P.CARLOS
L0043019	32-Ge	76	γ, xn	18.33	146.1	11	26.50	1487.		Nucl.Phys.A258,365(1976)	P.CARLOS
	32-Ge	76	γ, sn	15.34	110.3	10.	26.50	1120.	63.8	Nucl.Phys.A258,365(1976)	P.CARLOS
L0043017	32-Ge	76	γ, n	15.34	110.3	5.	26.50	733.		Nucl.Phys.A258,365(1976)	P.CARLOS
L0043017				25.64	25.4						
M0070011	32-Ge	76	γ, n	16.02	109.1	7.5	24.20	934.8	55.2	Vop.Teor.Y.Fiz.8,121(1982)	A.M.GORYACHEV
M0070011				22.42	74.9						
M0497005	32-Ge	76	γ, np	34.	2.2	8.5	39.00	20.	.6	Nucl.Phys.A213,371(1973)	J.J.MCCARTHY
L0043018	32-Ge	76	$\gamma, 2n$	19.95	52.9	8.	26.50	377.		Nucl.Phys.A258,365(1976)	P.CARLOS
L0043022	33-As	75	γ, xn	16.16	119.9	13.	26.20	1306.		Nucl.Phys.A258,365(1976)	P.CARLOS
L0043022				19.41	115.						
L0014002	33-As	75	γ, xn	16.22	97.27	11.	29.50	1130.		Phys.Rev.177,1745(1969)	B.L.BERMAN
L0014002				19.937	87.21						
	33-As	75	γ, xn	17.3	90.3	9.	23.00	800.		Phys.Rev.104,1334(1956)	P.F.YERGIN
	33-As	75	γ, sn	16.16	119.9	10.	26.20	1090.	62.7	Nucl.Phys.A258,365(1976)	P.CARLOS
L0014012	33-As	75	γ, sn	16.22	97.27	8.	29.50	909.	51.4	Phys.Rev.177,1745(1969)	B.L.BERMAN
L0043020	33-As	75	γ, n	16.16	119.9	6.5	26.20	872.		Nucl.Phys.A258,365(1976)	P.CARLOS
L0014003	33-As	75	γ, n	16.22	97.18	6.5	29.50	688.		Phys.Rev.177,1745(1969)	B.L.BERMAN
L0014003				27.989	17.38						
L0043021	33-As	75	$\gamma, 2n$	21.58	40.6	7.	26.20	217.		Nucl.Phys.A258,365(1976)	P.CARLOS
L0043021				25.37	27.2						
L0014004	33-As	75	$\gamma, 2n$	21.485	32.65	7.5	29.50	221.		Phys.Rev.177,1745(1969)	B.L.BERMAN
L0014004				21.556	31.39						
L0014004				26.44	19.32						
	34-Se		γ, xn	15.5	118.	5.2				Nuov.Cim.51B,199(1967)	S.COSTA
M0042005	34-Se	74	γ, n	15.71	89.	6.	24.20	639.2	37.	Izv.KAZSSR,6,16(1980)	A.M.GORYACHEV
M0070012	34-Se	74	γ, n	15.71	89.	6.5	24.40	639.2	37.	Vop.Teor.Y.Fiz.8,121(1982)	A.M.GORYACHEV
M0023002	34-Se	76	γ, abs	16.05	164.	5.9	19.70	922.1	60.8	Probl.Yad.Fiz.8,106(1978)	G.M.GUREVICH
M0023002				12.5	75.5						
M0023002				15.1	155.5						
L0043025	34-Se	76	γ, xn	15.34	108.2	12.5	26.50	1177.		Nucl.Phys.A258,365(1976)	P.CARLOS
L0043025				20.76	96.4						
	34-Se	76	γ, xn	15.9	109.	9.				Izv.AN SSSR,39,134(1975)	A.M.GORYACHEV

EXFOR	Nucl	A	Reac	E_{max} MeV	σ_{max} mb	FWHM MeV	E_{int} MeV	σ_{int} MeV * mb	σ^1_{int} mb	Reference	Author
	34-Se	76	γ,sn	15.34	108.2	10.5	26.50	1010.	57.	Nucl.Phys.A258.365(1976)	P.CARLOS
L0043023	34-Se	76	γ,n	15.34	108.2	7.5	26.50	815.		Nucl.Phys.A258.365(1976)	P.CARLOS
L0043023				17.51	105.8						
M0070013	34-Se	76	γ,n	15.42	108.1	8.5	24.2	938.4	54.9	Vop.Teor.Y.Fiz.8.121(1982)	A.M.GORYACHEV
M0070013				21.82	68.						
L0043024	34-Se	76	γ,2n	21.58	35.7	6.5	26.50	181.		Nucl.Phys.A258.365(1976)	P.CARLOS
L0043024				24.56	31.2						
M0042006	34-Se	77	γ,n	15.82	105.3	8.5	24.40	944.9	56.3	Izv.KAZSSR.6.16(1980)	A.M.GORYACHEV
M0070014	34-Se	77	γ,n	15.82	105.3	8.5	24.40	944.7	56.3	Vop.Teor.Y.Fiz.8.121(1982)	A.M.GORYACHEV
L0043028	34-Se	78	γ,xn	15.62	126.3	10.	26.50	1322.		Nucl.Phys.A258.365(1976)	P.CARLOS
L0043028				19.41	125.5						
	34-Se	78	γ,xn	16.2	132.	9.				Izv.AN SSSR.39.134(1975)	A.M.GORYACHEV
	34-Se	78	γ,sn	15.62	126.3	8.	26.50	1060.	61.4	Nucl.Phys.A258.365(1976)	P.CARLOS
L0043026	34-Se	78	γ,n	15.62	126.3	5.5	26.50	778.		Nucl.Phys.A258.365(1976)	P.CARLOS
M0070015	34-Se	78	γ,n	15.82	126.	8.5	24.20	1033.4	61.	Vop.Teor.Y.Fiz.8.121(1982)	A.M.GORYACHEV
L0043027	34-Se	78	γ,2n	21.58	47.5	7.5	26.50	272.		Nucl.Phys.A258.365(1976)	P.CARLOS
L0043031	34-Se	80	γ,xn	18.6	155.11	11.	28.10	1527.		Nucl.Phys.A258.365(1976)	P.CARLOS
L0043031				16.43	140.8						
	34-Se	80	γ,xn	16.7	142.	9.				Izv.AN SSSR.39.134(1975)	A.M.GORYACHEV
	34-Se	80	γ,sn	15.89	137.	7.5	28.10	1110.	65.9	Nucl.Phys.A258.365(1976)	P.CARLOS
L0043029	34-Se	80	γ,n	15.89	137.	6.	28.10	749.		Nucl.Phys.A258.365(1976)	P.CARLOS
M0070016	34-Se	80	γ,n	17.02	138.1	8.	24.20	1045.9	61.9	Vop.Teor.Y.Fiz 8.121(1982)	A.M.GORYACHEV
M0070016				15.62	132.9						
L0043030	34-Se	80	γ,2n	20.22	60.6	5.5	28.10	389.		Nucl.Phys.A258.365(1976)	P.CARLOS
L0043030	34-Se	80	γ,2n	19.14	54.3	5.5	28.10	389.		Nucl.Phys.A258.365(1976)	P.CARLOS
L0043030				21.04	52.8						
M0023003	34-Se	82	γ,abs	15.9	195.	5.1	19.90	1049.2	68.5	Probl.Yad.Fiz.8.106(1978)	G.M.GUREVICH
M0023003				12.	66.5						
L0043034	34-Se	82	γ,xn	18.05	190.9	7.	26.50	1521.		Nucl.Phys.A258.365(1976)	P.CARLOS
	34-Se	82	γ,xn	16.	152.	9.				Izv.AN SSSR.39.134(1975)	A.M.GORYACHEV
	34-Se	82	γ,sn	15.89	142.7	6.5	26.50	1130	66.4	Nucl.Phys.A258.365(1976)	P.CARLOS
L0043032	34-Se	82	γ,n	15.89	142.7	4.	26.50	727.		Nucl.Phys.A258.365(1976)	P.CARLOS
L0043032				23.47	17.8						
M0070017	34-Se	82	γ,n	16.22	151.8	8.	24.20	1087.7	64.7	Vop.Teor.Y.Fiz.8.121(1982)	A.M.GORYACHEV
M0070017				22.62	67.						
L0043033	34-Se	82	γ,2n	18.87	62.6	6.	26.50	397.		Nucl.Phys.A258.365(1976)	P.CARLOS
L0027002	37-Rb		γ,xn	16.805	194.	4.5	24.30	1242.		Nucl.Phys.A175.609(1971)	A.LEPRETRE
L0027017	37-Rb		γ,sn	16.805	194.	4.5	24.30	1147.	67.1	Nucl.Phys.A175.609(1971)	A.LEPRETRE
L0027003	37-Rb		γ,n	16.805	194.	4.5	24.30	1052.		Nucl.Phys.A175.609(1971)	A.LEPRETRE
L0027004	37-Rb		γ,2n	22.117	26.	>5	24.30	95.		Nucl.Phys.A175.609(1971)	A.LEPRETRE
	38-Sr		γ,xn	16.8	170.	9.				Nucl.Phys.A159.265(1970)	R.S.HICKS
L0027005	38-Sr		γ,xn	16.669	210.	7.	27.00	1553		Nucl.Phys.A175.609(1971)	A.LEPRETRE
L0027018	38-Sr		γ,sn	16.669	210.	5.5	27.00	1432.	80.3	Nucl.Phys.A175.609(1971)	A.LEPRETRE
L0027006	38-Sr		γ,n	16.669	210.	5.5	27.00	1311.		Nucl.Phys.A175.609(1971)	A.LEPRETRE
L0027007	38-Sr		γ,2n	25.113	24.	5.5	27.00	121.		Nucl.Phys.A175.609(1971)	A.LEPRETRE
L0027007				22.525	21.						
M0070018	38-Sr	84	γ,n	16.71	156.8	7.	24.40	1010.3	58.	Vop.Teor.Y.Fiz.8.121(1982)	A.M.GORYACHEV
	38-Sr	86	γ,xn	15.9	160.	5.	23.00	920.		Phys.Rev.104.1334(1956)	P.F.YERGIN
M0070019	38-Sr	86	γ,n	16.56	179.4	6.	24.40	1038.3	60.3	Vop.Teor.Y.Fiz.8.121(1982)	A.M.GORYACHEV
	38-Sr	87	γ,xn	15.8	146.	5.3	23.00	1000.		Phys.Rev.104.1334(1956)	P.F.YERGIN
M0070020	38-Sr	87	γ,n	16.75	195.8	4.5	24.40	1114.2	65.6	Vop.Teor.Y.Fiz.8.121(1982)	A.M.GORYACHEV
	38-Sr	88	γ,xn	16.3	201.	4.	23.00	1050.		Phys.Rev.104.1334(1956)	P.F.YERGIN
M0070021	38-Sr	88	γ,n	16.85	207.	5.	24.40	1112.8	64.7	Vop.Teor.Y.Fiz.8.121(1982)	A.M.GORYACHEV
L0027008	39-Y	89	γ,xn	16.669	225.	4.5	27.00	1427.		Nucl.Phys.A175.609(1971)	A.LEPRETRE
M0164002	39-Y	89	γ,xn	16.4	271.	3.7	30.00	1504.7	83.5	Izv.AN SSSR.34.2232(1970)	B.S.ISHKHANOV
M0164002				15.6	239.						
M0164002				17.	215.						
L0011002	39-Y	89	γ,xn	16.685	184.5	4.5	28.00	1158.		Phys.Rev.162.1098(1967)	B.L.BERMAN
	39-Y	89	γ,xn	16.3	191	4.	23.00	870.		Phys.Rev.104.1334(1956)	P.F.YERGIN
L0027019	39-Y	89	γ,sn	16.669	225.	4.5	27.00	1360.	76.5	Nucl.Phys.A175.609(1971)	A.LEPRETRE
	39-Y	89	γ,sn	16.	270.	3.7	29.00	1360.		Izv.AN SSSR.34.2232(1970)	B.S.ISHKHANOV
L0011018	39-Y	89	γ,sn	16.69	184.4	4.5	28.00	1059.	59.8	Phys.Rev.162.1098(1967)	B.L.BERMAN
L0027009	39-Y	89	γ,n	16.669	225.	4.5	27.00	1279.		Nucl.Phys.A175.609(1971)	A.LEPRETRE
L0011003	39-Y	89	γ,n	16.685	184.3	4.5	28.00	960		Phys.Rev.162.1098(1967)	B.L.BERMAN
L0059002	39-Y	89	γ,1n	17.118	211.31	4.	18.10	641.	40.	T.YOUNG.72	L.M.YOUNG
L0027010	39-Y	89	γ,2n	25.386	18.3	>8.	27.00	74.		Nucl.Phys.A175.609(1971)	A.LEPRETRE
L0011004	39-Y	89	γ,2n	23.344	19.38		28.00	99.		Phys.Rev.162.1098(1967)	B.L.BERMAN
L0011004				25.821	19.68						
	40-Zr		γ,xn	16.851	190.29	4.4	19.70	1079.		Phys.Rev.C36.1286(1987)	B.L.BERMAN
L0057004	40-Zr		γ,sn	16.851	190.29	4.4	19.70	991.	68.	Phys.Rev.C36.1286(1987)	B.L.BERMAN
L0057002	40-Zr		γ,n	16.373	158.92	>4.	19.70	903.		Phys.Rev.C36.1286(1987)	B.L.BERMAN
L0057003	40-Zr		γ,2n	17.329	26.92	>5.	19.70	88.		Phys.Rev.C36.1286(1987)	B.L.BERMAN
	40-Zr	90	γ,xn	16.5	205.	4.5				Nucl.Phys.A204.209(1973)	H.J.ASKIN
	40-Zr	90	γ,xn	16.	200.	3.7	28.00	950.		Yad.Fiz.14.27(1971)	B.S.ISHKHANOV
L0027011	40-Zr	90	γ,xn	16.669	215.	4.5	25.90	1309.		Nucl.Phys.A175.609(1971)	A.LEPRETRE
	40-Zr	90	γ,xn	16.5	175.	4.	22.50	1270.		Izv.AN SSSR.33.700(1969)	G.P.ANTROPOV
L0011005	40-Zr	90	γ,xn	16.724	180.	4.5	27.60	1158.		Phys.Rev.162.1098(1967)	B.L.BERMAN
	40-Zr	90	γ,xn	15.8	199.	4.5	23.00	980		Phys.Rev.104.1334(1956)	P.F.YERGIN
	40-Zr	90	γ,sn	16.	200.	3.7	28.00	930.		Yad.Fiz.14.27(1971)	B.S.ISHKHANOV
	40-Zr	90	γ,sn	16.67	215.	4.5	25.90	1260.	70.8	Nucl.Phys.A175.609(1971)	A.LEPRETRE
L0011019	40-Zr	90	γ,sn	16.724	180.	4.5	27.60	1060.	59.1	Phys.Rev.162.1098(1967)	B.L.BERMAN
L0027012	40-Zr	90	γ,n	16.669	215.	4.5	25.90	1211.		Nucl.Phys.A175.609(1971)	A.LEPRETRE
L0011006	40-Zr	90	γ,n	16.724	180.	4.5	27.60	962.		Phys.Rev.162.1098(1967)	B.L.BERMAN
	40-Zr	90	γ,2n	25.5	17.5	>8.				Phys.Rev.C13.1852(1976)	D.BRAJNIK
L0027013	40-Zr	90	γ,2n	24.568	19.	>8.	25.90	49.		Nucl.Phys.A175.609(1971)	A.LEPRETRE
L0027013				23.751	18.						
L0011007	40-Zr	90	γ,2n	25.124	22.6	>8.	27.60	98.		Phys.Rev.162.1098(1967)	B.L.BERMAN
M0125002	40-Zr	90	γ,p	21.5	30.	6.	30.50	159.1.	7.2	Phys.Lett.10.310(1964)	I.I.DUSHKOV
	40-Zr	90	γ,p	16.3	35.5	7.5				Phys.Rev.C13.1852(1976)	D.BRAJNIK
				20.3	33.3						
	40-Zr	91	γ,xn	16.	200.	4.2	22.50	1420.		Izv.AN SSSR.33.700(1969)	G.P.ANTROPOV
L0011008	40-Zr	91	γ,xn	16.84	188.29	4.5	30.00	1303.		Phys.Rev.162.1098(1967)	B.L.BERMAN
L0011008				21.021	85.31						
	40-Zr	91	γ,xn	16.5	200.	5.	23.00	1220.		Phys.Rev.104.1334(1956)	P.F.YERGIN
L0011020	40-Zr	91	γ,sn	16.84	188.25	4.5	30.00	1103.	65.4	Phys.Rev.162.1098(1967)	B.L.BERMAN
L0011009	40-Zr	91	γ,n	16.84	188.21	4.5	30.00	903.		Phys.Rev.162.1098(1967)	B.L.BERMAN
L0011010	40-Zr	91	γ,2n	21.65	30.4	9.	30.00	200.		Phys.Rev.162.1098(1967)	B.L.BERMAN
L0011010				23.37	25.75						
L0011010				24.88	24.3						
L0011011	40-Zr	92	γ,xn	17.459	207.5	6.5	27.80	1543.		Phys.Rev.162.1098(1967)	B.L.BERMAN

EXFOR	Nucl	A	Reac	E_{max} MeV	σ_{max} mb	FWHM MeV	E_{int} MeV	σ_{int} MeV * mb	σ^1_{int} mb	Reference	Author
	40-Zr	92	γ,xn	16.9	193.	5.5	23.00	1240.		Phys.Rev.104,1334(1956)	P.F.YERGIN
L0011021	40-Zr	92	γ,sn	154.911	177.24	6.5	27.80	1091.	64.2	Phys.Rev.162,1098(1967)	B.L.BERMAN
L0011012	40-Zr	92	γ,n	15.911	169.	4.	27.80	639.		Phys.Rev.162,1098(1967)	B.L.BERMAN
L0011013	40-Zr	92	$\gamma,2n$	17.924	69.74	6.	27.80	452.		Phys.Rev.162,1098(1967)	B.L.BERMAN
L0011013				21.021	58.11						
L0011013				23.576	28.14						
L0011014	40-Zr	94	γ,xn	16.99	244.5	5.	31.10	1767.		Phys.Rev.162,1098(1967)	B.L.BERMAN
L0011022	40-Zr	94	γ,sn	16.69	167.	5.	31.10	1121.	68.5	Phys.Rev.162,1098(1967)	B.L.BERMAN
L0011015	40-Zr	94	γ,n	15.15	135.9	3.5	31.10	508.		Phys.Rev.162,1098(1967)	B.L.BERMAN
L0011016	40-Zr	94	$\gamma,2n$	17.775	101.75	5.	31.10	578.1	29.7	Phys.Rev.162,1098(1967)	B.L.BERMAN
L0011016				23.04	40.5						
L0011016				25.6	32.7						
L0011017	40-Zr	94	$\gamma,3n$	28.3	12.9	4.5	31.10	33.		Phys.Rev.162,1098(1967)	B.L.BERMAN
L0027014	41-NB	93	γ,xn	17.622	207.	8.	24.30	1610.		Nucl.Phys.A175.609(1971)	A.LEPRETRE
	41-NB	93	γ,xn	17.	195.	6.5	23.00	1460.		Phys.Rev.104,1334(1956)	P.F.YERGIN
	41-NB	93	γ,sn	16.26	200.	6.5	24.30	1331.	78.5	Nucl.Phys.A175.609(1971)	A.LEPRETRE
L0027015	41-NB	93	γ,n	16.26	200.	4.	24.30	1052.		Nucl.Phys.A175.609(1971)	A.LEPRETRE
L0027016	41-NB	93	$\gamma,2n$	20.21	52.	6.5	24.30	279.		Nucl.Phys.A175.609(1971)	A.LEPRETRE
M0126002				23.03	26.						
M0126002				19.65	24.56						
M0126002				21.42	20.48						
M0126002				26.59	12.48						
L0032002	42-Mo	92	γ,xn	16.73	163.8	6.	29.50	1109.		Nucl.Phys.A227.427(1974)	H.BEIL
	42-Mo	92	γ,xn	16.4	170.	5.	30.00	1290.		Yad.Fiz.11,702(1970)	B.S.ISHKHANOV
L0032020	42-Mo	92	γ,sn	16.73	163.8	6.	29.50	1079.	57.4	Nucl.Phys.A227.427(1974)	H.BEIL
L0032003	42-Mo	92	γ,n	16.73	163.8	6.	29.50	1049.		Nucl.Phys.A227.427(1974)	H.BEIL
L0032004	42-Mo	92	$\gamma,2n$	25.67	8.2	>9.	29.50	30.		Nucl.Phys.A227.427(1974)	H.BEIL
L0032021	42-Mo	94	γ,xn	16.19	187.2	8.	28.40	1665.		Nucl.Phys.A227.427(1974)	H.BEIL
L0032005	42-Mo	94	γ,sn	16.19	189.5	6.5	28.40	1352.	78.3	Nucl.Phys.A227.427(1974)	H.BEIL
L0032006	42-Mo	94	γ,n	16.19	184.9	6.5	28.40	1039.		Nucl.Phys.A227.427(1974)	H.BEIL
L0032007	42-Mo	94	$\gamma,2n$	19.98	49.9	10.	28.40	313.		Nucl.Phys.A227.427(1974)	H.BEIL
L0032008	42-Mo	96	γ,xn	16.46	193.7	10.	27.80	1921.		Nucl.Phys.A227.427(1974)	H.BEIL
L0032022	42-Mo	96	γ,sn	16.46	192.1	6.5	27.80	1483.	87.6	Nucl.Phys.A227.427(1974)	H.BEIL
L0032009	42-Mo	96	γ,n	16.46	190.6	5.	27.80	1045.		Nucl.Phys.A227.427(1974)	H.BEIL
L0032010	42-Mo	96	$\gamma,2n$	19.17	67.9	6.5	27.80	438.		Nucl.Phys.A227.427(1974)	H.BEIL
L0032011	42-Mo	96	$\gamma,3n$	29.19	12.9		29.20	3.4		Nucl.Phys.A227.427(1974)	H.BEIL
L0032012	42-Mo	98	γ,xn	17.	235.4	8.	26.80	2100.		Nucl.Phys.A227.427(1974)	H.BEIL
	42-Mo	98	γ,xn	16.8	280.	5.	30.00	2000.		Yad.Fiz.11.702(1970)	B.S.ISHKHANOV
L0032023	42-Mo	98	γ,sn	15.37	195.8	7.	26.80	1518.	92.1	Nucl.Phys.A227.427(1974)	H.BEIL
L0032013	42-Mo	98	γ,n	15.37	194.7	5.	26.80	940.		Nucl.Phys.A227.427(1974)	H.BEIL
L0032014	42-Mo	98	$\gamma,2n$	19.17	86.	8.	26.80	574.		Nucl.Phys.A227.427(1974)	H.BEIL
L0032015	42-Mo	98	$\gamma,3n$	28.11	13.3	>5.	26.80	4.		Nucl.Phys.A227.427(1974)	H.BEIL
L0032015							28.90	22.			
L0032016	42-Mo	100	γ,xn	16.19	261.	8.	27.00	2270.		Nucl.Phys.A227.427(1974)	H.BEIL
	42-Mo	100	γ,sn	15.7	171.	7.5	27.00	1528.	93.6	Nucl.Phys.A227.427(1974)	H.BEIL
L0032017	42-Mo	100	γ,n	14.29	163.4	4.	27.00	811.		Nucl.Phys.A227.427(1974)	H.BEIL
	42-Mo	100	γ,nP	15.	180.	5.6	20.00	1110.		Nucl.Phys.60,343(1964)	R.W.GELLIE
L0032018	42-Mo	100	$\gamma,2n$	18.08	104.8	6.5	27.00	692.		Nucl.Phys.A227.427(1974)	H.BEIL
L0032019	42-Mo	100	$\gamma,3n$	28.38	22.5	>7.	27.00	25.		Nucl.Phys.A227.427(1974)	H.BEIL
L0032019				25.94	13.16						
L0032019				27.3	20.3						
L0035002	45-Rh	103	γ,xn	18.08	199.3	10.	25.80	1948.		Nucl.Phys.A219,39(1974)	A.LEPRETRE
L0035002				15.64	190.						
	45-Rh	103	γ,xn	16.5	205.	9.	23.00	1940.		Phys.Rev.104,1334(1956)	P.F.YERGIN
L0035041	45-Rh	103	γ,sn	15.64	190.9	8.	30.10	1568.	94.7	Nucl.Phys.A219,39(1974)	A.LEPRETRE
	45-Rh	103	γ,sn	17.5	280.	6.	20.00	2130.	123.	ZHETF,42,1502(1962)	BOGDANKEVICH
				14.8	200.						
L0035003	45-Rh	103	γ,n	15.64	190.	5.5	25.80	1188.		Nucl.Phys.A219,39(1974)	A.LEPRETRE
L0035004	45-Rh	103	$\gamma,2n$	19.44	66.	8.	25.80	380.		Nucl.Phys.A219,39(1974)	A.LEPRETRE
	45-Rh	103	γ,p	19.	8.	5.5	32.00	85.		ZHETF,45,38(1963)	B.S.ISHKHANOV
M0166003	45-Rh	103	γ,p	19.	8.	5.5	32.00	85.	3.9	Phys.Lett.10,310(1964)	B.S.ISHKHANOV
M0166003				29.	5.3						
L0035005	46-Pd		γ,xn	17.81	218.6	8.	21.30	1651.		Nucl.Phys.A219,39(1974)	A.LEPRETRE
L0035005				15.92	208.5						
L0035042	46-Pd		γ,sn	15.92	204.8	7.	21.30	1381.	88.5	Nucl.Phys.A219,39(1974)	A.LEPRETRE
L0035006	46-Pd		γ,n	15.92	201.1	5.	21.30	1111.		Nucl.Phys.A219,39(1974)	A.LEPRETRE
L0035007	46-Pd		$\gamma,2n$	18.9	73.5	>7.	21.30	270.		Nucl.Phys.A219,39(1974)	A.LEPRETRE
	46-Pd	108	γ,sn	15.7	210.	5.	25.00	1725.	104.	Yad.Fiz.9,241(1969)	S.V.DEMENTIJ
	46-Pd	108	γ,sn	15.7	215.	8.				Nucl.Phys.A139,501(1969)	T.K.DEAGUE
	46-Pd	108	γ,p	23.	10.	12.				Nucl.Phys.A139,501(1969)	T.K.DEAGUE
	46-Pd	110	γ,n	15.5	16.	7.				Nucl.Phys.A139,501(1969)	T.K.DEAGUE
	47-Ag		γ,abs	15.8	218.	7.5	35.00	2568.	130.	Phys.Rev.137.B576(1965)	J.M.WYCKOFF
L0035008	47-Ag		γ,xn	15.92	198.2	10.	24.90	1922.		Nucl.Phys.A219,39(1974)	A.LEPRETRE
L0035008				18.35	189.3						
L0035043	47-Ag		γ,sn	15.92	198.2	7.5	29.50	1643.	98.8	Nucl.Phys.A219,39(1974)	A.LEPRETRE
L0035009	47-Ag		γ,n	15.92	198.4	7.	24.90	1364.		Nucl.Phys.A219,39(1974)	A.LEPRETRE
L0035010	47-Ag		$\gamma,2n$	20.25	50.7	7.	24.90	279.		Nucl.Phys.A219,39(1974)	A.LEPRETRE
L0014005	47-Ag	107	γ,xn	16.066	159.59	9.5	29.50	1619.		Phys.Rev.177,1745(1969)	B.L.BERMAN
	47-Ag	107	γ,xn	16.	250.	6.5				ZHETF,42,1502(1962)	BOGDANKEVICH
L0014013	47-Ag	107	γ,sn	16.066	159.59	7.	29.50	1356.	78.7	Phys.Rev.177,1745(1969)	B.L.BERMAN
M0524002	47-Ag	107	γ,sn	16.1	195.98	7.5	30.00	1620.	95.3	Izv.AN SSSR,33,2074(1969)	B.S.ISHKHANOV
M0524002				17.7	189.35						
M0524002				24.1	65.33						
	47-Ag	107	γ,xn	16.	245.	5.				ZHETF,42,1502(1962)	BOGDANKEVICH
L0014006	47-Ag	107	γ,n	16.066	160.	5.5	29.50	1093.		Phys.Rev.177,1745(1969)	B.L.BERMAN
L0014006				24.892	41.87						
L0014007	47-Ag	107	$\gamma,2n$	21.176	46.36	5.	29.50	263.		Phys.Rev.177,1745(1969)	B.L.BERMAN
L0014007				26.131	20.36						
M0524003	47-Ag	109	γ,sn	15.9	175.62	5.5	29.00	1210.	72.6	Izv.AN SSSR,33,2074(1969)	B.S.ISHKHANOV
M0524003				13.8	138.39						
M0524003				17.3	138.39						
M0524003				19.6	86.93						
M0524003				24.3	48.61						
L0035011	48-Cd		γ,xn	16.46	231.		24.60	2046.	111.	Nucl.Phys.A219,39(1974)	A.LEPRETRE
	48-Cd		γ,xn	15.6	263.	5.1	27.00	1760.	111.	ZHETF,30,85591956)	B.I.GAVRILOV
L0035044	48-Cd		γ,sn	15.37	225.3	7.	26.20	1685.	106.	Nucl.Phys.A219,39(1974)	A.LEPRETRE
L0035012	48-Cd		γ,n	15.37	225.7	5.	24.60	1324.		Nucl.Phys.A219,39(1974)	A.LEPRETRE
L0035013	48-Cd		$\gamma,2n$	19.17	65.3	7.5	24.60	361.		Nucl.Phys.A219,39(1974)	A.LEPRETRE
L0035014	49-In	115	γ,xn	15.92	244.4	7.5	24.10	2026.		Nucl.Phys.A219,39(1974)	A.LEPRETRE
L0017002	49-In	115	γ,xn	15.601	265.49	7.5	31.10	2409.		Phys.Rev.186,1255(1969)	S.C.FULTZ

EXFOR	Nucl	A	Reac	E_{max} MeV	σ_{max} mb	FWHM MeV	E_{int} MeV	σ_{int} MeV * mb	σ_{int}^l mb	Reference	Author
L0035045	49-In	115	γ,sn	15.92	244.4	6.	29.50	1748.	108.	Nucl.Phys.A219,39(1974)	A.LEPRETRE
L0017029	49-In	115	γ,sn	15.601	264.77	4.5	31.10	1875.	113.	Phys.Rev.186,1255(1969)	S.C.FULTZ
	49-In	115	γ,sn	16.	310.	5.	23.00	2210.	119.	ZHETF.42.1502(1962)	BOGDANKEVICH
L0035015	49-In	115	γ,n	15.92	245.3	5.	24.10	1470.		Nucl.Phys.A219,39(1974)	A.LEPRETRE
L0017003	49-In	115	γ,n	15.291	264.7	4.	31.10	1354.		Phys.Rev.186,1255(1969)	S.C.FULTZ
L0035016	49-In	115	$\gamma,2n$	19.44	52.4	7.5	24.10	278.		Nucl.Phys.A219,39(1974)	A.LEPRETRE
L0017004	49-In	115	$\gamma,2n$	20.556	66.6	8.	31.10	508.		Phys.Rev.186,1255(1969)	S.C.FULTZ
L0017005	49-In	115	$\gamma,3n$	31.086	13.49		31.10	13.		Phys.Rev.186,1255(1969)	S.C.FULTZ
	50-Sn		γ,rn	16.	300.	5.	40.00	1640.	134.	Phys.Rev.112,554(1958)	E.G.FULLER
	50-Sn	112	γ,rn	15.8	295.	5.5	27.00	2230.		Yad.Fiz.20,233(1974)	YU.I.SOROKIN
	50-Sn	112	γ,sn	15.8	295.	5.5	27.00	1900.		Yad.Fiz.20,233(1974)	YU.I.SOROKIN
	50-Sn	112	γ,n	16.	340.	5.	21.00	1820.	152.	ZHETF.40.85(1961)	KUO CHI-DI
	50-Sn	114	γ,rn	15.7	265.	7.5	27.00	2260.		Izv.AN SSSR.39,114(1975)	YU.I.SOROKIN
	50-Sn	114	γ,sn	15.7	265.	7.	27.00	1860.	108.	Izv.AN SSSR.39,114(1975)	JU.I.SOROKIN
	50-Sn	116	γ,rn	15.6	260.	9.	27.00	2400.		Izv.AN SSSR.39,114(1975)	YU.I.SOROKIN
L0035017	50-Sn	116	γ,rn	15.44	277.3	7.5	22.10	1823.		Nucl.Phys.A219,39(1974)	A.LEPRETRE
L0017006	50-Sn	116	γ,rn	15.362	272.	6.	29.60	2083.		Phys.Rev.186,1255(1969)	S.C.FULTZ
L0017006				18.769	168.9						
L0017006				27.131	76.						
	50-Sn	116	γ,sn	15.6	260.	6.	27.00	2850.	110.	Izv.AN SSSR.39,114(1975)	YU.I.SOROKIN
L0035046	50-Sn	116	γ,sn	15.44	277.3	7.5	29.50	1630.	104.	Nucl.Phys.A219,39(1974)	A.LEPRETRE
L0017030	50-Sn	116	γ,sn	15.982	262.	4.	29.60	1669.	99.	Phys.Rev.186,1255(1969)	S.C.FULTZ
L0017030				27.131	55.						
L0035018	50-Sn	116	γ,n	15.44	277.3	7.5	22.10	1437.		Nucl.Phys.A219,39(1974)	A.LEPRETRE
L0017007	50-Sn	116	γ,n	15.362	272.	3.5	29.60	1255.		Phys.Rev.186,1255(1969)	S.C.FULTZ
L0017007				28.37	36.						
L0035019	50-Sn	116	$\gamma,2n$	20.07	51.4	>7.	22.10	193.		Nucl.Phys.A219,39(1974)	A.LEPRETRE
L0017008	50-Sn	116	$\gamma,2n$	20.008	60.	7.5	29.60	414.		Phys.Rev.186,1255(1969)	S.C.FULTZ
	50-Sn	117	γ,rn	15.4	260.	8.	27.00	2520.		Izv.AN SSSR.39,114(1975)	YU.I.SOROKIN
L0035020	50-Sn	117	γ,rn	15.37	266.5	9.	21.10	1774.		Nucl.Phys.A219,39(1974)	A.LEPRETRE
L0017009	50-Sn	117	γ,rn	15.601	262.55	8.	31.10	2446.		Phys.Rev.186,1255(1969)	S.C.FULTZ
	50-Sn	117	γ,sn	15.4	260.	5.5	27.00	1390.	110.	Izv.AN SSSR.39,114(1975)	YU.I.SOROKIN
L0035047	50-Sn	117	γ,sn	15.37	266.5	5.	21.10	1554.	102.	Nucl.Phys.A219,39(1974)	A.LEPRETRE
L0017031	50-Sn	117	γ,sn	15.601	262.67	5.	31.10	1894.	114.	Phys.Rev.186,1255(1969)	S.C.FULTZ
L0035021	50-Sn	117	γ,n	15.37	267.	4.	21.10	1334.		Nucl.Phys.A219,39(1974)	A.LEPRETRE
L0017010	50-Sn	117	γ,n	15.601	262.69	4.	31.10	1380.		Phys.Rev.186,1255(1969)	S.C.FULTZ
L0035022	50-Sn	117	$\gamma,2n$	19.17	70.1	5.	21.10	220.		Nucl.Phys.A219,39(1974)	A.LEPRETRE
L0017011	50-Sn	117	$\gamma,2n$	19.317	71.83	7.	31.10	476.		Phys.Rev.186,1255(1969)	S.C.FULTZ
L0017012	50-Sn	117	$\gamma,3n$	28.608	28.42		31.10	38.		Phys.Rev.186,1255(1969)	S.C.FULTZ
L0035023	50-Sn	118	γ,rn	15.31	286.4	7.5	21.60	1893.		Nucl Phys.A219,39(1974)	A.LEPRETRE
	50-Sn	118	γ,rn	15.5	290.	5.5	27.00	2460.		Yad.Fiz.20,233(1974)	YU.I.SOROKIN
L0017013	50-Sn	118	γ,rn	15.601	254.75	7.5	30.80	2424		Phys.Rev.186,1255(1969)	S.C.FULTZ
L0017013				17.769	225.3						
L0035048	50-Sn	118	γ,sn	15.31	286.4	5.	21.60	1635.	106.	Nucl.Phys.A219,39(1974)	A.LEPRETRE
	50-Sn	118	γ,sn	15.8	295.	5.5	27.00	1920.		Yad.Fiz.20,233(1974)	YU.I.SOROKIN
L0017032	50-Sn	118	γ,sn	15.601	254.75	5.5	30.80	1853.	110.	Phys.Rev.186,1255(1969)	S.C.FULTZ
L0035024	50-Sn	118	γ,n	15.31	286.4	4.	21.60	1377.		Nucl.Phys.A219,39(1974)	A.LEPRETRE
L0017014	50-Sn	118	γ,n	15.601	254.4	4.	30.80	1302.		Phys.Rev.186,1255(1969)	S.C.FULTZ
L0035025	50-Sn	118	$\gamma,2n$	19.39	68.5	4.5	21.60	258.		Nucl.Phys.A219,39(1974)	A.LEPRETRE
L0017015	50-Sn	118	$\gamma,2n$	19.008	77.75	8.	30.80	531.		Phys.Rev.186,1255(1969)	S.C.FULTZ
L0017016	50-Sn	118	$\gamma,3n$	30.157	19.57		30.80	20.		Phys.Rev.186,1255(1969)	S.C.FULTZ
	50-Sn	119	γ,rn	17.	270.	9.	31.10	2630.		Izv.AN SSSR.39,114(1975)	YU.I.SOROKIN
L0017017	50-Sn	119	γ,rn	15.369	259.49	8.	31.10	2728.		Phys.Rev.186,1255(1969)	S.C.FULTZ
	50-Sn	119	γ,sn	15.4	270.	6.	27.00	1420.	111.	Izv.AN SSSR.39,114(1975)	YU.I.SOROKIN
L0017033	50-Sn	119	γ,sn	15.369	259.97	5.	31.10	1993.	118	Phys.Rev.186,1255(1969)	S.C.FULTZ
L0017018	50-Sn	119	γ,n	15.369	260.24	3.5	31.10	1326.		Phys.Rev.186,1255(1969)	S.C.FULTZ
L0017019	50-Sn	119	$\gamma,2n$	17.769	94.41	6.	31.10	597.		Phys.Rev.186,1255(1969)	S.C.FULTZ
L0017020	50-Sn	119	$\gamma,3n$	29.538	22.57	3.5	31.10	69.		Phys.Rev.186,1255(1969)	S.C.FULTZ
L0017020				25.357	10.75						
L0035026	50-Sn	120	γ,rn	16.26	288.9	6.5	22.40	2169.		Nucl.Phys.A219,39(1974)	A.LEPRETRE
	50-Sn	120	γ,rn	15.3	295.	5.5	27.00	2060.		Yad.Fiz.20,233(1974)	YU.I.SOROKIN
L0017021	50-Sn	120	γ,rn	16.84	297.3	7.5	29.90	2771.		Phys.Rev.186,1255(1969)	S.C.FULTZ
L0035049	50-Sn	120	γ,sn	15.44	284.5	5.	29.50	1770.	113.	Nucl.Phys.A219,39(1974)	A.LEPRETRE
	50-Sn	120	γ,sn	15.3	295.	5.	27.00	2070.		Yad.Fiz.20,233(1974)	YU.I.SOROKIN
L0017034	50-Sn	120	γ,sn	15.291	281.54	4.5	29.90	2074.	124.	Phys.Rev.186,1255(1969)	S.C.FULTZ
L0035027	50-Sn	120	γ,n	14.9	289.1	4.	22.40	1371.		Nucl.Phys.A219,39(1974)	A.LEPRETRE
L0017022	50-Sn	120	γ,n	15.291	280.35	3.5	29.90	1389.		Phys.Rev.186,1255(1969)	S.C.FULTZ
L0035028	50-Sn	120	$\gamma,2n$	18.44	82.9	5.5	22.40	399.		Nucl.Phys.A219,39(1974)	A.LEPRETRE
L0017023	50-Sn	120	$\gamma,2n$	17.924	99.97	6.	29.90	673.		Phys.Rev.186,1255(1969)	S.C.FULTZ
L0017023				19.24	94.72						
L0017023				28.299	48.04						
L0017024	50-Sn	120	$\gamma,3n$	29.692	19.27		29.90	12.		Phys.Rev.186,1255(1969)	S.C.FULTZ
	50-Sn	122	γ,rn	16.3	320.	7.5	27.00	2940.		Izv.AN SSSR.39,114(1975)	YU.I.SOROKIN
	50-Sn	122	γ,sn	15.6	270.	5.	27.00	1510.	119.	Izv.AN SSSR.39,114(1975)	YU.I.SOROKIN
	50-Sn	124	γ,rn	16.2	340.	9.	27.00	2900.		Izv.AN SSSR.39,114(1975)	YU.I.SOROKIN
L0035029	50-Sn	124	γ,rn	15.92	344.9	5.5	21.60	2060.		Nucl.Phys.A219,39(1974)	A.LEPRETRE
L0017025	50-Sn	124	γ,rn	15.601	351.48	5.5	31.10	2790.		Phys.Rev.186,1255(1969)	S.C.FULTZ
	50-Sn	124	γ,sn	15.2	270.	5.5	27.00	1440.	114.	Izv.AN SSSR.39,114(1975)	YU.I.SOROKIN
L0035050	50-Sn	124	γ,sn	15.1	278.8.	5.	22.70	1558.	101.	Nucl.Phys.A219,39(1974)	A.LEPRETRE
L0017035	50-Sn	124	γ,sn	14.827	290.09	4.5	31.10	2010.	123.	Phys.Rev.186,1255(1969)	S.C.FULTZ
L0035030	50-Sn	124	γ,n	14.83	257.6	3.5	21.60	1056.		Nucl.Phys.A219,39(1974)	A.LEPRETRE
L0017026	50-Sn	124	γ,n	14.672	272.52	3.5	31.10	1285.		Phys.Rev.186,1255(1969)	S.C.FULTZ
L0035031	50-Sn	124	$\gamma,2n$	17.27	110.	5.	21.60	502.		Nucl.Phys.A219,39(1974)	A.LEPRETRE
L0017027	50-Sn	124	$\gamma,2n$	16.53	115.75	5.5	31.10	670.		Phys.Rev.186,1255(1969)	S.C.FULTZ
L0017028	50-Sn	124	$\gamma,3n$	30.157	19.36	>7.	31.10	55.		Phys.Rev.186,1255(1969)	S.C.FULTZ
L0035032	51-Sb		γ,rn	15.37	276.	7.5	25.70	2315.		Nucl.Phys.A219,39(1974)	A.LEPRETRE
L0035051	51-Sb		γ,sn	15.37	276.	5.5	29.50	1927.	119.	Nucl.Phys.A219,39(1974)	A.LEPRETRE
L0035033	51-Sb		γ,n	15.37	275.5	4.5	25.70	1539.		Nucl.Phys.A219,39(1974)	A.LEPRETRE
L0035034	51-Sb		$\gamma,2n$	19.17	61.4	6.5	25.70	388.		Nucl.Phys.A219,39(1974)	A.LEPRETRE
	51-Sb		γ,rn	15.	270.	4.8				Nucl.Phys.A430,99(1984)	R.P.RASSOOL
	51-Sb		γ,sn	18.	80.	>6.				Nucl.Phys.A430,99(1984)	R.P.RASSOOL
	51-Sb	121	γ,rn	15.8	275.	4.8	21.00	1473.		Nucl.Phys.A430,99(1984)	R.P.RASSOOL
M0273009	51-Sb	121	γ,n	15.	665.	5.	18.00	3287.	229.	Can.J.Phys.29,518(1951)	L.KATZ
	51-Sb	121	$\gamma,1n$	15.9	280.	5.				Nucl.Phys.A430,99(1984)	R.P.RASSOOL
	51-Sb	121	$\gamma,2n$	18.5	96.	>6.				Nucl.Phys.A430,99(1984)	R.P.RASSOOL
	51-Sb	123	γ,rn	15.3	275.	4.8	23.50	1350.		Nucl.Phys.A430,99(1984)	R.P.RASSOOL
	51-Sb	123	γ,sn	15.	270.	4.				Nucl.Phys.A430,99(1984)	R.P.RASSOOL
M0273010	51-Sb	123	γ,n	15.	362.	5.	18.00	1750.	121.9	Can.J.Phys.29,518(1951)	L.KATZ
	51-Sb	123	$\gamma,2n$	18.2	90.	6.				Nucl.Phys.A430,99(1984)	R.P.RASSOOL

EXFOR	Nucl	A	Reac	E_{max} MeV	σ_{max} mb	FWHM MeV	E_{int} MeV	σ_{int} MeV * mb	σ_{int}^1 mb	Reference	Author
L0035035	52-Te		γ, xn	15.64	313.5	8.	25.70	2636.		Nucl.Phys.A219,39(1974)	A.LEPRETRE
L0035052	52-Te		γ, sn	15.1	293.9	6.	25.70	2112.	134.	Nucl.Phys.A219,39(1974)	A.LEPRETRE
L0035036	52-Te		γ, n	15.1	290.1	4.5	25.70	1588.		Nucl.Phys.A219,39(1974)	A.LEPRETRE
L0035037	52-Te		$\gamma, 2n$	18.08	79.2	4.5	25.70	524.		Nucl.Phys.A219,39(1974)	A.LEPRETRE
L0042004	52-Te	124	γ, xn	14.8	287.7	7.5	26.50	2498.		Nucl.Phys.A258,350(1976)	A.LEPRETRE
	52-Te	124	γ, sn	14.8	287.7	7.	26.50	2022.	127.	Nucl.Phys.A258,350(1976)	A.LEPRETRE
L0042002	52-Te	124	γ, n	14.8	287.7	4.5	26.50	1546.		Nucl.Phys.A258,350(1976)	A.LEPRETRE
L0042003	52-Te	124	$\gamma, 2n$	18.87	80.1	7.5	26.50	476.		Nucl.Phys.A258,350(1976)	A.LEPRETRE
L0042007	52-Te	126	γ, xn	16.16	294.6	8.	24.80	2533.		Nucl.Phys.A258,350(1976)	A.LEPRETRE
	52-Te	126	γ, sn	15.07	288.9	6.	24.80	2023.	129.	Nucl.Phys.A258,350(1976)	A.LEPRETRE
L0042005	52-Te	126	γ, n	15.07	288.9	4.5	24.80	1513.		Nucl.Phys.A258,350(1976)	A.LEPRETRE
L0042006	52-Te	126	$\gamma, 2n$	18.05	95.9	4.	24.80	510.		Nucl.Phys.A258,350(1976)	A.LEPRETRE
L0042010	52-Te	128	γ, xn	16.16	336.1	7.	26.20	2732.		Nucl.Phys.A258,350(1976)	A.LEPRETRE
	52-Te	128	γ, sn	14.8	315.4	4.	26.20	2093.	134.	Nucl.Phys.A258,350(1976)	A.LEPRETRE
L0042008	52-Te	128	γ, n	14.8	315.4	4.	26.20	1454.		Nucl.Phys.A258,350(1976)	A.LEPRETRE
L0042009	52-Te	128	$\gamma, 2n$	18.05	115.	7.	26.20	639.		Nucl.Phys.A258,350(1976)	A.LEPRETRE
L0042013	52-Te	130	γ, xn	15.62	384.	7.	25.90	2893.		Nucl.Phys.A258,350(1976)	A.LEPRETRE
	52-Te	130	γ, sn	14.53	316.9	6.	25.90	2180.	139.	Nucl.Phys.A258,350(1976)	A.LEPRETRE
L0042011	52-Te	130	γ, n	14.53	316.9	4.5	25.90	1467.		Nucl.Phys.A258,350(1976)	A.LEPRETRE
L0042012	52-Te	130	$\gamma, 2n$	16.7	119.9	5.5	25.90	713.		Nucl.Phys.A258,350(1976)	A.LEPRETRE
	53-I	127	γ, xn	14.94	252.26		16.90	1043.		Bul.Am.Ph.Soc.31,855(1986)	B.L.BERMAN
	53-I	127	γ, xn	14.88	309.1	6.	24.90	2380.		Nucl.Phys.A133,417(1969)	R.BERGERE
L0009002	53-I	127	γ, xn	14.982	222.61	7.5	29.50	2171.		Phys.Rev.148,1198(1966)	R.L.BRAMBLETT
L0009002				17.15	203.						
L0057007	53-I	127	γ, xn	14.938	252.26	>5.	16.90	1043.		Phys.Rev.C36,1286(1987)	B.L.BERMAN
M0511002	53-I	127	γ, sn	15.2	289.53	5.9	22.40	1532.3	107.5	Phys.Rev.C39,1631(1989)	R.P.RASSOOL
	53-I	127	γ, sn	15.	254.	6.4				Phys.Rev.C36,1286(1987)	B.L.BERMAN
	53-I	127	γ, sn	14.94	252.26		16.90	1036.	74.	Phys.Rev.C36,1286(1987)	B.L.BERMAN
L0015022	53-I	127	γ, sn	14.88	309.	6.	24.90	1989.	128.	Nucl.Phys.A133,417(1969)	R.BERGERE
L0009009	53-I	127	γ, sn	14.982	221.48	5.5	29.50	1728.	105.	Phys.Rev.148,1198(1966)	R.L.BRAMBLETT
	53-I	127	γ, n	252.26	14.94		16.90	1030.		Bul.Am.Ph.Soc.31,855(1986)	B.L.BERMAN
L0015003	53-I	127	γ, n	14.88	309.1	5.	24.90	1601.		Nucl.Phys.A133,417(1969)	R.BERGERE
L0009003	53-I	127	γ, n	15.601	225.55	4.5	29.50	1285.		Phys.Rev.148,1198(1966)	R.L.BRAMBLETT
L0057005	53-I	127	γ, n	14.938	252.26		16.90	1030.		Phys.Rev.C36,1286(1987)	B.L.BERMAN
M0511003	53-I	127	$\gamma, 2n$	18.2	73.26	4.5	23.00	274.1	14.4	Phys.Rev.C39,1631(1989)	R.P.RASSOOL
	53-I	127	$\gamma, 2n$	21.35	16.85		16.90	6.		Bul.Am.Ph.Soc.31,855(1986)	B.L.BERMAN
L0015004	53-I	127	$\gamma, 2n$	18.68	69.9	7.5	23.00	390.		Nucl.Phys.A133,417(1969)	R.BERGERE
L0015004				26.57	34.4						
L0009004	53-I	127	$\gamma, 2n$	19.317	67.08	7.	29.50	443.		Phys.Rev.148,1198(1966)	R.L.BRAMBLETT
L0057006	53-I	127	$\gamma, 2n$	16.851	21.35		16.90	6.		Phys.Rev.C36,1286(1987)	B.L.BERMAN
L0015005	53-I	127	$\gamma, 3n$	30.65	12.2	>10.	31.20	31.		Nucl.Phys.A133,417(1969)	R.BERGERE
	53-I	127	$\gamma, 3n$	30.7	12.2	>10.	29.50	¡20.		Phys.Rev.148,1198(1966)	R.L.BRAMBLETT
L0035038	55-Cs	133	γ, xn	15.31	321.2	7.5	24.20	2484.		Nucl.Phys.A219,39(1974)	A.LEPRETRE
L0014008	55-Cs	133	γ, xn	15.291	296.01	8.	29.50	2505.		Phys.Rev.177,1745(1969)	B.L.BERMAN
L0035053	55-Cs	133	γ, sn	15.31	321.2	6.	24.20	2156.	137.	Nucl.Phys.A219,39(1974)	A.LEPRETRE
L0014014	55-Cs	133	γ, sn	15.291	296.01	6.	29.50	1986.	124.	Phys.Rev.177,1745(1969)	B.L.BERMAN
L0035039	55-Cs	133	γ, n	15.31	321.2	4.5	24.20	1828.		Nucl.Phys.A219,39(1974)	A.LEPRETRE
L0014009	55-Cs	133	γ, n	15.291	296.18	4.5	29.50	1475.		Phys.Rev.177,1745(1969)	B.L.BERMAN
L0035040	55-Cs	133	$\gamma, 2n$	18.71	61.6	6.5	24.20	328.		Nucl.Phys.A219,39(1974)	A.LEPRETRE
L0014010	55-Cs	133	$\gamma, 2n$	18.698	75.	6.	29.50	503.		Phys.Rev.177,1745(1969)	B.L.BERMAN
L0014010				19.937	68.85						
L0014010				25.511	31.55						
L0014011	55-Cs	133	$\gamma, 3n$	29.228	8.		29.50	8.		Phys.Rev.177,1745(1969)	B.L.BERMAN
L0024002	56-Ba		γ, xn	15.307	364.	6.	24.30	2619.		Nucl.Phys.A172,426(1971)	H.BEIL
L0024016	56-Ba		γ, sn	15.307	364.	4.	24.30	2248.	146.	Nucl.Phys.A172,426(1971)	H.BEIL
L0024003	56-Ba		γ, n	15.307	364.	4.	24.30	1877.		Nucl.Phys.A172,426(1971)	H.BEIL
L0024004	56-Ba		$\gamma, 2n$	18.031	63.	6.5	24.30	371.		Nucl.Phys.A172,426(1971)	H.BEIL
L0019004	56-Ba	138	γ, xn	15.291	337.69	7.	27.10	2536.		Phys.Rev.C2,2318(1970)	B.L.BERMAN
L0019008	56-Ba	138	γ, sn	15.291	337.27	4.5	27.10	2040.	130.	Phys.Rev.C2,2318(1970)	B.L.BERMAN
L0019005	56-Ba	138	γ, n	15.291	336.44	4.	27.10	1547.		Phys.Rev.C2,2318(1970)	B.L.BERMAN
M0367003	56-Ba	138	γ, n	15.33	353.86	4.5	21.20	1870.5	124.6	Izv.AN SSSR.55.953(1991)	S.N.BELJAEV
L0019006	56-Ba	138	$\gamma, 2n$	18.698	76.83	7.	27.10	490.		Phys.Rev.C2,2318(1970)	B.L.BERMAN
L0019007	56-Ba	138	$\gamma, 3n$	28.608	11.3		27.10	3.		Phys.Rev.C2,2318(1970)	B.L.BERMAN
L0019007							28.60	13.			
M0398004	57-La	139	γ, xn	15.37	420.	4.5	24.00	2510.	158.	Nucl.Phys.A191,305(1972)	T.K.DEAQUE
L0024005	57-La	139	γ, xn	15.307	340.	5.5	24.30	2269.		Nucl.Phys.A172,426(1971)	H.BEIL
	57-La	139	γ, xn	14.8	325.	4.	30.00	1760.		Phys.Rev.134,B557(1964)	L.B.RICE
	57-La	139	γ, xn	15.5	358.	6.5	21.20	1910.		Nucl.Phys.32,236(1962)	J.MILLER
L0024017	57-La	139	γ, sn	15.307	340.	4.	24.30	1978.	128.	Nucl.Phys.A172,426(1971)	H.BEIL
	57-La	139	γ, sn	14.5	305.	3.5	30.00	1360.		Phys.Rev.134,B557(1964)	L.B.RICE
L0012003	57-La	139	γ, n	14.88	363.7	4.	25.50	1873.4	125.1	Nucl.Phys.A121,463(1968)	R.BERGERE
L0024018	57-La	139	γ, n	15.307	340.	4.	24.30	1687.		Nucl.Phys.A172,426(1971)	H.BEIL
M0367004	57-La	139	γ, n	15.09	364.84	4.5	22.60	1981.5	129.8	Izv.AN SSSR.55.953(1991)	S.N.BELJAEV
L0024007	57-La	139	$\gamma, 2n$	18.848	53.0	8.	29.00	291.		Nucl.Phys.A172,426(1971)	H.BEIL
L0012004	57-La	139	$\gamma, 2n$	18.41	53.9	8.	24.30	291.		Nucl.Phys.A121,463(1968)	R.BERGERE
	57-La	139	$\gamma, 3n$	30.38	12.5	>10.	28.60	13.		Nucl.Phys.A172,426(1971)	H.BEIL
L0012005	57-La	139	$\gamma, 3n$	30.38	12.5	>10.	28.60	13.		Nucl.Phys.A121,463(1968)	R.BERGERE
L0024008	58-Ce		γ, xn	15.307	383.16	>5.	16.90	1561.9	111.7	Nucl.Phys.A172,426(1971)	H.BEIL
L0015023	58-Ce		γ, xn	14.88	369.1	5.5	30.00	2300.	140.	Nucl.Phys.A133,417(1969)	R.BERGERE
	58-Ce		γ, xn	15.9	381.5	5.5	21.20	1880.		Nucl.Phys.32,236(1962)	J.MILLER
L0015023	58-Ce		γ, sn	14.88	369.1	5.5	30.00	2300.	140.	Nucl.Phys.A133,417(1969)	R.BERGERE
L0024019	58-Ce		γ, sn	15.307	359.16	>5.	16.90	1495.1	107.3	Nucl.Phys.A172,426(1971)	H.BEIL
L0015007	58-Ce		γ, n	14.88	348.8	4.	23.30	1761.8	121.7	Nucl.Phys.A133,417(1969)	R.BERGERE
L0024009	58-Ce		γ, n	15.034	338.93	>5	16.90	1428.3	103.	Nucl.Phys.A172,426(1971)	H.BEIL
L0015008	58-Ce		$\gamma, 2n$	20.56	52.4	7.5	29.60	472.6	23.5	Nucl.Phys.A133,417(1969)	R.BERGERE
L0015008				15.69	27.1						
L0015008				18.96	51.4						
L0024010	58-Ce		$\gamma, 2n$	15.852	27.	>7.	16.90	66.6	4.3	Nucl.Phys.A172,426(1971)	H.BEIL
L0015009	58-Ce		$\gamma, 3n$	29.02	7.7	>6.	29.60	19.8	.7	Nucl.Phys.A133,417(1969)	R.BERGERE
L0042016	58-Ce	140	γ, xn	15.07	390.9	7.	26.50	2855.		Nucl.Phys.A258,350(1976)	A.LEPRETRE
	58-Ce	140	γ, sn	15.07	390.9	4.	26.50	2398.	153.	Nucl.Phys.A258,350(1976)	A.LEPRETRE
L0042014	58-Ce	140	γ, n	15.07	390.9	3.5	26.50	1941.		Nucl.Phys.A258,350(1976)	A.LEPRETRE
M0367005	58-Ce	140	γ, n	15.33	361.78	4.5	21.70	1825.5	120.7	Izv.AN SSSR,55.953(1991)	S.N.BELJAEV
M0367005				9.69	37.1						
L0042015	58-Ce	140	$\gamma, 2n$	20.49	65.5	8.	26.50	457.		Nucl.Phys.A258,350(1976)	A.LEPRETRE
L0042019	58-Ce	142	γ, xn	15.34	553.4	5.	23.50	3394.		Nucl.Phys.A258,350(1976)	A.LEPRETRE
	58-Ce	142	γ, sn	15.34	332.	6.	23.50	2208.	150.	Nucl.Phys.A258,350(1976)	A.LEPRETRE
L0042017	58-Ce	142	γ, n	12.91	186.1	4.	23.50	1022.		Nucl.Phys.A258,350(1976)	A.LEPRETRE
L0042018	58-Ce	142	$\gamma, 2n$	15.07	239.1	4.	23.50	1186.		Nucl.Phys.A258,350(1976)	A.LEPRETRE

EXFOR	Nucl	A	Reac	E_{max} MeV	σ_{max} mb	FWHM MeV	E_{int} MeV	σ_{int} MeV * mb	σ_{int}^1 mb	Reference	Author
M0398002	59-Pr	141	γ,xn	15.49	404.3	4.	24.00	1840.	121.	Nucl.Phys.A191,305(1972)	T.K.DEAQUE
L0024012	59-Pr	141	γ,xn	15.034	359.27	4.5	16.90	1422.	101.	Nucl.Phys.A172,426(1971)	H.BEIL
L0009005	59-Pr	141	γ,xn	14.982	332.66	4.5	29.80	2412.		Phys.Rev.148,1198(1966)	R.L.BRAMBLETT
L0057008	59-Pr	141	γ,xn	15.416	338.43	4.5	16.90	1143.6	77.3	Phys.Rev.C36,1286(1987)	B.L.BERMAN
	59-Pr	141	γ,xn	14.8 20.	315. 175.	9.	30.00	1760		Phys.Rev.134,B557(1964)	L.B.RICE
L0057008	59-Pr	141	γ,sn	15.416	338.43	4.5	16.90	1143.6	77.3	Phys.Rev.C36,1286(1987)	B.L.BERMAN
	59-Pr	141	γ,sn	14.9	450.	4.5				Nucl.Phys.A406,257(1983)	T.J.BOAL
	59-Pr	141	γ,sn	15.03	359.27	4.5	16.90	1422	101.	Nucl.Phys.A172,426(1971)	H.BEIL
L0009010	59-Pr	141	γ,sn	14.982	332.66	4.	29.80	2062.	128.	Phys.Rev.148,1198(1966)	R.L.BRAMBLETT
	59-Pr	141	γ,sn	14.8 20.	305. 170.	8.	30.00	1470.		Phys.Rev.134,B557(1964)	L.B.RICE
L0057008	59-Pr	141	γ,n	15.416	338.43	4.5	16.90	1143.6	77.3	Phys.Rev.C36,1286(1987)	B.L.BERMAN
L0024012	59-Pr	141	γ,n	15.034	359.27	4.5	16.90	1422.	101.	Nucl.Phys.A172,426(1971)	H.BEIL
L0009006	59-Pr	141	γ,n	14.982	335.56	4.	29.80	1717.		Phys.Rev.148,1198(1966)	R.L.BRAMBLETT
	59-Pr	141	γ,n	15.	380.	4.5	30.00	1790.		Phys.Rev.143,B730(1966)	B.C.COOK
M0367006	59-Pr	141	γ,n	15.09 9.81	355.97 35.57	4.5	23.50	1854.1	121.1	Izv.AN SSSR,55,953(1991)	S.N.BELJAEV
M0367006											
L0059003	59-Pr	141	γ,n	15.358	351.68	4.5	18.10	1395.	94.	T.YOUNG.72	L.M.YOUNG
M0345004	59-Pr	141	γ,n	15.52	359.5	4.5	17.60	1427.1	98.4	Yad.Konst.1.52(1993)	V.V.VARLAMOV
M0345004				14.61	326.7						
M0345004				14.94	344.9						
M0345004				16.06	308.7						
L0020002	59-Pr	141	$\gamma,1n$	15.39	352.	4.5	23.70	1713.		Phys.Rev.C2,1129(1970)	R.E.SUND
L0009007	59-Pr	141	$\gamma,2n$	19.937	59.34	5.	29.80	340.		Phys.Rev.148,1198(1966)	R.L.BRAMBLETT
L0009008	59-Pr	141	$\gamma,3n$	32.65	16.5	>4.	29.80	5.		Phys.Rev.148,1198(1966)	R.L.BRAMBLETT
L0009008							33.00	36.			
L0024013	60-Nd		γ,xn	15.307	402.33	4.5	18.00	1882.		Nucl.Phys.A172,426(1971)	H.BEIL
L0024020	60-Nd		γ,sn	15.307	319.9	4.5	18.00	1559.	112.	Nucl.Phys.A172,426(1971)	H.BEIL
L0024014	60-Nd		γ,n	14.626	252.19	4.	18.00	1236.		Nucl.Phys.A172,426(1971)	H.BEIL
L0024015	60-Nd		$\gamma,2n$	16.805	100.09	3.	18.00	323.		Nucl.Phys.A172,426(1971)	H.BEIL
L0025002	60-Nd	142	γ,xn	14.898	364.41	5.	20.20	1918.		Nucl.Phys.A172,437(1971)	P.CARLOS
L0025023	60-Nd	142	γ,sn	14.898	364.41	4.	20.20	1873.	126.	Nucl.Phys.A172,437(1971)	P.CARLOS
L0025003	60-Nd	142	γ,n	14.898	364.41	4.	20.20	1828.		Nucl.Phys.A172,437(1971)	P.CARLOS
M0367007	60-Nd	142	γ,n	15.03 19.62	377.02 115.75	4.5	22.60	1948.7	126.7	Izv.AN SSSR,55,953(1991)	S.N.BELJAEV
M0367007											
L0025004	60-Nd	142	$\gamma,2n$	19.938	30.7	>4.	20.20	45.		Nucl.Phys.A172,437(1971)	P.CARLOS
L0025005	60-Nd	143	γ,xn	15.443	369.22	6.	19.80	2054.		Nucl.Phys.A172,437(1971)	P.CARLOS
L0025024	60-Nd	143	γ,sn	15.443	346.92	4.5	19.80	1875.	130.	Nucl.Phys.A172,437(1971)	P.CARLOS
L0025006	60-Nd	143	γ,n	14.898	337.63	3.5	19.80	1696.		Nucl.Phys.A172,437(1971)	P.CARLOS
L0025007	60-Nd	143	$\gamma,2n$	17.622	65.05	9.	19.80	179.		Nucl.Phys.A172,437(1971)	P.CARLOS
L0025007				15.443	22.3						
L0025007				19.257	52.66						
L0025008	60-Nd	144	γ,xn	15.307	434.43	5.	20.20	2445.		Nucl.Phys.A172,437(1971)	P.CARLOS
L0025025	60-Nd	144	γ,sn	15.307	326.63	5.	20.20	1882.	128.	Nucl.Phys.A172,437(1971)	P.CARLOS
L0025009	60-Nd	144	γ,n	14.081	273.81	4.5	20.20	1319.		Nucl.Phys.A172,437(1971)	P.CARLOS
L0025010	60-Nd	144	$\gamma,2n$	16.396	139.06	4.5	20.20	563.		Nucl.Phys.A172,437(1971)	P.CARLOS
L0025011	60-Nd	145	γ,xn	15.579	476.73	4.5	20.20	2694.		Nucl.Phys.A172,437(1971)	P.CARLOS
L0025026	60-Nd	145	γ,sn	15.579	325.46	6.	20.20	2037.	147.	Nucl.Phys.A172,437(1971)	P.CARLOS
L0025012	60-Nd	145	γ,n	13.672	250.97	5.	20.20	1380.		Nucl.Phys.A172,437(1971)	P.CARLOS
L0025013	60-Nd	145	$\gamma,2n$	15.852	154.71	4.	20.20	657.		Nucl.Phys.A172,437(1971)	P.CARLOS
L0025014	60-Nd	146	γ,xn	15.034	457.88	5.	20.20	2587.		Nucl.Phys.A172,437(1971)	P.CARLOS
L0025027	60-Nd	146	γ,sn	15.307	311.63	4.5.	20.20	1920.	133.	Nucl.Phys.A172,437(1971)	P.CARLOS
	60-Nd	146	γ,sn	13.8	332.	4.1	23.00	2120.		Yad.Fiz.13,463(1971)	O.V.VASIL'EV
L0025015	60-Nd	146	γ,n	13.809	254.25	3.5	20.20	1253.		Nucl.Phys.A172,437(1971)	P.CARLOS
L0025016	60-Nd	146	$\gamma,2n$	16.124	177.75	3.5	20.20	667.		Nucl.Phys.A172,437(1971)	P.CARLOS
L0025017	60-Nd	148	γ,xn	15.715	467.8	5.5	18.80	2537.		Nucl.Phys.A172,437(1971)	P.CARLOS
	60-Nd	148	γ,xn	14.2 15.9	600. 545.	4.5				Yad.Fiz.10.460(1969)	O.V.VASIL'EV
L0025028	60-Nd	148	γ,sn	14.762	270.	7.	18.80	1702.	122.	Nucl.Phys.A172,437(1971)	P.CARLOS
	60-Nd	148	γ,sn	13.5 15.9	440. 275.	5.	22.00	2406.		Yad.Fiz.10.460(1969)	O.V.VASIL'EV
L0025018	60-Nd	148	γ,n	12.583	192.6	3.	18.80	867.		Nucl.Phys.A172,437(1971)	P.CARLOS
L0025019	60-Nd	148	$\gamma,2n$	15.715	214.8	3.5	18.80	835.		Nucl.Phys.A172,437(1971)	P.CARLOS
L0025020	60-Nd	150	γ,xn	15.579	456.33	7.	20.20	3185.		Nucl.Phys.A172,437(1971)	P.CARLOS
	60-Nd	150	γ,xn	15.9 14.7	605. 545.	4.5				Yad.Fiz.10.460(1969)	O.V.VASIL'EV
L0025029	60-Nd	150	γ,sn	15.579	270.84	8.	20.20	2011.	142.	Nucl.Phys.A172,437(1971)	P.CARLOS
L0025029				12.855	236.7						
	60-Nd	150	γ,sn	13.3 15.9	340. 335.	5.5	22.00	2213.		Yad.Fiz.10.460(1969)	O.V.VASIL'EV
L0025021	60-Nd	150	γ,n	12.31	236.7	3.	20.20	1174.		Nucl.Phys.A172,437(1971)	P.CARLOS
L0025022	60-Nd	150	$\gamma,2n$	15.579	185.49	5.	20.20	837.		Nucl.Phys.A172,437(1971)	P.CARLOS
	62-Sm		γ,xn	14.88	438.3	7.	25.20	3247.		Nucl.Phys.A133,417(1969)	R.BERGERE
L0015024	62-Sm		γ,sn	14.88	338.3	6.	25.20	2425.	164.	Nucl.Phys.A133,417(1969)	R.BERGERE
L0015011	62-Sm		γ,n	14.33	293.7	5.	25.20	1628.		Nucl.Phys.A133,417(1969)	R.BERGERE
L0015012	62-Sm		$\gamma,2n$	16.24	149.	5.	25.20	772.		Nucl.Phys.A133,417(1969)	R.BERGERE
L0015013	62-Sm		$\gamma,3n$	27.39	20.8	>10.	25.20	25.		Nucl.Phys.A133,417(1969)	R.BERGERE
L0015013							27.40	59.			
L0033002	62-Sm	144	γ,xn	15.37	403.	4.5	20.80	1970.		Nucl.Phys.A225,171(1974)	P.CARLOS
L0033017	62-Sm	144	γ,sn	15.37	391.5	4.5	20.80	1935.	126.	Nucl.Phys.A225,171(1974)	P.CARLOS
L0033003	62-Sm	144	γ,n	15.37	380.	4.	20.80	1900.		Nucl.Phys.A225,171(1974)	P.CARLOS
L0033004	62-Sm	144	$\gamma,2n$	20.79	31.7		20.80	35.		Nucl.Phys.A225,171(1974)	P.CARLOS
L0033004				16.19	20.5						
L0033005	62-Sm	148	γ,xn	15.64	408.5	6.	20.00	2498.		Nucl.Phys.A225,171(1974)	P.CARLOS
	62-Sm	148	γ,sn	14.1	335.	4.	22.00	2080.	137.	Yad.Fiz.13,463(1971)	O.V.VASIL'EV
L0033018	62-Sm	148	γ,sn	14.56	337.8	5.5	20.00	1942.	134.	Nucl.Phys.A225,171(1974)	P.CARLOS
L0033006	62-Sm	148	γ,n	14.56	331.1	5.5	20.00	1386.		Nucl.Phys.A225,171(1974)	P.CARLOS
L0033007	62-Sm	148	$\gamma,2n$	16.73	149.9	6.	20.00	556.		Nucl.Phys.A225,171(1974)	P.CARLOS
L0033008	62-Sm	150	γ,xn	15.92	449.2	6.	19.80	2687.		Nucl.Phys.A225,171(1974)	P.CARLOS
	62-Sm	150	γ,xn	15.9	500.	5.5				Yad.Fiz.10.460(1969)	O.V.VASIL'EV
	62-Sm	150	γ,sn	13.6	360.	5.5	23.00	2213.	203.	Yad.Fiz.10.460(1969)	O.V.VASIL'EV
L0033019	62-Sm	150	γ,sn	14.7	322.2	6.5	19.80	1991.	141.	Nucl.Phys.A225,171(1974)	P.CARLOS
L0033009	62-Sm	150	γ,n	14.15	302.3	4.	19.80	1295.		Nucl.Phys.A225,171(1974)	P.CARLOS
L0033010	62-Sm	150	$\gamma,2n$	16.32	179.	4.	19.80	696.		Nucl.Phys.A225,171(1974)	P.CARLOS
L0033010				19.03	114.9						
L0033011	62-Sm	152	γ,xn	16.32	432.1	7.5	20.00	2707.		Nucl.Phys.A225,171(1974)	P.CARLOS
L0033011				13.21	259.3						
	62-Sm	152	γ,xn	14.6	560.	5.5				Yad.Fiz.10.460(1969)	O.V.VASIL'EV

EXFOR	Nucl	A	Reac	E_{max} MeV	σ_{max} mb	FWHM MeV	E_{int} MeV	σ_{int} MeV * mb	σ^1_{int} mb	Reference	Author
				11.2	507.						
	62-Sm	152	γ, sn	11.2	507.	2.4	25.00	3079.	264.	Yad.Fiz.10.460(1969)	O.V.VASIL'EV
				14.7	502.						
L0033020	62-Sm	152	γ, sn	15.64	281.3	7.5	20.00	2026.	143.	Nucl.Phys.A225.171(1974)	P.CARLOS
L0033020				12.21	258.1						
L0033012	62-Sm	152	γ, n	12.53	257.3	4.5	20.00	1345.		Nucl.Phys.A225.171(1974)	P.CARLOS
L0033013	62-Sm	152	$\gamma, 2n$	16.86	178.5	4.	20.00	681.		Nucl.Phys.A225.171(1974)	P.CARLOS
M0073002	62-Sm	154	γ, abs	12.35	277.	7.5	20.00	1940.	286.	Nucl.Phys.A351.257(1981)	G.M.GUREVICH
M0073002				15.53	255.						
L0033014	62-Sm	154	γ, xn	16.19	420.3	8.5	21.10	2841.		Nucl.Phys.A225.171(1974)	P.CARLOS
L0033014				12.39	252.1						
	62-Sm	154	γ, xn	16.6	460.	5.5				Yad.Fiz.10.460(1969)	O.V.VASIL'EV
				11.	254.						
	62-Sm	154	γ, sn	15.3	400.	3.	23.00	2478.	202.	Yad.Fiz.10.460(1969)	O.V.VASIL'EV
				11.	254.						
L0033021	62-Sm	154	γ, sn	12.39	252.1	8.	21.10	2059.	144.	Nucl.Phys.A225.171(1974)	P.CARLOS
L0033021				15.92	248.8						
L0033015	62-Sm	154	γ, n	12.39	252.1	4.5	21.10	1277.		Nucl.Phys.A225.171(1974)	P.CARLOS
L0033016	62-Sm	154	$\gamma, 2n$	16.73	178.9	4.	21.10	782.		Nucl.Phys.A225.171(1974)	P.CARLOS
	63-Eu	151	γ, xn	16.	400.	6.				Nucl.Phys.A406.257(1983)	T.J.BOAL
	63-Eu	151	γ, sn	14.36	303.	5.1	24.50	1970.	133.	Nucl.Phys.A406.257(1983)	T.J.BOAL
	63-Eu	151	γ, sn	14.	285.	4.5	22.00	2020.	131.	Yad.Fiz.13.463(1971)	O.V.VASIL'EV
	63-Eu	153	γ, xn	16.5	340.	9.				Nucl.Phys.A406.257(1983)	T.J.BOAL
				12.8	230.						
L0016002	63-Eu	153	γ, xn	16.84	316.04	9.	28.90	3017.		Phys.Rev.185.1576(1969)	B.L.BERMAN
L0016002				12.814	239.22						
	63-Eu	153	γ, sn	12.8	240.	7.5	24.50	2000.	134.	Nucl.Phys.A406.257(1983)	T.J.BOAL
				15.	225.						
L0016018	63-Eu	153	γ, sn	15.601	259.78	8.	28.90	2273.	148.	Phys.Rev.185.1576(1969)	B.L.BERMAN
L0016018				12.814	239.22						
L0016003	63-Eu	153	γ, n	14.67	244.55	7.	28.90	1566.		Phys.Rev.185.1576(1969)	B.L.BERMAN
L0016003				12.814	239.31						
L0016004	63-Eu	153	$\gamma, 2n$	16.84	98.55	7.	28.90	670.		Phys.Rev.185.1576(1969)	B.L.BERMAN
L0016005	63-Eu	153	$\gamma, 3n$	27.679	17.68	3.	28.90	37.		Phys.Rev.185.1576(1969)	B.L.BERMAN
M0073003	64-Gd	156	γ, abs	12.23	296.	7.5	20.00	2070.	295.	Nucl.Phys.A351.257(1981)	G.M.GUREVICH
M0073003				15.33	296.						
	64-Gd	156	γ, xn	16.5	400.	7.5				Nucl.Phys.A406.257(1983)	T.J.BOAL
				13.	275.						
	64-Gd	156	γ, sn	15.	295.	7.5	24.50	2130.	144.	Nucl.Phys.A406.257(1983)	T.J.BOAL
				13.	275.						
	64-Gd	152	γ, sn	15.	259.	3.	22.00	1990.	135.	Yad.Fiz.13.463(1971)	O.V.VASIL'EV
				12.	147.						
	64-Gd	154	γ, sn	15.	250.	2.4	22.00	2000.	133.	Yad.Fiz.13.463(1971)	O.V.VASIL'EV
				11.9	161.						
	64-Gd	156	γ, sn	15.2	243.	2.6	22.00	2110.	142.	Yad.Fiz.13.463(1971)	O.V.VASIL'EV
				11.9	180.						
	64-Gd	158	γ, sn	14.9	249.	2.6	22.00	2160.	146.	Yad.Fiz.13.463(1971)	O.V.VASIL'EV
				11.7	165.						
L0016006	64-Gd	160	γ, xn	16.066	457.15	8.5	29.50	3748.		Phys.Rev.185.1576(1969)	B.L.BERMAN
L0016006				12.194	278.09						
L0016019	64-Gd	160	γ, sn	16.066	285.82	8.5	29.50	2533.	169.	Phys.Rev.185.1576(1969)	B.L.BERMAN
L0016019				12.194	278.09						
L0016007	64-Gd	160	γ, n	12.194	279.96	4.	29.50	1398.		Phys.Rev.185.1576(1969)	B.L.BERMAN
L0016008	64-Gd	160	$\gamma, 2n$	16.84	192.78	4.	29.50	1055.		Phys.Rev.185.1576(1969)	B.L.BERMAN
L0016009	64-Gd	160	$\gamma, 3n$	27.37	18.86	>7.	29.50	80.		Phys.Rev.185.1576(1969)	B.L.BERMAN
	65-Tb	159	γ, abs	17.	400.	5.5	19.00	3111.		ZHETF.42.1502(1962)	BOGDANKEVICH
				12.3	330.						
M0057003	65-Tb	159	γ, xn	16.8	459.	8.	23.00	3390.	213.7	Yad.Fiz.23.1145(1976)	B.I.GORYACHEV
M0057003				12.8	294.						
L0012006	65-Tb	159	γ, xn	16.24	344.9	8.5	27.40	3194.		Nucl.Phys.A121.463(1968)	R.BERGERE
L0012006				12.16	260.1						
	65-Tb	159	γ, xn	16.69	331.	7.	28.00	3187.		Phys.Rev.B133.869(1964)	R.L.BRAMBLETT
				12.35	259.						
M0057002	65-Tb	159	γ, sn	15.2	358.	7.	20.80	2475.7	170.1	Yad.Fiz.23.1145(1976)	B.I.GORYACHEV
M0057002				12.55	296.						
L0012019	65-Tb	159	γ, sn	15.69	285.8	8.	27.40	2557.	170.	Nucl.Phys.A121.463(1968)	R.BERGERE
L0012019				12.16	262.8						
L0005003	65-Tb	159	γ, sn	16.685	331.	6.5	28.00	2300.	151.	Phys.Rev.B133.869(1964)	R.L.BRAMBLETT
L0005003				12.349	259.						
L0012007	65-Tb	159	γ, n	12.16	265.5	7.	27.40	1936.		Nucl.Phys.A121.463(1968)	R.BERGERE
L0012007				15.42	262.1						
L0005004	65-Tb	159	γ, n	12.349	259.	5.	28.00	1413.		Phys.Rev.B133.869(1964)	R.L.BRAMBLETT
L0005004				15.136	251.						
L0012008	65-Tb	159	$\gamma, 2n$	17.05	101.	5.	27.40	605.		Nucl.Phys.A121.463(1968)	R.BERGERE
L0012008				24.67	38.4						
L0005005	65-Tb	159	$\gamma, 2n$	17.304	145.	5.	28.00	887.		Phys.Rev.B133.869(1964)	R.L.BRAMBLETT
L0005005				26.75	57.						
L0012009	65-Tb	159	$\gamma, 3n$	29.29	18.4	>10.	27.40	16.		Nucl.Phys.A121.463(1968)	R.BERGERE
M0073004	67-Ho	165	γ, abs	12.4	302.	6.	20.00	1860.	253.	Nucl.Phys.A351.257(1981)	G.M.GUREVICH
M0073004				15.66	282.						
	67-Ho	165	γ, abs	12.2	300.	6.				Pisma ZHETF.23.411(1976)	G.M.GUREVICH
				15.7	300.						
M0057004	67-Ho	165	γ, xn	16.7	508.	10.	22.00	3360.	218.	Yad.Fiz.23.1145(1976)	B.I.GORYACHEV
M0057004				12.5	310.						
L0016010	67-Ho	165	γ, xn	16.84	369.66	8.5	28.90	3355.		Phys.Rev.185.1576(1969)	B.L.BERMAN
L0016010				12.504	290.79						
L0012010	67-Ho	165	γ, xn	16.24	416.8	7.5	26.80	3667.		Nucl.Phys.A121.463(1968)	R.BERGERE
L0012010				12.16	322.4						
	67-Ho	165	γ, xn	16.3	395.	7.5				J.Phys.Et Rad.27.262(1966)	P.AXEL
				12.1	305.						
	67-Ho	165	γ, xn	15.8	365.	8.5				Phys.Rev.129.2723(1963)	R.L.BRAMBLETT
				12.1	275.						
L0016020	67-Ho	165	γ, sn	12.5	290.79	8.	28.90	2523.	166.	Phys.Rev.185.1576(1969)	B.L.BERMAN
L0016020				16.53	254.36						
L0012020	67-Ho	165	γ, sn	15.42	324.7	2.5	26.80	2871.	194.	Nucl.Phys.A121.463(1968)	R.BERGERE
L0012020				12.16	323.2						
	67-Ho	165	γ, sn	15.4	335.	7.5				J.Phys.Et Rad.27.262(1966)	P.AXEL
				12.1	305.						
	67-Ho	165	γ, sn	15.8	335.	8.5	28.00	2370.		Phys.Rev.129.2723(1963)	R.L.BRAMBLETT

EXFOR	Nucl	A	Reac	E_{max} MeV	σ_{max} mb	FWHM MeV	E_{int} MeV	σ_{int} MeV * mb	σ_{int}^1 mb	Reference	Author
M0057006 M0057006	67-Ho	165	γ, sn	12.1 16.7 12.5	295. 348. 308.	8.	20.00	3000.	218.	Yad.Fiz.23,1145(1976)	B.I.GORYACHEV
L0016011 L0016011	67-Ho	165	γ, n	12.504 14.982	290.91 265.41	6.	28.90	1735.		Phys.Rev.185,1576(1969)	B.L.BERMAN
L0012011 L0012011	67-Ho	165	γ, n	12.16 14.88	323.9 301.9	6.	26.80	2090.		Nucl.Phys.A121,463(1968)	R.BERGERE
	67-Ho	165	γ, n	12. 15.2	275. 275.	5.5				Phys.Rev.129,2723(1963)	R.L.BRAMBLETT
M0057005	67-Ho	165	$\gamma, 2n$	17.3	181.	5.	20.70	675.7	37.8	Yad.Fiz.23,1145(1976)	B.I.GORYACHEV
L0016012	67-Ho	165	$\gamma, 2n$	16.84	128.07	5.5	28.90	744.		Phys.Rev.185,1576(1969)	B.L.BERMAN
L0012012	67-Ho	165	$\gamma, 2n$	17.32	130.9	6.	26.80	766.		Nucl.Phys.A121,463(1968)	R.BERGERE
	67-Ho	165	$\gamma, 2n$	17.4	105.	4.5				J.Phys. Et Rad.27,262(1966)	P.AXEL
	67-Ho	165	$\gamma, 2n$	17.5	150.	5.5				Phys.Rev.129,2723(1963)	R.L.BRAMBLETT
L0016013	67-Ho	165	$\gamma, 3n$	28.299	21.21	>5.	28.90	44.		Phys.Rev.185,1576(1969)	B.L.BERMAN
L0012013 L0012013	67-Ho	165	$\gamma, 3n$	28.48	21.7	>10.	26.80 28.50	15. 45.		Nucl.Phys.A121,463(1968)	R.BERGERE
	68-Er		γ, xn	15.15 12.16	405.3 308.6	5.5	21.10	2973.		Nucl.Phys.A133,417(1969)	R.BERGERE
L0015025	68-Er		γ, sn	12.16 15.15	308.6 305.3	2.8	21.10	2387.	172.	Nucl.Phys.A133,417(1969)	R.BERGERE
L0015015 L0015015	68-Er		γ, n	12.16 14.88	308.6 259.3	5.5	21.10	1801.		Nucl.Phys.A133,417(1969)	R.BERGERE
L0015016 L0015016	68-Er		$\gamma, 2n$	16.78	126.1	5.5	21.10 27.40	586. 768.		Nucl.Phys.A133,417(1969)	R.BERGERE
L0015017	68-Er		$\gamma, 3n$	27.66	18.7	>15.	27.70	52.		Nucl.Phys.A133,417(1969)	R.BERGERE
M0057007 M0057007	68-Er	166	γ, xn	16.8 12.6	451. 297.	8.5	22.00	3560.	216.	Yad.Fiz.23,1145(1976)	B.I.GORYACHEV
M0057009 M0057009	68-Er	166	γ, sn	16. 12.6	358. 297.	7.5	20.00	3360.	216.	Yad.Fiz.23,1145(1976)	B.I.GORYACHEV
M0057008 M0057008 M0057008	68-Er	166	$\gamma, 2n$	18.1 17.4 19.1	182. 155. 152.	4.5	20.50	590.5	32.8	Yad.Fiz.23,1145(1976)	B.I.GORYACHEV
M0073005 M0073005	68-Er	168	γ, abs	15.25 12.01	342. 311.	7.5	20.00	2240.	307.	Nucl.Phys.A351,257(1981)	G.M.GUREVICH
M0318002 M0318002	70-Yb	170	γ, xn	15.82 12.62	379. 351.	7.	20.20	2492.7	175.7	Vop.Teor.Y.Fiz.5,42(1976)	A.M.GORYACHEV
M0318003 M0318003	70-Yb	171	γ, xn	15.42 12.42	389. 364.	6.5	20.20	2450.3	174.7	Vop.Teor.Y.Fiz.5,42(1976)	A.M.GORYACHEV
M0318004 M0318004	70-Yb	172	γ, xn	12.42 15.62	365. 360.	6.	20.20	2423.7	173.2	Vop.Teor.Y.Fiz.5,42(1976)	A.M.GORYACHEV
M0318005 M0318005	70-Yb	173	γ, xn	15.62 12.22	405. 372.	6.5	20.20	2494.9	178.	Vop.Teor.Y.Fiz.5,42(1976)	A.M.GORYACHEV
M0073006 M0073006	70-Yb	174	γ, abs	15.19 12.18	403. 400.	7.5	20.00	2690.	382.	Nucl.Phys.A351,257(1981)	G.M.GUREVICH
M0318006 M0318006	70-Yb	174	γ, xn	15.22 12.42	382. 345.	6.	20.20	2517.8	180.7	Vop.Teor.Y.Fiz.5,42(1976)	A.M.GORYACHEV
M0318007 M0318007	70-Yb	176	γ, xn	15.62 12.42	370. 369.	7.	20.20	2529.7	182.1	Vop.Teor.Y.Fiz.5,42(1976)	A.M.GORYACHEV
	71-Lu	175	γ, xn	15.15 12.43	431.4 315.4	8.	23.00	3142.		Nucl.Phys.A133,417(1969)	R.BERGERE
L0015026 L0015026	71-Lu	175	γ, sn	15.15 12.43	330.6 315.2	7.	23.00	2507.	173.	Nucl.Phys.A133,417(1969)	R.BERGERE
L0015019 L0015019	71-Lu	175	γ, n	12.43 14.6	315.4 302.4	6.	23.00	1872.		Nucl.Phys.A133,417(1969)	R.BERGERE
L0015020 L0015020	71-Lu	175	$\gamma, 2n$	16.78	132.3	5.5	23.00 28.50	635. 742.		Nucl.Phys.A133,417(1969)	R.BERGERE
L0015021	71-Lu	175	$\gamma, 3n$	27.39	25.4	>8.	28.50	65.		Nucl.Phys.A133,417(1969)	R.BERGERE
	71-Lu	175	γ, sn	12.4	270.	2.6	25.00	2900.	206.	Nucl.Phys.A121,463(1968)	R.BERGERE
	72-Hf	176	γ, xn	16.7 12.2	445. 385.	7.5				Yad.Fiz.26,465(1977)	A.M.GORYACHEV
M0007002 M0007002	72-Hf	176	γ, sn	12.42 15.04	374.7 356.9	6.5	20.00	2571.	184.	Yad.Fiz.26,465(1977)	A.M.GORYACHEV
M0073007 M0073007	72-Hf	178	γ, abs	12.37 14.58	415. 406.	7.5	20.00	2850.	399.	Nucl.Phys.A351,257(1981)	G.M.GUREVICH
	72-Hf	178	γ, abs	12.2 14.7	410. 400.	7.5				Pisma ZHETF,23,411(1976)	G.M.GUREVICH
	72-Hf	178	γ, xn	16. 12.	525. 395.	9.				Yad.Fiz.26,465(1977)	A.M.GORYACHEV
M0057010 M0057010	72-Hf	178	γ, xn	16. 12.7	561. 344.	7.	22.00	3080.	196.	Yad.Fiz.23,1145(1976)	B.I.GORYACHEV
M0007003 M0007003	72-Hf	178	γ, sn	12.54 15.79	387.5 355.3	6.5	20.00	2580.	185.	Yad.Fiz.26,465(1977)	A.M.GORYACHEV
M0057012 M0057012 M0057012	72-Hf	178	γ, sn	14.5 12.5 16.	379. 298. 318.	6.	20.00	3080.	196.	Yad.Fiz.23,1145(1976)	B.I.GORYACHEV
M0057011	72-Hf	178	$\gamma, 2n$	16.	246.	4.5	20.00	887.2	52.3	Yad.Fiz.23,1145(1976)	B.I.GORYACHEV
M0073008 M0073008	72-Hf	180	γ, abs	12.28 15.77	430. 409.	7.5	20.00	2720.	403.	Nucl.Phys.A351,257(1981)	G.M.GUREVICH
	72-Hf	180	γ, abs	12.2 15.6	440. 400.	7.5				Pisma ZHETF,23,411(1976)	G.M.GUREVICH
	72-Hf	180	γ, xn	15.9 12.5	575. 375.	9.				Yad.Fiz.26,465(1977)	A.M.GORYACHEV
M0007004 M0007004	72-Hf	180	γ, sn	12.54 15.29	372.4 353.7	7.	20.00	2535.	182.	Yad.Fiz.26,465(1977)	A.M.GORYACHEV
M0073009	73-Ta	181	γ, abs	14.54	409.	7.5	20.00	2840.	381.	Nucl.Phys.A351,257(1981)	G.M.GUREVICH
	73-Ta	181	γ, abs	12.5 15.	410. 410.	7.5				Pisma ZHETF,23,411(1976)	G.M.GUREVICH
	73-Ta	181	γ, xn	15.8 12.4	446. 380.	7.5				Austr.J.Phys.26,585(1973)	R.S.HICKS
	73-Ta	181	γ, xn	15.4 12.6	516. 370.	7.5				Pisma ZHETF,10,80(1969)	B.S.ISHKHANOV
L0012014 L0012014	73-Ta	181	γ, xn	15.42 12.43	510.2 371.	8.	25.20	3799.		Nucl.Phys.A121,463(1968)	R.BERGERE
	73-Ta	181	γ, xn	15.5 12.	558.2 354.	6.5				Izv.AN SSSR,31,336(1967)	G.P.ANTROPOV
	73-Ta	181	γ, xn	15.91 12.84	476. 300.	8.	24.60	3062.		Phys.Rev.129,2723(1963)	R.L.BRAMBLETT
	73-Ta	181	γ, xn	15.5 12.4	506. 420.	7.	23.00	3700.		ZHETF,42,1502(1962)	BOGDANKEVICH

86

EXFOR	Nucl	A	Reac	E_{max} MeV	σ_{max} mb	FWHM MeV	E_{int} MeV	σ_{int} MeV * mb	σ^1_{int} mb	Reference	Author
	73-Ta	181	γ, xn	17. 13.	388.9 293.8	8.	22.00	2970.		Nucl.Phys.32,236(1962)	J.MILLER
	73-Ta	181	γ, xn	12.45 15.45	415. 410.	6.5				Phys.Rev.112,560(1958)	E.G.FULLER
L0012021 L0012021	73-Ta	181	γ, sn	15.42 12.7	384.9 368.2	6.5	25.20	2983.	205.	Nucl.Phys.A121,463(1968)	R.BERGERE
L0003002 L0003002	73-Ta	181	γ, sn	15.91 12.814	446. 300.	5.5	24.60	2181.	149.	Phys.Rev.129,2723(1963)	R.L.BRAMBLETT
	73-Ta	181	γ, sn	15.0 12.	342.1 316.	7.5	20.00	2300.		Izv.AN SSSR.31,336(1967)	G.P.ANTROPOV
L0012015 L0012015	73-Ta	181	γ, n	12.7 14.06	367.1 356.2	5.	25.20	2180.		Nucl.Phys.A121,463(1968)	R.BERGERE
L0003003	73-Ta	181	γ, n	12.814	300.	4.	24.61	1300.		Phys.Rev.129,2723(1963)	R.L.BRAMBLETT
M0273011	73-Ta	181	γ, n	14.	80.	5.	18.00	396.5	29.3	Can.J.Phys.29,518(1951)	L.KATZ
L0012016	73-Ta	181	$\gamma, 2n$	16.5	158.7	4.5	25.20	790.		Nucl.Phys.A121,463(1968)	R.BERGERE
L0003004	73-Ta	181	$\gamma, 2n$	15.91	196.	4.	24.61	881.		Phys.Rev.129,2723(1963)	R.L.BRAMBLETT
	73-Ta	181	$\gamma, 2n$	16.	252.8	4.5	20.00	1100.		Izv.AN SSSR.31,336(1967)	G.P.ANTROPOV
L0012017 L0012017	73-Ta	181	$\gamma, 3n$	25.48	20.2	7.5	25.20 36.40	13. 137.		Nucl.Phys.A121,463(1968)	R.BERGERE
	74-W		γ, sn	15.2 12.6	328. 268.	2.7	21.30	2854.	203.	J.Physique.36,L-267(1975)	A.VEYSSIERE
	74-W		γ, p	23. 20.6	4.3 2.2	>15	33.00	50.		ZHETF.17,547(1962)	V.G.SHEVCHENKO
	74-W	182	γ, abs	12.5 15.	420. 390.	7.5				Pisma ZHETF.23,411(1976)	G.M.GUREVICH
M0073010	74-W	182	γ, abs	12.83	401.	7.5	20.00	2860.	401.	Nucl.Phys.A351,257(1981)	G.M.GUREVICH
	74-W	182	γ, xn	14.9 12.7	412. 290.	6.5	27.40	3680.		Yad.Fiz.17,3(1973)	YU.I.SOROKIN
	74-W	182	γ, sn	14.9 12.7	390. 290.	5.5	27.40	2780.		Yad.Fiz.17,3(1973)	YU.I.SOROKIN
M0025002 M0025002	74-W	182	γ, sn	15.02 13.02	427.5 420.9	6.	20.80	2885.9	202.3	Izv.AN KAZSSR.6,8(1978)	A.M.GORYACHEV
M0073011 M0073011	74-W	184	γ, abs	12.02 14.44	416. 407.	7.5	20.00	2780.	380.	Nucl.Phys.A351,257(1981)	G.M.GUREVICH
	74-W	184	γ, xn	15.2 12.7	525. 300.	6.5	27.40	4880.		Yad.Fiz.17,3(1973)	YU.I.SOROKIN
	74-W	184	γ, xn	15.6 12.7	640. 390.	7.5				Yad.Fiz.17,463(1973)	A.M.GORYACHEV
	74-W	184	γ, sn	14.3 12.7	400. 300.	5.5	27.40	2950.		Yad.Fiz.17,3(1973)	YU.I.SOROKIN
	74-W	184	γ, sn	15.6 12.7	412. 390.	7.				Yad.Fiz.17,463(1973)	A.M.GORYACHEV
M0025003 M0025003	74-W	184	γ, sn	13.42 15.02	432.1 426.2	7.	20.80	2954.8	208.4	Izv.AN KAZSSR.6,8(1978)	A.M.GORYACHEV
M0073012	74-W	186	γ, abs	13.47	449.	7.5	20.00	2900.	395.	Nucl.Phys.A351,257(1981)	G.M.GUREVICH
	74-W	186	γ, xn	15.6 12.7	645. 400.	6.5				Yad.Fiz.17,463(1973)	A.M.GORYACHEV
L0016014	74-W	186	γ, xn	14.982	612.222	6.	28.60	4502.		Phys.Rev.185,1576(1969)	B.L.BERMAN
	74-W	186	γ, sn	12.7 14.9	400. 385.	7.				Yad.Fiz.17,463(1973)	A.M.GORYACHEV
L0016021	74-W	186	γ, sn	14.672	391.13	6.	28.60	3004.	203.	Phys.Rev.185,1576(1969)	B.L.BERMAN
M0025004 M0025004	74-W	186	γ, sn	14.42 12.82	448.3 428.1	6.5	20.80	2974.2	210.4	Izv.AN KAZSSR.6,8(1978)	A.M.GORYACHEV
L0016015	74-W	186	γ, n	12.814	390.87	3.5	28.60	1655.		Phys.Rev.185,1576(1969)	B.L.BERMAN
L0016016	74-W	186	$\gamma, 2n$	15.756	256.28	4.	28.60	1200.		Phys.Rev.185,1576(1969)	B.L.BERMAN
L0016017	74-W	186	$\gamma, 3n$	28.299	38.03	>8.	28.60	149.		Phys.Rev.185,1576(1969)	B.L.BERMAN
	75-Re		γ, sn	15.2 12.6	375. 279.	2.8	21.60	3226.	227.	J.Physique.36,L-267(1975)	A.VEYSSIERE
	75-Re	185	γ, xn	15.9 12.7	520. 420.	7.				Yad.Fiz.17,463(1973)	A.M.GORYACHEV
	75-Re	185	γ, sn	12.7 14.9	420. 395.	6.				Yad.Fiz.17,463(1973)	A.M.GORYACHEV
	75-Re	187	γ, xn	15.2 12.7	600. 385.	7.				Yad.Fiz.17,463(1973)	A.M.GORYACHEV
	75-Re	187	γ, sn	12.7 14.8	385. 385.	6.				Yad.Fiz.17,463(1973)	A.M.GORYACHEV
	76-Os		γ, xn	13.3	430.	5.	27.00	2700.		Austr.J.Phys.30,677(1977)	S.SU
L0046004	76-Os	186	γ, xn	15.88	450.96	7.	19.70	2964.		Phys.Rev.C19,1205(1979)	B.L.BERMAN
	76-Os	186	γ, sn	15.88	450.96	6.	19.70	2508.	179.	Phys.Rev.C19,1205(1979)	B.L.BERMAN
L0046002	76-Os	186	γ, n	14.291	436.79	4.5	19.70	2040.		Phys.Rev.C19,1205(1979)	B.L.BERMAN
L0046003	76-Os	186	$\gamma, 2n$	16.613	145.44	4.	19.70	460.		Phys.Rev.C19,1205(1979)	B.L.BERMAN
L0046008 L0046008	76-Os	188	γ, xn	15.513 22.356	561. 184.91	6.5	30.40	4731.		Phys.Rev.C19,1205(1979)	B.L.BERMAN
	76-Os	188	γ, sn	14.05 23.	490.11 130.	5.5	30.40	3613.	239.	Phys.Rev.C19,1205(1979)	B.L.BERMAN
L0046005 L0046005	76-Os	188	γ, n	14.047 22.112	490.11 93.73	4.	30.40	2620.		Phys.Rev.C19,1205(1979)	B.L.BERMAN
L0046006	76-Os	188	$\gamma, 2n$	16.246	180.82	4.5	30.40	880.		Phys.Rev.C19,1205(1979)	B.L.BERMAN
L0046007	76-Os	188	$\gamma, 3n$	28.466	24.59	>8.	30.40	120.		Phys.Rev.C19,1205(1979)	B.L.BERMAN
L0046012	76-Os	189	γ, xn	15.269	615.68	5.5	29.90	4722.		Phys.Rev.C19,1205(1979)	B.L.BERMAN
	76-Os	189	γ, sn	14.05	492.2	4.5	29.90	3353.	228.	Phys.Rev.C19,1205(1979)	B.L.BERMAN
L0046009 L0046009	76-Os	189	γ, n	14.047 22.112	492.2 64.6	3.	29.90	2130.		Phys.Rev.C19,1205(1979)	B.L.BERMAN
L0046010	76-Os	189	$\gamma, 2n$	16.002	227.96	4.	29.90	1000.		Phys.Rev.C19,1205(1979)	B.L.BERMAN
L0046011	76-Os	189	$\gamma, 3n$	26.022	37.14	7.5	29.90	210.		Phys.Rev.C19,1205(1979)	B.L.BERMAN
L0046016	76-Os	190	γ, xn	15.024	589.05	4.	30.40	4602.		Phys.Rev.C19,1205(1979)	B.L.BERMAN
	76-Os	190	γ, xn	15.6 12.8	535. 420.	8.				Yad.Fiz.17,463(1973)	A.M.GORYACHEV
	76-Os	190	γ, sn	13.8 12.8	490.75 420.	4.	30.40	3229.	220.	Phys.Rev.C19,1205(1979)	B.L.BERMAN
	76-Os	190	γ, sn	15.6	360.	6.				Yad.Fiz.17,463(1973)	A.M.GORYACHEV
L0046013	76-Os	190	γ, n	13.802	490.75	4.	30.40	2010.		Phys.Rev.C19,1205(1979)	B.L.BERMAN
L0046014	76-Os	190	$\gamma, 2n$	16.124	224.	4.	30.40	1080.		Phys.Rev.C19,1205(1979)	B.L.BERMAN
L0046015	76-Os	190	$\gamma, 3n$	27.	30.35	5.5	30.40	140.		Phys.Rev.C19,1205(1979)	B.L.BERMAN
L0046020 L0046020	76-Os	192	γ, xn	14.78 24.067	643.62 199.18	5.5	29.90	4900.		Phys.Rev.C19,1205(1979)	B.L.BERMAN
	76-Os	192	γ, sn	13.31	480.29	5.	29.90	3306.	224.	Phys.Rev.C19,1205(1979)	B.L.BERMAN
L0046017 L0046017	76-Os	192	γ, n	13.314 24.067	480.29 57.99	3.5	29.90	1920.		Phys.Rev.C19,1205(1979)	B.L.BERMAN

EXFOR	Nucl	A	Reac	E_{max} MeV	σ_{max} mb	FWHM MeV	E_{int} MeV	σ_{int} MeV * mb	σ^1_{int} mb	Reference	Author
L0046018	76-Os	192	$\gamma,2n$	15.513	256.33	4.	29.90	1200.		Phys.Rev.C19,1205(1979)	B.L.BERMAN
L0046019	76-Os	192	$\gamma,3n$	27.489	35.01	7.	29.90	190.		Phys.Rev.C19,1205(1979)	B.L.BERMAN
	77-Ir		γ,sn	13.8	487.	5.1	21.90	2965.	211.	J.Physique,36,L-267(1975)	A.VEYSSIERE
M0049002	77-Ir	191	γ,xn	13.3	497.	7.5	20.30	3475.5	240.8	Yad.Fiz.27.1479(1978)	A.M.GORYACHEV
M0049002				15.9	480.						
M0049003	77-Ir	191	γ,sn	13.3	497.	5.	20.00	2757.	199.	Yad.Fiz.27.1479(1978)	A.M.GORYACHEV
M0008002	77-Ir	191	γ,sn	13.22	495.	5.	20.20	2580.4	205.9	Pisma ZHETF.26,107(1978)	A.M.GORYACHEV
M0049004	77-Ir	193	γ,xn	13.	551.	7.	20.20	3602.4	251.5	Yad.Fiz.27.1479(1978)	A.M.GORYACHEV
M0049004				15.6	539.						
M0049005	77-Ir	193	γ,sn	13.02	543.	5.	20.00	2835.	205.	Yad.Fiz.27.1479(1978)	A.M.GORYACHEV
M0008003	77-Ir	193	γ,sn	13.02	543.	4.5	20.20	2860.2	207.1	Pisma ZHETF.26,107(1978)	A.M.GORYACHEV
	78-Pt		γ,sn	13.7	512.	5.	20.30	3056.	228.	J.Physique,36,L-267(1975)	A.VEYSSIERE
M0049006	78-Pt	194	γ,xn	13.8	523.	7.	20.70	3457.4	239.4	Yad.Fiz.27.1479(1978)	A.M.GORYACHEV
M0049006				15.8	458.						
M0049007	78-Pt	194	γ,sn	13.8	523.	5.	20.00	2861.	210.	Yad.Fiz.27.1479(1978)	A.M.GORYACHEV
M0008004	78-Pt	194	γ,sn	13.82	511.1	5.	20.80	2867.4	204.5	Pisma ZHETF.26,107(1978)	A.M.GORYACHEV
M0049008	78-Pt	195	γ,xn	13.5	537.	7.	20.20	3392.9	238.2	Yad.Fiz.27.1479(1978)	A.M.GORYACHEV
M0049008				15.3	487.						
M0049009	78-Pt	195	γ,sn	13.5	537.	5.5	20.00	2797.	204.	Yad.Fiz.27.1479(1978)	A.M.GORYACHEV
M0008005	78-Pt	195	γ,sn	13.42	528.	5.	20.20	2835.3	206.1	Pisma ZHETF.26,107(1978)	A.M.GORYACHEV
M0049010	78-Pt	196	γ,xn	13.8	529.	6.5	20.80	3553.2	245.4	Yad.Fiz.27.1479(1978)	A.M.GORYACHEV
M0049010				15.6	504.						
M0049011	78-Pt	196	γ,sn	13.8	529.	4.5	20.00	2944.	213.	Yad.Fiz.27.1479(1978)	A.M.GORYACHEV
M0008006	78-Pt	196	γ,sn	13.82	522.5	5.	20.80	2864.3	205.3	Pisma ZHETF.26,107(1978)	A.M.GORYACHEV
M0049012	78-Pt	198	γ,xn	14.3	649.	6.	20.80	3990.1	277.3	Yad.Fiz.27.1479(1978)	A.M.GORYACHEV
M0049013	78-Pt	198	γ,sn	13.7	575.	5.	20.00	2813.	236.	Yad.Fiz.27.1479(1978)	A.M.GORYACHEV
M0008007	78-Pt	198	γ,sn	13.62	566.2	5.	20.80	3097.4	224.1	Pisma ZHETF.26,107(1978)	A.M.GORYACHEV
M0073013	79-Au	197	γ,abs	12.88	616.	5.5	20.00	3100	437.	Nucl.Phys.A351,257(1981)	G.M.GUREVICH
M0073013				10.65	296.						
	79-Au	197	γ,abs	13.5	540.	5.5				Pisma ZHETF.23,411(1976)	G.M.GUREVICH
	79-Au	197	γ,xn	13.5	494.15		16.90	2606.		Bul.Am.Ph.Soc.31,855(1986)	B.L.BERMAN
	79-Au	197	γ,xn	13.6	590.	7.	27.00	4200.		Izv.AN SSSR.37,1891(1973)	YU.I.SOROKIN
	79-Au	197	γ,xn	13.79	528.7.	7.	21.70	3546.		Nucl.Phys.A159,561(1970)	A.VEYSSIERE
	79-Au	197	γ,xn	13.64	549.	7.	24.70	3744.		Phys.Rev.127,1273(1962)	S.C.FULTZ
	79-Au	197	γ,xn	14.	491.8	6.	22.00	3000.		Nucl.Phys.32,236(1962)	J.MILLER
	79-Au	197	γ,xn	13.6	590.	5.				Phys.Rev.112,560(1958)	E.G.FULLER
L0057011	79-Au	197	γ,xn	13.504	494.15	>6	16.90	2606.		Phys.Rev.C36,1286(1987)	B.L.BERMAN
	79-Au	197	γ,sn	13.73	502.	4.76				Phys.Rev.C36,1286(1987)	B.L.BERMAN
	79-Au	197	γ,sn	13.5	494.15		16.90	2491.	194.	Bul.Am.Ph.Soc.31,855(1986)	B.L.BERMAN
	79-Au	197	γ,sn	13.6	590.	4.5	27.00	3150.		Izv.AN SSSR,37,1891(1973)	YU.I.SOROKIN
L0021010	79-Au	197	γ,sn	13.52	532.1	5.	21.70	3067.	217.	Nucl.Phys.A159,561(1970)	A.VEYSSIERE
L0002002	79-Au	197	γ,sn	13.64'	549.	4.	24.70	2967.	205.	Phys.Rev.127,1273(1962)	S.C.FULTZ
L0057009	79-Au	197	γ,n	13.504	494.15	>5.	16.90	1738.3	124.	Phys.Rev.C36,1286(1987)	B.L.BERMAN
	79-Au	197	γ,n	16.85	104.78		16.90	2376.		Bul.Am.Ph.Soc.31,855(1986)	B.L.BERMAN
L0021003	79-Au	197	γ,n	13.52	529.2	4.5	21.70	2588.		Nucl.Phys.A159,561(1970)	A.VEYSSIERE
L0002003	79-Au	197	γ,n	13.641	549.	4.5	24.70	2190.		Phys.Rev.127,1273(1962)	S.C.FULTZ
L0057010	79-Au	197	$\gamma,2n$	16.851	104.78	>6.	16.90	115.3	7.1	Phys.Rev.C36,1286(1987)	B.L.BERMAN
L0021004	79-Au	197	$\gamma,2n$	16.78	106.7	7.	27.10	671.		Nucl.Phys.A159,561(1970)	A.VEYSSIERE
L0002004	79-Au	197	$\gamma,2n$	17.329	136.	6.	24.7	777.		Phys.Rev.127,1273(1979)	S.C.FULTZ
	79-Au	197	$\gamma,2n$	17.	105.	>5.	26.90	671.		Bul.Am.Ph.Soc.31,855(1986)	B.L.BERMAN
L0021005	79-Au	197	$\gamma,3n$	27.12	13.6	>6.	27.10	24.		Nucl.Phys.A159,561(1970)	A.VEYSSIERE
	80-Hg		γ,sn	13.7	582.	4.4	21.10	3133.	227.	J.Physique,36,L-267(1975)	A.VEYSSIERE
	80-Hg	201	γ,p	26.	4.3	11.	32.00	40.		Phys.Rev.127,2198(1962)	J.H.CARVER
	81-Tl		γ,abs	14.	648.	4.6	27.00	3770.	266.	ZHETF,30,859(1956)	B.I.GAVRILOV
	81-Tl	203	γ,sn	14.2	490.	3.7	20.00	2610.	185.	Izv.AN SSSR,34,116(1969)	G.P.ANTROPOV
	81-Tl	205	γ,sn	14.1	490.	3.7	20.00	2780.	187.	Izv.AN SSSR,34,116(1969)	G.P.ANTROPOV
	82-Pb		γ,xn	14.1	660.	5.5	24.00	3910.		J.Phys.Soc.Jap.25,655(1968)	T.TOMIMASU
	82-Pb		γ,xn	13.7	657.5	5.5	27.00	4100.		Nucl.Phys.32,236(1962)	J.MILLER
	82-Pb		γ,xn	13.4	670.	6.				J.Phys.Rad.,22.529(1961)	J.MILLER
L0057014	82-Pb		γ,xn	13.504	613.02	>5.	16.90	3192.		Phys.Rev.C36,1286(1987)	B.L.BERMAN
	82-Pb		γ,sn	13.5	613.		16.90	3047.	249.	Phys.Rev.C36,1286(1987)	B.L.BERMAN
L0057012	82-Pb		γ,n	13.504	613.28	4.2	16.90	2902.	137.9	Phys.Rev.C36,1286(1987)	B.L.BERMAN
L0057013	82-Pb		$\gamma,2n$	16.851	93.56	>5.	16.90	145.		Phys.Rev.C36,1286(1987)	B.L.BERMAN
	82-Pb	206	γ,xn	13.4	460.	6.	27.00	3930.		Izv.AN SSSR.37,156(1973)	YU.I.SOROKIN
L0007002	82-Pb	206	γ,xn	13.743	530.	5.	26.40	3441		Phys.Rev.B136,126(1964)	R.R.HARVEY
	82-Pb	206	γ,xn	13.4	460.	4.5	27.00	3210.		Izv.AN SSSR.37,156(1973)	YU.I.SOROKIN
L0007014	82-Pb	206	γ,sn	13.743	530.	4.	26.40	2909.	203	Phys.Rev.B136,126(1964)	R.R.HARVEY
L0007003	82-Pb	206	γ,n	13.743	529.	4.	28.00	2220.		Phys.Rev.B136,126(1964)	R.R.HARVEY
L0007004	82-Pb	206	$\gamma,2n$	18.233	82.	8.	28.00	560.		Phys.Rev.B136,126(1964)	R.R.HARVEY
L0007004				16.685	75.						
L0007004				17.304	81.						
L0007004				20.247	57.						
L0007005	82-Pb	207	γ,xn	13.743	500.	4.5	26.40	3267.		Phys.Rev B136,126(1964)	R.R.HARVEY
L0007005				25.511	163.						
L0007015	82-Pb	207	γ,sn	13.743	500.	4.	26.40	2718.	191.	Phys.Rev.B136,126(1964)	R.R.HARVEY
L0007015				25.202	160.						
L0007006	82-Pb	207	γ,n	13.743	500.	4.	28.00	2050.		Phys.Rev.B136,126(1964)	R.R.HARVEY
L0007007	82-Pb	207	$\gamma,2n$	17.459	94.	8.	28.00	600.		Phys.Rev.B136,126(1964)	R.R.HARVEY
M0345005	82-Pb	208	γ,xn	13.71	666.6	>5.	14.80	2096.5	167.9	Yad.Konst.1,52(1993)	V.V.VARLAMOV
	82-Pb	208	γ,xn	13.	510.	6.	27.00	4320.		Izv.AN SSSR.37,156(1973)	YU.I.SOROKIN
M0400002	82-Pb	208	γ,xn	13.355	884.367	4.5	17.20	3260.	242.8	Yad.Fiz.12.682(1970)	B.S.ISHKHANOV
M0400002				9.775	246.32						
M0400002				10.195	335.148						
M0400002				11.235	511.042						
M0400002				11.655	645.379						
M0400002				12.295	680.685						
M0400002				12.815	812.486						
M0400002				16.035	633.47						
M0399004	82-Pb	208	γ,xn	13.77	645.	4.	18.90	3387.		Nucl.Phys.A159,561(1970)	A.VEYSSIERE
M0399004	82-Pb	208	γ,xn	13.04	820.	4.5	16.50	3329.4	257.8	Pisma ZHETF,7,210(1968)	B.I.GORYACHEV
M0399004				12.46	650.						
M0399004				14.52	800.						
M0399004				15.39	710.						
L0007008	82-Pb	208	γ,xn	13.433	518.	4.	26.40	3496.		Phys.Rev.B136,126(1964)	R.R.HARVEY
M0399002	82-Pb	208	γ,xn	12.86	760.	4.5	22.00	4813.1	348.	Pisma ZHETF,7,210(1968)	B.I.GORYACHEV
M0399002				15.1	690.						
M0399002				16.48	470.						
M0399002				17.81	420.						
M0399002				20.85	280.						
M0345005	82-Pb	208	γ,sn	13.32	641.	>5.	14.80	2096.5	167.9	Yad.Konst.1,52(1993)	V.V.VARLAMOV
M0345005				9.99	158.2						

EXFOR	Nucl	A	Reac	E_{max} MeV	σ_{max} mb	FWHM MeV	E_{int} MeV	σ_{int} MeV * mb	σ_{int}^{1} mb	Reference	Author
M0345005				11.31	354.8						
M0345005				13.32	641.						
	82-Pb	208	γ, sn	13.	510.	4.5	27.00	3280.		Izv.AN SSSR,37,156(1973)	YU.I.SOROKIN
L0021011	82-Pb	208	γ, sn	13.37	642.	4.	18.90	3059.	229.	Nucl.Phys.A159,561(1970)	A.VEYSSIERE
L0007016	82-Pb	208	γ, sn	13.433	518.	4.	26.40	2636.	189.	Phys.Rev.B136,B26(1964)	R.R.HARVEY
M0345005	82-Pb	208	γ, n	13.32	641.	>5.	14.80	2096.5	167.9	Yad.Konst.1,52(1993)	V.V.VARLAMOV
M0345005				9.99	158.2						
M0345005				11.31	354.8						
M0345005				13.32	641.						
L0021007	82-Pb	208	γ, n	13.5	645.	3.5	18.90	2731.		Nucl.Phys.A159,561(1970)	A.VEYSSIERE
L0007009	82-Pb	208	γ, n	13.433	518.	3.5	26.40	1776.		Phys.Rev.B136,126(1964)	R.R.HARVEY
L0007009							28.00	1960.			
M0367008	82-Pb	208	γ, n	13.56	618.89	4.5	21.20	2909.8	215.4	Izv.AN SSSR,55,953(1991)	S.N.BELJAEV
M0367008				7.58	58.23						
M0367008				10.05	147.68						
L0059004	82-Pb	208	γ, n	13.34	651.96	4.	14.90	2090.	165.	T.YOUNG,72	L.M.YOUNG
L0059004				10.005	133.41						
L0059004				11.305	320.35						
L0021008	82-Pb	208	$\gamma, 2n$	16.53	92.	8.	18.90	328.		Nucl.Phys.A159,561(1970)	A.VEYSSIERE
L0021008							21.67	52.			
L0007010	82-Pb	208	$\gamma, 2n$	16.995	127.	9.	26.40	860.		Phys.Rev.B136,126(1964)	R.R.HARVEY
L0021009	82-Pb	208	$\gamma, 3n$	29.95	23.	11.	37.80	197.		Nucl.Phys.A159,561(1970)	A.VEYSSIERE
	82-Pb	208	γ, p	24.8	3.1					Nucl.Phys.A246,365(1975)	K.SHODA
	83-Bi	209	γ, abs	13.5	630.	4.5				Pisma ZHETF,23,411(1976)	G.M.GUREVICH
	83-Bi	209	γ, xn	14.	625.	5.5	27.00	4600.		Izv.AN SSSR,37,1891(1973)	YU.I.SOROKIN
L0007011	83-Bi	209	γ, xn	13.588	544.	5.5	26.40	3772.		Phys.Rev.B136,126(1964)	R.R.HARVEY
	83-Bi	209	γ, xn	13.9	537.	5.9	27.00	3960.		ZHETF,30,855(1957)	B.I.GAVRILOV
	83-Bi	209	γ, xn	14.5	743.8	5.				Izv.AN SSSR,31,336(1967)	G.P.ANTROPOV
	83-Bi	209	γ, xn	13.9	656.9	6.	22.00	3730.		Nucl.Phys.32,236(1962)	J.MILLER
	83-Bi	209	γ, sn	13.6	625.	4.5	27.00	3470.		Izv.AN SSSR,37,1891(1973)	YU.I.SOROKIN
L0007017	83-Bi	209	γ, sn	13.588	544.	4.	26.40	3058.	214.	Phys.Rev.B136,126(1964)	R.R.HARVEY
	83-Bi	209	γ, sn	13.8	537.	4.8	27.00	3120.		ZHETF,30,855(1957)	B.I.GAVRILOV
	83-Bi	209	γ, sn	14.5	682.3	5.	20.00	3400.		Izv.AN SSSR,31,336(1967)	G.P.ANTROPOV
L0007012	83-Bi	209	γ, n	13.588	544.	3.5	26.40	2344.		Phys.Rev.B136,126(1964)	R.R.HARVEY
L0059005	83-Bi	209	γ, n	13.113	658.82	4.5	14.80	2129.	170.	T.YOUNG,72	L.M.YOUNG
L0059005				11.757	362.82						
L0007013	83-Bi	209	$\gamma, 2n$	17.614	121.	8.	26.40	714.		Phys.Rev.B136,126(1964)	R.R.HARVEY
M0195002	88-Ra	226	γ, F	15.	.95	5.5	20.00	5.2	.4	Yad.Fiz.13,934(1971)	E.A.ZHAGROV
M0015002	89-Ac	227	γ, F	14.	3.02	>6.	15.50	13.3	1.1	Yad.Fiz.27,301(1978)	V.E.ZHUCHKO
M0090002	90-Th	232	γ, abs	13.5	469.	6.	18.00	2920.	231.	Nucl.Phys.A273,326(1976)	G.M.GUREVICH
M0090002				11.7	401.						
	90-Th	232	γ, abs	13.5	480.	6.				Pisma ZHETF,20,741(1974)	G.M.GUREVICH
				10.9	190.						
L0050005	90-Th	232	γ, xn	14.34	969.84	6.	18.30	5606.		Phys.Rev.C21,1215(1980)	J.T.CALDWELL
L0031002	90-Th	232	γ, xn	14.43	747.	7.	16.30	3888.		Nucl.Phys.A199,45(1973)	A.VEYSSIERE
L0031002				11.18	429.						
	90-Th	232	γ, sn	14.34	549.	4.8	18.30	3483.	276.	Phys.Rev.C21,1215(1980)	J.T.CALDWELL
				11.27	443.41						
L0031014	90-Th	232	γ, sn	13.89	436.	7.5	16.30	2705.	228.	Nucl.Phys.A199,45(1973)	A.VEYSSIERE
L0031014				11.72	394.						
L0050002	90-Th	232	γ, n	11.27	443.41	5.	18.30	1660.		Phys.Rev.C21,1215(1980)	J.T.CALDWELL
L0031003	90-Th	232	γ, n	11.45	373.	5.5	16.30	1730.		Nucl.Phys.A199,45(1973)	A.VEYSSIERE
L0031003		232		13.89	183.						
L0031003		232		15.79	81.						
L0050003	90-Th	232	$\gamma, 2n$	14.34	348.52	4.5	18.30	1450.		Phys.Rev.C21,1215(1980)	J.T.CALDWELL
L0031004	90-Th	232	$\gamma, 2n$	14.97	243.	4.5	16.30	787.		Nucl.Phys.A199,45(1973)	A.VEYSSIERE
M0491002	90-Th	232	γ, F	14.2	54.		102.00	1024.7	28.8	Nucl.Phys.A472,533(1987)	A.LEPRETRE
M0449002	90-Th	232	γ, F	11.5	33.5		11.90	98.	10.4	Phys.Rev.C34,1397(1986)	H.X.ZHANG
M0449002				6.2	15.5						
L0050004	90-Th	232	γ, F	14.34	63.93	7.	18.30	370.		Phys.Rev.C21,1215(1980)	J.T.CALDWELL
L0050004				6.39	12.44						
L0031005	90-Th	232	γ, F	14.16	46.	7.	16.30	188.		Nucl.Phys.A199,45(1973)	A.VEYSSIERE
L0031005				10.94	23.						
	90-Th	232	γ, F	14.5	48.	6.	19.00	320.		Yad.Fiz.13,934(1971)	E.A.ZHAGROV
L0058004	92-U	233	γ, xn	13.85	1528.	7.	17.80	9000.		Phys.Rev.C34,2201(1986)	B.L.BERMAN
	92-U	233	γ, sn	13.85	483.	7.	17.80	3024.	239.	Phys.Rev.C34,2201(1986)	B.L.BERMAN
				11.4	421.						
L0058003	92-U	233	γ, n	11.4	134.	3.	17.80	580.		Phys.Rev.C34,2201(1986)	B.L.BERMAN
L0058003				16.79	63.						
L0058002	92-U	233	γ, F	13.85	419.	6.	17.80	2444.		Phys.Rev.C34,2201(1986)	B.L.BERMAN
L0058007	92-U	234	γ, xn	14.33	1421.	7.	18.30	8676.		Phys.Rev.C34,2201(1986)	B.L.BERMAN
L0058007				11.39	998.						
	92-U	234	γ, sn	11.88	482.	6.	18.30	3317.	270.	Phys.Rev.C34,2201(1986)	B.L.BERMAN
				13.84	464.						
L0058006	92-U	234	γ, n	11.88	249.	5.	18.30	1060.		Phys.Rev.C34,2201(1986)	B.L.BERMAN
L0058005	92-U	234	γ, F	14.33	384.	6.5	18.30	2260.		Phys.Rev.C34,2201(1986)	B.L.BERMAN
L0058005				11.39	250.						
M0090003	92-U	235	γ, abs	13.4	487.	7.	18.00	2990.	238.	Nucl.Phys.A273,326(1976)	G.M.GUREVICH
M0090003				11.2	450.						
	92-U	235	γ, abs	13.6	460.	7.				Pisma ZHETF,20,741(1974)	G.M.GUREVICH
				11.	430.						
L0050009	92-U	235	γ, xn	13.84	1486.9	7.	18.30	8889.		Phys.Rev.C21,1215(1980)	J.T.CALDWELL
	92-U	235	γ, snf	10.9	364.	2.5	19.00	3560.	303.	J.Physique,24,974(1964)	P.BOUNIN
	92-U	235	γ, sn	14.34	520.	6.	18.30	3497.	277.	Phys.Rev.C21,1215(1980)	J.T.CALDWELL
				10.9	488.						
L0050006	92-U	235	γ, n	10.9	264.8	3.5	18.30	1140.		Phys.Rev.C21,1215(1980)	J.T.CALDWELL
L0050007	92-U	235	$\gamma, 2n$	14.83	63.4	5.	18.30	202.		Phys.Rev.C21,1215(1980)	J.T.CALDWELL
L0050007				17.28	52.5						
M0503002	92-U	235	γ, F	13.5	336.33	4.	20.00	1791.	116.7	Phys.Rev.C29,2346(1984)	H.RIES
L0050008	92-U	235	γ, F	13.84	390.1	5.5	18.30	2160.		Phys.Rev.C21,1215(1980)	J.T.CALDWELL
M0300002	92-U	235	γ, F	13.9	331.04	7.5	104.40	3706.9	191.7	CDFE/Fis2.87	V.V.VARLAMOV
L0050013	92-U	236	γ, xn	14.338	1205.5	6.5	18.30	7168.		Phys.Rev.C21,1215(1980)	J.T.CALDWELL
L0050013				11.886	778.7						
	92-U	236	γ, sn	14.34	455.	6.	18.30	3156.	252.	Phys.Rev.C21,1215(1980)	J.T.CALDWELL
L0050010	92-U	236	γ, n	11.395	290.9	4.	18.30	1256.		Phys.Rev.C21,1215(1980)	J.T.CALDWELL
L0050011	92-U	236	$\gamma, 2n$	14.828	125.6	3.	18.30	450.		Phys.Rev.C21,1215(1980)	J.T.CALDWELL
L0050011				13.847	122.5						
L0050012	92-U	236	γ, F	14.338	252.5	7.	18.30	1450.		Phys.Rev.C21,1215(1980)	J.T.CALDWELL
L0050012				11.886	156.2						

EXFOR	Nucl	A	Reac	E_{max} MeV	σ_{max} mb	FWHM MeV	E_{int} MeV	σ_{int} MeV * mb	σ^1_{int} mb	Reference	Author
M0090004	92-U	238	$\gamma.abs$	13.6	441.	6.5	18.00	2950.	229.	Nucl.Phys.A273.326(1976)	G.M.GUREVICH
M0090004				11.1	399.						
M0090004				22.7	149.						
	92-U	238	$\gamma.abs$	13.5	450.	6.5				Pisma ZHETF.20.741(1974)	G.M.GUREVICH
				10.9	400.						
L0050017	92-U	238	$\gamma.xn$	14.338	1221.81	7.	18.30	7465.		Phys.Rev.C21.1215(1980)	J.T.CALDWELL
L0050017				11.395	750.76						
	92-U	238	$\gamma.xn$	14.02	1100.	6.5	18.30	6351.		Nucl.Phys.A199.45(1973)	A.VEYSSIERE
				11.31	600.						
	92-U	238	$\gamma.sn$	13.48	519.	7.	18.30	3575.	286.	Phys.Rev.C21.1215(1980)	J.T.CALDWELL
				11.4	481.						
L0031015	92-U	238	$\gamma.sn$	14.02	435.	6.5	18.30	3017.	242.	Nucl.Phys.A199.45(1973)	A.VEYSSIERE
L0031015				11.31	416.						
L0050014	92-U	238	$\gamma.n$	11.395	374.71	3.	18.30	1358.		Phys.Rev.C21.1215(1980)	J.T.CALDWELL
L0031011	92-U	238	$\gamma.n$	11.31	317.	3.	18.30	1199.		Nucl.Phys.A199.45(1973)	A.VEYSSIERE
L0050015	92-U	238	$\gamma.2n$	13.479	280.79	3.	18.30	1132.		Phys.Rev.C21.1215(1980)	J.T.CALDWELL
L0031012	92-U	238	$\gamma.2n$	14.29	207.	4.5	18.30	899.		Nucl.Phys.A199.45(1973)	A.VEYSSIERE
M0491004	92-U	238	$\gamma.F$	25.	35.2		104.00	1421.7	28.9	Nucl.Phys.A472,533(1987)	A.LEPRETRE
M0503003	92-U	238	$\gamma.F$	15.	149.22	5.	30.00	943.7	59.3	Phys.Rev.C29.2346(1984)	H.RIES
M0503003				12.	86.53						
L0050016	92-U	238	$\gamma.F$	14.338	175.58	8.5	18.30	1085.		Phys.Rev.C21.1215(1980)	J.T.CALDWELL
L0050016				11.395	113.1						
M0017007	92-U	238	$\gamma.F$	13.9	162.	6.	20.00	1104.1	81.	Yad.Fiz.30.910(1979)	I.S.KORECKAYA
	92-U	238	$\gamma.F$	14.	152.	6.5				Phys.Rev.C14.1499(1976)	ARRUDA-NeTO
L0031013	92-U	238	$\gamma.F$	14.02	154.	7.	18.30	919.		Nucl.Phys.A199.45(1973)	A.VEYSSIERE
L0031013				11.04	90.						
	92-U	238	$\gamma.F$	14.	110.	6.4	19.00	760.		Yad.Fiz.13.334(1971)	E.A.ZHAGROV
M0300003	92-U	238	$\gamma.F$	14.4	164.55	7.	105.00	2574.7	113.7	CDFE/Fis2.87	V.V.VARLAMOV
M0300003				11.4	102.27						
L0058011	93-Np	237	$\gamma.xn$	14.34	1790.	7.	18.30	10909.		Phys.Rev.C34,2201(1986)	B.L.BERMAN
L0058011				11.4	1195.						
L0031006	93-Np	237	$\gamma.xn$	14.43	1376.	7.	16.60	7792.		Nucl.Phys.A199.45(1973)	A.VEYSSIERE
				11.4	441.						
L0031006				11.18	987.						
	93-Np	237	$\gamma.sn$	14.34	590.	6.5	18.30	3799.	298.	Phys.Rev.C34,2201(1986)	B.L.BERMAN
				11.4	481.						
	93-Np	237	$\gamma.sn$	14.43	472.	7.	16.60	2795.	233.	Nucl.Phys.A199.45(1973)	A.VEYSSIERE
				11.18	396.						
L0058008	93-Np	237	$\gamma.n$	12.38	212.	5.5	18.30	1172.		Phys.Rev.C34,2201(1986)	B.L.BERMAN
L0031007	93-Np	237	$\gamma.n$	12.26	211.	7.	16.60	1013.		Nucl.Phys.A199.45(1973)	A.VEYSSIERE
L0058009	93-Np	237	$\gamma.2n$	14.34	130.	5.	18.30	349.		Phys.Rev.C34,2201(1986)	B.L.BERMAN
L0031008	93-Np	237	$\gamma.2n$	16.06	73.	>5.	16.60	121.		Nucl.Phys.A199.45(1973)	A.VEYSSIERE
L0058010	93-Np	237	$\gamma.F$	13.85	350.	6.	18.30	2278.		Phys.Rev.C34,2201(1986)	B.L.BERMAN
L0058010				11.4	280.						
L0031009	93-Np	237	$\gamma.F$	14.16	290.	7.	16.60	1661.		Nucl.Phys.A199.45(1973)	A.VEYSSIERE
L0031009				11.18	220.						
M0090005	94-Pu	239	$\gamma.abs$	13.4	447.	6	18.00	2970.	232.	Nucl.Phys.A273.326(1976)	G.M.GUREVICH
	94-Pu	239	$\gamma.abs$	12.	450.	6.				Pisma ZHETF.20.741(1974)	G.M.GUREVICH
L0058015	94-Pu	239	$\gamma.xn$	13.84	1674.	6.5	17.80	9806.		Phys.Rev.C34,2201(1986)	B.L.BERMAN
L0058015				11.88	1336.						
	94-Pu	239	$\gamma.sn$	11.4	515.	5.5	17.80	2930.	235	Phys.Rev.C34,2201(1986)	B.L.BERMAN
				13.8	474.						
L0058012	94-Pu	239	$\gamma.n$	11.39	208.	3.5	17.80	631.		Phys.Rev.C34,2201(1986)	B.L.BERMAN
L0058013	94-Pu	239	$\gamma.2n$	13.35	64.	3.5	17.80	153.		Phys.Rev.C34,2201(1986)	B.L.BERMAN
L0058014	94-Pu	239	$\gamma.F$	13.84	359.	6.5	17.80	2146.		Phys.Rev.C34,2201(1986)	B.L.BERMAN
L0058014				11.88	293.						
	94-Pu	240	$\gamma.F$	14.5	340.	7.1				Phys.Rev.C23,2104(1981)	H.THIERENS
	94-Pu	244	$\gamma.F$	14.	250.	7.1	30.00	1860.		Phys.Rev.C27,1117(1983)	H.THIERENS
M0017005	95-Am	241	$\gamma.F$	14.	336.	7.	20.00	2291.	169.3	Yad.Fiz.30.910(1979)	I.S.KORECKAYA
M0017006	95-Am	243	$\gamma.F$	13.9	350.	8.	20.00	2228.1	174.	Yad.Fiz.30.910(1979)	I.S.KORECKAYA

90

References To Appendix A

[A.1]   A. V. Varlamov, V. V. Varlamov, D. S. Rudenko, and M. E. Stepanov, "Atlas of giant dipole resonance paramaters and graphs of photonuclear reaction cross-sections," Technical Report No. INDC (NDS)-394 (1999), International Atomic Energy Agency, Vienna.

[A.2]   V. V. Varlamov and V. V. Sapunenko, "Photonuclear data index 1976 - 1995," Technical Report No. Izdatel'stvo Moskovskogo Universiteta (1996), Moscow State University, Moscow, Russia.

[A.3]   S. S. Dietrich and B. L. Berman, "Atlas of photoneutron cross-sections obtained with monoenergetic photons," Atomic Data and Nuclear Data Tables **38**, 199 (1988).

[A.4]   E. G. Fuller and H. Gerstenberg, "Photonuclear data - abstract sheets 1955-1982," Report of the US National Bureau of Standards, NBSIR 83-2742, vol. I-XV (1983-1986), National Institute for Standards and Technology, Gaithersburg, MD.

Appendix B

Graphical Presentation

The IAEA Photonuclear Data Library includes 164 isotopes. Data for each isotope are illustrated in several figures accompanied by a short explanatory text. For users convenience, an Index of nuclei is given below.

Table Appendix B.1: INDEX OF NUCLEI

NUCLEUS	PAGE	NUCLEUS	PAGE	NUCLEUS	PAGE	NUCLEUS	PAGE	NUCLEUS	PAGE
H-2	95	Ca-44	130	Ge-73	164	Cd-106	197	Pr-141	300
Be-9	96	Ca-46	131	Ge-74	165	Cd-108	198	Sm-144	301
C-12	97	Ca-48	132	Ge-76	166	Cd-110	199	Sm-147	232
C-13	99	Ti-46	133	Sr-84	167	Cd-111	200	Sm-148	233
N-14	100	Ti-47	134	Sr-86	168	Cd-112	201	Sm-149	234
N-15	101	Ti-48	135	Sr-87	169	Cd-113	202	Sm-150	235
O-16	102	Ti-49	136	Sr-88	170	Cd-114	203	Sm-151	236
O-17	104	Ti-50	137	Sr-90	171	Cd-116	204	Sm-152	237
O-18	105	V-51	138	Zr-90	172	Sn-112	205	Sm-154	238
Na-23	106	Cr-50	139	Zr-91	173	Sn-115	206	Tb-158	239
Mg-24	107	Cr-52	140	Zr-92	174	Sn-114	207	Tb-159	240
Mg-25	108	Cr-53	141	Zr-93	175	Sn-116	208	Ho-165	241
Mg-26	109	Cr-54	142	Zr-94	176	Sn-117	209	Ta-181	242
Al-27	110	Mn-55	143	Zr-96	177	Sn-118	210	W-180	244
Si-27	111	Fe-54	145	Nb-93	178	Sn-119	211	W-182	245
Si-28	112	Fe-56	146	Nb-94	179	Sn-120	212	W-183	246
Si-29	113	Fe-57	147	Mo-92	180	Sn-122	213	W-184	247
Si-30	114	Fe-58	148	Mo-94	181	Sn-124	214	W-186	248
S-32	115	Co-59	149	Mo-95	182	Sb-121	215	Au-197	249
S-33	116	Ni-58	150	Mo-96	183	Sb-123	216	Pb-206	2251
S-34	117	Ni-60	151	Mo-97	184	Te-120	217	Pb-207	252
S-36	118	Ni-61	152	Mo-98	185	Te-122	218	Pb-208	253
Cl-35	119	Ni-62	153	Mo-100	186	Te-123	219	Bi-209	255
Cl-37	120	Ni-64	154	Pd-102	187	Te-124	220	Th-232	256
Ar-36	121	Cu-63	155	Pd-104	188	Te-125	221	U-233	257
Ar-38	122	Cu-65	156	Pd-105	189	Te-126	222	U-234	258
Ar-40	123	Zn-64	157	Pd-106	190	Te-128	223	U-235	259
K-39	124	Zn-66	158	Pd-107	191	Te-130	224	U-236	260
K-40	125	Zn-67	159	Pd-108	192	I-127	225	U-238	261
K-41	126	Zn-68	160	Pd-110	193	I-129	226	Pu-238	262
Ca-40	127	Zn-70	161	Ag-107	194	Cs-133	227	Pu-239	263
Ca-42	128	Ge-70	162	Ag-108	195	Cs-135	228	Pu-241	264
Ca-43	129	Ge-72	163	Ag-109	196	Cs-137	229		

The figures are organized as follows. For each isotope we give its abundance and threshold energies of the most important photonuclear reactions. This is followed by several figures with experimental data. if available, along with recommended evaluated data. References to experimental data are shown in figures in the EXFOR style, with full list of references given at the end of the present Appendix. Recommended evaluated data are displayed as curves, denoted as BOFOD, CNDC, JENDL. KAERI and LANL, according to the name of the original library.

It should be noted that the figures do not show emission spectra in view of practical non-availability of experimental data. However, evaluated emission spectra are included in the ENDF-6 numerical data files that can be obtained from the Web or upon request from the IAEA Nuclear Data Section as explained in Sec. 6.4.

To summarize, the ENDF-6 numerical data files of the IAEA Photonuclear Data Library contain the following information:

- cross sections,

- spectra of emitted particles,

- angular distributions of emitted particles, and

- production cross sections, including activation cross sections.

$\gamma + {}^2\mathrm{H}$

Abundance	Threshold Energies (MeV)								
(%)	γ,n	γ,p	γ,t	γ,He-3	γ,α	γ,2n	γ,np	γ,2p	γ,3n
0.01	2.22	*	*	*	*	*	*	*	*

Deuteron's low photoneutron threshold (2.22 MeV) makes it an important potential neutron source in applications that include heavy water. Because of its light mass, the nuclear theories described in this report are unsuitable for modeling deuteron photodisintegration. Instead, use was made of models of Marshall + Guth [Mar50] and Partovi [Par64]. Furthermore, the evaluation was closely based on the measurements of [Ale68, All55, Bar52a, Bar52b, Bir85, Bis50, Deb92, Gal60, Hal53, Hou50, Kec56, McM55, Mor89, Phi50, Sne50, Waf51, Wha56]. Angular distributions of the photoneutrons are provided in the evaluation. Further details are given in [Mur94].

$$\gamma + {}^9\text{Be}$$

Abundance (%)	Threshold Energies (MeV)							
	$\gamma,\text{n}+2\alpha$	γ,p	γ,t	$\gamma,\text{He-3}$	$\gamma,\text{2n}$	γ,np	$\gamma,\text{2p}$	$\gamma,\text{3n}$
100.00	1.67	16.89	17.69	21.18	20.56	18.92	29.34	31.24
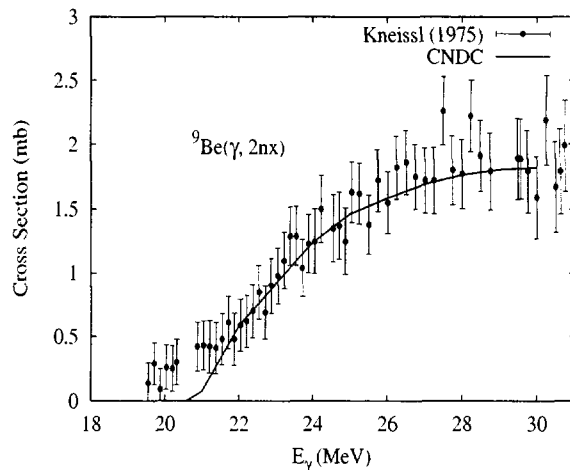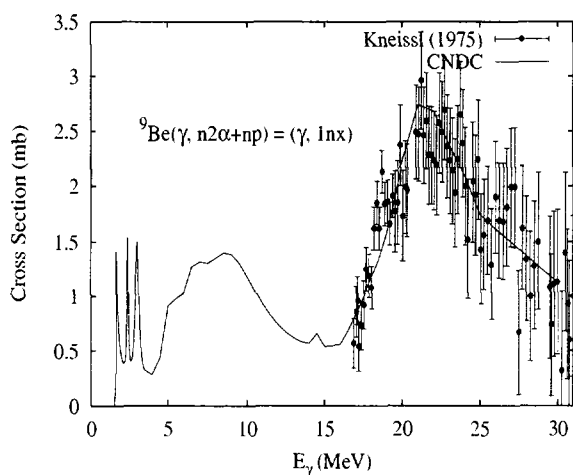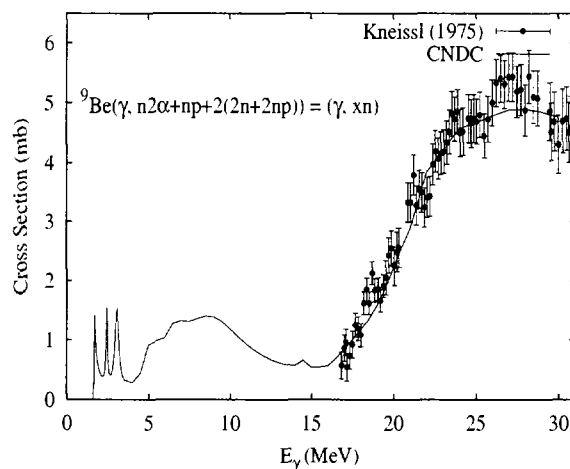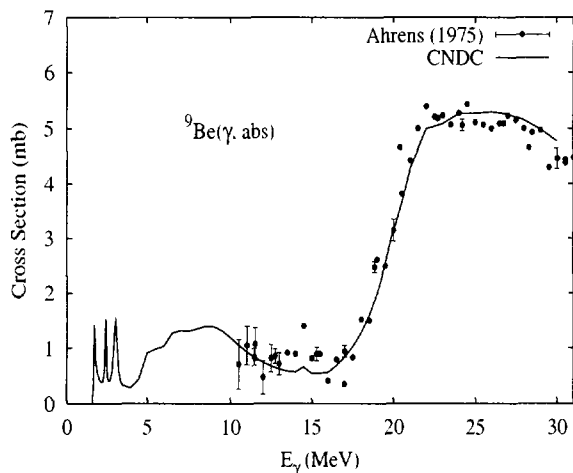
The measured data of $\sigma(\gamma,\text{abs})$ are taken from J.Ahrens [Ahr75] and the photonuclear data of $(\gamma, 1n)$, $(\gamma, 2n)$, (γ,np) reactions are taken from U.kneissl [Kne75], R.D.Edge [Edg57], J.H.Gibbons [Gib59], W.John [Joh62] and M.Fujishiro [Fuj82] . The experimental data were evaluated to guide the model calculation with code GLUNF [Zha99] up to 30 MeV, in which the file 6 in ENDF/B-VI format are given with full energy balance. However, below 16 MeV, the model calculation could not reproduce the experimental data of the $(\gamma, 1n)$ reaction, while these data have been performed by T.Fukohari [Fuk99] by using GDR multiple Lorentzian fitting, which have been adopted in this work.

At low energy (< 30 MeV), the giant-dipole resonance is the dominant excitation mechanism, in this energy region a simple isotropic approximation was used for the angular distribution of outgoing particles. The double differential cross sections include $(\gamma, 1n)$, $(\gamma, 2n)^7\text{Be}$, $(\gamma,np)^7\text{Li}$ reaction channels. In the $(\gamma,np)^7\text{Li}$ * reaction channel, the spectra of neutron, proton, ^7Li and gamma as well as gamma-Multiplicity are involved in the file 6.

Abundance (%)	Threshold Energies (MeV)								
	γ,n	γ,p	γ,t	$\gamma,\text{He-3}$	γ,α	$\gamma,2\text{n}$	γ,np	$\gamma,2\text{p}$	$\gamma,3\text{n}$
98.89	18.72	15.96	27.37	26.28	7.37	31.84	27.41	27.19	53.13
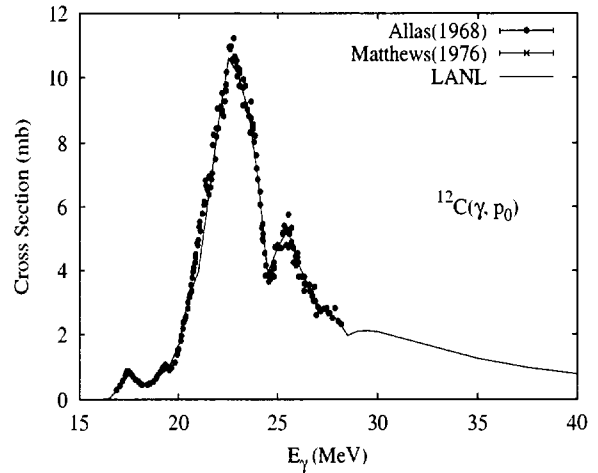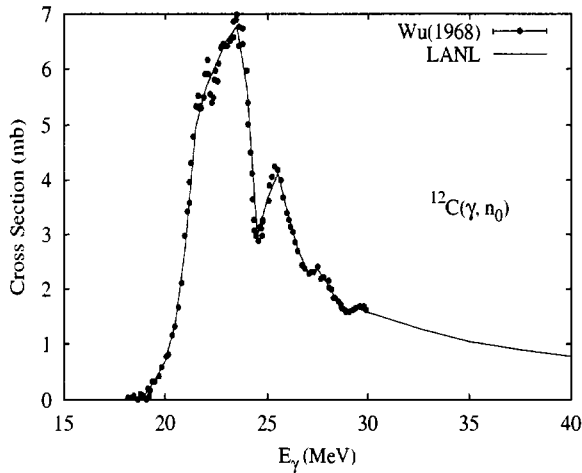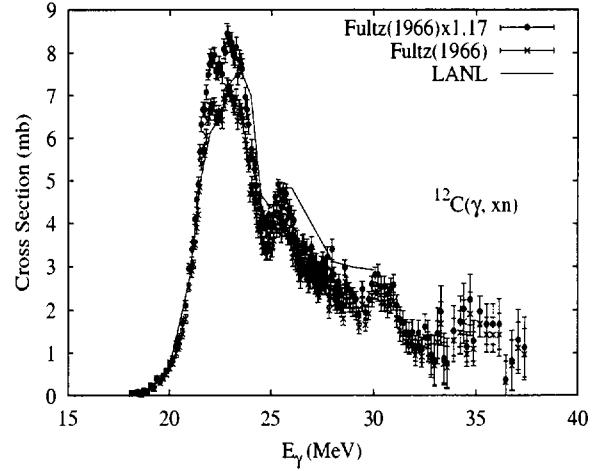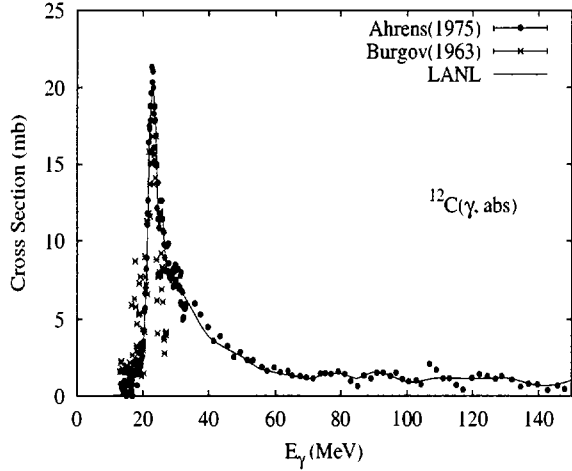
Our evaluation of photonuclear reactions on carbon follows, to a large extent, the analysis described by Fuller [Ful85].

The photoabsorption cross section was evaluated based on the data of Ahrens [Ahr75], that extend up to 150 MeV. Below 30 MeV, a constant value of 0.7 mb was subtracted from these data, as recommended by Fuller.

The Hauser-Feshbach statistical theory cannot be immediately applied in the analysis of photonuclear reactions on carbon, since there are significant contributions from direct reactions. In particular the (γ,n_0) and (γ,p_0) processes, which result in the residual nucleus being left in its ground state, account for a significant fraction of the photonuclear cross section (particularly for incident energies below 30 MeV). Therefore we first evaluate the (γ,n_0) and (γ,p_0) cross sections from the available experimental data. We adopt Fuller's recommendations [Ful85] in the GDR region; at higher energies our evaluation is based on the Matthews [Mat76] data at 60, 80, and 100 MeV for (γ,p_0) reactions, and we assume an equal cross section for the (γ,n_0) reactions at these high energies motivated by the concept of QD reaction mechanism. We used dipole angular distribution shapes (the only non-zero Legendre coefficient being a2) taken from Fuller. This describes the angular distribution in the GDR region. Although it is not appropriate at higher energies, where forward peaking is observed [Cha95a], our present evaluation is probably adequate

for most applications since the (γ,n_0) and (γ,p_0) reactions become very small in magnitude at higher incident energies.

The remaining cross section after (γ,n_0) and (γ,p_0) processes have occurred is modeled with the GNASH code, and represented in the ENDF file using MT5. Preequilibrium and compound decay processes are included. The resulting neutron emission contribution, when added to the (γ,n_0) cross section, was compared with Fuller's evaluation based on a renormalization of Fultz's data [Ful66] by a factor 1.17. Reasonable agreement for neutron production was obtained in the GDR peak, though the calculations appeared to somewhat overpredict neutron production (by as much as 30%) by 30 MeV. This failing is due to the difficulties in using a Hauser-Feshbach code to model reactions on light nuclei. Finally, GNASH calculations [Cha95a] of proton emission spectra for 60 MeV incident photons agreed well with the DDX data of McGeorge [McG86].

$$\gamma + {}^{13}\text{C}$$

Abundance (%)	Threshold Energies (MeV)								
	γ,n	γ,p	γ,t	γ,He-3	γ,α	γ,2n	γ,np	γ,2p	γ,3n
1.11	4.95	17.53	23.88	24.41	10.65	23.67	20.90	31.63	36.79
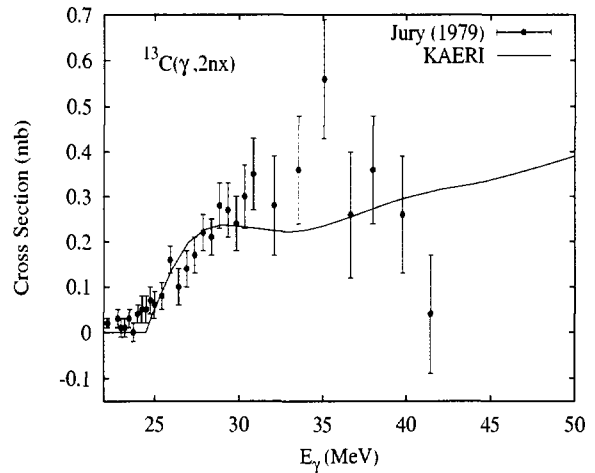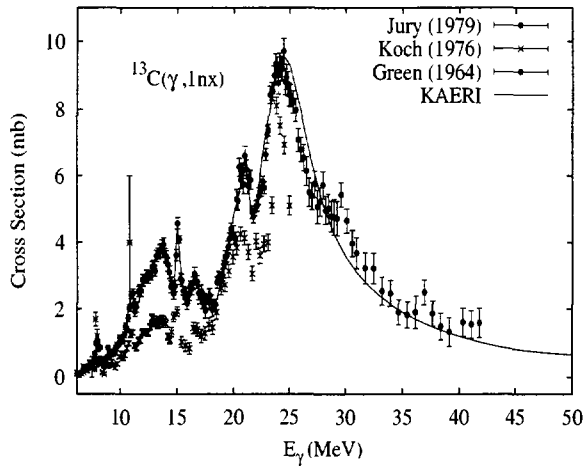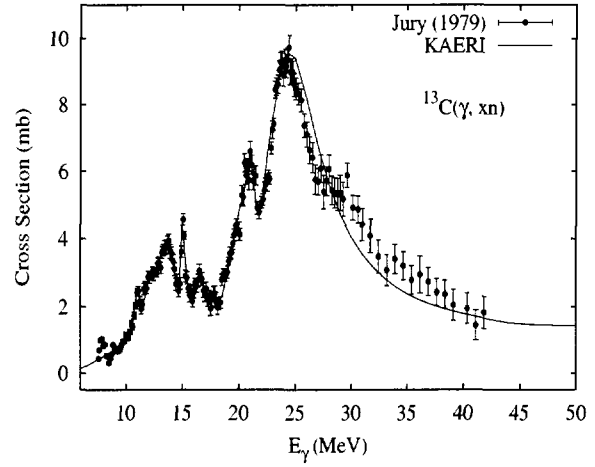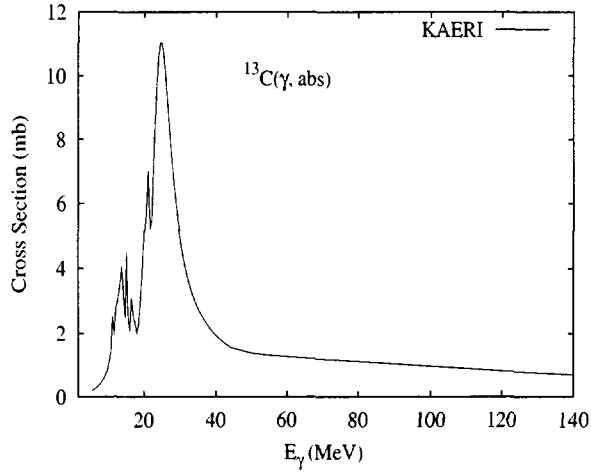
The photoabsorption cross section has not been measured. However, there are experimental data for the (γ, 1nx), (γ, 2nx) and (γ, xn) reaction cross sections [Jur79, Koc76, Gre64]. We relied on the GUNF and GNASH codes to infer the photoabsorption cross section in the GDR regime, in order to model accurately Jury's (γ, 1nx) data. The photoabsorption cross section above the GDR, up to 140 MeV, was obtained from QD model calculations using the theory of Chadwick.

The calculated results of the emission channels by the GNASH code are in good agreement with the Jury data for the (γ, 1nx), (γ, 2nx) and (γ, xn) cross sections.

Abundance	Threshold Energies (MeV)								
(%)	γ,n	γ,p	γ,t	γ,He-3	γ,α	γ,2n	γ,np	γ,2p	γ,3n
99.63	10.55	7.55	22.74	20.74	11.61	30.62	12.50	25.08	46.24
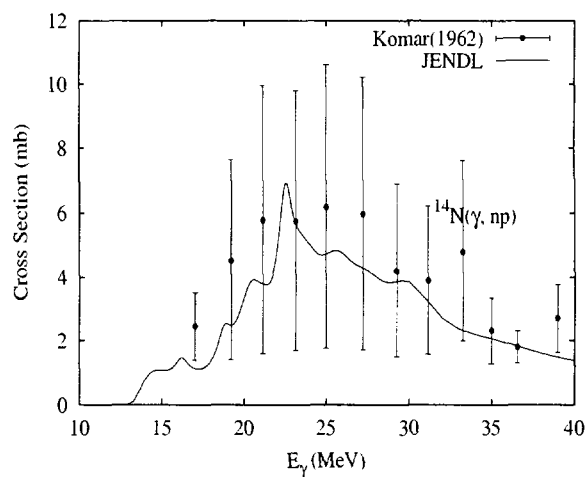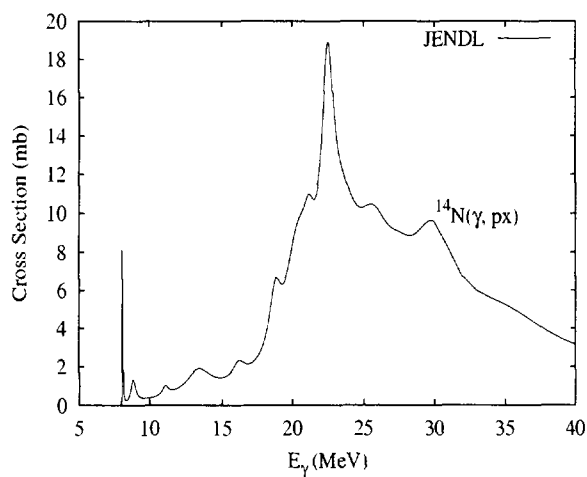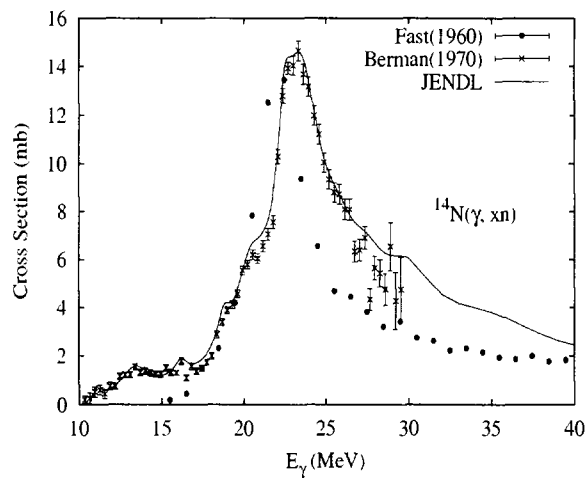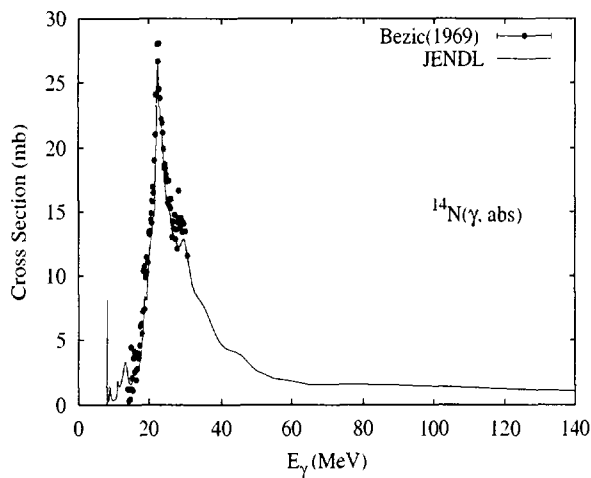
The photoabsorption cross section was measured by Bezic et al. [Bez69] and was analyzed between 15 and 31 MeV. Above 31 MeV, the cross section was estimated based on measurements of ${}^{16}\text{O}$ and ${}^{12}\text{C}$. Total photoneutron production data below 30 MeV [Ber70] were analyzed consistently together with other reaction channels [Kom62]. Above 30 MeV, the cross section was calculated with a GDR plus QD models [Mur91].

$$\gamma + {}^{15}\text{N}$$

Abundance	Threshold Energies (MeV)								
(%)	γ,n	γ,p	γ,t	γ,He-3	γ,α	γ,2n	γ,np	γ,2p	γ,3n
0.37	10.83	10.21	14.85	28.20	10.99	21.39	18.38	31.04	41.45
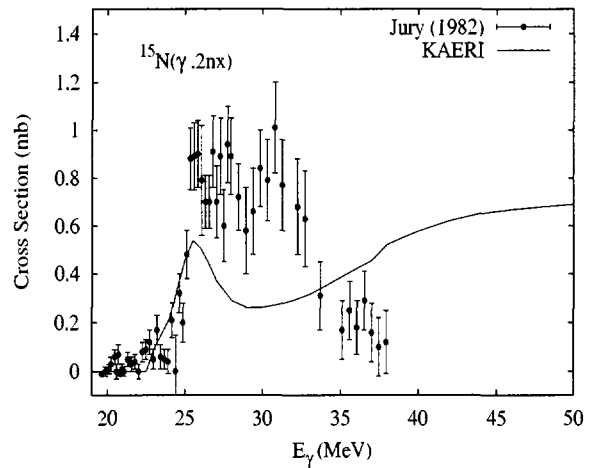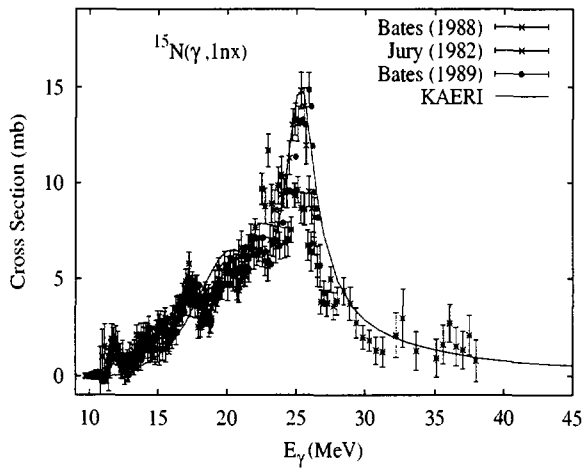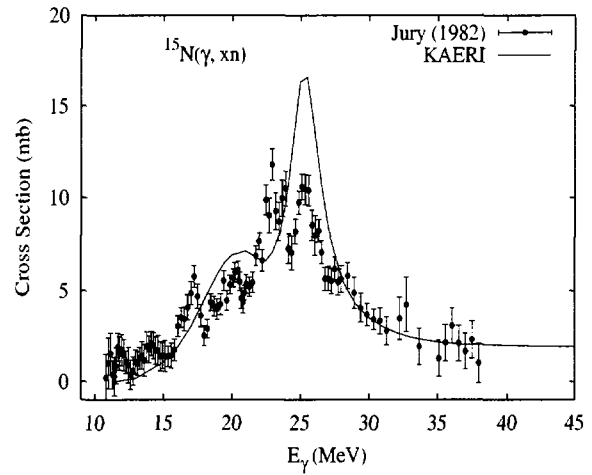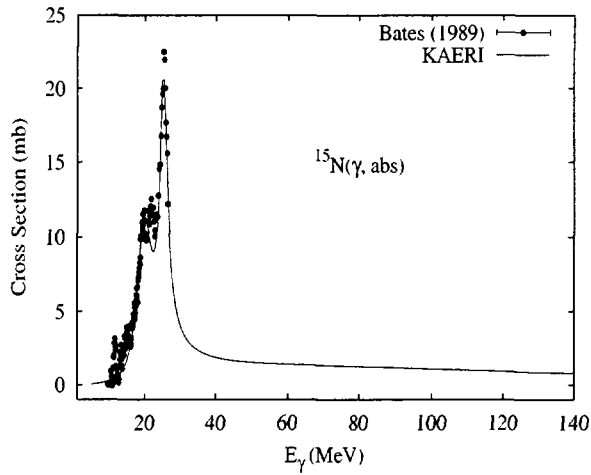
The photoabsorption cross section was evaluated based on the experimental data of Bates [Bat89], up to 35 MeV. Above this energy, the absorption cross section was calculated from the QD model.

The calculated results of the emission channel by the GNASH code are in agreement with the experimental data of Bates [Bat88] for (γ, 1nx) reaction cross sections, but are larger than the measurements of Jury [Jur82] for the (γ,xn) and (γ,2nx) reaction cross sections.

$$\gamma + {}^{16}\text{O}$$

Abundance (%)	Threshold Energies (MeV)								
	γ,n	γ,p	γ,t	$\gamma,\text{He-3}$	γ,α	$\gamma,2n$	γ,np	$\gamma,2p$	$\gamma,3n$
99.76	15.66	12.13	25.03	22.79	7.16	28.89	22.96	22.34	52.06
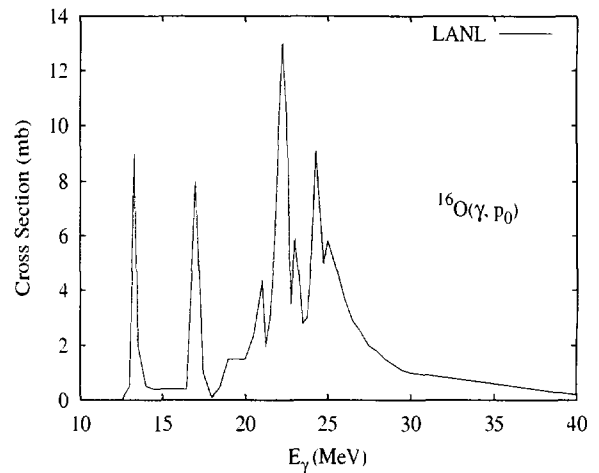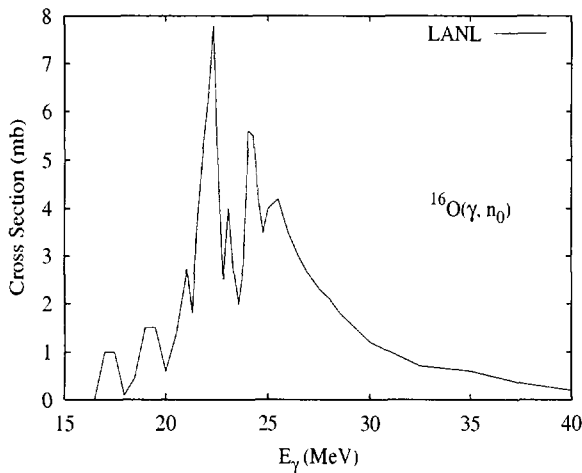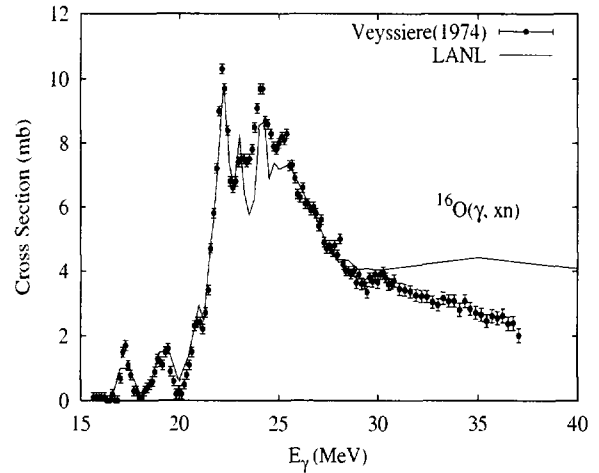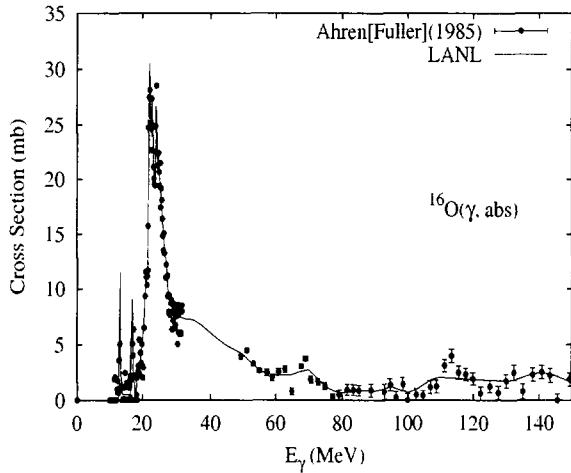
Our evaluation of photonuclear reactions on oxygen follows, to a large extent, the analysis described by Fuller [Ful85].

The photoabsorption cross section was evaluated based on the data of Ahrens [Ahr75], that extend up to 150 MeV. Below 30 MeV, a constant value of 2.78 mb was subtracted from these data, as recommended by Fuller, in order to make these data consistent with the sum of other (γ,n), (γ,p), etc. data. However, no such subtraction was made for energies above 50 MeV since this would result in negative cross sections, and a smooth transition was used for the absorption cross section from 30 to 50 MeV.

The Hauser-Feshbach statistical theory cannot be immediately applied in the analysis of photonuclear reactions on oxygen, since there are significant contributions from direct reactions. In particular the (γ,n_0) and (γ,p_0) processes, which result in the residual nucleus being left in its ground state, account for a significant fraction of the photonuclear cross section (particularly for incident energies below 30 MeV). Therefore we first evaluate the (γ,n_0) and (γ,p_0) cross sections from the available experimental data. We adopt Fuller's recommendations for these data. In the case of the p_0 data, these are based on the inverse process of proton capture. These evaluations were extended to 45 MeV based on Phillips' [Phi79] measurements for n_0 and the p_0 results shown in this same paper which are of the same magnitude from 30-45 MeV. Above 45 MeV, because

of a lack of other information, we based the n_0,p_0 cross sections on those for carbon [Mat76], since the carbon and oxygen n_0, p_0 data are of similar magnitude to oxygen at 30 MeV.

For the n_0 and p_0 cross sections we provide angular distributions using Legendre polynomials. These were obtained from Phillip's paper [Phi79], for both n_0 and p_0. (Note that Phillips' text describing the p_0 polynomials is not consistent with the data in his figure 7; Phillips advised us to use the graphical data rather than that based on the text.) Above 40 MeV, these angular distributions were simply extended, unmodified, up to 150 MeV. This is not physically correct [Cha95a], though its impact in transport calculations will be generally small due to the small magnitude of n_0, p_0 cross sections above 40 MeV.

The remaining cross section after (γ,n_0) and (γ,p_0) processes have occurred is modeled with the GNASH code, and represented in the ENDF file using MT5. Preequilibrium and compound decay processes are included. The resulting neutron emission contribution, when added to the (γ,n_0) cross section, was compared with Fuller's evaluation, and other measurements [Vey74, Ber80, Kne75] and good agreement was obtained.

$$\gamma + {}^{17}O$$

| Abundance	Threshold Energies (MeV)								
(%)	γ,n	γ,p	γ,t	γ,He-3	γ,α	γ,2n	γ,np	γ,2p	γ,3n
0.04	4.14	13.78	18.62	18.76	6.36	19.81	16.27	25.26	33.03
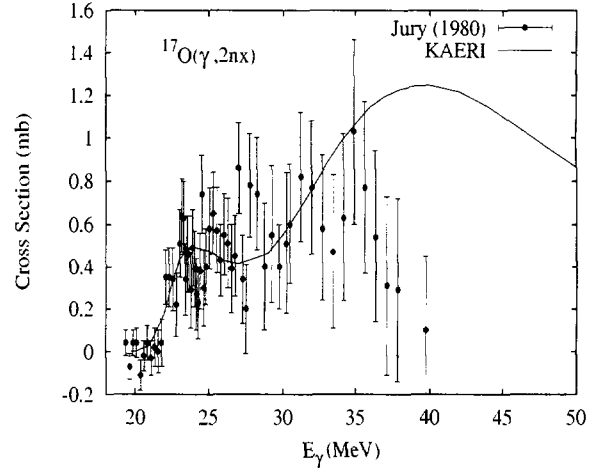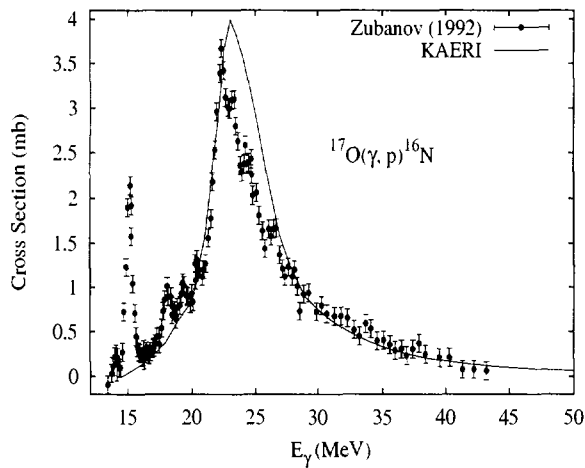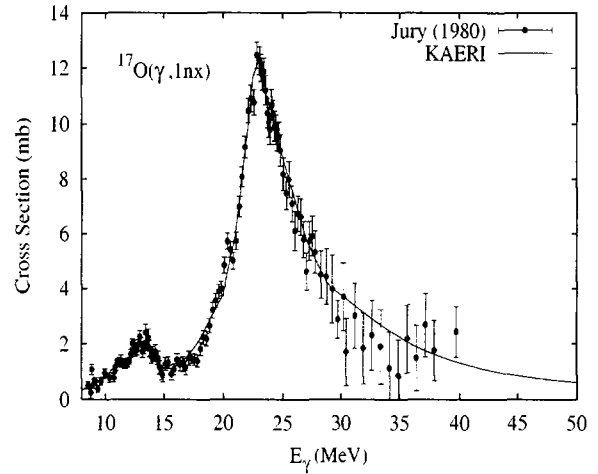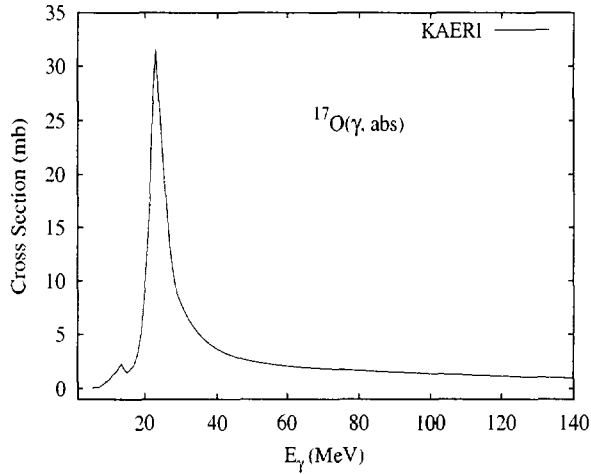
The photoabsorption cross section has not been measured. However, there are experimental data for (γ, 1nx), (γ, p), (γ, 2nx) and (γ, xn) reaction cross sections by Jury [Jur80]. We relied on the GUNF and GNASH codes to infer the absorption cross section in the GDR regime, so as to model accurately the Jury's measured data. The absorption cross section above the GDR, up to 140 MeV, was taken from QD model calculations.

The calculated results for the emission channels by the GNASH code are in good agreement with the Jury data for (γ, 1nx), (γ, 2nx) and (γ, xn) reaction cross sections. Overall agreement was also seen for the calculated results for (γ, p) reaction cross sections with the experimental data of Zubanov [Zub92] except the sharp resonance at 15.2 MeV, which is due to the direct capture mechanism.

$\gamma + {}^{18}\mathrm{O}$

Abundance	Threshold Energies (MeV)								
(%)	γ,n	γ,p	γ,t	γ,He-3	γ,α	γ,2n	γ,np	γ,2p	γ,3n
0.20	8.04	15.94	15.83	25.59	6.23	12.19	21.82	29.05	27.85
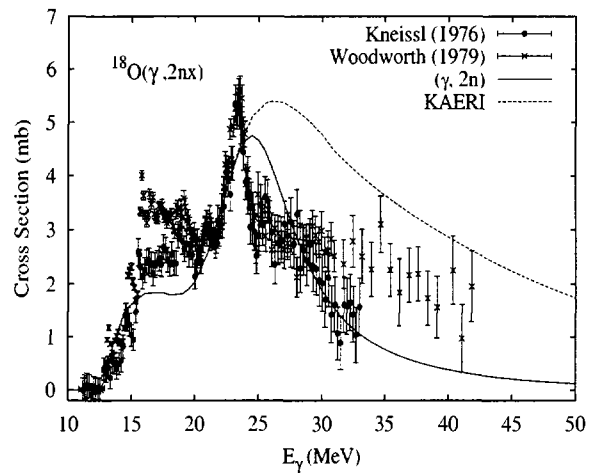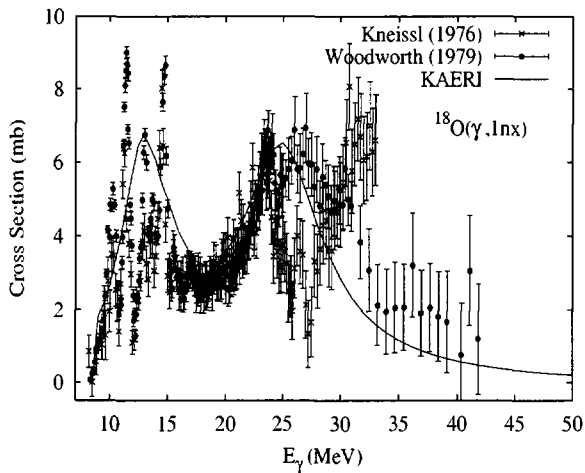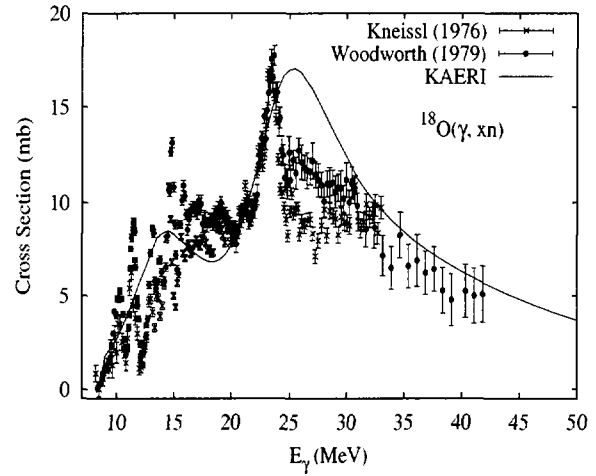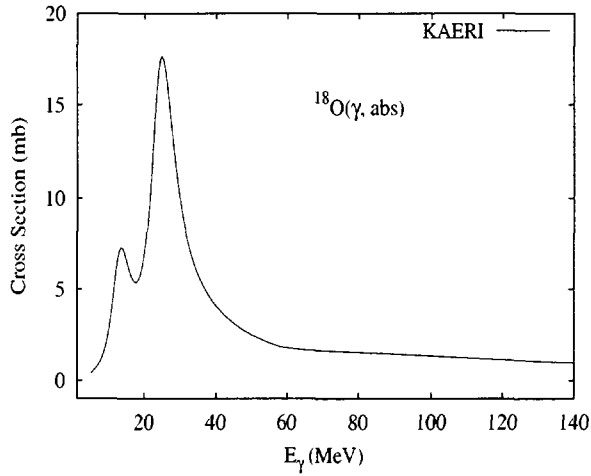
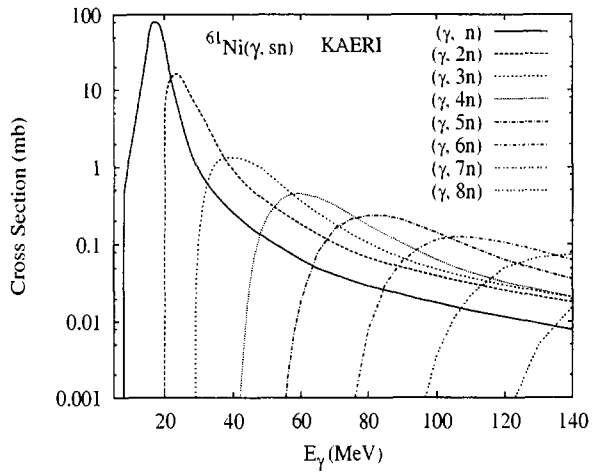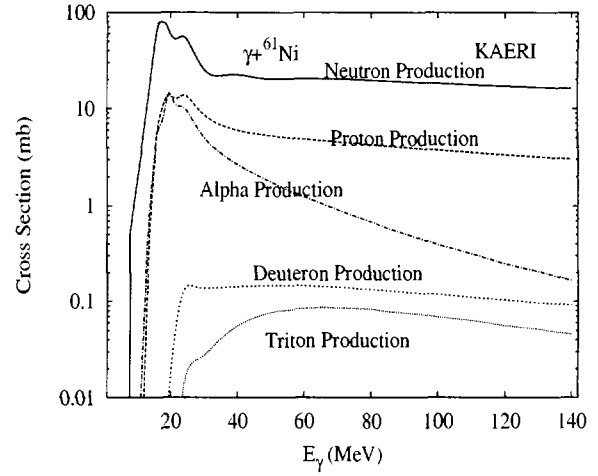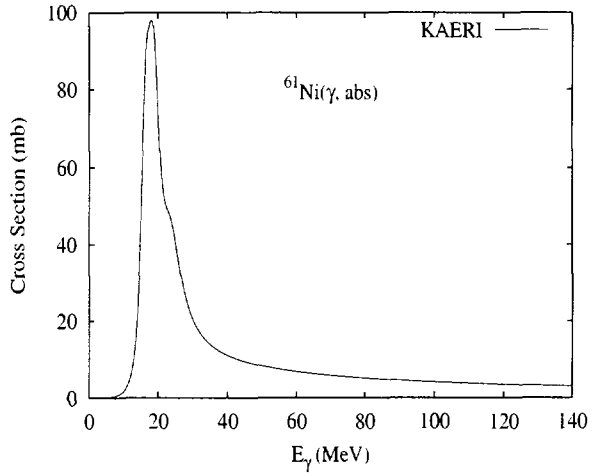
The photoabsorption cross section has not been measured. However, there are experimental data for the (γ, 1nx), (γ, 1p), (γ, 2nx) and (γ, xn) reaction cross sections by Woodworth [Woo79] and Kneissl [Kne76]. We relied on the GUNF and GNASH codes to infer the photoabsorption cross section in the GDR regime, in order to reproduce the measured data of Woodworth and Kneissl consistently. The photoabsorption cross section above the GDR, up to 140 MeV, was obtained from QD model calculations using the theory of Chadwick. The calculated results are basically in agreement with the experimental data for (γ, 1nx), (γ, 1p), (γ, 2nx) and (γ, xn) reaction cross sections. However, as expected, the statistical approach is not adequate to represent the sharp resonance structures typically seen in light nuclei.

$\gamma + {}^{23}\mathrm{Na}$

Abundance (%)	Threshold Energies (MeV)								
	γ,n	γ,p	γ,t	$\gamma,\mathrm{He}\text{-}3$	γ,α	$\gamma,2n$	γ,np	$\gamma,2p$	$\gamma,3n$
100.00	12.42	8.79	17.43	24.45	10.47	23.49	19.16	24.06	40.59
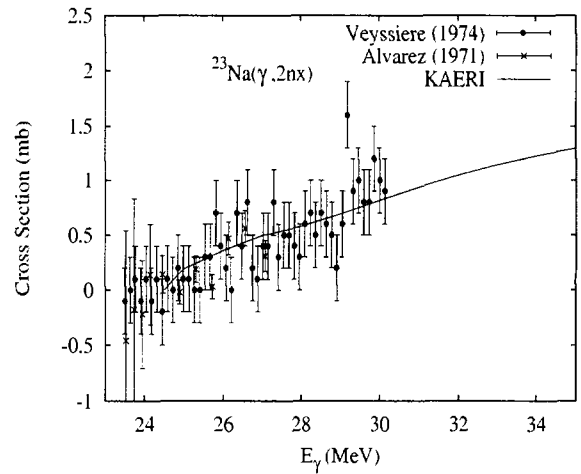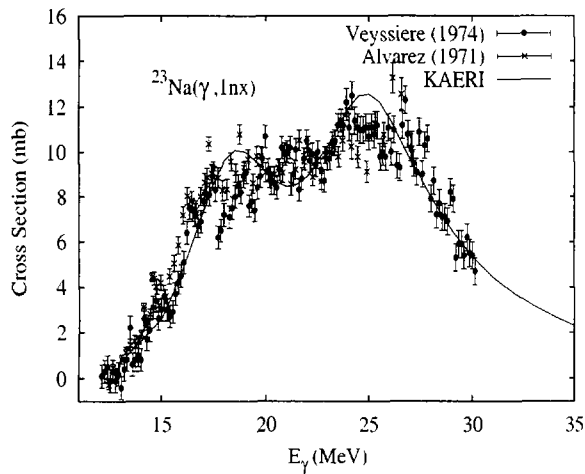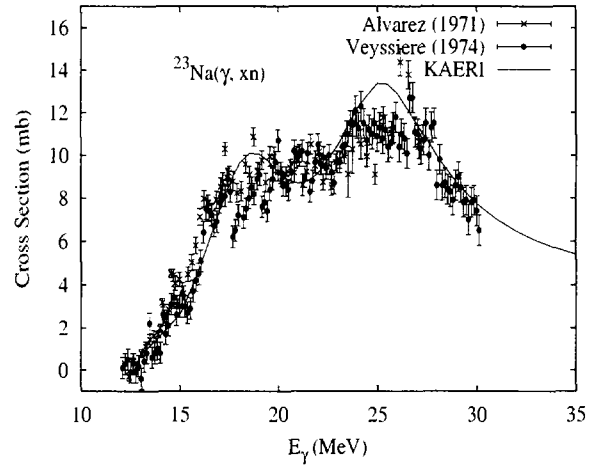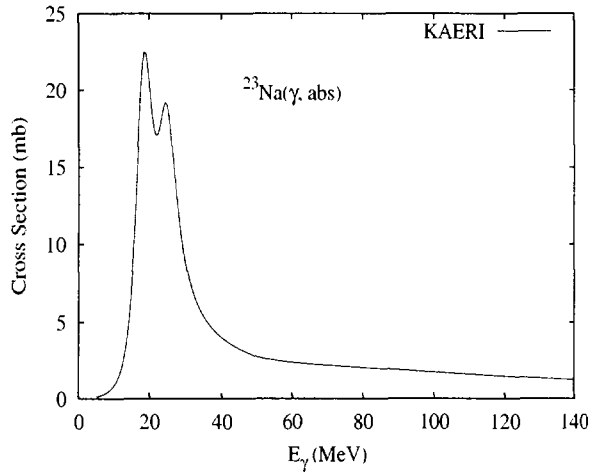
The photoabsorption cross section has not been measured. However, there are experimental data for the (γ, 1nx), (γ, 2nx), (γ, sn) and (γ, xn) reaction cross sections [Alv71, Vey74]. We relied on the GUNF and GNASH codes to infer the photoabsorption cross section in the GDR regime, in order to model accurately Veyssiere's (γ, 1nx) data. The photoabsorption cross section above the GDR, up to 140 MeV, was obtained from QD model calculations using the theory of Chadwick.

The calculated results of the emission channels by the GNASH code reproduce fairly well all the available experimental data for (γ, 1nx), (γ, 2nx), (γ, sn) and (γ, xn) reaction cross sections.

$$\gamma + {}^{24}\text{Mg}$$

Abundance	Threshold Energies (MeV)								
(%)	γ,n	γ,p	γ,t	γ,He-3	γ,α	γ,2n	γ,np	γ,2p	γ,3n
78.99	16.53	11.69	26.69	23.13	9.31	29.68	24.11	20.48	49.06
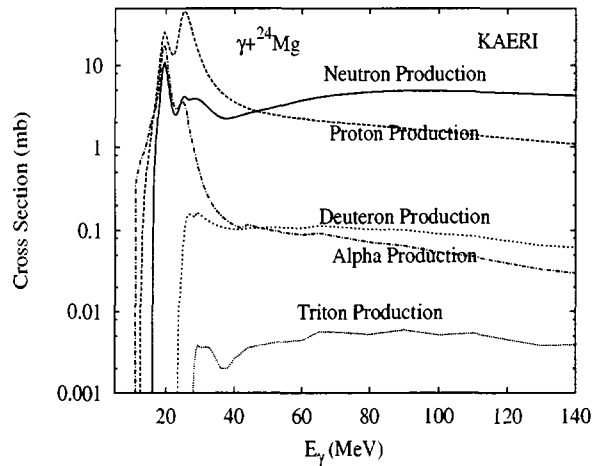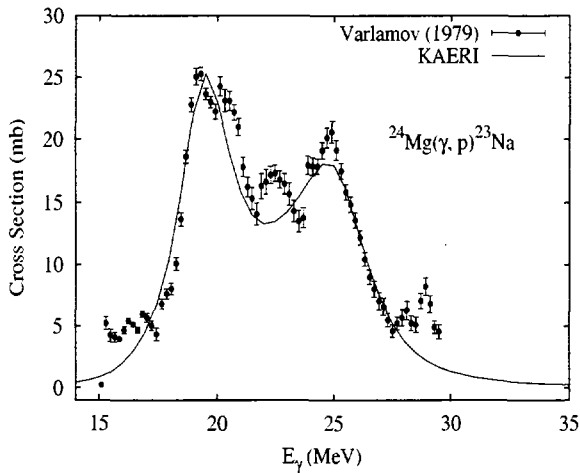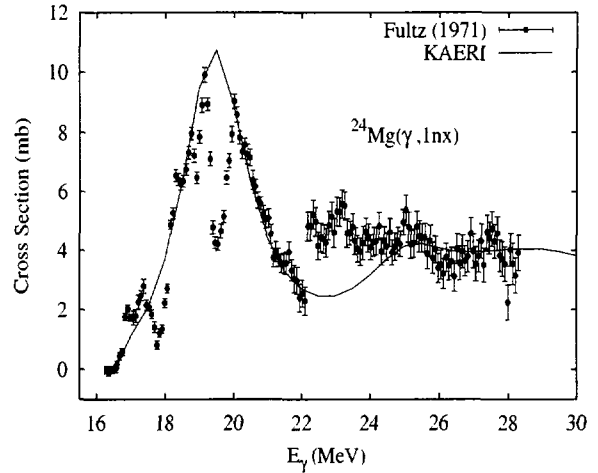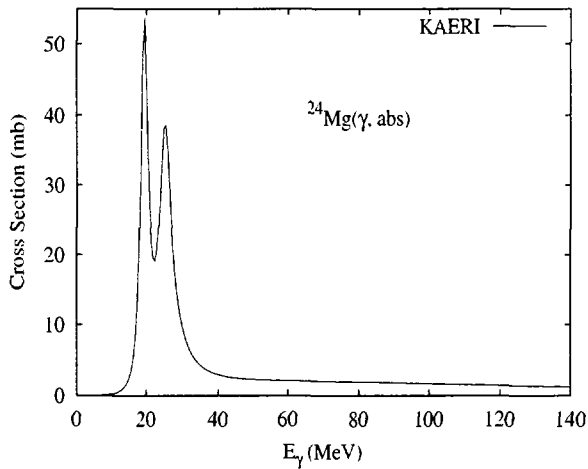
The photoabsorption cross section has not been measured. However, there are experimental data for the (γ, 1nx) [Ful71], and (γ, 1p) [Var79b] reaction cross sections. We relied on the GUNF and GNASH codes to infer the photoabsorption cross section in the GDR regime, in order to model accurately the (γ, 1nx) and (γ, 1p) cross sections. The photoabsorption cross section above the GDR, up to 140 MeV, was obtained from QD model calculations using the theory of Chadwick. The calculated results of the emission channels by the GNASH code show reasonable agreement with both channels measured.

$\gamma + {}^{25}\mathrm{Mg}$

Abundance (%)	Threshold Energies (MeV)								
	γ,n	γ,p	γ,t	$\gamma,\mathrm{He\text{-}3}$	γ,α	$\gamma,2\mathrm{n}$	γ,np	$\gamma,2\mathrm{p}$	$\gamma,3\mathrm{n}$
10.00	7.33	12.06	22.96	20.10	9.88	23.86	19.02	22.61	37.01
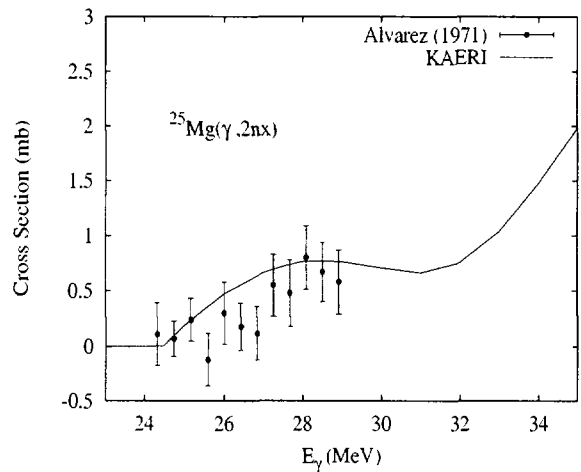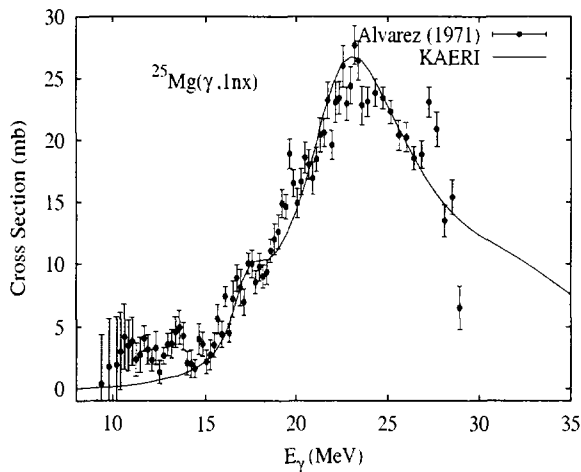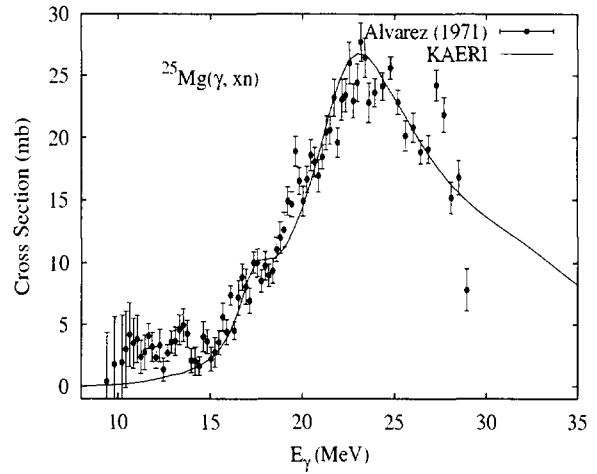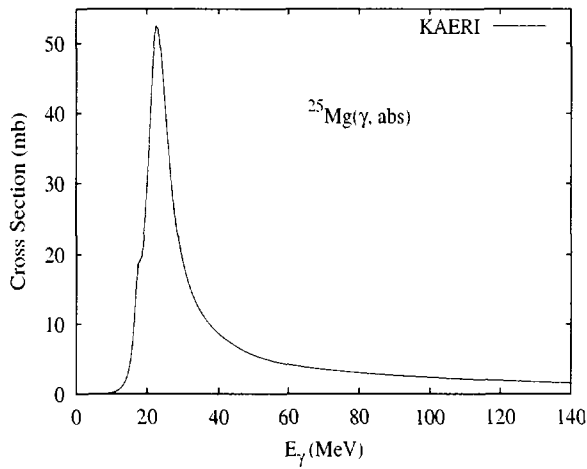
The photoabsorption cross section has not been measured. However, there are experimental data for the $(\gamma, 1\mathrm{nx})$, $(\gamma, 2\mathrm{nx})$, (γ, sn) and (γ, xn) reaction cross sections [Alv71]. We relied on the GUNF and GNASH codes to infer the photoabsorption cross section in the GDR regime, in order to model accurately Alvarez's data. The photoabsorption cross section above the GDR, up to 140 MeV, was obtained from QD model calculations using the theory of Chadwick.

The calculated results of the emission channels by the GNASH code are in good agreement with the experimental data for all measured channels.

$$\gamma + {}^{26}\mathrm{Mg}$$

Abundance (%)	Threshold Energies (MeV)								
	γ,n	γ,p	γ,t	γ,He-3	γ,α	γ,2n	γ,np	γ,2p	γ,3n
11.01	11.09	14.14	21.63	25.99	10.61	18.42	23.15	24.84	34.95
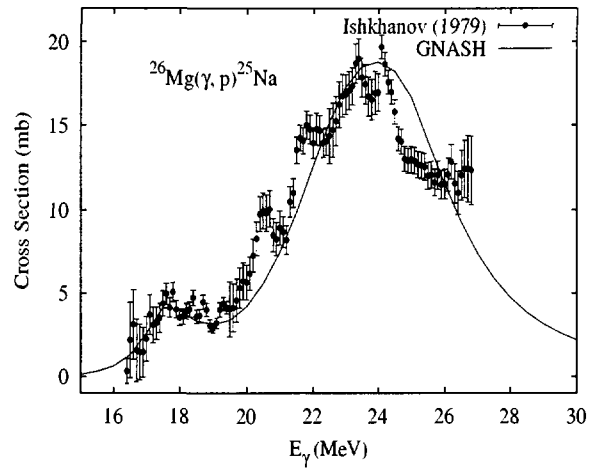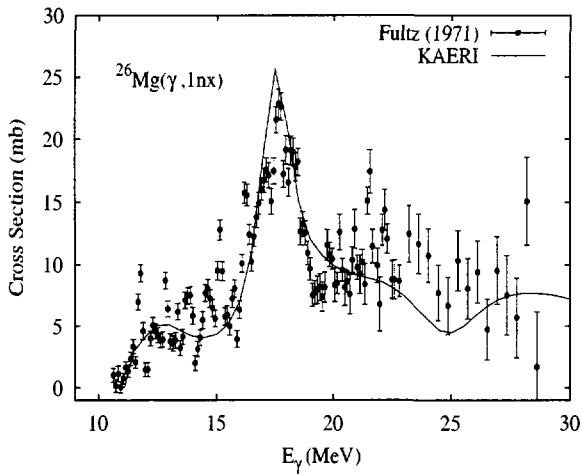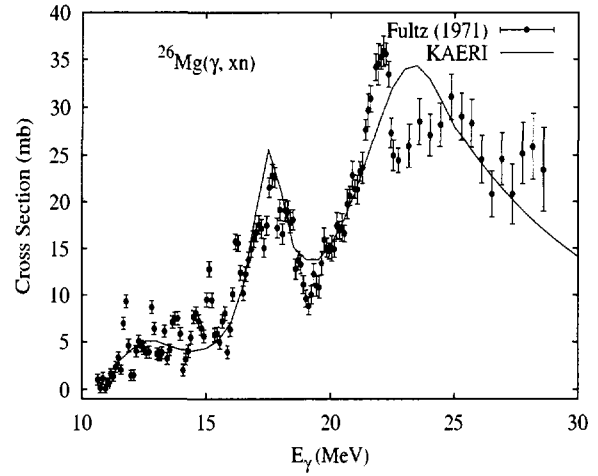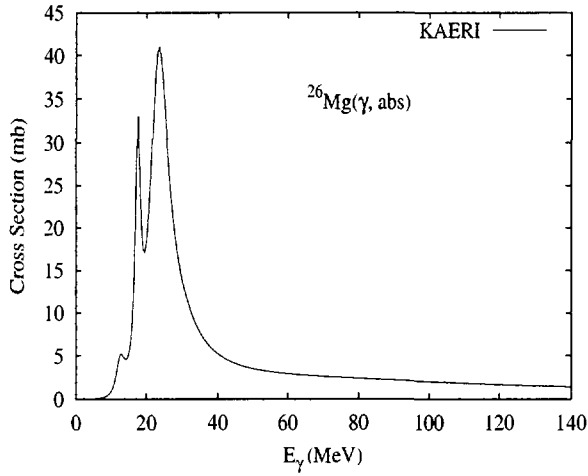
The photoabsorption cross section has not been measured. However, there are experimental data for the (γ, 1nx), (γ, 1p), (γ, 2n), (γ, sn) and (γ, xn) reaction cross sections [Ful71, Ish79]. We relied on the GUNF and GNASH codes to infer the photoabsorption cross section in the GDR regime, in order to reproduce the overall shapes of the experimental data. The photoabsorption cross section above the GDR, up to 140 MeV, was obtained from QD model calculations using the theory of Chadwick.

The calculated results of the emission channels by the GNASH code are basically in agreement with the experimental data for the (γ, 1nx), (γ, 1p), (γ, 2n), (γ, sn) and (γ, xn) reaction cross sections.

Abundance	Threshold Energies (MeV)								
(%)	γ,n	γ,p	γ,t	γ,He-3	γ,α	γ,2n	γ,np	γ,2p	γ,3n
100.00	13.06	8.27	18.21	23.71	10.09	24.42	19.36	22.41	41.36
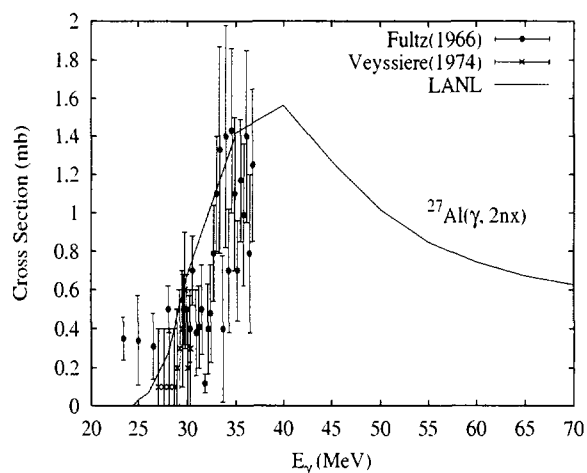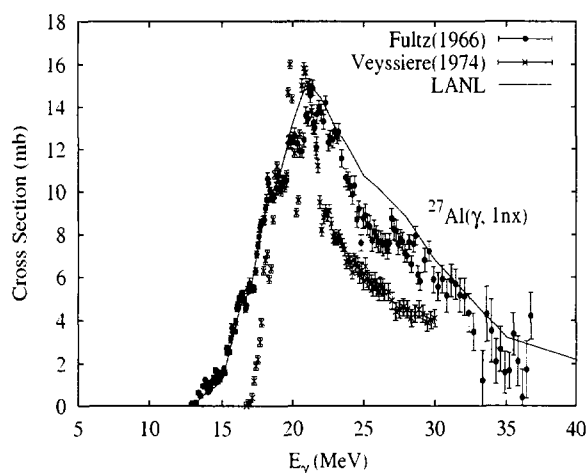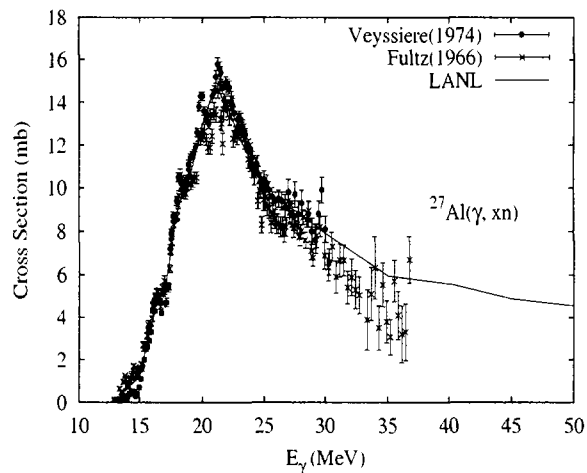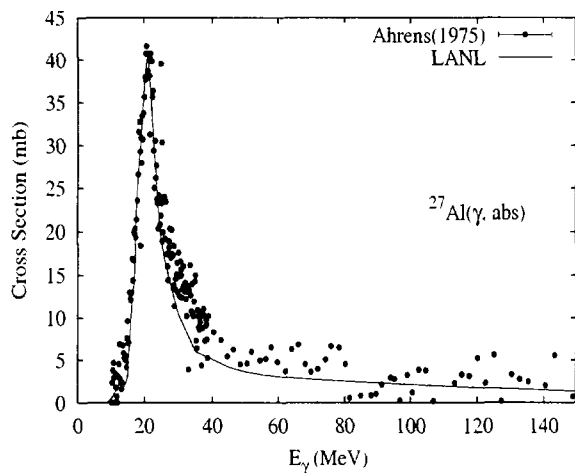
Available data are summarized by Varlamov [Var96]. The photoabsorption cross section was evaluated based on the data of Ahrens [Ahr75], that extend up to 150 MeV. However, above about 35 MeV, the evaluation used directly theoretical predictions from the QD model of Chadwick [Cha91]. Between approximately 30-40 MeV, the evaluation under-predicted the Ahrens absorption data. This was done since the evaluated neutron production in this energy range, based on GNASH predictions, somewhat over-predicted the photoneutron production measurements (see below), and it was felt that it is important to have as accurate as possible predictions of photoneutron production; increasing the absorption cross section here would lead to a worse discrepancy with the photoneutron production data.

Input level density parameters for the GNASH calculations were "tuned" so as to give an accurate representation of data at the GDR peak [i.e. at 21 MeV, a neutron production of about 15mb in agreement with [Ful66, Vey74]; a proton production about 16mb (experiment = 17.5 mb [Var96]]; and an alpha production of 11 mb, with the sum adding up to 41 mb as predicted by Ahrens [Ahr75]].

$\gamma + {}^{27}\mathrm{Si}$

Abundance	Threshold Energies (MeV)								
(%)	γ,n	γ,p	γ,t	γ,He-3	γ,α	γ,2n	γ,np	γ,2p	γ,3n
0.00	13.31	7.46	27.28	13.38	9.34	32.36	18.83	13.77	47.35
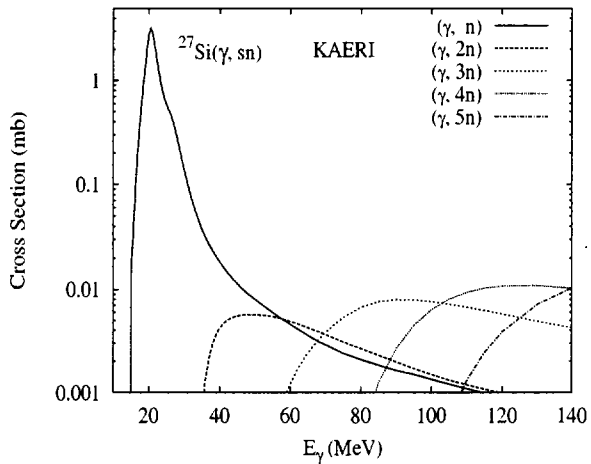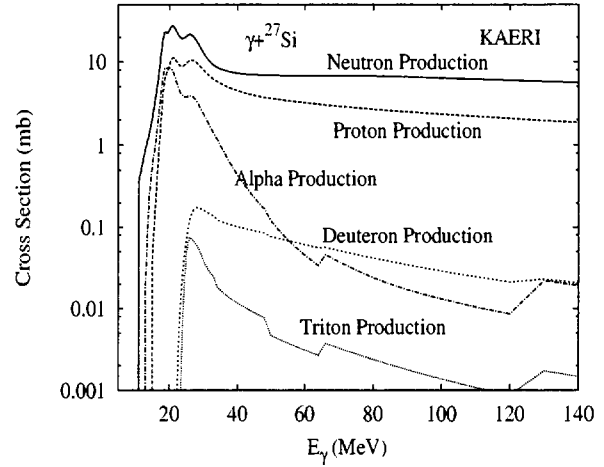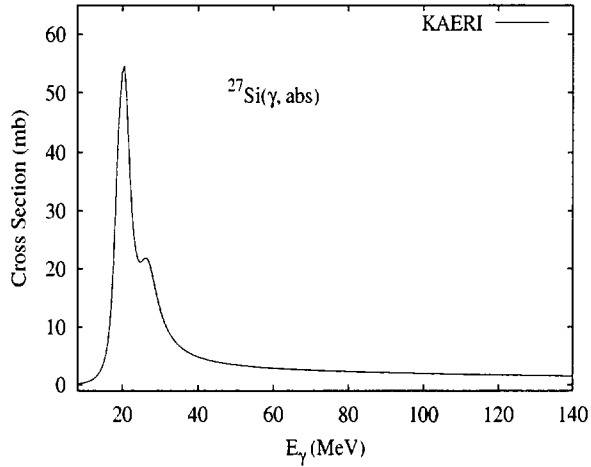
There are no experimental data available. The photoabsorption cross section was obtained from GDR and QD model calculations, adopting the GDR parameters of ${}^{28}\mathrm{Si}$. The neutron, proton, deuteron, triton and alpha emission cross sections, as well as production cross sections, were calculated by the GNASH code.

$$\gamma + {}^{28}\text{Si}$$

Abundance (%)	Threshold Energies (MeV)								
	γ,n	γ,p	γ,t	γ,He-3	γ,α	γ,2n	γ,np	γ,2p	γ,3n
92.23	17.18	11.58	27.53	23.23	9.98	30.49	24.64	19.86	49.53
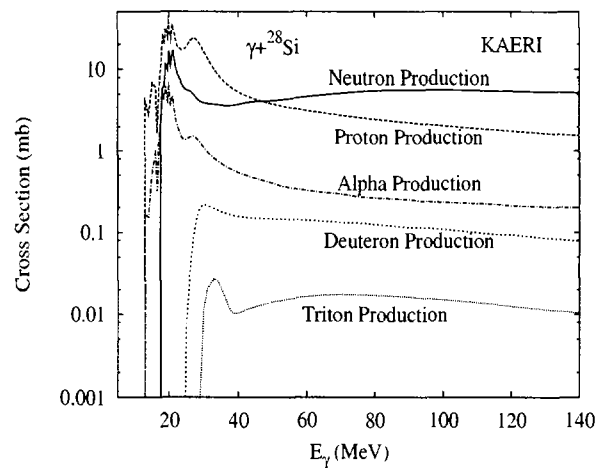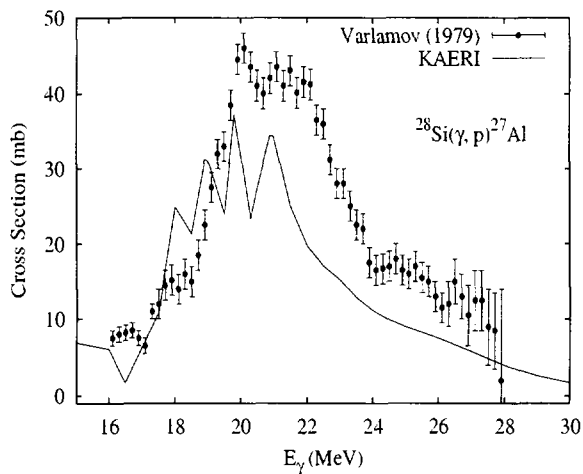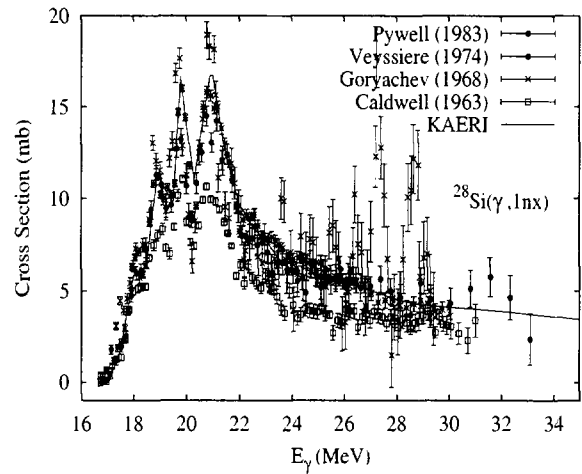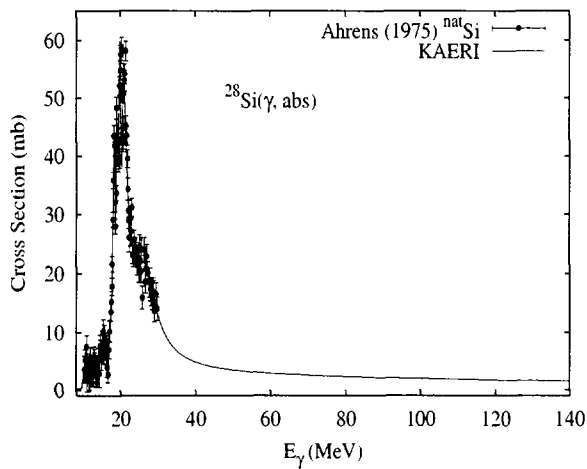
The photoabsorption cross section was evaluated based on the measurements of Ahrens [Ahr75] for ^{nat}Si. Above about 35 MeV, and up to 140 MeV, the absorption cross section was calculated from the QD model. Experimental data for (γ, 1nx) reaction cross section are available [Pyw83, Vey74, Cal63, Gor68].

The calculated results of the emission channels by the GNASH code are in good agreement with the experimental data of Pywell [Pyw83] and Veyssiere [Vey74] for the (γ, 1nx) reaction cross section, but are lower than the experimental data of Varlamov [Var79a] for the (γ, 1p) reaction cross section.

$$\gamma + {}^{29}\text{Si}$$

Abundance	Threshold Energies (MeV)								
(%)	γ,n	γ,p	γ,t	γ,He-3	γ,α	γ,2n	γ,np	γ,2p	γ,3n
4.67	8.47	12.33	24.63	20.61	11.13	25.65	20.06	21.89	38.96
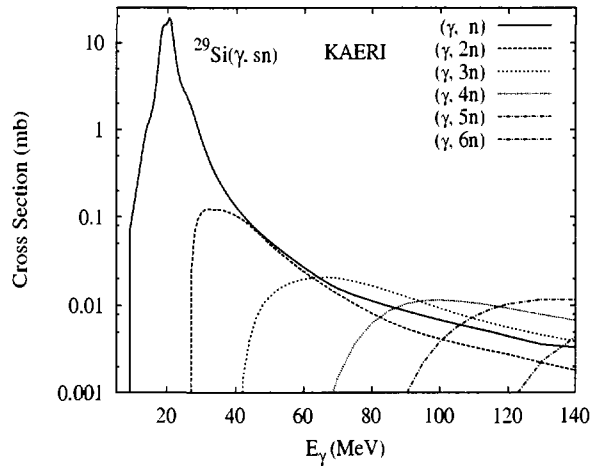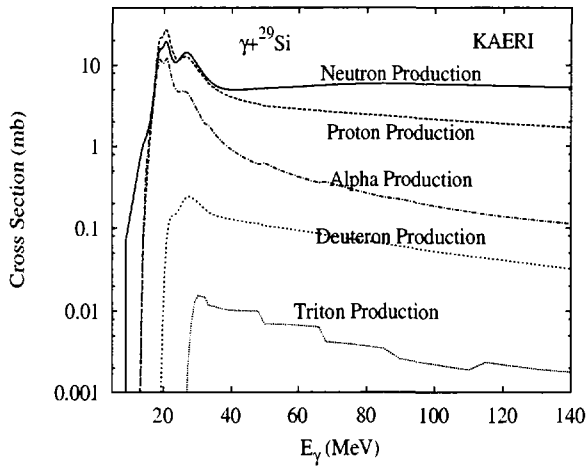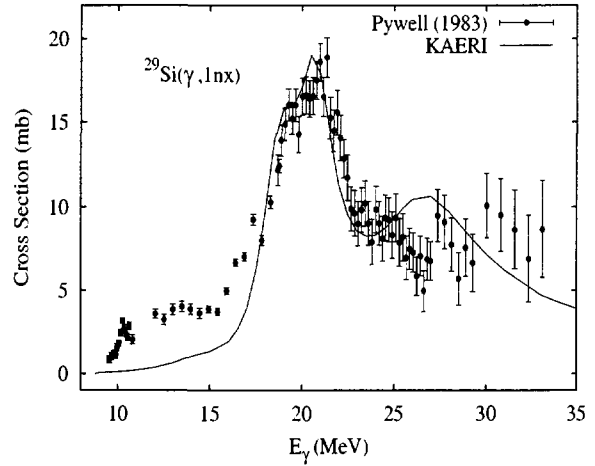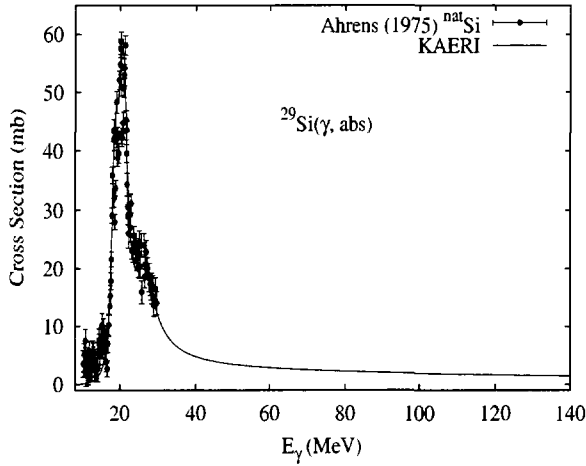
The photoabsorption cross section was evaluated based on the measurements of Ahrens' [Ahr75] for ^{nat}Si. Above about 35 MeV, and up to 140 MeV, the absorption cross section was calculated from the QD model.

The calculated results of the emission channels by the GNASH code reproduce fairly well the experimental data for the (γ, 1nx) reaction cross section [Pyw83].

$\gamma + {}^{30}\text{Si}$

Abundance (%)	Threshold Energies (MeV)								
	γ,n	γ,p	γ,t	$\gamma,\text{He-3}$	γ,α	$\gamma,2n$	γ,np	$\gamma,2p$	$\gamma,3n$
3.10	10.61	13.51	22.19	24.78	10.64	19.08	22.94	23.99	36.26
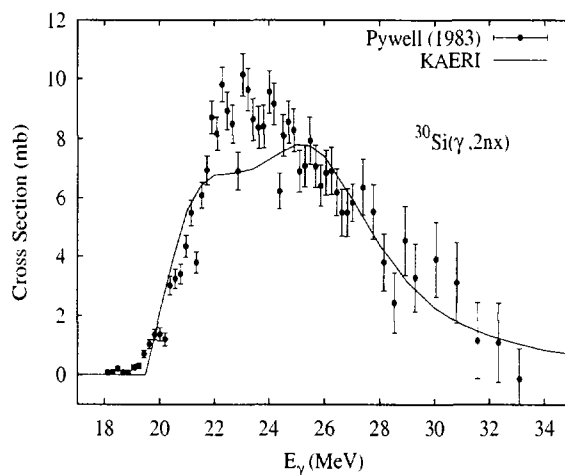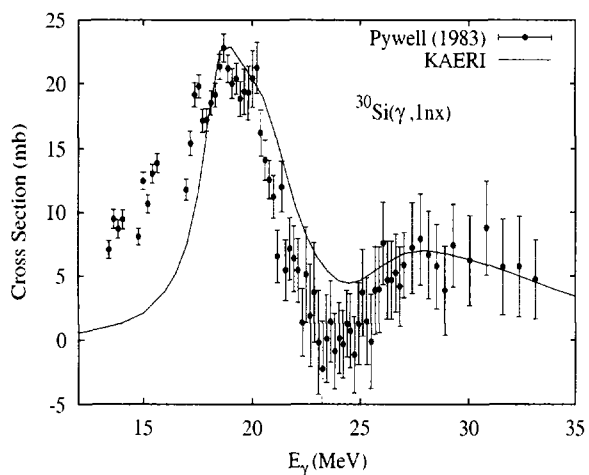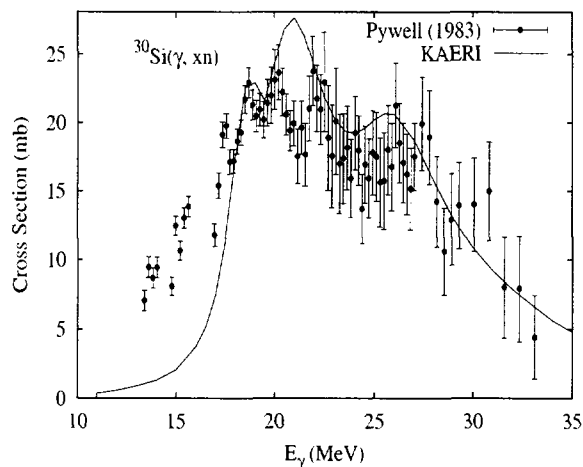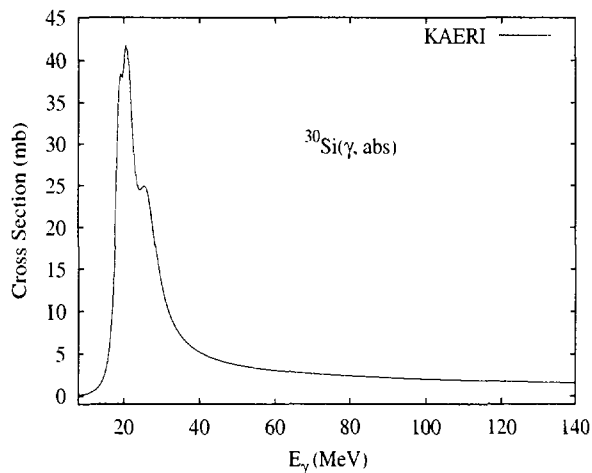
The photoabsorption cross section has not been measured. However, there are experimental data [Pyw83] for the $(\gamma, 1nx)$, $(\gamma, 2nx)$ and (γ, xn) reaction cross sections. We relied on the GUNF and GNASH codes to infer the absorption cross section in the GDR regime, so as to reproduce the overall shapes of the Pywell's measurements. The absorption cross section above the GDR, up to 140 MeV, was taken from QD model calculations.

The calculated results of the emission channels by the GNASH code are basically in agreement with the experimental data for $(\gamma, 1nx)$, $(\gamma, 2nx)$ and (γ, xn) reaction cross sections.

$$\gamma + {}^{32}\text{S}$$

Abundance	Threshold Energies (MeV)								
(%)	γ,n	γ,p	γ,t	$\gamma,$He-3	γ,α	$\gamma,2n$	γ,np	$\gamma,2p$	$\gamma,3n$
95.02	15.04	8.86	24.01	19.05	6.95	28.10	21.18	16.16	47.07
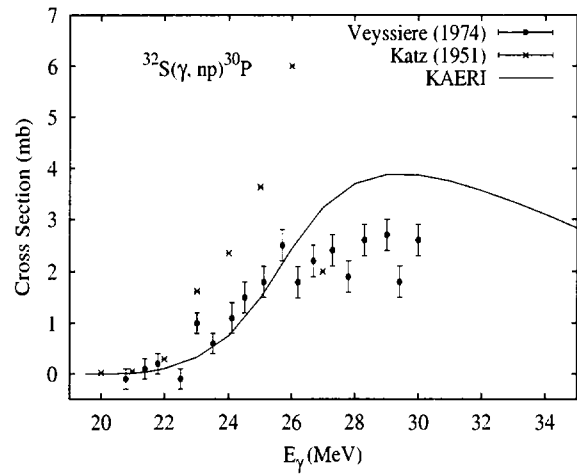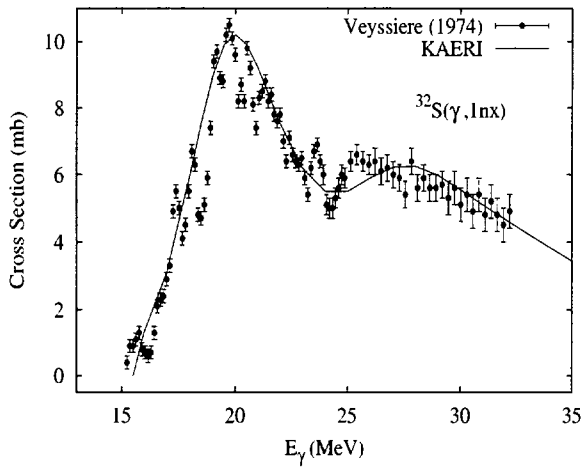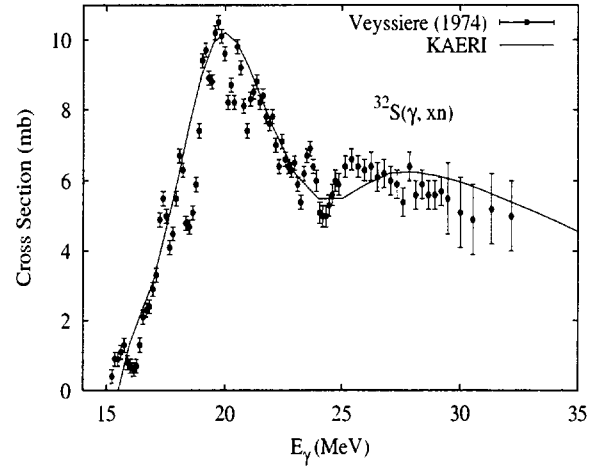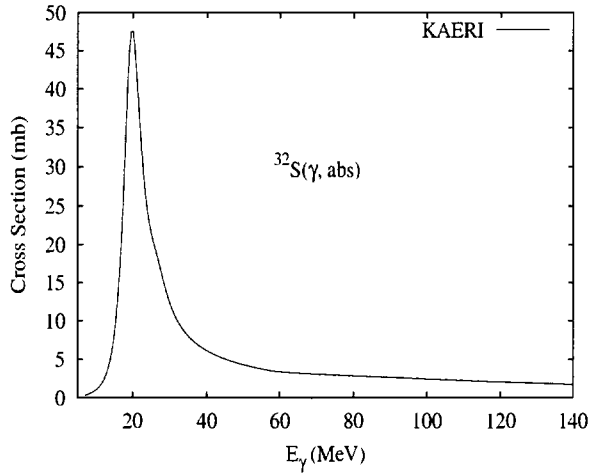
The photoabsorption cross section has not been measured. However, there are experimental data for the $(\gamma, \ln x)$, (γ, np), $(\gamma, 2n)$ and (γ, xn) reaction cross sections [Vey74]. We relied on the GUNF and GNASH codes to infer the photoabsorption cross section in the GDR regime, in order to model accurately Veyssiere's data. The photoabsorption cross section above the GDR, up to 140 MeV, was obtained from QD model calculations using the theory of Chadwick.

The calculated results of the emission channels by the GNASH code are in good agreement with the Veyssiere data for $(\gamma, \ln x)$, (γ, np), $(\gamma, 2n)$ and (γ, xn) reaction cross sections.

$\gamma + {}^{33}\text{S}$

Abundance (%)	Threshold Energies (MeV)								
	γ,n	γ,p	γ,t	$\gamma,\text{He-3}$	γ,α	$\gamma,2n$	γ,np	$\gamma,2p$	$\gamma,3n$
0.75	8.64	9.57	21.34	17.08	7.12	23.68	17.51	18.21	36.74
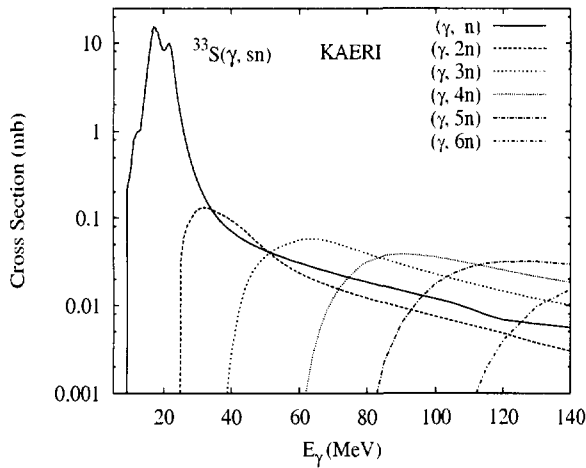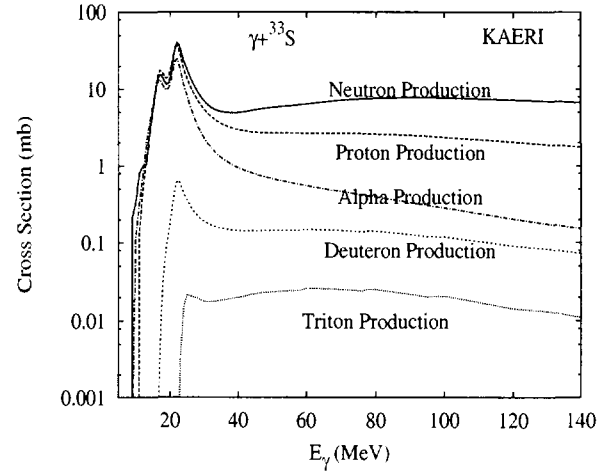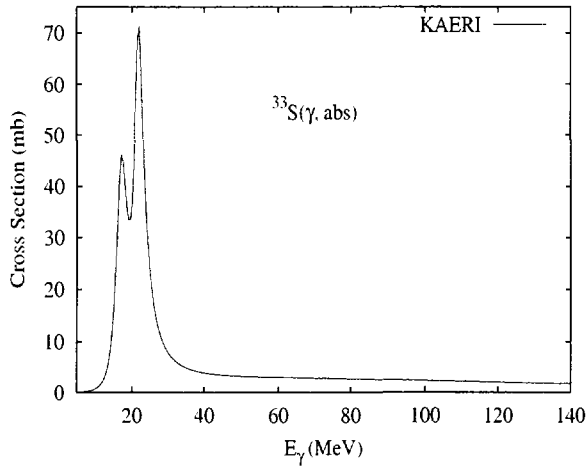
There are no experimental data available. The photoabsorption cross section was obtained from GDR and QD model calculations, adopting the GDR parameters of ${}^{34}\text{S}$. The neutron, proton, deuteron, triton and alpha emission cross sections, as well as production cross sections, were calculated by the GNASH code.

$$\gamma + {}^{34}\text{S}$$

Abundance	Threshold Energies (MeV)								
(%)	γ,n	γ,p	γ,t	γ,He-3	γ,α	γ,2n	γ,np	γ,2p	γ,3n
4.21	11.42	10.88	20.44	21.91	7.92	20.06	20.99	20.43	35.10
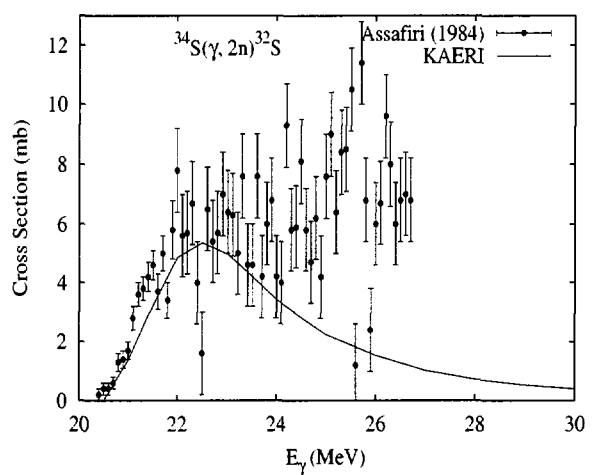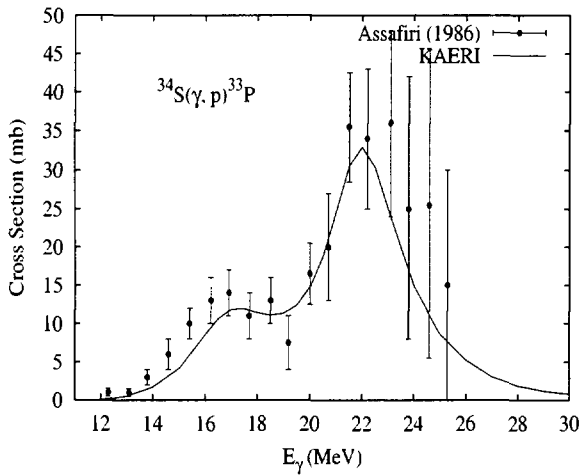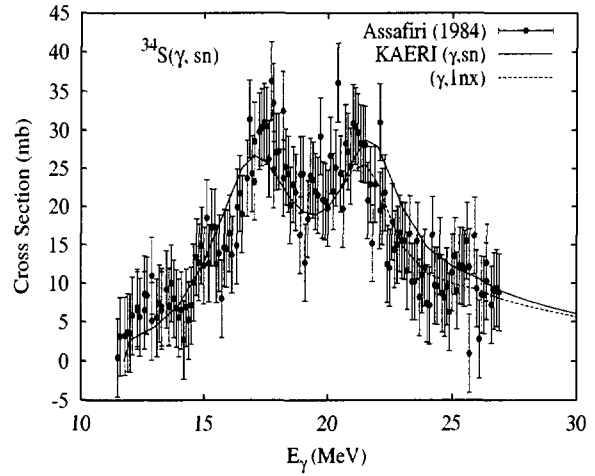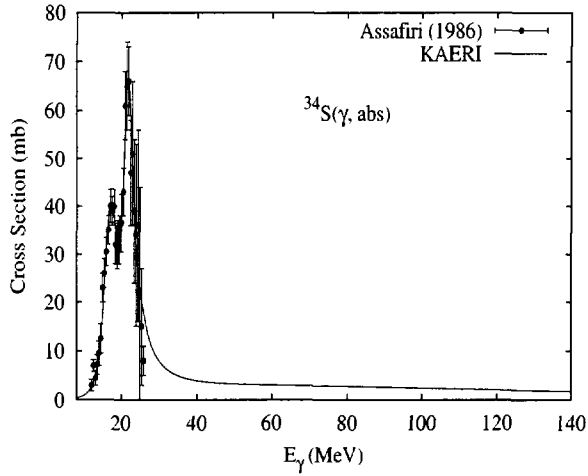
The photoabsorption cross section was evaluated based on the experimental data of Assafiri [Ass86], up to 35 MeV. Above this energy, the absorption cross section was calculated from the QD model.

The calculated results of the emission channels by the GNASH code are in good agreement with the experimental data [Ass84] for the (γ, sn) and (γ, p) reaction cross sections, but there are some gaps between calculations and measurements for (γ, 2n) reaction cross sections above around 25 MeV of photon energies.

$$\gamma + {}^{36}S$$

Abundance	Threshold Energies (MeV)								
(%)	γ,n	γ,p	γ,t	γ,He-3	γ,α	γ,2n	γ,np	γ,2p	γ,3n
0.02	9.89	13.10	19.28	25.10	9.01	16.87	21.47	25.28	28.29

There are no experimental data available. The photoabsorption cross section was obtained from GDR and QD model calculations, adopting the GDR parameters of ^{34}S. The neutron, proton, deuteron, triton and alpha emission cross sections, as well as production cross sections, were calculated by the GNASH code.

118

Abundance	Threshold Energies (MeV)								
(%)	γ,n	γ,p	γ,t	γ,He-3	γ,α	γ,2n	γ,np	γ,2p	γ,3n
75.77	12.65	6.37	17.95	19.64	7.00	24.15	17.79	17.25	39.90
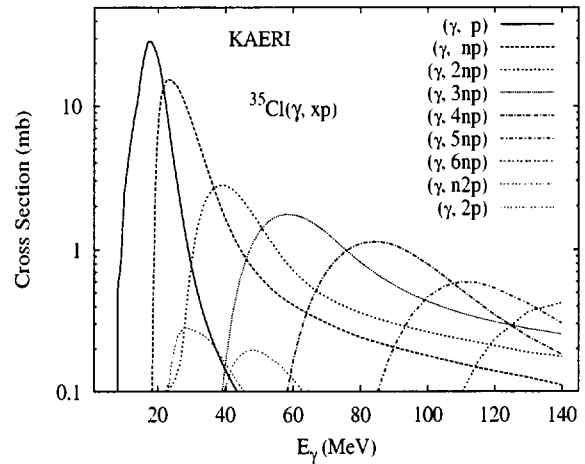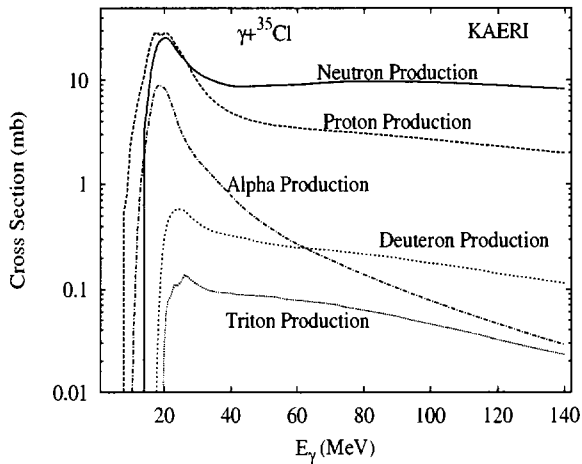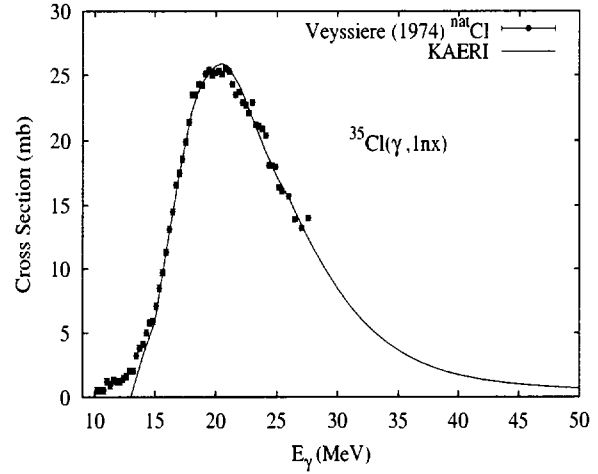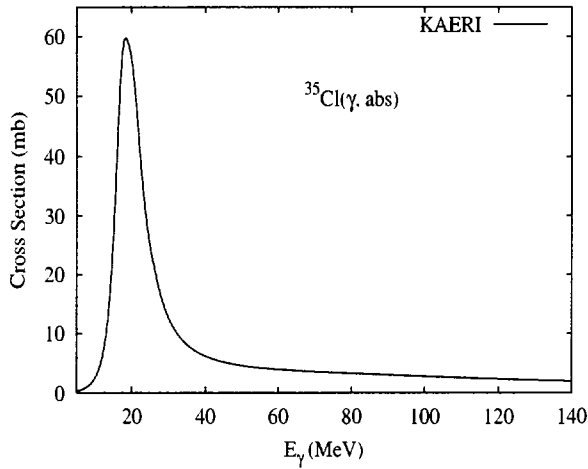
The photoabsorption cross section has not been measured. However, for ^{nat}Cl, there are experimental data for the $(\gamma, 1nx)$, $(\gamma, 2nx)$ and (γ, xn) reaction cross sections [Vey74]. We relied on the GUNF and GNASH codes to infer the photoabsorption cross section in the GDR regime, in order to model accurately the $(\gamma, 1nx)$ data. The photoabsorption cross section above the GDR, up to 140 MeV, was obtained from QD model calculations using the theory of Chadwick. The neutron, proton, deuteron, triton and alpha emission cross sections, as well as production cross sections, were calculated by the GNASH code.
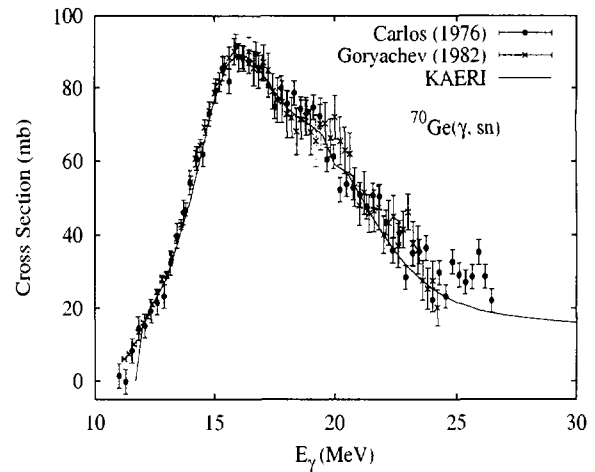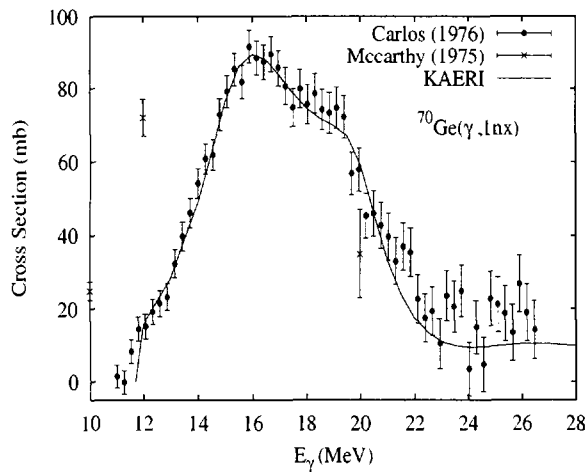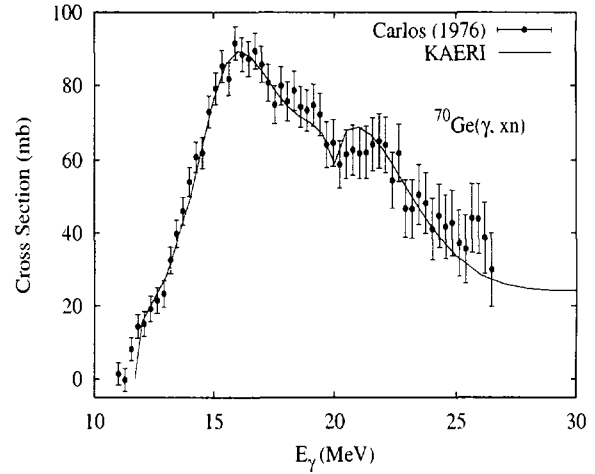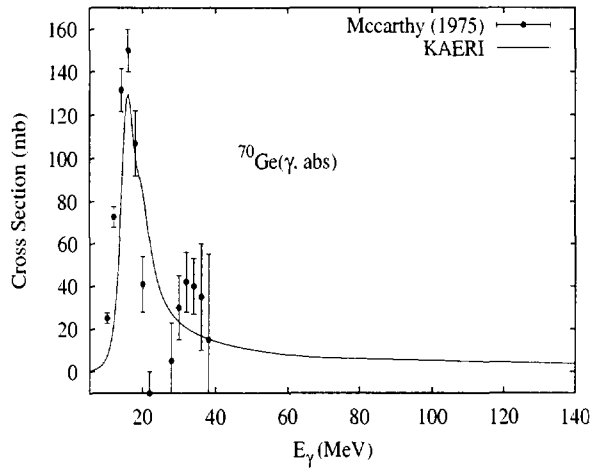
$\gamma + {}^{37}\text{Cl}$

Abundance (%)	Threshold Energies (MeV)								
	γ,n	γ,p	γ,t	$\gamma,\text{He-3}$	γ,α	$\gamma,2n$	γ,np	$\gamma,2p$	$\gamma,3n$
24.23	10.31	8.39	16.78	22.14	7.85	18.89	18.28	21.48	31.54
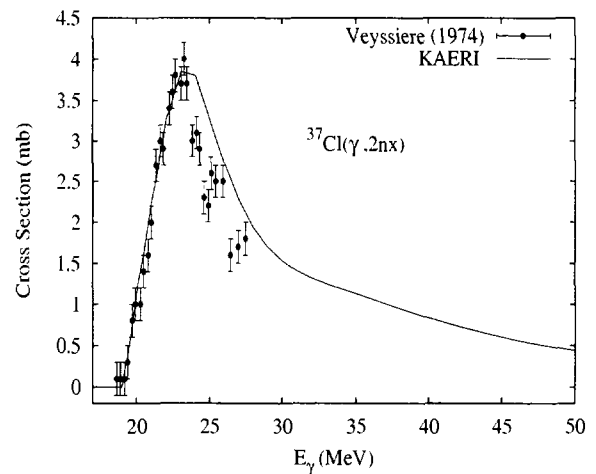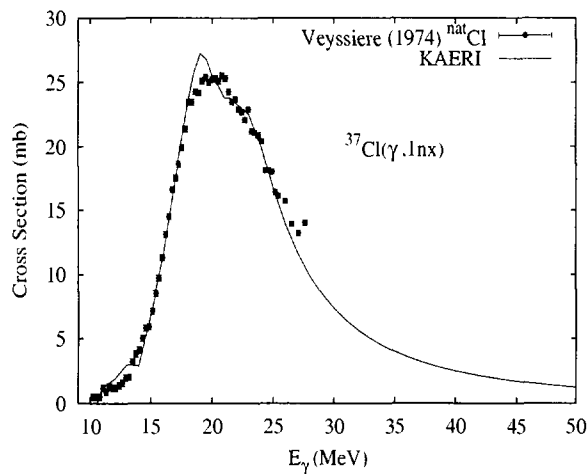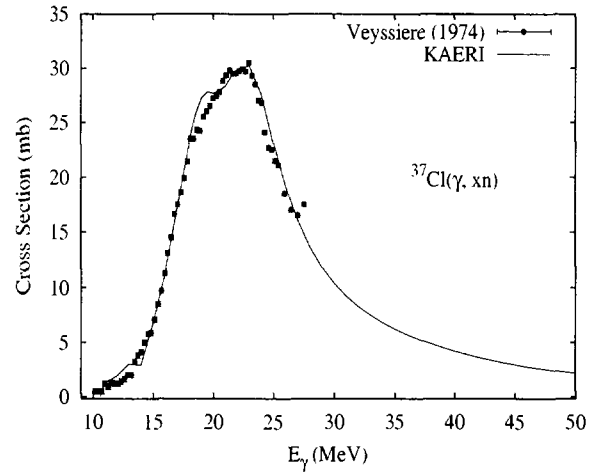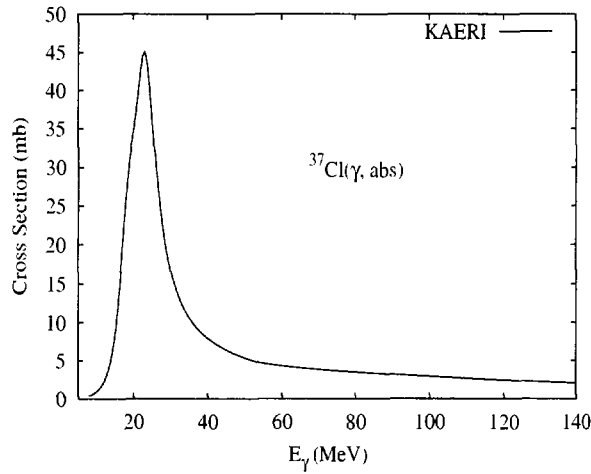
The photoabsorption cross section has not been measured. However, for ^{nat}Cl, there are experimental data for the (γ, 1nx), (γ, 2nx) and (γ, xn) reaction cross sections [Vey74]. We relied on the GUNF and GNASH codes to infer the photoabsorption cross section in the GDR regime, in order to model accurately the (γ, 1nx) data. The photoabsorption cross section above the GDR, up to 140 MeV, was obtained from QD model calculations using the theory of Chadwick.

The calculated results of the emission channels by the GNASH are in agreement with the experimental data of ^{nat}Cl for the (γ, 1nx), (γ, 2nx), and (γ, xn) reaction cross sections.

$\gamma + {}^{36}\text{Ar}$

Abundance (%)	Threshold Energies (MeV)								
	γ,n	γ,p	γ,t	$\gamma,\text{He-3}$	γ,α	$\gamma,\text{2n}$	γ,np	$\gamma,\text{2p}$	$\gamma,\text{3n}$
0.34	15.25	8.51	24.18	18.58	6.64	27.99	21.15	14.88	45.06
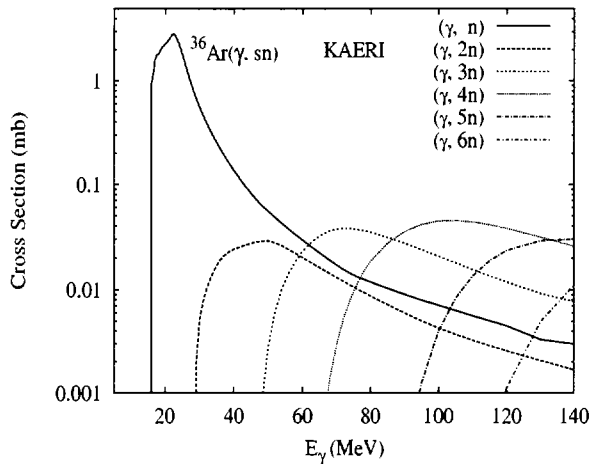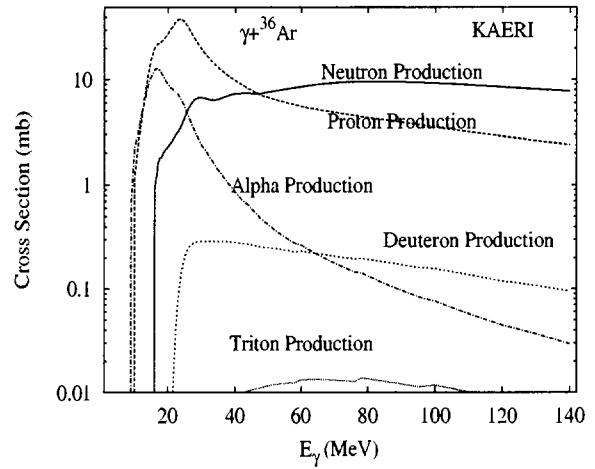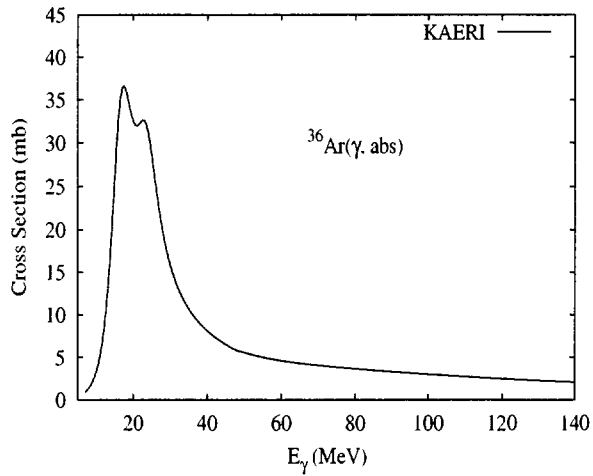
There are no experimental data available. The photoabsorption cross section was obtained from GDR and QD model calculations, adopting the GDR parameters of ${}^{40}\text{Ar}$. The neutron, proton, deuteron, triton and alpha emission cross sections, as well as production cross sections, were calculated by the GNASH code.

$\gamma + {}^{38}\text{Ar}$

Abundance (%)	Threshold Energies (MeV)								
	γ,n	γ,p	γ,t	$\gamma,\text{He-3}$	γ,α	$\gamma,2n$	γ,np	$\gamma,2p$	$\gamma,3n$
0.06	11.84	10.24	20.65	20.80	7.21	20.63	20.55	18.63	35.88

There are no experimental data available. The photoabsorption cross section was obtained from GDR and QD model calculations, adopting the GDR parameters of ${}^{40}\text{Ar}$. The neutron, proton, deuteron, triton and alpha emission cross sections, as well as production cross sections, were calculated by the GNASH code.

γ + ^{40}Ar

Abundance	Threshold Energies (MeV)								
(%)	γ,n	γ,p	γ,t	γ,He-3	γ,α	γ,2n	γ,np	γ,2p	γ,3n
99.60	9.87	12.53	18.23	23.07	6.80	16.47	20.60	22.76	28.30
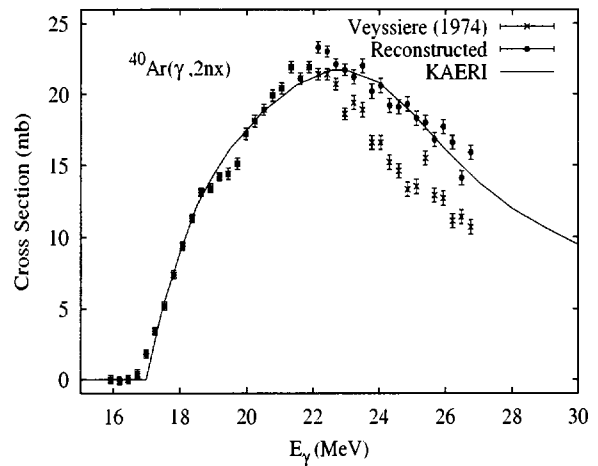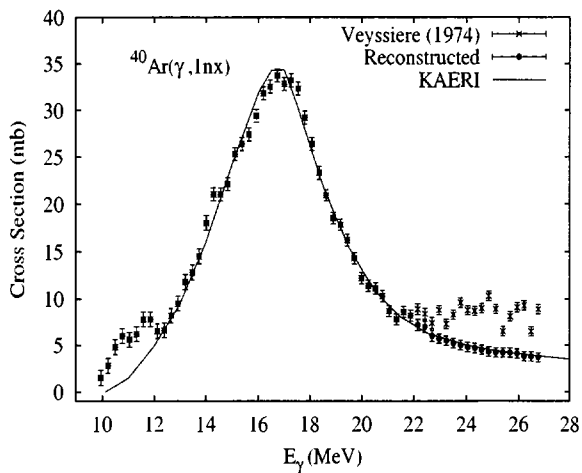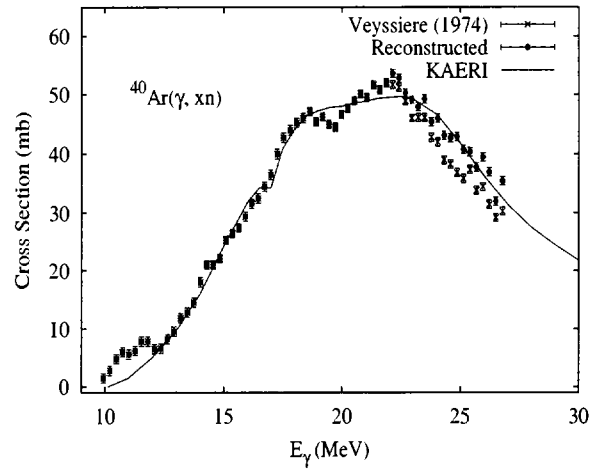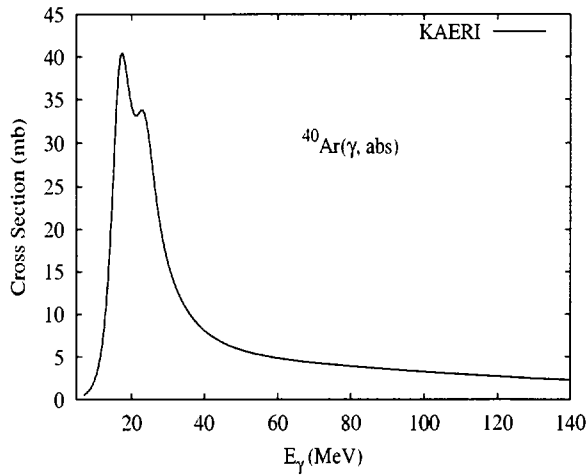
There are no experimental data for the absorption cross section. However, experimental data are available for (γ, 1nx), (γ, 2nx), and (γ, xn) reaction cross sections [Vey74]. We relied on the GUNF and GNASH codes to infer the photoabsorption cross section in the GDR regime, so as to model accurately the (γ, xn) data. The photoabsorption cross section above the GDR, up to 140 MeV, was obtained from QD model calculations using the theory of Chadwick.

The calculated results of the emission channels by the GNASH code are in good agreement with all the photoneutron reaction data below 22 MeV. However, above 22 MeV the calculated cross section for the (γ, 1nx) channel is smaller, and that for the (γ, 2nx) channel is larger than the experimental data. New reference photoneutron cross sections were reconstructed by adding the excess of (γ, 1nx) cross section [(γ, 1nx)$_{expt}$ - (γ, 1nx)$_{calc}$], to the (γ, 2nx) cross section above 22 MeV.

$$\gamma + {}^{39}\mathrm{K}$$

Abundance	Threshold Energies (MeV)								
(%)	γ,n	γ,p	γ,t	$\gamma,\mathrm{He}\text{-}3$	γ,α	$\gamma,2n$	γ,np	$\gamma,2p$	$\gamma,3n$
93.26	13.08	6.38	18.53	19.22	7.22	25.15	18.22	16.62	40.60
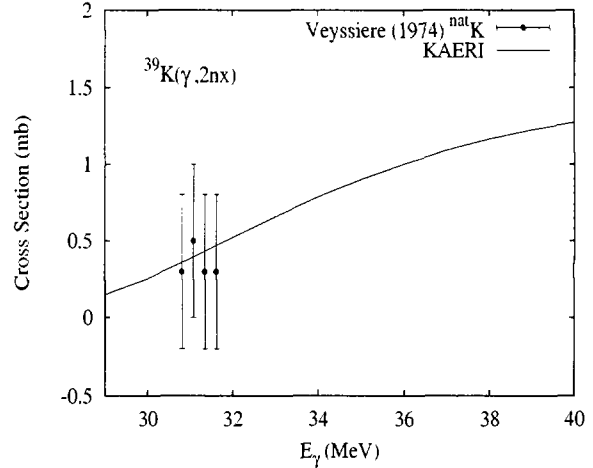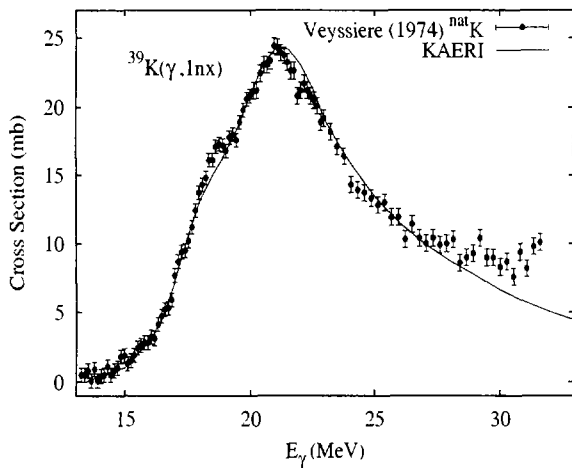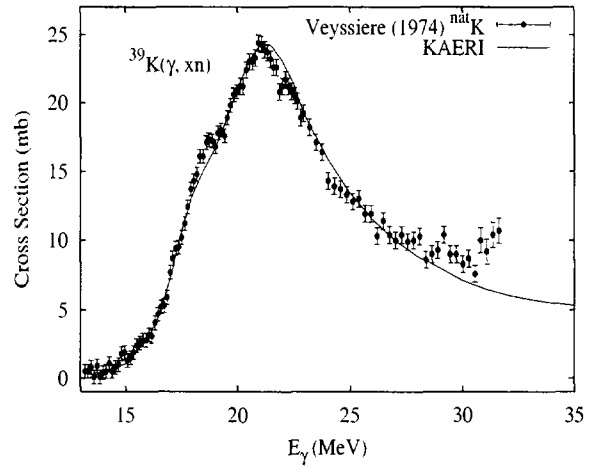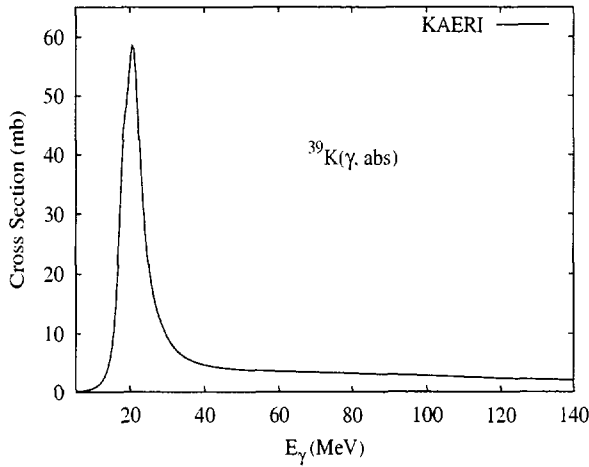
The photoabsorption cross section has not been measured. However, for ${}^{nat}\mathrm{K}$, there are experimental data for the $(\gamma,\,1nx)$, $(\gamma,\,2nx)$ and $(\gamma,\,xn)$ reaction cross sections [Vey74]. We relied on the GUNF and GNASH codes to infer the photoabsorption cross section in the GDR regime, in order to model accurately the $(\gamma,\,1nx)$ data. The photoabsorption cross section above the GDR, up to 140 MeV, was obtained from QD model calculations using the theory of Chadwick. The neutron, proton, deuteron, triton and alpha emission cross sections, as well as production cross sections, were calculated by the GNASH code.

$$\gamma + {}^{40}\mathrm{K}$$

Abundance (%)	Threshold Energies (MeV)								
	γ,n	γ,p	γ,t	γ,He-3	γ,α	γ,2n	γ,np	γ,2p	γ,3n
0.01	7.80	7.58	17.54	16.70	6.44	20.88	14.18	18.31	32.95
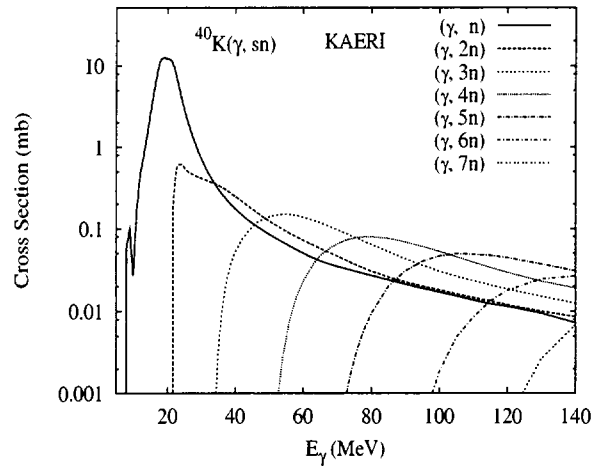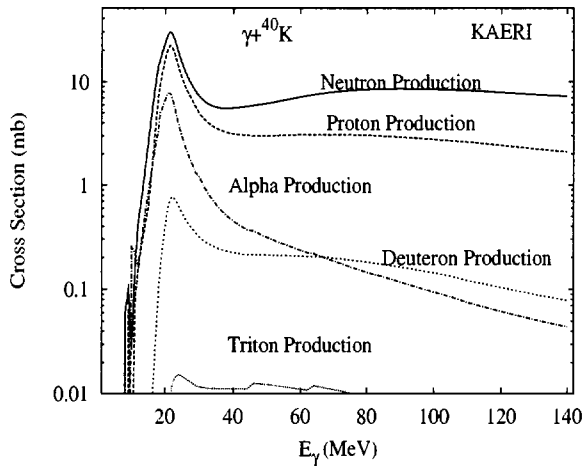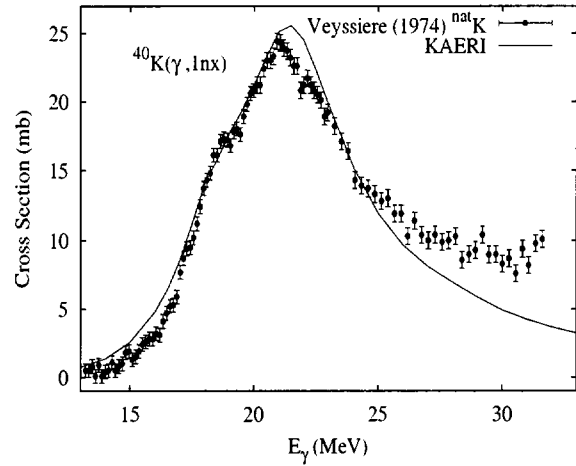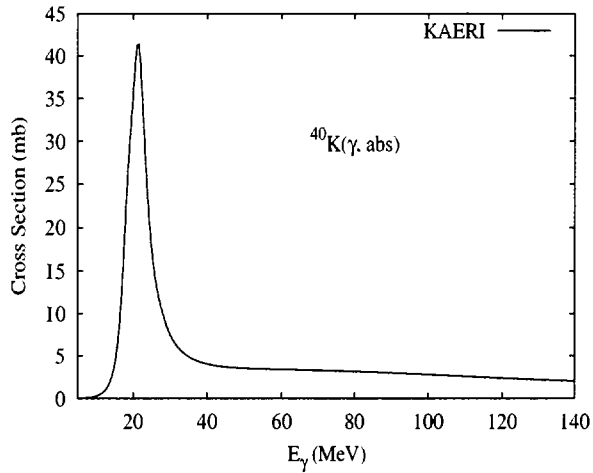
The photoabsorption cross section has not been measured. The photoabsorption cross section was obtained from GDR and QD model calculations, adopting the GDR parameters of ${}^{39}\mathrm{K}$. The neutron, proton, deuteron, triton and alpha emission cross sections, as well as production cross sections, were calculated by the GNASH code. The calculated results for the ${}^{40}\mathrm{K}(\gamma, \mathrm{1nx})$ are lower than the ${}^{nat}\mathrm{K}$ data above 25 MeV, where the ${}^{39}\mathrm{K}(\gamma, \mathrm{2n})$ reaction channel opens.

$\gamma + {}^{41}\mathrm{K}$

Abundance	Threshold Energies (MeV)								
(%)	γ,n	γ,p	γ,t	γ,He-3	γ,α	γ,2n	γ,np	γ,2p	γ,3n
6.73	10.10	7.81	15.79	20.69	6.22	17.89	17.68	20.33	30.97
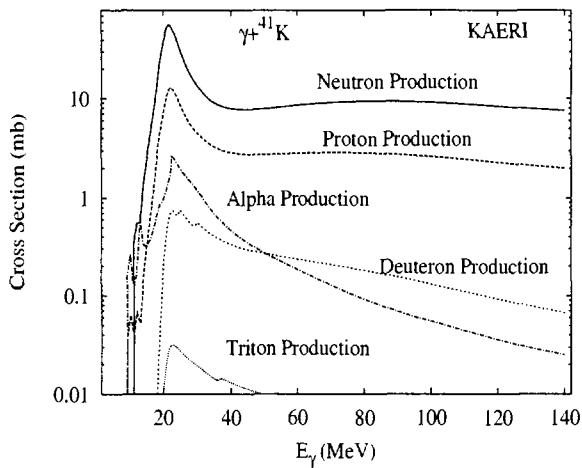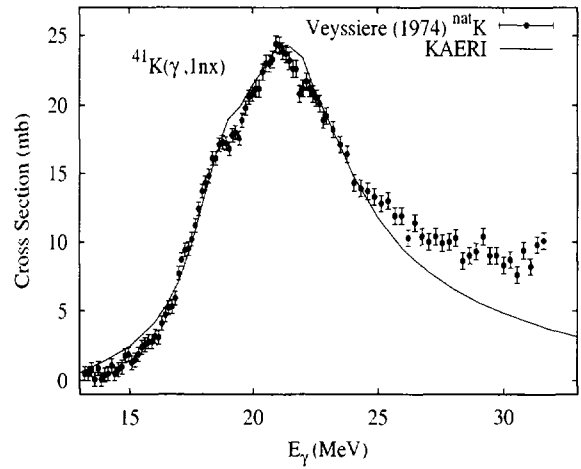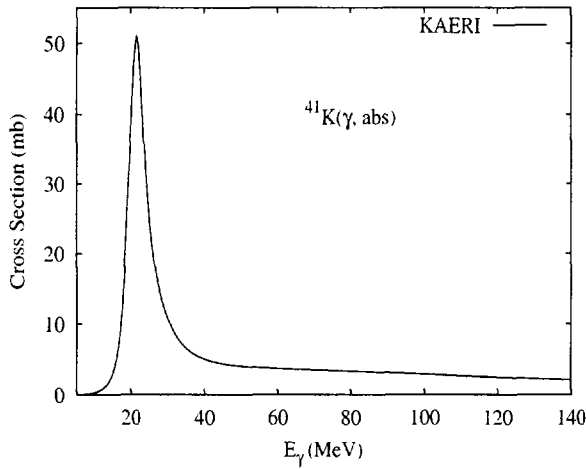
The photoabsorption cross section has not been measured. The photoabsorption cross section was obtained from GDR and QD model calculations, The neutron, proton, deuteron, triton and alpha emission cross sections, as well as production cross sections, were calculated by the GNASH code. The calculated results for the ${}^{41}\mathrm{K}(\gamma, \mathrm{1nx})$ are lower than the ${}^{nat}\mathrm{K}$ data above 25 MeV, where the ${}^{39}\mathrm{K}(\gamma, \mathrm{2n})$ reaction channel opens.

126

$\gamma + {}^{40}\mathrm{Ca}$

Abundance (%)	Threshold Energies (MeV)								
	γ,n	γ,p	γ,t	$\gamma,$He-3	γ,α	$\gamma,2n$	γ,np	$\gamma,2p$	$\gamma,3n$
96.94	15.64	8.33	25.00	18.83	7.04	28.93	21.40	14.71	45.90
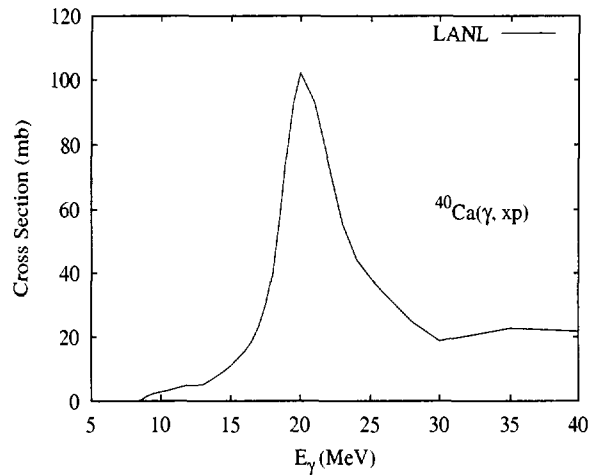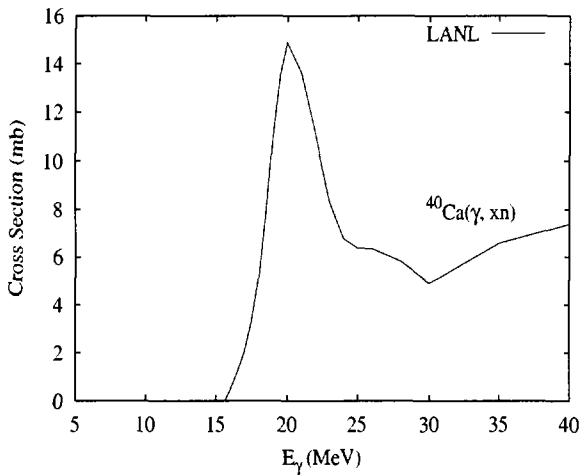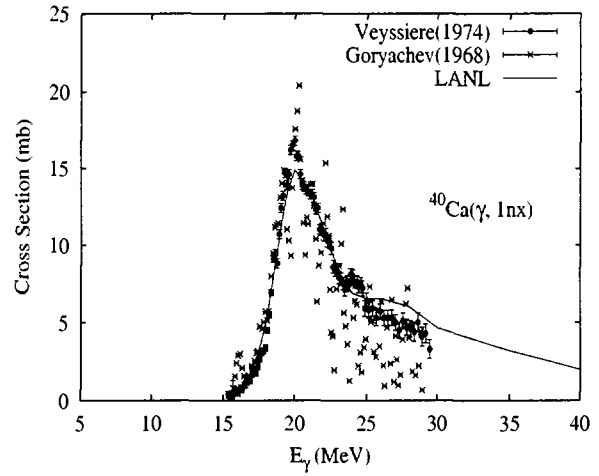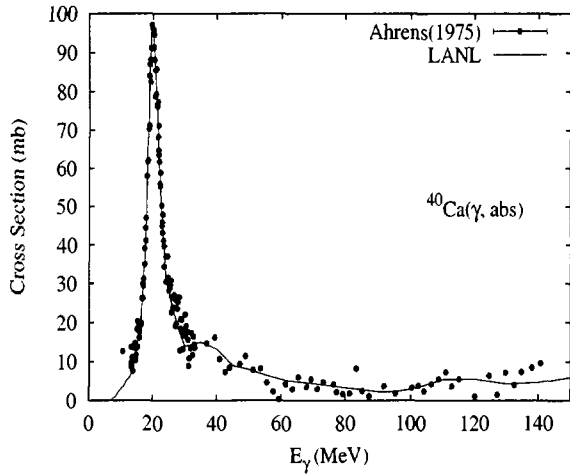
Available data are summarized by Varlamov [Var96]. The photoabsorption cross section was evaluated based on the data of Ahrens [Ahr75], that extend up to 150 MeV. At 60 MeV, the value for the absorption cross section was consistent with that used by Ryckbosch et al. [Ryc90].

The total photoabsorption cross section is used as an input into the GNASH calculations. These calculations then predict the branching to photoneutron, photoproton, etc. emission. The calculated photoneutron production was compared with measurements of Veyssiere [Vey74]. The calculations, after a level density adjustment for ${}^{39}\mathrm{Ca}$, predicted the (γ,xn) data well, with the exception of the 25-30 MeV region where the calculated photoneutron production appears to be about 20% too high.

Measurement [Ryc90] of the inclusive photoproton spectrum for 62 MeV Ca(γ,xp) at 90° provide a useful test of the preequilibrium emission following QD absorption. These data are amongst the very few for essentially monochromatic photons. The calculations, in the preequilibrium region, agree very well with the measurements. This is important since the comparison tests not only the preequilibrium model, but also the angular distribution systematics [Cha95b]. In this particular case, where the systematics predict only a small forward peaking, the calculations at 90 ° account for the data.

$$\gamma + {}^{42}\text{Ca}$$

Abundance	Threshold Energies (MeV)								
(%)	γ,n	γ,p	γ,t	γ,He-3	γ,α	γ,2n	γ,np	γ,2p	γ,3n
0.65	11.48	10.28	19.69	20.24	6.26	19.84	20.37	18.09	35.49
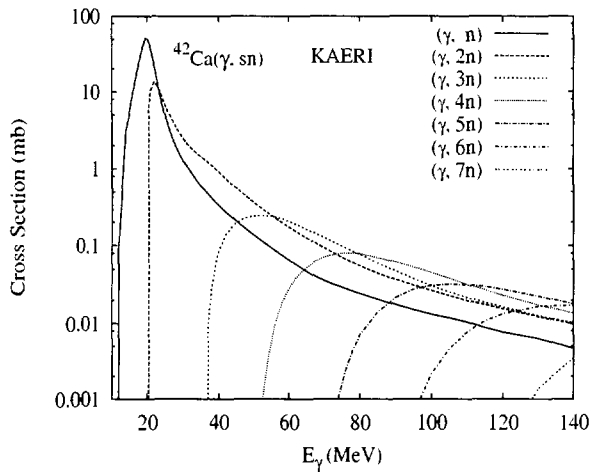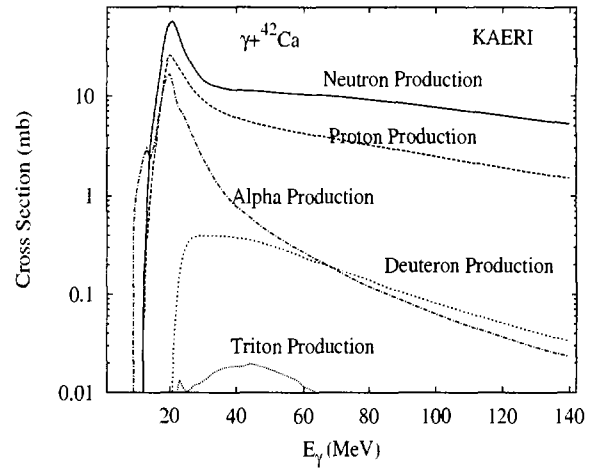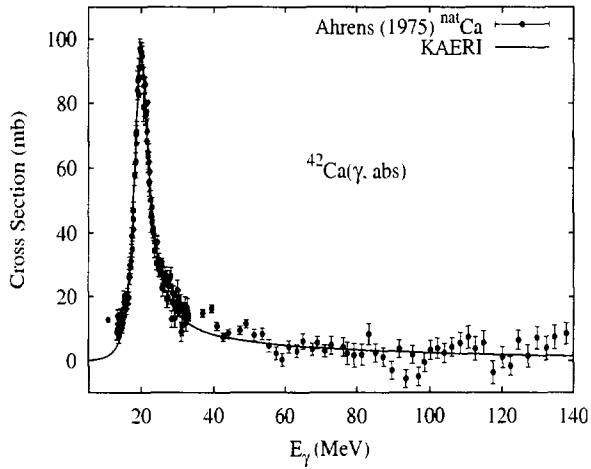
There are no experimental data available. The photoabsorption cross section was obtained from GDR and QD model calculations, adopting the GDR parameters of ${}^{40}\text{Ca}$. The neutron, proton, deuteron, triton and alpha emission cross sections, as well as production cross sections, were calculated by the GNASH code.

$\gamma + {}^{43}\text{Ca}$

Abundance	Threshold Energies (MeV)								
(%)	γ,n	γ,p	γ,t	$\gamma,\text{He-3}$	γ,α	$\gamma,\text{2n}$	γ,np	$\gamma,\text{2p}$	$\gamma,\text{3n}$
0.14	7.93	10.68	19.82	18.30	7.59	19.41	18.21	19.92	27.78
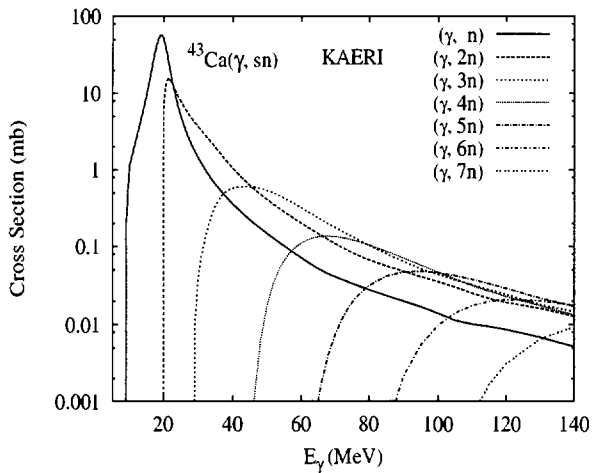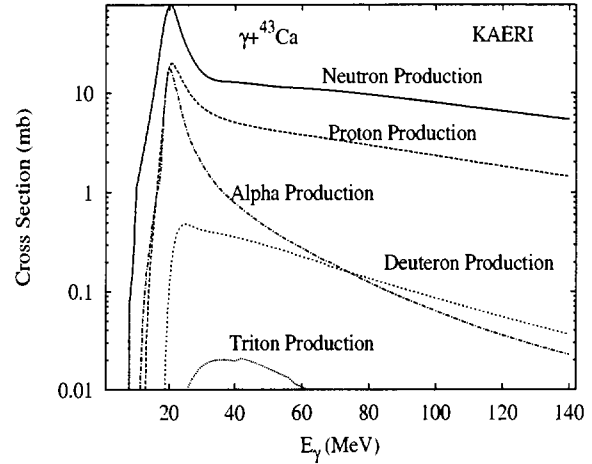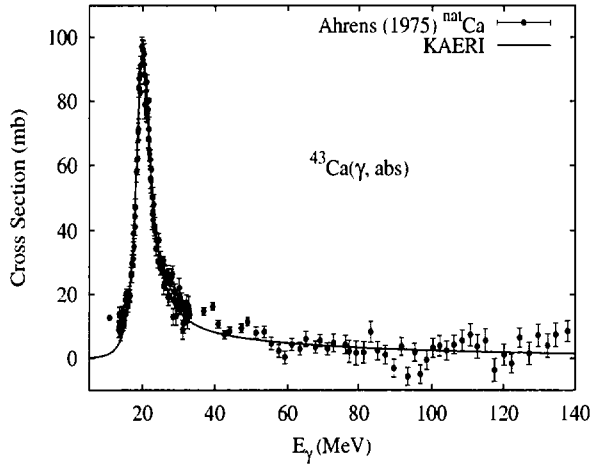
There are no experimental data available. The photoabsorption cross section was obtained from GDR and QD model calculations, adopting the GDR parameters of ${}^{40}\text{Ca}$. The neutron, proton, deuteron, triton and alpha emission cross sections, as well as production cross sections, were calculated by the GNASH code.

$\gamma + {}^{44}\text{Ca}$

Abundance (%)	Threshold Energies (MeV)								
	γ,n	γ,p	γ,t	$\gamma,\text{He-3}$	γ,α	$\gamma,2n$	γ,np	$\gamma,2p$	$\gamma,3n$
2.09	11.13	12.17	20.86	23.33	8.86	19.06	21.81	21.63	30.55
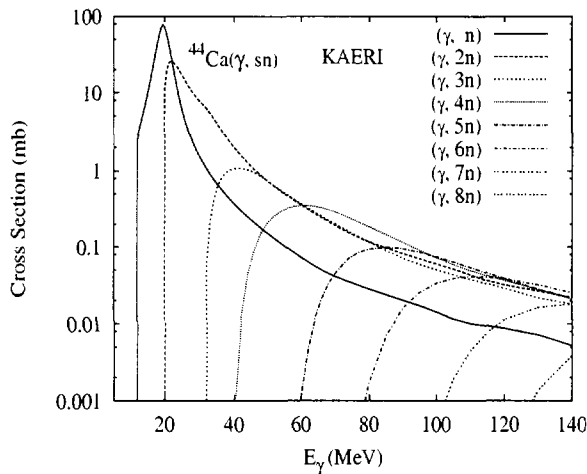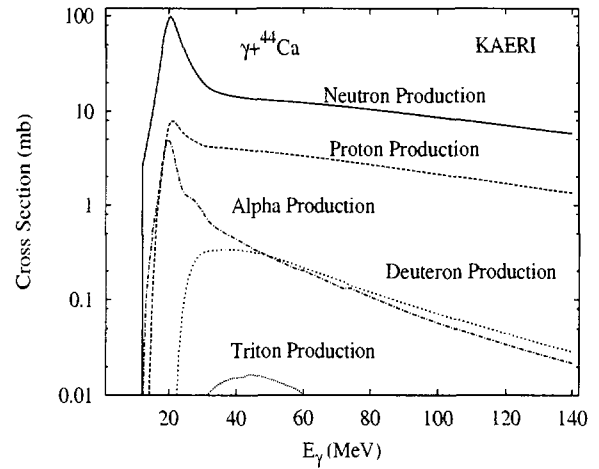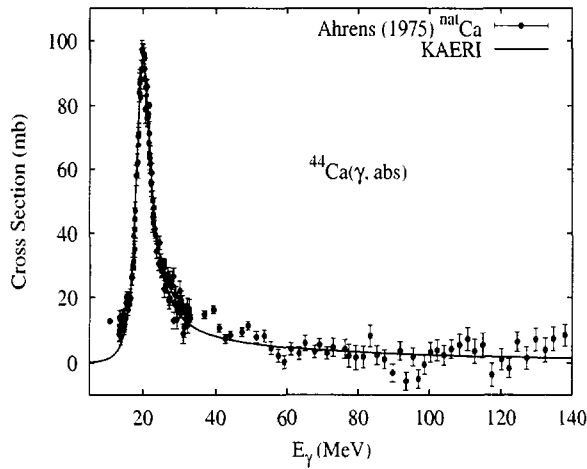
There are no experimental data available. The photoabsorption cross section was obtained from GDR and QD model calculations, adopting the GDR parameters of ${}^{40}\text{Ca}$. The neutron, proton, deuteron, triton and alpha emission cross sections, as well as production cross sections, were calculated by the GNASH code.

$\gamma + {}^{46}\mathrm{Ca}$

Abundance	Threshold Energies (MeV)								
(%)	γ,n	γ,p	γ,t	γ,He-3	γ,α	γ,2n	γ,np	γ,2p	γ,3n
0.00	10.40	13.82	21.50	26.09	11.15	17.81	22.69	25.46	28.95
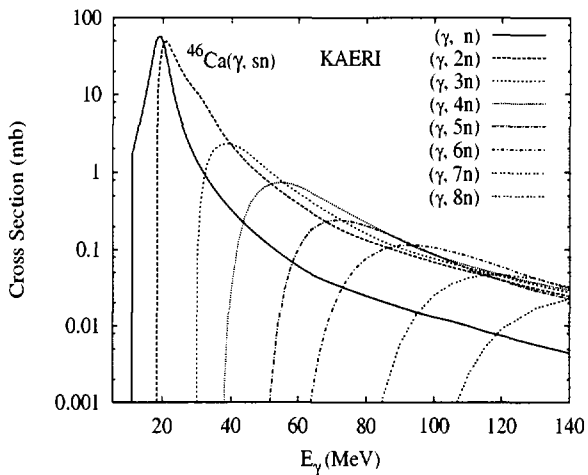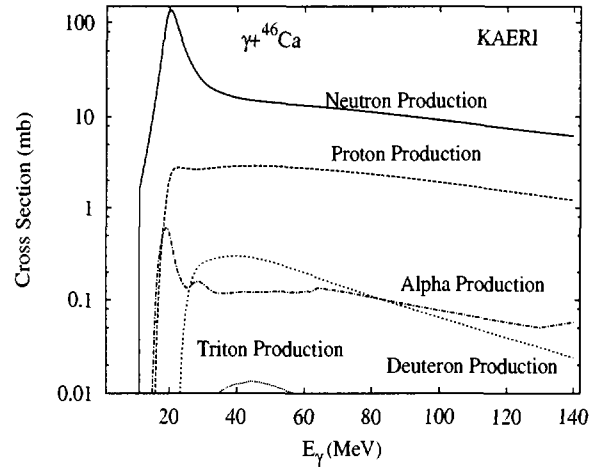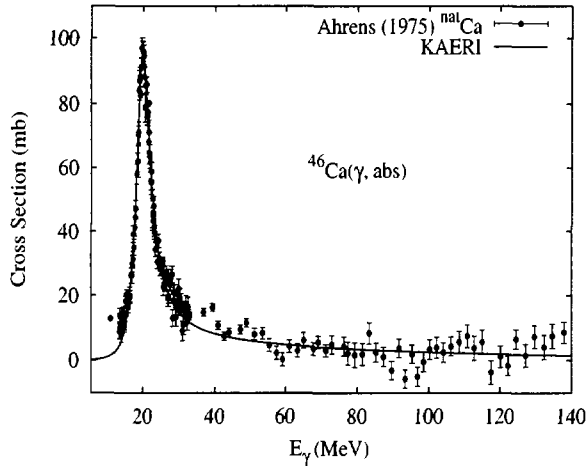
There are no experimental data available. The photoabsorption cross section was obtained from GDR and QD model calculations, adopting the GDR parameters of ${}^{40}\mathrm{Ca}$. The neutron, proton, deuteron, triton and alpha emission cross sections, as well as production cross sections, were calculated by the GNASH code.

$\gamma + {}^{48}\text{Ca}$

Abundance (%)	Threshold Energies (MeV)								
	γ,n	γ,p	γ,t	$\gamma,\text{He-3}$	γ,α	$\gamma,2n$	γ,np	$\gamma,2p$	$\gamma,3n$
0.19	9.94	15.81	22.55	29.43	14.38	17.22	24.16	29.07	27.62

There are no experimental data available. The photoabsorption cross section was obtained from GDR and QD model calculations, adopting the GDR parameters of ${}^{40}\text{Ca}$. The neutron, proton, deuteron, triton and alpha emission cross sections, as well as production cross sections, were calculated by the GNASH code.

| Abundance	Threshold Energies (MeV)								
(%)	γ,n	γ,p	γ,t	$\gamma,\text{He-3}$	γ,α	$\gamma,2n$	γ,np	$\gamma,2p$	$\gamma,3n$
8.00	13.19	10.34	22.89	20.65	8.00	22.72	21.67	17.23	39.02
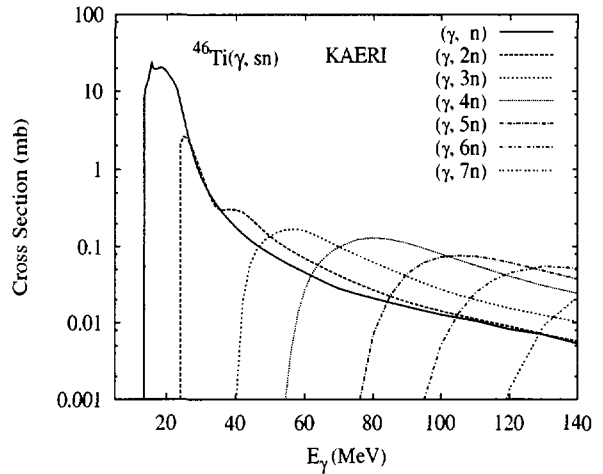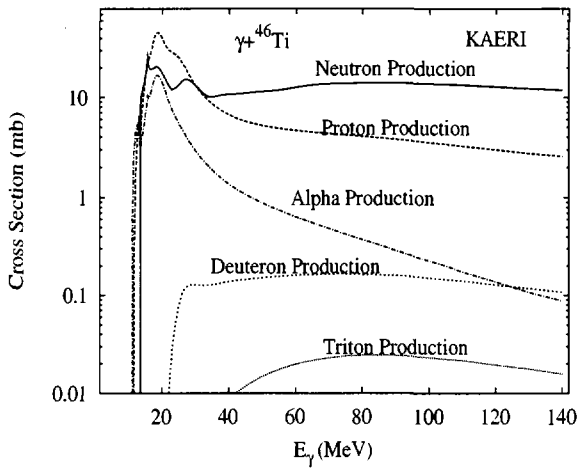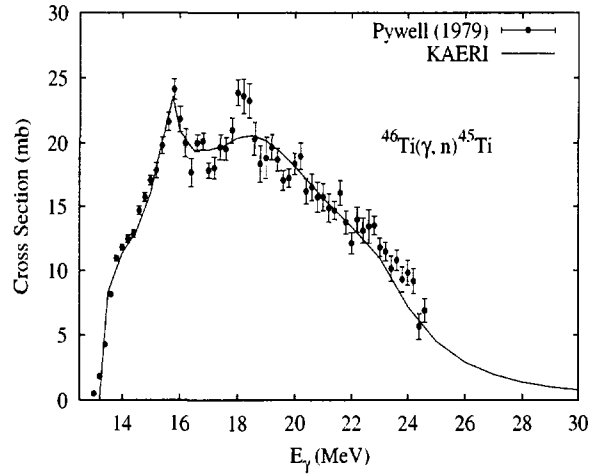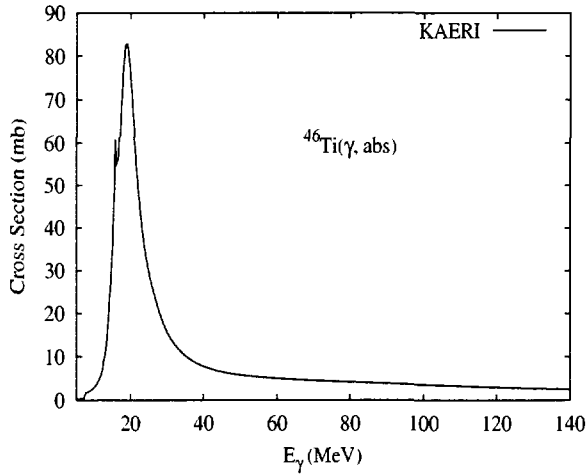
The photoabsorption cross section has not been measured. However, there are experimental data for the (γ, 1n) reaction cross section [Pyw79a]. We relied on the GUNF and GNASH codes to infer the photoabsorption cross section in the GDR regime, in order to model accurately the (γ, 1n) data. The photoabsorption cross section above the GDR, up to 140 MeV, was obtained from QD model calculations using the theory of Chadwick. The neutron, proton, deuteron, triton and alpha emission cross sections, as well as production cross sections, were calculated by the GNASH code.

$$\gamma + {}^{47}\text{Ti}$$

Abundance	Threshold Energies (MeV)								
(%)	γ,n	γ,p	γ,t	γ,He-3	γ,α	γ,2n	γ,np	γ,2p	γ,3n
7.30	8.88	10.46	22.07	18.39	8.95	22.07	19.22	18.70	31.60
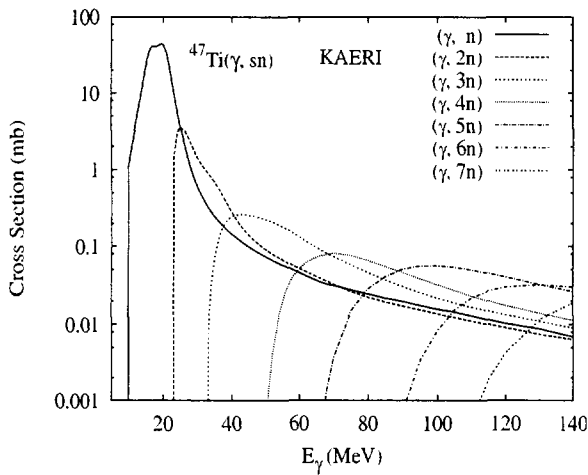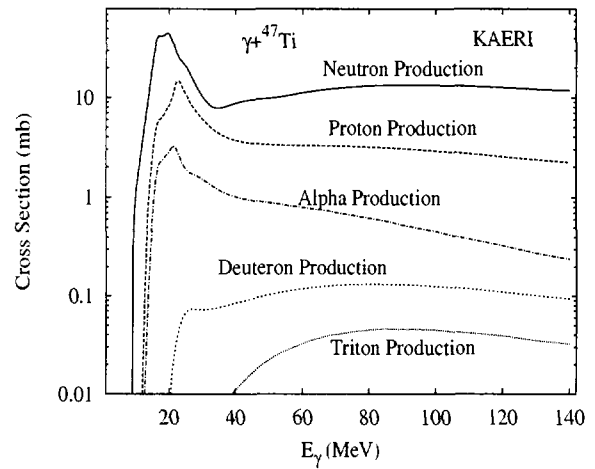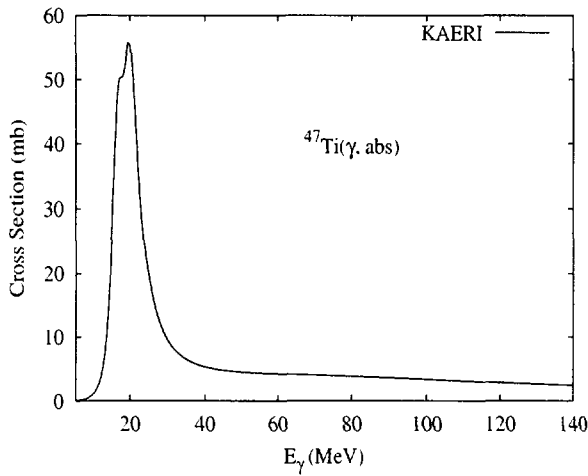
There no experimental data available. The photoabsorption cross section was obtained from GDR and QD model calculations, adopting the GDR parameters of ^{48}Ti. The neutron, proton, deuteron, triton and alpha emission cross sections, as well as production cross sections, were calculated by the GNASH code.

$$\gamma + {}^{48}\text{Ti}$$

| Abundance (%)	Threshold Energies (MeV)								
	γ,n	γ,p	γ,t	$\gamma,\text{He-3}$	γ,α	$\gamma,\text{2n}$	γ,np	$\gamma,\text{2p}$	$\gamma,\text{3n}$
73.80	11.63	11.45	22.37	22.61	9.44	20.50	22.09	19.92	33.69
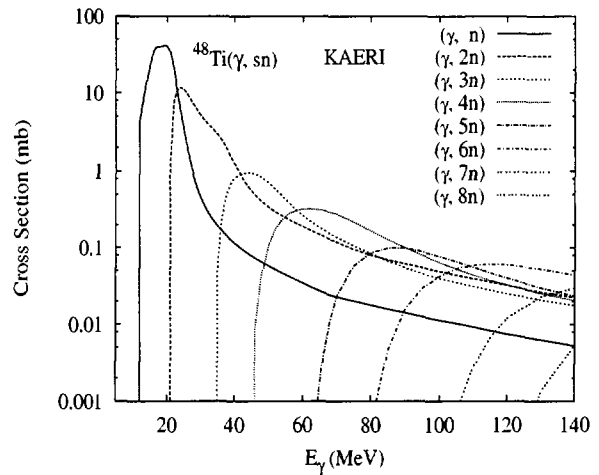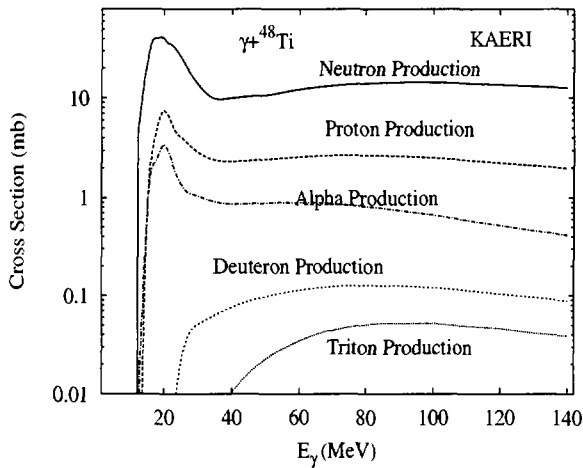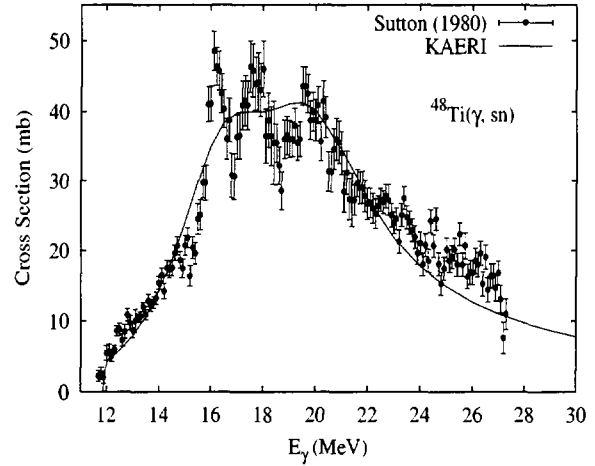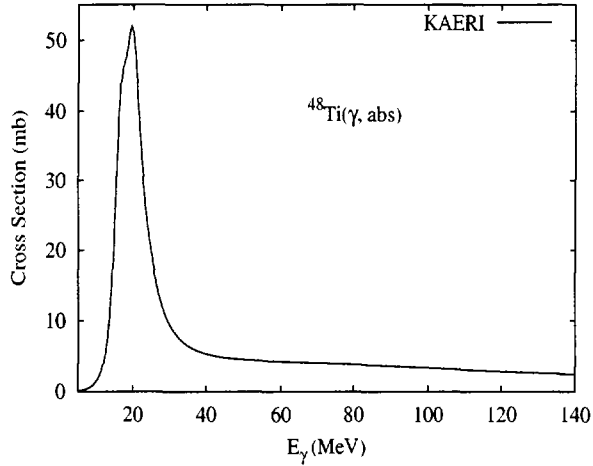
The photoabsorption cross section has not been measured. However, there are experimental data for the (γ, xn) reaction cross section [Sut80]. We relied on the GUNF and GNASH codes to infer the photoabsorption cross section in the GDR regime, in order to model accurately the (γ, xn) data. The photoabsorption cross section above the GDR, up to 140 MeV, was obtained from QD model calculations using the theory of Chadwick. The neutron, proton, deuteron, triton and alpha emission cross sections, as well as production cross sections, were calculated by the GNASH code.

γ + ^{49}Ti

Abundance (%)	Threshold Energies (MeV)								
	γ,n	γ,p	γ,t	γ,He-3	γ,α	γ,2n	γ,np	γ,2p	γ,3n
5.50	8.14	11.36	21.75	20.35	10.17	19.77	19.59	20.79	28.65
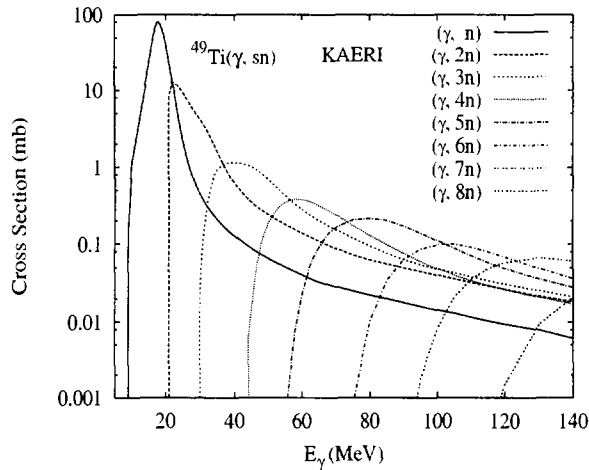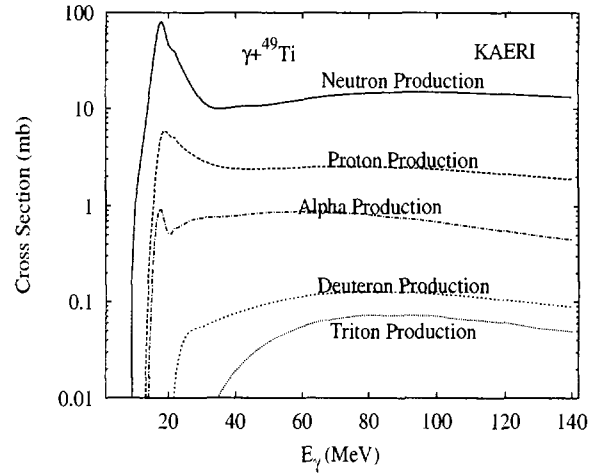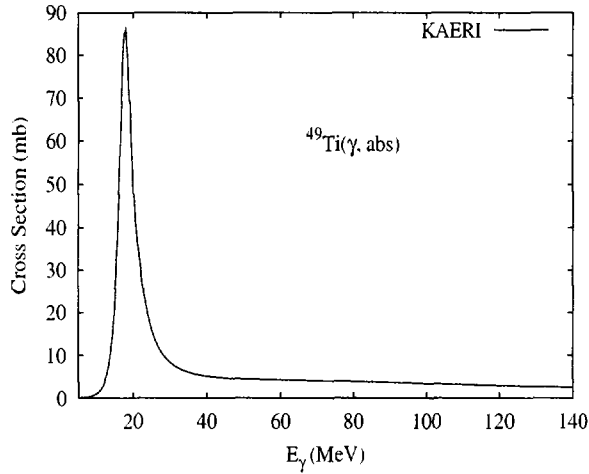
There no experimental data available. The photoabsorption cross section was obtained from GDR and QD model calculations, adopting the GDR parameters of ^{48}Ti. The neutron, proton, deuteron, triton and alpha emission cross sections, as well as production cross sections, were calculated by the GNASH code.

$$\gamma + {}^{50}\text{Ti}$$

Abundance (%)	Threshold Energies (MeV)								
	$\gamma,$n	$\gamma,$p	$\gamma,$t	$\gamma,$He-3	γ,α	$\gamma,$2n	$\gamma,$np	$\gamma,$2p	$\gamma,$3n
5.40	10.94	12.16	22.05	24.01	10.71	19.08	22.29	21.79	30.71
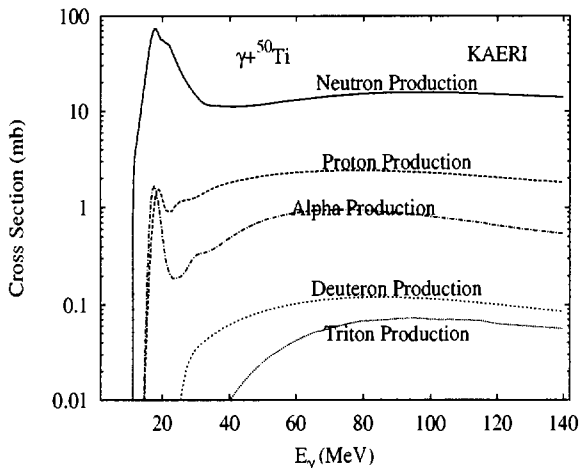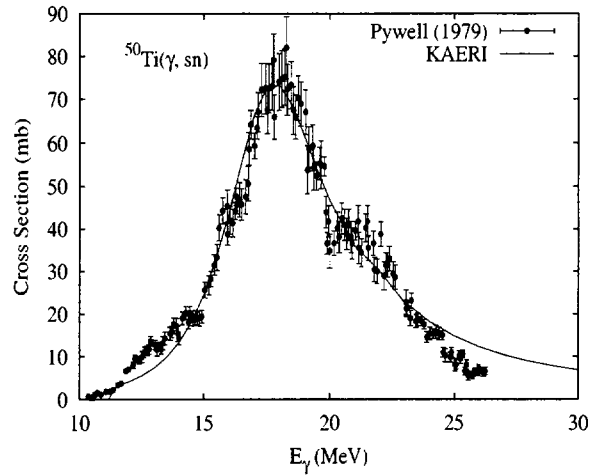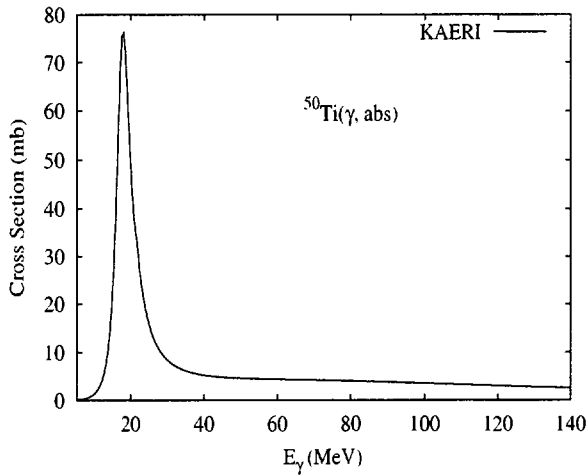
The photoabsorption cross section has not been measured. However, there are experimental data for the (γ, xn) reaction cross section [Pyw79b]. We relied on the GUNF and GNASH codes to infer the photoabsorption cross section in the GDR regime, in order to model accurately the (γ, xn) data. The photoabsorption cross section above the GDR, up to 140 MeV, was obtained from QD model calculations using the theory of Chadwick. The neutron, proton, deuteron, triton and alpha emission cross sections, as well as production cross sections, were calculated by the GNASH code.

$$\gamma + {}^{51}\text{V}$$

Abundance	Threshold Energies (MeV)								
(%)	γ,n	γ,p	γ,t	γ,He-3	γ,α	γ,2n	γ,np	γ,2p	γ,3n
99.75	11.05	8.06	18.66	22.64	10.29	20.39	19.00	20.22	31.94
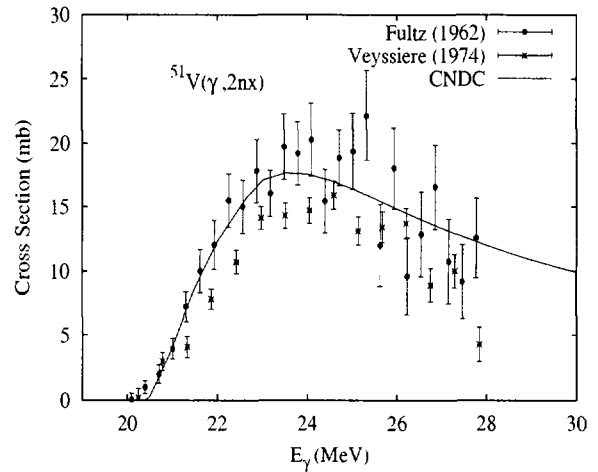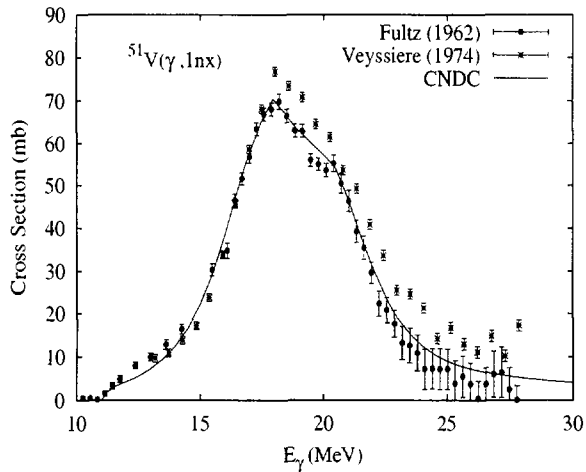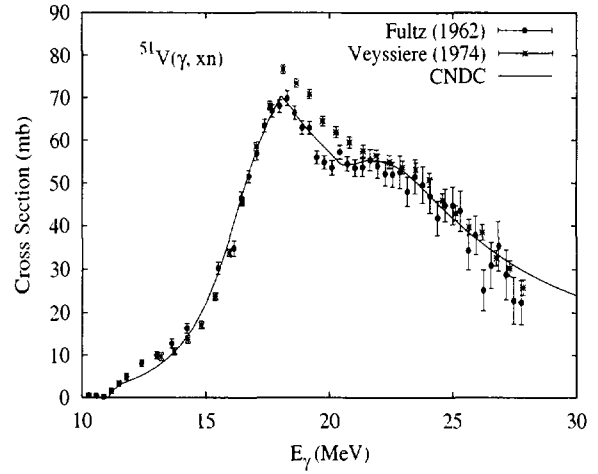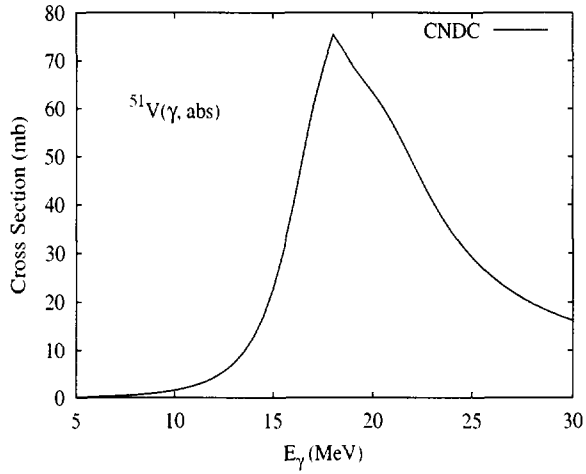
The photoabsorption cross section has not been measured. However, there are experimental data for the (γ, 1nx), (γ, 2nx) and (γ, xn) reaction cross sections [Ful62a, Vey74]. We relied on GUNF code [Zha98] to infer the photoabsorption cross section in the GDR regime, in order to model accurately the available experimental data [Ful62a, Vey74].

138

$$\gamma + {}^{50}\text{Cr}$$

Abundance (%)	Threshold Energies (MeV)								
	γ,n	γ,p	γ,t	γ,He-3	γ,α	γ,2n	γ,np	γ,2p	γ,3n
4.34	13.00	9.59	23.20	20.26	8.56	23.58	21.14	16.35	39.92
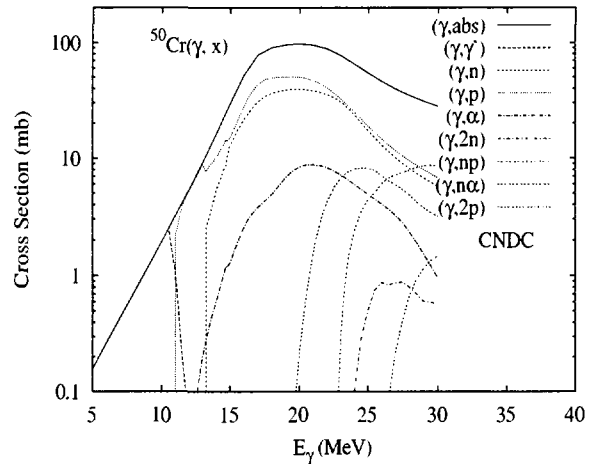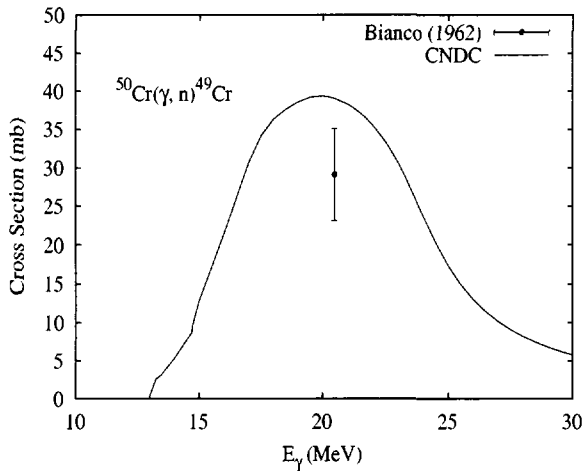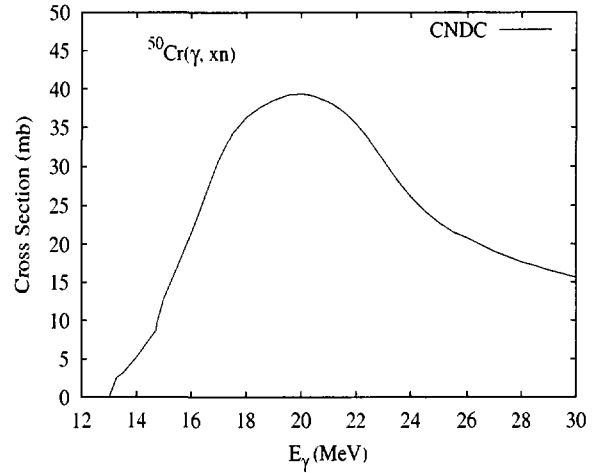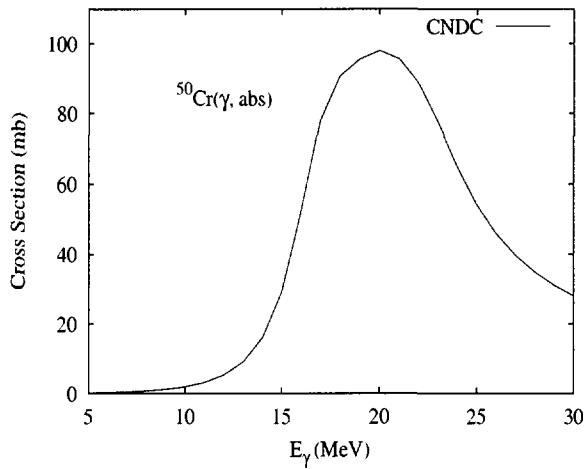
The photoabsorption cross section has not been measured. However, the (γ,1n) reaction was measured at 20.5 MeV [Bia62]. The experimental data for ${}^{52}\text{Cr}(\gamma,$ xn) were also used to guide the model calculation.

The APOM code [She92] is used to determine the optical potential parameters for neutrons. The optical potential parameters for charged particles p,α, ${}^{3}\text{He}$, d, and t, were taken from [Per76]. We relied on GUNF code [Zha98] to infer the photoabsorption cross section in the GDR regime, in order to model accurately the available experimental data.
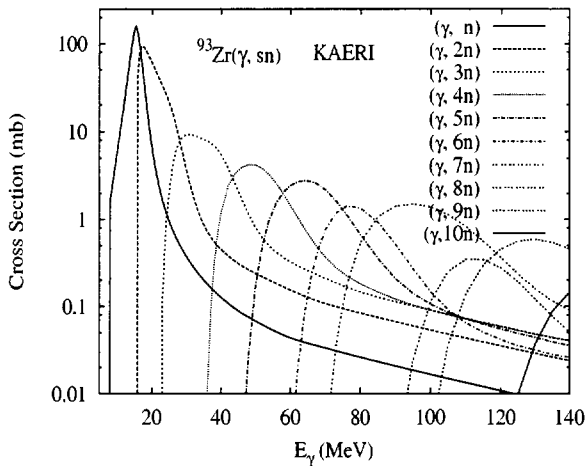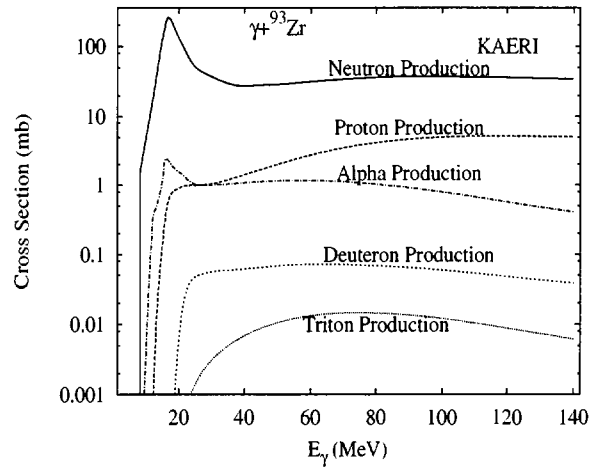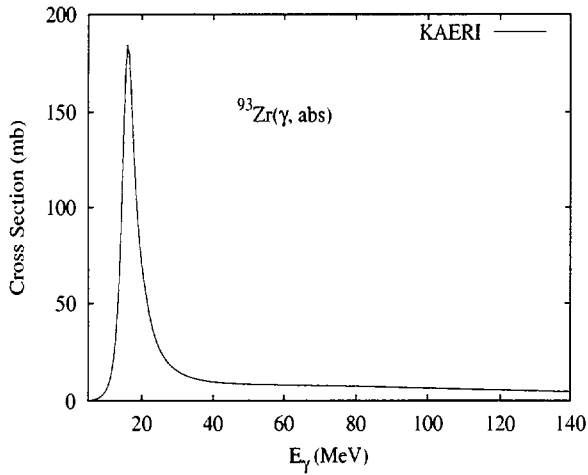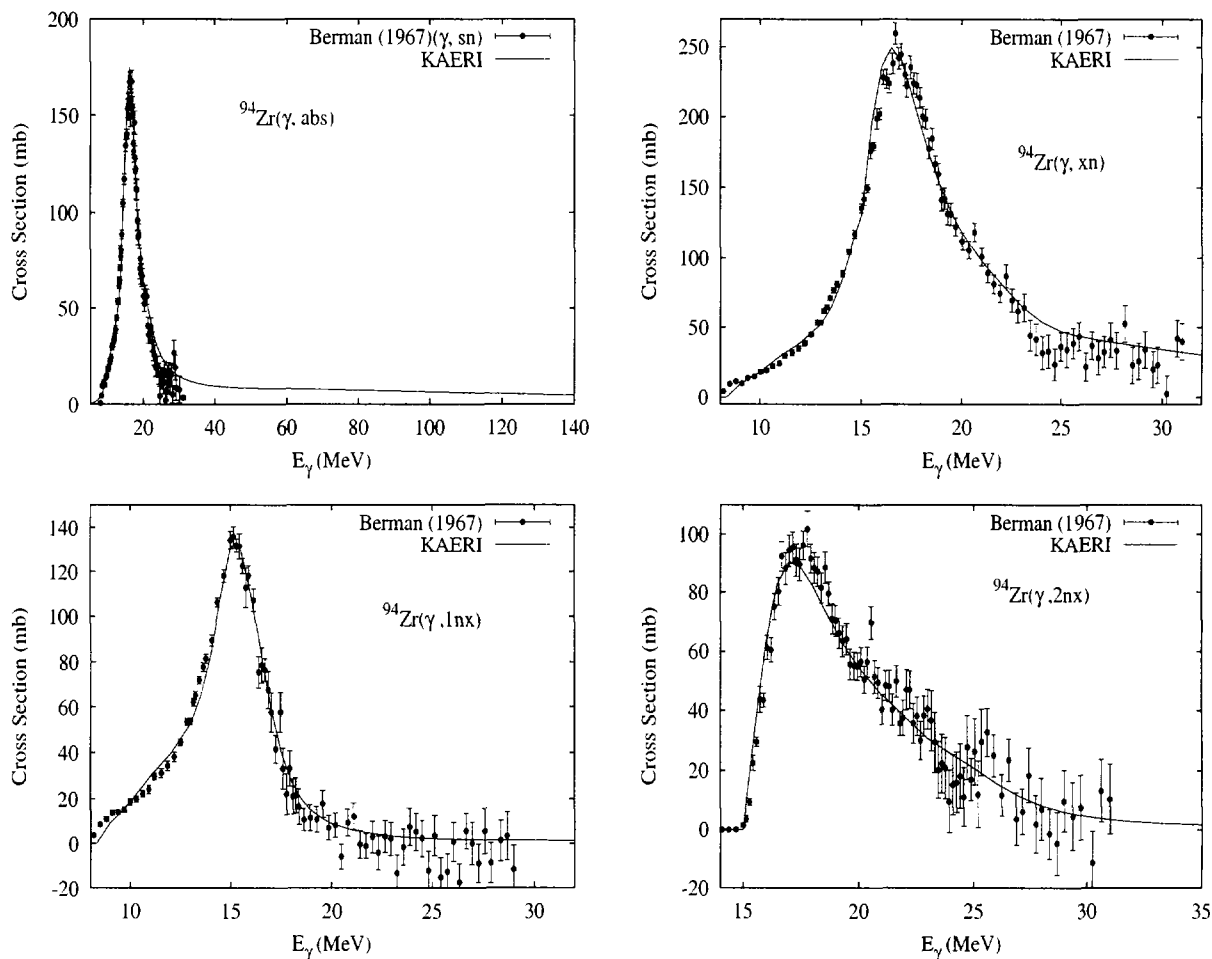
$$\gamma + {}^{52}\text{Cr}$$

Abundance (%)	Threshold Energies (MeV)								
	γ,n	γ,p	γ,t	$\gamma,\text{He-3}$	γ,α	$\gamma,2n$	γ,np	$\gamma,2p$	$\gamma,3n$
83.79	12.04	10.50	22.41	21.79	9.35	21.30	21.56	18.57	34.30
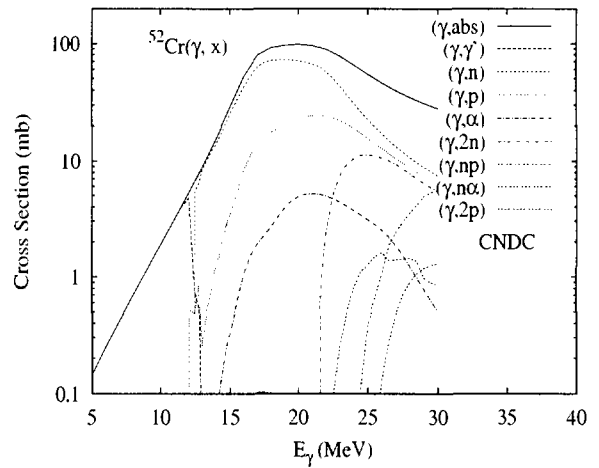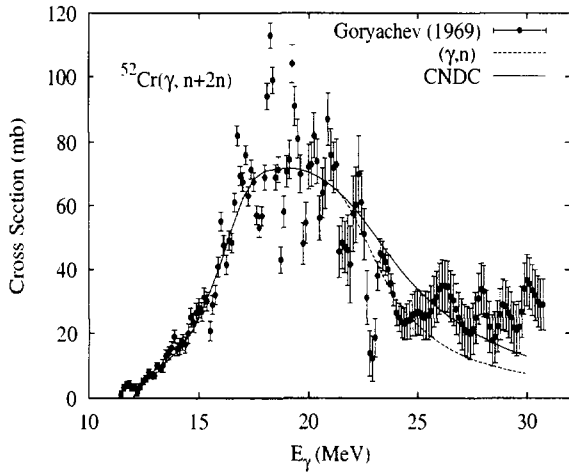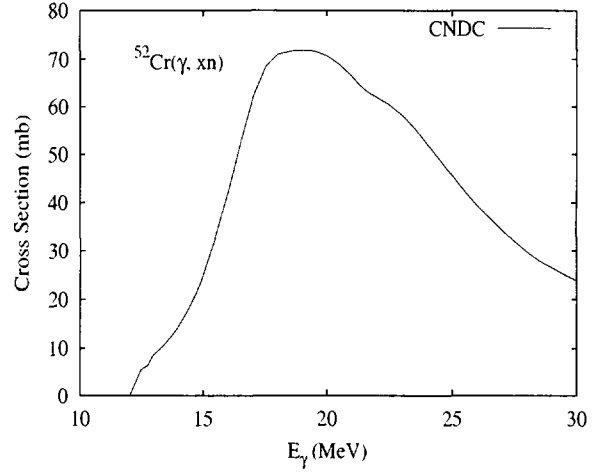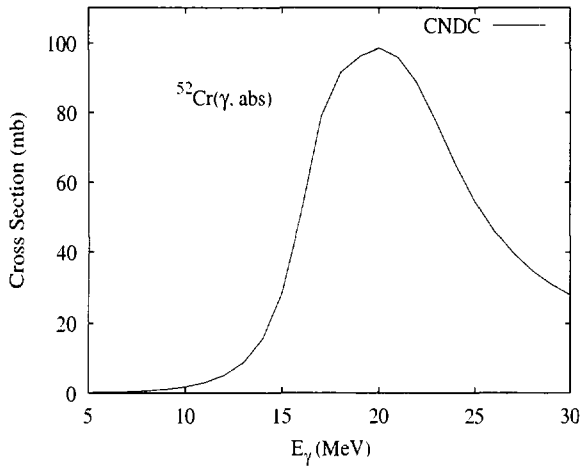
The photoabsorption cross section has not been measured. However, there are experimental data for the (γ, 1nx), and (γ, 2nx) reaction cross sections [Gor69]. We relied on GUNF code [Zha98] to infer the photoabsorption cross section in the GDR regime, in order to model accurately the available experimental data. The APOM code [She92], was used to obtain the neutron optical potential parameters by fitting experimental data for the total and nonelastic scattering cross sections and for the elastic scattering angular distributions of n + ^{nat,50,52,53,54}Cr reactions. The optical potential parameters for charged particles p, α, ^{3}He, d, and t, were taken from [Per76].

140

$\gamma + {}^{53}\mathrm{Cr}$

Abundance (%)	Threshold Energies (MeV)								
	γ,n	γ,p	γ,t	$\gamma,$He-3	γ,α	$\gamma,2n$	γ,np	$\gamma,2p$	$\gamma,3n$
9.50	7.94	11.13	21.01	18.79	9.15	19.98	18.44	20.13	29.24
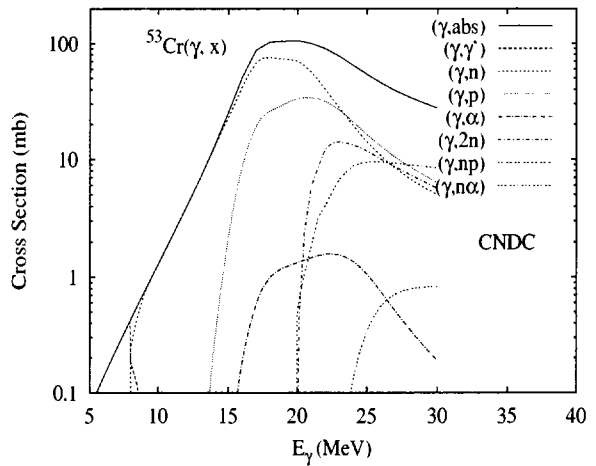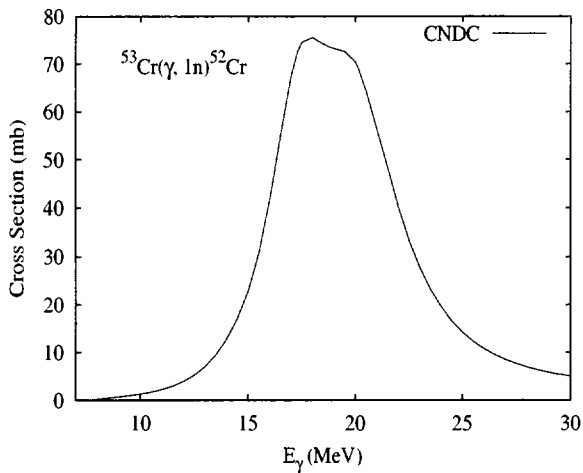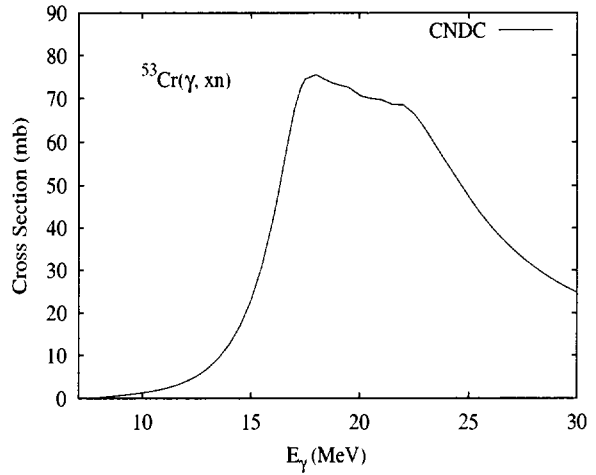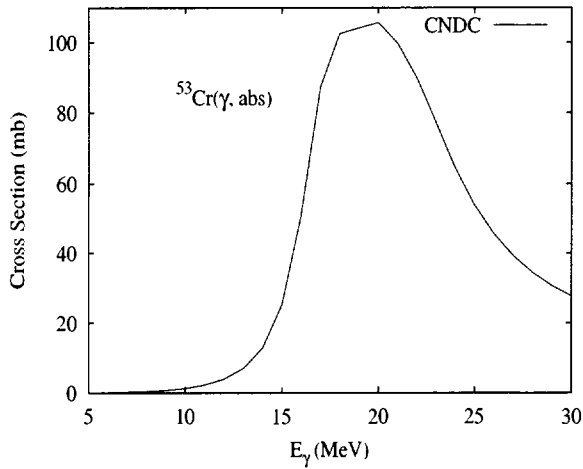
There are no experimental data available. The photoabsorption cross section was obtained from GDR model calculations using the GUNF code [Zha98]. Neutron optical potential parameters were determined from the APOM code [She92] fittings of neutron nuclear data for $nat,50,52$Cr. Optical potential parameters for charged particles, p, α, ^{3}He, d, and t were obtained from [Per76].

$\gamma + {}^{54}\mathrm{Cr}$

Abundance (%)	Threshold Energies (MeV)								
	γ,n	γ,p	γ,t	$\gamma,$He-3	γ,α	$\gamma,2n$	γ,np	$\gamma,2p$	$\gamma,3n$
2.37	9.72	12.37	19.68	22.13	7.93	17.66	20.85	22.04	29.70

There are no experimental data available. The photoabsorption cross section was obtained from GDR model calculations using the GUNF code [Zha98]. Neutron optical potential parameters were determined from the APOM code [She92] fittings of neutron nuclear data for ^{nat,50,52}Cr. Optical potential parameters for charged particles, p, α, ^{3}He, d, and t were obtained from [Per76].

142

Abundance	Threshold Energies (MeV)								
(%)	γ,n	γ,p	γ,t	$\gamma,\text{He-3}$	γ,α	$\gamma,\text{2n}$	γ,np	$\gamma,\text{2p}$	$\gamma,\text{3n}$
100.00	10.23	8.07	17.24	21.20	7.93	19.16	17.79	20.44	31.22
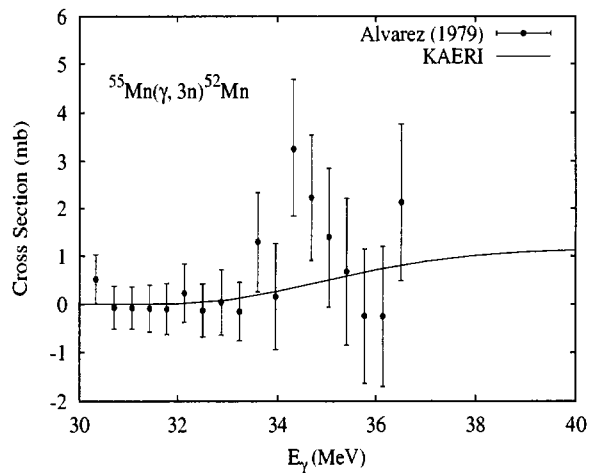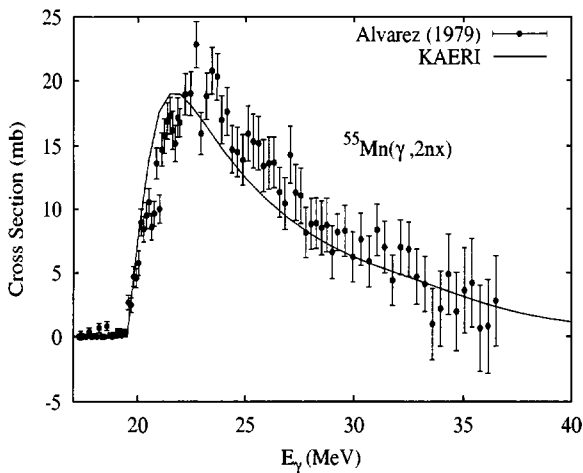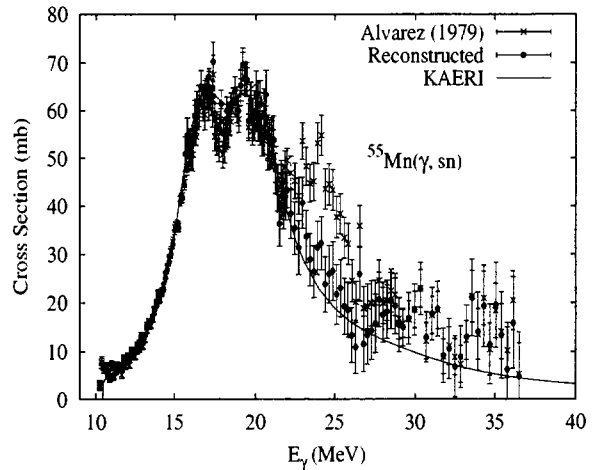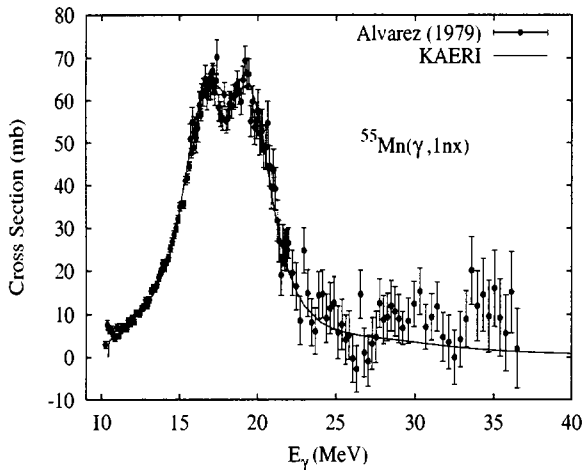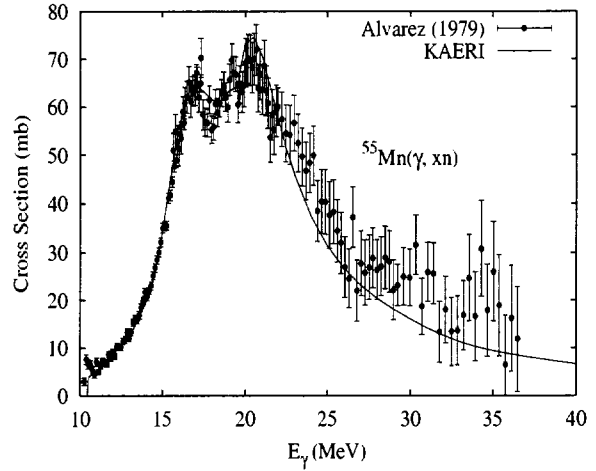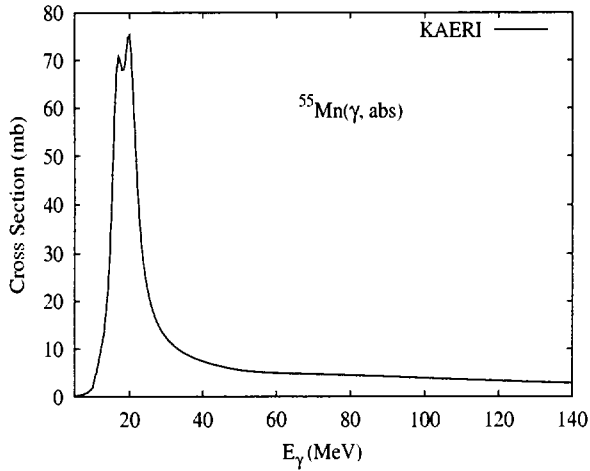
The photoabsorption cross section has not been measured. However, the experimental data [Alv79] were given for $(\gamma,\text{ 1nx})$, $(\gamma,\text{ 2nx})$, $(\gamma,\text{ 3nx})$, $(\gamma,\text{ sn})$ and $(\gamma,\text{ xn})$ reaction cross sections. Since the original $(\gamma,\text{ sn})$ data of Alvarez are not consistent with the $(\gamma,\text{ 1nx})$ and $(\gamma,\text{2nx})$ above 25 MeV, new $(\gamma,\text{ sn})$ reference data were constructed by adding $(\gamma,\text{ 1nx})$ and

(γ,2nx) data. We relied on the GUNF and GNASH codes to infer the photoabsorption cross section in the GDR regime, in order to model accurately the reconstructed (γ, sn) data. The photoabsorption cross section above the GDR, up to 140 MeV, was obtained from QD model calculations using the theory of Chadwick.

The calculated results of the emission channels by the GNASH code are basically in agreement with the experimental data for (γ, 1nx), (γ, 2nx), (γ, 3nx) and (γ, xn) as well as the reconstructed (γ, sn) reaction.

$\gamma + {}^{54}\text{Fe}$

Abundance (%)	Threshold Energies (MeV)								
	γ,n	γ,p	γ,t	$\gamma,\text{He-3}$	γ,α	$\gamma,2n$	γ,np	$\gamma,2p$	$\gamma,3n$
5.90	13.38	8.85	22.96	19.73	8.42	24.06	20.91	15.41	40.25
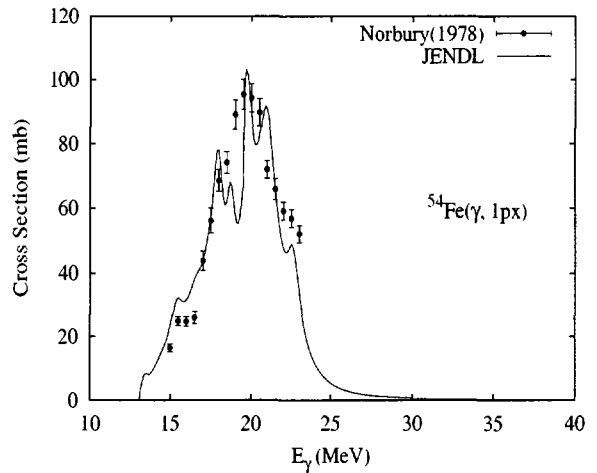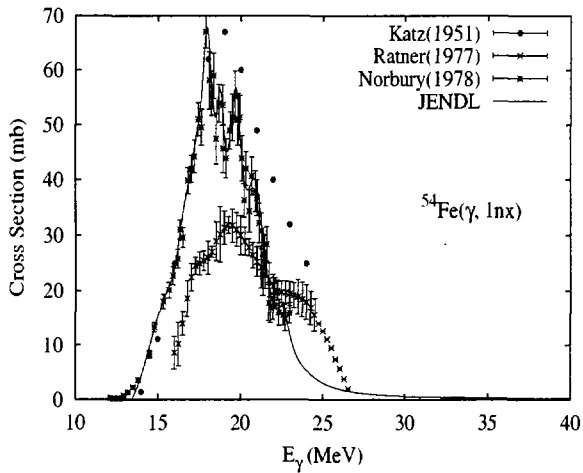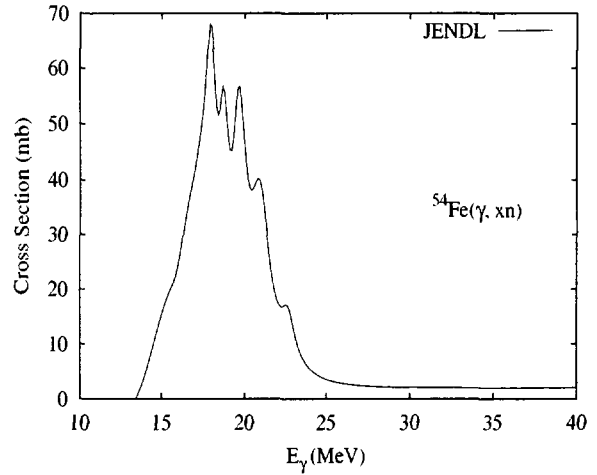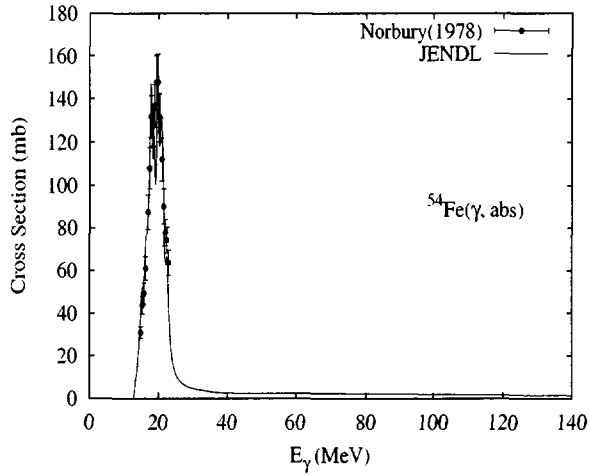
Photonuclear reactions were evaluated using ALICE-F [Fuk93] code calculations together with experimental data. Input model parameters were adjusted so as to improve the quality of the calculated results compared with data [Nor78]. Photoabsorption was modeled as a sum of GDR and QD components [Cha91].

$$\gamma + {}^{56}\text{Fe}$$

Abundance	Threshold Energies (MeV)								
(%)	γ,n	γ,p	γ,t	γ,He-3	γ,α	γ,2n	γ,np	γ,2p	γ,3n
91.72	11.20	10.18	20.87	20.25	7.61	20.50	20.41	18.25	33.87
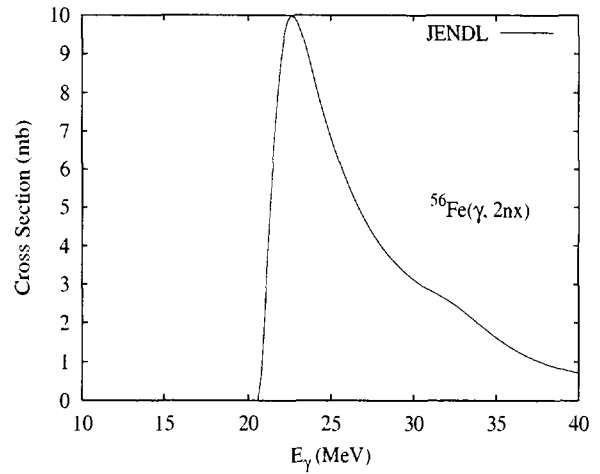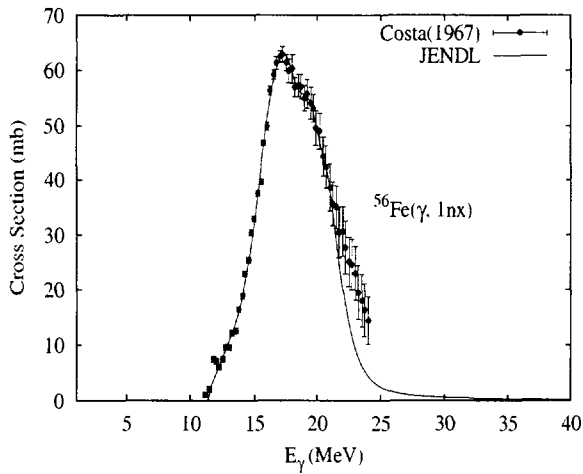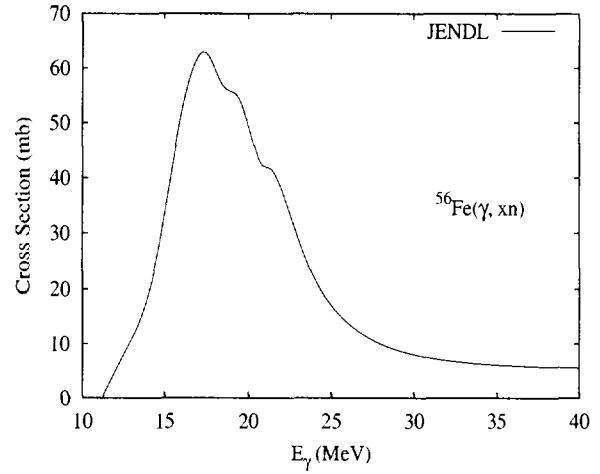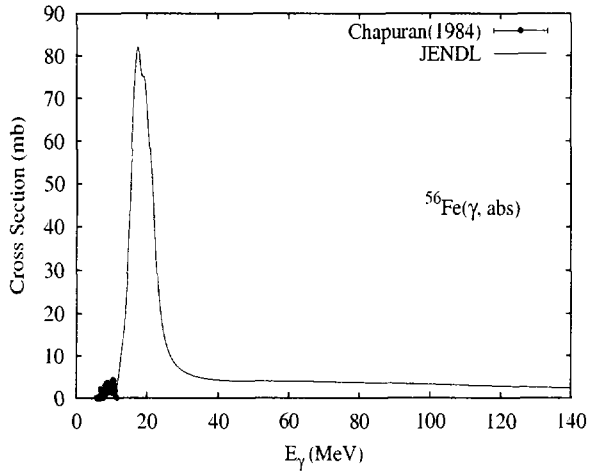
Photonuclear reactions were evaluated using ALICE-F [Fuk93] code calculations together with experimental data. Input model parameters were adjusted so as to improve the quality of the calculated results compared with data [Cos67]. Photoabsorption was modeled as a sum of GDR and QD components [Cha91].

$\gamma + {}^{57}\mathrm{Fe}$

Abundance (%)	Threshold Energies (MeV)								
	γ,n	γ,p	γ,t	γ,He-3	γ,α	γ,2n	γ,np	γ,2p	γ,3n
2.10	7.65	10.56	19.58	18.18	7.32	18.84	17.83	19.65	28.14
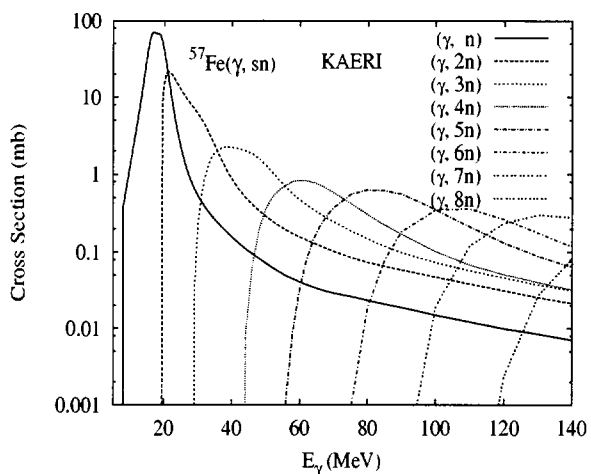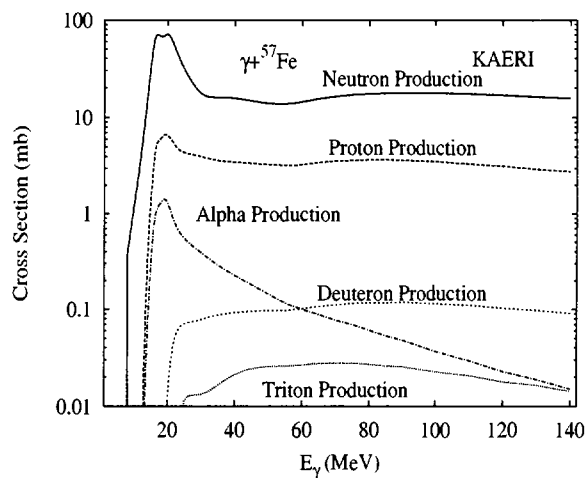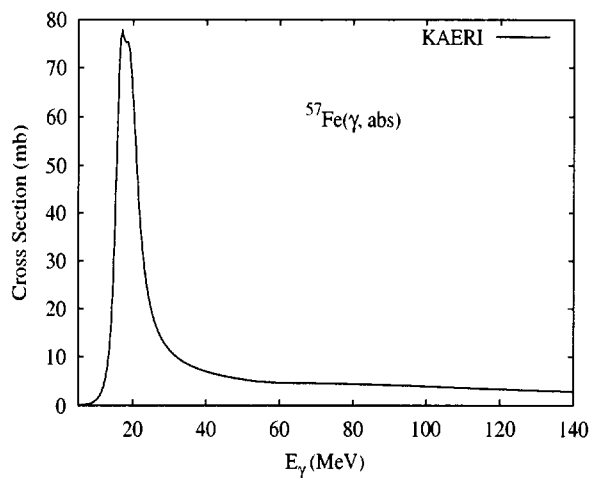
There are no experimental data available. The photoabsorption cross section was obtained from GDR and QD model calculations, adopting the GDR parameters of ${}^{56}\mathrm{Fe}$. The neutron, proton, deuteron, triton and alpha emission cross sections, as well as production cross sections, were calculated by the GNASH code.

$\gamma + {}^{58}\text{Fe}$

Abundance (%)	Threshold Energies (MeV)								
	γ,n	γ,p	γ,t	$\gamma,\text{He-3}$	γ,α	$\gamma,2n$	γ,np	$\gamma,2p$	$\gamma,3n$
0.28	10.04	11.95	19.39	21.98	7.65	17.69	20.60	21.44	28.89
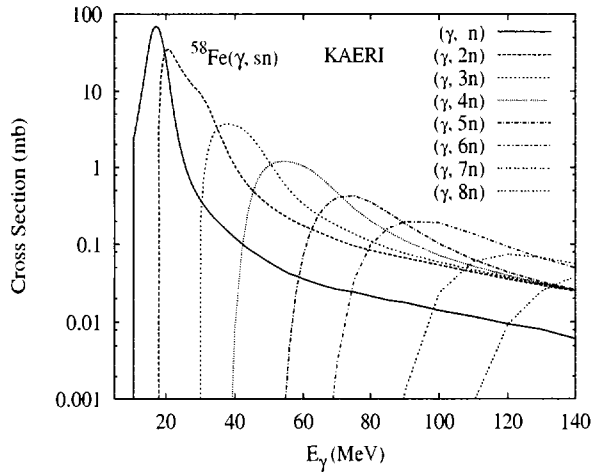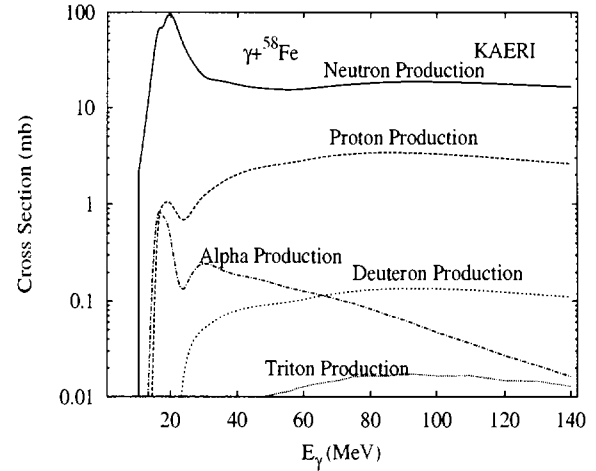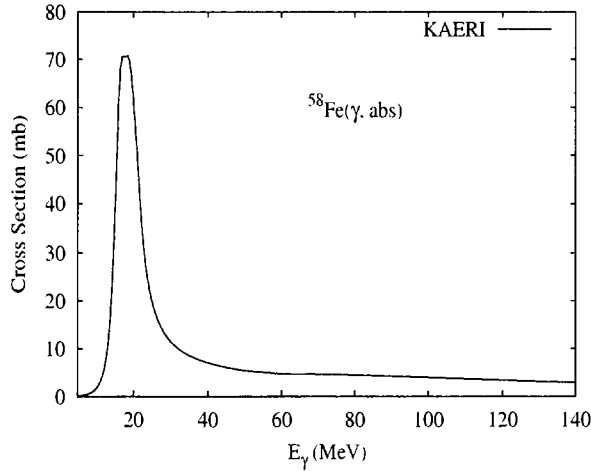
There are no experimental data available. The photoabsorption cross section was obtained from GDR and QD model calculations, adopting the GDR parameters of ${}^{56}\text{Fe}$. The neutron, proton, deuteron, triton and alpha emission cross sections, as well as production cross sections, were calculated by the GNASH code.

$$\gamma + {}^{59}\text{Co}$$

| Abundance (%)	Threshold Energies (MeV)								
	γ,n	γ,p	γ,t	γ,He-3	γ,α	γ,2n	γ,np	γ,2p	γ,3n
100.00	10.45	7.36	16.57	20.25	6.94	19.03	17.41	19.32	30.40
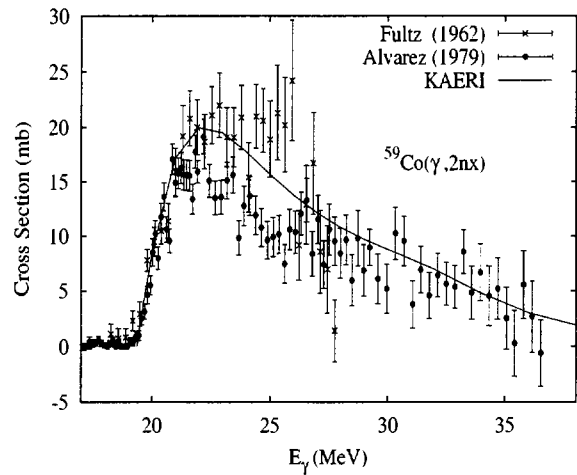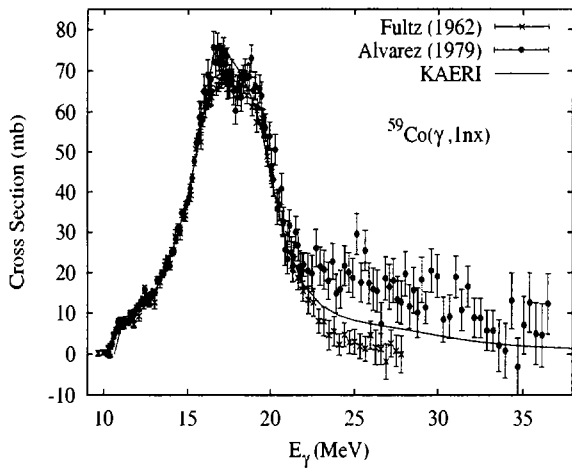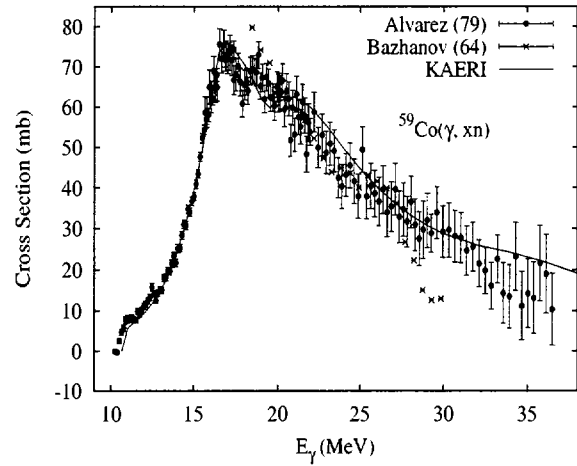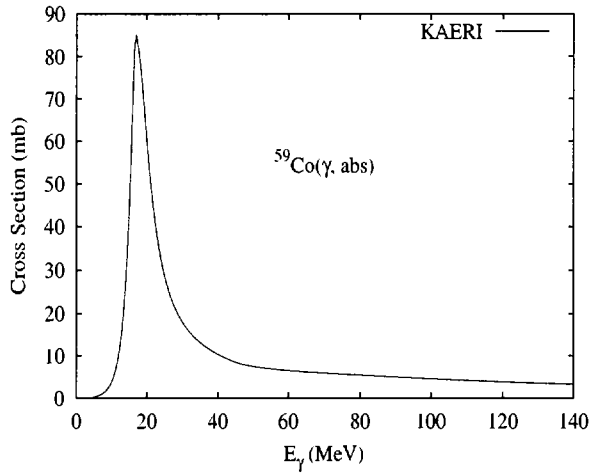
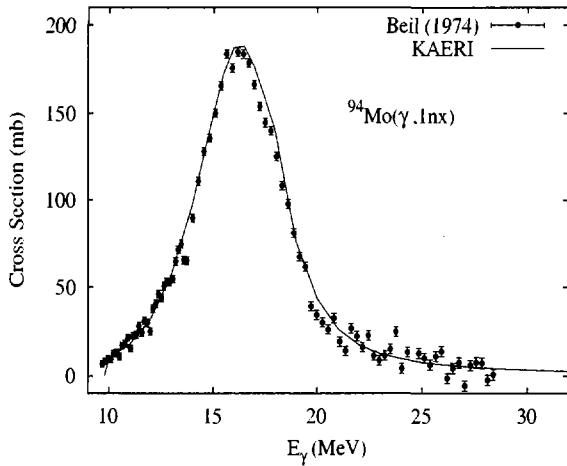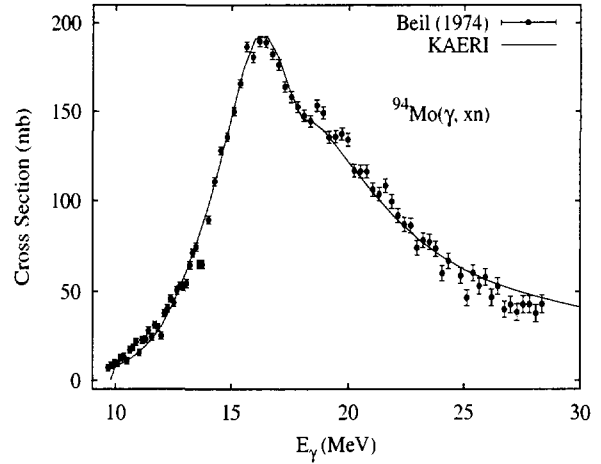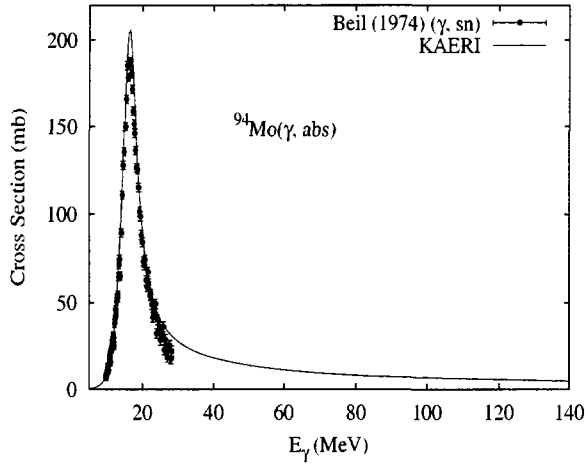

The photoabsorption cross section has not been measured. However, there are experimental data for the (γ, 1nx) and (γ, 2nx) reaction cross sections by Fultz and Alvarez [Ful62a, Alv79], (γ, 3nx) cross section by Alvarez [Alv79], and (γ, xn) reaction cross section by [Baz64, Alv79]. We relied on the GUNF and GNASH codes to infer the photoabsorption cross section in the GDR regime, in order to model accurately the (γ, xn) data of Alvarez. The photoabsorption cross section above the GDR, up to 140 MeV, was obtained from QD model calculations using the theory of Chadwick.

The calculated results of the emission channels by the GNASH code are in good agreement with the experimental data.

$$\gamma + {}^{58}\text{Ni}$$

Abundance	Threshold Energies (MeV)								
(%)	γ,n	γ,p	γ,t	$\gamma,\text{He-3}$	γ,α	$\gamma,2n$	γ,np	$\gamma,2p$	$\gamma,3n$
68.08	12.22	8.17	21.15	17.68	6.40	22.47	19.55	14.20	39.11
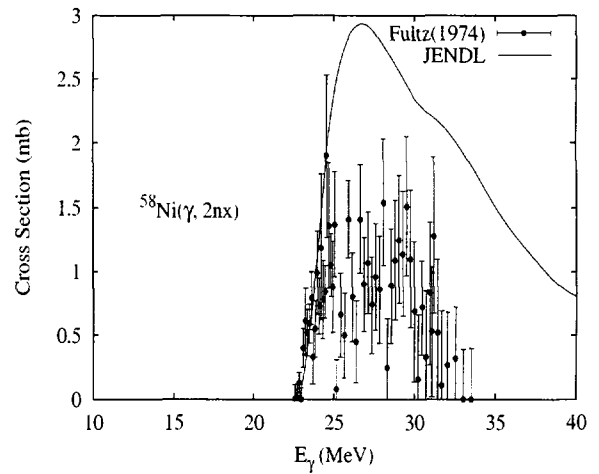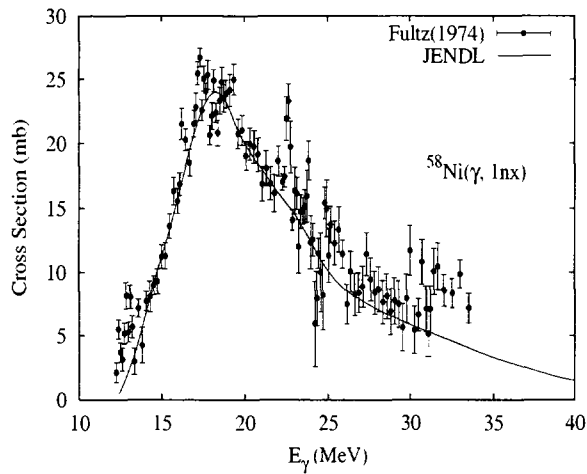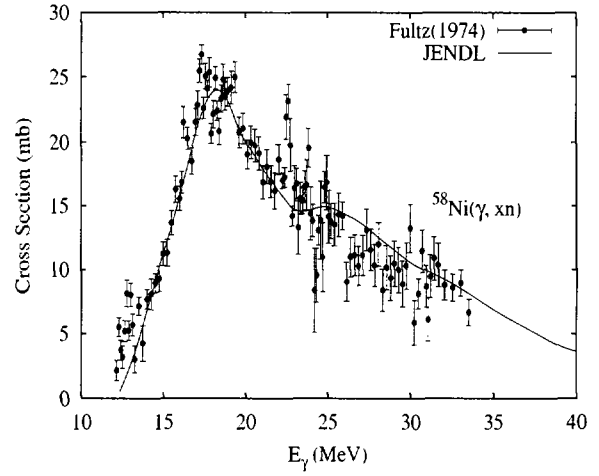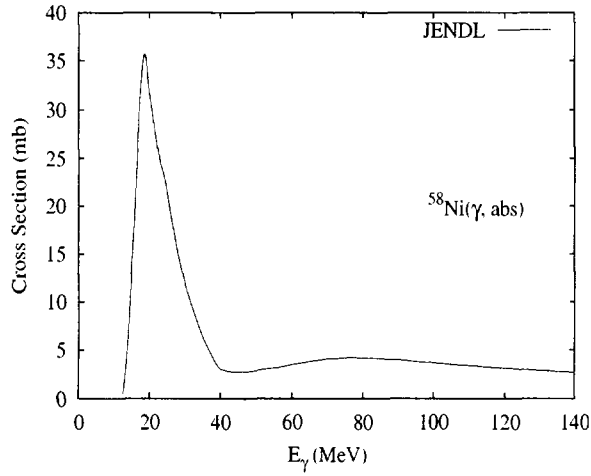
Photonuclear reactions were evaluated using ALICE-F [Fuk93] code calculations together with experimental data. Input model parameters were adjusted so as to improve the quality of the calculated results compared with data [Ful74]. Photoabsorption was modeled as a sum of GDR and QD components [Cha91].

$\gamma + {}^{60}\text{Ni}$

| Abundance (%)	Threshold Energies (MeV)								
	γ,n	γ,p	γ,t	$\gamma,\text{He-3}$	γ,α	$\gamma,2n$	γ,np	$\gamma,2p$	$\gamma,3n$
26.22	11.39	9.53	20.08	19.22	6.29	20.39	19.99	16.90	32.61
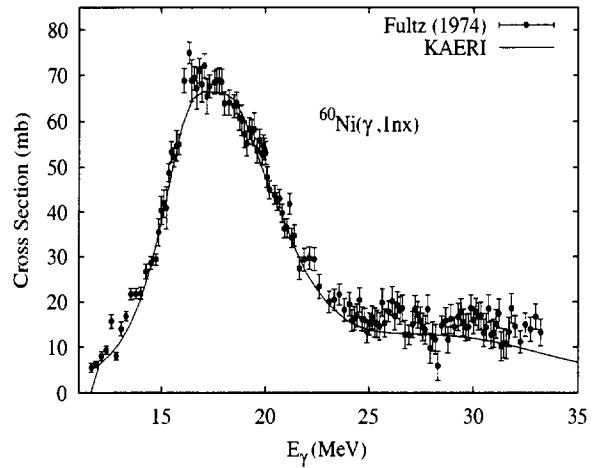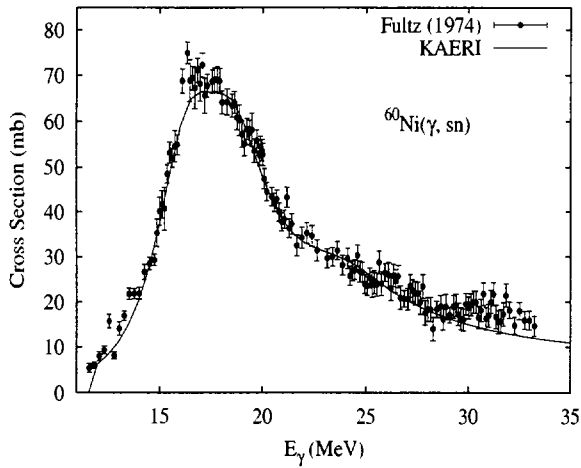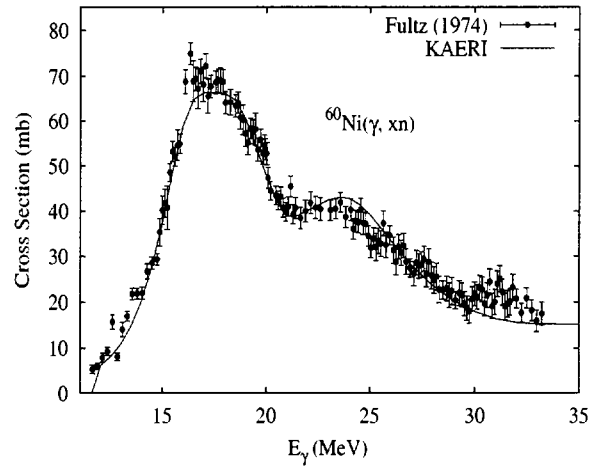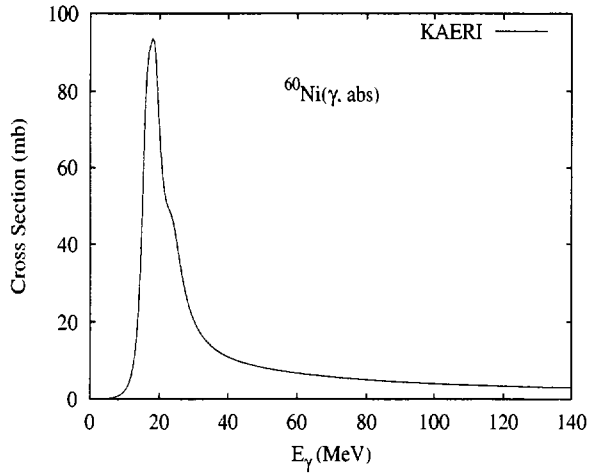
The photoabsorption cross section has not been measured. However, there are experimental data for the (γ, 1nx), (γ, 2nx), (γ, sn) and (γ, xn) reaction cross sections [Ful74]. We relied on the GUNF and GNASH codes to infer the photoabsorption cross section in the GDR regime, in order to model accurately the (γ, sn) data. The photoabsorption cross section above the GDR, up to 140 MeV, was obtained from QD model calculations using the theory of Chadwick.

The calculated results of the emission channels by the GNASH code are in good agreement with the experimental data.

$\gamma + {}^{61}\text{Ni}$

Abundance (%)	Threshold Energies (MeV)								
	γ,n	γ,p	γ,t	γ,He-3	γ,α	γ,2n	γ,np	γ,2p	γ,3n
1.14	7.82	9.86	19.33	17.00	6.47	19.21	17.35	18.14	28.21

There are no experimental data available. The photoabsorption cross section was obtained from GDR and QD model calculations, adopting the GDR parameters of ${}^{60}\text{Ni}$. The neutron, proton, deuteron, triton and alpha emission cross sections, as well as production cross sections, were calculated by the GNASH code.

$\gamma + {}^{62}\text{Ni}$

Abundance	Threshold Energies (MeV)								
(%)	γ,n	γ,p	γ,t	γ,He-3	γ,α	γ,2n	γ,np	γ,2p	γ,3n
3.63	10.60	11.14	19.47	21.02	7.02	18.42	20.46	19.92	29.81
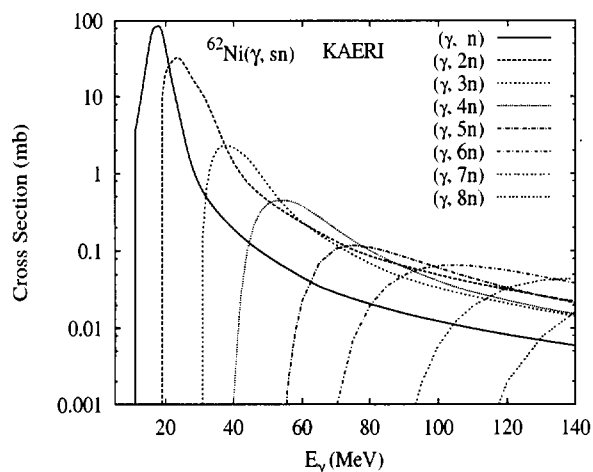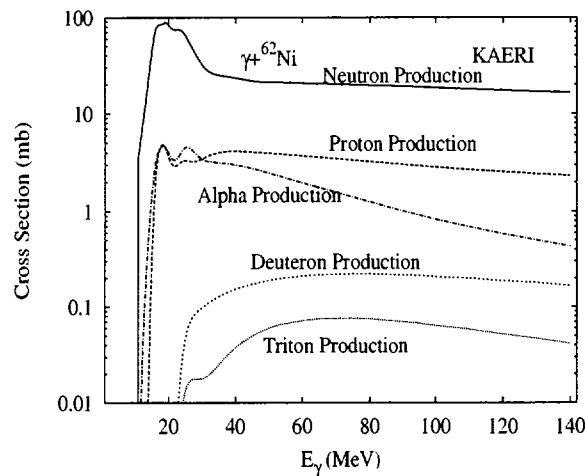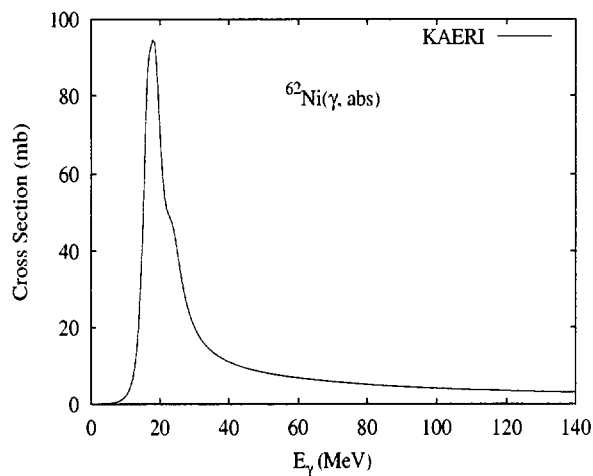
There are no experimental data available. The photoabsorption cross section was obtained from GDR and QD model calculations, adopting the GDR parameters of ${}^{60}\text{Ni}$. The neutron, proton, deuteron, triton and alpha emission cross sections, as well as production cross sections, were calculated by the GNASH code.

$\gamma + {}^{64}$Ni

Abundance	Threshold Energies (MeV)								
(%)	γ,n	γ,p	γ,t	γ,He-3	γ,α	γ,2n	γ,np	γ,2p	γ,3n
0.93	9.66	12.55	19.15	23.11	8.12	16.50	21.04	22.78	27.09
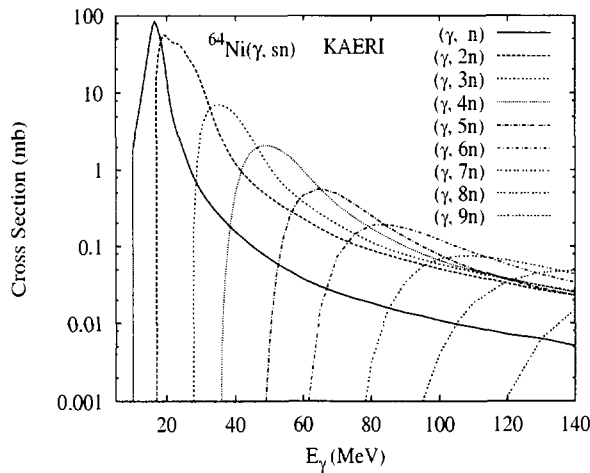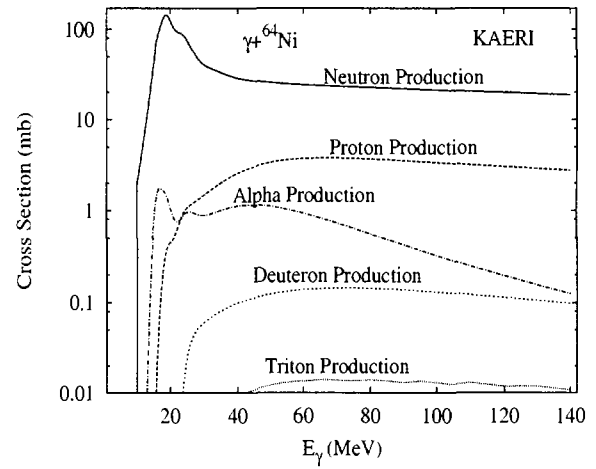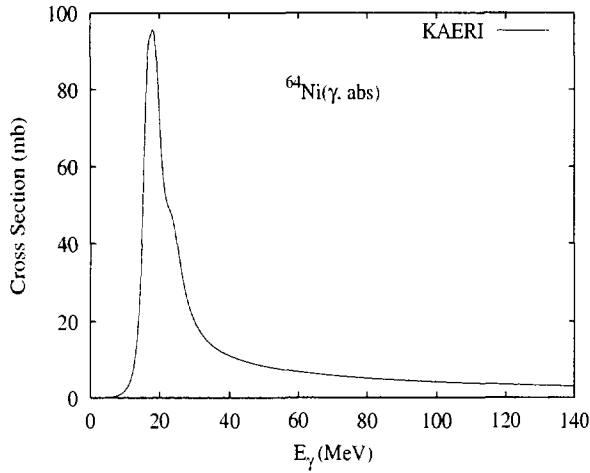
There are no experimental data available. The photoabsorption cross section was obtained from GDR and QD model calculations, adopting the GDR parameters of ^{60}Ni. The neutron, proton, deuteron, triton and alpha emission cross sections, as well as production cross sections, were calculated by the GNASH code.

$$\gamma + {}^{63}\text{Cu}$$

Abundance (%)	Threshold Energies (MeV)								
	γ,n	γ,p	γ,t	γ,He-3	γ,α	γ,2n	γ,np	γ,2p	γ,3n
69.17	10.85	6.12	16.06	18.86	5.78	19.74	16.72	17.26	31.45
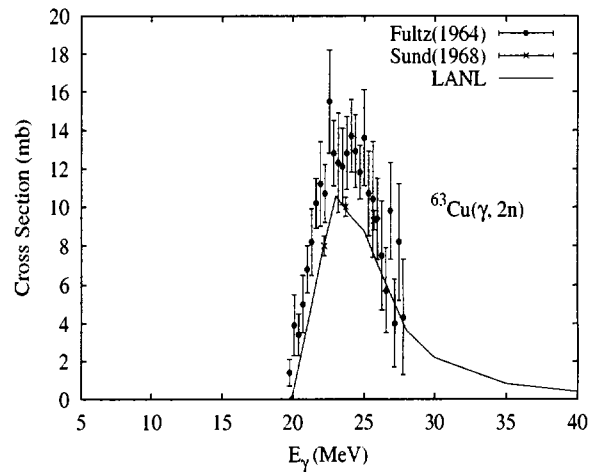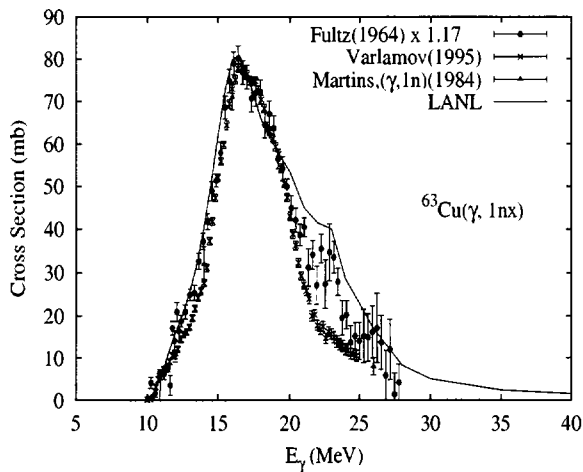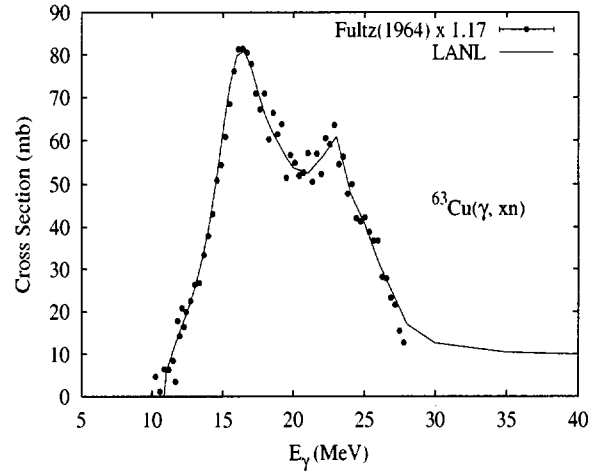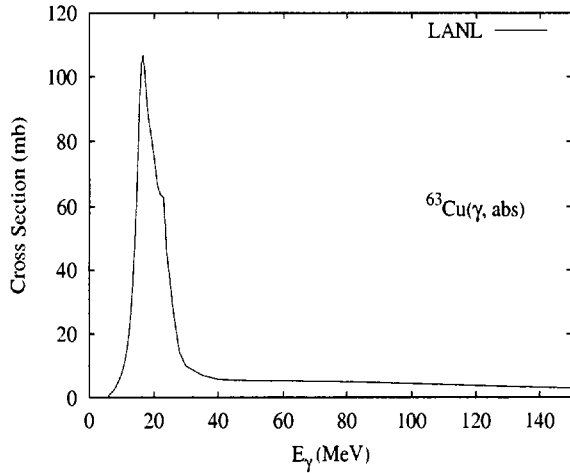
Available data are summarized by Varlamov [Var96]. No data exist for the total absorption cross section, for ^{63}Cu. However, data do exist for the photoneutron cross section [Ful64], and the GNASH code predicts the ratio of (γ,abs) to (γ,n) and (γ,p), etc. Thus, we relied on the GNASH code to infer the absorption cross section in the GDR regime, so as to model accurately the Fultz (γ,xn) measured data [Ful64]. We followed recommendations from IAEA CRP members at the JAERI CRP to renormalize the Livermore Fultz data and absorption cross section by 1.17. This led to agreement with Varlamov [Var95]. The total absorption cross section above the GDR, up to 150 MeV, was taken from QD model calculations using the theory of Chadwick [Cha91]. The (γ,xn) data agreed with Fultz [Ful64] x1.17. The (γ,1nx) data were in fairly good agreement with those of Fultz x 1.17 [Ful64], Varlamov [Var95], and Martins [Mar84], though were on the high side of the data near 23 MeV. Likewise, the (γ,2n) were low at 23 MeV compared to the Fultz x 1.17 data, but these 2 defects compensated each other and (γ,xn) agreed with data.

$$\gamma + {}^{65}\text{Cu}$$

Abundance (%)	Threshold Energies (MeV)								
	γ,n	γ,p	γ,t	γ,He-3	γ,α	γ,2n	γ,np	γ,2p	γ,3n
30.83	9.91	7.45	15.47	20.77	6.79	17.83	17.11	20.00	28.68
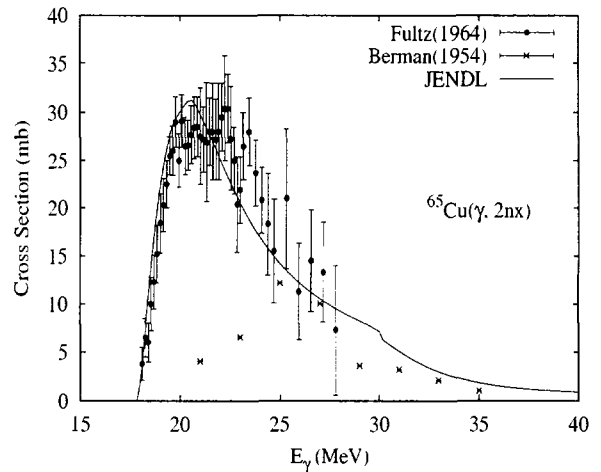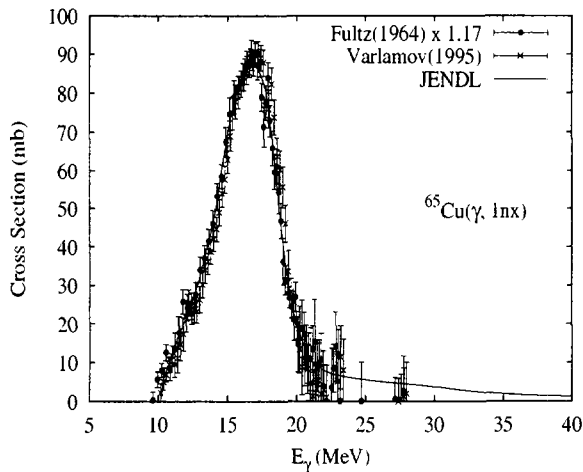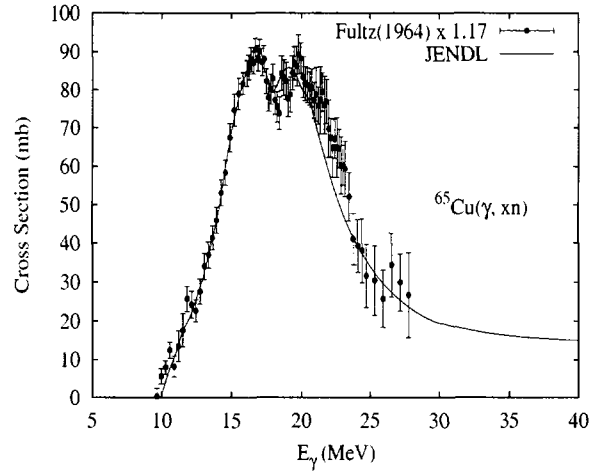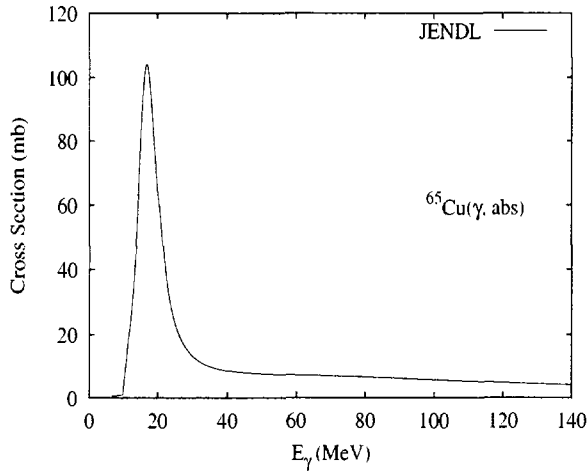
Photonuclear reactions were evaluated using ALICE-F [Fuk93] code calculations together with experimental data [Ful64, Var95]. Renormalization was applied to the Livermore Fultz's data up by 17% in accordance with a suggestion of IAEA Third Research Co-ordination Meeting on Compilation and Evaluation of Photonuclear Data for Applications on 25-29 October 1999. This led to agreement with the Varlamov's (γ,1nx) reaction cross section [Var95]. Photoabsorption was modeled as a sum of GDR and QD components [Cha91].

$\gamma + {}^{64}\mathrm{Zn}$

Abundance (%)	Threshold Energies (MeV)								
	γ,n	γ,p	γ,t	γ,He-3	γ,α	γ,2n	γ,np	γ,2p	γ,3n
48.60	11.86	7.71	18.97	16.71	3.96	20.97	18.57	13.83	33.87
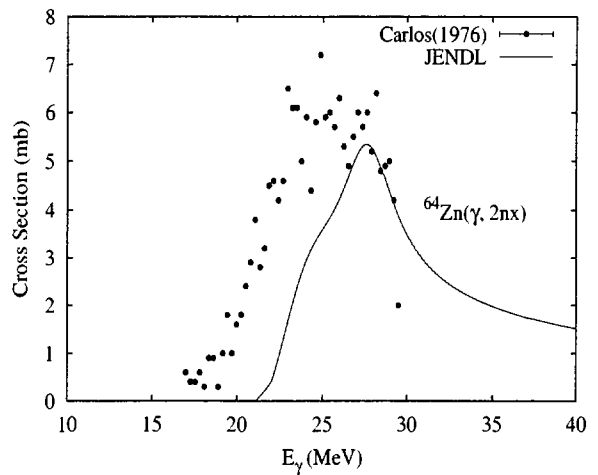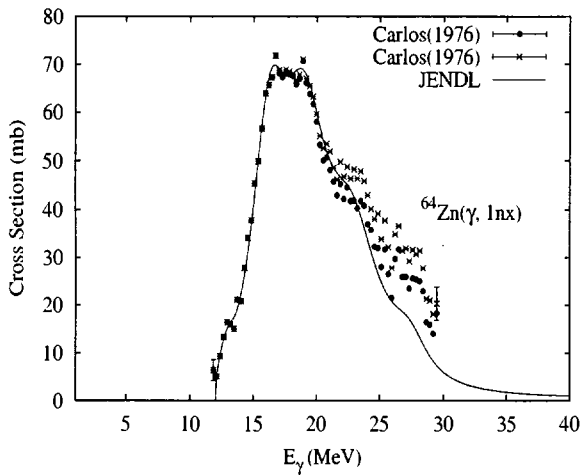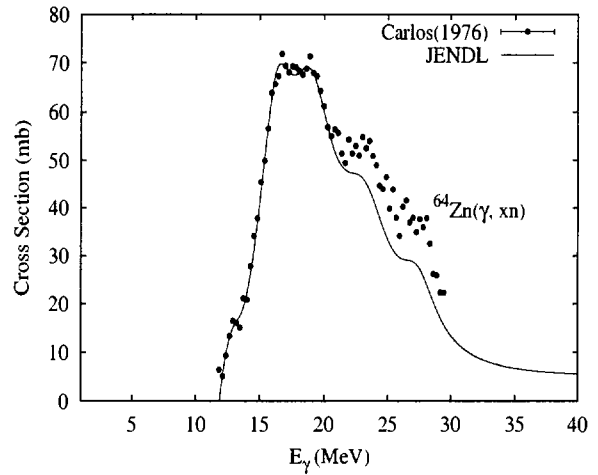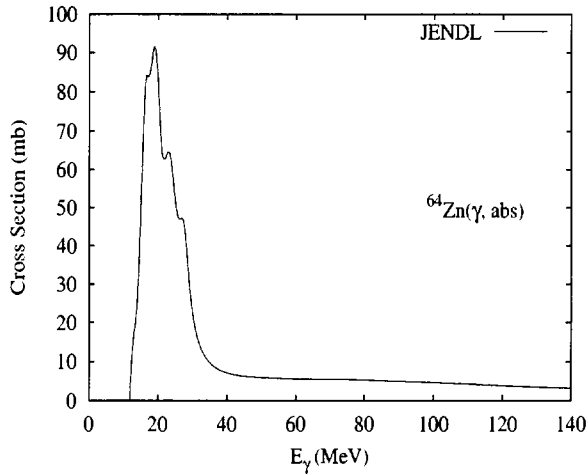
Photonuclear reactions were evaluated using ALICE-F [Fuk93] code calculations together with experimental data. Input model parameters were adjusted so as to improve the quality of the calculated results compared with data [Car76]. Photoabsorption was modeled as a sum of GDR and QD components [Cha91].

$\gamma + {}^{66}\text{Zn}$

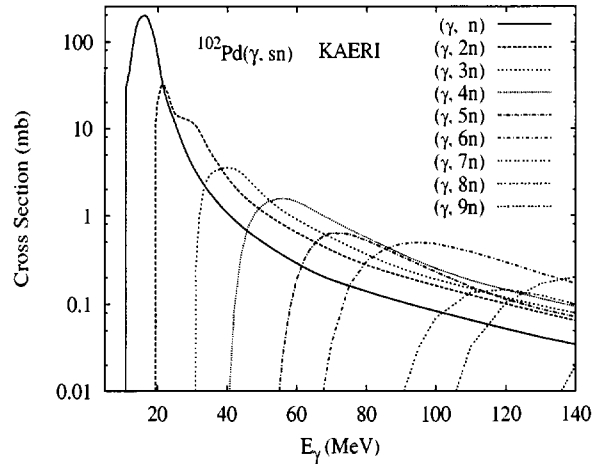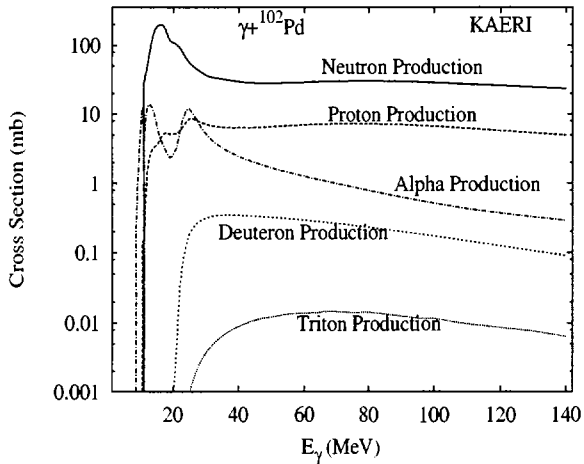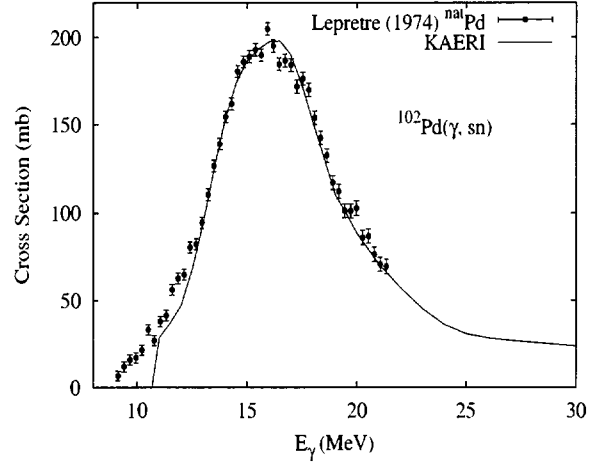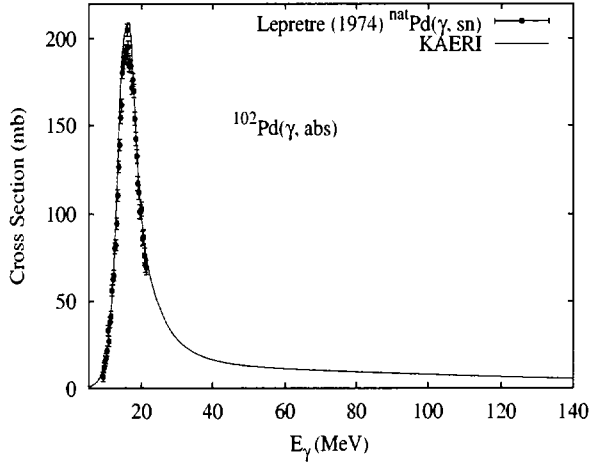| Abundance	Threshold Energies (MeV)								
(%)	γ,n	γ,p	γ,t	$\gamma,\text{He-3}$	γ,α	$\gamma,2n$	γ,np	$\gamma,2p$	$\gamma,3n$
27.90	11.06	8.93	18.27	18.32	4.58	19.04	18.84	16.38	30.90
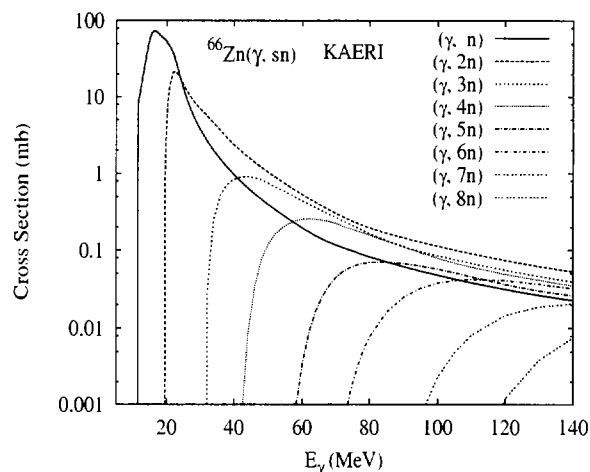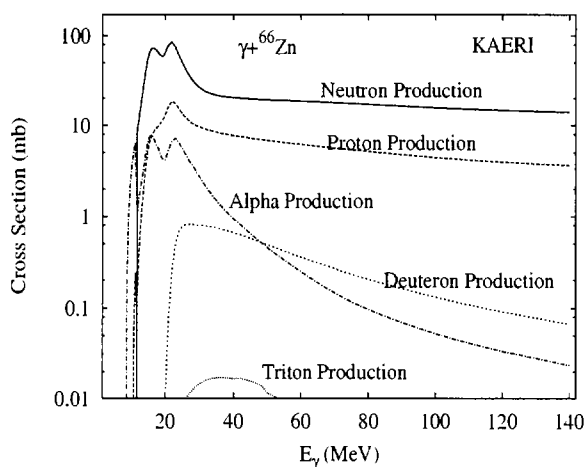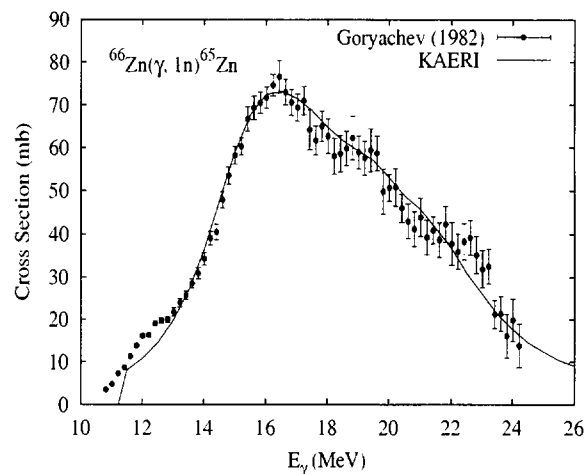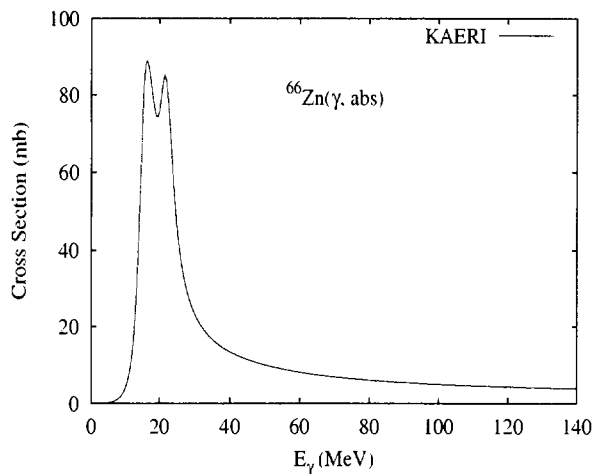
The photoabsorption cross section has not been measured. However, there are experimental data for the $(\gamma, 1n)$ reaction cross section [Gor82]. We relied on the GUNF and GNASH codes to infer the photoabsorption cross section in the GDR regime, in order to model accurately the $(\gamma, 1n)$ data. The photoabsorption cross section above the GDR, up to 140 MeV, was obtained from QD model calculations using the theory of Chadwick. The neutron, proton, deuteron, triton and alpha emission cross sections, as well as production cross sections, were calculated by the GNASH code.

$\gamma + {}^{67}\text{Zn}$

Abundance (%)	Threshold Energies (MeV)								
	γ,n	γ,p	γ,t	$\gamma,\text{He-3}$	γ,α	$\gamma,2n$	γ,np	$\gamma,2p$	$\gamma,3n$
4.10	7.05	8.91	17.41	15.71	4.79	18.11	15.98	17.33	26.09
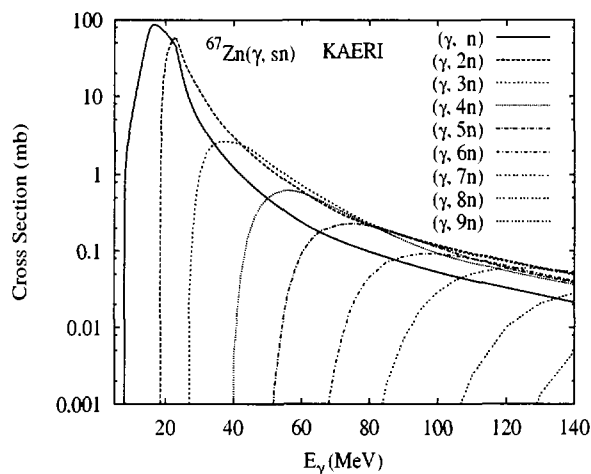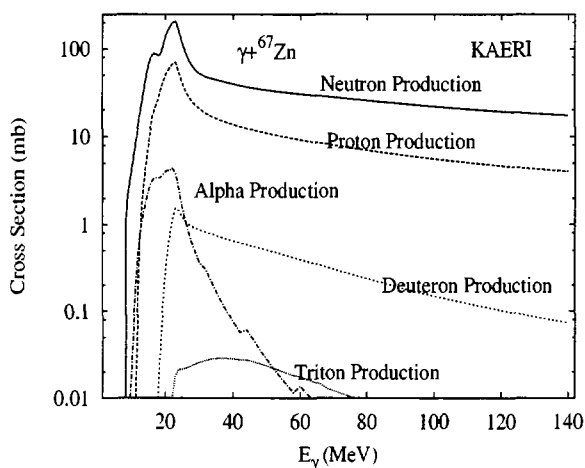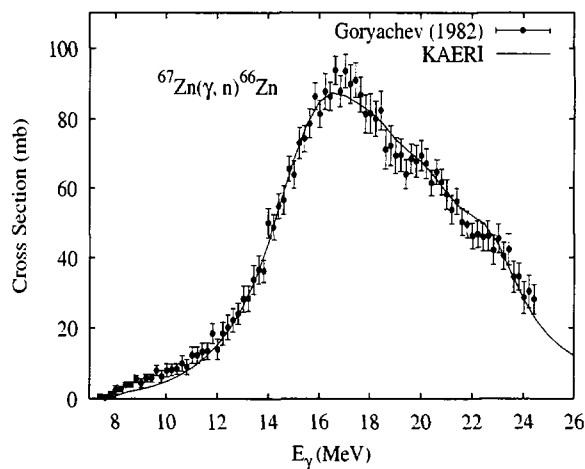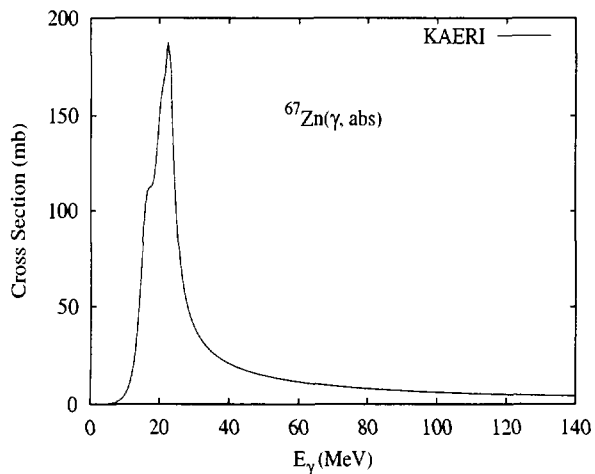
The photoabsorption cross section has not been measured. However, there are experimental data for the $(\gamma, 1n)$ reaction cross section [Gor82]. We relied on the GUNF and GNASH codes to infer the photoabsorption cross section in the GDR regime, in order to model accurately the $(\gamma, 1n)$ data. The photoabsorption cross section above the GDR, up to 140 MeV, was obtained from QD model calculations using the theory of Chadwick. The neutron, proton, deuteron, triton and alpha emission cross sections, as well as production cross sections, were calculated by the GNASH code.

$\gamma + {}^{68}\text{Zn}$

Abundance (%)	Threshold Energies (MeV)								
	γ,n	γ,p	γ,t	$\gamma,\text{He-3}$	γ,α	$\gamma,2n$	γ,np	$\gamma,2p$	$\gamma,3n$
18.80	10.20	9.99	17.69	19.81	5.33	17.25	19.11	18.56	28.31
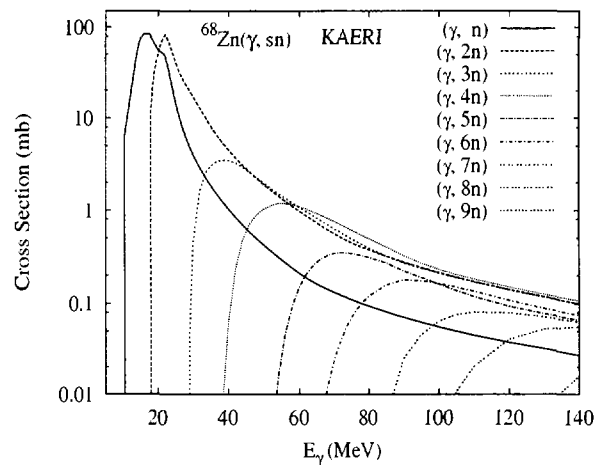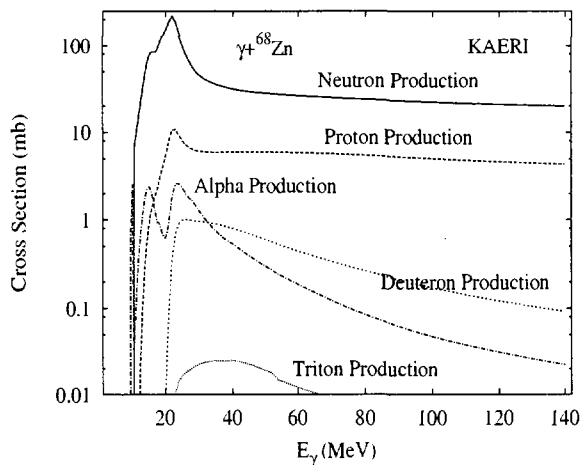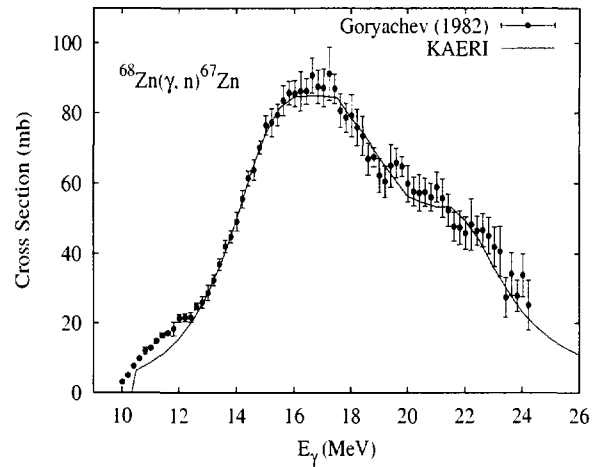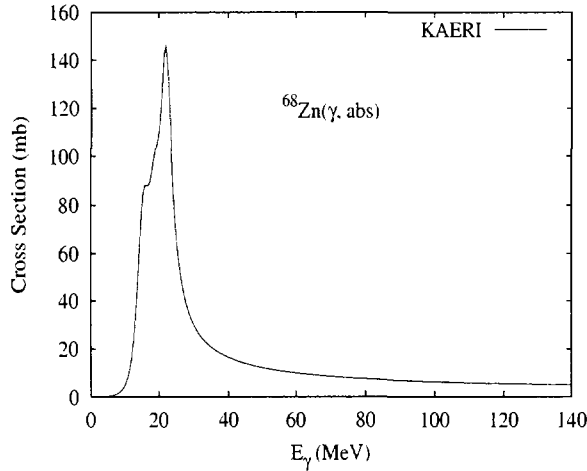
The photoabsorption cross section has not been measured. However, there are experimental data for the $(\gamma, 1n)$ reaction cross section [Gor82]. We relied on the GUNF and GNASH codes to infer the photoabsorption cross section in the GDR regime, in order to model accurately the $(\gamma, 1n)$ data. The photoabsorption cross section above the GDR, up to 140 MeV, was obtained from QD model calculations using the theory of Chadwick. The neutron, proton, deuteron, triton and alpha emission cross sections, as well as production cross sections, were calculated by the GNASH code.
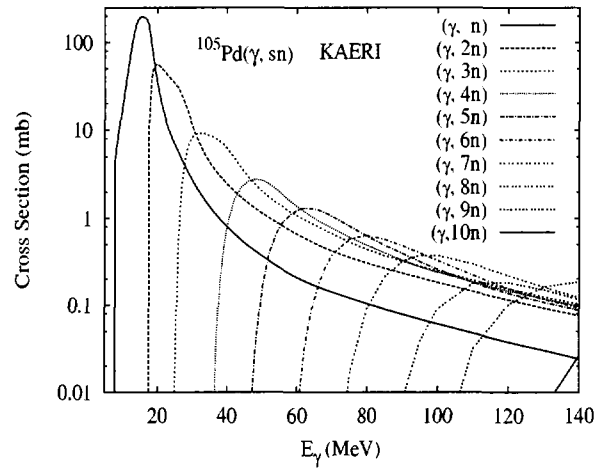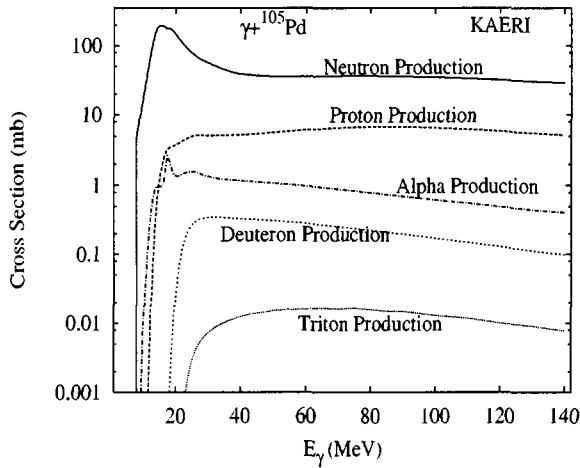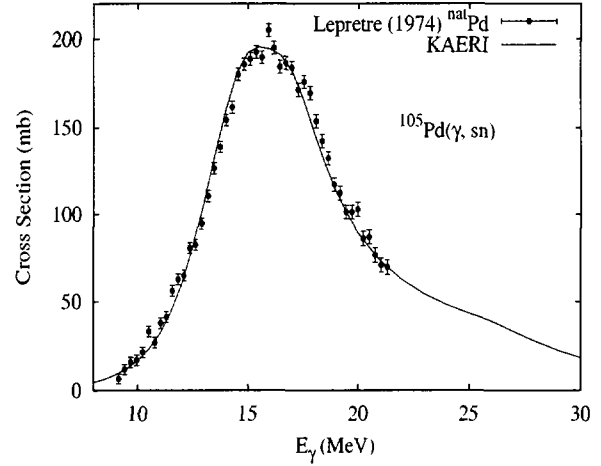
$\gamma + {}^{70}\mathbf{Zn}$

Abundance	Threshold Energies (MeV)								
(%)	γ,n	γ,p	γ,t	$\gamma,\text{He-3}$	γ,α	$\gamma,2n$	γ,np	$\gamma,2p$	$\gamma,3n$
0.60	9.22	11.11	17.21	20.75	5.96	15.70	19.38	20.66	25.90
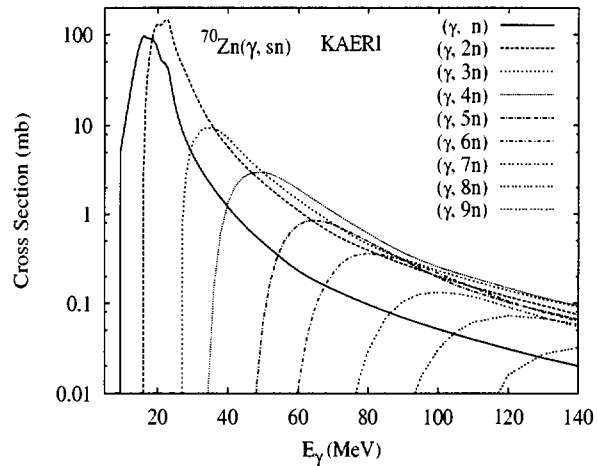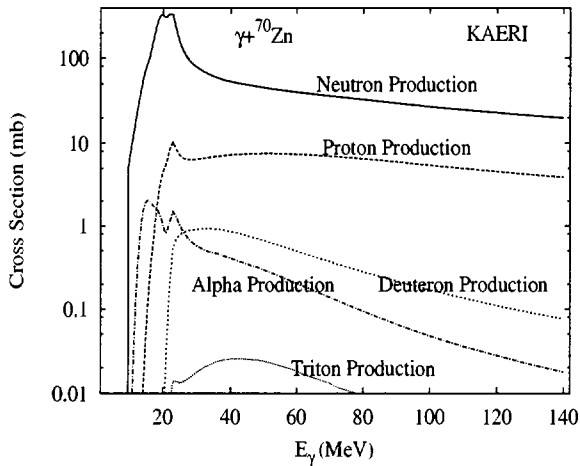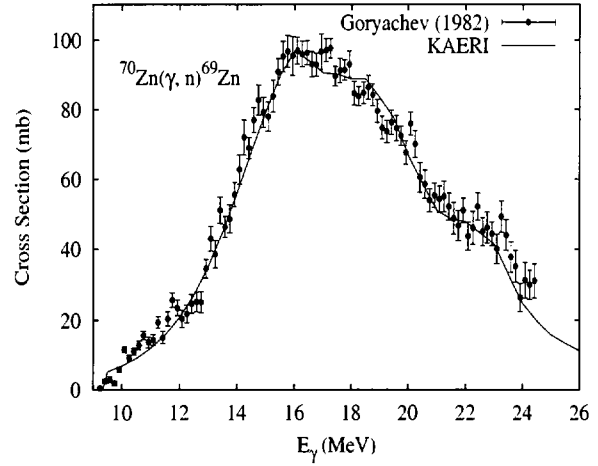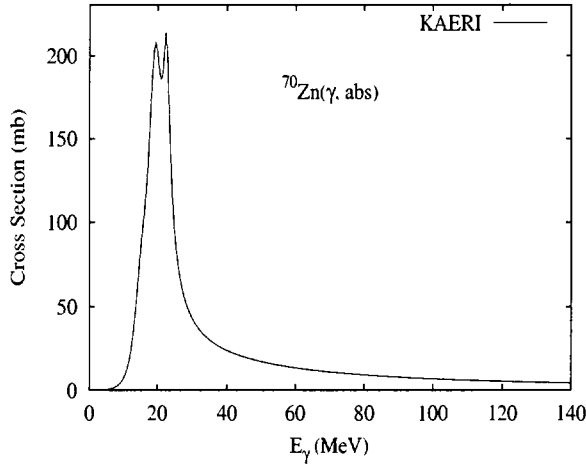
The photoabsorption cross section has not been measured. However, there are experimental data for the $(\gamma, 1n)$ reaction cross section [Gor82]. We relied on the GUNF and GNASH codes to infer the photoabsorption cross section in the GDR regime, in order to model accurately the $(\gamma, 1n)$ data. The photoabsorption cross section above the GDR, up to 140 MeV, was obtained from QD model calculations using the theory of Chadwick. The neutron, proton, deuteron, triton and alpha emission cross sections, as well as production cross sections, were calculated by the GNASH code.
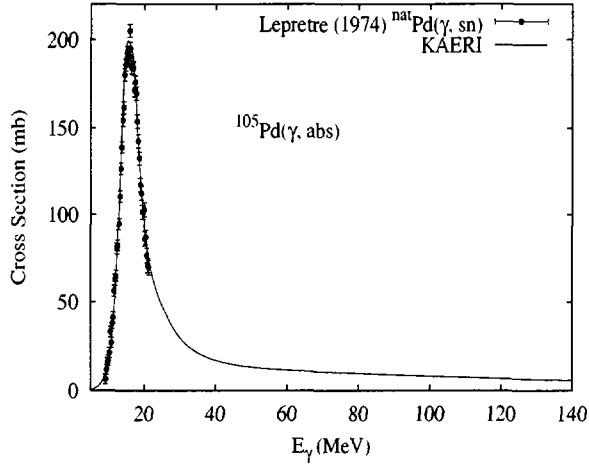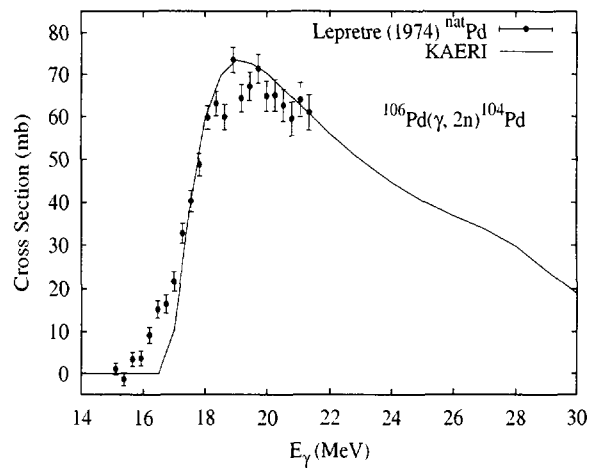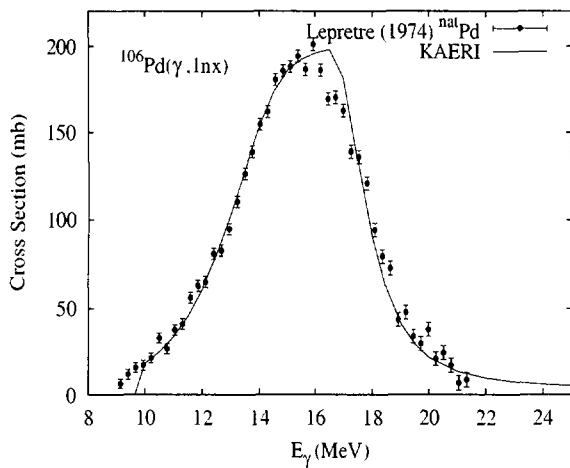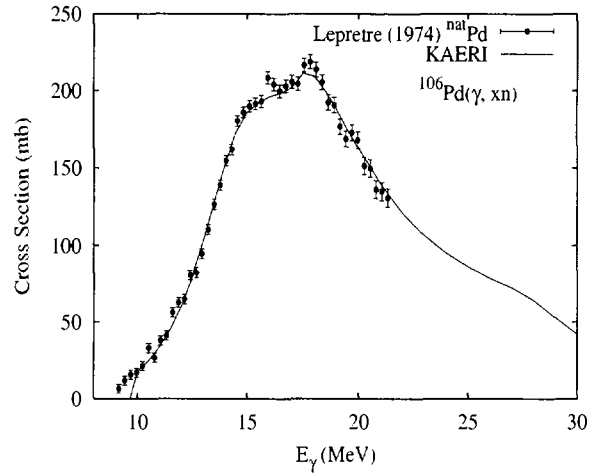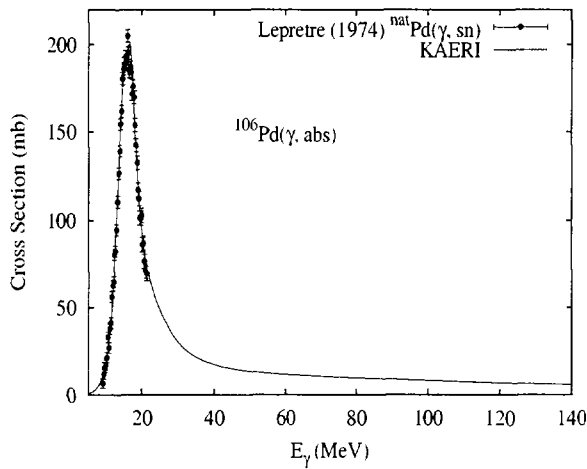
$\gamma + {}^{70}\mathbf{Ge}$

Abundance	Threshold Energies (MeV)								
(%)	γ,n	γ,p	γ,t	γ,He-3	γ,α	γ,2n	γ,np	γ,2p	γ,3n
21.23	11.54	8.53	18.63	17.61	4.09	19.73	18.84	15.13	32.12

The experimental data of absorption cross section and (γ, 1nx), (γ, 1p), (γ, np), (γ, 2nx) reaction cross sections were given by Mccarthy [Mcc75]. However, his absorption cross section has a small number of data points and a peak with large errors above 30 MeV, and his (γ, 1nx) cross section has different threshold, shape, and magnitude than the others. The experimental data of Carlos [Car76] and Goryachev [Gor82] were also given for (γ, 1nx), (γ, 2nx), (γ, sn) and (γ, xn) reaction cross sections. We relied on the GUNF and GNASH codes to infer the absorption cross section in the GDR regime, so as to model accurately the (γ, sn) reaction measured data of Carlos. The absorption cross section above the GDR, up to 140 MeV, was taken from QD model calculations.

The calculated results of the emission channels by the GNASH code are in good agreement with all the measured reaction data of Carlos and Goryachev.

$$\gamma + {}^{72}\text{Ge}$$

Abundance	Threshold Energies (MeV)								
(%)	γ,n	γ,p	γ,t	γ,He-3	γ,α	γ,2n	γ,np	γ,2p	γ,3n
27.66	10.75	9.73	18.21	19.10	5.00	18.16	19.04	17.60	29.70

The experimental data of absorption cross section and (γ, 1nx), (γ, 1p), (γ, np), (γ, 2nx) reaction cross sections were given by Mccarthy [Mcc75]. However, his absorption cross section has a small number of data points and a peak with large errors above 30 MeV, and his (γ, 1nx) cross section has different threshold, shape, and magnitude than the others. The experimental data of Carlos [Car76] and Goryachev [Gor82] were also given for (γ, 1nx), (γ, 2nx), (γ, sn) and (γ, xn) reaction cross sections. We relied on the GUNF and GNASH codes to infer the absorption cross section in the GDR regime, so as to model accurately the (γ, sn) reaction measured data. The absorption cross section above the GDR, up to 140 MeV, was taken from QD model calculations.

The calculated results of the emission channels by the GNASH code are in good agreement with the experimental data of Carlos.

$\gamma + {}^{73}\text{Ge}$

Abundance	Threshold Energies (MeV)								
(%)	γ,n	γ,p	γ,t	$\gamma,\text{He-3}$	γ,α	$\gamma,2n$	γ,np	$\gamma,2p$	$\gamma,3n$
7.73	6.78	9.99	17.34	16.67	5.30	17.53	16.52	18.55	24.95
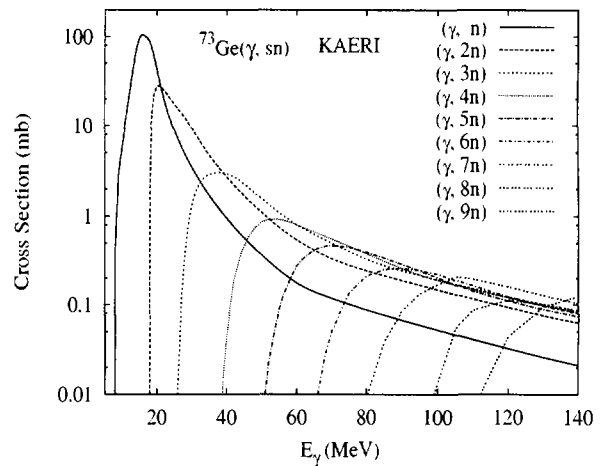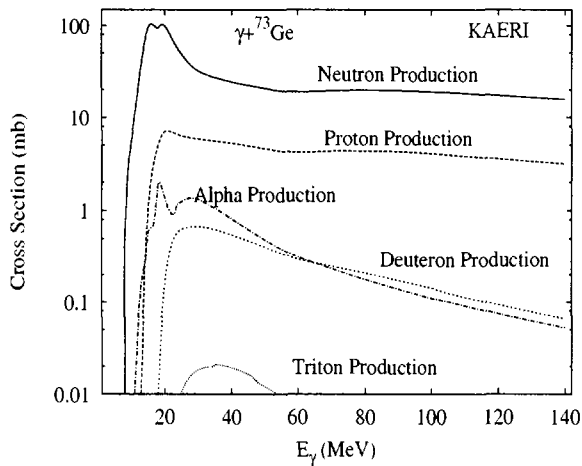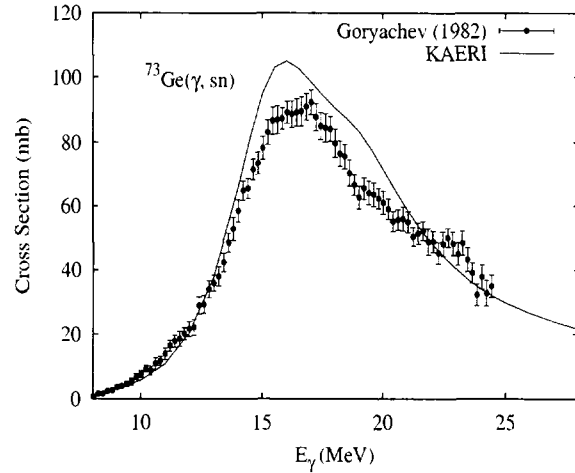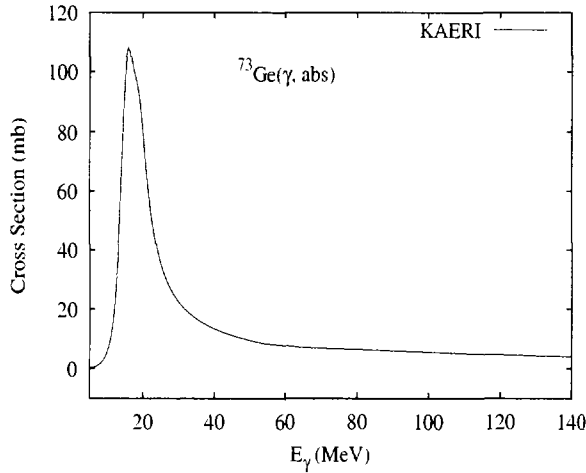
The photoabsorption cross section has not been measured. However, there are experimental data for the (γ, sn) reaction cross sections by Goryachev [Gor82]. By analyzing the Goryachev and Carlos's data for ${}^{72,74}\text{Ge}$, the cross sections for (γ, sn) reaction were scaled up to have 110 mb at 16 MeV. The GUNF and GNASH codes were used to to infer the absorption cross section in the GDR regime, so as to model accurately the reconstructed (γ, sn) reaction of Goryachev. The photoabsorption cross section above the GDR, up to 140 MeV, was obtained from QD model calculations using the theory of Chadwick.

$$\gamma + {}^{74}\text{Ge}$$

Abundance	Threshold Energies (MeV)								
(%)	γ,n	γ,p	γ,t	γ,He-3	γ,α	γ,2n	γ,np	γ,2p	γ,3n
35.94	10.20	11.01	18.23	21.03	6.29	16.98	20.19	19.87	27.73

The experimental data of absorption cross section and (γ, 1nx), (γ, 1p), (γ, np), (γ, 2nx) reaction cross sections were given by Mccarthy [Mcc75]. However, his absorption cross section has a small number of data points and a peak with large errors above 30 MeV, and his (γ, 1nx) cross section has different threshold, shape, and magnitude than the others. The experimental data of Carlos [Car76] and Goryachev [Gor82] were also given for (γ, 1nx), (γ, 2nx), (γ, sn) and (γ, xn) reaction cross sections. We relied on the GUNF and GNASH codes to infer the absorption cross section in the GDR regime, so as to model accurately the (γ, sn) reaction measured data. The absorption cross section above the GDR, up to 140 MeV, was taken from QD model calculations.

The calculated results of the emission channels by the GNASH code are in good agreement with the experimental data of Carlos and Goryachev.

$\gamma + {}^{76}\text{Ge}$

Abundance	Threshold Energies (MeV)								
(%)	γ,n	γ,p	γ,t	$\gamma,\text{He-3}$	γ,α	$\gamma,2n$	γ,np	$\gamma,2p$	$\gamma,3n$
7.44	9.43	12.04	18.46	22.74	7.51	15.93	20.52	22.08	26.13
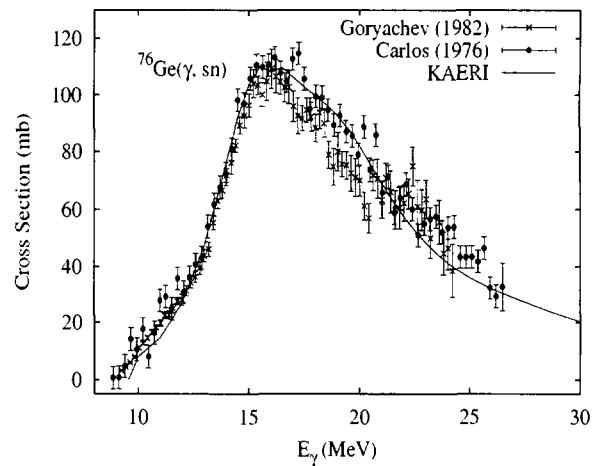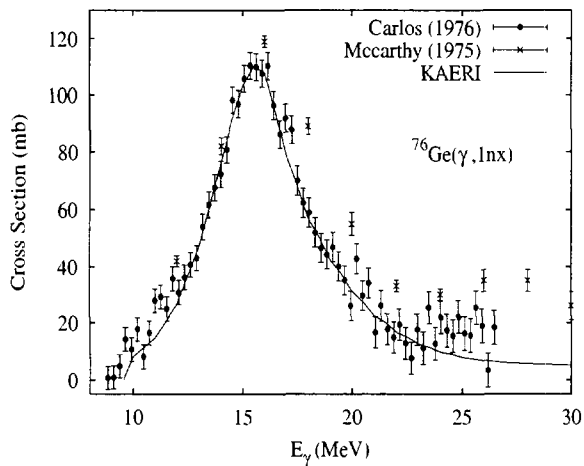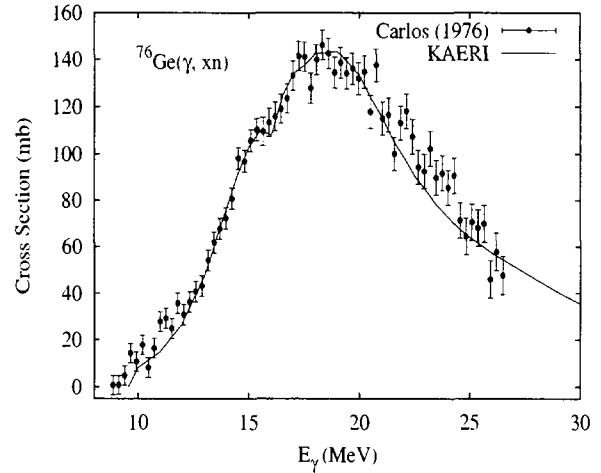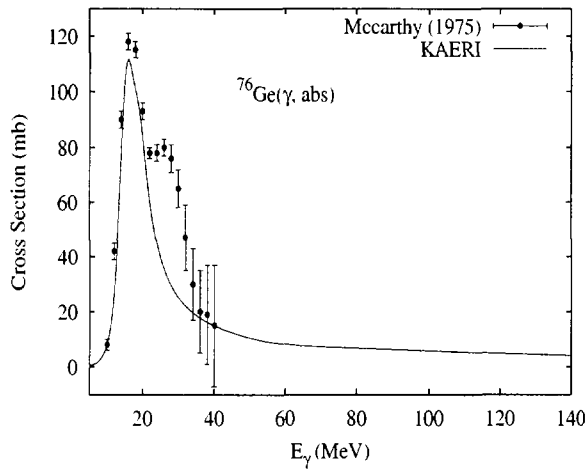
The experimental data of absorption cross section and $(\gamma, 1nx)$, $(\gamma, 1p)$, (γ, np), $(\gamma, 2nx)$ reaction cross sections were given by Mccarthy [Mcc75]. However, his absorption cross section has a small number of data points and a peak with large errors above 30 MeV, and his $(\gamma, 1nx)$ cross section has different threshold, shape, and magnitude than the others. The experimental data of Carlos [Car76] and Goryachev [Gor82] were also given for $(\gamma, 1nx)$, $(\gamma, 2nx)$, (γ, sn) and (γ, xn) reaction cross sections. We relied on the GUNF and GNASH codes to infer the absorption cross section in the GDR regime, so as to model accurately the (γ, sn) reaction measured data. The absorption cross section above the GDR, up to 140 MeV, was taken from QD model calculations.

The calculated results of the emission channels by the GNASH code are in good agreement with the experimental data of Carlos and Goryachev.

Abundance	Threshold Energies (MeV)								
(%)	γ,n	γ,p	γ,t	$\gamma,$He-3	γ,α	$\gamma,2n$	γ,np	$\gamma,2p$	$\gamma,3n$
0.56	11.93	8.88	20.13	17.88	5.17	20.79	19.80	14.63	33.39
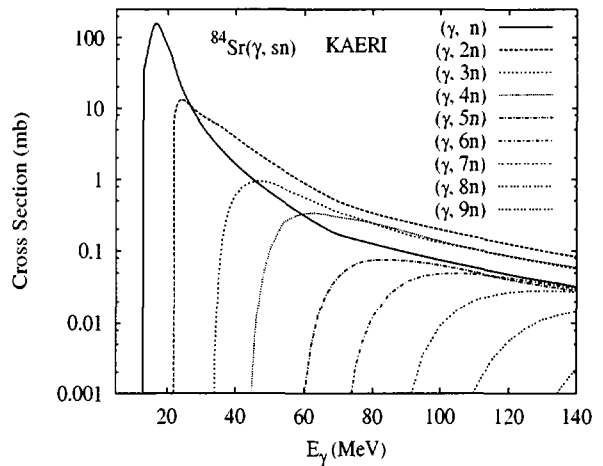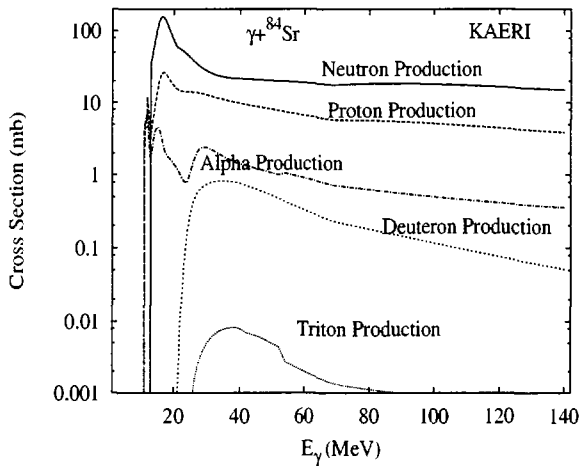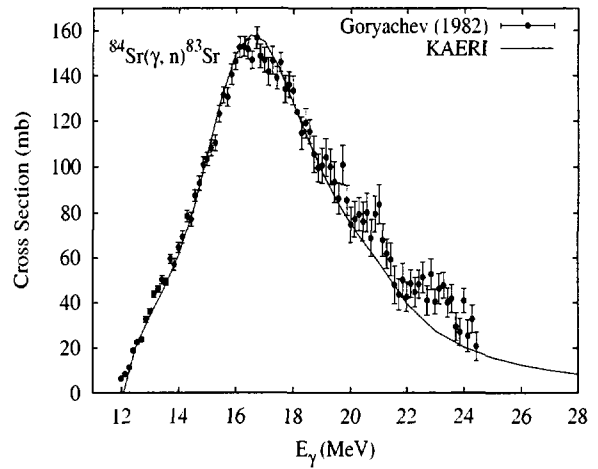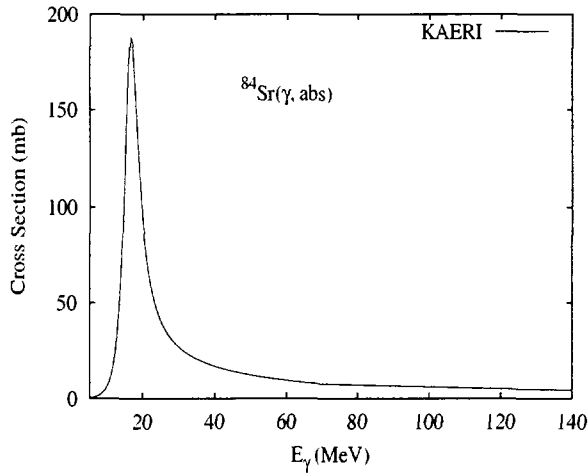
The photoabsorption cross section has not been measured. However, there are experimental data for the $(\gamma, 1n)$ reaction cross section [Gor82]. We relied on the GUNF and GNASH codes to infer the photoabsorption cross section in the GDR regime, in order to model accurately the $(\gamma, 1n)$ data. The photoabsorption cross section above the GDR, up to 140 MeV, was obtained from QD model calculations using the theory of Chadwick.

$\gamma + {}^{86}\text{Sr}$

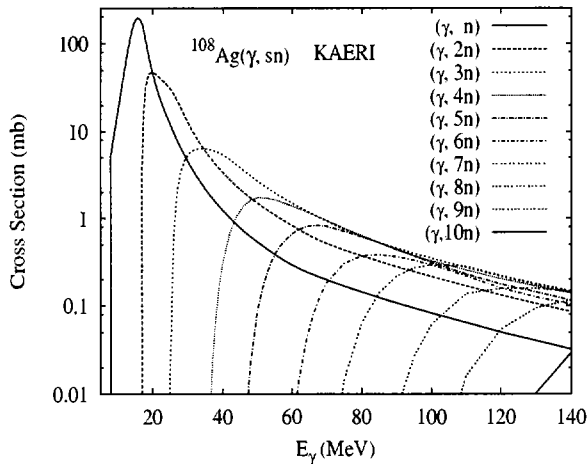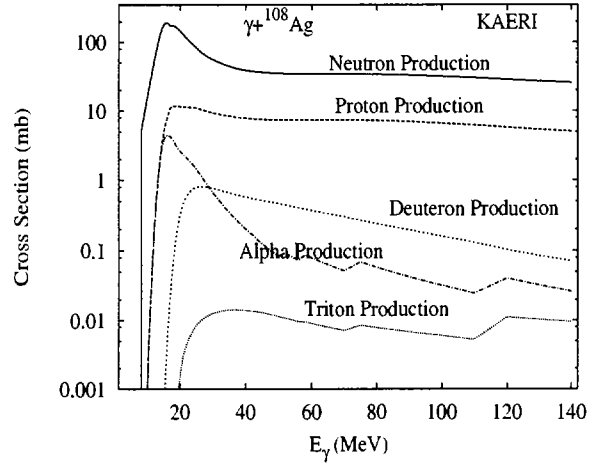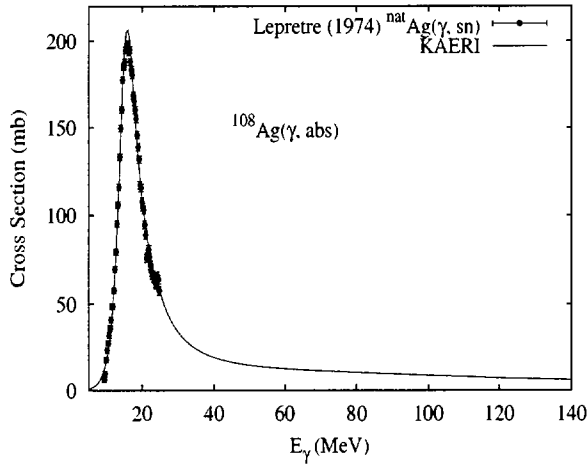| Abundance	Threshold Energies (MeV)								
(%)	γ,n	γ,p	γ,t	$\gamma,\text{He-3}$	γ,α	$\gamma,2n$	γ,np	$\gamma,2p$	$\gamma,3n$
9.86	11.49	9.64	20.42	19.47	6.35	20.02	20.13	16.67	31.95

The photoabsorption cross section has not been measured. However, there are experimental data for the $(\gamma, 1n)$ reaction cross section [Gor82]. We relied on the GUNF and GNASH codes to infer the photoabsorption cross section in the GDR regime, in order to model accurately the $(\gamma, 1n)$ data. The photoabsorption cross section above the GDR, up to 140 MeV, was obtained from QD model calculations using the theory of Chadwick.

γ + ^{87}Sr

Abundance	Threshold Energies (MeV)								
(%)	γ,n	γ,p	γ,t	γ,He-3	γ,α	γ,2n	γ,np	γ,2p	γ,3n
7.00	8.43	9.42	20.08	17.38	7.32	19.92	18.07	17.98	28.45
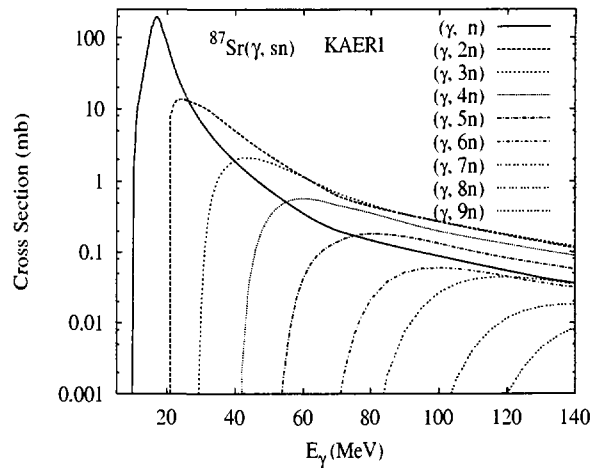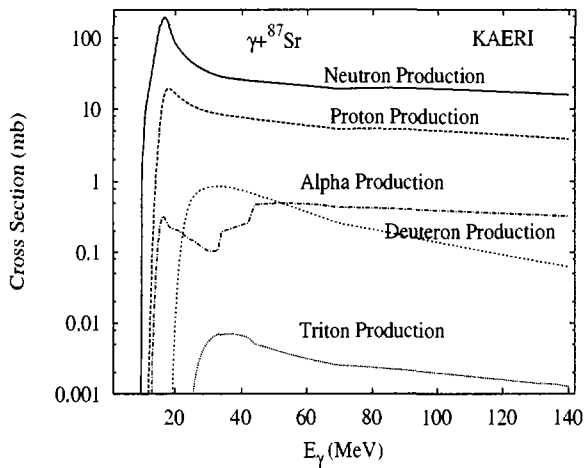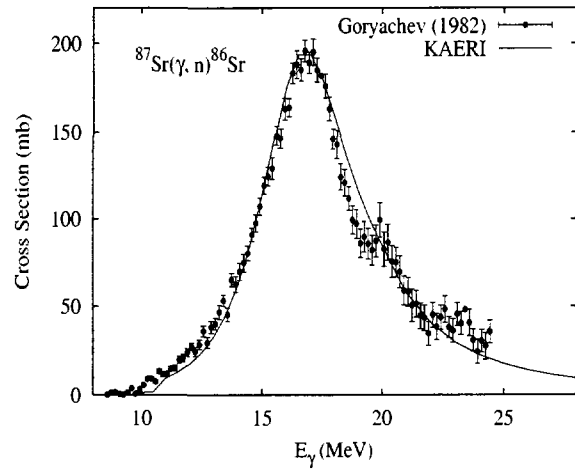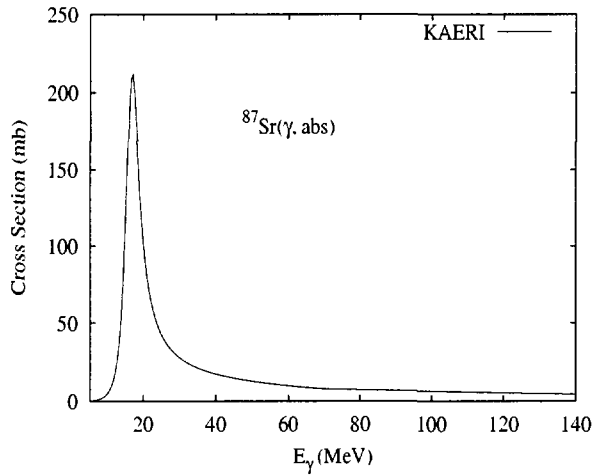
The photoabsorption cross section has not been measured. However, there are experimental data for the (γ, 1n) reaction cross section [Gor82]. We relied on the GUNF and GNASH codes to infer the photoabsorption cross section in the GDR regime, in order to model accurately the (γ, 1n) data. The photoabsorption cross section above the GDR, up to 140 MeV, was obtained from QD model calculations using the theory of Chadwick.

$\gamma + {}^{88}\text{Sr}$

Abundance (%)	Threshold Energies (MeV)								
	γ,n	γ,p	γ,t	γ,He-3	γ,α	γ,2n	γ,np	γ,2p	γ,3n
82.58	11.11	10.61	20.70	21.37	7.91	19.54	20.53	19.23	31.03
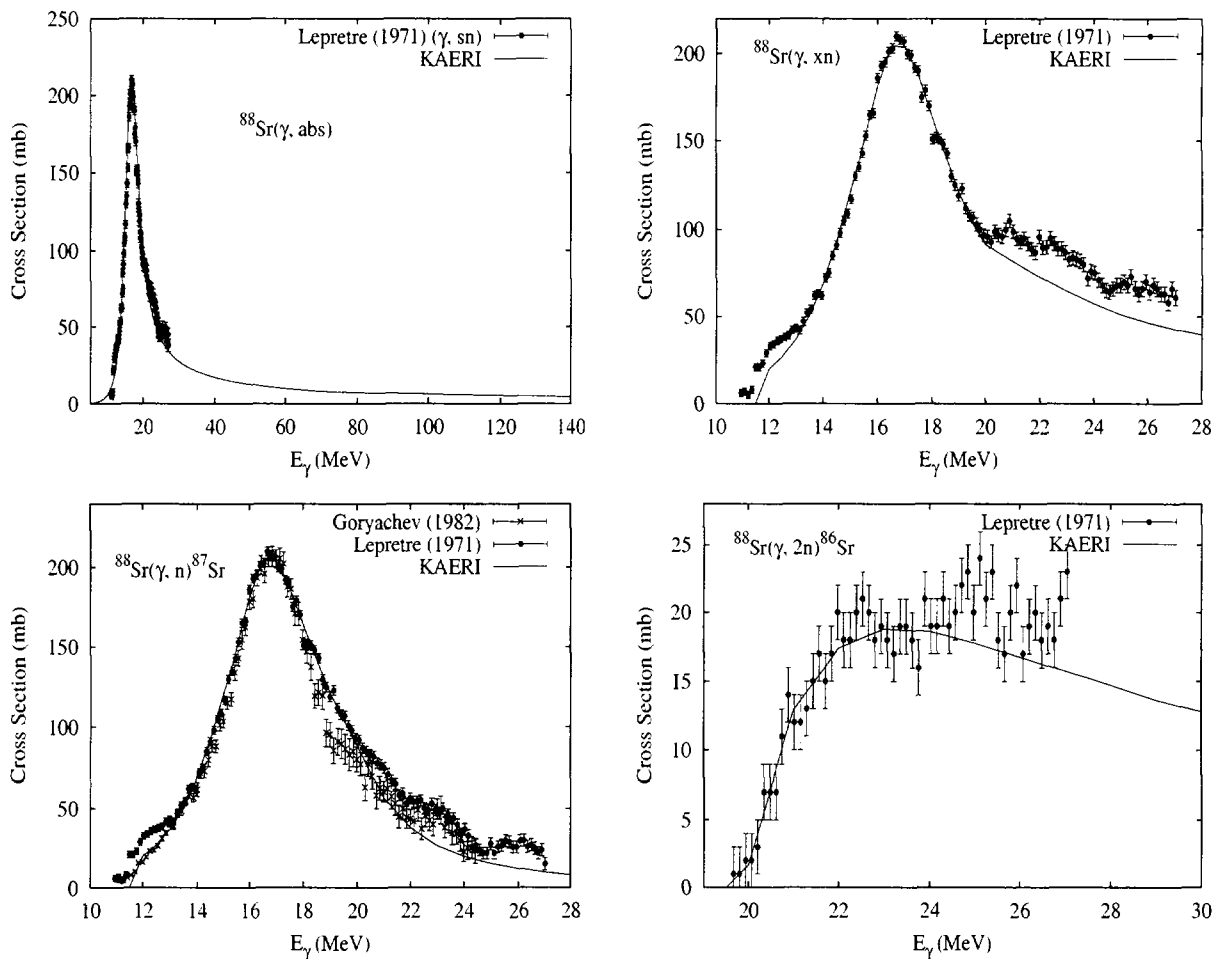
The photoabsorption cross section has not been measured. However, for ${}^{nat}\text{Sr}$, there are experimental data for the (γ, 1nx), (γ, 2nx), (γ, sn) and (γ, xn) reaction cross sections [Lep71]. Experimental data were also reported [Gor82] for the (γ, 1n) cross section of ${}^{88}\text{Sr}$. We relied on the GUNF and GNASH codes to infer the photoabsorption cross section in the GDR regime, in order to model accurately Lepretre's (γ, sn) data. The photoabsorption cross section above the GDR, up to 140 MeV, was obtained from QD model calculations using the theory of Chadwick.

The calculated results of the emission channels by the GNASH code are in good agreement with the experimental data.
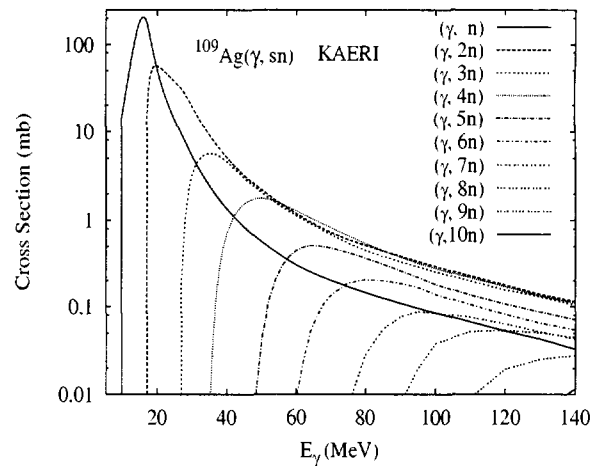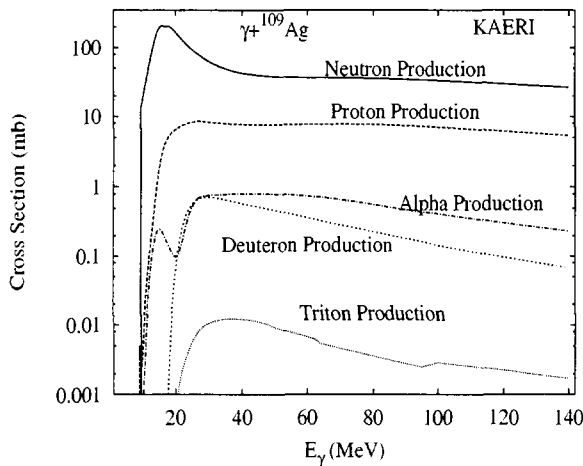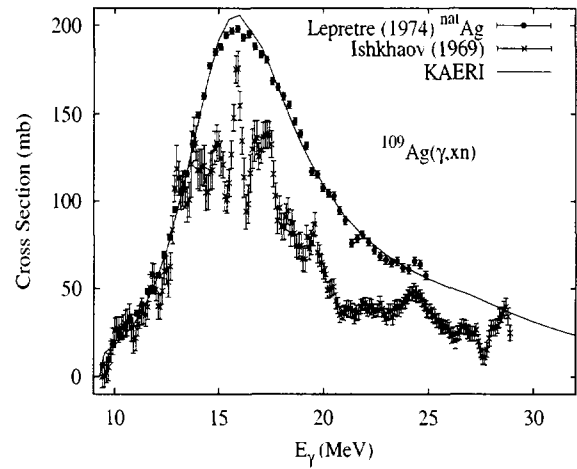
170

$\gamma + {}^{90}\text{Sr}$

Abundance	Threshold Energies (MeV)								
(%)	γ,n	γ,p	γ,t	$\gamma,\text{He-3}$	γ,α	$\gamma,2\text{n}$	γ,np	$\gamma,2\text{p}$	$\gamma,3\text{n}$
0.00	7.80	11.52	16.30	20.17	5.11	14.17	18.70	20.83	25.28
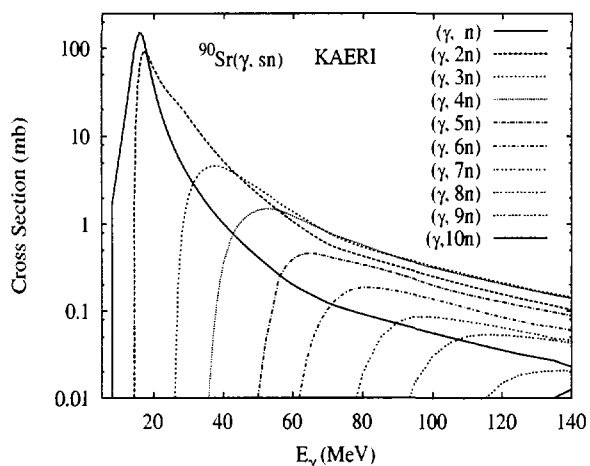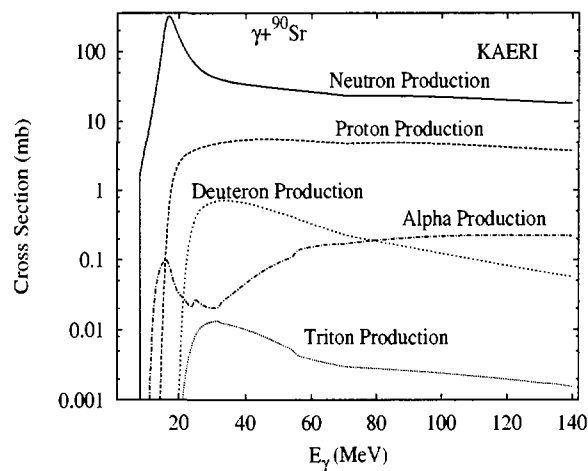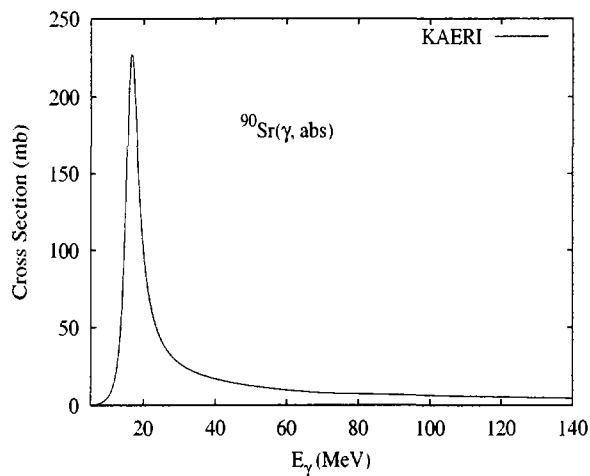
There are no experimental data available. The photoabsorption cross section was obtained from GDR and QD model calculations, adopting the GDR parameters of ${}^{88}\text{Sr}$. The neutron, proton, deuteron, triton and alpha emission cross sections, as well as production cross sections, were calculated by the GNASH code.

γ + ^{90}Zr

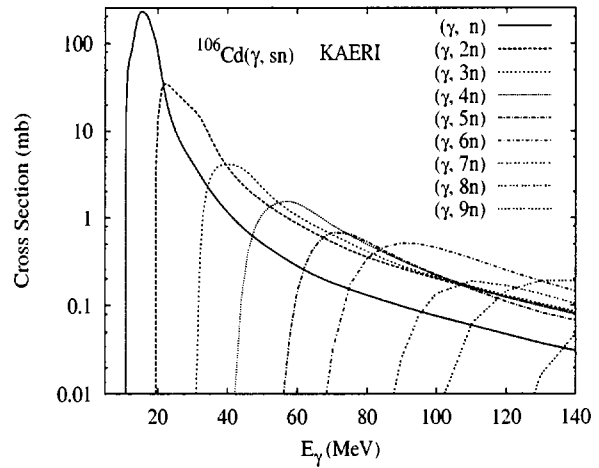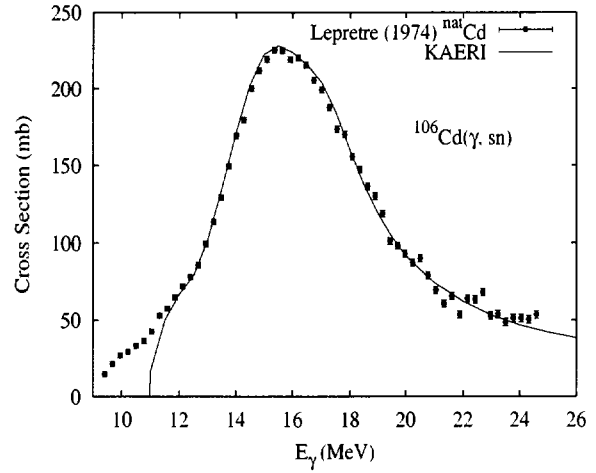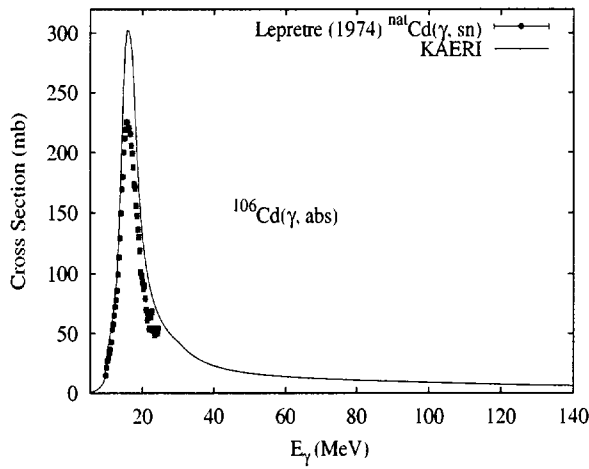| Abundance (%)	Threshold Energies (MeV)								
	γ,n	γ,p	γ,t	γ,He-3	γ,α	γ,2n	γ,np	γ,2p	γ,3n
51.45	11.97	8.36	20.71	18.83	6.68	21.29	19.84	15.43	33.64
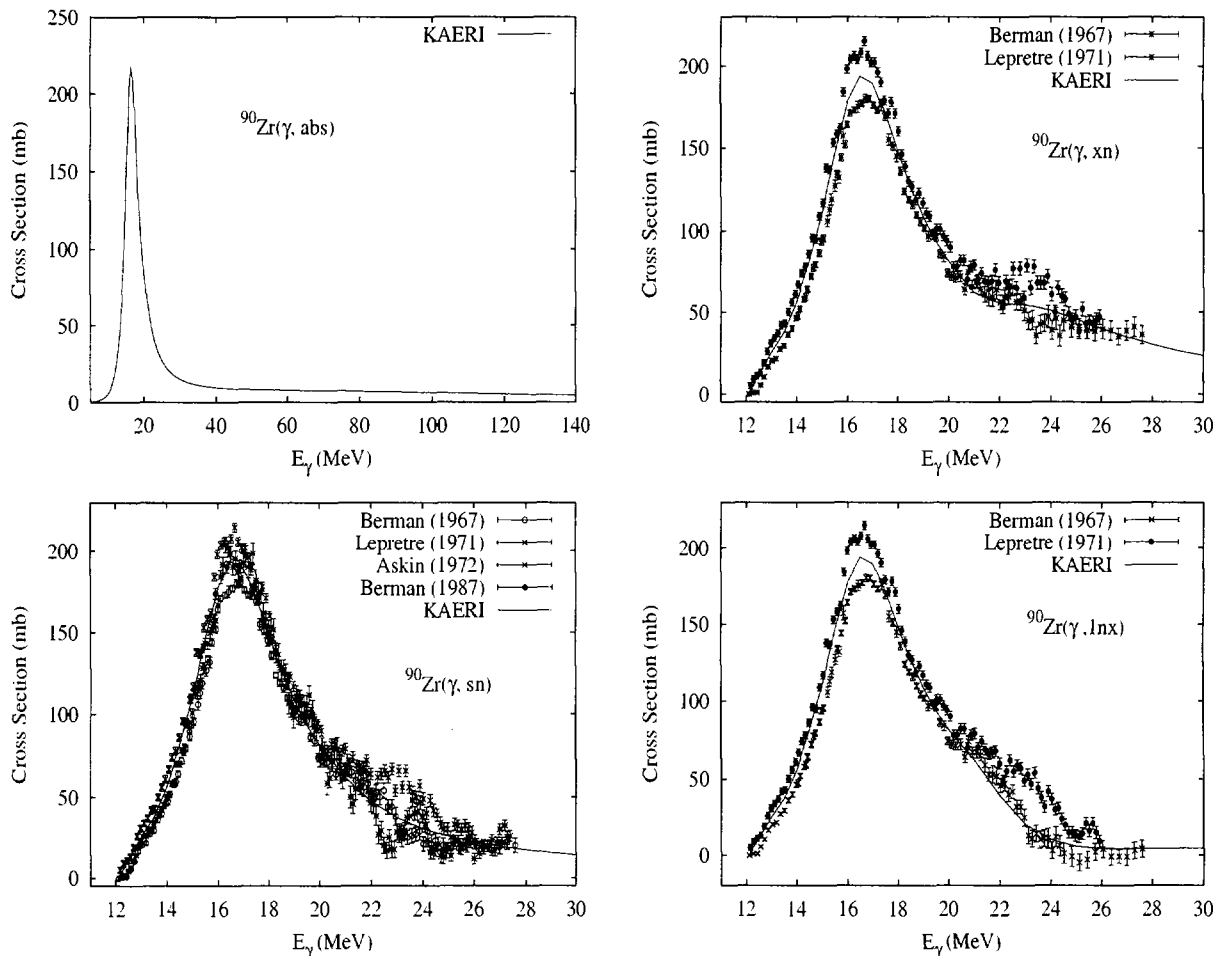
The photoabsorption cross section has not been measured. However, there are experimental data for (γ, 1nx), (γ, 2nx), (γ, sn) and (γ, xn) reaction cross sections by Berman [Ber67] and Lepretre [Lep71], and for (γ, sn) by Ashkin [Ask72]. Lepretre's data is different from Berman's and Askin's data in the magnitudes. Berman [Ber87] remeasured the (γ, sn) reaction cross section near the peak of the giant dipole resonance for natural Zr in 1987. We relied on the GUNF and GNASH codes to infer the photoabsorption cross section in the GDR regime, in order to model accurately the (γ, sn) data of Berman measured in 1987. The photoabsorption cross section above the GDR, up to 140 MeV, was obtained from QD model calculations using the theory of Chadwick. The calculated results of the emission channels by the GNASH code are in overall agreement with the experimental data of (γ, 1nx), (γ, 2nx) and (γ, xn) reaction cross sections.

$\gamma + {}^{91}\text{Zr}$

Abundance (%)	Threshold Energies (MeV)								
	γ,n	γ,p	γ,t	$\gamma,\text{He-3}$	γ,α	$\gamma,2n$	γ,np	$\gamma,2p$	$\gamma,3n$
11.22	7.19	8.69	18.55	14.91	5.44	19.17	15.55	16.26	28.48
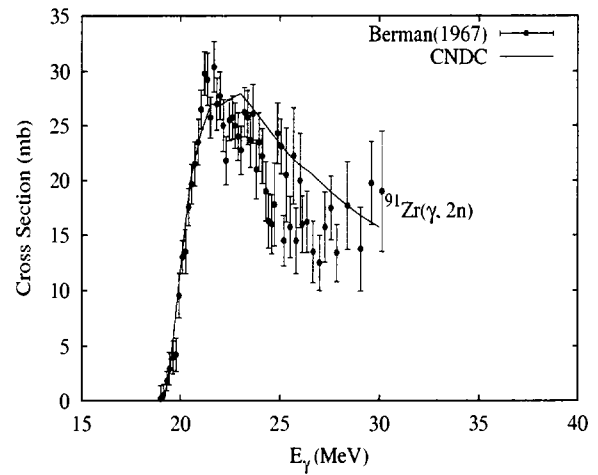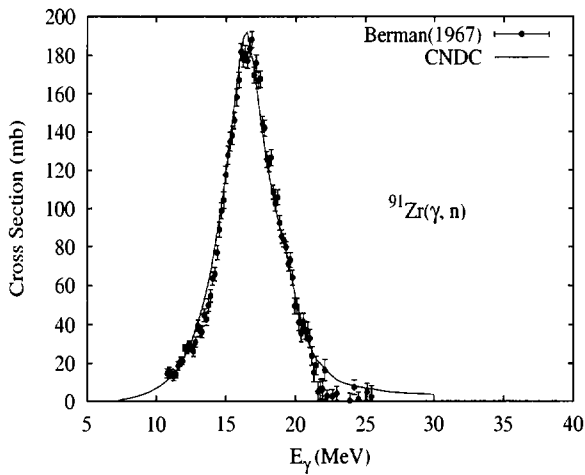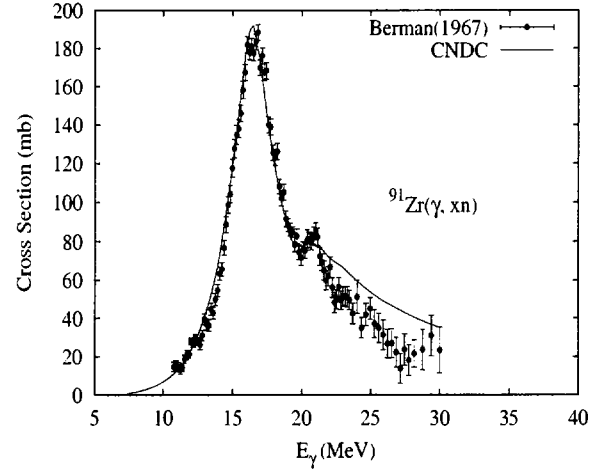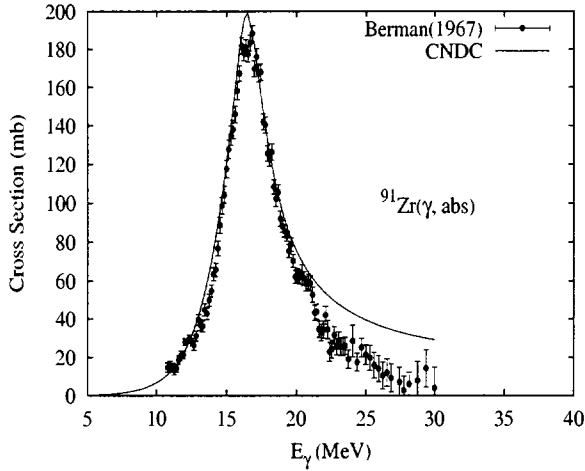
The photoabsorption cross section has not been measured. However, there are experimental data for the $(\gamma, 1nx)$, $(\gamma, 2nx)$ and (γ, xn) reaction cross sections [Ber67]. We relied on GUNF code [Zha98] to infer the photoabsorption cross section in the GDR regime, in order to model accurately the available experimental data.

$$\gamma + {}^{92}\text{Zr}$$

Abundance	Threshold Energies (MeV)								
(%)	γ,n	γ,p	γ,t	$\gamma,\text{He-3}$	γ,α	$\gamma,2n$	γ,np	$\gamma,2p$	$\gamma,3n$
17.15	8.64	9.40	15.70	17.18	2.97	15.83	17.33	17.09	27.80

The photoabsorption cross section has not been measured. However, there are experimental data for the $(\gamma, 1nx)$, $(\gamma, 2nx)$ and (γ, xn) reaction cross sections [Ber67]. We relied on GUNF code [Zha98] to infer the photoabsorption cross section in the GDR regime, in order to model accurately the available experimental data.

174

$\gamma + {}^{93}\text{Zr}$

Abundance	Threshold Energies (MeV)								
(%)	γ,n	γ,p	γ,t	γ,He-3	γ,α	γ,2n	γ,np	γ,2p	γ,3n
0.00	6.73	9.58	15.58	16.11	3.33	15.37	16.13	18.05	22.56

There are no experimental data available. The photoabsorption cross section was obtained from GDR and QD model calculations, adopting the GDR parameters of ^{94}Zr. The neutron, proton, deuteron, triton and alpha emission cross sections, as well as production cross sections, were calculated by the GNASH code.
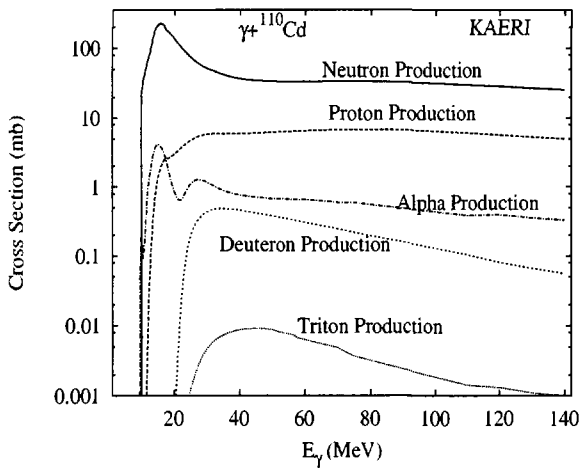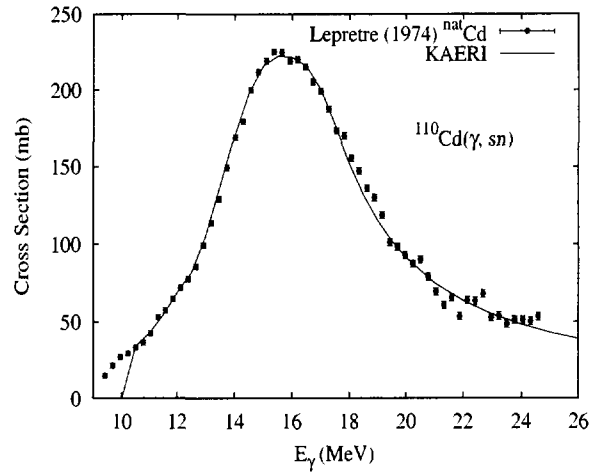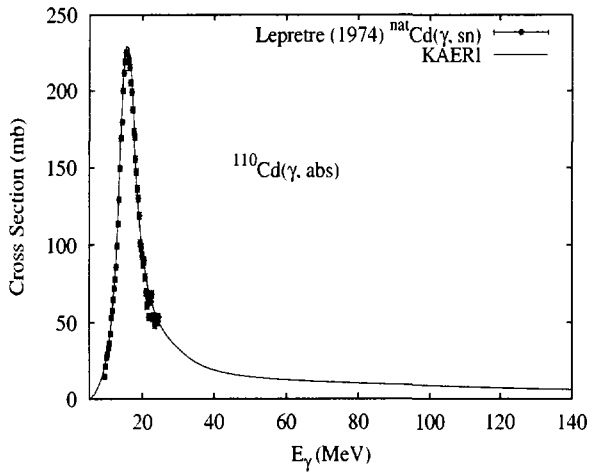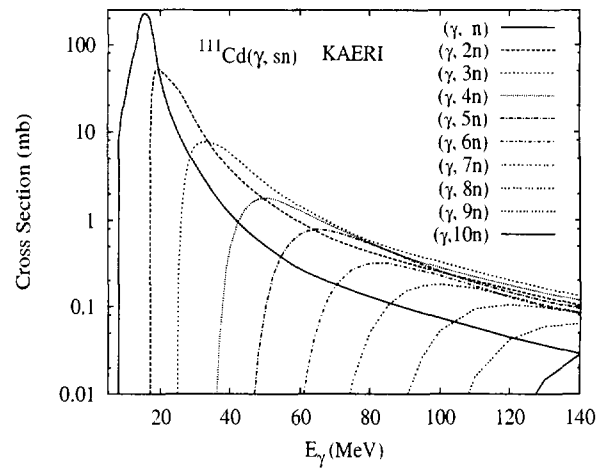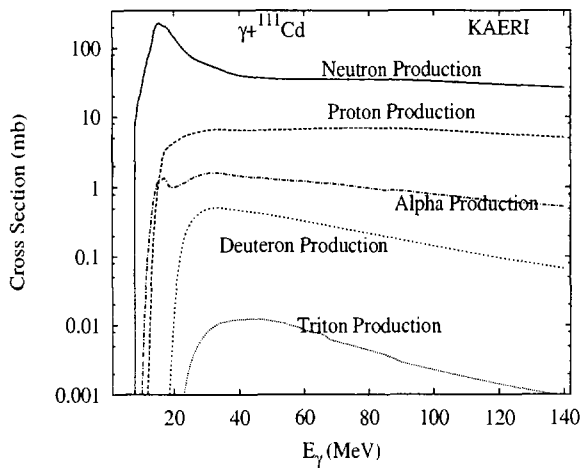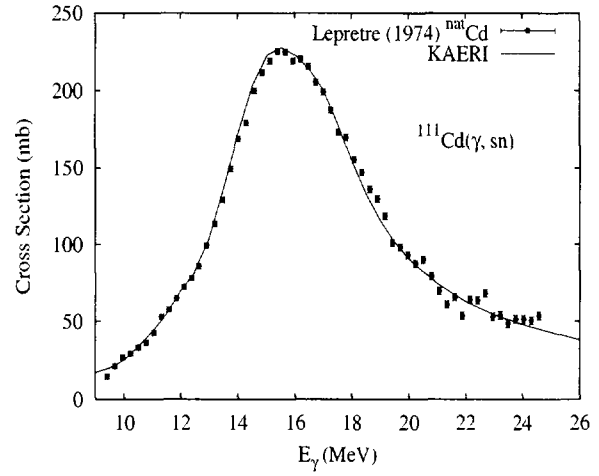
$\gamma + {}^{94}\mathrm{Zr}$

Abundance (%)	Threshold Energies (MeV)								
	$\gamma,$n	$\gamma,$p	$\gamma,$t	$\gamma,$He-3	γ,α	$\gamma,$2n	$\gamma,$np	$\gamma,$2p	$\gamma,$3n
17.38	8.22	10.31	15.87	18.55	3.75	14.95	17.80	18.92	23.59

The photoabsorption cross section has not been measured. However, there are experimental data for the (γ, 1nx), (γ, 2nx), (γ, sn), and (γ, xn) reaction cross sections [Ber67]. We relied on the GUNF and GNASH codes to infer the photoabsorption cross section in the GDR regime, in order to model accurately the (γ, sn) data. The photoabsorption cross section above the GDR, up to 140 MeV, was obtained from QD model calculations using the theory of Chadwick.

The calculated results of the emission channels by the GNASH code are in good agreement with the experimental data for (γ, 1nx), (γ, 2nx) and (γ, xn) reaction cross sections.

176

$\gamma + {}^{96}\text{Zr}$

Abundance (%)	Threshold Energies (MeV)								
	γ,n	γ,p	γ,t	$\gamma,\text{He-3}$	γ,α	$\gamma,2n$	γ,np	$\gamma,2p$	$\gamma,3n$
2.80	7.85	11.52	16.15	20.21	4.94	14.32	18.45	21.18	22.54
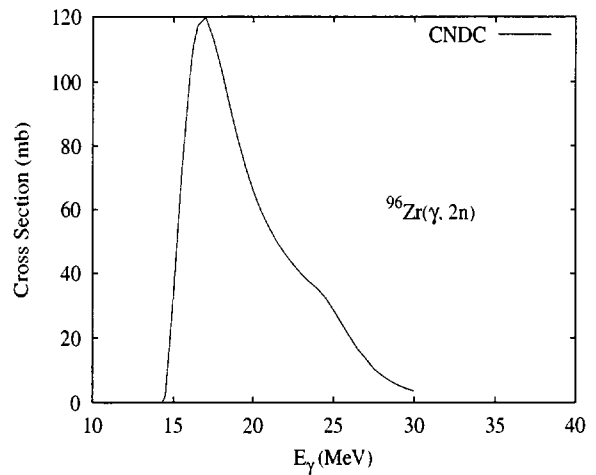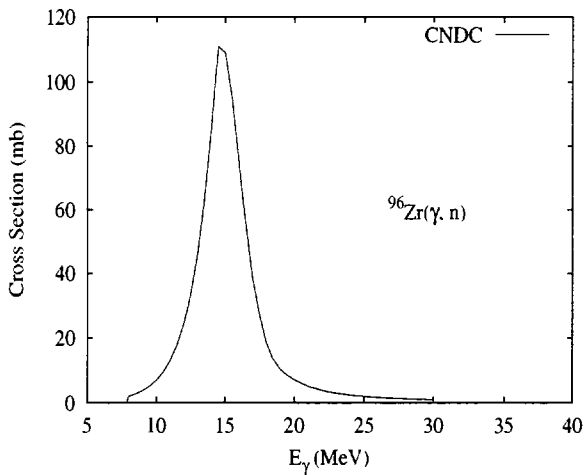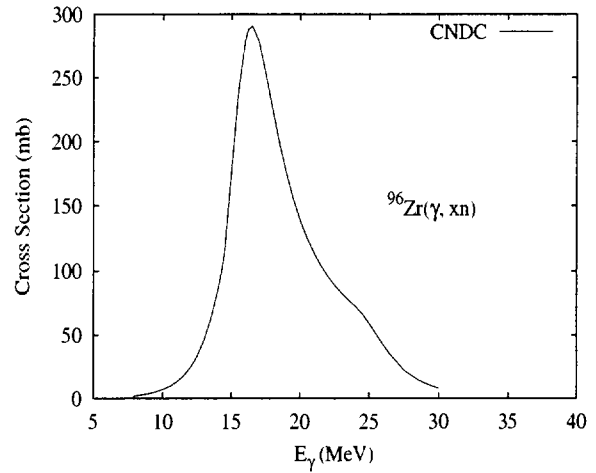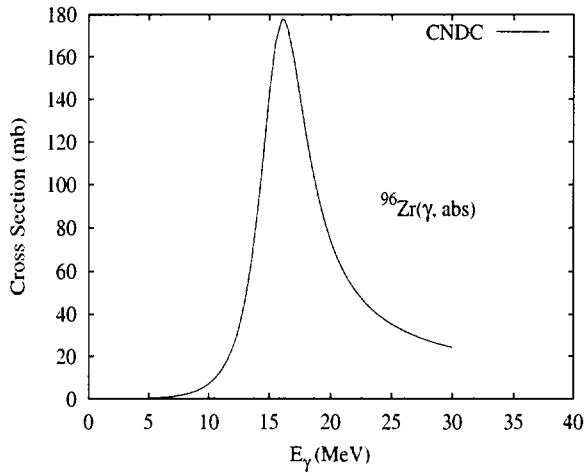
There are no experimental data available. The photoabsorption cross section was obtained from GDR model calculations using the GUNF code [Zha98], adopting the same model parameters as for the $\gamma +$ ${}^{90,91,92,94}\text{Zr}$ reactions.

γ + ^{93}Nb

Abundance (%)	Threshold Energies (MeV)								
	γ,n	γ,p	γ,t	γ,He-3	γ,α	γ,2n	γ,np	γ,2p	γ,3n
100.00	8.83	6.04	13.39	15.65	1.93	16.71	14.68	15.44	28.77
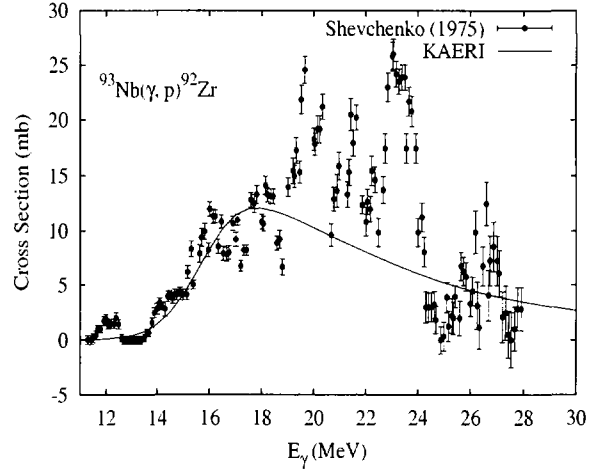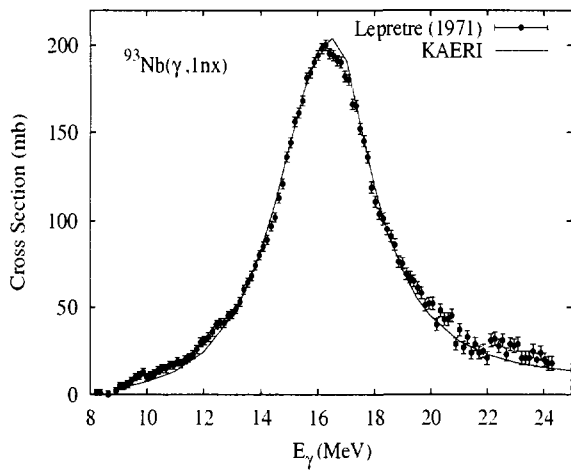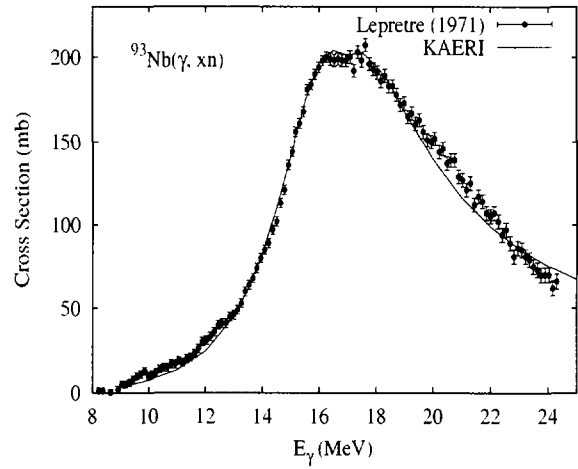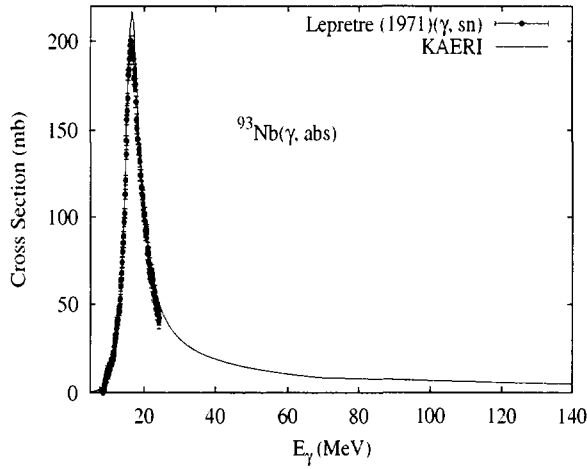
The photoabsorption cross section has not been measured. However, there are experimental data for the (γ, 1nx), (γ, 2nx), (γ, sn) and (γ, xn) reaction cross sections by Lepretre [Lep71], and (γ, 1p) reaction cross section by Shevchenko [She75]. We relied on the GUNF and GNASH codes to infer the photoabsorption cross section in the GDR regime, in order to model accurately the (γ, sn) data. The photoabsorption cross section above the GDR, up to 140 MeV, was obtained from QD model calculations using the theory of Chadwick.

The calculated results of the emission channels by the GNASH code are in good agreement with the experimental data for (γ, 1nx) and (γ, xn) reaction cross sections. For the (γ, 1p) reaction cross section, the calculated results are in good agreement with the experimental data below 18 MeV, but are lower than the experiment above that. A possible explanation is that the experiment may include the (γ, np) channel.

$\gamma + {}^{94}\text{Nb}$

Abundance	Threshold Energies (MeV)								
(%)	γ,n	γ,p	γ,t	$\gamma,\text{He-3}$	γ,α	$\gamma,2n$	γ,np	$\gamma,2p$	$\gamma,3n$
0.00	7.23	6.54	13.42	14.95	2.30	16.06	13.27	16.11	23.94
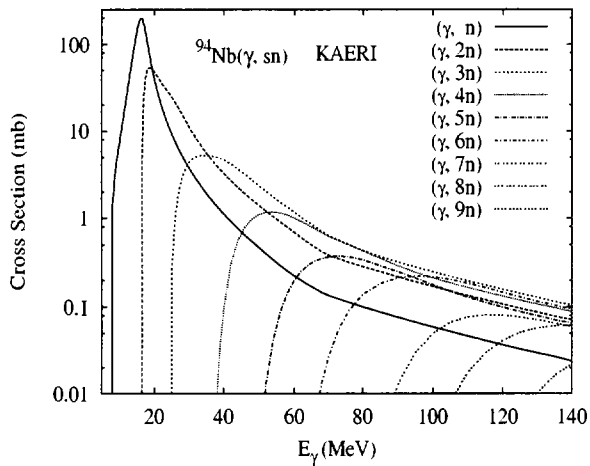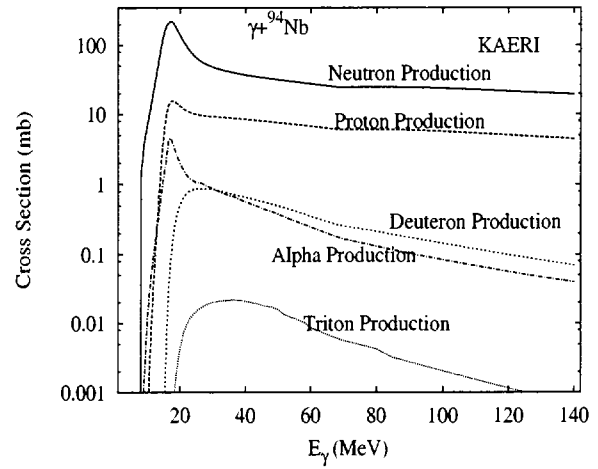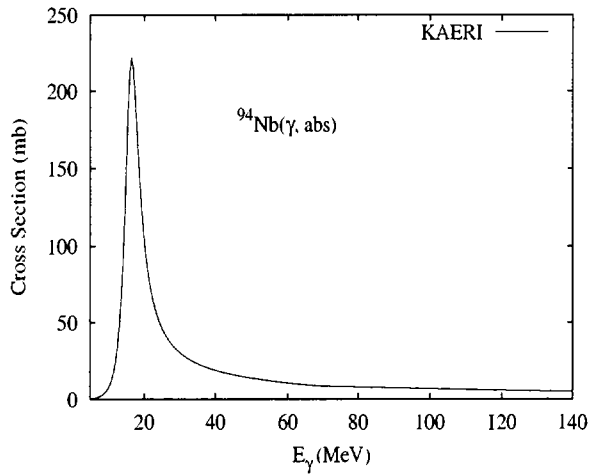
There are no experimental data available. The photoabsorption cross section was obtained from GDR and QD model calculations, adopting the GDR parameters of ${}^{93}\text{Nb}$. The neutron, proton, deuteron, triton and alpha emission cross sections, as well as production cross sections, were calculated by the GNASH code.

γ + ^{92}Mo

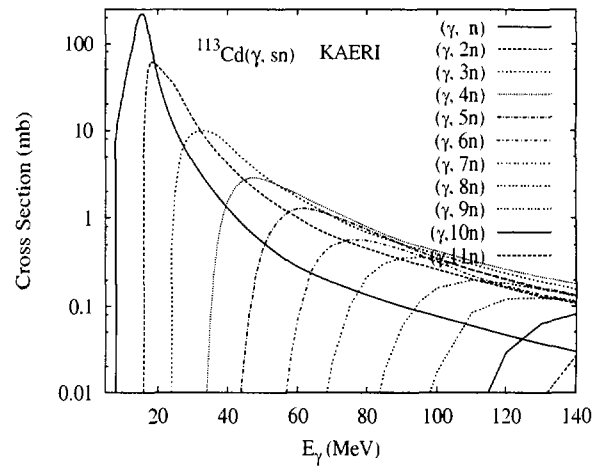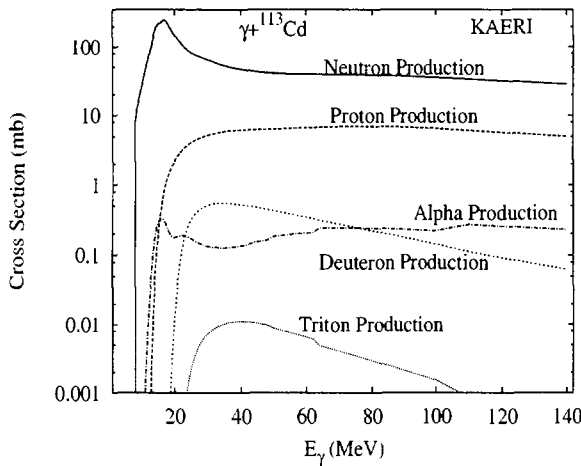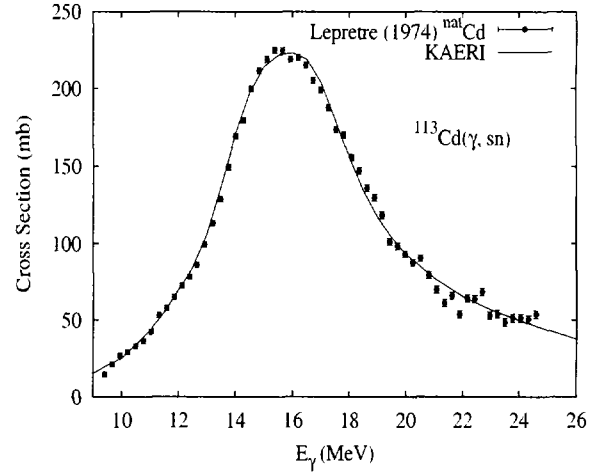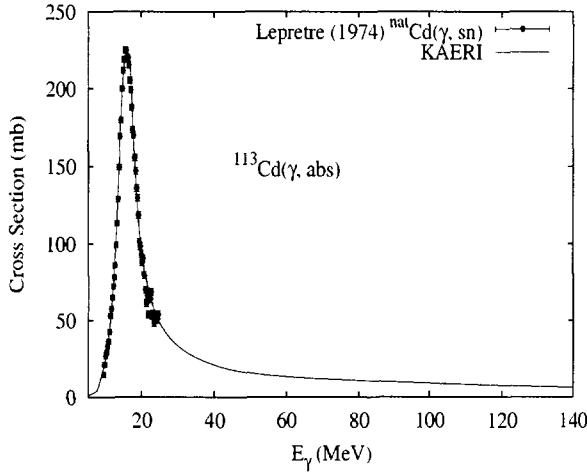| Abundance (%)	Threshold Energies (MeV)								
	γ,n	γ,p	γ,t	γ,He-3	γ,α	γ,2n	γ,np	γ,2p	γ,3n
14.84	12.67	7.46	21.18	16.87	5.61	22.78	19.51	12.62	36.02
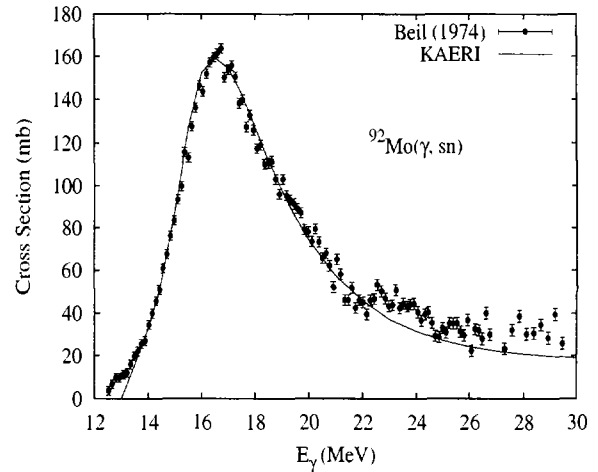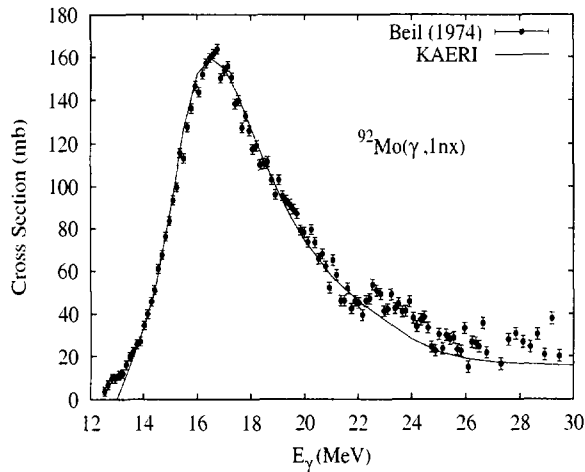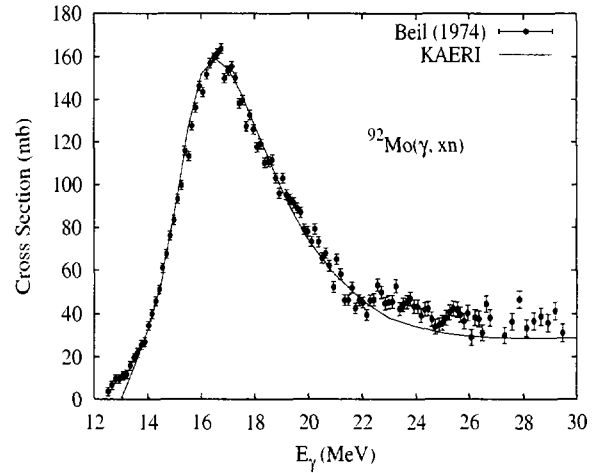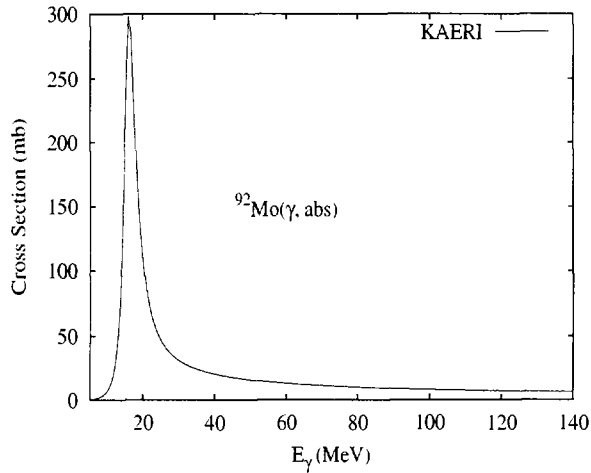
The photoabsorption cross section has not been measured. However, there are experimental data for the (γ, 1nx), (γ, 2nx), (γ, sn), and (γ, xn) reaction cross sections [Bei74]. We relied on the GUNF and GNASH codes to infer the photoabsorption cross section in the GDR regime, in order to model accurately the (γ, sn) data. The photoabsorption cross section above the GDR, up to 140 MeV, was obtained from QD model calculations using the theory of Chadwick.

The calculated results of the emission channels by the GNASH code are in good agreement with the experimental data.

$\gamma + {}^{94}\text{Mo}$

Abundance	Threshold Energies (MeV)								
(%)	γ,n	γ,p	γ,t	$\gamma,\text{He-3}$	γ,α	$\gamma,\text{2n}$	γ,np	$\gamma,\text{2p}$	$\gamma,\text{3n}$
9.25	9.68	8.49	16.72	15.45	2.07	17.75	17.32	14.53	30.42
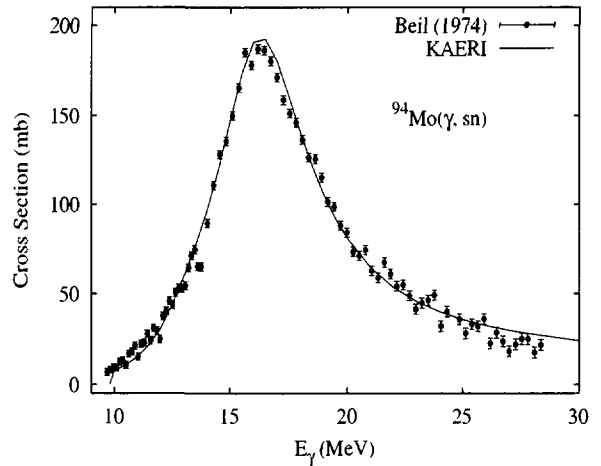
The photoabsorption cross section has not been measured. However, there are experimental data for the (γ, 1nx), (γ, 2nx), (γ, sn), and (γ, xn) reaction cross sections [Bei74]. We relied on the GUNF and GNASH codes to infer the photoabsorption cross section in the GDR regime, in order to model accurately the (γ, sn) data. The photoabsorption cross section above the GDR, up to 140 MeV, was obtained from QD model calculations using the theory of Chadwick.

The calculated results of the emission channels by the GNASH code are in good agreement with the experimental data.

$\gamma + {}^{95}\text{Mo}$

Abundance	Threshold Energies (MeV)								
(%)	γ,n	γ,p	γ,t	$\gamma,\text{He-3}$	γ,α	$\gamma,2n$	γ,np	$\gamma,2p$	$\gamma,3n$
15.92	7.37	8.63	16.21	14.18	2.24	17.05	15.86	15.17	25.11
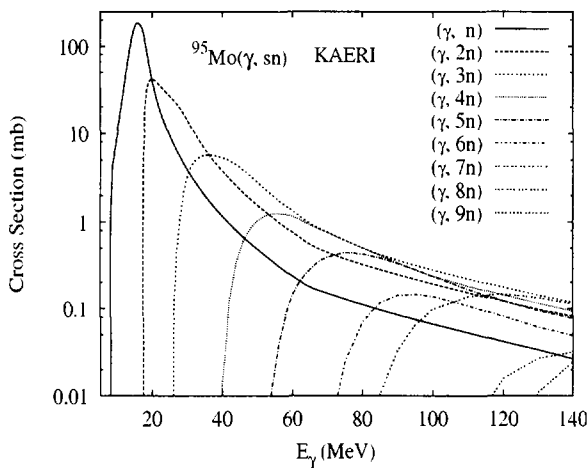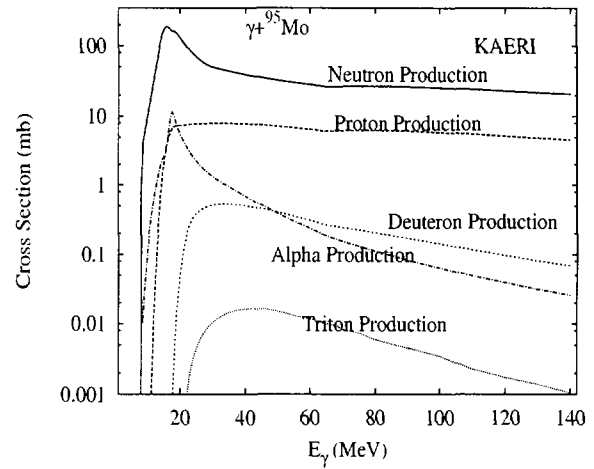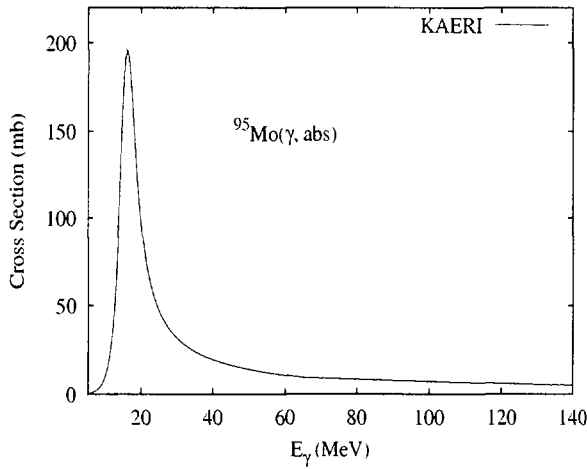
There are no experimental data available. The photoabsorption cross section was obtained from GDR and QD model calculations, adopting the GDR parameters of ${}^{96}\text{Mo}$. The neutron, proton, deuteron, triton and alpha emission cross sections, as well as production cross sections, were calculated by the GNASH code.
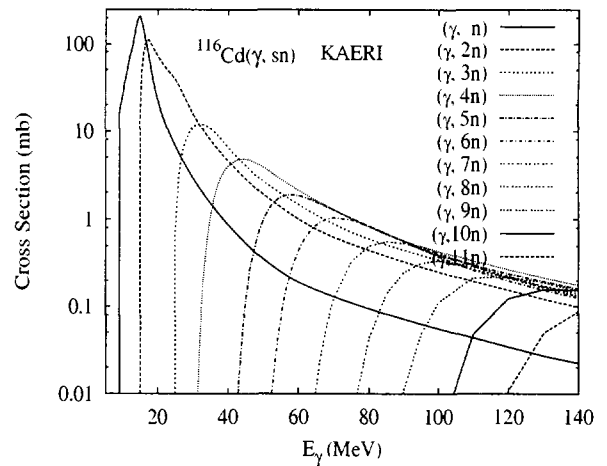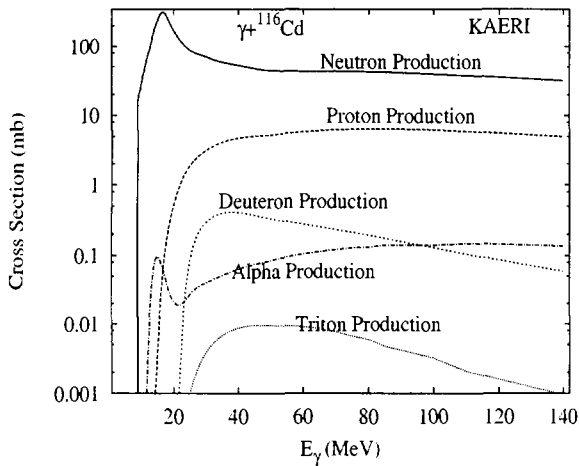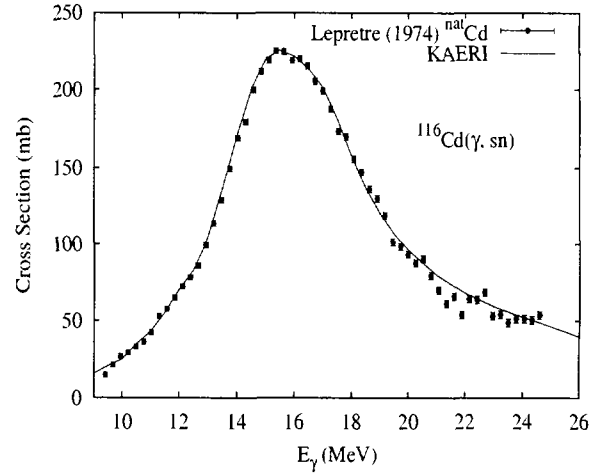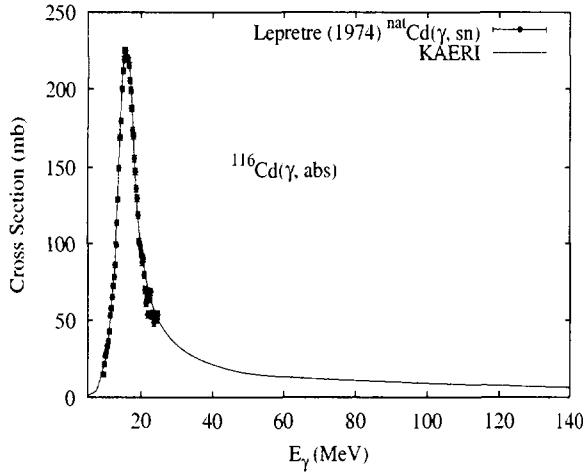
$\gamma + {}^{96}\text{Mo}$

Abundance	Threshold Energies (MeV)								
(%)	γ,n	γ,p	γ,t	$\gamma,\text{He-3}$	γ,α	$\gamma,2n$	γ,np	$\gamma,2p$	$\gamma,3n$
16.68	9.15	9.30	16.53	16.60	2.76	16.52	17.78	16.10	26.20
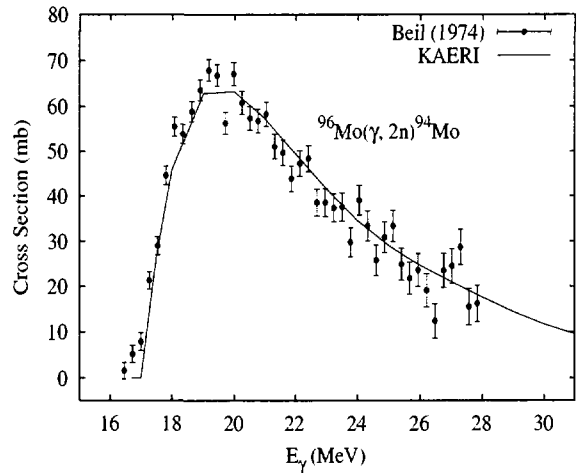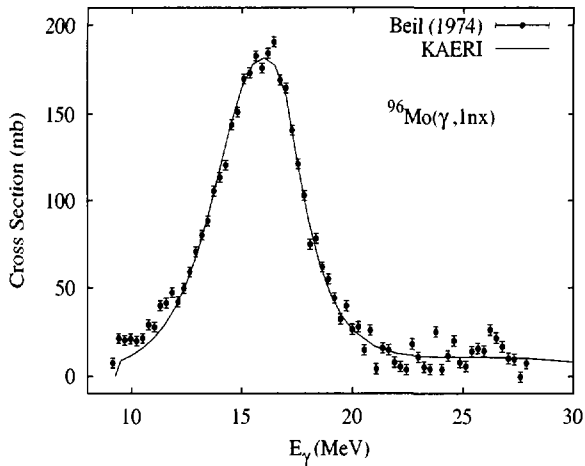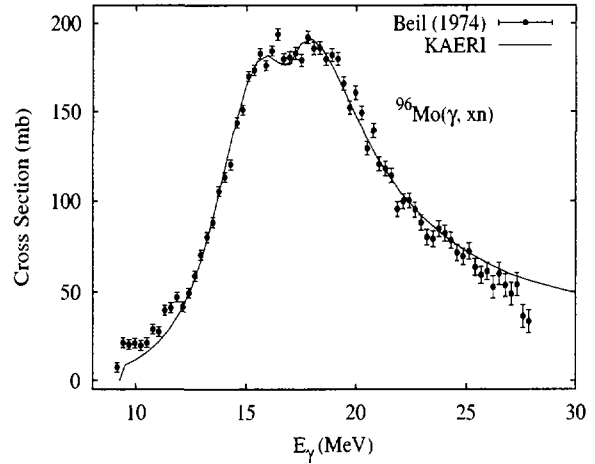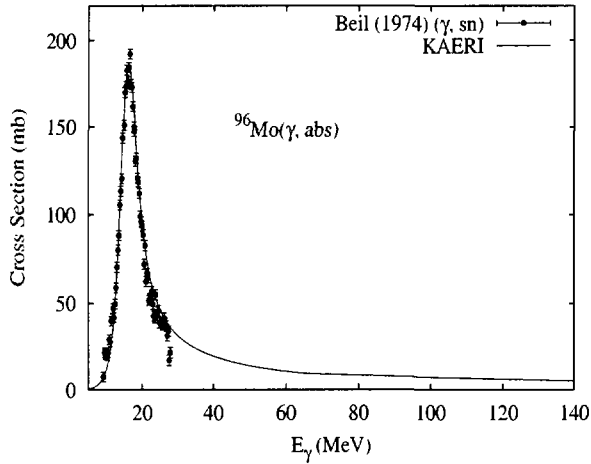
The photoabsorption cross section has not been measured. However, there are experimental data for the $(\gamma, 1nx)$, $(\gamma, 2nx)$, (γ, sn), and (γ, xn) reaction cross sections [Bei74]. We relied on the GUNF and GNASH codes to infer the photoabsorption cross section in the GDR regime, in order to model accurately the (γ, sn) data. The photoabsorption cross section above the GDR, up to 140 MeV, was obtained from QD model calculations using the theory of Chadwick.

The calculated results of the emission channels by the GNASH code are in good agreement with the experimental data.

$\gamma + {}^{97}\text{Mo}$

Abundance (%)	Threshold Energies (MeV)								
	γ,n	γ,p	γ,t	$\gamma,$He-3	γ,α	$\gamma,2n$	γ,np	$\gamma,2p$	$\gamma,3n$
9.55	6.82	9.23	16.12	15.21	2.85	15.98	16.12	16.46	23.34
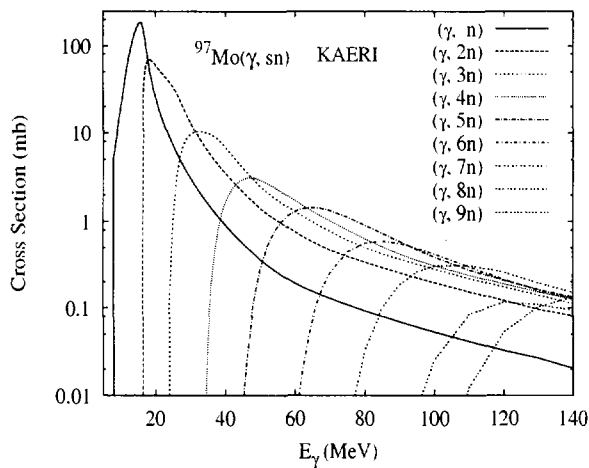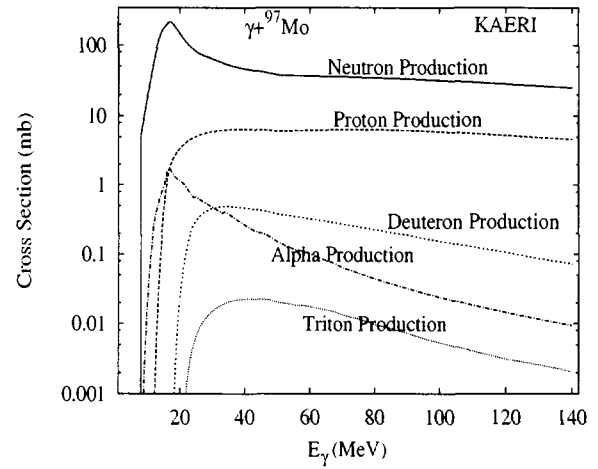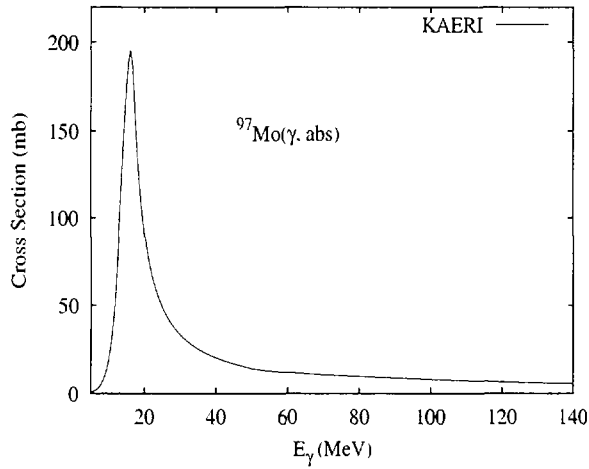
There are no experimental data available. The photoabsorption cross section was obtained from GDR and QD model calculations, adopting the GDR parameters of ^{98}Mo. The neutron, proton, deuteron, triton and alpha emission cross sections, as well as production cross sections, were calculated by the GNASH code.

$$\gamma + {}^{98}\text{Mo}$$

Abundance	Threshold Energies (MeV)								
(%)	γ,n	γ,p	γ,t	γ,He-3	γ,α	γ,2n	γ,np	γ,2p	γ,3n
24.13	8.64	9.79	16.28	17.39	3.27	15.46	17.87	17.25	24.62
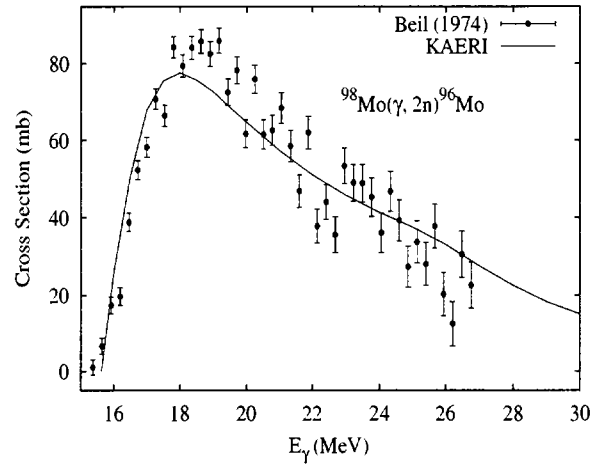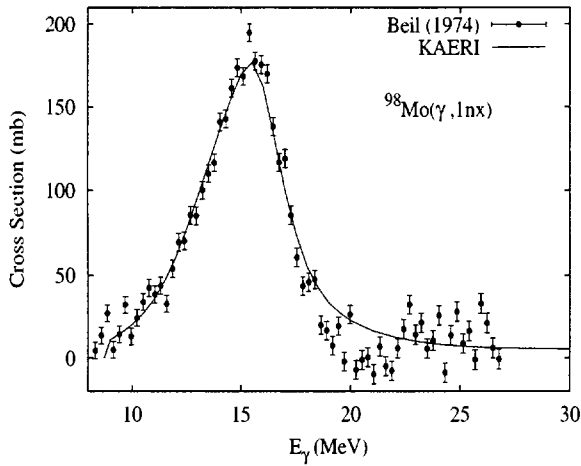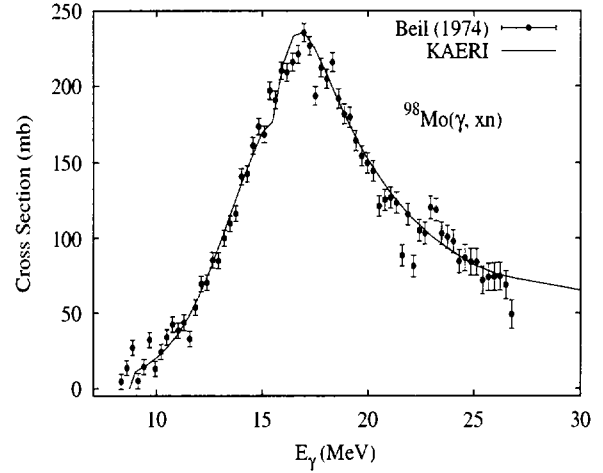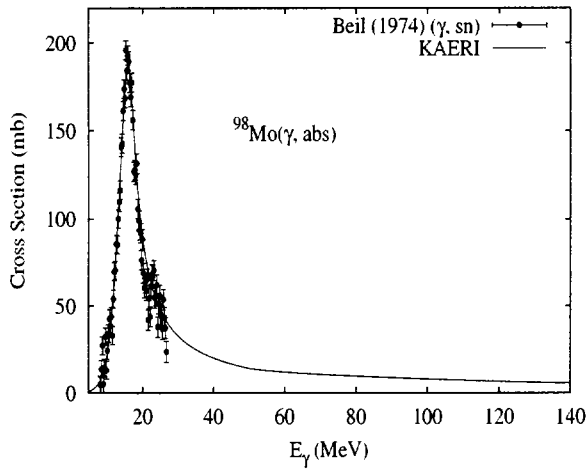
The photoabsorption cross section has not been measured. However, there are experimental data for the (γ, 1nx), (γ, 2nx), (γ, 3nx), (γ, sn), and (γ, xn) reaction cross sections [Bei74]. We relied on the GUNF and GNASH codes to infer the photoabsorption cross section in the GDR regime, in order to model accurately the (γ, sn) data. The photoabsorption cross section above the GDR, up to 140 MeV, was obtained from QD model calculations using the theory of Chadwick.

The calculated results of the emission channels by the GNASH code are in good agreement with the experimental data.

$\gamma + {}^{100}\text{Mo}$

Abundance	Threshold Energies (MeV)								
(%)	γ,n	γ,p	γ,t	γ,He-3	γ,α	γ,2n	γ,np	γ,2p	γ,3n
9.63	8.29	11.15	15.53	18.17	3.17	14.22	18.02	19.48	22.86
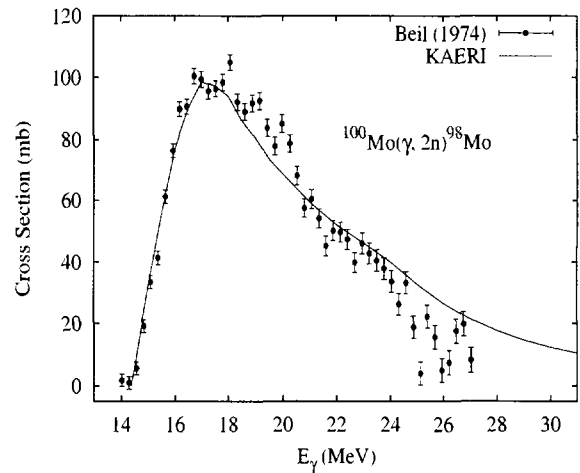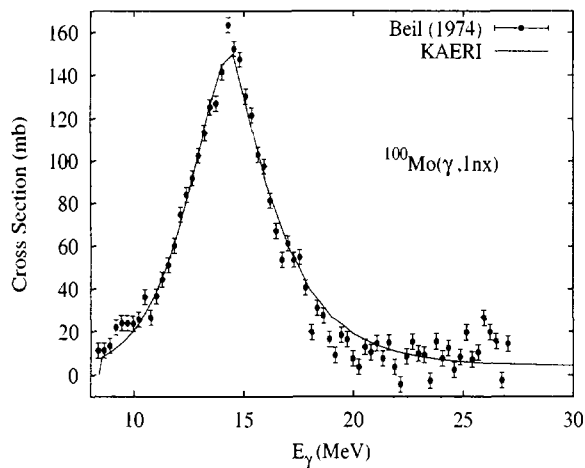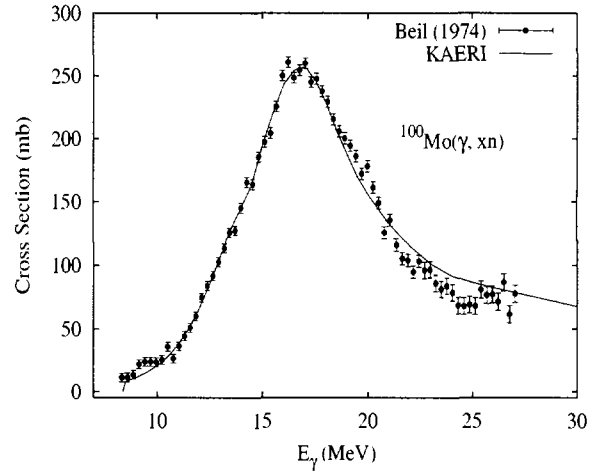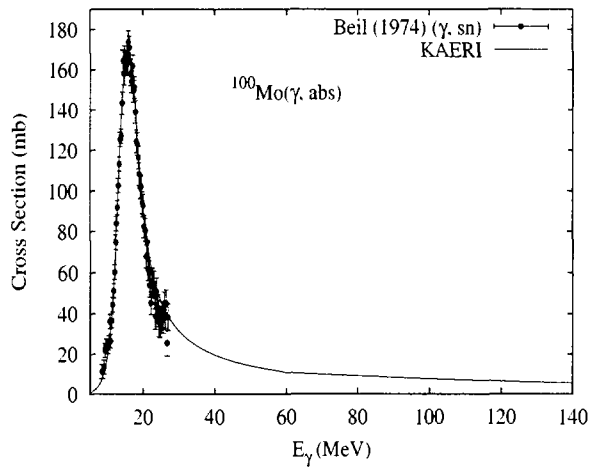
The photoabsorption cross section has not been measured. However, there are experimental data for the (γ, 1nx), (γ, 2nx), (γ, 3nx), (γ, sn), and (γ, xn) reaction cross sections [Bei74]. We relied on the GUNF and GNASH codes to infer the photoabsorption cross section in the GDR regime, in order to model accurately the (γ, sn) data. The photoabsorption cross section above the GDR, up to 140 MeV, was obtained from QD model calculations using the theory of Chadwick.

The calculated results of the emission channels by the GNASH code are in good agreement with the experimental data.

$\gamma + {}^{102}\text{Pd}$

Abundance (%)	Threshold Energies (MeV)								
	γ,n	γ,p	γ,t	$\gamma,$He-3	γ,α	$\gamma,2n$	γ,np	$\gamma,2p$	$\gamma,3n$
1.02	10.56	7.80	17.35	15.23	2.12	18.84	17.69	13.28	29.94

The photoabsorption cross section has not been measured. However, for ^{nat}Pd, there are experimental data for the $(\gamma, 1\text{nx})$, $(\gamma, 2\text{nx})$, (γ, sn) and (γ, xn) reaction cross sections [Lep74]. We relied on the GUNF and GNASH codes to infer the photoabsorption cross section in the GDR regime, in order to model accurately the (γ, sn) data. The photoabsorption cross section above the GDR, up to 140 MeV, was obtained from QD model calculations using the theory of Chadwick. The neutron, proton, deuteron, triton and alpha emission cross sections, as well as production cross sections, were calculated by the GNASH code.
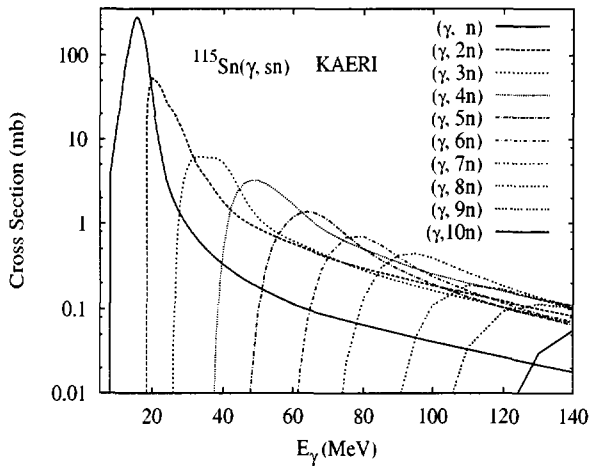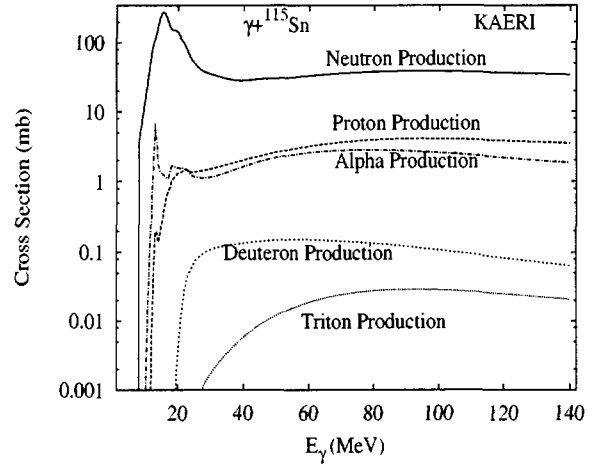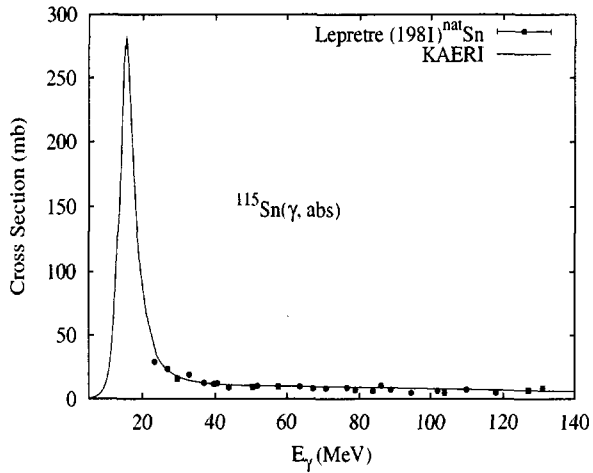
$\gamma + {}^{104}\text{Pd}$

Abundance (%)	Threshold Energies (MeV)								
	γ,n	γ,p	γ,t	$\gamma,\text{He-3}$	γ,α	$\gamma,2n$	γ,np	$\gamma,2p$	$\gamma,3n$
11.14	9.99	8.66	16.93	16.37	2.60	17.62	17.93	14.87	28.18

The photoabsorption cross section has not been measured. However, for ${}^{nat}\text{Pd}$, there are experimental data for the $(\gamma, 1nx)$, $(\gamma, 2nx)$, (γ, sn) and (γ, xn) reaction cross sections [Lep74]. We relied on the GUNF and GNASH codes to infer the photoabsorption cross section in the GDR regime, in order to model accurately the (γ, sn) data. The photoabsorption cross section above the GDR, up to 140 MeV, was obtained from QD model calculations using the theory of Chadwick. The neutron, proton, deuteron, triton and alpha emission cross sections, as well as production cross sections, were calculated by the GNASH code.
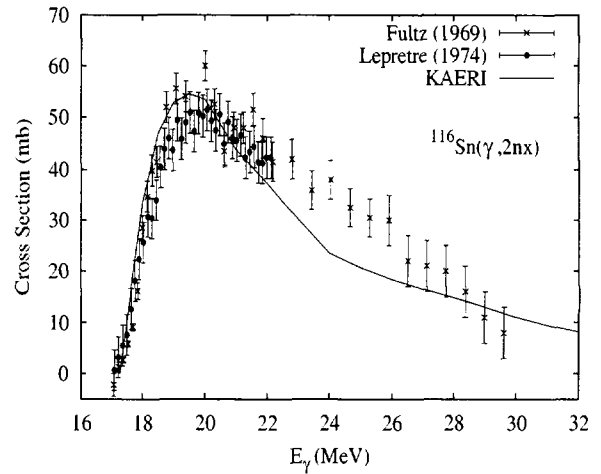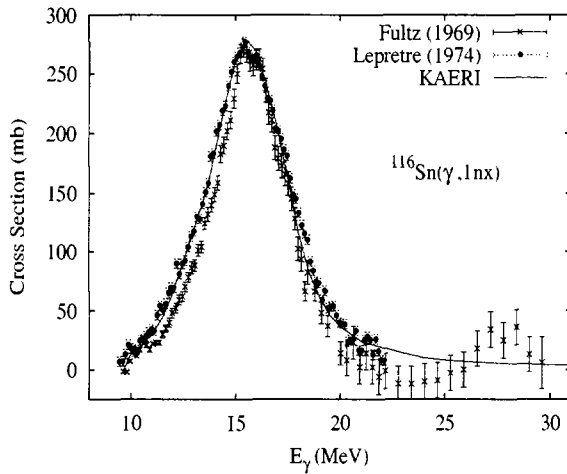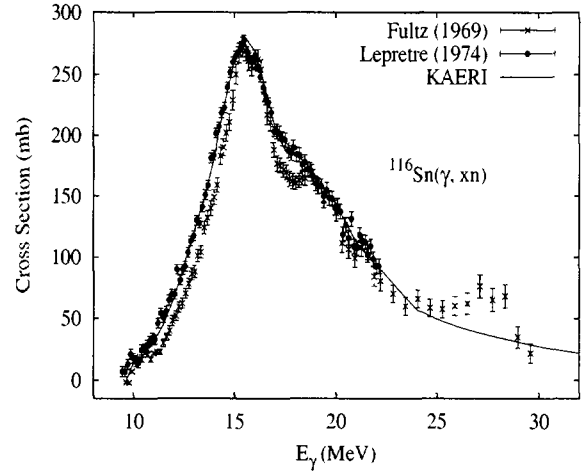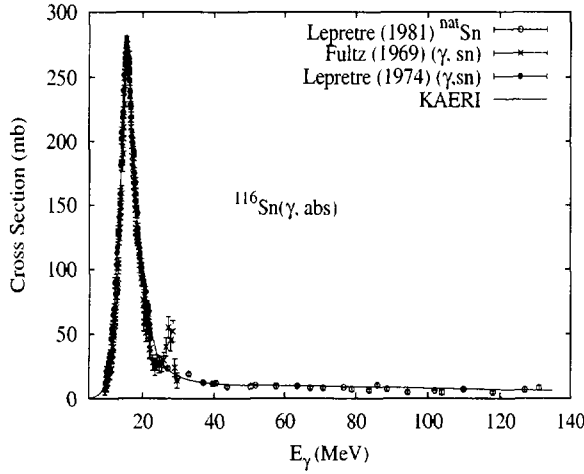
$\gamma + {}^{105}\text{Pd}$

Abundance (%)	Threshold Energies (MeV)								
	γ,n	γ,p	γ,t	$\gamma,\text{He-3}$	γ,α	$\gamma,2n$	γ,np	$\gamma,2p$	$\gamma,3n$
22.33	7.09	8.75	16.54	14.25	2.89	17.09	15.75	15.73	24.71

The photoabsorption cross section has not been measured. However, for ^{nat}Pd, there are experimental data for the (γ, 1nx), (γ, 2nx), (γ, sn) and (γ, xn) reaction cross sections [Lep74]. We relied on the GUNF and GNASH codes to infer the photoabsorption cross section in the GDR regime, in order to model accurately the (γ, sn) data. The photoabsorption cross section above the GDR, up to 140 MeV, was obtained from QD model calculations using the theory of Chadwick. The neutron, proton, deuteron, triton and alpha emission cross sections, as well as production cross sections, were calculated by the GNASH code.
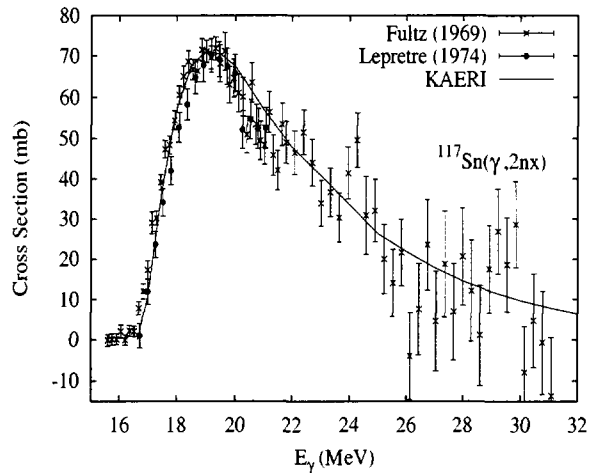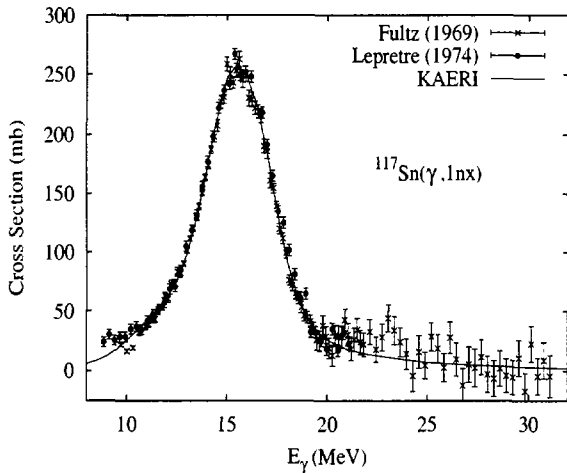
189

$\gamma + {}^{106}\text{Pd}$

Abundance (%)	Threshold Energies (MeV)								
	γ,n	γ,p	γ,t	γ,He-3	γ,α	γ,2n	γ,np	γ,2p	γ,3n
27.33	9.56	9.35	16.83	17.58	3.23	16.66	18.32	16.39	26.65

The photoabsorption cross section has not been measured. However, for ^{nat}Pd, there are experimental data for the (γ, 1nx), (γ, 2nx), (γ, sn) and (γ, xn) reaction cross sections [Lep74]. We relied on the GUNF and GNASH codes to infer the photoabsorption cross section in the GDR regime, in order to model accurately the (γ, sn) data. The photoabsorption cross section above the GDR, up to 140 MeV, was obtained from QD model calculations using the theory of Chadwick. The neutron, proton, deuteron, triton and alpha emission cross sections, as well as production cross sections, were calculated by the GNASH code.

γ + ^{107}Pd

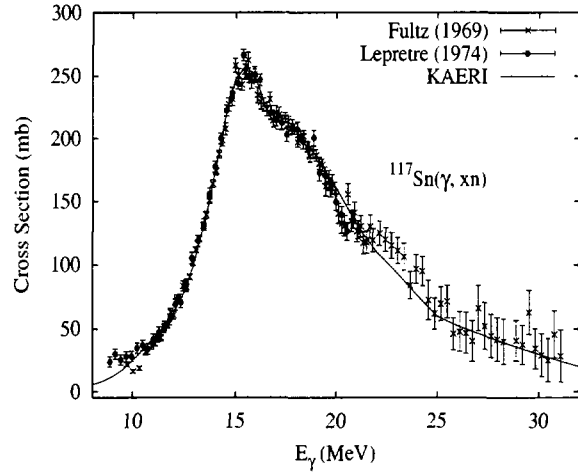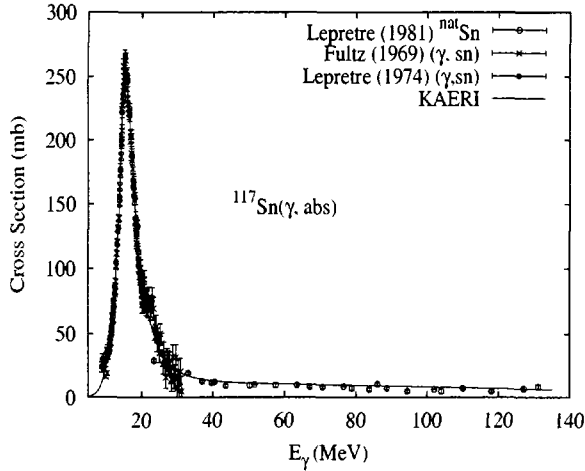| Abundance	Threshold Energies (MeV)								
(%)	γ,n	γ,p	γ,t	γ,He-3	γ,α	γ,2n	γ,np	γ,2p	γ,3n
0.00	6.54	9.30	16.37	15.21	3.54	16.10	15.89	17.02	23.20

The photoabsorption cross section has not been measured. However, for ^{nat}Pd, there are experimental data for the (γ, 1nx), (γ, 2nx), (γ, sn) and (γ, xn) reaction cross sections [Lep74]. We relied on the GUNF and GNASH codes to infer the photoabsorption cross section in the GDR regime, in order to model accurately the (γ, sn) data. The photoabsorption cross section above the GDR, up to 140 MeV, was obtained from QD model calculations using the theory of Chadwick. The neutron, proton, deuteron, triton and alpha emission cross sections, as well as production cross sections, were calculated by the GNASH code.
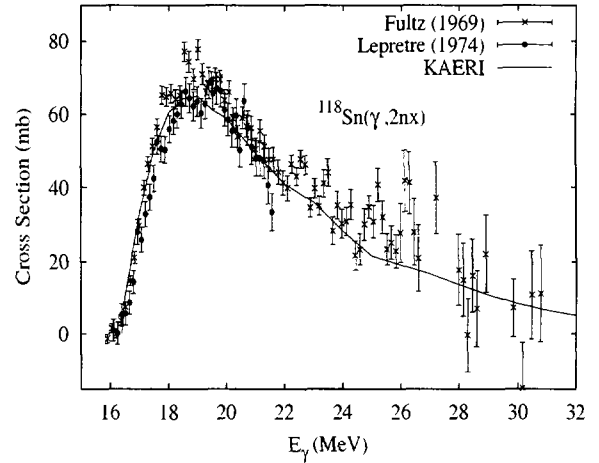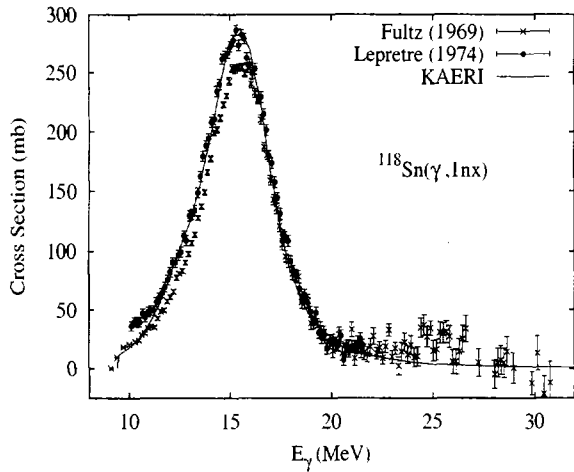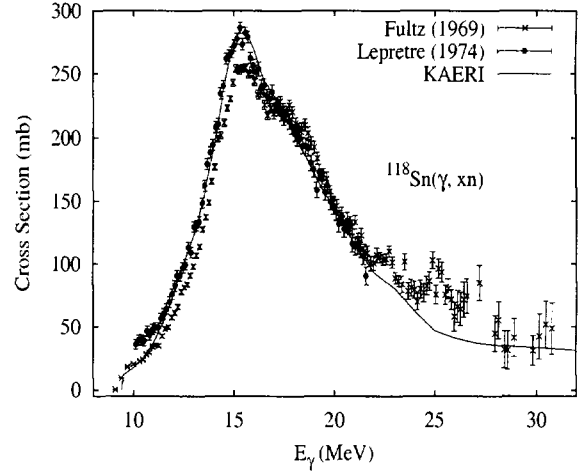
γ + ^{108}Pd

Abundance			Threshold Energies (MeV)						
(%)	γ,n	γ,p	γ,t	γ,He-3	γ,α	γ,2n	γ,np	γ,2p	γ,3n
26.46	9.22	9.95	16.62	18.52	3.85	15.76	18.52	17.78	25.32

The photoabsorption cross section has not been measured. However, for ^{nat}Pd, there are experimental data for the (γ, 1nx), (γ, 2nx), (γ, sn) and (γ, xn) reaction cross sections [Lep74]. We relied on the GUNF and GNASH codes to infer the photoabsorption cross section in the GDR regime, in order to model accurately the (γ, sn) data. The photoabsorption cross section above the GDR, up to 140 MeV, was obtained from QD model calculations using the theory of Chadwick. The neutron, proton, deuteron, triton and alpha emission cross sections, as well as production cross sections, were calculated by the GNASH code.
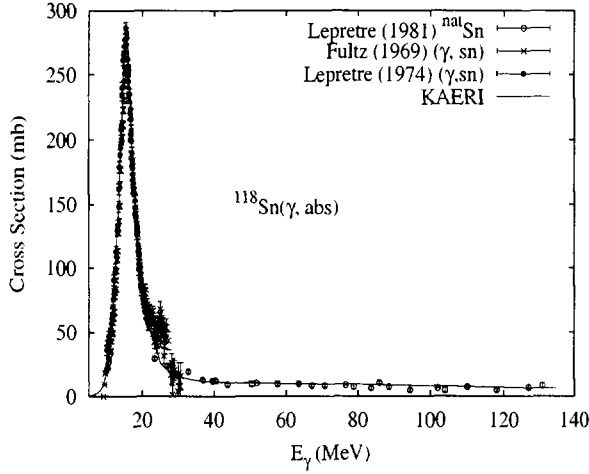
$\gamma + {}^{110}\text{Pd}$

Abundance (%)	Threshold Energies (MeV)								
	γ,n	γ,p	γ,t	$\gamma,\text{He-3}$	γ,α	$\gamma,2n$	γ,np	$\gamma,2p$	$\gamma,3n$
11.72	8.81	10.61	16.43	19.57	4.44	14.96	18.63	19.16	24.19

The photoabsorption cross section has not been measured. However, for ${}^{nat}\text{Pd}$, there are experimental data for the $(\gamma, 1nx)$, $(\gamma, 2nx)$, (γ, sn) and (γ, xn) reaction cross sections [Lep74]. We relied on the GUNF and GNASH codes to infer the photoabsorption cross section in the GDR regime, in order to model accurately the (γ, sn) data. The photoabsorption cross section above the GDR, up to 140 MeV, was obtained from QD model calculations using the theory of Chadwick. The neutron, proton, deuteron, triton and alpha emission cross sections, as well as production cross sections, were calculated by the GNASH code.
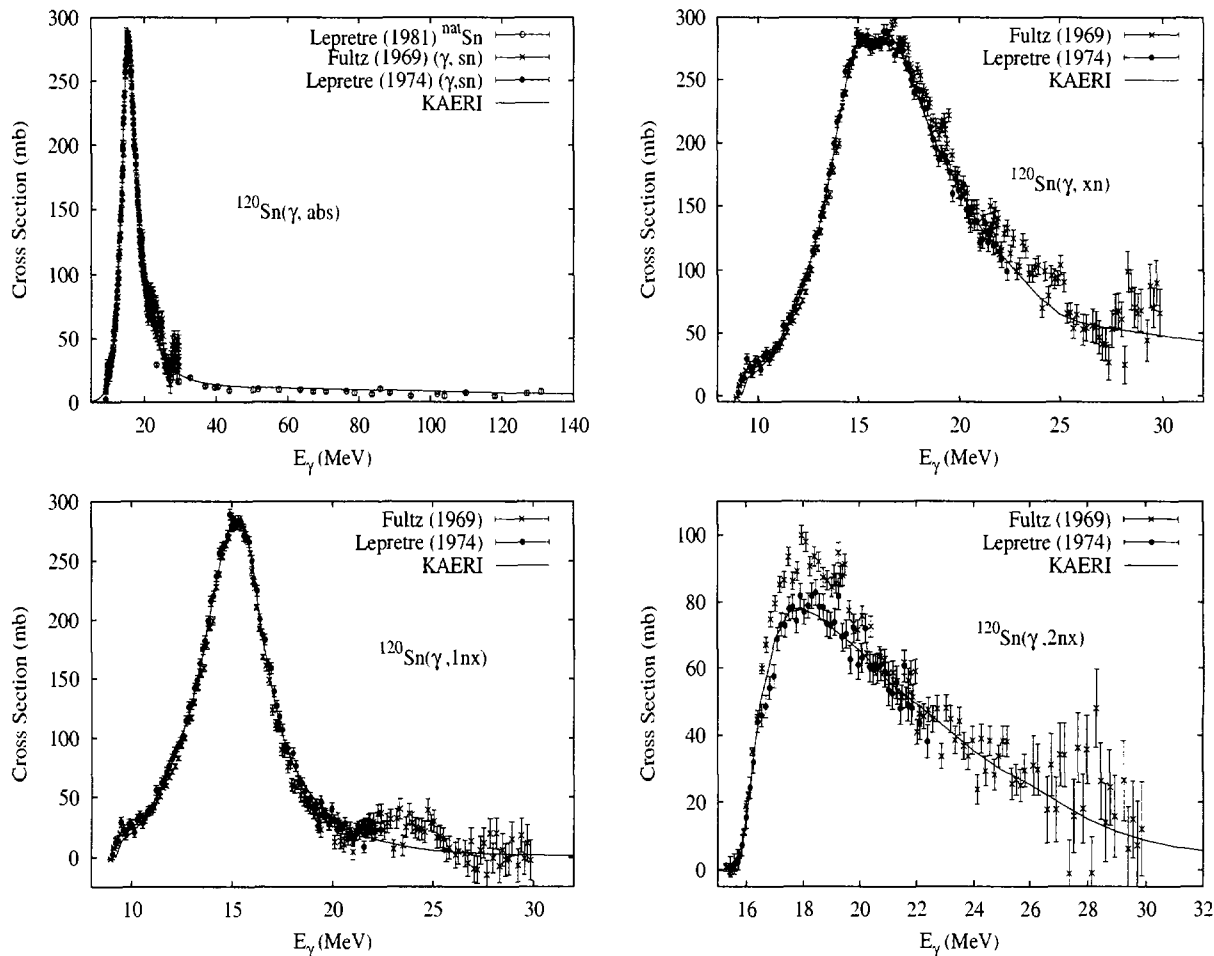
$$\gamma \ + \ ^{107}\text{Ag}$$

Abundance	Threshold Energies (MeV)								
(%)	γ,n	γ,p	γ,t	γ,He-3	γ,α	γ,2n	γ,np	γ,2p	γ,3n
51.84	9.54	5.79	13.96	16.39	2.81	17.47	15.35	15.14	27.51
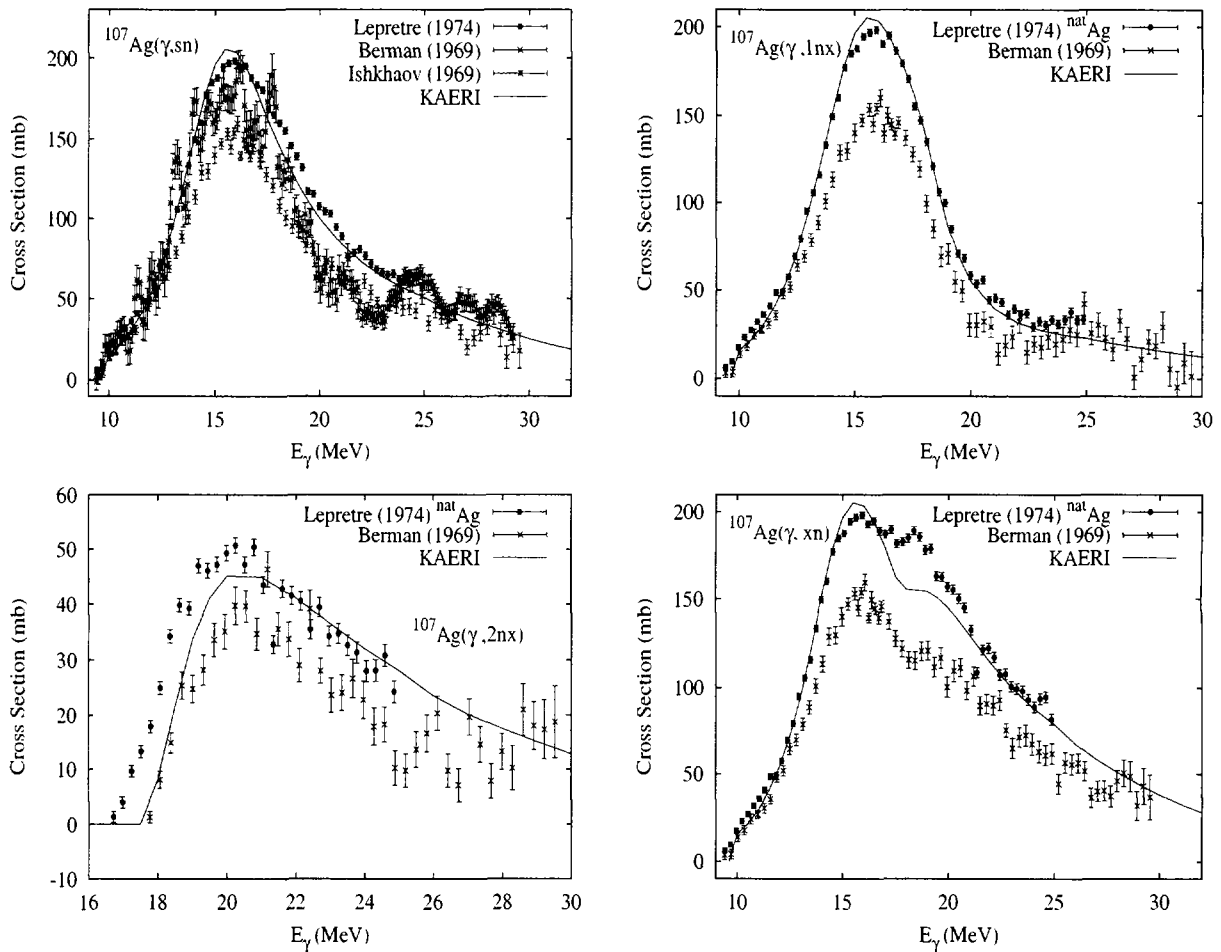
The photoabsorption cross section has not been measured. However, there are experimental data for the (γ, 1nx), (γ, 2nx), (γ, sn), and (γ, xn) reaction cross sections from [Ber69b], and for the (γ, sn) from [Ish69]. Experimental data for ^{nat}Ag were reported for the (γ, 1nx), (γ, 2nx), (γ, sn) and (γ, xn) cross sections [Lep74]. Ishkhanov's and Lepretre's data agree fairly well in magnitude. By comparing those with that of neighboring nuclei such as Pd and Cd, the results of Lepretre were selected as reference. We relied on the GUNF and GNASH codes to infer the photoabsorption cross section in the GDR regime, in order to model accurately Lepretre's (γ, sn) data. The photoabsorption cross section above the GDR, up to 140 MeV, was obtained from QD model calculations using the theory of Chadwick.

The calculated results of the emission channels by the GNASH code are in good agreement with all the experimental data of Lepretre.

γ + ^{108}Ag

Abundance	Threshold Energies (MeV)								
(%)	γ,n	γ,p	γ,t	γ,He-3	γ,α	γ,2n	γ,np	γ,2p	γ,3n
0.00	7.27	6.52	14.14	14.69	3.08	16.81	13.06	15.82	24.74

The photoabsorption cross section has not been measured. However, there are experimental data, for ^{nat}Ag, for the (γ, 1nx), (γ, 2nx), (γ, sn), and (γ, xn) reaction cross sections [Lep74]. The photoabsorption cross section was obtained from GDR and QD model calculations, adopting the GDR parameters of ^{109}Ag. The neutron, proton, deuteron, triton and alpha emission cross sections, as well as production cross sections, were calculated by the GNASH code.

$$\gamma + {}^{109}\text{Ag}$$

Abundance (%)	Threshold Energies (MeV)								
	γ,n	γ,p	γ,t	γ,He-3	γ,α	γ,2n	γ,np	γ,2p	γ,3n
48.16	9.19	6.49	13.76	17.29	3.30	16.46	15.71	16.44	25.99
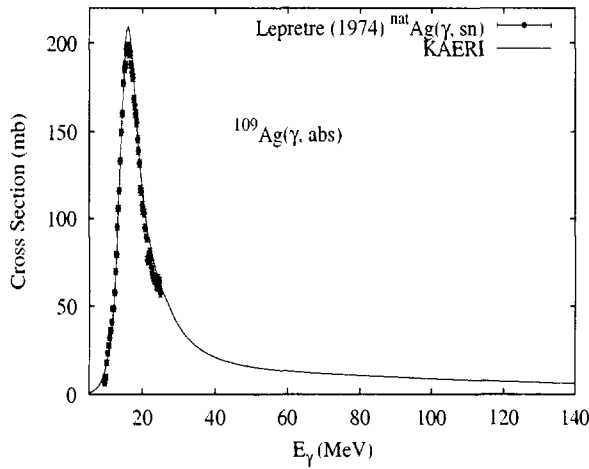
The photoabsorption cross section has not been measured. However, there are experimental data, for ^{nat}Ag, for the (γ, 1nx), (γ, 2nx), (γ, sn), and (γ, xn) reaction cross sections [Lep74], which were used as reference. We relied on the GUNF and GNASH codes to infer the photoabsorption cross section in the GDR regime, in order to model accurately Lepretre's (γ, sn) data. The photoabsorption cross section above the GDR, up to 140 MeV, was obtained from QD model calculations using the theory of Chadwick.

The calculated results of the emission channels by the GNASH code are in good agreement with all the experimental data of Lepretre.

γ + ^{106}Cd

Abundance	Threshold Energies (MeV)								
(%)	γ,n	γ,p	γ,t	γ,He-3	γ,α	γ,2n	γ,np	γ,2p	γ,3n
1.25	10.87	7.35	17.30	14.60	1.64	19.30	17.38	12.32	30.70

The photoabsorption cross section has not been measured. However, for ^{nat}Cd, there are experimental data for the (γ, 1nx), (γ, 2nx), (γ, sn) and (γ, xn) reaction cross sections [Lep74]. We relied on the GUNF and GNASH codes to infer the photoabsorption cross section in the GDR regime, in order to model accurately the (γ, sn) data. The photoabsorption cross section above the GDR, up to 140 MeV, was obtained from QD model calculations using the theory of Chadwick. The neutron, proton, deuteron, triton and alpha emission cross sections, as well as production cross sections, were calculated by the GNASH code.
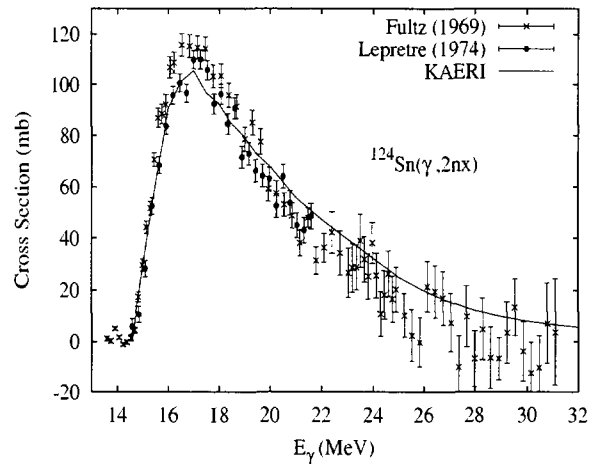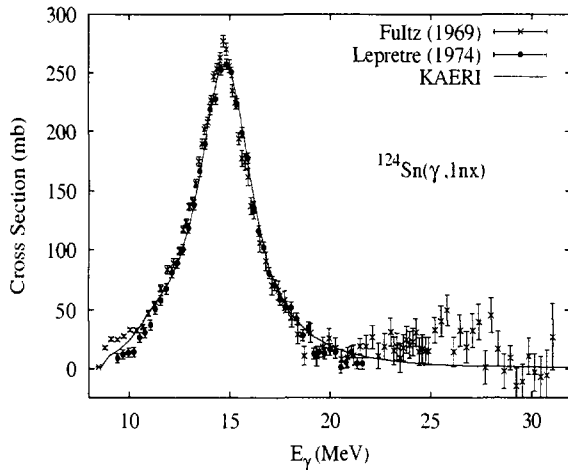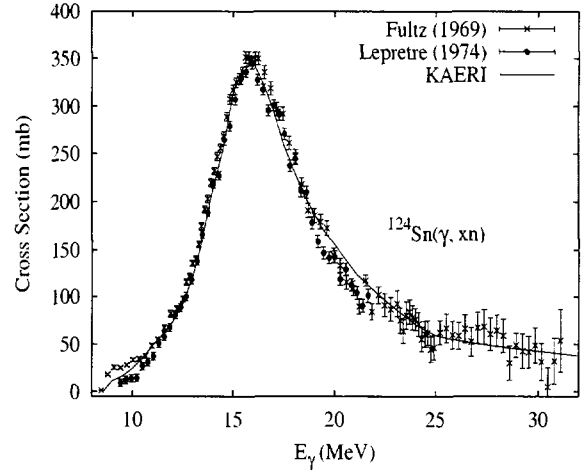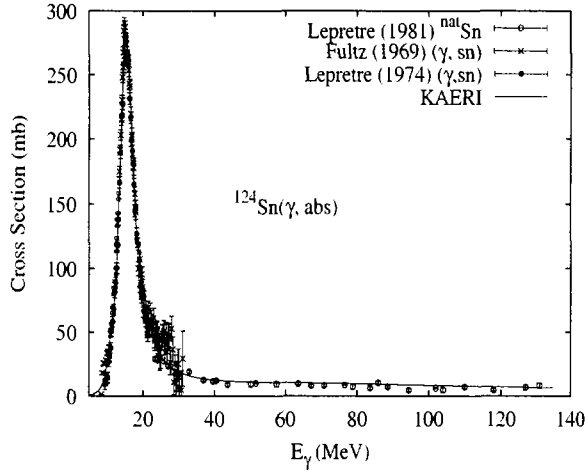
γ + ^{108}Cd

Abundance	Threshold Energies (MeV)								
(%)	γ,n	γ,p	γ,t	$\gamma,$He-3	γ,α	$\gamma,2n$	γ,np	$\gamma,2p$	$\gamma,3n$
0.89	10.33	8.14	17.12	15.77	2.28	18.26	17.67	13.92	29.13

The photoabsorption cross section has not been measured. However, for ^{nat}Cd, there are experimental data for the (γ, 1nx), (γ, 2nx), (γ, sn) and (γ, xn) reaction cross sections [Lep74]. We relied on the GUNF and GNASH codes to infer the photoabsorption cross section in the GDR regime, in order to model accurately the (γ, sn) data. The photoabsorption cross section above the GDR, up to 140 MeV, was obtained from QD model calculations using the theory of Chadwick. The neutron, proton, deuteron, triton and alpha emission cross sections, as well as production cross sections, were calculated by the GNASH code.
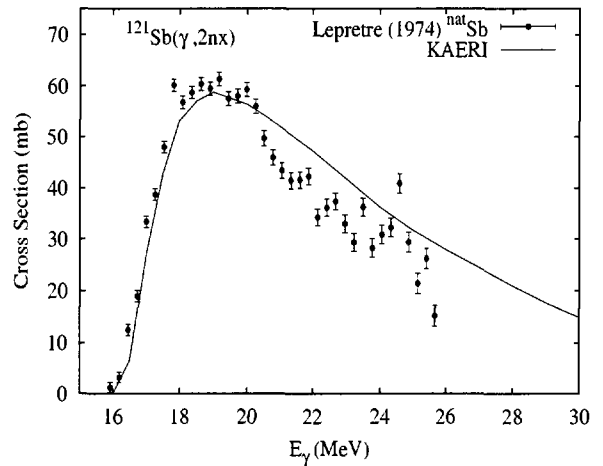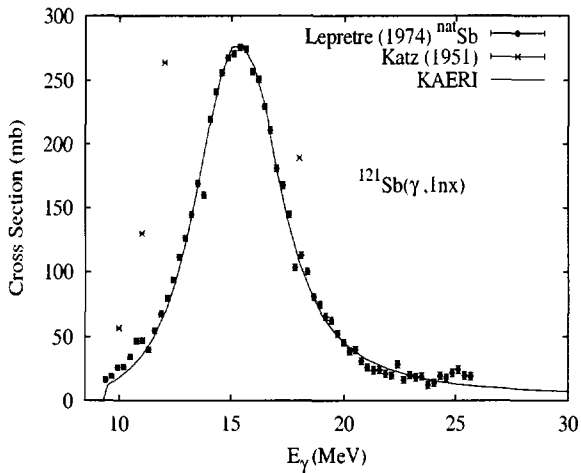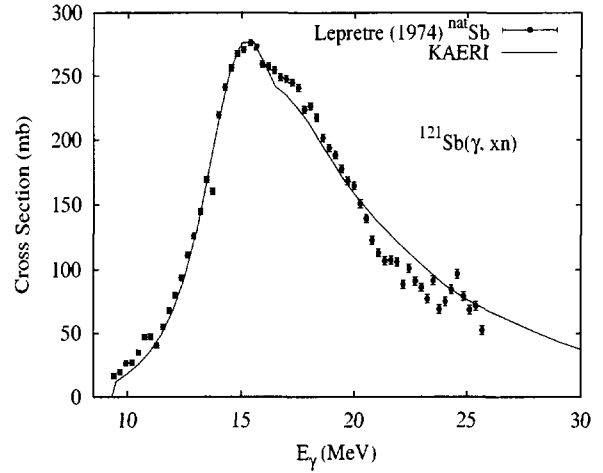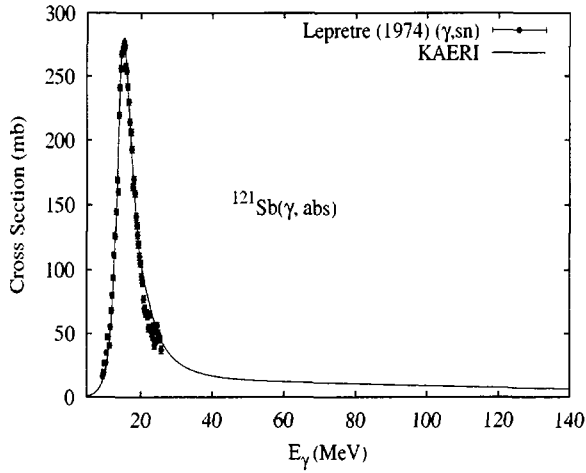
$$\gamma + \text{}^{110}\text{Cd}$$

Abundance	Threshold Energies (MeV)								
(%)	γ,n	γ,p	γ,t	γ,He-3	γ,α	γ,2n	γ,np	γ,2p	γ,3n
12.49	9.92	8.92	16.89	16.91	2.87	17.24	18.11	15.41	27.58

The photoabsorption cross section has not been measured. However, for ^{nat}Cd, there are experimental data for the (γ, 1nx), (γ, 2nx), (γ, sn) and (γ, xn) reaction cross sections [Lep74]. We relied on the GUNF and GNASH codes to infer the photoabsorption cross section in the GDR regime, in order to model accurately the (γ, sn) data. The photoabsorption cross section above the GDR, up to 140 MeV, was obtained from QD model calculations using the theory of Chadwick. The neutron, proton, deuteron, triton and alpha emission cross sections, as well as production cross sections, were calculated by the GNASH code.

$\gamma + {}^{111}\text{Cd}$

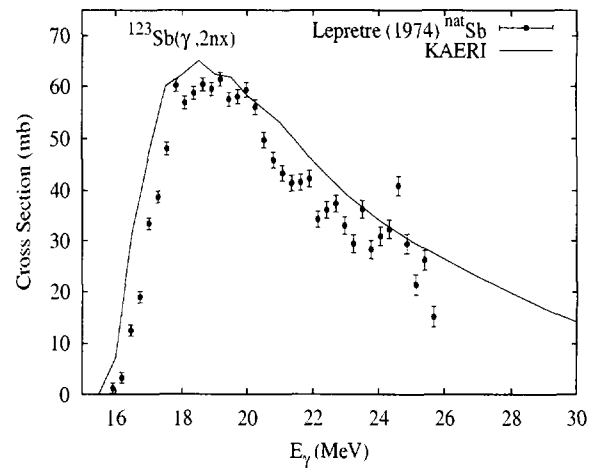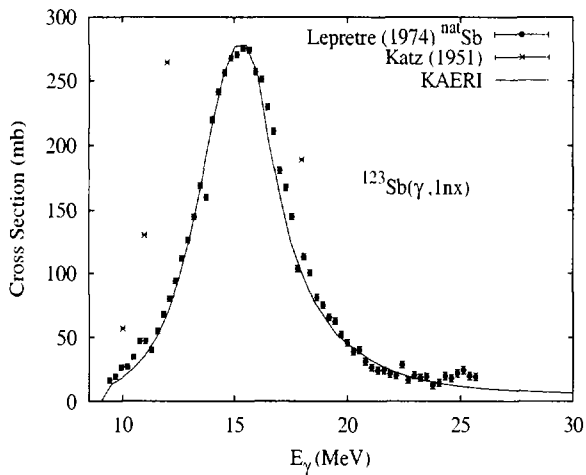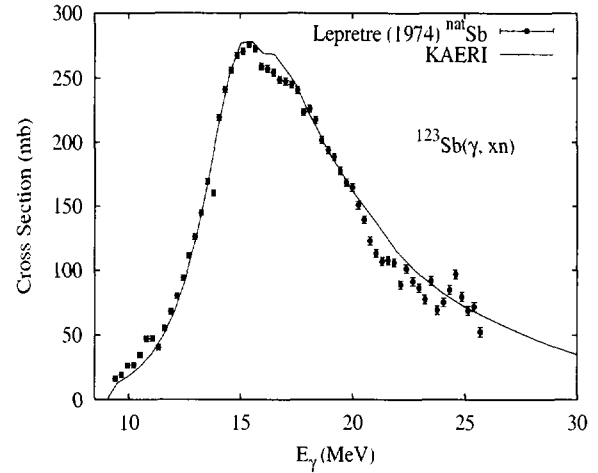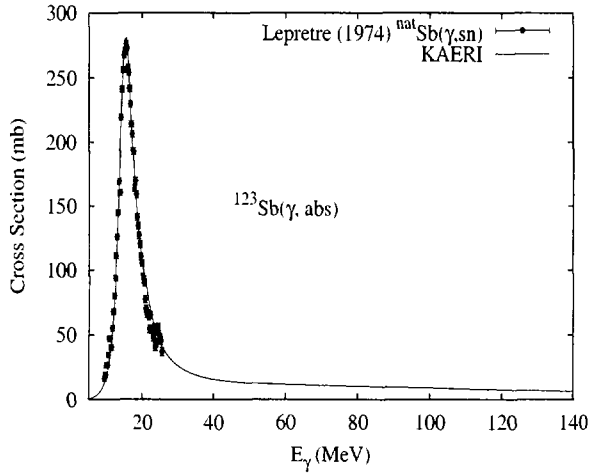| Abundance (%)	Threshold Energies (MeV)								
	γ,n	γ,p	γ,t	$\gamma,\text{He-3}$	γ,α	$\gamma,2n$	γ,np	$\gamma,2p$	$\gamma,3n$
12.80	6.97	9.08	16.60	14.66	3.30	16.89	15.89	16.23	24.22

The photoabsorption cross section has not been measured. However, for ${}^{nat}\text{Cd}$, there are experimental data for the $(\gamma, 1\text{nx})$, $(\gamma, 2\text{nx})$, (γ, sn) and (γ, xn) reaction cross sections [Lep74]. We relied on the GUNF and GNASH codes to infer the photoabsorption cross section in the GDR regime, in order to model accurately the (γ, sn) data. The photoabsorption cross section above the GDR, up to 140 MeV, was obtained from QD model calculations using the theory of Chadwick. The neutron, proton, deuteron, triton and alpha emission cross sections, as well as production cross sections, were calculated by the GNASH code.

$\gamma + {}^{112}\text{Cd}$

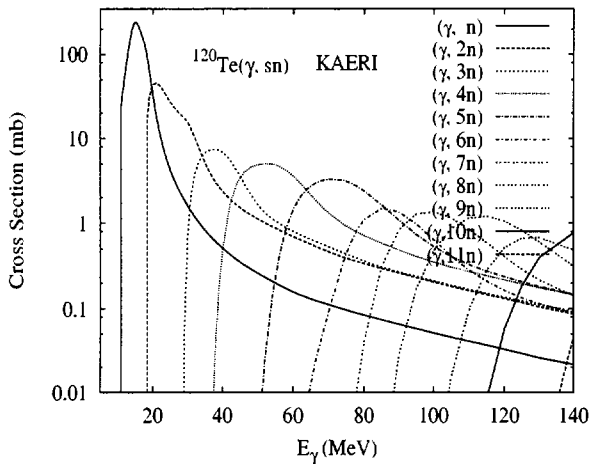| Abundance (%)	Threshold Energies (MeV)								
	γ,n	γ,p	γ,t	$\gamma,\text{He-3}$	γ,α	$\gamma,2\text{n}$	γ,np	$\gamma,2\text{p}$	$\gamma,3\text{n}$
24.13	9.40	9.65	16.81	17.91	3.48	16.37	18.48	16.81	26.29

The photoabsorption cross section has not been measured. However, for ^{nat}Cd, there are experimental data for the $(\gamma, \text{1nx})$, $(\gamma, \text{2nx})$, (γ, sn) and (γ, xn) reaction cross sections [Lep74]. We relied on the GUNF and GNASH codes to infer the photoabsorption cross section in the GDR regime, in order to model accurately the (γ, sn) data. The photoabsorption cross section above the GDR, up to 140 MeV, was obtained from QD model calculations using the theory of Chadwick. The neutron, proton, deuteron, triton and alpha emission cross sections, as well as production cross sections, were calculated by the GNASH code.

$\gamma + {}^{113}\mathrm{Cd}$

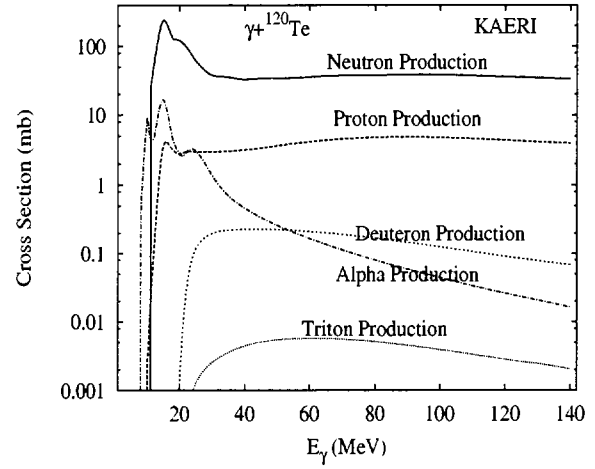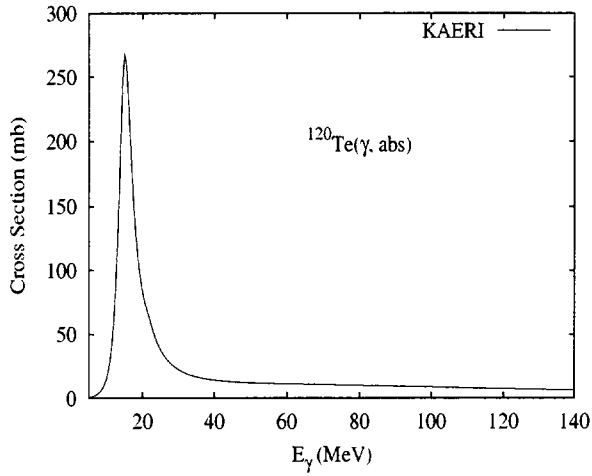| Abundance	Threshold Energies (MeV)								
(%)	γ,n	γ,p	γ,t	γ,He-3	γ,α	γ,2n	γ,np	γ,2p	γ,3n
12.22	6.54	9.72	16.54	15.64	3.87	15.94	16.19	17.60	22.91

The photoabsorption cross section has not been measured. However, for ^{nat}Cd, there are experimental data for the (γ, 1nx), (γ, 2nx), (γ, sn) and (γ, xn) reaction cross sections [Lep74]. We relied on the GUNF and GNASH codes to infer the photoabsorption cross section in the GDR regime, in order to model accurately the (γ, sn) data. The photoabsorption cross section above the GDR, up to 140 MeV, was obtained from QD model calculations using the theory of Chadwick. The neutron, proton, deuteron, triton and alpha emission cross sections, as well as production cross sections, were calculated by the GNASH code.

$\gamma + {}^{114}\mathrm{Cd}$

Abundance (%)	Threshold Energies (MeV)								
	γ,n	γ,p	γ,t	γ,He-3	γ,α	γ,2n	γ,np	γ,2p	γ,3n
28.73	9.04	10.27	16.75	18.92	4.10	15.58	18.76	18.27	24.98

The photoabsorption cross section has not been measured. However, for ${}^{nat}\mathrm{Cd}$, there are experimental data for the (γ, 1nx), (γ, 2nx), (γ, sn) and (γ, xn) reaction cross sections [Lep74]. We relied on the GUNF and GNASH codes to infer the photoabsorption cross section in the GDR regime, in order to model accurately the (γ, sn) data. The photoabsorption cross section above the GDR, up to 140 MeV, was obtained from QD model calculations using the theory of Chadwick. The neutron, proton, deuteron, triton and alpha emission cross sections, as well as production cross sections, were calculated by the GNASH code.
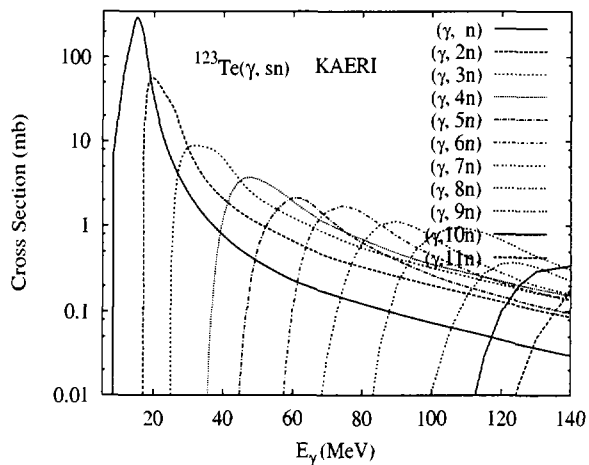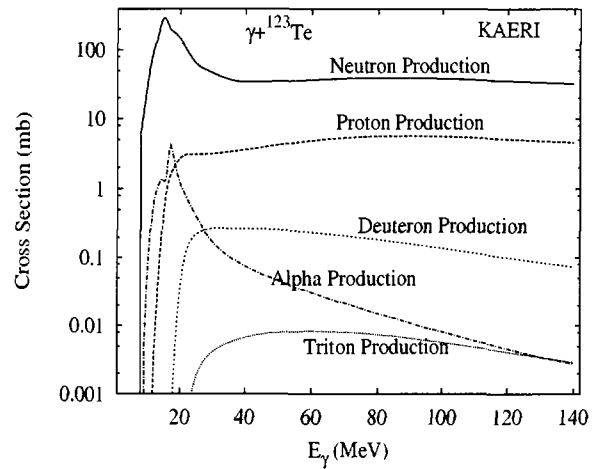
$\gamma + {}^{116}\text{Cd}$

Abundance (%)	Threshold Energies (MeV)								
	γ,n	γ,p	γ,t	γ,He-3	γ,α	γ,2n	γ,np	γ,2p	γ,3n
7.49	8.70	11.06	16.63	19.97	4.81	14.84	19.12	19.84	23.88

The photoabsorption cross section has not been measured. However, for ^{nat}Cd, there are experimental data for the (γ, 1nx), (γ, 2nx), (γ, sn) and (γ, xn) reaction cross sections [Lep74]. We relied on the GUNF and GNASH codes to infer the photoabsorption cross section in the GDR regime, in order to model accurately the (γ, sn) data. The photoabsorption cross section above the GDR, up to 140 MeV, was obtained from QD model calculations using the theory of Chadwick. The neutron, proton, deuteron, triton and alpha emission cross sections, as well as production cross sections, were calculated by the GNASH code.
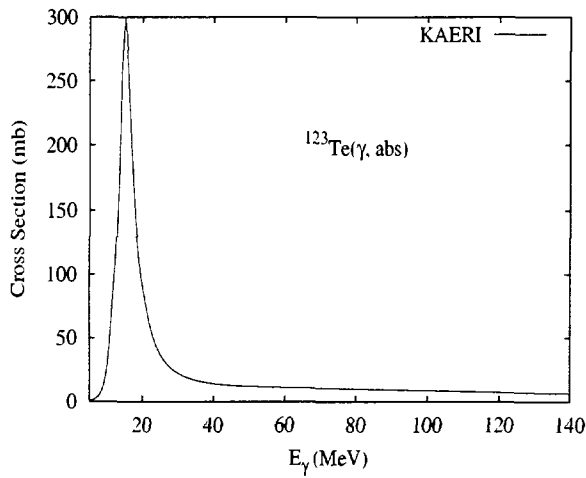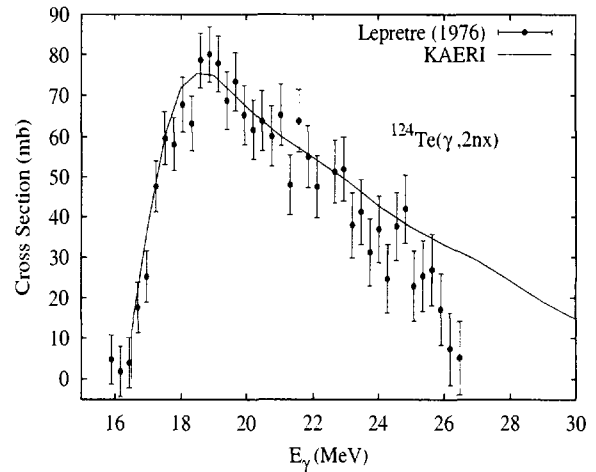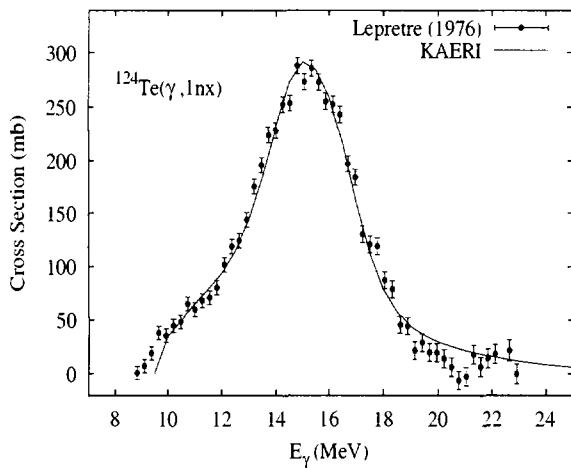
$$\gamma + \, ^{112}\text{Sn}$$

Abundance (%)	Threshold Energies (MeV)								
	$\gamma,$n	$\gamma,$p	$\gamma,$t	$\gamma,$He-3	γ,α	$\gamma,$2n	$\gamma,$np	$\gamma,$2p	$\gamma,$3n
0.97	10.79	7.56	17.12	15.08	1.83	18.97	17.61	12.89	30.24
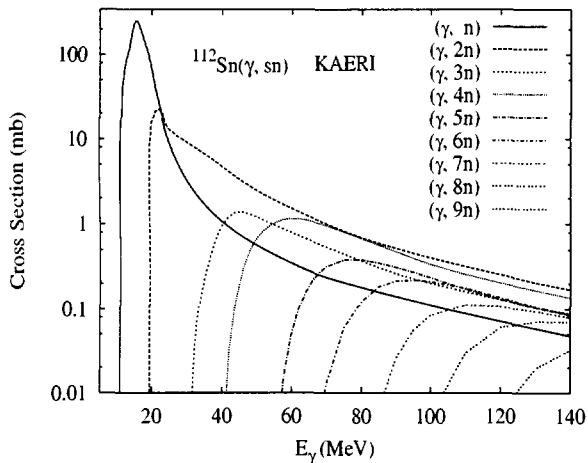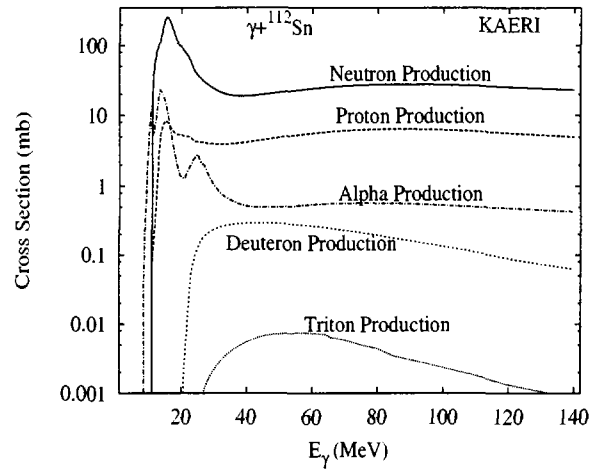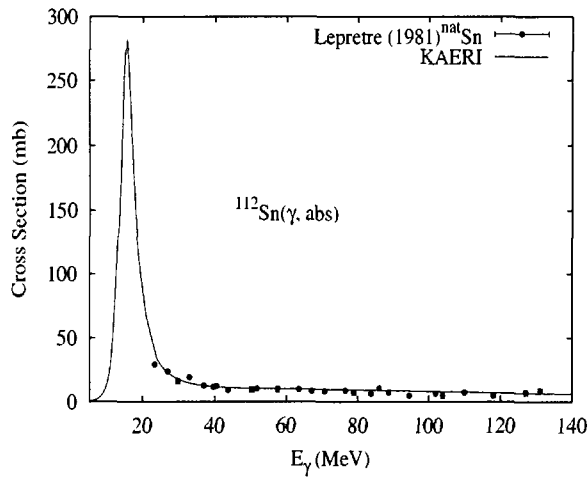
Measurements of the photoabsorption cross section, above 25 MeV, are available for ^{nat}Sn [Lep81]. The GUNF code was used to infer the photoabsorption cross section in the GDR regime, adopting the GDR parameters of ^{116}Sn. The photoabsorption cross section above the GDR, up to 140 MeV, was obtained from QD model calculations using the theory of Chadwick. The neutron, proton, deuteron, triton and alpha emission cross sections, as well as production cross sections, were calculated by the GNASH code.
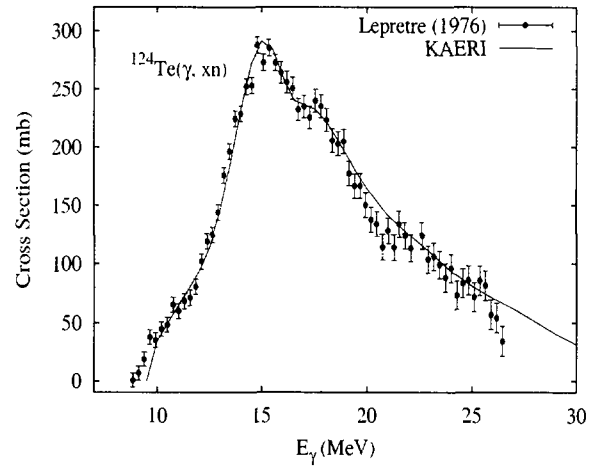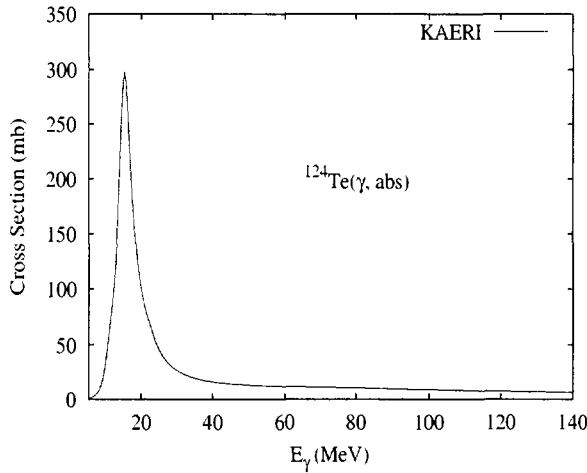
$\gamma + {}^{114}\text{Sn}$

Abundance (%)	Threshold Energies (MeV)								
	γ,n	γ,p	γ,t	$\gamma.\text{He-3}$	γ,α	$\gamma,2n$	γ,np	$\gamma,2p$	$\gamma,3n$
0.65	10.30	8.48	17.12	16.24	2.63	18.04	17.93	14.56	28.83

Measurements of the photoabsorption cross section, above 25 MeV, are available for ^{nat}Sn [Lep81]. The GUNF code was used to infer the photoabsorption cross section in the GDR regime, adopting the GDR parameters of ^{116}Sn. The photoabsorption cross section above the GDR, up to 140 MeV, was obtained from QD model calculations using the theory of Chadwick. The neutron, proton, deuteron, triton and alpha emission cross sections, as well as production cross sections, were calculated by the GNASH code.

Abundance	Threshold Energies (MeV)								
(%)	γ,n	γ,p	γ,t	γ,He-3	γ,α	γ,2n	γ,np	γ,2p	γ,3n
0.36	7.55	8.75	16.99	14.38	3.21	17.85	16.03	15.56	25.59

Measurements of the photoabsorption cross section, above 25 MeV, are available for ^{nat}Sn [Lep81]. The GUNF code was used to infer the photoabsorption cross section in the GDR regime, adopting the GDR parameters of ^{116}Sn. The photoabsorption cross section above the GDR, up to 140 MeV, was obtained from QD model calculations using the theory of Chadwick. The neutron, proton, deuteron, triton and alpha emission cross sections, as well as production cross sections, were calculated by the GNASH code.

$\gamma + {}^{116}\text{Sn}$

Abundance (%)	Threshold Energies (MeV)								
	γ,n	γ,p	γ,t	$\gamma,\text{He-3}$	γ,α	$\gamma,2n$	γ,np	$\gamma,2p$	$\gamma,3n$
14.53	9.56	9.28	17.11	17.41	3.37	17.11	18.32	16.08	27.41

There are no measurements of the photoabsorption cross section in the GDR energy region. Lepretre [Lep74] and Fultz [Ful69] measured the $(\gamma, 1nx)$, $(\gamma, 2nx)$, (γ, sn) and (γ, xn) reaction cross sections. Lepretre [Lep81] also measured the photoabsorption cross section for ${}^{nat}\text{Sn}$ from 25 MeV to 135 MeV. We relied on the GUNF and GNASH codes to infer the photoabsorption cross section in the GDR regime, using Lepretre's two measurements [Lep81, Lep74], in order to model all the photonuclear cross sections consistently. The photoabsorption cross section above the GDR, up to 140 MeV, was obtained from QD model calculations using the theory of Chadwick. The neutron, proton, deuteron, triton and alpha emission cross sections, as well as production cross sections, were calculated by the GNASH code.

$$\gamma + {}^{117}\text{Sn}$$

Abundance (%)	Threshold Energies (MeV)								
	γ,n	γ,p	γ,t	$\gamma,\text{He-3}$	γ,α	$\gamma,2n$	γ,np	$\gamma,2p$	$\gamma,3n$
7.68	6.94	9.44	16.78	15.31	3.77	16.51	16.22	16.89	24.05

There are no measurements of the photoabsorption cross section in the GDR energy region. Lepretre [Lep74] and Fultz [Ful69] measured the (γ, 1nx), (γ, 2nx), (γ, sn) and (γ, xn) reaction cross sections. Lepretre [Lep81] also measured the photoabsorption cross section for ${}^{nat}\text{Sn}$ from 25 MeV to 135 MeV. We relied on the GUNF and GNASH codes to infer the photoabsorption cross section in the GDR regime, using Lepretre's two measurements [Lep81, Lep74], in order to model all the photonuclear cross sections consistently. The photoabsorption cross section above the GDR, up to 140 MeV, was obtained from QD model calculations using the theory of Chadwick. The neutron, proton, deuteron, triton and alpha emission cross sections, as well as production cross sections, were calculated by the GNASH code.

209

$$\gamma + {}^{118}\text{Sn}$$

Abundance (%)	Threshold Energies (MeV)								
	γ,n	γ,p	γ,t	$\gamma,\text{He-3}$	γ,α	$\gamma,2n$	γ,np	$\gamma,2p$	$\gamma,3n$
24.22	9.33	10.00	17.07	18.49	4.06	16.27	18.76	17.51	25.83

There are no measurements of the photoabsorption cross section in the GDR energy region. Lepretre [Lep74] and Fultz [Ful69] measured the (γ, 1nx), (γ, 2nx), (γ, sn) and (γ, xn) reaction cross sections. Lepretre [Lep81] also measured the photoabsorption cross section for ${}^{nat}\text{Sn}$ from 25 MeV to 135 MeV. We relied on the GUNF and GNASH codes to infer the photoabsorption cross section in the GDR regime, using Lepretre's two measurements [Lep81, Lep74], in order to model all the photonuclear cross sections consistently. The photoabsorption cross section above the GDR, up to 140 MeV, was obtained from QD model calculations using the theory of Chadwick. The neutron, proton, deuteron, triton and alpha emission cross sections, as well as production cross sections, were calculated by the GNASH code.

$$\gamma \ + \ ^{119}\text{Sn}$$

Abundance (%)	Threshold Energies (MeV)								
	γ,n	γ,p	γ,t	$\gamma,\text{He-3}$	γ,α	$\gamma,2n$	γ,np	$\gamma,2p$	$\gamma,3n$
8.58	6.49	10.13	16.77	16.28	4.40	15.81	16.48	18.23	22.76
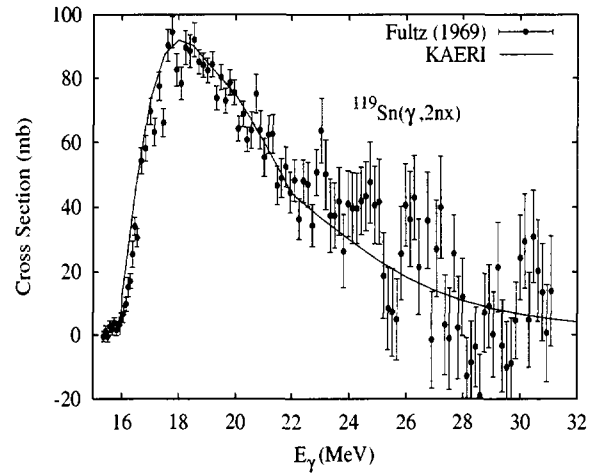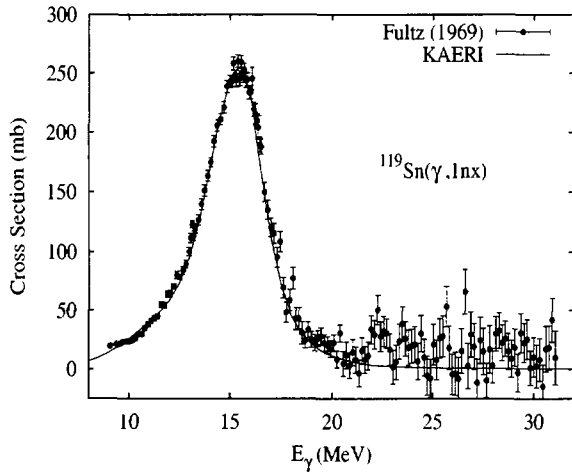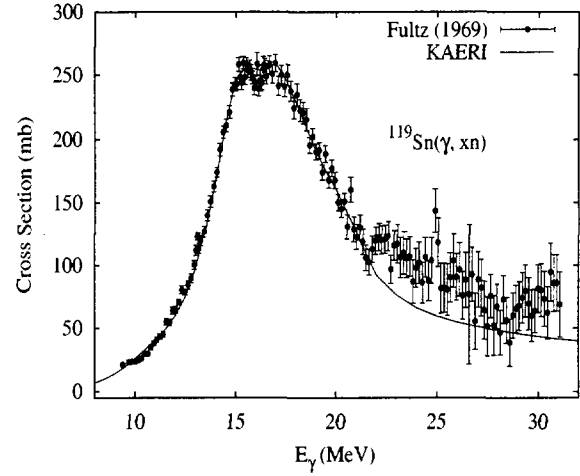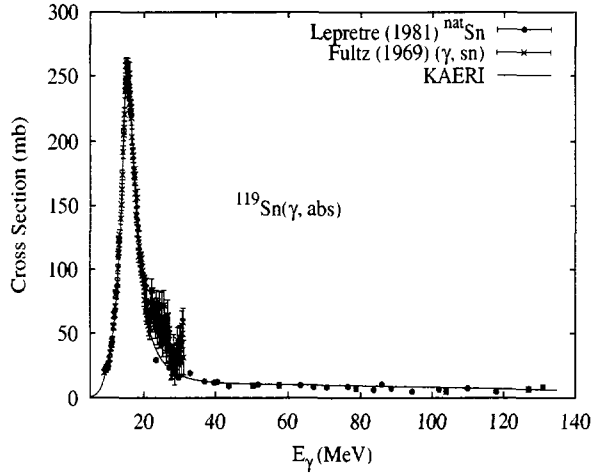
There are no measurements of the photoabsorption cross section in the GDR energy region. Fultz [Ful69] measured the $(\gamma, 1nx)$, $(\gamma, 2nx)$, (γ, sn) and (γ, xn) reaction cross sections. Lepretre [Lep81] measured the photoabsorption cross section for ^{nat}Sn from 25 MeV to 135 MeV. We relied on the GUNF and GNASH codes to infer the photoabsorption cross section in the GDR regime, using Fultz's and Lepretre's measurements [Ful69, Lep81], in order to model all the photonuclear cross sections consistently. The photoabsorption cross section above the GDR, up to 140 MeV, was obtained from QD model calculations using the theory of Chadwick. The neutron, proton, deuteron, triton and alpha emission cross sections, as well as production cross sections, were calculated by the GNASH code.

$$\gamma + {}^{120}\text{Sn}$$

Abundance (%)	Threshold Energies (MeV)								
	γ,n	γ,p	γ,t	γ,He-3	γ,α	γ,2n	γ,np	γ,2p	γ,3n
32.59	9.11	10.66	17.11	19.62	4.81	15.59	19.23	18.97	24.92

There are no measurements of the photoabsorption cross section in the GDR energy region. Lepretre [Lep74] and Fultz [Ful69] measured the (γ, 1nx), (γ, 2nx), (γ, sn) and (γ, xn) reaction cross sections. Lepretre [Lep81] also measured the photoabsorption cross section for ^{nat}Sn from 25 MeV to 135 MeV. We relied on the GUNF and GNASH codes to infer the photoabsorption cross section in the GDR regime, using Lepretre's two measurements [Lep81, Lep74], in order to model all the photonuclear cross sections consistently. The photoabsorption cross section above the GDR, up to 140 MeV, was obtained from QD model calculations using the theory of Chadwick. The neutron, proton, deuteron, triton and alpha emission cross sections, as well as production cross sections, were calculated by the GNASH code.

$$\gamma + {}^{122}\text{Sn}$$

Abundance (%)	Threshold Energies (MeV)								
	γ,n	γ,p	γ,t	γ,He-3	γ,α	$\gamma,2n$	γ,np	$\gamma,2p$	$\gamma,3n$
4.63	8.81	11.39	17.16	20.94	5.66	14.98	19.51	20.55	24.09
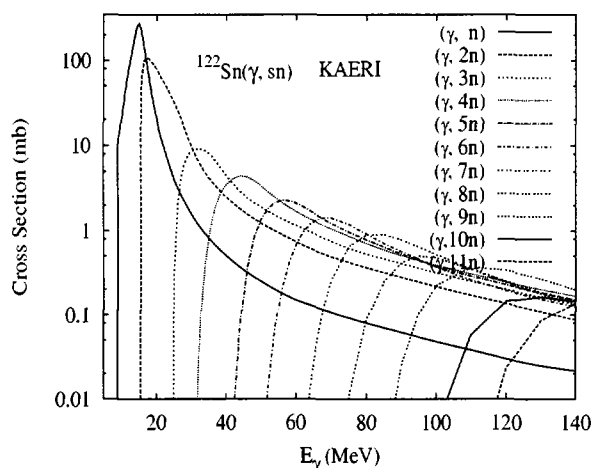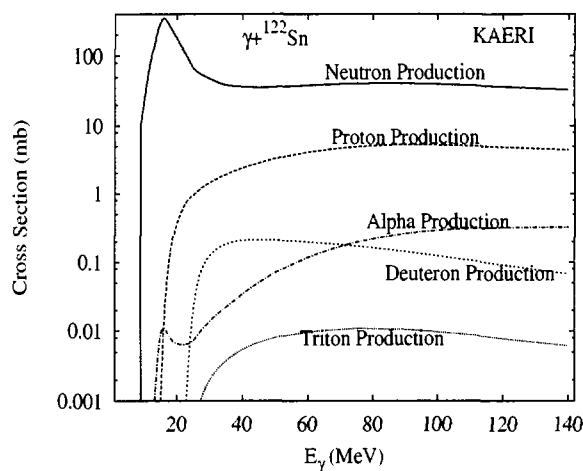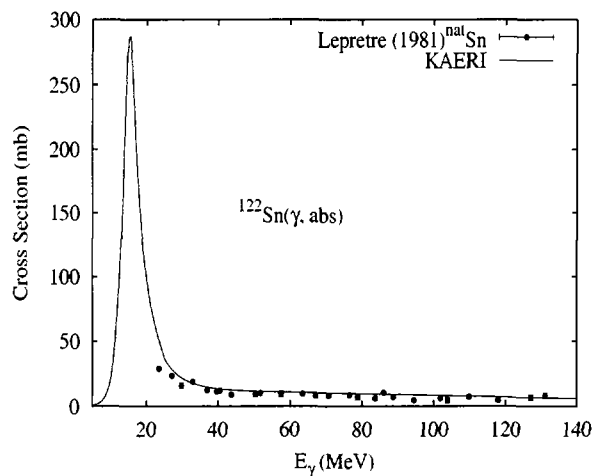
Measurements of the photoabsorption cross section, above 25 MeV, are available for ${}^{nat}\text{Sn}$ [Lep81]. The GUNF code was used to infer the photoabsorption cross section in the GDR regime, adopting the GDR parameters of ${}^{116}\text{Sn}$. The photoabsorption cross section above the GDR, up to 140 MeV, was obtained from QD model calculations using the theory of Chadwick. The neutron, proton, deuteron, triton and alpha emission cross sections, as well as production cross sections, were calculated by the GNASH code.

$$\gamma + {}^{124}\text{Sn}$$

| Abundance	Threshold Energies (MeV)								
(%)	γ,n	γ,p	γ,t	γ,He-3	γ,α	γ,2n	γ,np	γ,2p	γ,3n
5.79	8.49	12.11	17.35	22.22	6.69	14.43	20.02	21.83	23.25

There are no measurements of the photoabsorption cross section in the GDR energy region. Lepretre [Lep74] and Fultz [Ful69] measured the (γ, 1nx), (γ, 2nx), (γ, sn) and (γ, xn) reaction cross sections. Lepretre [Lep81] also measured the photoabsorption cross section for ^{nat}Sn from 25 MeV to 135 MeV. We relied on the GUNF and GNASH codes to infer the photoabsorption cross section in the GDR regime, using Lepretre's two measurements [Lep81, Lep74], in order to model all the photonuclear cross sections consistently. The photoabsorption cross section above the GDR, up to 140 MeV, was obtained from QD model calculations using the theory of Chadwick. The neutron, proton, deuteron. triton and alpha emission cross sections, as well as production cross sections, were calculated by the GNASH code.

$\gamma + {}^{121}\mathrm{Sb}$

Abundance	Threshold Energies (MeV)								
(%)	γ,n	γ,p	γ,t	γ,He-3	γ,α	γ,2n	γ,np	γ,2p	γ,3n
57.36	9.24	5.78	12.89	17.29	3.07	16.26	14.88	16.44	25.81

The photoabsorption cross section has not been measured. However, for ${}^{nat}\mathrm{Sb}$, there are experimental data for the (γ, 1nx), (γ, 2nx), (γ, sn) and (γ, xn) reaction cross sections [Lep74]. Katz reported a few points for the (γ, 1n) reaction cross section [Kat51]. We relied on the GUNF and GNASH codes to infer the photoabsorption cross section in the GDR regime, in order to model accurately the (γ, sn) data. The photoabsorption cross section above the GDR, up to 140 MeV, was obtained from QD model calculations using the theory of Chadwick.

The calculated results of the emission channels by the GNASH code are in good agreement with all the experimental data of Lepretre.

$$\gamma + {}^{123}\text{Sb}$$

Abundance (%)	Threshold Energies (MeV)								
	γ,n	γ,p	γ,t	γ,He-3	γ,α	γ,2n	γ,np	γ,2p	γ,3n
42.64	8.97	6.57	13.07	18.36	3.92	15.77	15.38	17.96	25.01

The photoabsorption cross section has not been measured. However, for ^{nat}Sb, there are experimental data for the (γ, 1nx), (γ, 2nx), (γ, sn) and (γ, xn) reaction cross sections [Lep74]. Katz reported a few points for the (γ, 1n) reaction cross section [Kat51]. We relied on the GUNF and GNASH codes to infer the photoabsorption cross section in the GDR regime, in order to model accurately the (γ, sn) data. The photoabsorption cross section above the GDR, up to 140 MeV, was obtained from QD model calculations using the theory of Chadwick.

The calculated results of the emission channels by the GNASH code are in good agreement with all the experimental data of Lepretre.

$\gamma + {}^{120}\text{Te}$

Abundance	Threshold Energies (MeV)								
(%)	γ,n	γ,p	γ,t	γ,He-3	γ,α	γ,2n	γ,np	γ,2p	γ,3n
0.10	10.28	7.20	15.69	13.92	0.28	17.88	16.75	12.31	28.49

There are no experimental data available. The photoabsorption cross section was obtained from GDR and QD model calculations, adopting the GDR parameters of ^{124}Te. The neutron, proton, deuteron, triton and alpha emission cross sections, as well as production cross sections, were calculated by the GNASH code.
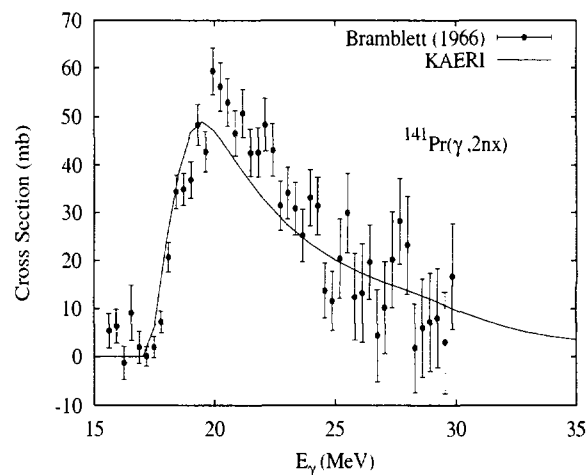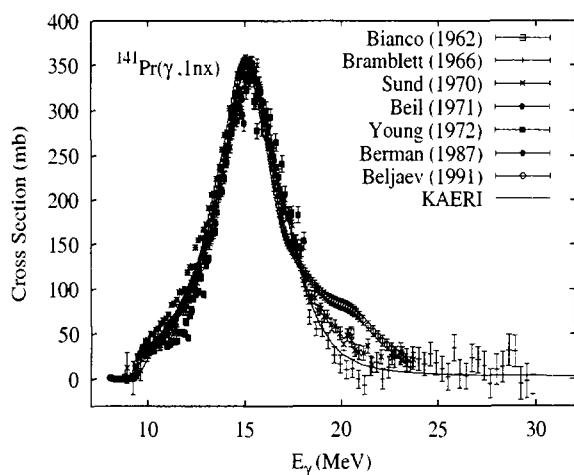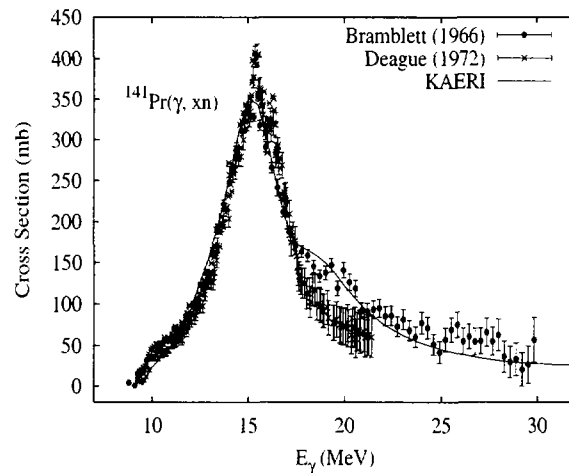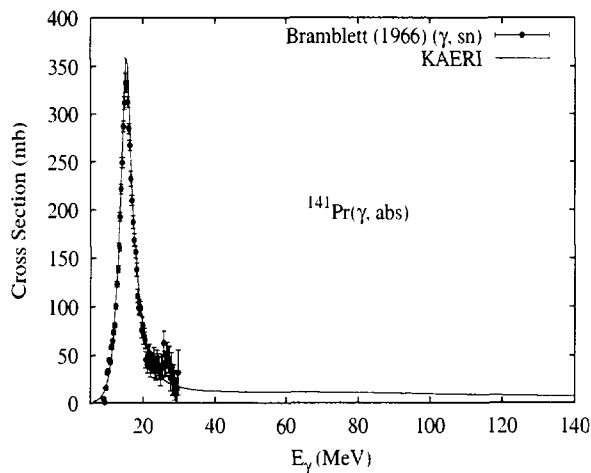
$\gamma + {}^{122}\text{Te}$

Abundance (%)	Threshold Energies (MeV)								
	γ,n	γ,p	γ,t	$\gamma,\text{He-3}$	γ,α	$\gamma,2n$	γ,np	$\gamma,2p$	$\gamma,3n$
2.59	9.83	8.00	15.78	15.17	1.08	17.06	17.24	13.78	27.34
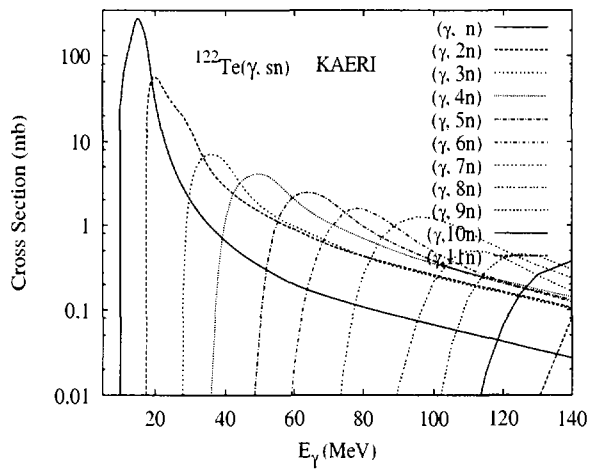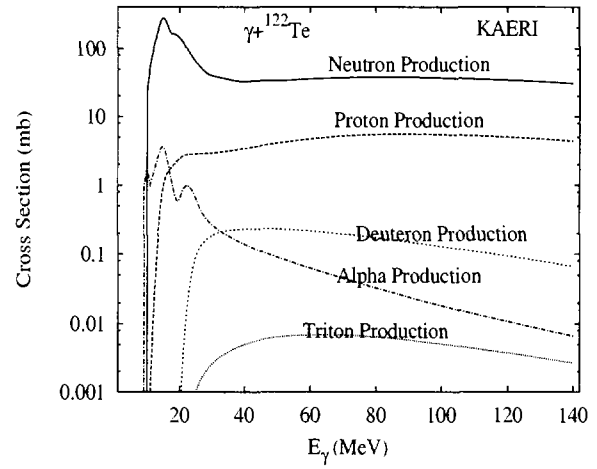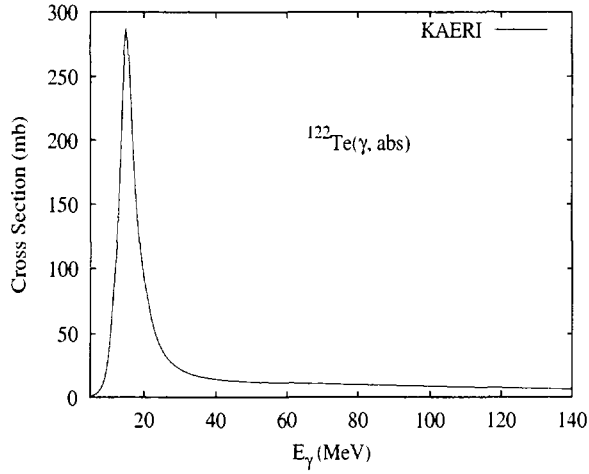
There are no experimental data available. The photoabsorption cross section was obtained from GDR and QD model calculations, adopting the GDR parameters of ${}^{124}\text{Te}$. The neutron, proton, deuteron, triton and alpha emission cross sections, as well as production cross sections, were calculated by the GNASH code.

$$\gamma + {}^{123}\text{Te}$$

Abundance	Threshold Energies (MeV)								
(%)	γ,n	γ,p	γ,t	γ,He-3	γ,α	γ,2n	γ,np	γ,2p	γ,3n
0.91	6.94	8.13	15.70	13.00	1.53	16.76	14.94	14.55	24.00

There are no experimental data available. The photoabsorption cross section was obtained from GDR and QD model calculations, adopting the GDR parameters of ^{124}Te. The neutron, proton, deuteron, triton and alpha emission cross sections, as well as production cross sections, were calculated by the GNASH code.

$\gamma + {}^{124}\text{Te}$

| Abundance (%)	Threshold Energies (MeV)								
	γ,n	γ,p	γ,t	$\gamma,\text{He-3}$	γ,α	$\gamma,2n$	γ,np	$\gamma,2p$	$\gamma,3n$
4.79	9.43	8.59	15.88	16.25	1.85	16.36	17.56	15.16	26.19

The photoabsorption cross section has not been measured. However, there are experimental data for the $(\gamma, 1nx)$, $(\gamma, 2nx)$ and (γ, xn) reaction cross sections [Lep76]. We relied on the GUNF and GNASH codes to infer the photoabsorption cross section in the GDR regime, in order to model accurately the (γ, xn) channel data. The photoabsorption cross section above the GDR, up to 140 MeV, was obtained from QD model calculations using the theory of Chadwick.

The calculated results of the emission channels by the GNASH code are in good agreement with the data for the $(\gamma, 1nx)$, $(\gamma, 2nx)$ and (γ, xn) cross sections.

$$\gamma + {}^{125}\text{Te}$$

Abundance	Threshold Energies (MeV)								
(%)	γ,n	γ,p	γ,t	γ,He-3	γ,α	γ,2n	γ,np	γ,2p	γ,3n
7.12	6.57	8.69	15.65	14.01	2.25	16.00	15.16	15.78	22.93
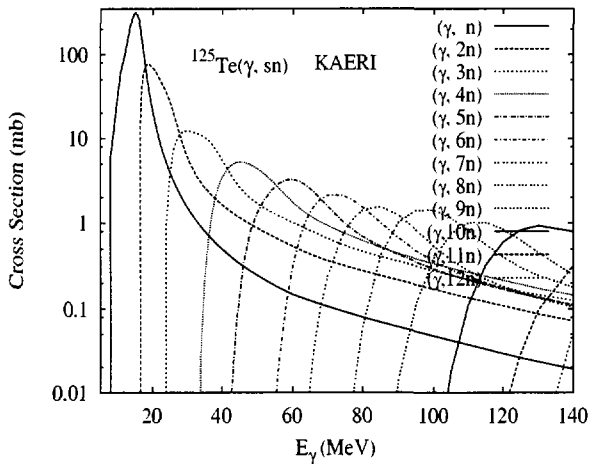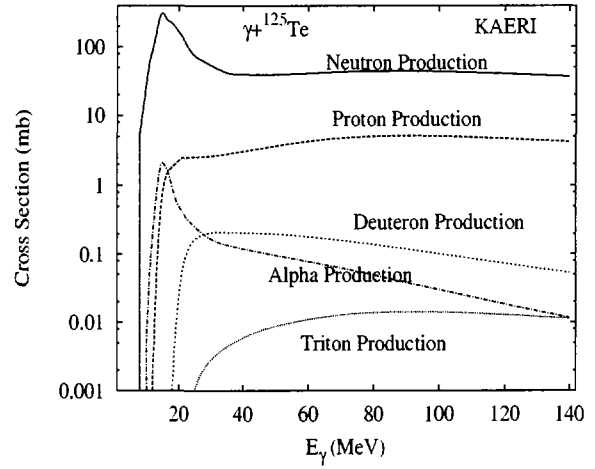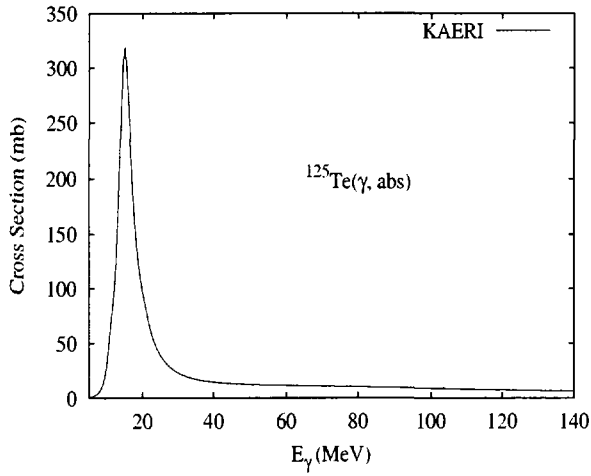
There are no experimental data available. The photoabsorption cross section was obtained from GDR and QD model calculations, adopting the GDR parameters of ${}^{126}\text{Te}$. The neutron, proton, deuteron, triton and alpha emission cross sections, as well as production cross sections, were calculated by the GNASH code.

$\gamma + {}^{126}\mathrm{Te}$

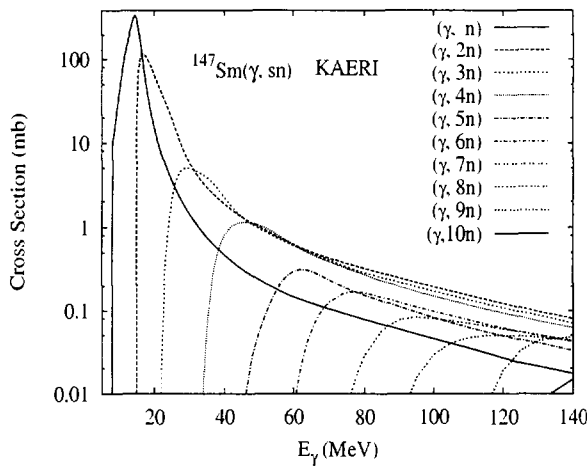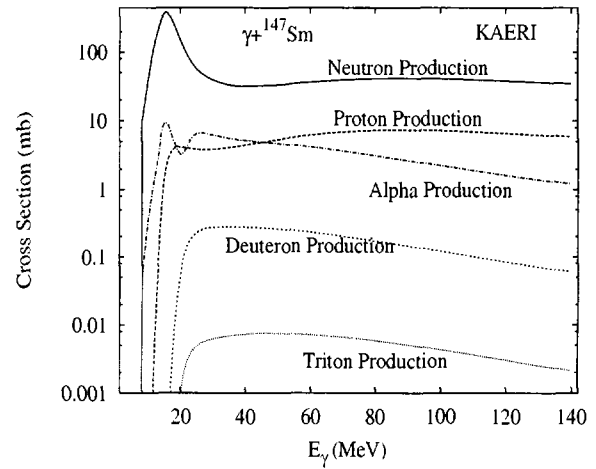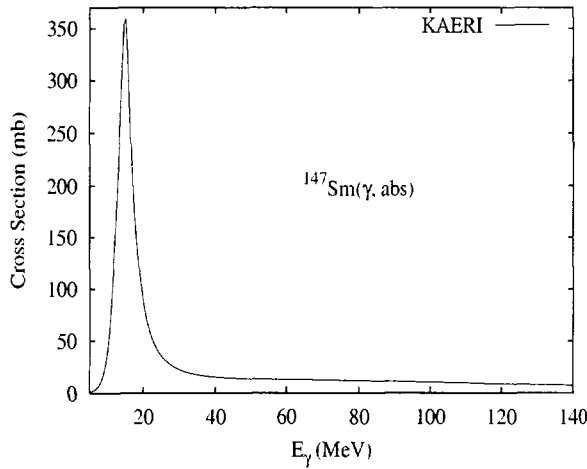| Abundance (%)	Threshold Energies (MeV)								
	γ,n	γ,p	γ,t	$\gamma,\mathrm{He\text{-}3}$	γ,α	$\gamma,2n$	γ,np	$\gamma,2p$	$\gamma,3n$
18.93	9.11	9.10	15.79	17.18	2.55	15.68	17.81	16.41	25.11

The photoabsorption cross section has not been measured. However, there are experimental data for the $(\gamma, 1nx)$, $(\gamma, 2nx)$ and (γ, xn) reaction cross sections [Lep76]. We relied on the GUNF and GNASH codes to infer the photoabsorption cross section in the GDR regime, in order to model accurately the (γ, xn) channel data. The photoabsorption cross section above the GDR, up to 140 MeV, was obtained from QD model calculations using the theory of Chadwick.

The calculated results of the emission channels by the GNASH code are in good agreement with the data for the $(\gamma, 1nx)$, $(\gamma, 2nx)$ and (γ, xn) cross sections.

$$\gamma + {}^{128}\text{Te}$$

Abundance	Threshold Energies (MeV)								
(%)	γ,n	γ,p	γ,t	γ,He-3	γ,α	γ,2n	γ,np	γ,2p	γ,3n
31.70	8.78	9.58	15.68	18.02	3.18	15.07	17.95	17.55	24.18

The photoabsorption cross section has not been measured. However, there are experimental data for the (γ, 1nx), (γ, 2nx) and (γ, xn) reaction cross sections [Lep76]. We relied on the GUNF and GNASH codes to infer the photoabsorption cross section in the GDR regime, in order to model accurately the (γ, xn) channel data. The photoabsorption cross section above the GDR, up to 140 MeV, was obtained from QD model calculations using the theory of Chadwick.

The calculated results of the emission channels by the GNASH code are in good agreement with the data for the (γ, 1nx), (γ, 2nx) and (γ, xn) cross sections.

$\gamma + {}^{130}\mathrm{Te}$

| Abundance	Threshold Energies (MeV)								
(%)	γ,n	γ,p	γ,t	γ,He-3	γ,α	γ,2n	γ,np	γ,2p	γ,3n
33.87	8.41	10.01	15.59	18.78	3.75	14.50	18.10	18.60	23.28

The photoabsorption cross section has not been measured. However, there are experimental data for the (γ, 1nx), (γ, 2nx) and (γ, xn) reaction cross sections [Lep76]. We relied on the GUNF and GNASH codes to infer the photoabsorption cross section in the GDR regime, in order to model accurately the (γ, xn) channel data. The photoabsorption cross section above the GDR, up to 140 MeV, was obtained from QD model calculations using the theory of Chadwick.

The calculated results of the emission channels by the GNASH code are in good agreement with the data for the (γ, 1nx), (γ, 2nx) and (γ, xn) cross sections.
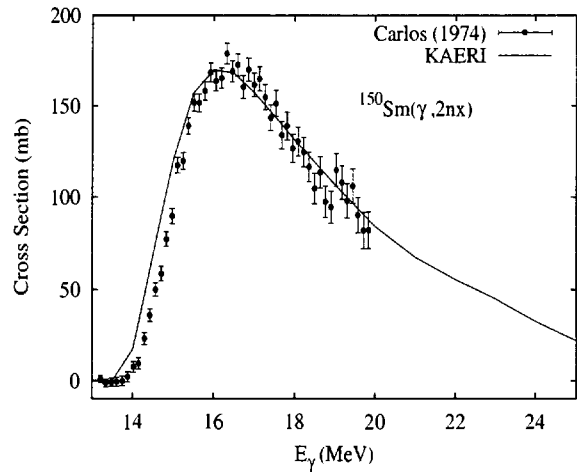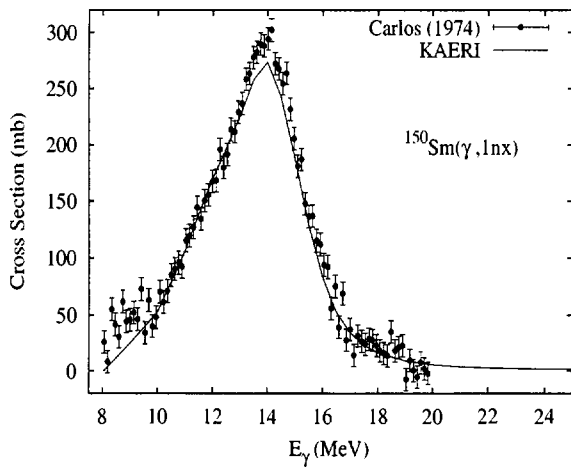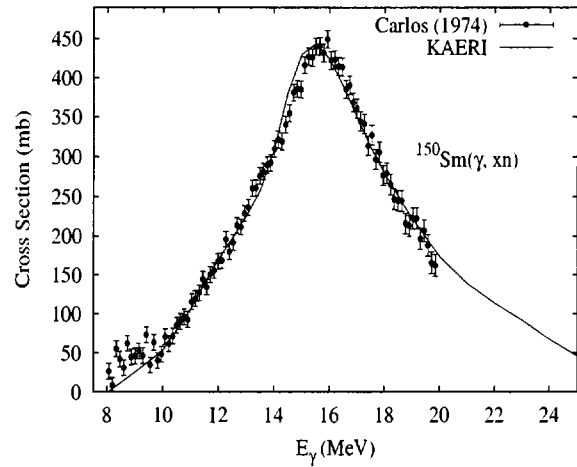
$$\gamma + {}^{127}\text{I}$$

Abundance (%)	Threshold Energies (MeV)								
	γ,n	γ,p	γ,t	γ,He-3	γ,α	γ,2n	γ,np	γ,2p	γ,3n
100.00	9.14	6.20	13.41	16.29	2.18	16.28	15.32	15.30	25.83
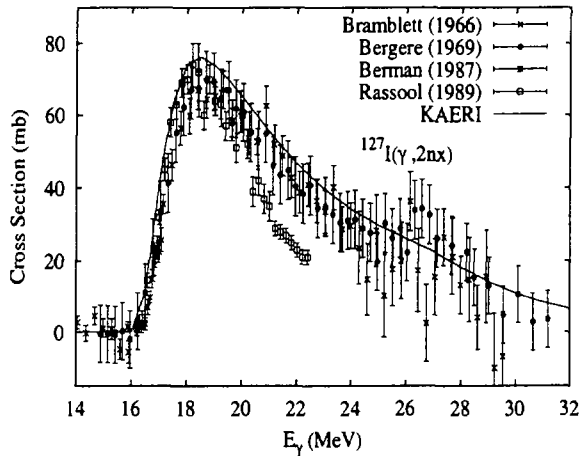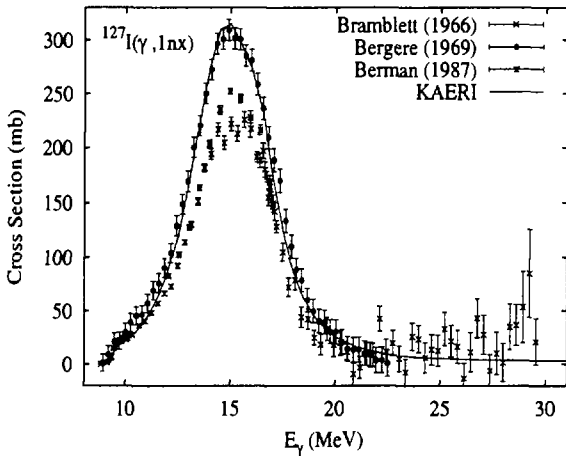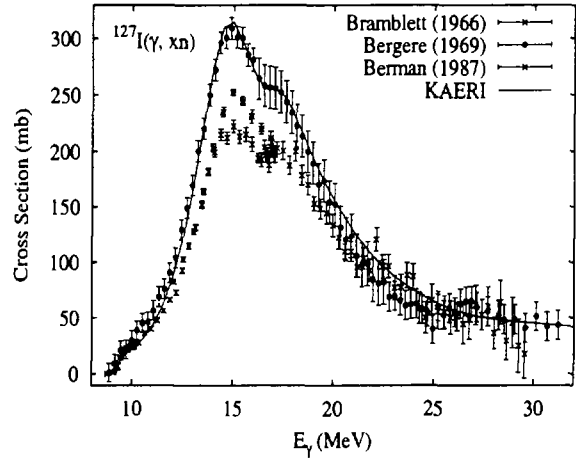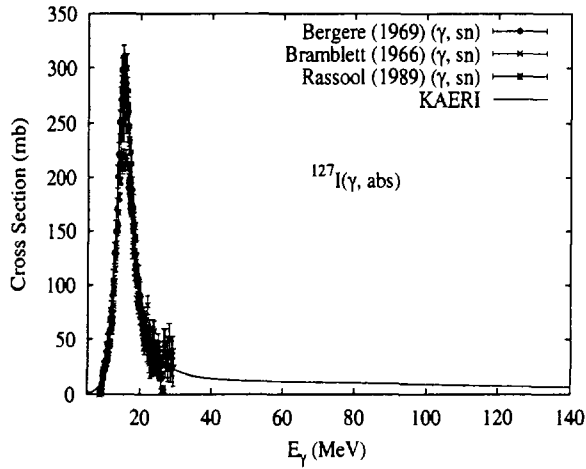
The photoabsorption cross section has not been measured. However, there are experimental data for the (γ, 1nx), (γ, 2nx), (γ,sn) and (γ, xn) reaction cross sections, from Bramblett [Bra66], Bergere [Ber69a] and Berman [Ber87]. Bramblett also reported the (γ, 3nx) cross section, and Rassool [Ras89] the (γ, 2nx) and (γ, xn) cross sections. All the measurements present good agreement as the shapes of the cross sections are concerned, but not in their magnitudes. Bramblett's and Rassool's data have good agreement in the magnitude of the (γ, sn) cross section. We relied on the GUNF and GNASH codes to infer the photoabsorption cross section in the GDR regime, in order to model accurately Bramblett's (γ, sn) data. The photoabsorption cross section above the GDR, up to 140 MeV, was obtained from QD model calculations using the theory of Chadwick.

The calculated results of the emission channels by the GNASH code are in good agreement with Bramblett's experimental data for the (γ, 1nx), (γ, 2nx), and (γ, xn) cross sections.

$$\gamma + {}^{129}\text{I}$$

Abundance (%)	Threshold Energies (MeV)								
	γ,n	γ,p	γ,t	γ,He-3	γ,α	γ,2n	γ,np	γ,2p	γ,3n
0.00	8.84	6.80	13.39	17.04	2.67	15.67	15.58	16.38	24.81
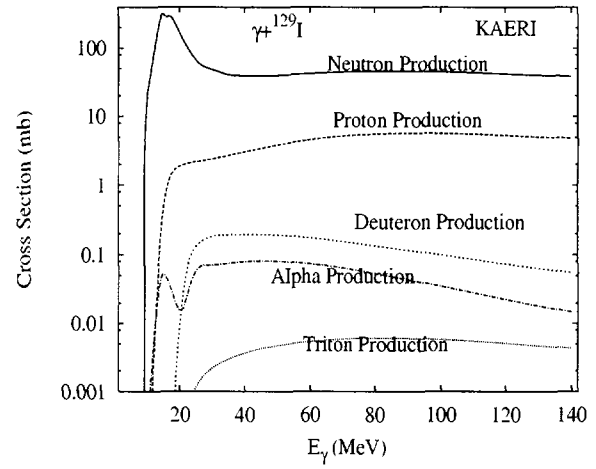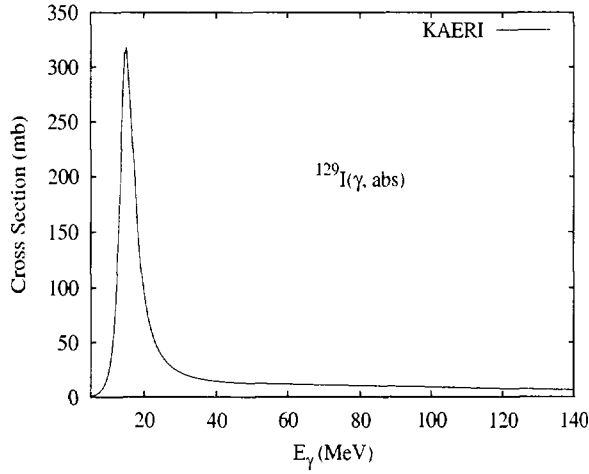
There are no experimental data available. The photoabsorption cross section was obtained from GDR and QD model calculations, adopting the GDR parameters of ^{127}I. The neutron, proton, deuteron, triton and alpha emission cross sections, as well as production cross sections, were calculated by the GNASH code.

$$\gamma + {}^{133}\text{Cs}$$

| Abundance	Threshold Energies (MeV)								
(%)	γ,n	γ,p	γ,t	γ,He-3	γ,α	γ,2n	γ,np	γ,2p	γ,3n
100.00	8.99	6.08	13.15	16.12	2.00	16.15	15.02	15.21	25.45
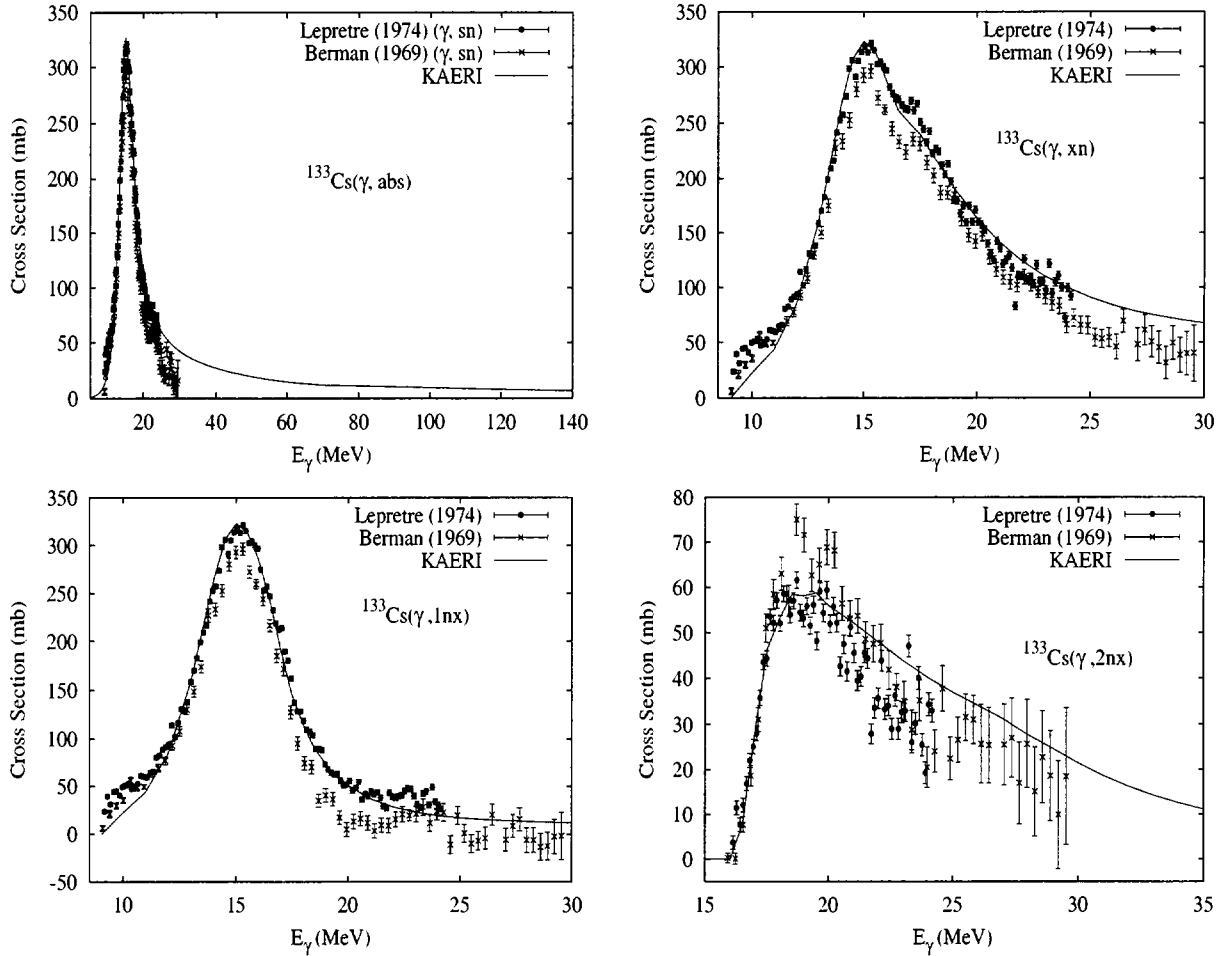
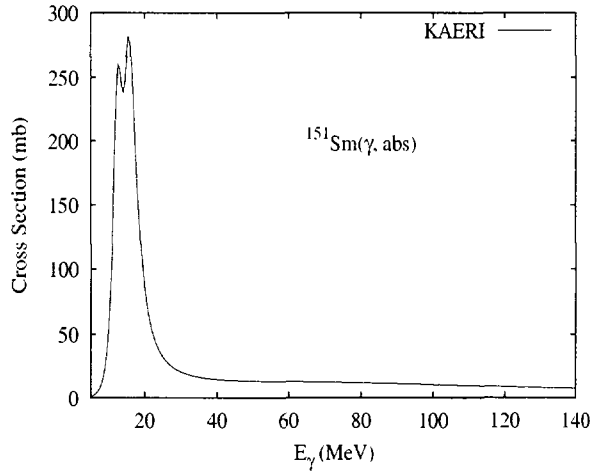

The photoabsorption cross section has not been measured. However, there are experimental data for the (γ, 1nx), (γ, 2nx), (γ,sn) and (γ, xn) reaction cross sections [Lep74, Ber69b]. Berman also reported the (γ, 3nx) cross section. All the measurements present good agreement as the shapes of the cross sections are concerned, but not in their magnitudes. However, based on the analysis [Mar97, Wol84] of the systematic differences between Saclay and Livermore data, Lepretre's measurements were used as reference. We relied on the GUNF and GNASH codes to infer the photoabsorption cross section in the GDR regime, in order to model accurately Lepretre's (γ, sn) data. The photoabsorption cross section above the GDR, up to 140 MeV, was obtained from QD model calculations using the theory of Chadwick. The calculated results of the emission channels by the GNASH code are in good agreement with the experimental data of Lepretre for (γ, 1nx), (γ, 2nx), and (γ, xn) cross sections.

$\gamma + {}^{135}\text{Cs}$

Abundance (%)	Threshold Energies (MeV)								
	γ,n	γ,p	γ,t	$\gamma,\text{He-3}$	γ,α	$\gamma,2n$	γ,np	$\gamma,2p$	$\gamma,3n$
0.00	8.83	6.83	13.32	16.88	2.63	15.72	15.36	16.35	24.71
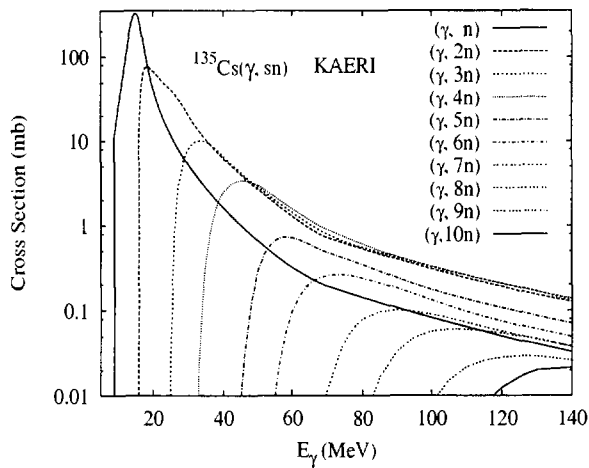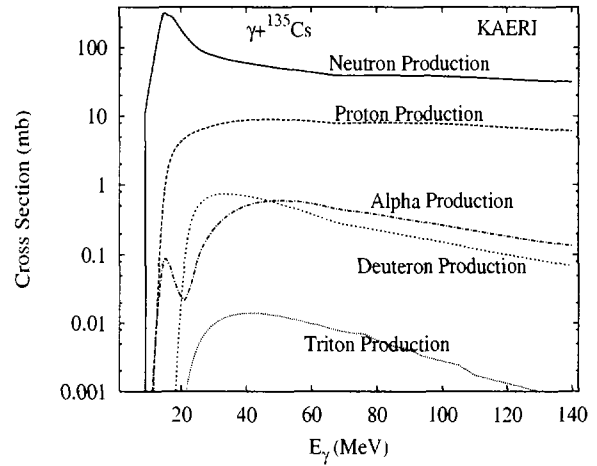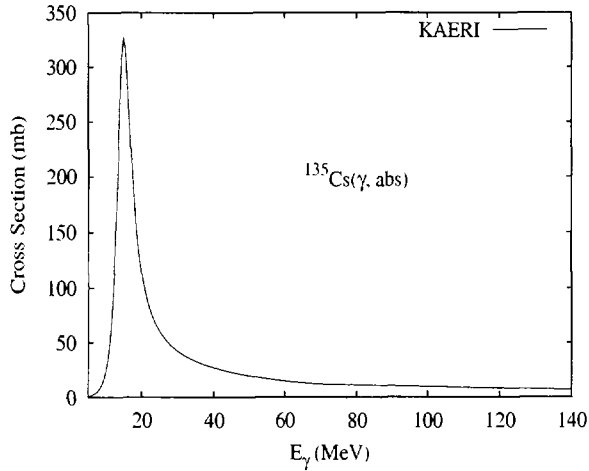
There are no experimental data available. The photoabsorption cross section was obtained from GDR and QD model calculations, adopting the GDR parameters of ^{133}Cs. The neutron, proton, deuteron, triton and alpha emission cross sections, as well as production cross sections, were calculated by the GNASH code.

$\gamma + {}^{137}\text{Cs}$

Abundance (%)	Threshold Energies (MeV)								
	γ,n	γ,p	γ,t	γ,He-3	γ,α	γ,2n	γ,np	γ,2p	γ,3n
0.00	8.27	7.42	13.38	17.50	3.09	15.04	15.41	17.31	23.86

There are no experimental data available. The photoabsorption cross section was obtained from GDR and QD model calculations, adopting the GDR parameters of ${}^{133}\text{Cs}$. The neutron, proton, deuteron, triton and alpha emission cross sections, as well as production cross sections, were calculated by the GNASH code.

γ + ^{141}Pr

| Abundance (%)	Threshold Energies (MeV)								
	γ,n	γ,p	γ,t	γ,He-3	γ,α	γ,2n	γ,np	γ,2p	γ,3n
100.00	9.40	5.23	13.40	14.43	1.32	17.32	14.41	13.37	27.10

The photoabsorption cross section has not been measured. However, there are six different measurements of the (γ 1nx) reaction cross section [Bia62, Bra66, Sun70, Bei71, You72, Ber87, Bel91]. Bramblett also measured the (γ, 2nx), (γ, 3nx), (γ, sn) and (γ, xn) cross sections. Deague [Dea72] measured the (γ, xn) reaction cross section [Dea72]. Bramblett's measurements were chosen as the reference data, since most of the photoneutron reactions were included. We relied on the GUNF and GNASH codes to infer the photoabsorption cross section in the GDR regime, in order to model accurately Bramblett's (γ, 1nx) data. The photoabsorption cross section above the GDR, up to 140 MeV, was obtained from QD model calculations using the theory of Chadwick.

The calculated results of the emission channels by the GNASH code are in good agreement with the Bramblett data for the (γ, 1nx), (γ, 2nx), (γ, sn), and (γ, xn) cross sections.

$\gamma + {}^{144}\mathrm{Sm}$

Abundance (%)	Threshold Energies (MeV)								
	γ,n	γ,p	γ,t	$\gamma,\mathrm{He}\text{-}3$	γ,α	$\gamma,2\mathrm{n}$	γ,np	$\gamma,2\mathrm{p}$	$\gamma,3\mathrm{n}$
3.10	10.52	6.29	16.45	12.70	-0.07	19.13	16.25	10.59	30.25
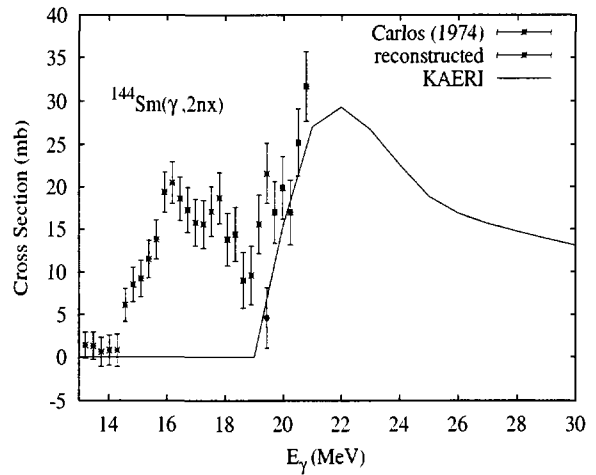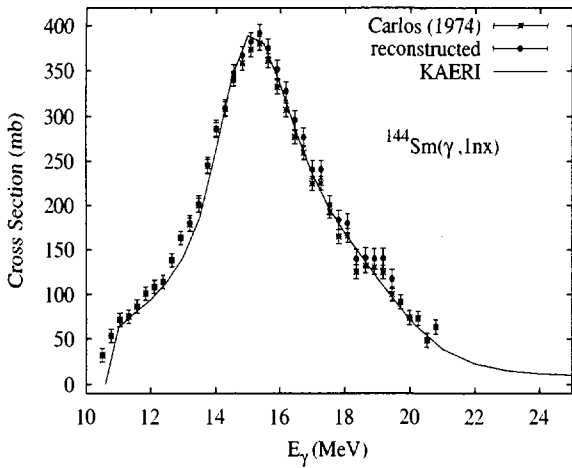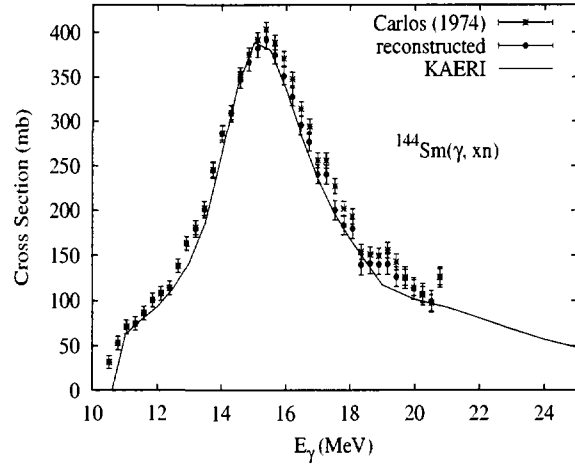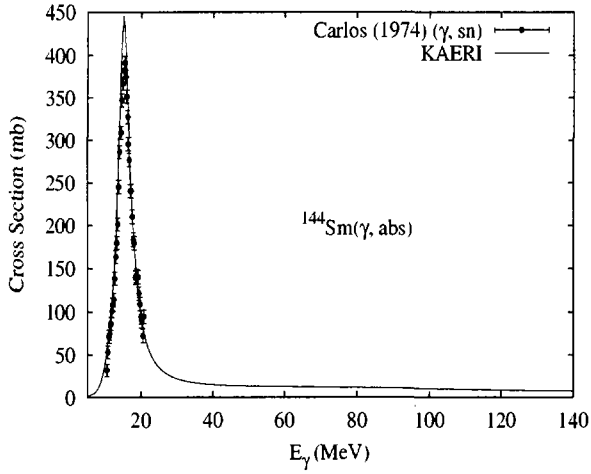
The photoabsorption cross section has not been measured. However, there are experimental data for the $(\gamma,\ 1\mathrm{nx})$, $(\gamma,\ 2\mathrm{nx})$, $(\gamma,\ \mathrm{sn})$ and $(\gamma,\ \mathrm{xn})$ reaction cross section [Car74]. However, the $(\gamma,\ 2\mathrm{nx})$ reaction data do not correspond to the threshold energy of $(\gamma,\ 2\mathrm{n}+2\mathrm{np})$, 19.13 MeV. The $(\gamma,\ 1\mathrm{nx})$, $(\gamma,\ 2\mathrm{nx})$ and $(\gamma,\ \mathrm{xn})$ reaction data were fixed by converting $(\gamma,\ 2\mathrm{nx})$ cross sections below the threshold energy into the $(\gamma,\ 1\mathrm{nx})$ cross sections. We relied on the GUNF and GNASH codes to infer the photoabsorption cross section in the GDR regime, in order to model accurately the $(\gamma,\ \mathrm{sn})$ reaction data. The photoabsorption cross section above the GDR, up to 140 MeV, was obtained from QD model calculations using the theory of Chadwick.

The calculated results of the emission channels by the GNASH code are in good agreement with the fixed experimental data for $(\gamma,\ 1\mathrm{nx})$, $(\gamma,\ 2\mathrm{nx})$ and $(\gamma,\ \mathrm{xn})$ reaction cross sections.

$\gamma + {}^{147}\text{Sm}$

Abundance	Threshold Energies (MeV)								
(%)	γ,n	γ,p	γ,t	γ,He-3	γ,α	γ,2n	γ,np	γ,2p	γ,3n
15.00	6.35	7.11	12.80	10.45	-2.31	14.76	13.36	12.41	21.52

There are no experimental data available. The photoabsorption cross section was obtained from GDR and QD model calculations, adopting the GDR parameters of ^{148}Sm. The neutron, proton, deuteron, triton and alpha emission cross sections, as well as production cross sections, were calculated by the GNASH code.

γ + ^{148}Sm

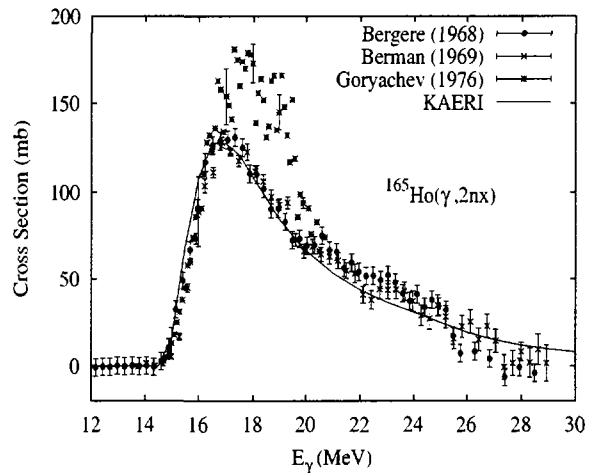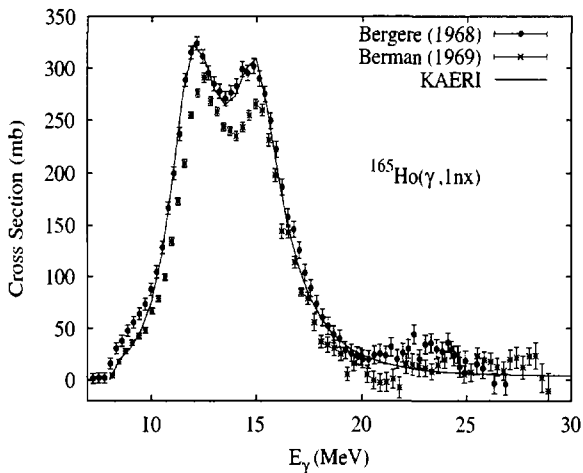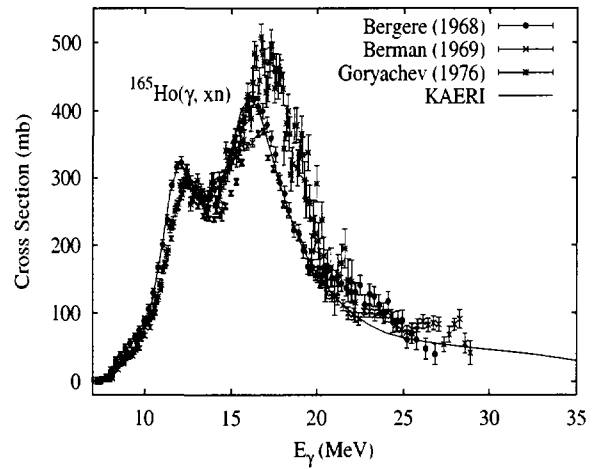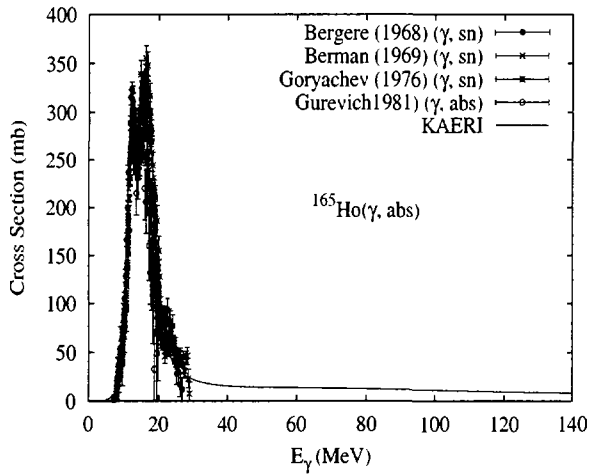| Abundance	Threshold Energies (MeV)								
(%)	γ,n	γ,p	γ,t	γ,He-3	γ,α	γ,2n	γ,np	γ,2p	γ,3n
11.30	8.14	7.58	13.02	12.84	-1.99	14.49	15.25	12.99	22.90

The photoabsorption cross section has not been measured. However, there are experimental data for the (γ, 1nx), (γ, 2nx), (γ, sn) and (γ, xn) reaction cross sections [Car74]. We relied on the GUNF and GNASH codes to infer the photoabsorption cross section in the GDR regime, in order to model accurately the (γ, sn) data. The photoabsorption cross section above the GDR, up to 140 MeV, was obtained from QD model calculations using the theory of Chadwick.

The calculated results of the emission channels by the GNASH code are in good agreement with the data for the (γ, 1nx), (γ, 2nx) and (γ, xn) cross sections.

$$\gamma + {}^{149}\text{Sm}$$

Abundance	Threshold Energies (MeV)								
(%)	γ,n	γ,p	γ,t	γ,He-3	γ,α	γ,2n	γ,np	γ,2p	γ,3n
13.80	5.87	7.56	12.64	11.14	-1.87	14.01	13.45	13.57	20.36
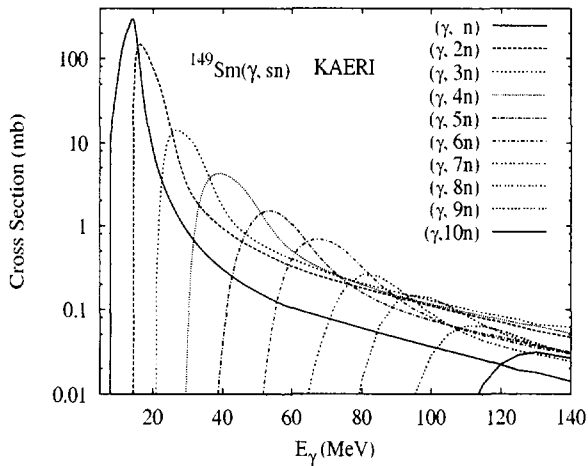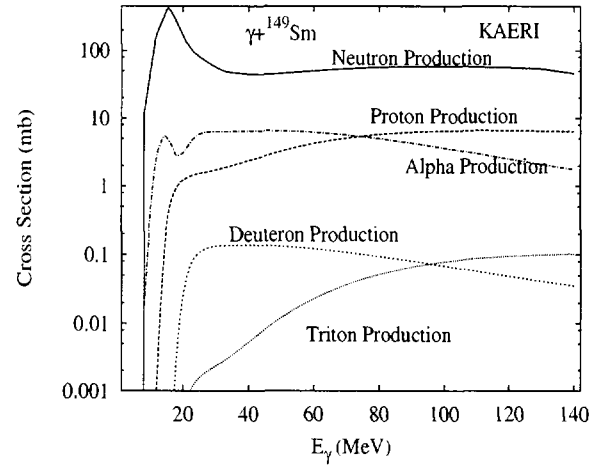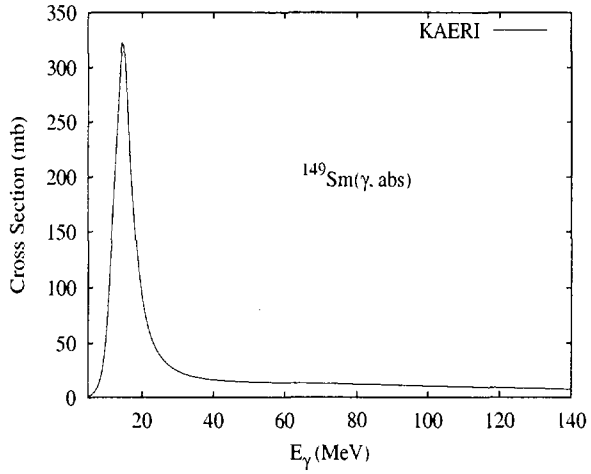
There are no experimental data available. The photoabsorption cross section was obtained from GDR and QD model calculations, adopting the GDR parameters of ${}^{150}\text{Sm}$. The neutron, proton, deuteron, triton and alpha emission cross sections, as well as production cross sections, were calculated by the GNASH code.

$\gamma + {}^{150}\text{Sm}$

Abundance	Threshold Energies (MeV)								
(%)	γ,n	γ,p	γ,t	γ,He-3	γ,α	γ,2n	γ,np	γ,2p	γ,3n
7.40	7.99	8.28	12.96	13.84	-1.45	13.86	15.55	14.22	22.00

The photoabsorption cross section has not been measured. However, there are experimental data for the (γ, 1nx), (γ, 2nx), (γ, sn) and (γ, xn) reaction cross sections [Car74]. We relied on the GUNF and GNASH codes to infer the photoabsorption cross section in the GDR regime, in order to model accurately the (γ, sn) data. The photoabsorption cross section above the GDR, up to 140 MeV, was obtained from QD model calculations using the theory of Chadwick.

The calculated results of the emission channels by the GNASH code are in good agreement with the data for the (γ, 1nx), (γ, 2nx) and (γ, xn) cross sections.

$\gamma + {}^{151}\mathrm{Sm}$

Abundance	Threshold Energies (MeV)								
(%)	$\gamma,$n	$\gamma,$p	$\gamma,$t	$\gamma,$He-3	γ,α	$\gamma,$2n	$\gamma,$np	$\gamma,$2p	$\gamma,$3n
0.00	5.60	8.27	12.66	12.10	-1.14	13.58	13.87	14.78	19.46
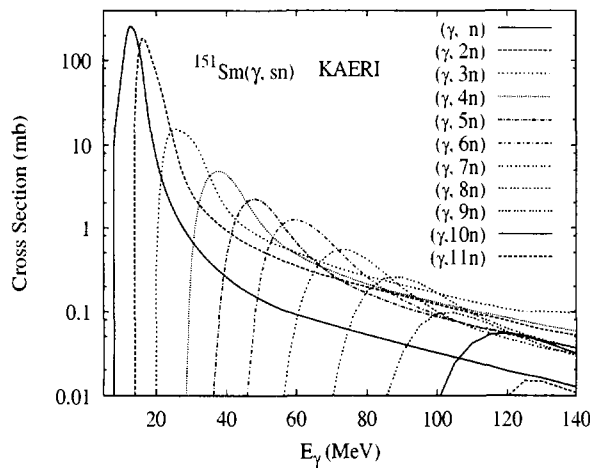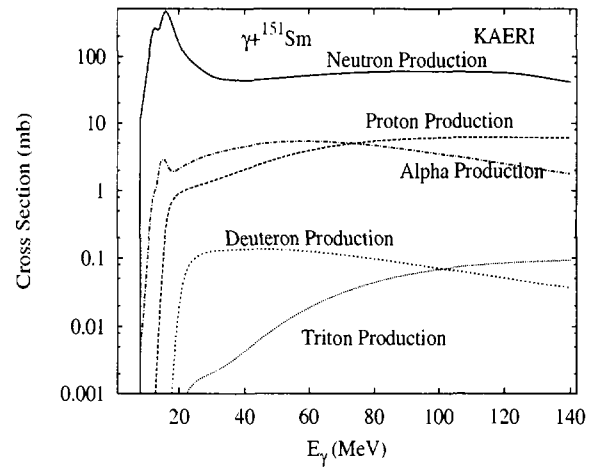
There are no experimental data available. The photoabsorption cross section was obtained from GDR and QD model calculations, adopting the GDR parameters of $^{152}\mathrm{Sm}$. The neutron, proton, deuteron, triton and alpha emission cross sections, as well as production cross sections, were calculated by the GNASH code.

$\gamma + {}^{152}\mathrm{Sm}$

| Abundance | Threshold Energies (MeV) | | | | | | | | |
(%)	γ,n	γ,p	γ,t	$\gamma,\mathrm{He\text{-}3}$	γ,α	$\gamma,\mathrm{2n}$	γ,np	$\gamma,\mathrm{2p}$	$\gamma,\mathrm{3n}$
26.70	8.26	8.66	13.65	15.32	-0.22	13.86	16.53	15.66	21.84

The photoabsorption cross section has not been measured. However, there are experimental data for the (γ, 1nx), (γ, 2nx), (γ, sn) and (γ, xn) reaction cross sections [Car74]. We relied on the GUNF and GNASH codes to infer the photoabsorption cross section in the GDR regime, in order to model accurately the (γ, sn) data. The photoabsorption cross section above the GDR, up to 140 MeV, was obtained from QD model calculations using the theory of Chadwick.

The calculated results of the emission channels by the GNASH code are in good agreement with the data for the (γ, 1nx), (γ, 2nx) and (γ, xn) cross sections.

$\gamma + {}^{154}\mathrm{Sm}$

Abundance (%)	Threshold Energies (MeV)								
	$\gamma,$n	$\gamma,$p	$\gamma,$t	$\gamma,$He-3	γ,α	$\gamma,$2n	$\gamma,$np	$\gamma,$2p	$\gamma,$3n
22.70	7.97	9.09	14.02	16.44	1.20	13.83	16.56	16.88	22.09
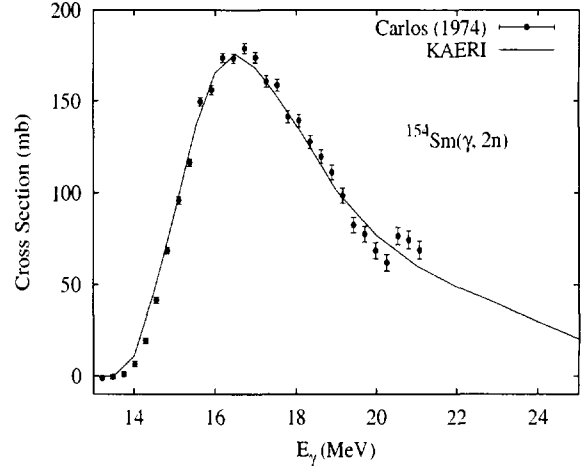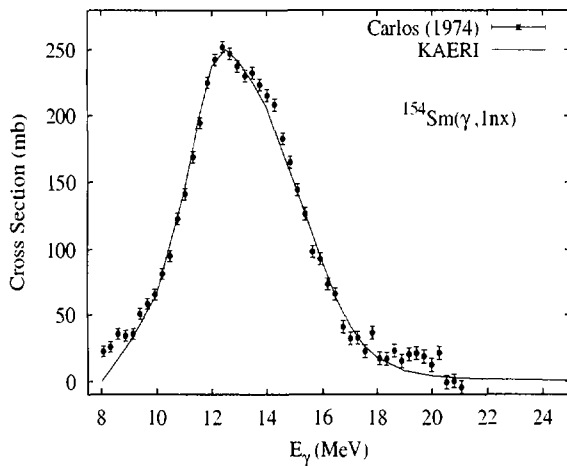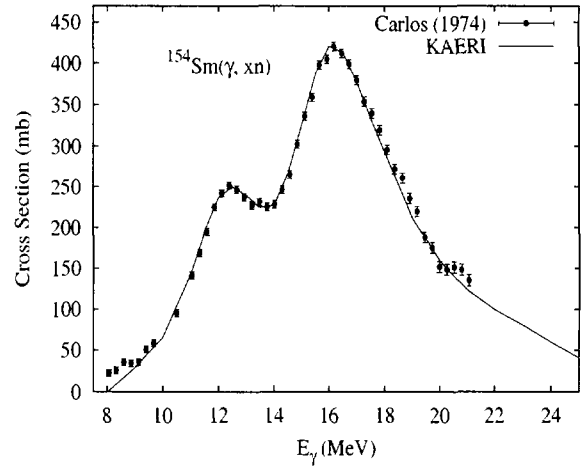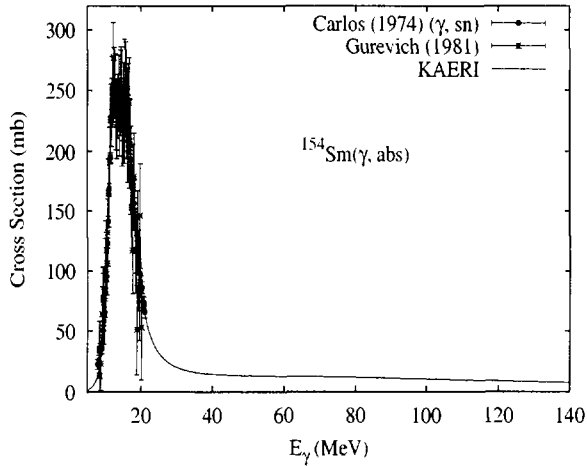
The experimental data for absorption cross section were given by Gurevich [Gur81]. Carlos [Car74] measured the (γ, lnx), $(\gamma, \mathrm{2nx})$, (γ, sn) and (γ, xn) reaction cross section. Gurecvich's absorption cross section has larger errors than Carlos's (γ, sn) data. We relied on the GUNF and GNASH codes to infer the photoabsorption cross section in the GDR regime, in order to model accurately Carlos's (γ, sn) data. The photoabsorption cross The absorption cross section above the GDR, up to 140 MeV, was taken from QD model calculations.

The calculated results of the emission channels by the GNASH code are in good agreement with the experimental data for (γ, lnx), $(\gamma, \mathrm{2nx})$ and (γ, xn) reaction cross sections.

$\gamma + {}^{158}\text{Tb}$

Abundance	Threshold Energies (MeV)								
(%)	γ,n	γ,p	γ,t	$\gamma,\text{He-3}$	γ,α	$\gamma,2n$	γ,np	$\gamma,2p$	$\gamma,3n$
0.00	6.78	5.94	12.35	12.58	0.16	15.52	12.29	13.96	22.43
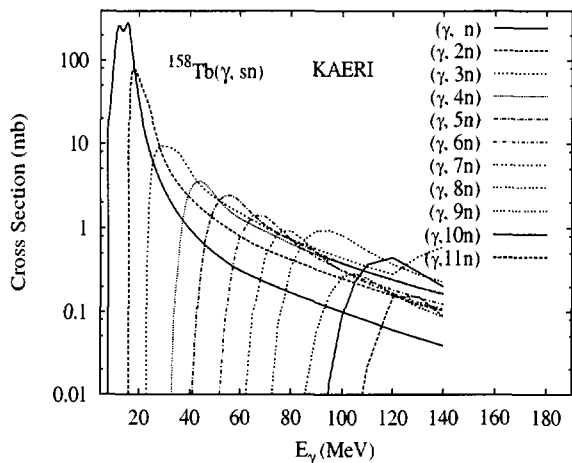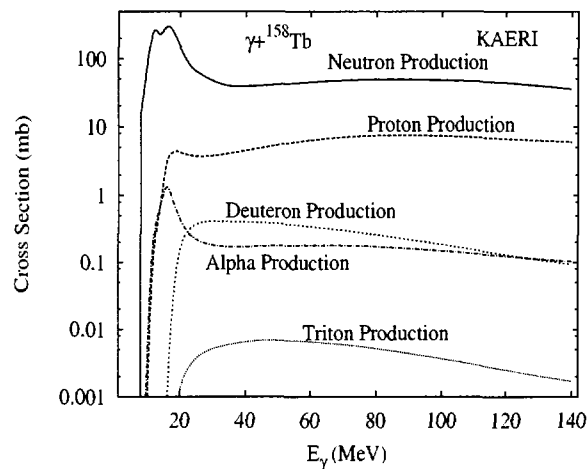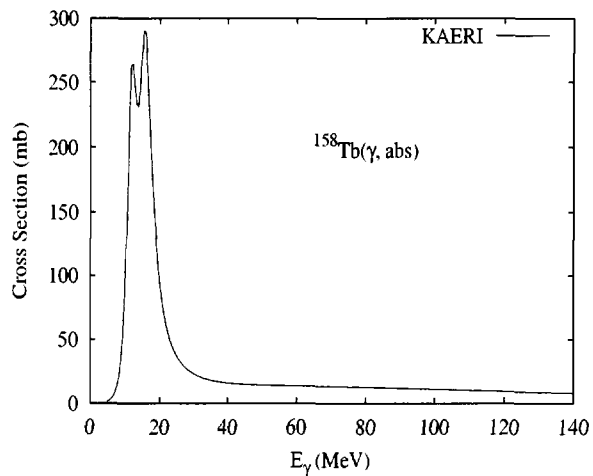
There are no experimental data available. The photoabsorption cross section was obtained from GDR and QD model calculations, adopting the GDR parameters of ${}^{159}\text{Tb}$. The neutron, proton, deuteron, triton and alpha emission cross sections, as well as production cross sections, were calculated by the GNASH code.

$\gamma + {}^{159}\text{Tb}$

Abundance (%)	Threshold Energies (MeV)								
	γ,n	γ,p	γ,t	$\gamma,\text{He-3}$	γ,α	$\gamma,2n$	γ,np	$\gamma,2p$	$\gamma,3n$
100.00	8.13	6.13	11.95	14.38	0.14	14.91	14.07	14.65	23.65
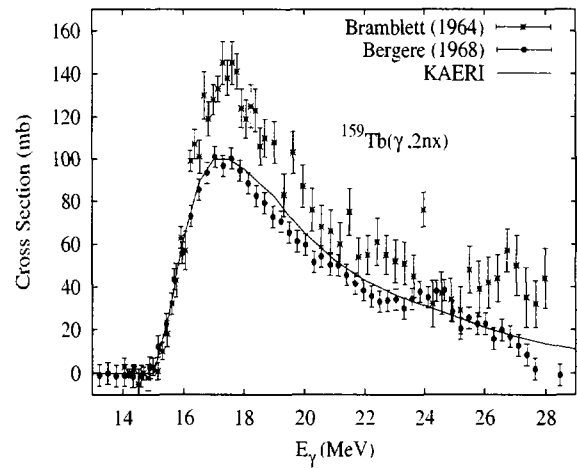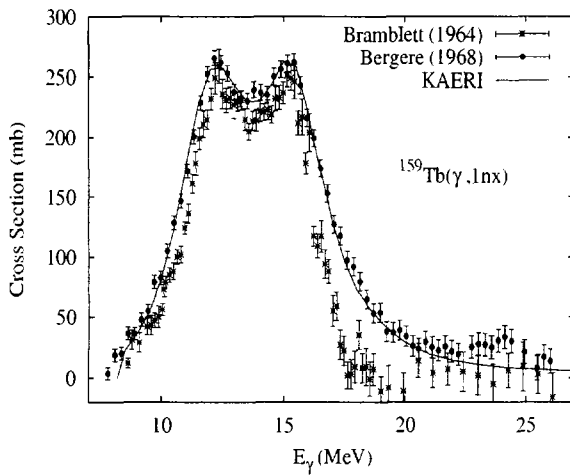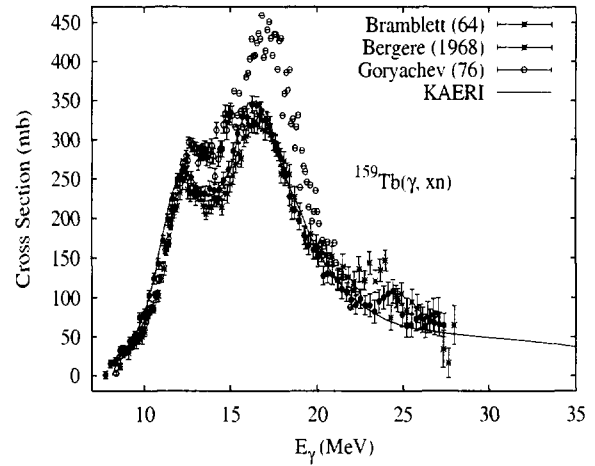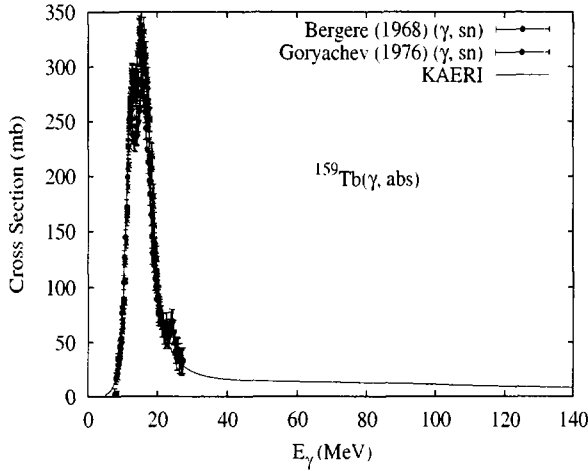
The photoabsorption cross section has not been measured. However, there are experimental data for the (γ, 1nx), (γ, 2nx) and (γ, xn) reaction cross sections [Bra64, Ber68]. Bergere also reported the (γ, sn) cross section, and Goryachev [Gor76] reported both the (γ, sn) and (γ, xn) cross sections. The experiments present good agreement on the shape of the cross sections but their magnitudes are different. We relied on the GUNF and GNASH codes to infer the photoabsorption cross section in the GDR regime, in order to model accurately Bergere's (γ, sn) data. The photoabsorption cross section above the GDR, up to 140 MeV, was obtained from QD model calculations using the theory of Chadwick.

The calculated results of the emission channels by the GNASH code are in good agreement with the Bergere data for the (γ, 1nx), (γ, 2nx) and (γ, xn) cross sections.

$$\gamma + {}^{165}\text{Ho}$$

Abundance (%)	Threshold Energies (MeV)								
	γ,n	γ,p	γ,t	γ,He-3	γ,α	γ,2n	γ,np	γ,2p	γ,3n
100.00	7.99	6.22	11.67	14.16	-0.14	14.66	13.88	14.79	23.07

The photoabsorption cross section was measured by Gurevich [Gur76, Gur80]. Bergere [Ber68] and Berman [Ber69c] measured the (γ, 1nx), (γ, 2nx), (γ, 3nx), (γ, sn) and (γ, xn) reaction cross sections. Goryachev [Gor76] reported results for the (γ, 2nx), (γ, sn) and (γ, xn) cross sections. Gurecvich's absorption cross sections are lower and have larger errors than the other (γ, sn) data above 10 MeV. We relied on the GUNF and GNASH codes to infer the photoabsorption cross section in the GDR regime, in order to model accurately Bergere's (γ, sn) data. The photoabsorption cross section above the GDR, up to 140 MeV, was obtained from QD model calculations using the theory of Chadwick.

The calculated results of the emission channels by the GNASH code are in good agreement with the Bergere data for the (γ, 1nx), (γ, 2nx) and (γ, xn) cross sections.

$\gamma + {}^{181}\text{Ta}$

Abundance	Threshold Energies (MeV)								
(%)	γ,n	γ,p	γ,t	$\gamma.\text{He-3}$	γ,α	$\gamma,2n$	γ,np	$\gamma,2p$	$\gamma,3n$
99.99	7.58	5.94	10.95	13.04	-1.53	14.22	13.33	13.91	22.13
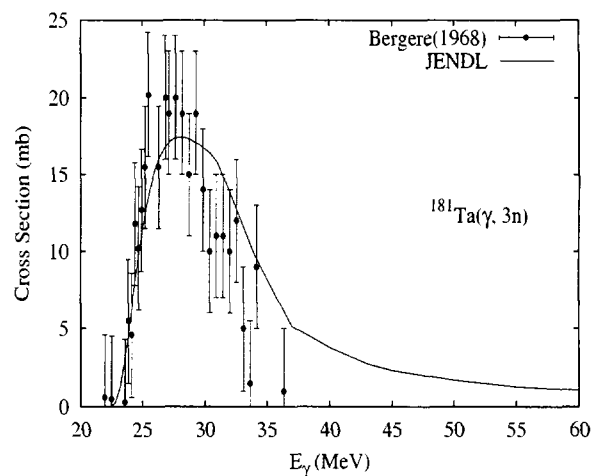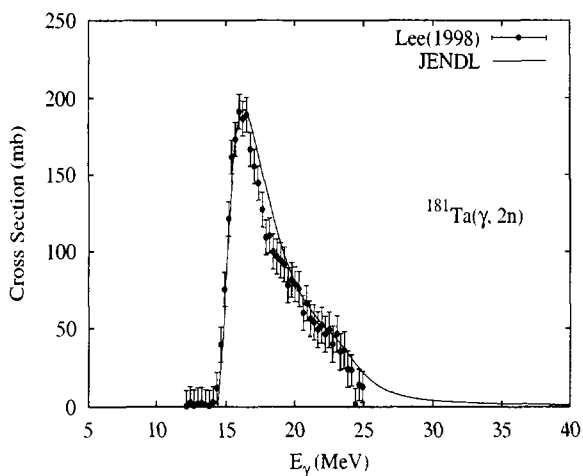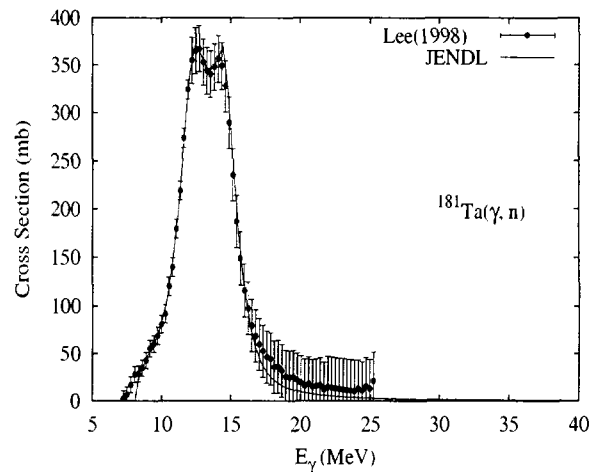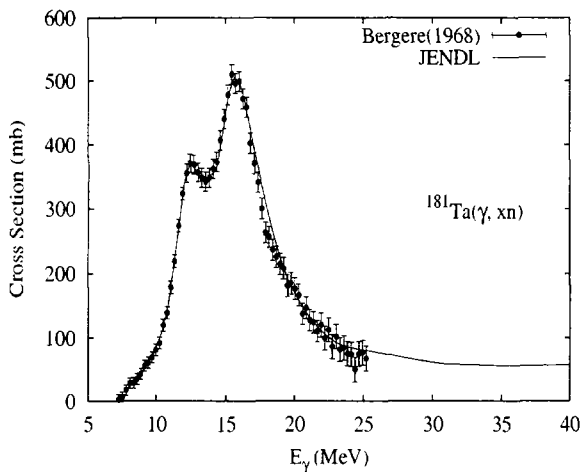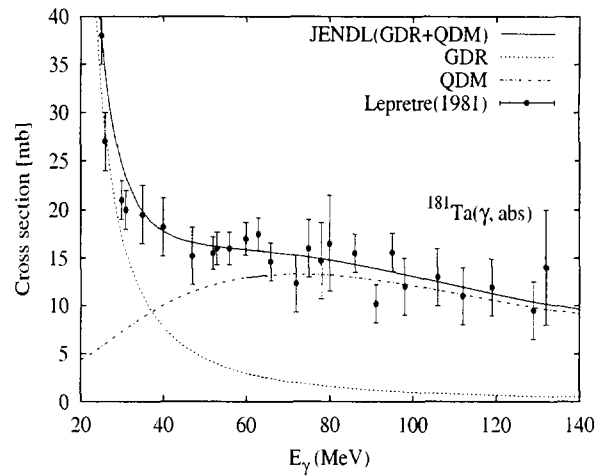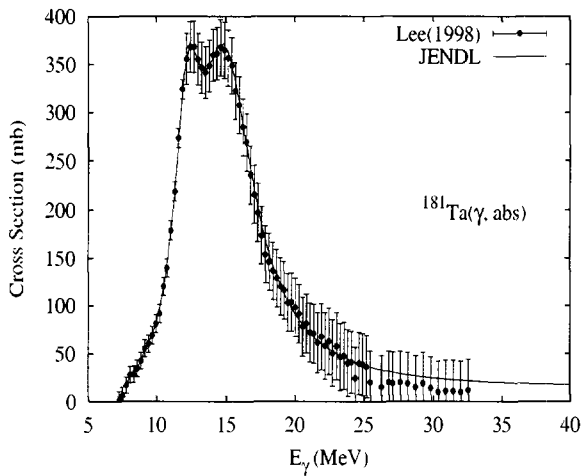
A study by Sao Paulo laboratory [Mar97, Wol84] showed that the differences between the Saclay [Ber68] and Livermore [Bra63] photoneutron cross sections arose from the incomplete separation of the partial cross section from the total neutron counts (neutron multiplicities sorting). It is noted that the neutron multiplicity sorting at Livermore is correct, while the excess (γ,n)

cross section in the Saclay measurement is caused by interpreting each (γ,2n) event as two (γ,n) events. However, the magnitude of the Livermore data is too low by a factor of 1.22. According to these arguments, new reference experimental data for (γ,n) and (γ,2n) are constructed as is (γ,abs) from Livermore measurements, but the (γ,3n) and (γ,xn) Saclay data remain unchanged [Lee98]. The reconstructed photoabsorption cross section are fitted by the GDR below 40 MeV, and by Levinger parameter of L = 6.5 with the Pauli-blocking effect [Cha91] which reproduces Lepretre's data [Lep81] well.

The ALICE-F [Fuk92] code was adopted for the theoretical evaluation of decaying processes by the use of the evaluated photoabsorption cross sections given as input, with the default parameters and options in principle except the level density parameter, which was adjusted as 11. The calculated results reproduce the experimental data of all the photoneutron cross sections consistently.

$$\gamma + {}^{180}\text{W}$$

Abundance	Threshold Energies (MeV)								
(%)	γ,n	γ,p	γ,t	$\gamma,\text{He-3}$	γ,α	$\gamma,2n$	γ,np	$\gamma,2p$	$\gamma,3n$
0.12	8.41	6.57	12.87	11.69	-2.51	15.35	14.48	11.78	23.57

There are no experimental data available. The photoabsorption cross section was obtained from GDR model calculations using the GUNF code [Zha98], adopting the same model parameters of ${}^{182,184,186}\text{W}$.

244

$$\gamma + {}^{182}\text{W}$$

Abundance	Threshold Energies (MeV)								
(%)	γ,n	γ,p	γ,t	γ,He-3	γ,α	γ,2n	γ,np	γ,2p	γ,3n
26.30	8.07	7.10	12.83	12.71	-1.77	14.75	14.67	13.04	23.16
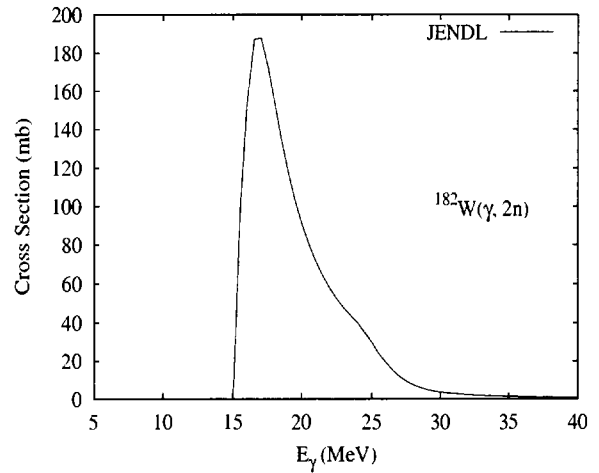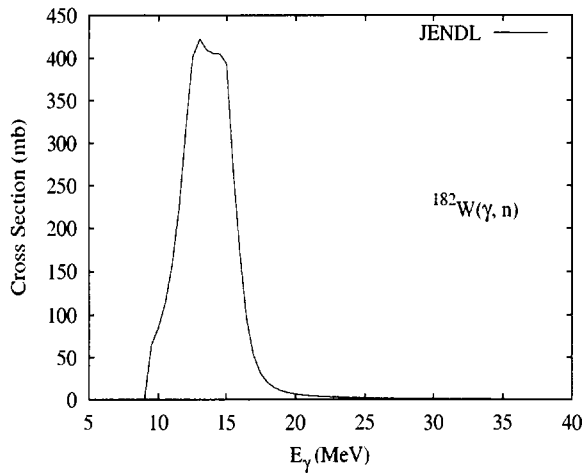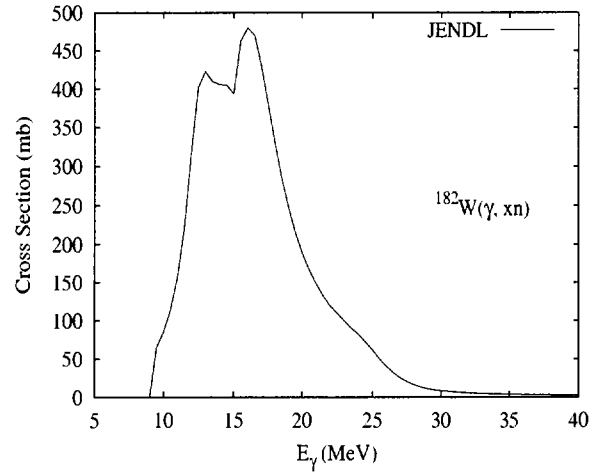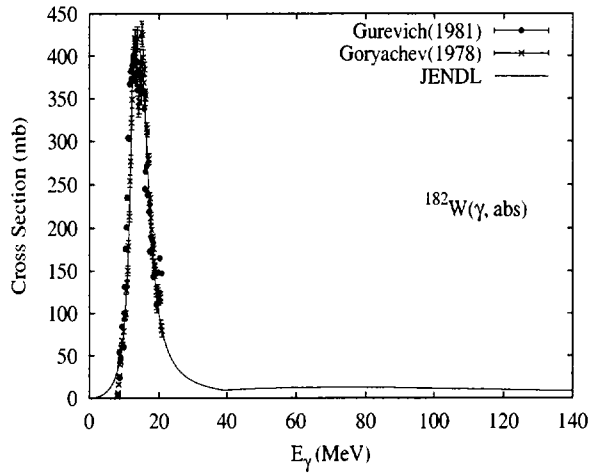
Photonuclear reactions were evaluated using ALICE-F [Fuk93] code calculations together with experimental data. Input model parameters were adjusted so as to improve the quality of the calculated results compared with data [Gor78, Gur81]. Photoabsorption was modeled as a sum of GDR and QD components [Cha91].

$$\gamma + {}^{183}\text{W}$$

Abundance	Threshold Energies (MeV)								
(%)	γ,n	γ,p	γ,t	γ,He-3	γ,α	γ,2n	γ,np	γ,2p	γ,3n
14.28	6.19	7.22	12.38	11.51	-1.68	14.26	13.29	13.53	20.94

There are no experimental data available. The photoabsorption cross section was obtained from GDR model calculations using the GUNF code [Zha98], adopting the same model parameters of ${}^{182,184,186}\text{W}$.

246

$$\gamma + {}^{184}\text{W}$$

Abundance	Threshold Energies (MeV)								
(%)	γ,n	γ,p	γ,t	$\gamma,\text{He-3}$	γ,α	$\gamma,2n$	γ,np	$\gamma,2p$	$\gamma,3n$
30.70	7.41	7.70	12.22	13.22	-1.66	13.60	14.63	14.23	21.67
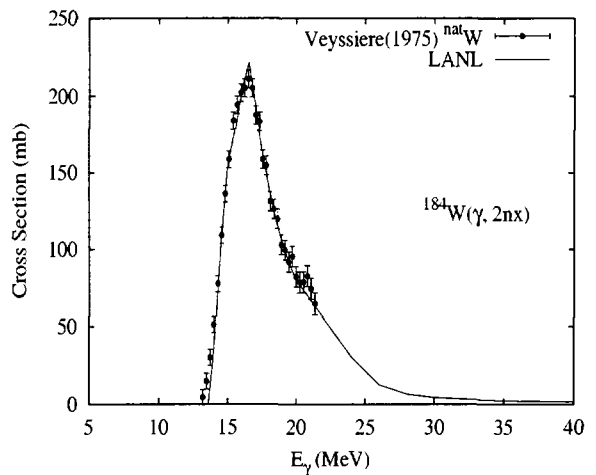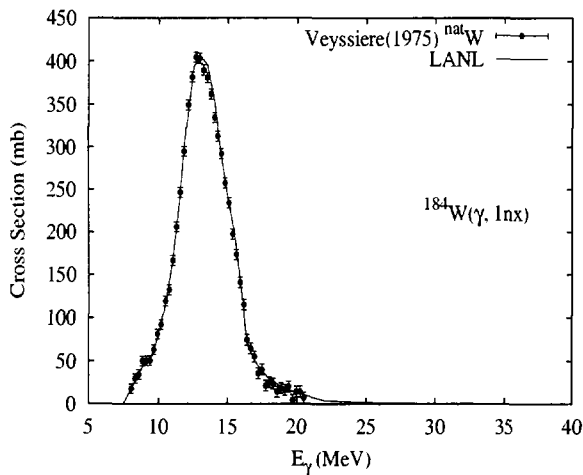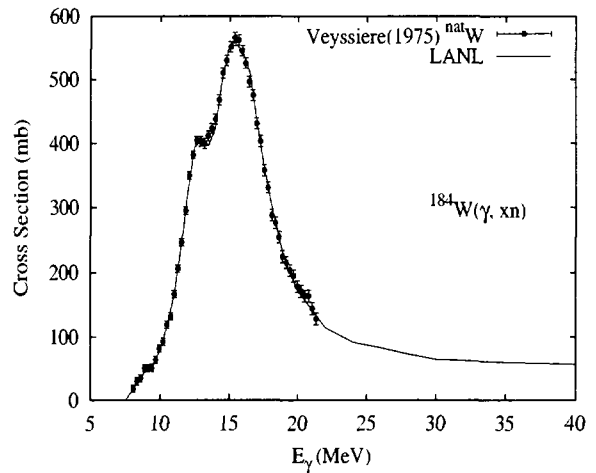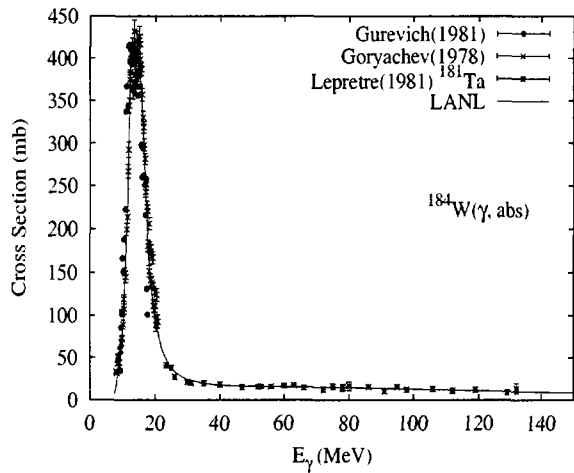
In the evaluation, the calculated photoabsorption cross section using GDR Lorentzian and QD parameters was modified slightly to better agree with the elemental tungsten photoabsorption cross section from Saclay [Vey75]. Use was made of the total Ta absorption cross section data of Lepretre et al [Lep81] to guide the QD model calculation of the absorption cross section, giving a Levinger parameter of L=6.7. (No such data exists for W, but we expect W and Ta experimental data to be similar). Good agreement was obtained with $(\gamma,1n)$ and $(\gamma,2n)$ elemental W experimental data from Saclay [Vey75], as well as neutron multiplicity data on Ta [Lep81]. The GNASH input parameter describing the preequilibrium exciton level density was modified to optimize agreement with the measured data.

$$\gamma + {}^{186}\text{W}$$

Abundance	Threshold Energies (MeV)								
(%)	γ,n	γ,p	γ,t	$\gamma,\text{He-3}$	γ,α	$\gamma,\text{2n}$	γ,np	$\gamma,\text{2p}$	$\gamma,\text{3n}$
28.60	7.19	8.40	12.17	14.16	-1.12	12.95	15.03	15.59	20.36
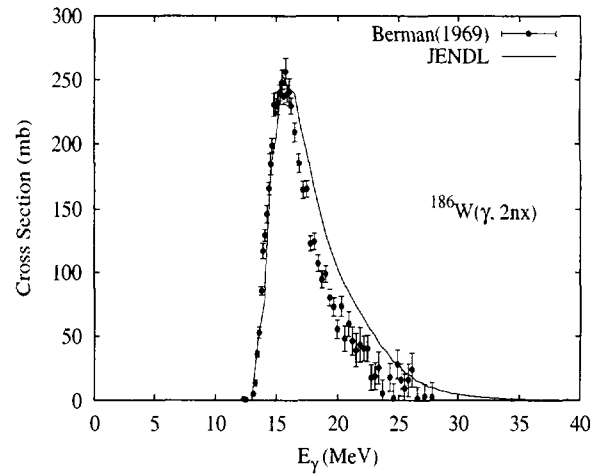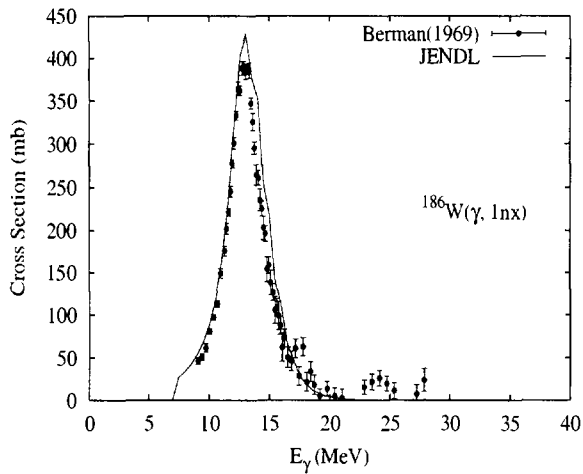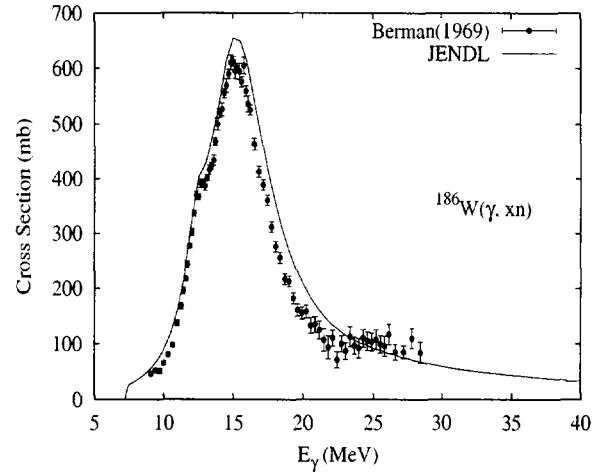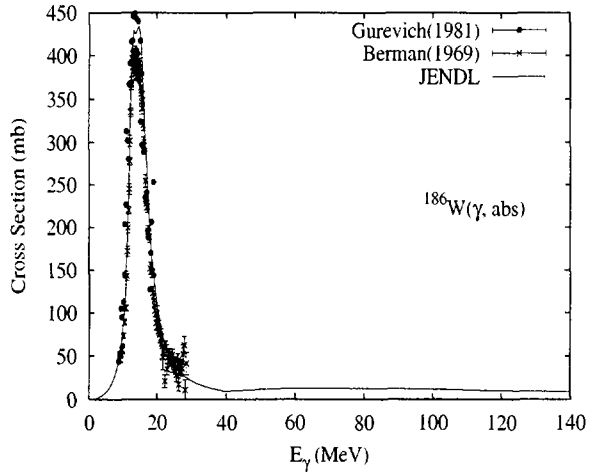
Photonuclear reactions were evaluated using ALICE-F [Fuk93] code calculations together with experimental data. Input model parameters were adjusted so as to improve the quality of the calculated results compared with data [Gur81, Ber69b]. Photoabsorption was modeled as a sum of GDR and QD components [Cha91].

$\gamma + {}^{197}\mathrm{Au}$

Abundance	Threshold Energies (MeV)								
(%)	γ,n	γ,p	γ,t	$\gamma,$He-3	γ,α	$\gamma,2n$	γ,np	$\gamma,2p$	$\gamma,3n$
100.00	8.07	5.78	11.33	13.56	-0.95	14.71	13.70	14.04	23.08
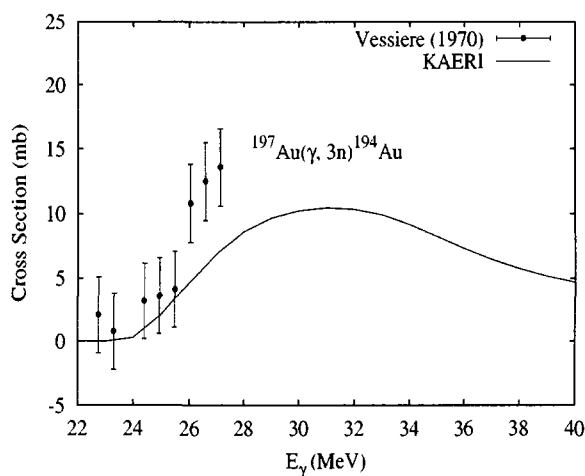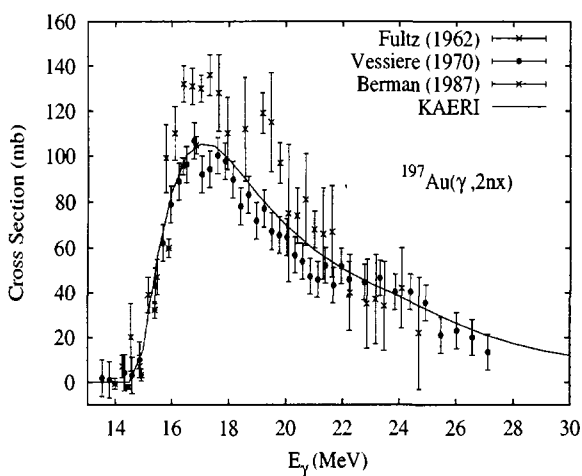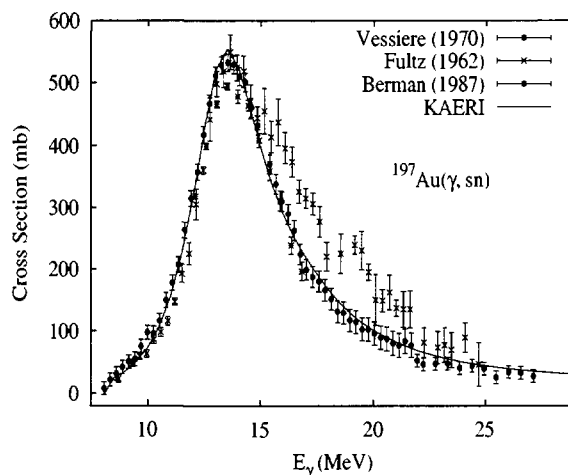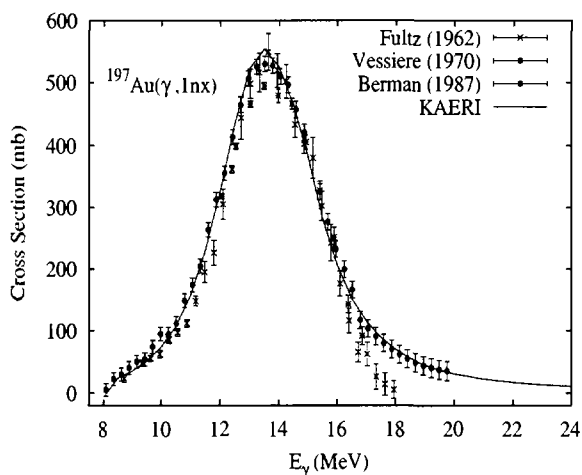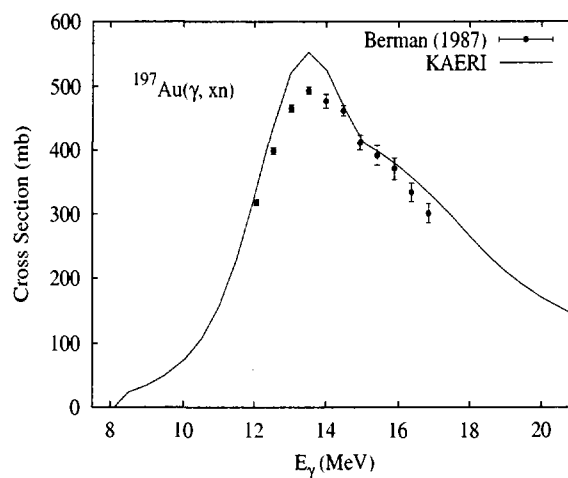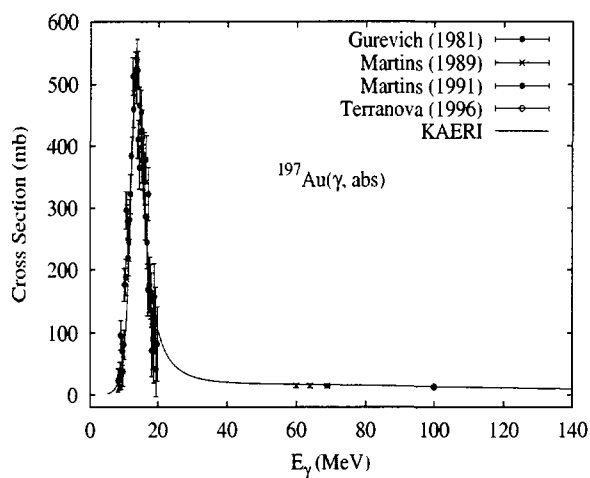
The experimental data for absorption cross section were given by Gurevich [Gur81], Terranova [Ter96] and Martins [Mar89, Mar91], respectively. Fultz [Ful62b], Veyssiere [Vey70] and Berman [Ber87] measured the $(\gamma, 1nx)$, $(\gamma, 2nx)$ and (γ, sn) reaction cross sections. Berman also gave the experimental data of (γ, sn) reaction cross section. Among these data, Veyssiere's and

249

Fultz's data have good agreement in their magnitudes of the (γ, sn) cross sections. We relied on the GUNF and GNASH codes to infer the photoabsorption cross section in the GDR regime, in order to model accurately Veyssiere's (γ, sn) data. The photoabsorption cross section above the GDR, up to 140 MeV, was obtained from QD model calculations using the theory of Chadwick.

The calculated results of the emission channels by the GNASH code are in overall agreement with the absorption cross sections data of Gurevich, Terranova and Martins, and in good agreement with the $(\gamma, 1nx)$, $(\gamma, 2nx)$ and $(\gamma, 3nx)$ data of Veyssiere.

$$\gamma + {}^{206}\text{Pb}$$

| Abundance (%)	Threshold Energies (MeV)								
	γ,n	γ,p	γ,t	γ,He-3	γ,α	γ,2n	γ,np	γ,2p	γ,3n
24.10	8.09	7.25	12.97	13.45	-1.14	14.82	14.80	13.67	23.21
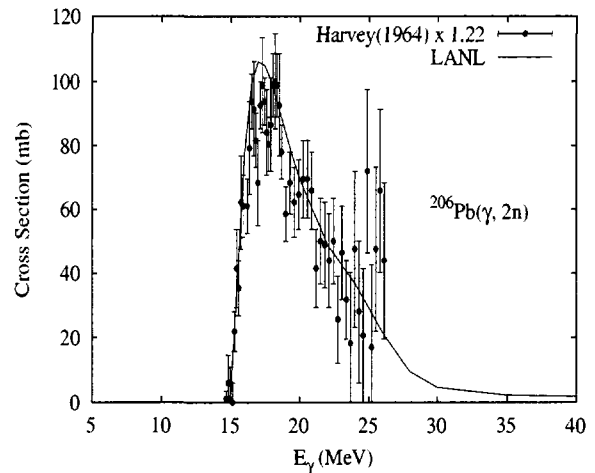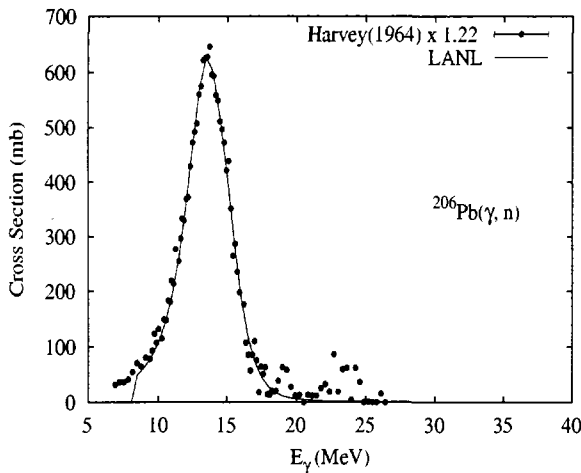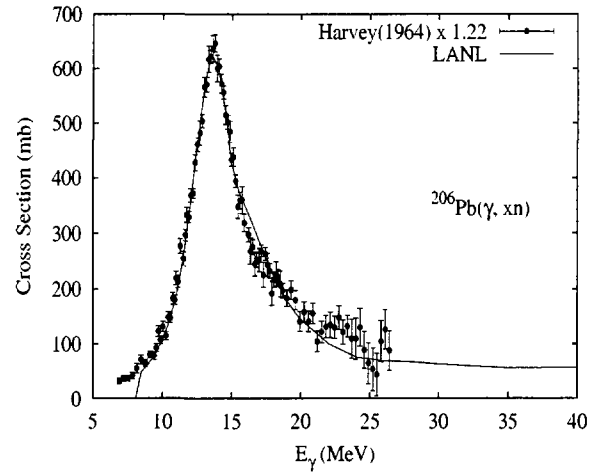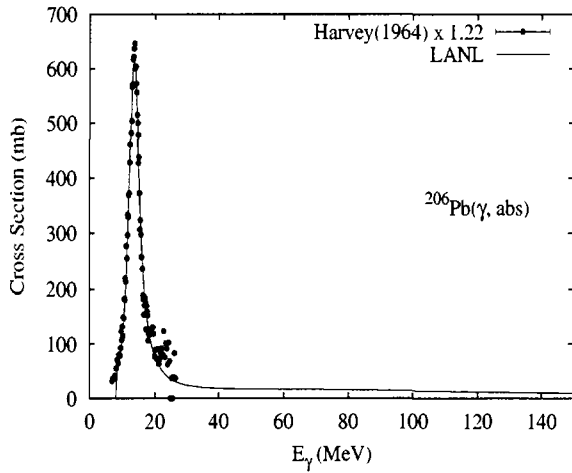
For photonuclear reactions on lead, there are systematical differences between some of the important measurements of neutron production. Specifically, the results from Saclay are significantly higher than those from Livermore. Berman [Ber87] concluded that the earlier Livermore measurements on lead [Har64] were too low. We have adopted Berman's view that the Livermore [Har64] data for ${}^{206}\text{Pb}$ need to be renormalized up by 22%.

Thus, photoabsorption was evaluated based on the GDR parameters given by Dietrich and Berman [Die88], which were a fit to Harvey's data [Har64], but the peak was increased by 22%. Above the GDR, in the QD regime, we then evaluated the absorption cross section up to 150 MeV based on model calculations [Cha91].

The GNASH calculations gave results for the (γ,1n), (γ,2n), and (γ,xn) cross sections that were in excellent agreement with the data [Har64], after it was also scaled by 22%.

$\gamma + {}^{207}\mathrm{Pb}$

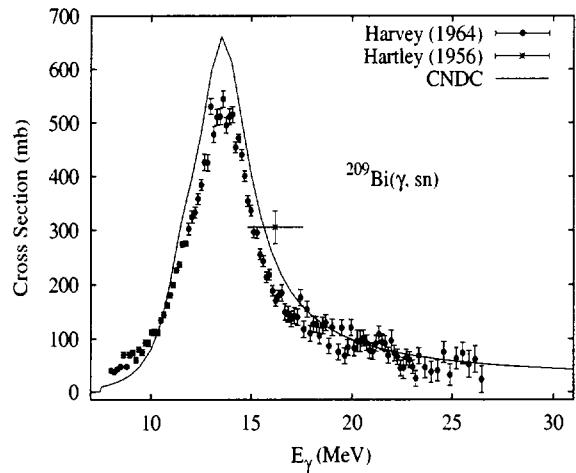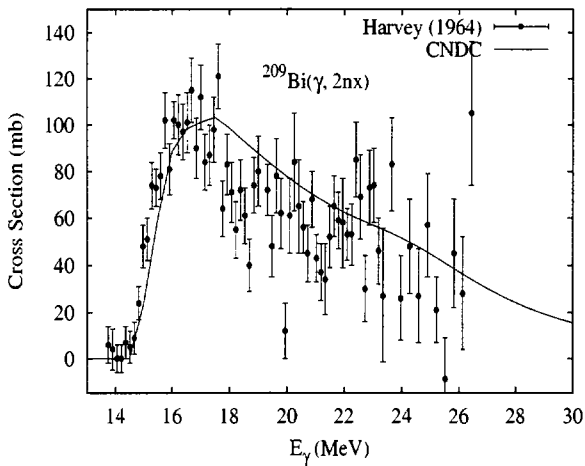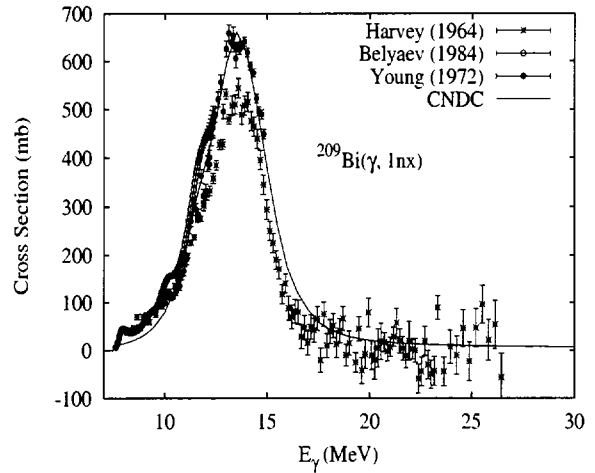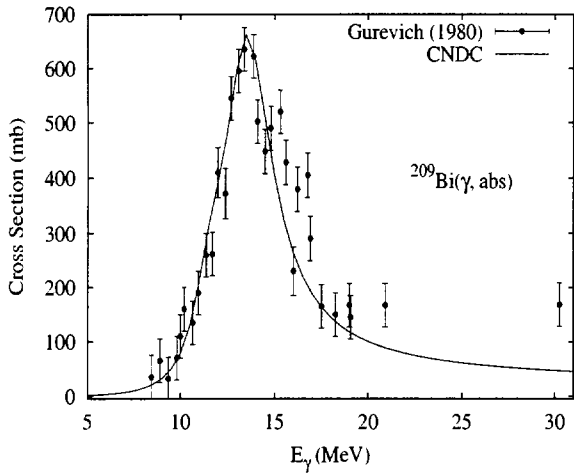| Abundance (%)	Threshold Energies (MeV)								
	γ,n	γ,p	γ,t	$\gamma,\mathrm{He\text{-}3}$	γ,α	$\gamma,2n$	γ,np	$\gamma,2p$	$\gamma,3n$
22.10	6.74	7.49	13.06	12.69	-0.39	14.83	13.99	14.74	21.56
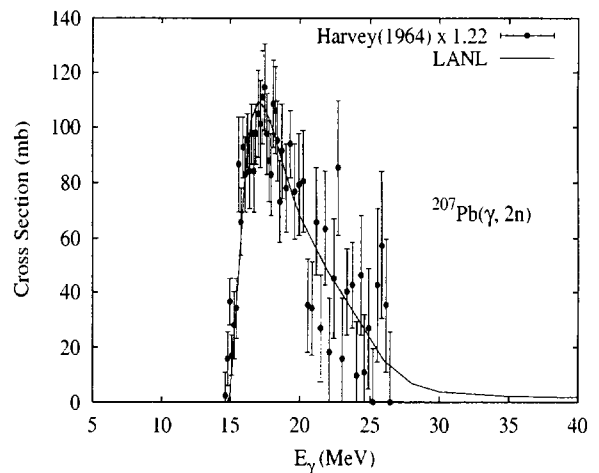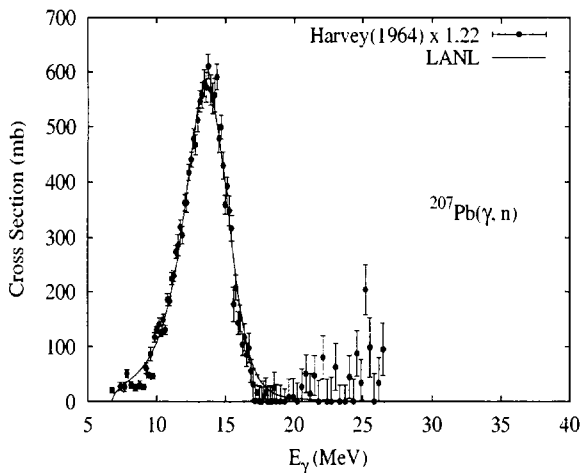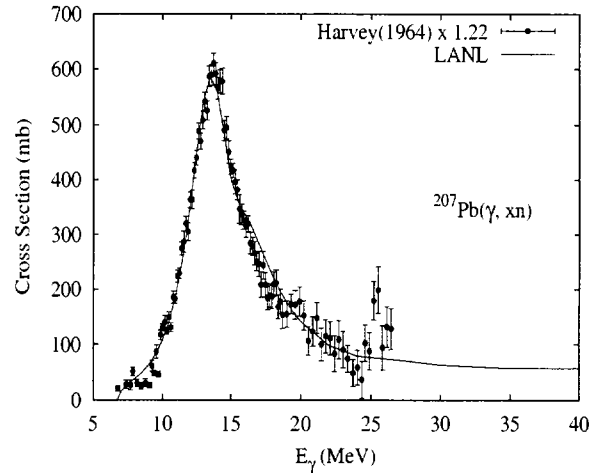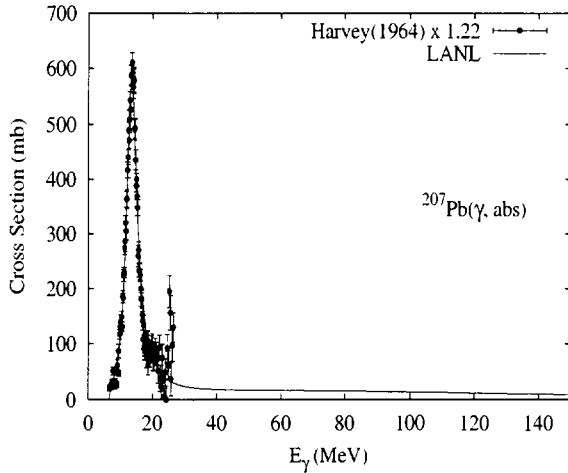
For photonuclear reactions on lead, there are systematical differences between some of the important measurements of neutron production. Specifically, the results from Saclay are significantly higher than those from Livermore. Berman [Ber87] concluded that the earlier Livermore measurements on lead [Har64] were too low. We have adopted Berman's view that the Livermore [Har64] data for ${}^{207}\mathrm{Pb}$ need to be renormalized up by 22%.

Thus, photoabsorption was evaluated based on the GDR parameters given by Dietrich and Berman [Die88] which were a fit to Harvey's data [Har64] , but the peak was increased by 22%. Above the GDR, in the QD regime, we then evaluated the absorption cross section up to 150 MeV based on model calculations [Cha91].

The GNASH calculations gave results for the $(\gamma,1n)$, $(\gamma,2n)$, and (γ,xn) cross sections that were in excellent agreement with the data [Har64] , after it was also scaled by 22%.

$$\gamma + {}^{208}\mathrm{Pb}$$

Abundance (%)	Threshold Energies (MeV)								
	γ,n	γ,p	γ,t	$\gamma,\mathrm{He\text{-}3}$	γ,α	$\gamma,2n$	γ,np	$\gamma,2p$	$\gamma,3n$
52.40	7.37	8.01	12.88	14.39	-0.52	14.11	14.85	15.38	22.19
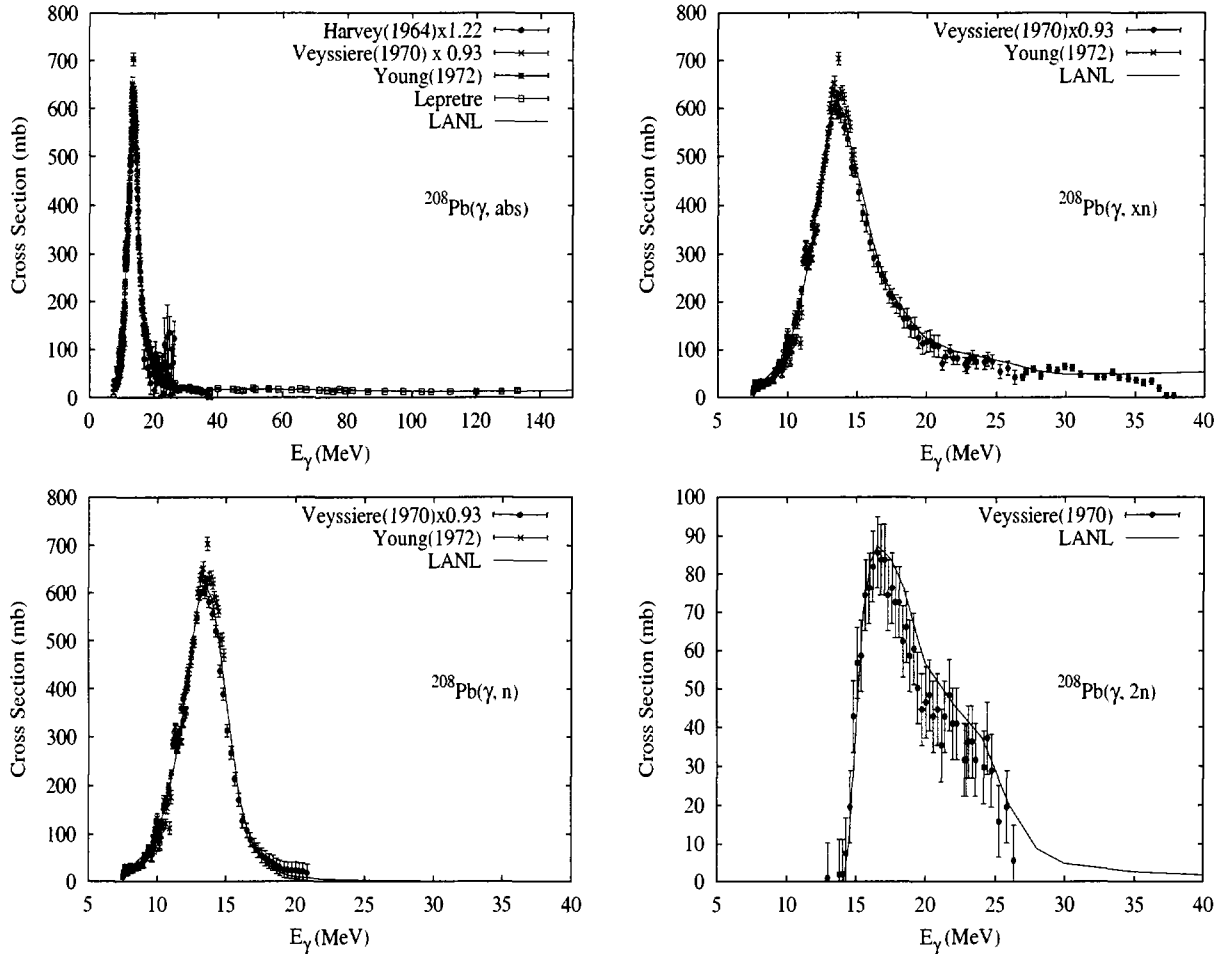
For photonuclear reactions on lead, there are systematical differences between some of the important measurements of neutron production. Specifically, the results from Saclay are significantly higher than those from Livermore. Berman [Ber87] concluded that the earlier Livermore measurements on lead [Har64] were too low. We have adopted Berman's view that the Saclay data [Vey70] need to be renormalized down by 7%, and the Livermore [Har64] data for ^{208}Pb need to be renormalized up by 22%. The photoabsorption cross section was calculated from a Lorentzian line shape modified on the low-energy tail where deviations from experimental data are seen. Above the GDR, in the QD regime, we then evaluated the absorption cross section up to 150 MeV based on experimental data [Lep81] and model calculations [Cha91].

Our resulting evaluation is in good agreement with (renormalized) data [Har64, Vey70, You72, Lep81] for neutron production and for the photonuclear absorption cross section up to 150 MeV. Our results for $(\gamma,1n),(\gamma,2n)$, $(\gamma,3n)$ reactions exhibit the following features: $(\gamma,1n)$ is in good agreement with data [Vey70, You72, Ber87]; $(\gamma,2n)$ agrees reasonably with data [Vey70, You72] though appears somewhat high in the 17-25 MeV range); $(\gamma,3n)$ agrees reasonably with data [Vey70],though appears somewhat low in the 25-30 MeV range. We attempted to improve agreement with the $(\gamma,2n)$ and $(\gamma,3n)$ measurements but were unable to do so using a consistent set of input model parameters.

We have also compared [Cha95a] calculated multiplicities for neutron and proton emission with the measurements of Lepretre [Lep82](See Fig. 4.3 in Sec. 4.2.3). Our calculations describe the correct partitioning of ejectiles among preequilibrium and equilibrium emission, and between neutrons and protons. These measurements are invaluable for testing the preequilibrium modeling in our calculation, since direct measurements of the nucleon emission spectra from monoenergetic photons do not exist for lead. The large Coulomb barrier in lead is responsible for the excess of fast preequilibrium neutrons compared to protons; at the highest energies the differences are reduced. In general the slow neutron multiplicity is much larger than the fast reaction multiplicities, since preequilibrium decay accounts for at most the first two emissions, with the subsequent sequential particle decays coming from compound-nucleus emission.

$$\gamma + {}^{209}\text{Bi}$$

Abundance (%)	Threshold Energies (MeV)								
	γ,n	γ,p	γ,t	γ,He-3	γ,α	γ,2n	γ,np	γ,2p	γ,3n
100.00	7.46	3.80	9.42	10.94	-3.14	14.35	11.17	11.81	22.44
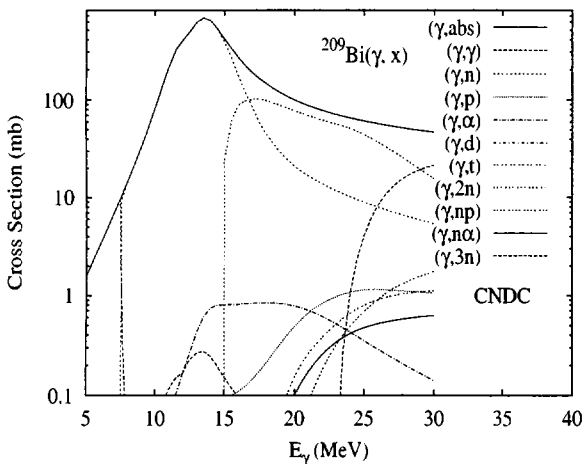
The photoabsorption [Gur80], as well as the photonuclear cross sections for (γ, 1nx), (γ, 2nx), (γ, xn), and (γ, sn) reactions [Har64, Bel85, You72] were measured. We relied on GUNF code [Zha98] to infer the photoabsorption cross section in the GDR regime, in order to model accurately the experimental data [Gur80, Har64].

$\gamma + {}^{232}\text{Th}$

Abundance (%)	Threshold Energies (MeV)								
	γ,n	γ,p	γ,t	$\gamma,\text{He-3}$	γ,α	$\gamma,2\text{n}$	γ,np	$\gamma,2\text{p}$	$\gamma,3\text{n}$
100.00	6.44	7.75	10.41	12.15	-4.08	11.56	13.31	13.25	18.35
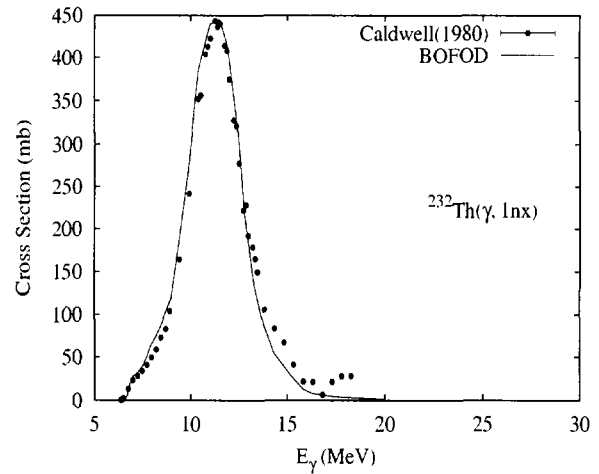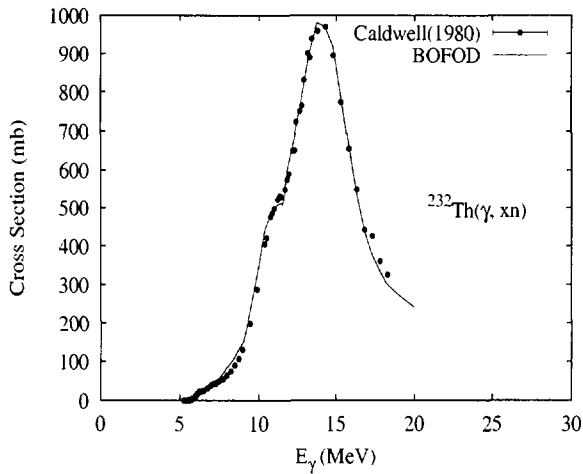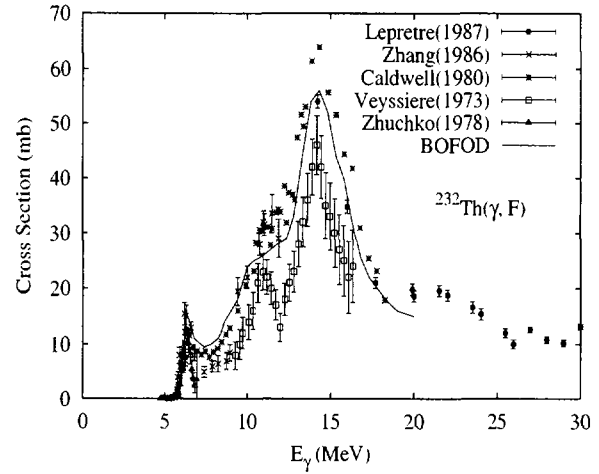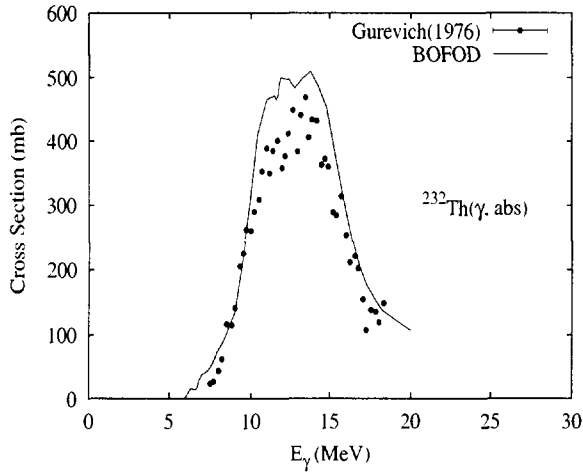
Experimental information is available for the photoabsorption [Gur76], photofission [Vey73, Cal80a, Zha86, Zhu78b, Lep87], and (γ, xn), (γ, 1nx), and (γ, 2nx) cross sections [Cal80a, Vey73]. For a complete reference list of photofission cross sections see [Blo99a]. The photofission cross section presents large differences between some of the important measurements, in the energy range below 10 MeV. In the GDR range there are systematical differences between the Livermore [Cal80a] and the Saclay data [Vey73]. The evaluation adopted the Saclay data for photoneutron production as reference, in order to obtain the relevant parameters of the statistical model [Blo99b]. The widths for radiative, neutron and fission decays were taken from the description of the photofission cross section below 6 MeV [Sto97]. The calculated results are in good agreement with the experimental data for (γ, xn), ((γ, 1nx) and (γ, 2nx) reactions [Cal80a].

Abundance (%)	Threshold Energies (MeV)								
	γ,n	γ,p	γ,t	$\gamma,\text{He-3}$	γ,α	$\gamma,\text{2n}$	γ,np	$\gamma,\text{2p}$	$\gamma,\text{3n}$
0.00	5.74	6.30	10.20	8.88	-4.91	13.01	11.87	11.48	18.90
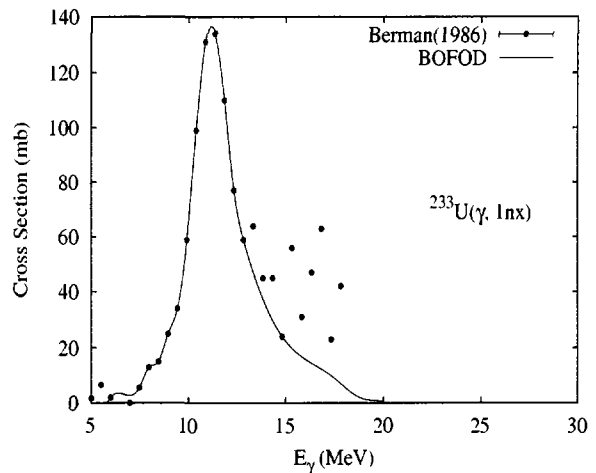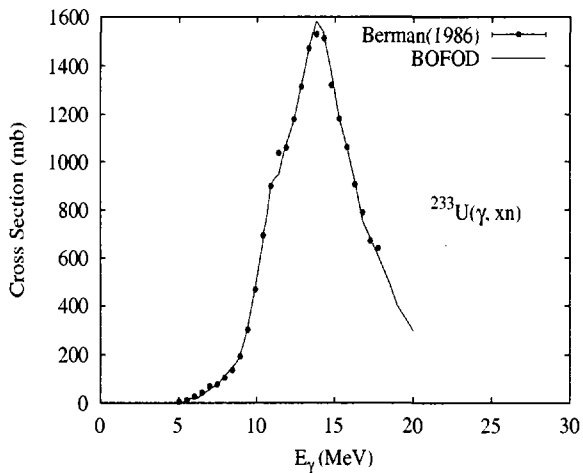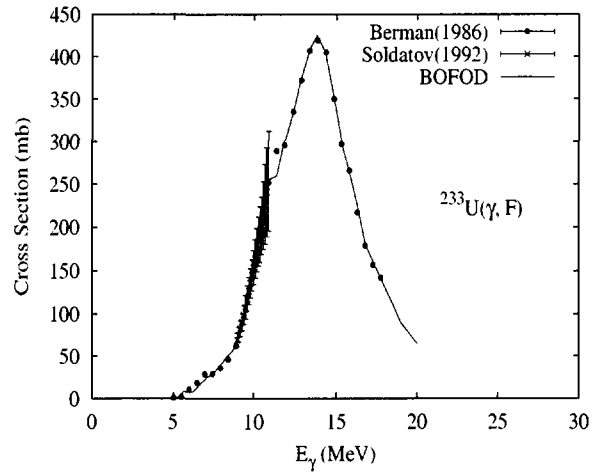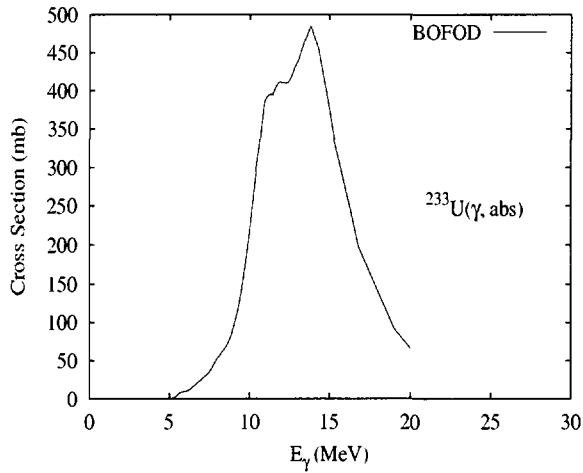
Experimental information is available for the photofission, (γ, xn), and $(\gamma, \text{1nx})$ cross sections [Ber86]. For a complete reference list of photofission cross sections see [Blo99a]. The evaluation adopted the Livermore data for photofission and photoneutron production as reference, in order to obtain the relevant parameters of the statistical model [Blo99b]. The widths for radiative, neutron and fission decays were taken from the description of the photofission cross section below 10 MeV [Sol92]. The calculated results are in good agreement with the experimental data for photofission and photoneutron production [Ber86] in the GDR region. Below 10 MeV the calculated results agree well with experimental data from [Sol92].
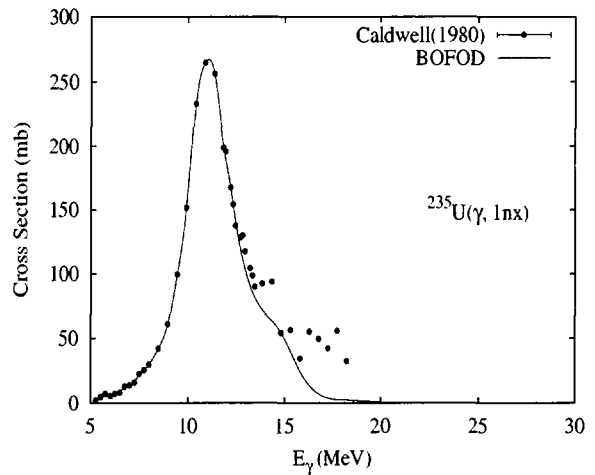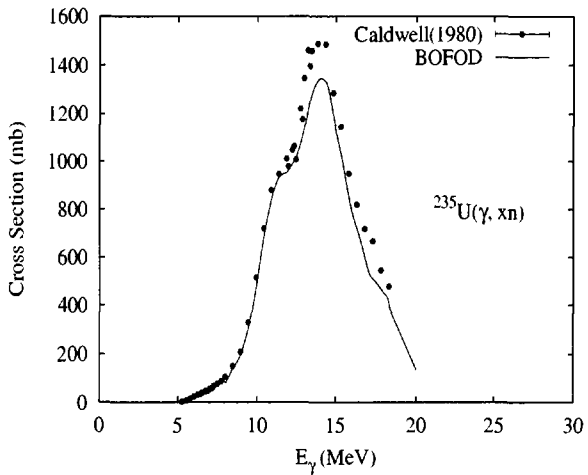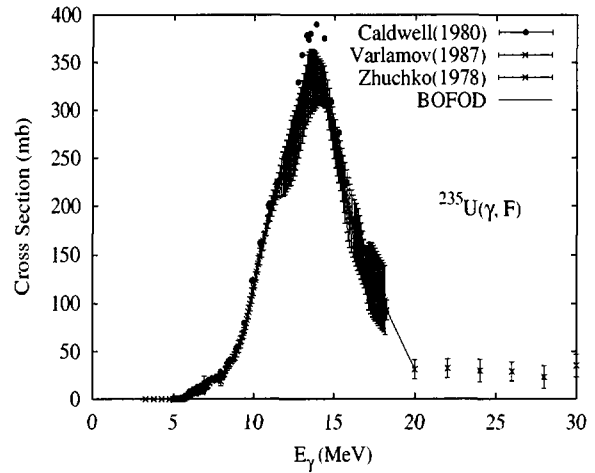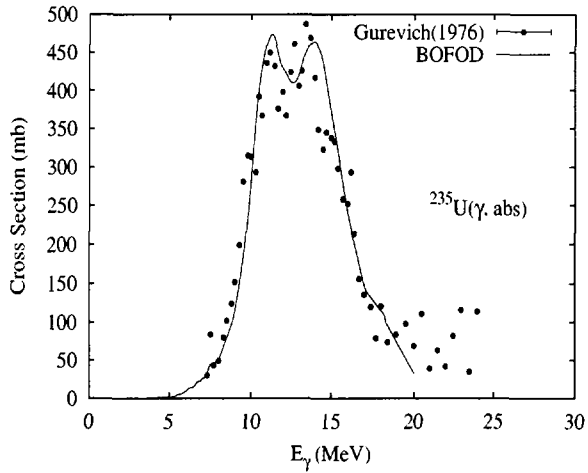
$$\gamma + {}^{234}\mathrm{U}$$

Abundance	Threshold Energies (MeV)								
(%)	γ,n	γ,p	γ,t	γ,He-3	γ,α	γ,2n	γ,np	γ,2p	γ,3n
0.01	6.84	6.63	10.23	10.60	-4.86	12.59	13.14	11.88	19.85
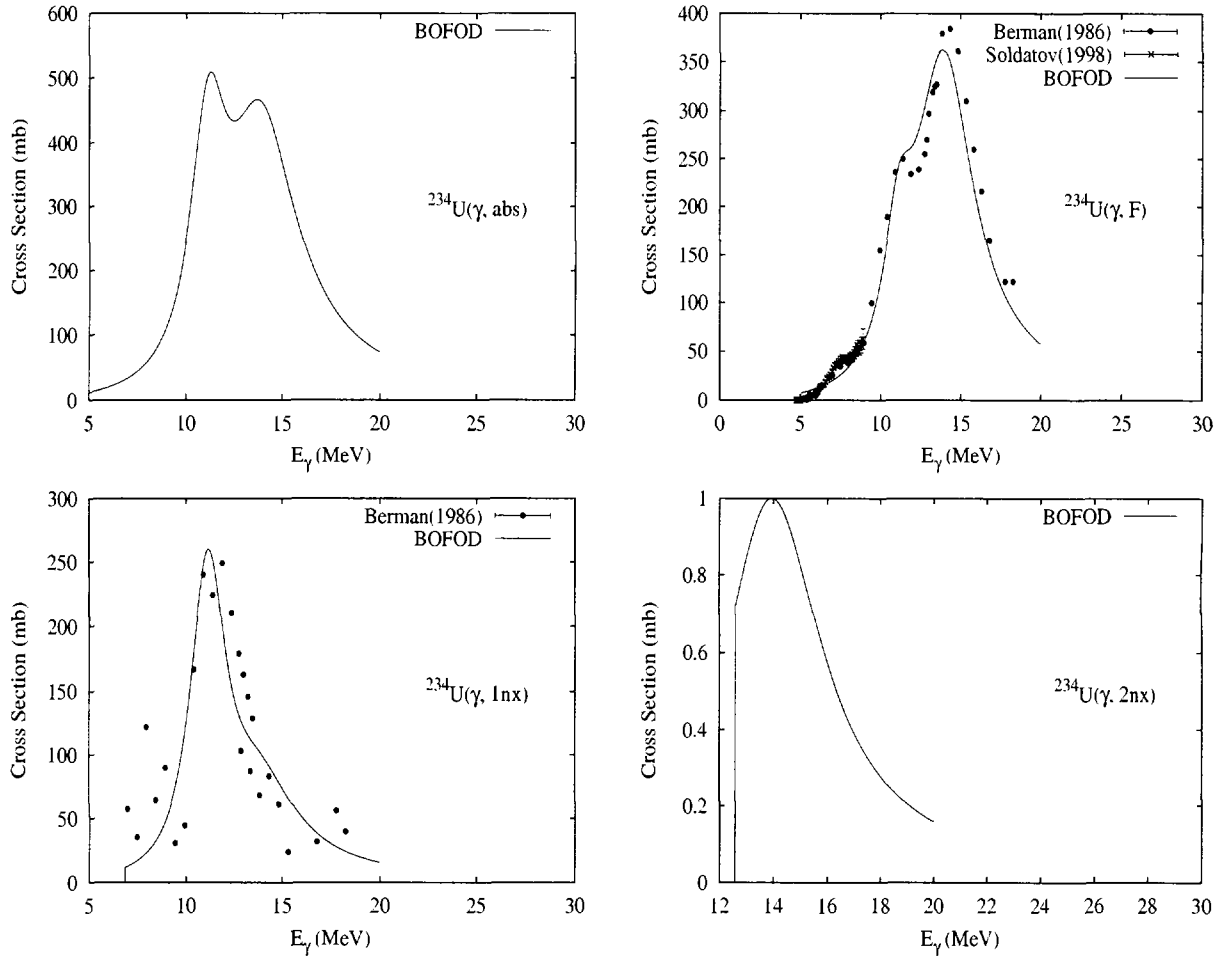
Experimental information is available for the photofission [Sol98, Ber86], (γ, xn), and (γ, 1nx) cross sections [Ber86]. For a complete reference list of photofission cross sections see [Blo99a]. The evaluation adopted the Livermore data for photofission and photoneutron production as reference, in order to obtain the relevant parameters of the statistical model [Blo99b]. The widths for radiative, neutron and fission decays were taken from the description of the photofission cross section below 9 MeV [Sol98]. The calculated results are in good agreement with the experimental data for photofission and photoneutron production [Ber86] in the GDR region. Below 10 MeV the calculated results agree well with experimental data from [Sol98].

$$\gamma + {}^{235}\text{U}$$

Abundance	Threshold Energies (MeV)								
(%)	γ,n	γ,p	γ,t	γ,He-3	γ,α	γ,2n	γ,np	γ,2p	γ,3n
0.72	5.30	6.71	9.96	9.46	-4.68	12.14	11.93	12.39	17.89

Experimental information is available for the photoabsorption [Gur76], photofission [Cal80b, Cal80a, Zhu78b], (γ, xn), and (γ, 1nx) cross sections [Cal80a]. For a complete reference list of photofission cross sections see [Blo99a]. The evaluation adopted the Caldwell's data for the (γ, 1nx), and Varlamov's photofission data as reference below 14 MeV, in order to obtain the relevant parameters of the statistical model [Blo99b]. The widths for radiative, neutron and fission decays were taken from the description of the (γ, 1nx) cross section below 14 MeV [Cal80a].
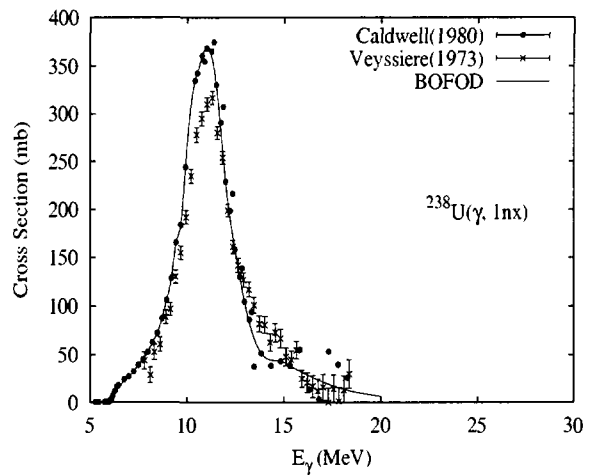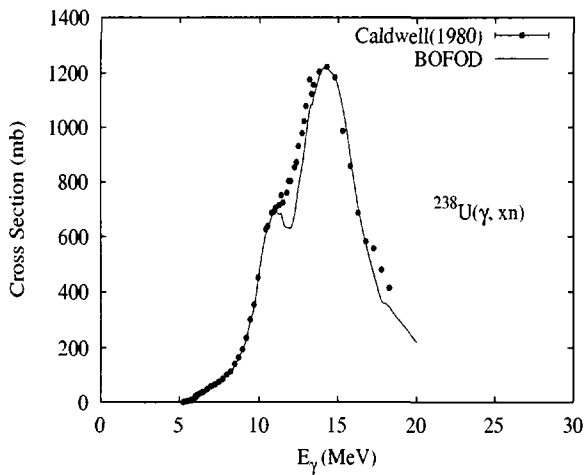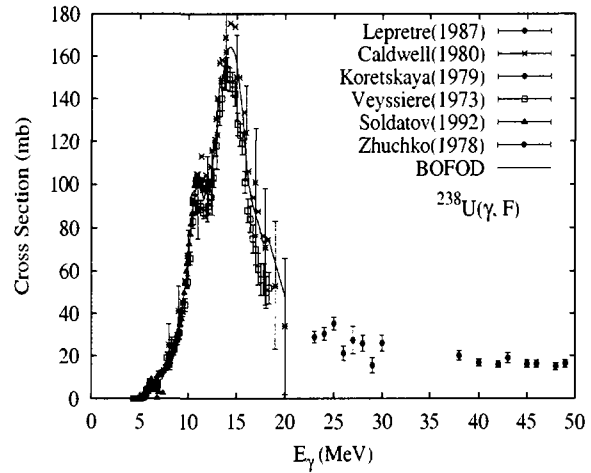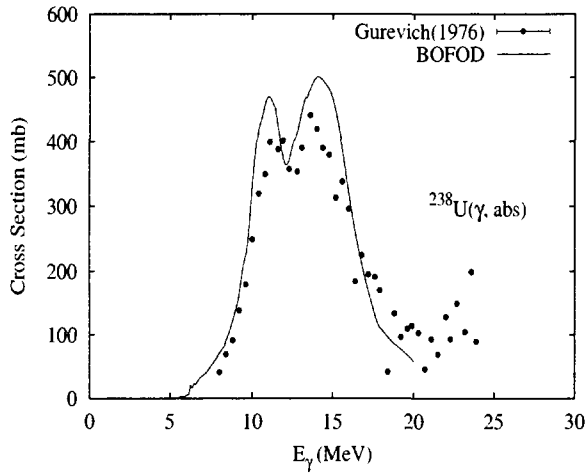
$$\gamma + {}^{236}\mathrm{U}$$

Abundance	Threshold Energies (MeV)								
(%)	γ,n	γ,p	γ,t	$\gamma,\mathrm{He}\text{-}3$	γ,α	$\gamma,2n$	γ,np	$\gamma,2p$	$\gamma,3n$
0.00	6.55	7.18	9.99	11.22	-4.57	11.84	13.25	12.74	18.69
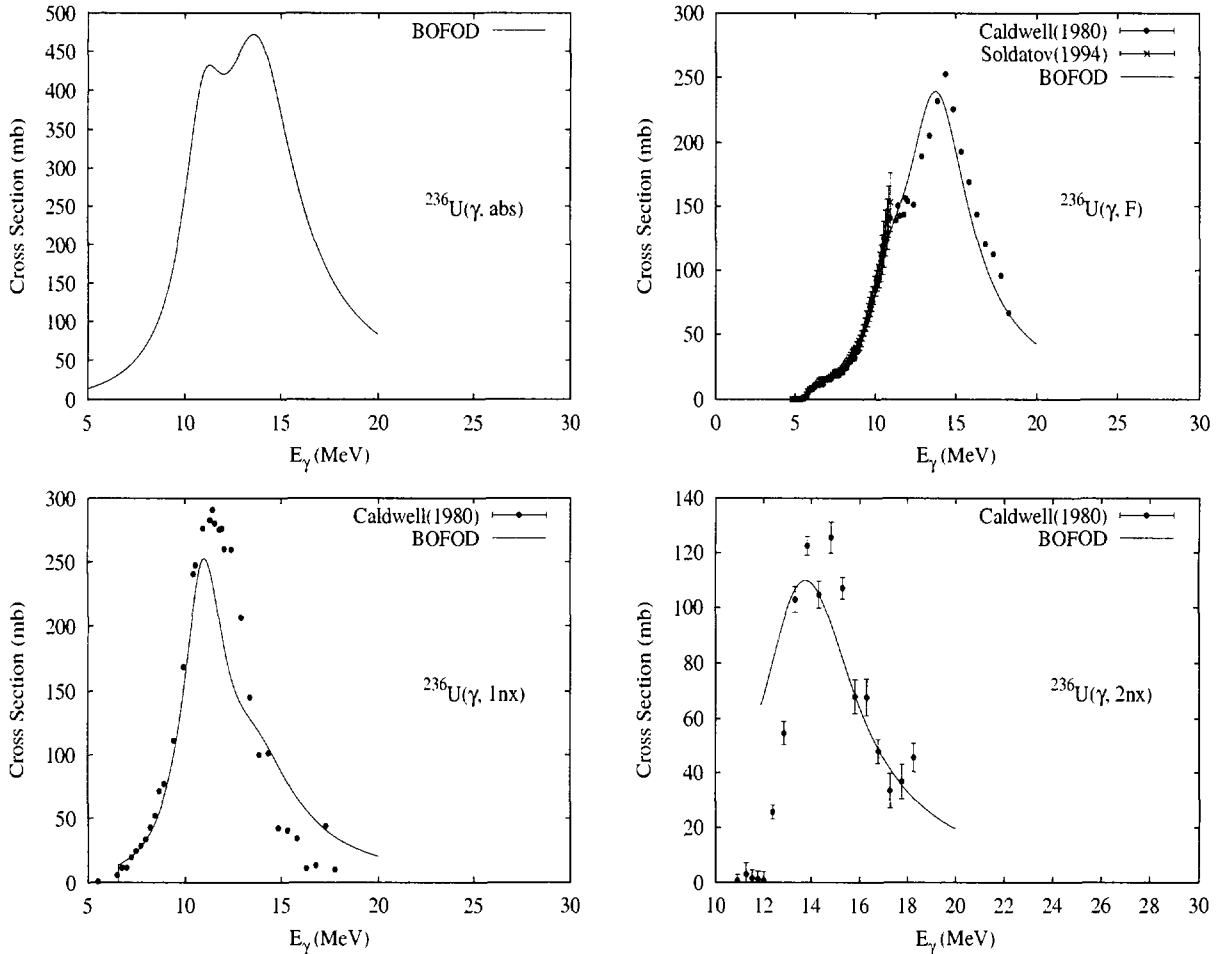
Experimental information is available for the photofission [Cal80b, Cal80a, Zhu78b, Zhu78a, Rud88, Sol94], (γ, xn), (γ, 1nx), and (γ, 2nx) cross sections [Cal80a]. For a complete reference list of photofission cross sections see [Blo99a]. The evaluation adopted the Livermore data for (γ, 1nx) [Cal80a], and both the Livermore and Obninsk data for photofission [Cal80a, Sol94] as reference below 12 MeV, in order to obtain the relevant parameters of the statistical model [Blo99b]. The widths for radiative, neutron and fission decays were taken from the description of the photofission cross section below 10 MeV [Sol94]. The calculated results are in good agreement with the experimental data for photofission [Cal80a, Sol94], and for (γ, xn), (γ, 1nx), and (γ, 2nx) cross sections below 12 MeV. In the 12 to 14 MeV range the evaluated data for the photoneutron production are lower than the experiment.

$$\gamma + {}^{238}\text{U}$$

Abundance (%)	Threshold Energies (MeV)								
	γ,n	γ,p	γ,t	γ,He-3	γ,α	γ,2n	γ,np	γ,2p	γ,3n
99.27	6.15	7.62	9.97	11.88	-4.27	11.28	13.39	13.01	17.82

Experimental information is available for the photoabsorption [Gur76], photofission [Vey73, Cal80b, Cal80a, Zhu78b, Sol92], and (γ, xn), (γ, 1nx), and (γ, 2nx) cross sections [Cal80a, Vey73]. For a complete reference list of reaction cross sections see [Blo99a]. The evaluation adopted the Livermore data for (γ, 1nx) and (γ, xn) [Cal80a], and both the Livermore and Obninsk data for photofission [Cal80a] and [Sol92] as reference below 14 MeV, in order to obtain the relevant parameters of the statistical model [Blo99b]. The widths for radiative, neutron and fission decays were taken from the description of the(γ, 1nx) cross section below 14 MeV [Cal80a], and the photofission cross section below 10 MeV [Sol92]. In general, the results are in reasonable agreement with experimental data [Gur76] for photoabsorption cross section and for (γ,xn), (γ,1nx), (γ,2nx) and (γ,F) reactions for gamma-ray energy below 20 MeV.

$\gamma + {}^{238}\mathrm{Pu}$

Abundance	Threshold Energies (MeV)								
(%)	γ,n	γ,p	γ,t	$\gamma,\mathrm{He\text{-}3}$	γ,α	$\gamma,\mathrm{2n}$	γ,np	$\gamma,\mathrm{2p}$	$\gamma,\mathrm{3n}$
0.00	7.00	6.00	9.83	9.69	-5.59	12.86	12.57	10.86	20.21
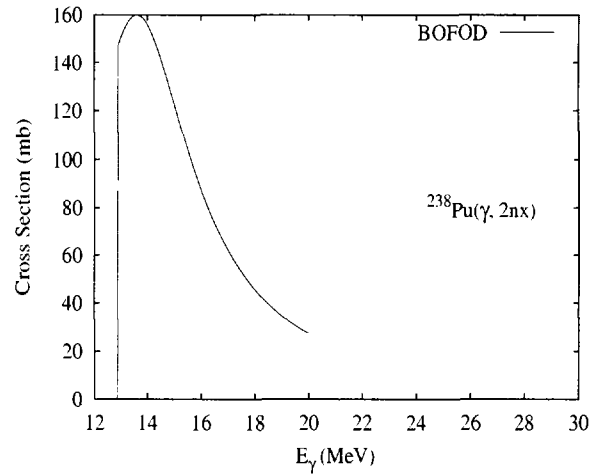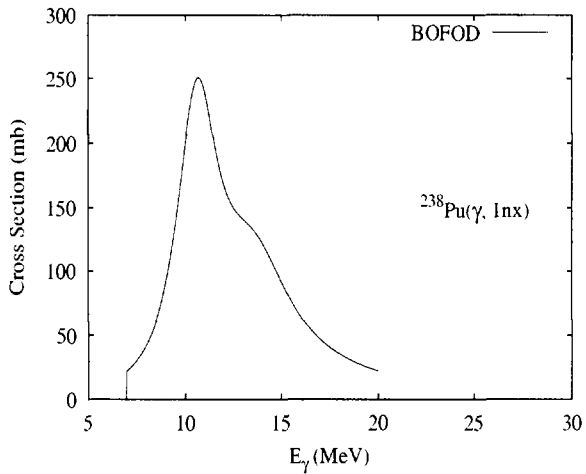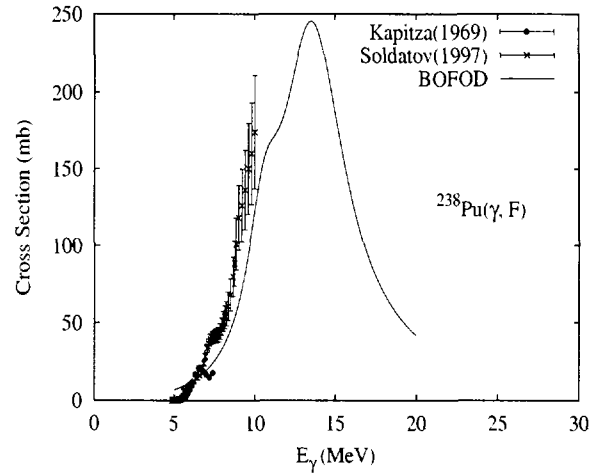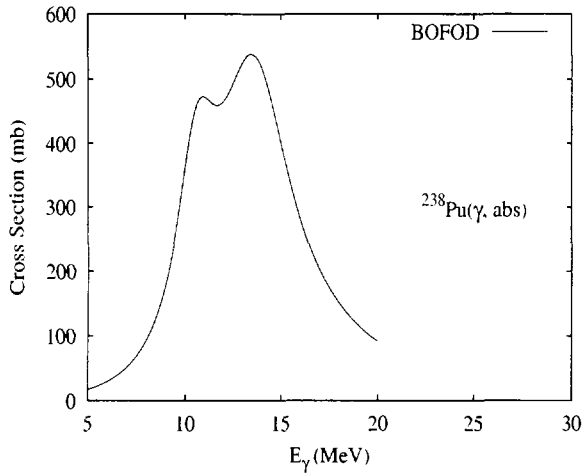
There are two measurements of the photofission cross sections [Kap69, Sol97]. The evaluation used statistical model parameters based on a systematics of neighboring nuclei [Blo99b]. The radiative-decay, neutron and fission widths were taken from description of (γ, F) reaction [Sol97] below 10 MeV.

$\gamma + {}^{239}\mathrm{Pu}$

Abundance (%)	Threshold Energies (MeV)								
	γ,n	γ,p	γ,t	$\gamma,\mathrm{He}\text{-}3$	γ,α	$\gamma,2\mathrm{n}$	γ,np	$\gamma,2\mathrm{p}$	$\gamma,3\mathrm{n}$
0.00	5.65	6.16	9.74	8.79	-5.24	12.65	11.64	11.38	18.51
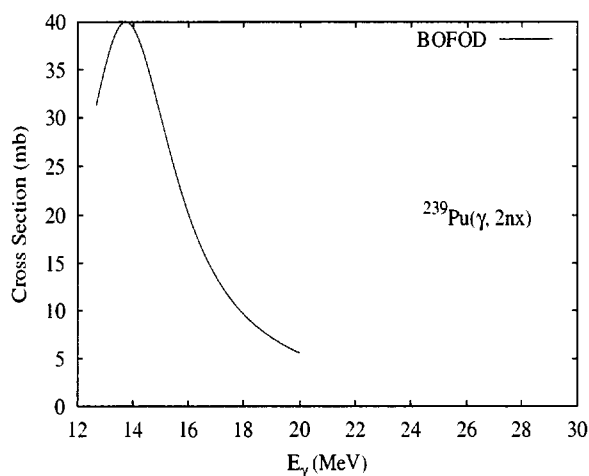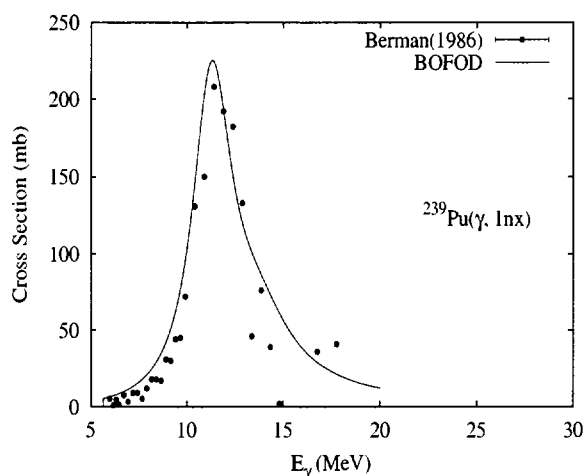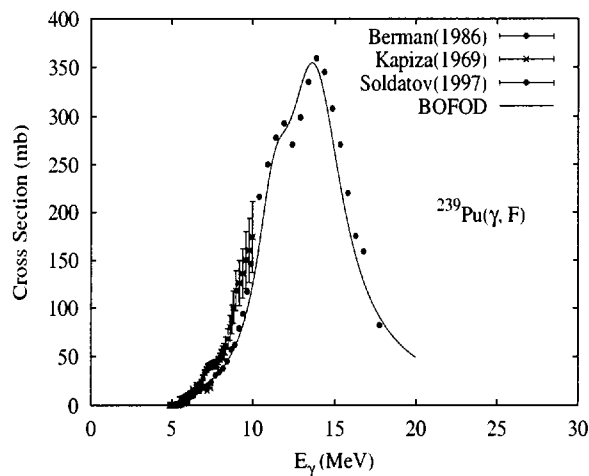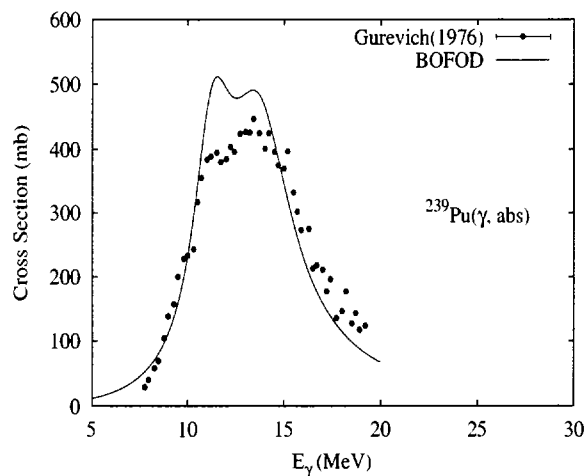
Experimental information is available for the photoabsorption [Gur76], photofission ([Ber86, Zhu78b, Sol92], and (γ, xn), (γ, 1nx), and (γ, 2nx) cross sections [Ber86]. For a complete reference list of photofission cross sections see [Blo99a]. The evaluation adopted the Livermore data for photoneutron production as reference, in order to obtain the relevant parameters of the statistical model [Blo99b]. The widths for radiative, neutron and fission decays were taken from the description of the photofission cross section below 10 MeV [Sol92].

$\gamma + {}^{241}\text{Pu}$

Abundance (%)	Threshold Energies (MeV)								
	γ,n	γ,p	γ,t	$\gamma,\text{He-3}$	γ,α	$\gamma,2n$	γ,np	$\gamma,2p$	$\gamma,3n$
0.00	5.24	6.66	9.45	9.29	-5.14	11.78	11.72	12.20	17.42
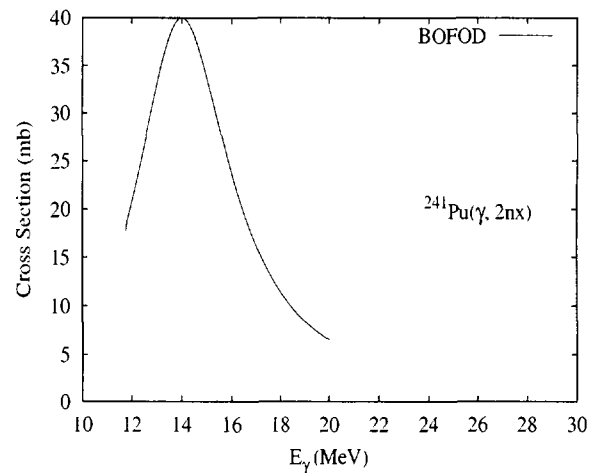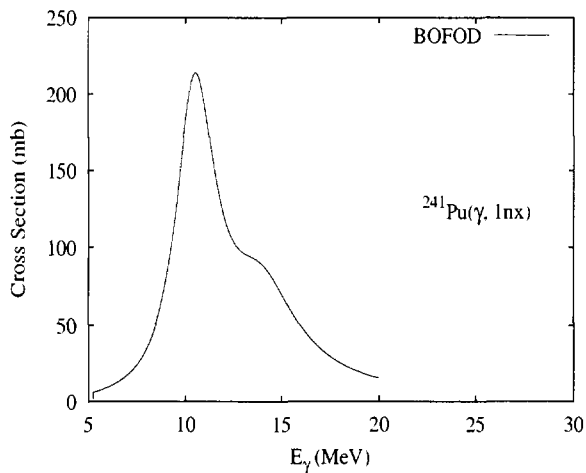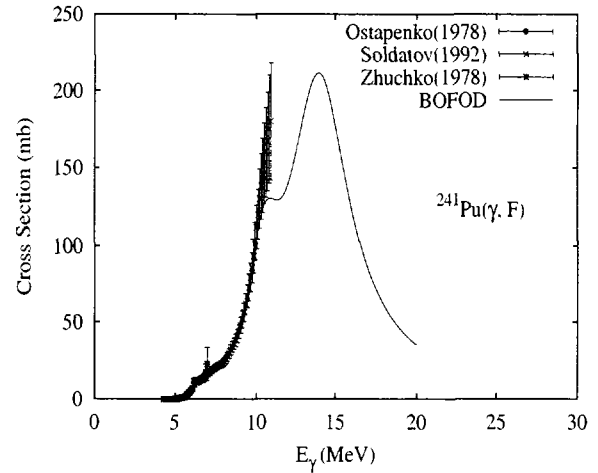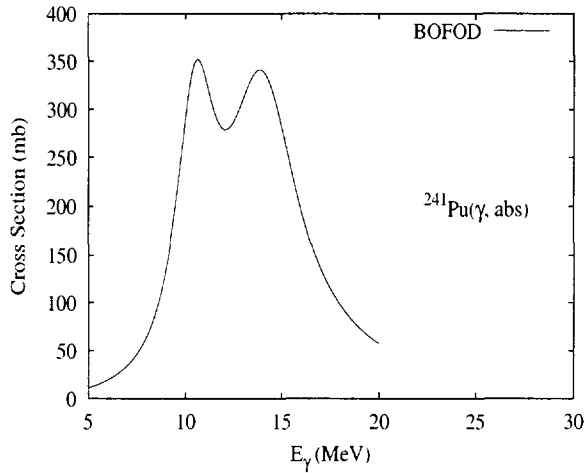
Experimental information is available only for the photofission cross section [Sol92, Zhu78a, Ost78]. The evaluation adopted both the Soldatov and Zhuchko data [Sol92, Zhu78a] for photofission below 12 MeV as reference, in order to obtain the relevant parameters of the statistical model [Blo99b]. The widths for radiative, neutron and fission decays were taken from the description of the photofission cross section below 10 MeV [Sol92].

References To Appendix B

[Ahr75] J. Ahrens, H. Borchert, K. Czock, H. Eppler, H. Gimm, H. Gundrum, M. Kroning, P. Riehn, G. Ram, A. Zieger, and B. Ziegler, "Total nuclear photon absorption cross sections for some light elements", Nucl. Phys. A **251**, 479 (1975), EXFOR M0372.

[Ale68] I. Alexandrov, Soviet Phys. **JETP 6**, 472 (1568).

[All55] L. J. Allen, Phys. Rev. **98**, 705 (1955).

[Alv71] R. Alvarez, B. Berman, D. Lasher, T. Phillips, and S. Fultz, "Photoneutron cross sections for 23-Na and 25-Mg", Phys. Rev. C **4**, 1673 (1971), EXFOR L0022.

[Alv79] R. Alvarez, B. Berman, D. Faul, F. Lewis-jr, and P. Meyer, "Photoneutron cross sections for 55Mn and 59Co", Phys. Rev. C **20**, 128 (1979), EXFOR L0028.

[Ask72] H. Askin, J. Allen, R. Hicks, R. Petty, and M. Thompson, "Isotopic mixing in the isobaric analogue states of Zr-90", in Conf. Nucl. Structure Studies, Sendai, Japan, 1972 (1972), EXFOR M0360.

[Ass84] Y. Assafiri, G. Egan, and M. Thompson, "Photoneutron Cross Section of ^{34}S", Nucl. Phys. **A413**, 416 (1984), EXFOR M0506.

[Ass86] Y. Assafiri, G. Egan, and M. Thompson, "Photoproton Cross Section of ^{34}S", Nucl. Phys. **A460**, 455 (1986), EXFOR M0510.

[Bar52a] C. Barnes, Phys. Rev. **86**, 359 (1952).

[Bar52b] J. Barns, Phys. Rev. **86**, 359 (1952).

[Bat88] A. Bates, R. Rassool, E. Milne, and M. Thompson, "N-15 photoneutron cross section", Phys. Rev. C **40**, 506 (1988), EXFOR G0012.

[Bat89] A. Bates, R. Rassool, E. Milne, M. Thompson, and K. Mcneil, "N-15 photoneutron cross section", Phys. Rev. C **40**, 506 (1989), EXFOR M0264.

[Baz64] E. Bazhanov, A. Komar, and A. Kulikov, "Photoneutrons from Li-6 and Co-59", Zh. Eksp. Teor. Fiz. **46**, 1497 (1964), EXFOR M0106.

[Bei71] H. Beil, R. Bergere, P. Carlos, A. Lepretre, and A. Veyssiere, "Giant dipole resonance in N = 82 nuclei", Nucl. Phys. A **172**, 426 (1971), EXFOR L0024.

[Bei74] H. Beil, R. Bergere, P. Carlos, A. Lepretre, A. Miniac, and A. Veyssiere, "A study of the photoneutron contribution to the giant dipole resonance in doubly even Mo isotopes", Nucl. Phys. A **227**, 427 (1974), EXFOR L0032.

[Bel85] S. Belyaev, A. Kozin, A. Nechkin, V. Semenov, and S. Semenko, "On photoabsorption cross sections of Pr, Bi, and Ta isotopes in the energy region $E_\gamma < 12$ MeV", Yad. Fiz. **42**, 1050 (1985), EXFOR M0146.

[Bel91] S. Beljaev and V. Semenov, "Analysis of the intermediate structure in the (γ,n)- cross sections on nuclei with N=82", Izv. Akad. Nauk SSSR,ser. Fiz. **55**, 953 (1991), EXFOR M0367.

[Ber67] B. Berman, J. Caldwell, R. Harvey, M. Kelly, R. Bramblett, and S. Fultz, "Photoneutron cross sections for Zr-90,Zr-91, Zr-92,Zr-94, and Y-89", Phys. Rev. **162**, 1098 (1967), EXFOR L0011.

[Ber68] R. Bergere, H. Beil, and A. Veyssiere, "Photoneutron cross sections of La, Tb, Ho and Ta", Nucl. Phys. A **121**, 463 (1968), EXFOR L0012.

[Ber69a] R. Bergere, H. Beil, P. Carlos, and A. Veyssiere, "Photoneutron cross sections of I, Ce, Sm, Er, and Lu", Nucl. Phys. A **133**, 417 (1969), EXFOR L0015.

[Ber69b] B. Berman, R. Bramblett, J. Caldwell, H. Davis, M. Kelly, and S. Fultz, "Photoneutron cross sections for As-75,Ag-107, and Cs-133", Phys. Rev. **177**, 1745 (1969), EXFOR L0014.

[Ber69c] B. Berman, M. Kelly, R. Bramblett, J. Caldwell, H. Davis, and S. Fultz, "Giant resonance in deformed nuclei, photoneutron cross sections for Eu-153, Gd-160, Ho-165, and W-186", Phys. Rev. **185**, 1576 (1969), EXFOR L0016.

[Ber70] B. Berman, S. Fultz, J. Caldwell, M. Kelly, and S. Dietrich, "Photoneutron cross sections for Ba-138 and N-14", Phys. Rev. C **2**, 2318 (1970), EXFOR L0019.

[Ber80] B. Berman, D. Faul, P. Meyer, and D. Olson, "Photoneutron cross sections for He-4", Phys. Rev. C **22**, 2273 (1980), EXFOR L0051.

[Ber86] B. Berman, J. Caldwell, E. Dowdy, S. Dietrich, P. Meyer, and R. Alvarez, "Photofission and photoneutron cross sections and photofission neutron multiplicities for 233U, 234U, 237Np, and 239Pu", Phys. Rev. C **34**, 2201 (1986), EXFOR L0058.

[Ber87] B. Berman, R. Pywell, S. Dietrich, M. Thompson, K. Mcneil, and J. Jury, "Absolute photoneutron cross sections for Zr, I, Pr, Au, and Pb", Phys. Rev. C **36**, 1286 (1987), EXFOR L0057.

[Bez69] N. Bezic, Nucl. Phys. **A128**, 426 (1969).

[Bia62] W. Bianco and W. Stephens, "Photonuclear activation by 20.5-MeV γ rays", Phys. Rev. **126**, 709 (1962), EXFOR L0037.

[Bir85] Y. Birenbaum, S. Kahane, and R. Moreh, "Absolute cross section for the photodisintegration of deuterium", Phys. Rev. C **32**, 1825 (1985), EXFOR M0488.

[Bis50] G. Bishop, Phys. Rev. **80**, 211 (1950).

[Blo99a] A. Blokhin, "The evaluation of photonuclear cross-section data for the Th-232, U-233,234,235,236,238, and Pu-238,239,241 nuclei in the γ-ray energy up to 20 MeV", YK **2** (1999), in press.

[Blo99b] A. Blokhin, "The XGFISS code for analysis of photonuclear cross-sections for actinide nuclei", YK **2** (1999), in press.

[Bra63] R. Bramblett, J. Caldwell, G. Auchampaugh, and S. Fultz, "Photoneutron cross sections of Ta-181 and Ho-165", Phys. Rev. **129**, 2723 (1963), EXFOR L0003.

[Bra64] R. Bramblett, J. Caldwell, R. Harvey, and S. Fultz, "Photoneutron cross sections of Tb-159 and O-16", Phys. Rev. B **133**, 869 (1964), EXFOR L0005.

[Bra66] R. Bramblett, J. Caldwell, B. Berman, R. Harvey, and S. Fultz, "Photoneutron cross sections of Pr-141 and I-127 from threshold to 33 MeV", Phys. Rev. **148**, 1198 (1966), EXFOR L0009.

[Cal63] J. Caldwell, R. Harvey, R. Bramblett, and S. Fultz, "(γ,n) cross sections for O-16 and Si-28", Phys. Lett. **6**, 213 (1963), EXFOR L0004.

[Cal80a] J. Caldwell, E. Dowdy, B. Berman, R. Alvarez, and P. Meyer, "Giant resonance for the actinide nuclei: photoneutron and photofission cross sections for 235U, 236U, 238U, and 232Th", Phys. Rev. C **21**, 1215 (1980), EXFOR L0050.

[Cal80b] J. Caldwell and et al., Nucl. Sci. Eng. **73**, 153 (1980).

266

[Car74] P. Carlos, H. Beil, R. Bergere, A. Lepretre, A. Deminiac, and A. Veyssiere, "The giant dipole resonance in the transition region of the samariam isotopes", Nucl. Phys. A **225**, 171 (1974), EXFOR L0033.

[Car76] P. Carlos, H. Beil, R. Bergere, J. Fagot, A. Lepretre, A. Veyssiere, and G. Solodukhov, "A study of the photoneutron contribution to the giant dipole resonance of nuclei in the A = 64 - 86 mass region", Nucl. Phys. A **258**, 365 (1976), EXFOR M0364.

[Cha91] M. Chadwick, P. Oblozinsky, P. Hodgson, and G. Reffo, "Pauli-blocking in the Quasideuteron Model of Photoabsorption", Phys. Rev. C **44**, 814 (1991).

[Cha95a] M. B. Chadwick and P. G. Young, "Preequilibrium model for photonuclear reactions up to the pion threshold", Acta Physica Slovacia **45**, 633 (1995).

[Cha95b] M. B. Chadwick, P. G. Young, and S. Chiba, "Photonuclear angular distribution systematics in the quasideuteron regime", Journal of Nuclear Science and Technology **32**, 1154 (1995).

[Cos67] S. Costa, Nuovo Cimento **LI B**, 5891 (1967).

[Dea72] T. Deague and R. Stewart, "The photoneutron cross sections of La-139 and Pr-141", Nucl. Phys. A **191**, 305 (1972), EXFOR M0398.

[Deb92] P. Debevec, Phys. Rev. **C45**, 904 (1992).

[Die88] S. S. Dietrich and B. L. Berman, "Atlas of photonuetron cross sections obtained with monoenergetic photons", Atomic Data and Nuclear Data Tables **38**, 199 (1988).

[Edg57] R. Edge, "The (γ,n) reaction in Be-9 at intermediate energies", Nucl. Phys. **2**, 485 (1957), EXFOR M0444.

[Fuj82] M. Fujishiro, T. Tabata, K. Okamoto, and T. Tsujimoto, "Cross section of the reaction Be-9(γ,n) near threshold", Can. J. Phys. **60**, 1672 (1982), EXFOR M0438.

[Fuk92] T. Fukahori, "ALICE-F Calculation of Nuclear Data up to 1 GeV", in Proc. of the Specialists' Meeting on High Energy Nuclear Data, number JAERI-M 92-039, page 114, 3-4 October 1991, JAERI, Tokai, Japan, JAERI, Tokai, Ibaraki-ken, Japan (1992).

[Fuk93] T. Fukahori, Nucl. Data. News **82**, 41 (1993), (in Japanese).

[Fuk99] T. Fukahori, Private Communication (1999).

[Ful62a] S. Fultz, R. Bramblett, J. Caldwell, N. Hansen, and C. Jupiter, "Photoneutron cross sections for V-51 and Co-59", Phys. Rev. **128**, 2345 (1962), EXFOR L0001.

[Ful62b] S. Fultz, R. Bramblett, J. Caldwell, and N. Kerr, "Photoneutron cross-section measurements on gold using nearly monochromatic photons", Phys. Rev. **127**, 1273 (1962), EXFOR L0002.

[Ful64] S. Fultz, R. Bramlett, J. Caldwell, and R. Harvey, "Photoneutron cross sections for natural Cu, Cu-63, and Cu-65", Phys. Rev. B **133**, 1149 (1964), EXFOR L0006.

[Ful66] S. Fultz, J. Caldwell, B. Berman, R. Bramblett, and R. Harvey, "Photoneutron cross sections for C-12 and Al-27", Phys. Rev. **143**, 790 (1966), EXFOR L0010.

[Ful69] S. Fultz, B. Berman, J. Caldwell, R. Bramblett, and M. Kelly, "Photoneutron cross sections for Sn-116, Sn-117, Sn-118, Sn-119, Sn-120, Sn-124, and indium", Phys. Rev. **186**, 1255 (1969), EXFOR L0017.

[Ful71] S. Fultz, R. Alvarez, B. Berman, M. Kelly, D. Lasher, T. Phillips, and J. Elhinney, "Photoneutron cross sections for 24-Mg, 26-Mg, and natural magnesium", Phys. Rev. C **4**, 149 (1971), EXFOR L0026.

[Ful74] S. Fultz, R. Alvarez, B. Berman, and P. Meyer, "Photoneutron cross sections of 58-Ni and 60-Ni", Phys. Rev. C **10**, 608 (1974), EXFOR L0034.

[Ful85] E. G. Fuller, "Photonuclear reaction cross-sections for C-12, N-14 and O-16", Physics Reports **127**, 187 (1985).

[Gal60] J. Galey, "Photodisintegration of the deuteron with 94 MeV bremsstrahlung radiation", Phys. Rev. **117**, 763 (1960), EXFOR M0459.

[Gib59] J. Gibbons, R. Macklin, J. Marion, and H. Schmidt, "Precision measurement of the Be-9(γ,n) cross section", Phys. Rev. **114**, 1319 (1959), EXFOR M0441.

[Gor68] B. Goryachev, B. Ishkhanov, V. Shevchenko, and B. Yuryev, "Structure of cross section of the (γ,n) reaction on nuclei Si-28, S-32, and Ca-40", Yad. Fiz. **2**, 1168 (1968), EXFOR M0397.

[Gor69] B. Goryachev, B. Ishkhanov, I. Kapitonov, I. Piskarev, V. Shevchenko, and O. Shevchenko, "The structure of photoneutron cross sections of V-51, Cr-52, and Co-59 in the field of giant dipole resonance", Izv. Akad. Nauk SSSR,ser. Fiz. **33**, 1736 (1969), EXFOR M0093.

[Gor76] B. Goryachev, Y. Kuznetsov, V. Orlin, N. Pozhidaeva, and V. Shevchenko, "Giant resonance in strongly deformed nuclei Tb-159, Ho-165, Er-166, and Hf-178", Yad. Fiz. **23**, 1145 (1976), EXFOR M0057.

[Gor78] A. Goryachev and G. Zalesnyy, "Giant dipole resonance of W-182,184,186 isotopes and the shape of transitional nuclei with A=170-198", Izv. An Kaz. Ssr, Ser. Fiz.-mat. **6**, 8 (1978), EXFOR M0025.

[Gor82] A. Goryachev and G. Zalesnyy, "The studing of the photoneutron reactions cross sections in the region of the giant dipole resonanse in zinc, germanium, selenium, and strontium isotopes", Vopr. Teor. I Yad. Fiz. **8**, 121 (1982), EXFOR M0070.

[Gre64] L. Green and D. Donahue, "Photoneutron cross sections with monoenergetic neutron-capture γ rays", Phys. Rev. **135**, 701 (1964), EXFOR M0217.

[Gur76] G. Gurevich, L. Lazareva, V. Mazur, and G. Solodukhov, "About the width of giant resonance in the γ quanta absorption cross sections in the range of nuclei with A=150-200", Zh. Eksp. Teor. Fiz.,Pis'ma Red. **23**, 411 (1976), EXFOR M0056.

[Gur80] G. Gurevich, L. Lazareva, V. Mazur, S. Merkulov, and G. Solodukhov, "Total photoabsorption cross sections for high-Z elements in the energy range 7-20 MeV", Nucl. Phys. A **338**, 97 (1980), EXFOR M0041.

[Gur81] G. Gurevich, L. Lazareva, V. Mazur, S. Merkulov, G. Solodukhov, and V. Tyutin, "Total nuclear photoabsorption cross sections in the region 150<a<190", Nucl. Phys. A **351**, 257 (1981), EXFOR M0073.

[Hal53] J. Halpern, Phys. Rev. **91**, 934 (1953).

[Har64] R. Harvey, J. Caldwell, R. Bramblett, and S. Fultz, "Photoneutron cross sections of Pb-206, Pb-207, Pb-208 and Bi-209", Phys. Rev. B **136**, 126 (1964), EXFOR L0007.

[Hou50] P. Hough, Phys. Rev. **80**, 1069 (1950).

[Ish69] B. Ishkhanov, I. Kapitonov, E. Lazutin, I. Piskarev, and O. Shevchenko, "Photoneutron cross section of silver isotopes", Izv. Akad. Nauk SSSR,ser. Fiz. **33**, 2074 (1969), EXFOR M0524.

[Ish79] B. Ishkhanov, I. Kapitonov, V. Orlin, I. Piskarev, V. Shvedunov, and V. Varlamov, "Decay channels of the giant dipole resonance in Mg-26", Nucl. Phys. A **313**, 317 (1979), EXFOR M0002.

[Joh62] W. John and J. Prosser, "Photodisintegration cross section of beryllium near threshold", Phys. Rev. **127**, 231 (1962), EXFOR M0442.

[Jur79] J. Jury, B. Berman, D. Faul, P. Meyer, K. Mcneill, and J. Woodworth, "Photoneutron cross sections for 13C", Phys. Rev. C **19**, 1684 (1979), EXFOR L0048.

[Jur80] J. Jury, B. Berman, D. Faul, P. Meyer, and J. Woodworth, "Photoneutron cross sections for 17O", Phys. Rev. C **21**, 503 (1980), EXFOR L0049.

[Jur82] J. Jury, B. Berman, J. Woodworth, N. Thompson, R. Pywell, and K. Mcneill, "Photoneutron cross sections for 15N", Phys. Rev. C **26**, 777 (1982), EXFOR L0053.

[Kap69] S. Kapitza, N. Rabotnov, G. Smirenkin, A. Soldatov, L. Usachev, and Y. Tsipenyuk, "Photofission of even-even nuclei and structure of fission barrier", Zh. Eksp. Teor. Fiz.,Pis'ma Red. **9**, 128 (1969), EXFOR M0186.

[Kat51] L. Katz and A. Cameron, "The solution of X-ray activation curves for photonuclear cross sections", Can. J. Phys. **29**, 518 (1951), EXFOR M0273.

[Kec56] J. Keck, Phys.Rev. **101**, 360 (1956).

[Kne75] U. Kneissl, G. Kuhl, K. Leister, and A. Weller, "Photoneutron cross sections for 9Be obtained with quasi-monoenergetic photons", Nucl. Phys. A **247**, 91 (1975), EXFOR L0040.

[Kne76] U. Kneissl, K. Leister, H. Neidel, and A. Weller, "Photoneutron cross sections for 18O", Nucl. Phys. A **272**, 125 (1976), EXFOR L0045.

[Koc76] R. Koch and H. Thies, "The photoneutron cross section in C-13", Nucl. Phys. A **272**, 296 (1976), EXFOR M0363.

[Kom62] A. Komar, B. Bochagov, and V. Fadeev, "Fission of U-238 nuclei by photons of continuous spectra with E_γ max =35 MeV and neutrons with energies equal 14 MeV", Dokl. Akad. Nauk SSSR **146**, 1051 (1962), EXFOR M0170.

[Lee98] Y. O. Lee, T. Fukahori, and J. Chang, "Evaluation of Photonuclear Reaction Data on Tantalum-181 up to 140 MeV", Journal of Nuclear Science and Technology **35**, 685 (1998).

[Lep71] A. Lepretre, H. Beil, R. Bergere, P. Carlos, A. Veyssiere, and M. Sugawara, "The giant dipole states in the A = 90 mass region", Nucl. Phys. A **175**, 609 (1971), EXFOR L0027.

[Lep74] A. Lepretre, H. Beil, R. Bergere, P. Carlos, A. Deminiac, and A. Veyssiere, "A study of the giant dipole resonance of vibrational nuclei in the 103-a-133 mass region", Nucl. Phys. A **219**, 39 (1974), EXFOR L0035.

[Lep76] A. Lepretre, H. Beil, R. Bergere, P. Carlos, J. Fagot, A. Miniac, A. Veyssiere, and H. Miyase, "A study of the giant dipole resonance in doubly even tellurium and cerium isotopes", Nucl. Phys. A **258**, 350 (1976), EXFOR L0042.

[Lep81]   A. Lepretre, H. Beil, R. Bergere, P. Carlos, J. Fagot, A. DeMiniac, and Veyssiere, "The measurements of the total photonuclear cross sections from 30 MeV to 140 MeV for Sn, Ce, Ta, Pb and U nuclei", Nucl. Phys. A **367**, 237 (1981).

[Lep82]   A. Lepretre, H. Beil, R. Bergere, P. Carlos, J. Fagot, A. Veyssiere, and I. Halpern, "Analysis of neutron multiplicities in photo-nuclear reactions from 30 to 140 MeV in heavy-elements", Nucl. Phys. A **390**, 221 (1982).

[Lep87]   A. Lepretre, R. Bergere, P. Bourgeois, P. Carlos, J. Fagot, J. Fallou, P. Garganne, A. Veyssiere, H. Ries, R. Gobel, U. Kneissl, G. Mank, H. Stroher, W. Wilke, D. Ryckbosch, and J. Jury, "Absolute photofission cross sections for Th-232 and U-235,238 measured with monochromatic tagged photons (20 MeV < E_{gamma} < 110 MeV)", Nucl. Phys. A **472**, 533 (1987), EXFOR M0491.

[Mar50]   J. Marshall and E. Guth, Phys. Rev. **78**, 738 (1950).

[Mar84]   M. Martins, E. Hayward, G. Lamaze, X. Maruyama, F. Schima, and E. Wolynec, "Experimental test of bremsstrahlung cross section", Phys. Rev. C **30**, 1855 (1984), EXFOR M0473.

[Mar89]   J. Martins, E. Moreira, O. Tavares, J. Vieira, J. Filho, R. Bernabei, S. D'angelo, M. Pascale, C. Shaerf, and B. Girolami, "Nuclear fission of Au-197, Pb-nat, and Bi-209 induced by polarized and monocromatic photons of 60 and 64 MeV", Nuovo Cimento A **101**, 789 (1989), EXFOR M0402.

[Mar91]   J. Martins, E. Moreira, O. Tavares, J. Vieira, L. Casano, A. D'angelo, C. Schaerf, M. Terranova, D. Babusci, and B. Girolami, "Absolute photofission cross section of Au-197, Pb-nat, Bi-209, Th-232, U-238, and U-235 nuclei by 69-MeV monochromatic and polarized photons", Phys. Rev. C **44**, 354 (1991), EXFOR M0388.

[Mar97]   M. N. Martins, "Compilation and Evaluation of Photonuclear Data for Applications", in P. Oblozinský, editor, Summary Report of IAEA 1-st Research Coordination Meeting, number INDC(NDS)-364, International Atomic Energy Agency, Vienna, Austria, Obninsk, Russian Federation, December 7-10, 1996 (1997).

[Mat76]   J. Matthews, D. Findlay, S. Gardiner, and R. Owens, "High energy photoprotons from light nuclei", Nucl. Phys. A **267**, 51 (1976), EXFOR M0425.

[Mcc75]   J. Mccarthy, R. Morrison, and H. Molen, "Systematic study of the photodisintegration of Ge-70, Ge-72, Ge-74, and Ge-76", Phys. Rev. C **11**, 772 (1975), EXFOR M0496.

[McG86]   J. C. McGeorge and et al., "The ^{12}C(γ,p) reaction at E_γ=60 and E_γ=80 MeV", Phys. Lett. B **179**, 212 (1986).

[McM55]   W. McMurray, Proc. Phys. Soc. **68A**, 181 (1955).

[Mor89]   R. Moreh, T. Kennett, and W. Prestwich, "H-2 absolute cross section at 2754 KeV", Phys. Rev. C **39**, 1247 (1989), EXFOR M0453.

[Mur91]   T. Murata, in Proc.Int.Conf. on Nuclear Data for Science and Technology, Julich, page 955 (1991).

[Mur94]   T. Murata, Technical Report JAERI-M 94-019 (1994).

[Nor78]   J. Norbury, M. Thompson, K. Shoda, and H. Tsubota, "Photoneutron cross section of Fe-54", Amer. J. Phys. **31**, 471 (1978), EXFOR M0507.

270

[Ost78] Y. Ostapenko, G. Smirenkin, A. Soldatov, V. Zhuchko, and Y. Tsipenyuk, "Yields and cross sections of photofission for isotopes Th, U, Np, and Am in energy range from 4.5 MeV to 7.0 MeV", Technical Report YK-3(30), Inst. Fizicheskikh Problem, Moscow (1978), EXFOR M0004.

[Par64] F. Partovi, Ann. Physics **27**, 79 (1964).

[Per76] C. M. Perey and F. G. Perey, "Compilation of Phenomenological Optical Model Parameters", Atomic Data and Nucl. Data Tables **17**, 1 (1976).

[Phi50] J. Phillips, Phys. Rev. **80**, 326 (1950).

[Phi79] T. W. Phillips and R. G. Johnson, "Evidence for the isovector giant quadrupole resonance in 16O from the $16O(\gamma,n_0)15O$ reaction", Physical Review **C20**, 1689 (1979).

[Pyw79a] R. Pywell and M. Thompson, "Isospin splitting in the giant dipole resonance in Ti-46", Nucl. Phys. A **318**, 461 (1979), EXFOR M0370.

[Pyw79b] R. Pywell, M. Thompson, and R. Hicks, "A measurement of the Ti-50(γ,n) and Ti-50(γ,n_0) cross sections", Nucl. Phys. A **325**, 116 (1979), EXFOR M0326.

[Pyw83] R. Pywell, B. Berman, J. Jury, J. Woodworth, K. Mcneill, and N. Thompson, "Photoneutron cross sections for the silicon isotopes", Phys. Rev. C **27**, 960 (1983), EXFOR L0055.

[Ras89] R. Rassool and M. Thompson, "Absolute photoneutron cross section of I-127", Phys. Rev. C **39**, 1631 (1989), EXFOR G0013.

[Rud88] V. Rudnikov, G. Smirenkin, A. Soldatov, and S. Juhaz, "Angular anisotropy of photofission of even-even nuclei at above barrier energies", Yad. Fiz. **48**, 646 (1988), EXFOR M0447.

[Ryc90] D. Ryckbosch, L. Vanhoorebeke, R. Vandevyver, F. Desmet, J. O. Adler, D. Nilsson, B. Schroder, and R. Zorro, "Determination of the absorption mechanism in photon-induced preequilibrium reactions", Phys. Rev. C **42**, 444 (1990).

[She75] V. Shevchenko, "Photodisintegration of atomic nuclei in the giant dipole resonance region", Fiz. Elem. Chastic At. Jadra **2**, 243 (1975), EXFOR M0126.

[She92] Q. Shen, Commu. of Nucl. Data Prog. **7**, 43 (1992).

[Sne50] A. Snell, Phys. Rev. **80**, 637 (1950).

[Sol92] A. Soldatov and G. Smirenkin, Yad. Fiz. **55**, 3153 (1992).

[Sol94] A. Soldatov, Yad. Fiz. **58**, 224 (1994).

[Sol97] A. Soldatov, YK **3-4**, 3 (1997).

[Sol98] A. Soldatov, Phys. of Atomic Nuclei **61(8)**, 1325 (1998).

[Sto97] A. Storozhenko and et al., "Neutron Spectroscopy, Nuclear Structure, and related Topics", in Proc. 5th Intern. Seminar on Neutron-Nucleus Interactions (ISINN-5), page 337, Dubna (1997).

[Sun70] R. Sund, V. Verbinski, H. Weber, and L. Kull, "141-Pr (γ,n) cross section from threshold to 24 MeV", Phys. Rev. C **2**, 1129 (1970), EXFOR L0020.

[Sut80] R. Sutton, M. Thompson, M. Sugawara, K. Shoda, T. Saito, and H. Tsubota, "A study of photoreactions in Ti-48", Nucl. Phys. A **339**, 125 (1980), EXFOR M0532.

[Ter96] M. Terranova, O. Tavares, G. Kezerashvili, V. Kiselev, A. Milov, N. Muchnoi, A. Naumenkov, V. Petrov, I. Protopopov, E. Simonov, E. Paiva, and E. Moreira, "Fissility of Bi, Pb, Au, Pt, W, V, and Ti nuclei mesured with 100 MeV compton backscattering photons", J. Of Physics, G **22**, 511 (1996), EXFOR M0390.

[Var79a] V. Varlamov, B. Ishkhanov, I. Kapitonov, A. Panov, and V. Shvedunov, "The investigation of contributions of various configurations in giant dipole resonance of Si-28 nucleus", Izv. Akad. Nauk SSSR,ser. Fiz. **43**, 186 (1979), EXFOR M0003.

[Var79b] V. Varlamov, B. Ishkhanov, I. Kapitonov, Y. Prokopchuk, and V. Shvedunov, "On the effect of nucleons from various shells in formation of the giant dipole resonance of the Mg-24 nucleus", Yad. Fiz. **30**, 1185 (1979), EXFOR M0001.

[Var95] V. Varlamov, N. Efimkin, B. Ishkhanov, V. Sapunenko, and M. Stepanov, "Evaluation of Cu-63,65(γ,np) and Cu-63,65(γ,p) reaction cross sections in the energy range of giant dipole resonance and isospin splitting of the GDR of Cu nuclei", Izv. Akad. Nauk SSSR,ser. Fiz. **59**, 222 (1995), EXFOR M0374.

[Var96] V. V. Varlamov and V. V. Sapunenko, "Photonuclear Data Index 1976 - 1995", Technical Report Izdatel'stvo Moskovskogo Universiteta, Moscow State University, Moscow, Russia (1996).

[Vey70] A. Veyssiere, H. Beil, R. Bergere, P. Carlos, and A. Lepretre, "Photoneutron cross sections of 208-Pb and 197-Au", Nucl. Phys. A **159**, 561 (1970), EXFOR L0021.

[Vey73] A. Veyssiere, H. Beil, R. Bergere, P. Carlos, and A. Lepretre, "A study of the photofission and photoneutron processes in the giant dipole resonance of 232-Th, 238-U and 237-Np", Nucl. Phys. A **199**, 45 (1973), EXFOR L0031.

[Vey74] A. Veyssiere, H. Beil, R. Bergere, P. Carlos, A. Lepretre, and A. Miniac, "A study of the photoneutron contribution to the giant dipole resonance of s-d shell nuclei", Nucl. Phys. A **227**, 513 (1974), EXFOR L0039.

[Vey75] A. Veyssiere, H. Beil, R. Bergere, P. Carlos, A. Lepretre, and A. Deminiac, "Study of giant dipole resonance in A=190 transition region", J. de Physique Lettres **36**, L267 (1975).

[Waf51] H. Waffler, Helv. Phys. Acta **24**, 483 (1951).

[Wha56] B. Whalin, Phys. Rev. **101**, 377 (1956).

[Wol84] E. Wolynec, A. R. V. Martinez, P. Gouffon, Y. Miyao, V. A. Serrao, and M. N. Martins, Phys. Rev. C **29**, 1137 (1984).

[Woo79] J. Woodworth, K. Mcneill, J. Jury, R. Alvarez, B. Berman, D. Faul, and P. Meyer, "Photoneutron cross sections for 18O", Phys. Rev. C **19**, 1667 (1979), EXFOR L0047.

[You72] L. Young, Photoneutron cross-sections and spectra from monoenergetic photons on yttrium, praseodymium, lead, and bismuth in the giant-resonance, Ph.D. thesis (1972), EXFOR L0059.

[Zha86] H. Zhang, T. Yeh, and H. Lancman, "Photofission cross section of Th-232", Phys. Rev. C **34**, 1397 (1986), EXFOR M0449.

[Zha98] J. Zhang, "Illustration of Photonuclear Data Calc. with GUNF Code", Commu. of Nucl. Data Prog. **19**, 33 (1998).

[Zha99] J. Zhang, "Illustration of Photonuclear Data Calc. with GLUNF Code", Commu. of Nucl. Data Prog. **22** (1999).

[Zhu78a] V. Zhuchko, Y. Ostapenko, G. Smirenkin, A. Soldatov, and Y. Tsipenyuk, "Fission fragments angular distribution for the photofission of U-235", Yad. Fiz. **27**, 1420 (1978), EXFOR M0016.

[Zhu78b] V. Zhuchko, Y. Ostapenko, G. Smirenkin, A. Soldatov, and Y. Tsipenyuk, "Investigation of probability of the near-threshold fission of Th, U, Np, Pu, Am isotopes by bremsstrahlung γ quanta", Yad. Fiz. **28**, 1170 (1978), EXFOR M0078.

[Zub92] D. Zubanov, Phys. Rev. C **45**, 174 (1992).

CONTRIBUTORS TO DRAFTING AND REVIEW

Blokhin, A.I.   Nuclear Data Center
                   Institute of Physics and Power Engineering
                   Bondarenko Sq. 1
                   249 020 Obninsk, Kaluga Region
                   Russian Federation
                   E-mail: blokhin@ippe.rssi.ru

Chadwick, M.B.   Group T-2, MS B243
                   Los Alamos National Laboratory
                   Los Alamos, NM 87545
                   USA
                   E-mail: mbchadwick@lanl.gov

Fukahori, T.   Nuclear Data Center
                   Japan Atomic Energy Research Institute
                   Tokai-mura, Naka-gun
                   Ibaraki-ken 319-1195
                   Japan
                   E-mail: fukahori@ndc.tokai.jaeri.go.jp

Han, Y.   Nuclear Data Evaluation Laboratory
                   Korea Atomic Energy Research Institute
                   P.O. Box 105
                   Yusung, Taejon 305-600
                   Republic of Korea
                   Note: On leave from CNDC, Beijing
                   E-mail: hans@mipsa.ciae.ac.cn

Lee, Y.-O.   Nuclear Data Evaluation Laboratory
                   Korea Atomic Energy Research Institute
                   P.O. Box 105
                   Yusung, Taejon 305-600
                   Republic of Korea
                   E-mail: yolee@lui.kaeri.re.kr

Martins, M.N.   Instituto de Física
                   Universidade de São Paulo
                   Caixa Postal 66318
                   05315-970 Sao Paulo
                   Brazil
                   E-mail: martins@if.usp.br

S.F. Mughabghab   Dept of Advanced Technology
Brookhaven National Laboratory
P.O. Box 5000
Upton. NY 11973-5000
USA
E-mail: mugabgab@bnl.gov

Obložinský. P.   Nuclear Data Section
International Atomic Energy Agency
Wagramerstrasse 5, P.O. Box 100
A-1400 Vienna
Austria
E-mail: oblozinsky@iaeand.iaea.or.at

Varlamov, V.V.   Centre for Photonuclear Experiments Data
(CDFE–Centr Dannykh Fotoyadernykh Eksperimentov)
Institute of Nuclear Physics
Moscow State University
Vorob'evy Gory
119 899 Moscow
Russian Federation
E-mail: varlamov@cdfe.npi.msu.su
E-mail: varlamov@depni.npi.msu.su

Yu. B.   China Nuclear Data Center
Atomic Energy Institute
P.O. Box 275(41)
Beijing
China
E-mail: baosheng@mipsa.ciae.ac.cn

Zhang, J.   China Nuclear Data Center
Atomic Energy Institute
P.O. Box 275(41)
Beijing
China
E-mail: zhangjs@mipsa.ciae.ac.cn